Lithostratigraphy, palynostratigraphy and basin analysis of the Late Cretaceous to early Tertiary Paparoa Group, Greymouth Coalfield, New Zealand

A thesis
submitted in fulfilment
of the requirements for the Degree
of

Doctor of Philosophy

in the

University of Canterbury

by

Simon David Ward

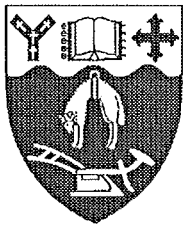

University of Canterbury

1997

Frontispiece

The deposition of the basal conglomerate was followed
by conditions that permitted the formation of mud and sand layers,
and occasional bands of coarser material,
and numerous beds of vegetable matter.

So far as the writer can judge,
the facts are best accounted for by supposing that
a freshwater lake or marsh was formed in a basin-like area,
which may be called the Paparoa Coal Basin.

Percy Gates Morgan
The Geology of the Greymouth Subdivision
North Westland
New Zealand Geological Survey Bulletin 13
1911

Abstract

The Paparoa Group of the Greymouth Coalfield, (West Coast, South Island, New Zealand) comprises a wholly terrestrial sequence of alternating fluvial and lacustrine strata deposited in a Late Cretaceous to Early Tertiary rift basin (the Paparoa Basin). Stratigraphic and tectonic evolution of the Paparoa Basin was determined from the lithologic record of 200 drillholes, and chronostratigraphic control was obtained from palynological identification of the Cretaceous–Tertiary Boundary (KTB).

Basin fill comprises three lithosomes, which were distinguished using lithofacies and geophysical log character. Coal measure lithosomes comprise pebble–cobble conglomerate, poorly sorted carbonaceous sandstone, siltstone, carbonaceous mudstone and coal, and represent fluvial and mire environments. Mudstone lithosomes comprise massive silty mudstone with rare plant fragments and freshwater bivalves, and represent lacustrine environments. Transitional lithosomes comprise coarsening upwards packets of moderate–well sorted fine to medium non-carbonaceous sandstone and rare conglomerates interbedded with massive mudstone. Lithofacies and unit geometry indicated these strata were deposited as progradational deltas in shallow lakes.

Lithostratigraphic unit definitions were revised in accordance with the lithosome framework. Five Formations and five members were recognised within the reinstated Paparoa Group: Jay Fm.; Ford Fm. (including the Ford Transitional Member); Rewanui Fm. (comprising Rewanui Coal Measure Member, Waiomo Mudstone Member and Morgan Coal Measure Member); Goldlight Fm. (including the Goldlight Transitional Member) and Dunollie Fm. The Ford and Goldlight Transitional Members are newly established to incorporate transitional lithosomes within the Ford Fm. and Goldlight Fm. Correlation of all units below the Rewanui Coal Measure Member (CMM) was revised, with Morgan CMM and Waiomo MM in the west of Greymouth Coalfield being transferred to Jay Fm. and Ford Fm. respectively.

Revised isopach models for all units (excluding Dunollie Fm.) were constructed using manual and numerical modelling techniques. Maximum present-day thickness of the Paparoa Group (excluding Dunollie Fm.) is 758.6m, and average thickness is 290m. Successively younger units onlap greater areas of basement, and basin geometry becomes simpler with time. Unit thicknesses were decompacted to account for differential burial of 1.75km (west coast) to 4.75km (eastern basin margin). Average thickness reduction during burial was 27%, and there was up to 290m of compaction. Compaction from cover strata deposition was greater than syndepositional compaction within the Paparoa Group.

The KTB was identified in 16 drillholes in the western Greymouth Coalfield. Key floral events were the extinction of *Tricolpites lilliei* and other rare large and/or ornamented angiosperm pollen taxa, and the rise in abundance of *Triorites minor*. The occurrence of diagnostic taxa was controlled by lithofacies and floral diversity in addition to sample age. Total spore proportions of palynofloras declined across the KTB, though dominant conifer and spore taxa were unaffected. There was a brief decline in angiosperm and conifer diversity c.4m above the KTB. Average palynoflora diversity was unchanged across the KTB, and no mass extinction event was recognised.

The interval between the KTB and the upper contact of Rewanui CMM varied throughout the western Greymouth Coalfield, and was controlled by syndepositional faulting. The position of the KTB was predicted in all western drillholes, and major coal seams were found to occur at predictable intervals beneath the estimated KTB position. At the time of the KTB, the western Paparoa Basin was occupied by a floodplain and mire-dominated environment intersected by rivers and associated crevasse splays.

Two principal sediment sources fed into the Paparoa Basin. The northeastern axial sandy fluvial system carried granite-derived detritus whereas the northwestern basin margin supplied sand and gravel derived from Paleozoic Greenland Group basement. Sediment flux from both sources declined during lacustrine deposition, however elongate to lobate deltas marked persistent sources of coarse clastic influx into the lake basins. During Goldlight Fm. deposition, sediment transport in the south of the basin was reversed. Minor sediment entered the Paparoa Basin from the southwest, but the eastern basin margin was not a significant sediment source.

Tectonic history of the Paparoa Basin was reconstructed from decompacted isopach patterns. Persistent sediment entry points were interpreted as transfer zones between normal faults. Unit thickness patterns were controlled by two orientations of normal faults: WNW/ESE and NNE/SSW. The steep eastern basin margin comprised a NNE/SSW aligned segmented fault zone, whereas there was block faulting along the western basin margin. The southwestern basin margin was flexural. Initial extension was oblique, resulting in reactivation of older (WNW/ESE) structures. Increasing dominance of the NNE/SSW faults during Paparoa Group deposition represented slight anticlockwise rotation of the extension direction.

Basin fill style was determined by the interaction of the two sediment sources and the two prominent fault orientations. Structural constraint of sediment entry points, and small scale normal faults within the basin, determined the position of fluvial systems within the basin during coal measure deposition, and the location and geometry of deltaic deposits during lacustrine episodes.

The Paparoa Basin is the largest basin within the West Coast Rift System, which comprises a colinear segmented rift system of extensional basins and rift gaps. Extension was initiated in the latest Cretaceous, at c.70Ma, approximately 10Ma after commencement of opening of the Tasman Sea, and related basin formation at Ohai Coalfield and in Taranaki. The West Coast Rift System may therefore contain the record of a previously unrecognised latest Cretaceous tectonic event.

Table of Contents

Section 1.

Chapter 1. Introduction

Chapter 2. Paparoa Group lithostratigraphy

Chapter 3. Revision of isopach models

Chapter 4. Decompacted isopach models and basin evolution

Chapter 5. Cretaceous-Tertiary Boundary palynostratigraphy, Rapahoe Sector

Chapter 6. Applications of palynostratigraphy and palynology to basin analysis

Chapter 7. Evolution of sediment transport within the Paparoa Basin

Chapter 8. Tectonic evolution of the Paparoa Basin

Chapter 9. Summary, discussion and conclusions

Part 2. Appendices

Appendix 4. Data preparation for decompaction analysis

Appendix 5. Palynological sampling and zonation

Appendix 6. Description and analysis of Greymouth Coalfield palynofloras

Section 3. Data tables

Section 4. Papers

Map pocket

List of abbreviations used in text

AFTA	Apatite Fission Track Analysis
CCNZ	Coal Corporation of New Zealand Ltd.
CM	Coal Measures
CMM	Coal Measure Member
CRA	Coal Research Association
CRL	Coal Research Ltd.
CRS	Coal Resources Survey
CV	Calorific value (MJ/Kg)
DH	drillhole
ECS	Eastern Compositional Suite
eoh	end of hole
Fm.	Formation
GCL	Greymouth Coal Ltd.
GCOL	Greymouth Coal Operating Ltd. (formerly GCL)
IGNS	Institute of Geological and Nuclear Sciences Ltd. (formerly NZGS)
KTB	Cretaceous – Tertiary Boundary
MM	Mudstone Member
MoE	Ministry of Energy (now Energy and Resources Division, Ministry of Commerce)
NZGS	New Zealand Geological Survey
SCM	State Coal Mines
UCP	University of Canterbury Palynology collection no.
UoC	University of Canterbury
VM	Volatile matter
VR	Vitrinite reflectance
VRF	Vitrinite reflectance and fluorescence
WCS	Western Compositional Suite

Acknowledgements

This project was supported financially by a University of Canterbury Postgraduate Scholarship, the former Canterbury Coal Research Group, the Department of Geological Sciences, and the Mason Trust Fund. Other financial support was by way of temporary employment with Coal Corporation of New Zealand Ltd. and Coal Research Ltd., and teaching opportunities within the Department of Geological Sciences.

Stuart Henley (Solid Energy) and Frank Taylor (GCOL) provided access to drillhole, mapping and geophysical data, plus a wealth of field and underground experience. Paul Caffyn divulged his wisdom on the geology of many mysterious places, and provided some crucial field observations. Staff of the Ministry of Commerce in Wellington gave access to official records, and supplied some geophysical data. Simon Nathan (IGNS) kindly supplied copies of older drillhole logs and maps. I particularly wish to thank the many geologists who have logged core in Greymouth over the years.

The *TECHBASE* database, without which this project could not have happened, was the product of Murry Cave (formerly MoC) and Bill Leask, of Ian R. Brown Associates, who supplied the software. Training was provided by Pete Manning, and Ian Brown and his staff were always happy to help with problems.

This project benefitted from paleobotanical and palynological discussions with Bob Spicer, Judy Parrish, Kirk Johnson, Ian Raine, John Lovis, Ian Daniel, Malcolm Warnes, Liz Kennedy and Nick Moore. Coaly matters were discussed with Nigel Newman, Joan Esterle, Jane Shearer and Tim Moore. Don Wise, John Bradshaw and Malcolm Laird gave of their time to entertain tectonic and stratigraphic thoughts. Peter Kamp kindly supplied a manuscript on fission track analysis. Doug Lewis and Dave MacKinnon assisted with supervision and read various bits of the manuscript. Helen Lever cheerfully offered to proof-read the appendices - hope you enjoy the bribe.

The technical and secretarial staff of the Department of Geological Sciences happily provided assistance. I would particularly like to thank Kerry Swanson for getting me started in the palynology lab all those years ago and Michael Finnemore for dragging us out of the computing dark ages. Assistance on the West Coast came from Richard Cotton, the Small family, Chris Cowan (and helicopter), Rob Boyd, Robin Simpson Hamish McLauchlan and the many people who provided mine keys.

To my former room-mates Rob Ferguson and Adriaan Bal, thanks heaps for everything over the years (who could call the Canterbury Plains was flat and boring now?), and thanks to all the students around the place who have made the department a great place to work, especially Steve Beresford for his timeless observation "You never finish your thesis, just one day you hand it in."

The project was initiated, supported and supervised by Jane Newman, who without a doubt makes the best cheesecakes this side of the Alpine Fault! What more could you ask for in a supervisor? Many thanks for everything, Jane, I have enjoyed every minute.

Finally, to Mum and Dad, Felicity, Craig and Morgan, and Anna and Nick (thanks for putting up with me), Cadfael and Zebbie, thanks for being there, and for not asking the obvious (when...?) question too often.

Part 1.

Chapters 1 – 9

Chapter 1. Introduction

1.1 Location of study area

Greymouth Coalfield is located at the southern end of the Paparoa Range, in the central West Coast region of the South Island, New Zealand (Figure 1.1). Coal-bearing strata include the Eocene Brunner Coal Measures, and the Late Cretaceous to Paleocene Paparoa Group, which is the subject of this thesis. Greymouth Coalfield contains New Zealand's premier resource of low ash, low sulphur bituminous coal (Barry et al. 1994).

Reviews of the physiography, vegetation, climate and cultural features of the Greymouth Coalfield and environs were presented by Gage (1952) and Bowman et al. (1984), and are not repeated here. The coalfield is divided into two Sectors, the western Rapahoe Sector and the eastern Mt. Davy Sector (Figure 1.1). Sectors encompass prospecting and mining licence blocks, and adjacent areas which are geologically continuous (Bowman 1982). Though defined geographically, the sectors also highlight major geological variation within the coalfield.

1.2 A history of geological investigation, Greymouth Coalfield

The early history of discovery and exploration of the Greymouth Coalfield was reviewed by Gage (1952, p. 5). The earliest definition of "Paparoa Beds" may be found in Morgan (1911, p. 50–51), who also recognised that these beds, while definitely below the well-known and extensively mined Brunner beds, "cannot be correlated with any other coal-bearing strata in New Zealand" (p. 53). The first comprehensive treatment of Greymouth Coalfield geology was presented by Gage (1952), who reported the results of an extensive field investigation carried out between 1938 and 1944 by the New Zealand Geological Survey (NZGS). This study encompassed topographic surveying, geological mapping, stratigraphy, structure and analysis of coal properties and resources.

The Greymouth Coalfield Bulletin (Gage 1952) was a benchmark achievement in New Zealand's economic geology, both in the context of regional geology and the broader implications for coal rank and hydrocarbon generation from coal (Kear 1994), and has formed the foundation for all subsequent work.

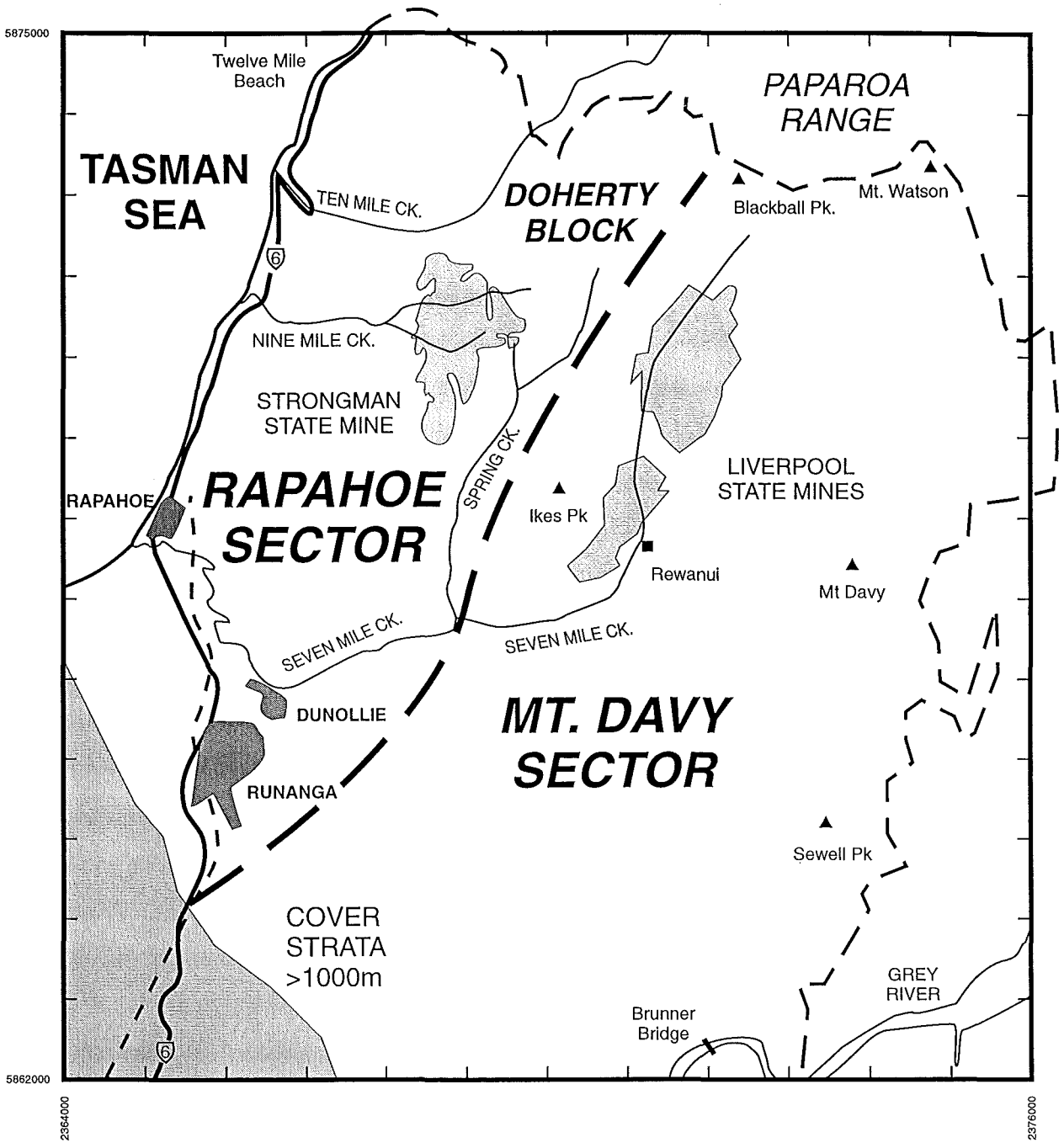

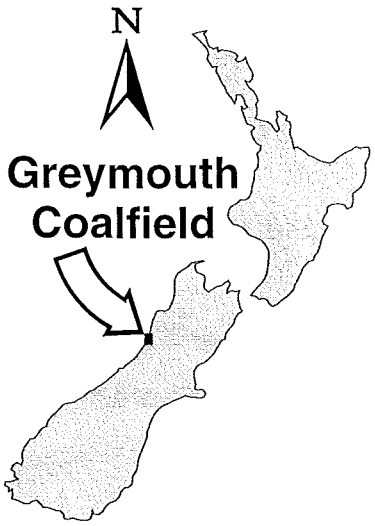

State Highway 6
railway
outcrop extent of coal measures
rivers and streams

Grid ticks = 1km
Grid numbers = New Zealand Map Grid
NZMS 260 J31 & K31

Figure 1.1 Location map, Greymouth Coalfield. Coalfield limits are defined by outcrop, coast, and sedimentary cover to the southwest.

During the period 1945–1978, geological activity in Greymouth Coalfield was undertaken by State Coal Mines, NZGS and Japanese mining interests. A wealth of data collected in the Strongman and Liverpool State Mines (Figure 1.1) was reviewed by Thorburn (1981a, b). These reports synthesised structure, stratigraphy and coal seam geometry for mining areas which are now exhausted and inaccessible, and are a valuable source of subsurface information. A revised, 1:63360 scale geological map for the Greymouth area was presented by Nathan (1978), which encompassed an earlier revision of lithostratigraphic nomenclature (Nathan 1974). An investigation of Late Cretaceous and Cenozoic sedimentary basins throughout New Zealand was started by NZGS in 1978. The West Coast volume (Nathan et al. 1986) provided an overview of the regional context of Greymouth Coalfield geology.

The next phase of investigation in Greymouth Coalfield was the 1979–1984 Coal Resources Survey (CRS) programme undertaken by the Mines Division, Ministry of Energy (Bowman 1982; Bowman et al. 1984). The aims of the CRS were to define remaining resources and to identify mining targets for possible future development (Bowman et al. 1984, p. 2). 22km of new drilling data was obtained from 49 drillholes spaced on a c.1km grid, many of which were fully cored and geophysically logged. The programme identified c.640Mt of in-ground coal resources (Bowman et al. 1984, p. 205) concentrated in several areas, namely the southern Rapahoe Sector, the Doherty Block, the upper Seven Mile Ck. area, and the central Mt. Davy Sector (Figure 1.1).

Coincident with the CRS programme was an upsurge in academic interest in Greymouth Coalfield and other West Coast coalfields, culminating in Ph.D. theses by J. Newman (1985) and N. Newman (1988). These studies, parts of which are summarised in Newman (1987) and Newman & Newman (1992), expanded the knowledge of diverse fields such as coal petrology, paleoenvironmental analysis and geochemistry. More recently, thesis research in Greymouth Coalfield has encompassed organic metamorphism and sandstone diagenesis (Boyd 1993; Boyd & Lewis 1995), coal seam palynology (Ward et al. 1995; Moore 1996a,b) and structural geology (McNee 1996).

Geological exploration and research in Greymouth Coalfield continues to the present-day. Resource targets identified by the CRS are presently being developed by Greymouth Coal Operating Ltd. (GCOL) and Solid Energy, and investigations continue in other parts of the coalfield (e.g. Caffyn 1994). Recent research activity has focussed on controls on coal seam distribution and properties (e.g. Ward 1995, 1996; T. Moore 1996), and development of techniques for vitrinite reflectance and fluorescence measurement (Newman & Ward 1996; Newman 1997).

1.3 Synthesis of Greymouth Coalfield geology

"It is widely acknowledged that the high level of geological complexity inherent at Greymouth is considerably greater than that normally experienced in most producing coalfields elsewhere" (Bowman et al. 1984, p. 2).

The 1:63360 geological map for Greymouth Coalfield and its accompanying description (Nathan 1978), which is referred to throughout this thesis as Figure 1.2, is included in the map pocket for ease of reference. The following synthesis of the geology of Greymouth Coalfield was compiled from Gage (1952), Nathan (1978), and Bowman et al. (1984).

Basement in Greymouth Coalfield comprises Paleozoic (c.500Ma) Greenland Group greywacke and argillite metasediments (lower greenschist facies). Greenland Group rocks are strongly deformed, with steep dips, ENE to NNW isoclinal folding and penetrative cleavage. Unconformably overlying basement in restricted areas of the coalfield is the mid-Cretaceous Pororari Group, a fanglomerate sequence deposited in rift basins associated with regional extension and metamorphic core complex formation to the north of Greymouth Coalfield (Laird 1988).

Two coal measure sequences unconformably overlie basement or Pororari Group (where present). The Late Cretaceous to early Paleocene Paparoa Group, which is the subject of this thesis, comprises a mostly conformable sequence of four coal-bearing coarse-grained intervals (conglomerates to carbonaceous mudstone and coal) and three non-carbonaceous fine grained intervals (mostly mudstone and siltstone). All Paparoa Group strata are of terrestrial origin, and were deposited in basins of limited extent. Thickness varies from c.100m in the west to >1000m in the east.

Unconformably overlying Paparoa Group, and basement in some parts of the coalfield, is the Eocene Brunner Coal Measures (CM), a quartz-rich sandy to conglomeratic sequence with widespread coal seams. Thickness of Brunner CM varies from <10m to 120m. In some places, thin Paleocene Brunner CM is apparently conformable upon the uppermost Paparoa Group unit (Newman 1985). Unlike Paparoa Group strata, Brunner CM are widespread in the Westland and Nelson area (Nathan et al. 1986).

Above Brunner CM is an Eocene to Oligocene sequence of marginal marine to shelf sediments, comprising the Rapahoe and Nile Groups of Nathan (1974). Total thickness of these strata varies from 1000m (west) to c.3000m (east), though erosion has removed this sequence from all but the western, southern and eastern margins of the coalfield. Sediments of the Rapahoe and Nile Groups occur throughout the Westland region. At Greymouth Coalfield, these strata are unconformably overlain by the Miocene Blue Bottom Group (marine), which is conformably overlain by non-marine gravels of the Pliocene Old Man Group. Quaternary valley fills and marine terrace deposits form the youngest deposits in the study area.

The basins in which the above sequence was deposited were inverted and deformed by Neogene to Recent compressional tectonics. Greymouth Coalfield is the central portion of a large, south-southwest plunging asymmetrical anticline with a steep eastern limb and gently dipping western limb. The axis of inversion (the Brunner – Mt. Davy Anticline) corresponds with the locus of maximum subsidence during the Late Cretaceous to Oligocene.

Greymouth Coalfield is pervasively faulted, with numerous NNE/SSW oriented normal and reverse faults (throws up to 100m) disrupting the sequence. Fault blocks vary in width from a few hundred metres to c.3km, and there is gentle folding within the larger blocks. Fault spacing recorded in underground mines varies from 10m to 2400m (Bowman et al. 1984, p. 95). Minor structural disruption is prevalent, and there is shearing and slickensiding associated with most coaly horizons. Coarse clastic beds, which are indurated, tend to be less deformed.

1.4 Opportunities for research in Greymouth Coalfield

Existing basin–wide studies of Greymouth Coalfield (Gage 1952; Bowman et al. 1984; Newman 1985) present a vast amount of data and interpretation, and numerous explanations for the observed geological features within the study area. Many of the conclusions reached were elegantly stated, and were confirmed by the present project. However, conclusions were arrived at by intuitive rather than deductive reasoning, as summarised by Bowman et al. (1984, p. 2):

"In particular, geological models used to explain the evolution of the coalfield and the distribution of coal have been constructed on the basis of a number of important assumptions. As such they are largely conjectural but they do incorporate all the currently available data and as such represent reasonable "best fit" models."

The above statement highlights the need to incorporate all available data. However, one notable absence from the extensive CRS report is a drillhole data summary. Stratigraphic contacts were located by the geologists responsible for logging the core, and unit thicknesses were derived from those contact locations. These data were used for isopach construction without verification of contact placement, or systematic correction for structural complications. Newman (1985) revised the CRS lithostratigraphy in selected drillholes, and made corrections where steeper dips were present. However, some faulted sections remained unrecognised or unconfirmed until the present project.

Sedimentological information derived from cored drillholes in Greymouth Coalfield was previously under-utilised. Traditionally, seam correlation models were constructed using stratigraphic columns comprising key contact locations and the positions and thickness of coal seams, and no use was made of information from the sediments above, below or between coal seams. During more recent investigations (Bowman et al. 1984; Newman 1985, 1987), sedimentological interpretations were enhanced by systematic descriptions of texture and composition, enabling the general patterns of alternating fluvial and lacustrine sedimentation within Greymouth Coalfield to be defined. However, deltaic deposits, which would be expected to be present in such a sequence, have not been consistently recognised or described.

A second source of data which was previously under-utilised is geophysical logging. Since 1979, suites of geophysical logs have been routinely obtained from exploration drillholes. Such data were used for interpretation of stratigraphic sequences in non-cored (open) drillholes, and detailed geophysical logs for seam intervals were used for coal resource studies (e.g. seam thickness), but there has been no comprehensive use of geophysical data for lithostratigraphic or sedimentological investigations.

One aspect of coalfield investigation which remained undefined during previous studies was chronostratigraphy, and Bowman et al. (1984, p. 40) conceded that "some control on the age of sediments, which could for example refine the correlation of coal seams, would be of enormous value". Preliminary palynostratigraphic investigations (Raine 1981, 1984) indicated that the Cretaceous Tertiary Boundary (KTB) lies within the coalfield, however no further work was undertaken at the time. Other palynological applications, such as interpretation of coal-forming vegetation and paleoclimate, had received no attention.

The above review indicates that, while general features of Greymouth Coalfield geology were well documented, thorough synthesis, description and interpretation of data was lacking. Within existing data sets, there was significant potential for further investigation, and collection of additional data (particularly palynological) was required. "Conjectural" conclusions, which dominated previous studies, required testing by rigorous geological investigation and construction of logical inferences founded upon all available data and the relevant state of geological knowledge.

1.5 Scope of this thesis

This thesis is an exercise in basin analysis. The scope of the thesis encompasses those aspects of previous work where further investigation was needed, namely drillhole sedimentology, geophysical data interpretation, data synthesis and basin modelling, and collection of new palynological data. Initially, the investigation was to focus on the economically-significant Rewanui Coal Measure Member (CMM), which contains c.80% of known coal resources in Greymouth Coalfield (Bowman et al. 1984, Figure 49). The initial objective was to integrate outcrop data, drillhole sedimentology and palynology with seam geometry records, in order to determine controls on coal seam distribution. However, as preliminary work progressed, three problems became apparent.

Firstly, in order to understand the Rewanui CMM, the unit had to be clearly defined, and this was not possible with the existing lithostratigraphic framework. Consequently, there was uncertainty about the distribution and thickness of the unit. Secondly, sedimentary structures were found to be poorly developed in core and generally poor in outcrop, limiting the ability to undertake detailed sedimentological analysis. Thirdly, there was an inverse relationship between drillhole and outcrop data availability (i.e. good outcrop but limited drillhole data in the Mt. Davy Sector, vice versa in the Rapahoe Sector). Geological differences between the two sectors precluded integration of field and subsurface data as initially envisaged.

Much of the drillhole data available for the southern Rapahoe Sector had been obtained since completion of previous studies (Bowman 1981; Bowman et al 1984; Newman 1985, 1987), and further investigation of this area was clearly warranted.

Thus, the scope of the thesis was broadened to firstly address problems inherent in existing lithostratigraphic nomenclature and definitions, and secondly, to undertake additional study of the southern Rapahoe Sector. The emphasis of the thesis was therefore shifted from a detailed study of one unit, to comprehensive basin analysis of all relevant units, with the emphasis on utilising subsurface (drillhole) data. Particular emphasis was still given to study of the Rewanui CMM, because of the economic interest in that unit, and the good data availability. Field investigations were limited to observations of specific geological features not present in the drillhole database.

The large size of the drillhole data set, including much quantitative data, required development of new research tools to enable data to be accessed and assimilated efficiently. This project represents the first comprehensive application of computer-based data management, reduction and reporting techniques to the study of Greymouth Coalfield geology. Use of numerical techniques allowed many aspects of the present study to progress from the qualitative interpretations of previous workers, to quantification of basinal features, and statistical testing of relationships. Computer techniques also required a structured framework for data collection, which enabled many errors in the drillhole database to be detected.

1.6 Objectives

The broad objectives of this thesis are (1) to test assumptions and conclusions proposed by previous studies, (2) to enhance the utilisation and interpretation of existing data, and (3) to add new data which would increase the understanding of the geology of the Paparoa Group, and the basin in which it accumulated (which is referred to as the Paparoa Basin). To achieve these objectives, three themes of investigation are followed. The first theme is lithostratigraphy, which addresses the following specific objectives:

- subdivision of the sequence based on lithological criteria and geophysical log character
- revision of the lithostratigraphic nomenclature and definitions
- location of stratigraphic contacts in all drillholes, and determination of unit thicknesses, accounting for post-depositional structural disruption

The second theme pursued in this thesis is basin modelling, which addresses:

- construction of isopach models
- the effects of Paleogene burial on lithostratigraphy
- the controls on lithostratigraphic patterns: tectonic subsidence vs. compaction

The final theme pursued in this thesis is palynology, which addresses:

- location of the Cretaceous – Tertiary Boundary at a reconnaissance level throughout the Rapahoe Sector
- description of paleovegetation from mire and non-mire environments
- paleoenvironmental and paleoclimatic interpretation
- applications of palynostratigraphy to lithostratigraphy and coal seam correlation

Integration of the above investigations addresses the following aspects of basin analysis:

- sediment transport history
- controls on deltaic sedimentation
- tectonic evolution of the basin

The final objectives are to present an integrated model for the evolution of the Paparoa Basin and its sedimentary fill, and to highlight how and why the character of the Paparoa Group differs from basin–fill predicted by conventional tectonostratigraphic models.

1.7 Stratigraphic data sources

The primary source of stratigraphic data for this study comprises 200 drillholes, which contain information for c.57km of stratigraphic section. Data sources and drillhole locations are listed in Appendix 9, and a location map is given in Figure 1.3 (map pocket). More than 550 other drillholes are present in the coalfield, but these are mostly short (<50m), or intersect units not covered in this study, and were omitted. High quality lithological logs are available for newer drillholes (post–1978), whereas logs for older drillholes are of lower quality, and often only grainsize was recorded.

Lithological and stratigraphic data were coded and entered into a database established by the Energy and Resources Division, Ministry of Commerce. Subsequently, data were reformatted into the Greymouth Coalfield Database (Ian R. Brown Associates Ltd. 1992) which operates under the *TECHBASE*® software package (MINEsoft 1996). A routine was developed for transfer of data between *TECHBASE* and *ROCKWORKS*™ *LOGGER*® for construction of graphic logs, editing of existing records and addition of new data. Records for 35 drillholes were either added to the database or significantly revised, and data for all other drillholes were verified against original lithological log data.

1.8 Thesis structure

This thesis is presented in four parts. **Part 1**, which comprises nine chapters, constitutes the body of the thesis proper. **Part 2** (Appendices 1–8) presents reviews, methods and ancillary research necessary to develop the arguments and analyses presented in Part 1. **Part 3** (Appendices 9–14) comprises drillhole, lithostratigraphic and palynological data on which the thesis is based. **Part 4** comprises three papers published during the course of this investigation, which addressed paleoenvironmental and paleofloral controls on coal seam genesis and distribution within the Rapahoe Sector.

Throughout the thesis, the components of chapters within Part 1 are referred to as Sections (e.g. Section 1.1), components of appendices are denoted "Appendix X.X" (e.g. Appendix 1.1), and tables and figures within all appendices are prefixed with "A" (e.g. Figure A1.1). Papers in Part 4 are referred to as Ward 1995, Ward et al. 1995, and Ward 1996.

Chapter 2. Paparoa Group lithostratigraphy

2.1 Introduction

The objective of this chapter is to define and describe the vertical succession of Paparoa Group strata present in Greymouth Coalfield. Lithostratigraphic subdivision of the Paparoa Group at Greymouth Coalfield is well established (Figure 2.1), and is reviewed in Appendix 1. However, Newman (1985) recognised that the distinction of Coal Measures Members from Mudstone Members was not always straightforward. The lithostratigraphic nomenclature largely reflects data available in c.1945, and is inadequate to account for the complex lateral and vertical inter-relationships between many units, as discussed in Appendix 1.2.1–1.2.6.

This chapter presents a means of objective subdivision for the Paparoa Group (Section 2.3), a resolution of existing problems of definition and correlation (Sections 2.4–2.6) and a revised suite of definitions for the Paparoa Group and its constituent formations and members (Sections 2.7, 2.8).

2.2 Summary of lithostratigraphic problems

The following lithostratigraphic problems are addressed in this chapter:

- identification of Dunollie CMM / Goldlight MM contact
- definition of Goldlight MM; whether sandy strata should be included
- location of Dunollie CMM / Rewanui CMM contact in the northwest
- definition of Rewanui CMM to account for compositional variation
- definition and correlation of "transitional" strata beneath Rewanui CMM
- lateral relationship between Morgan CMM and Waiomo MM
- correlation of basal conglomerates at Twelve Mile Beach

Other stratigraphic problems identified in Appendix 1 which are beyond the scope of this thesis are the resolution of the Brunner CM / Paparoa Group contact, the significance of Paleocene Brunner CM at Greymouth Coalfield, and the higher order nomenclature for Brunner CM throughout the West Coast region.

Group	Formation	Member
Mawheranui	Brunner CM	
	Paparoa CM	Dunollie CMM
		Goldlight MM
		Rewanui CMM
		Waiomo MM
		Morgan CMM
		Ford MM
		Jay CMM
Pororari	Hawks Crag Breccia	

A. Nathan (1974, 1978)

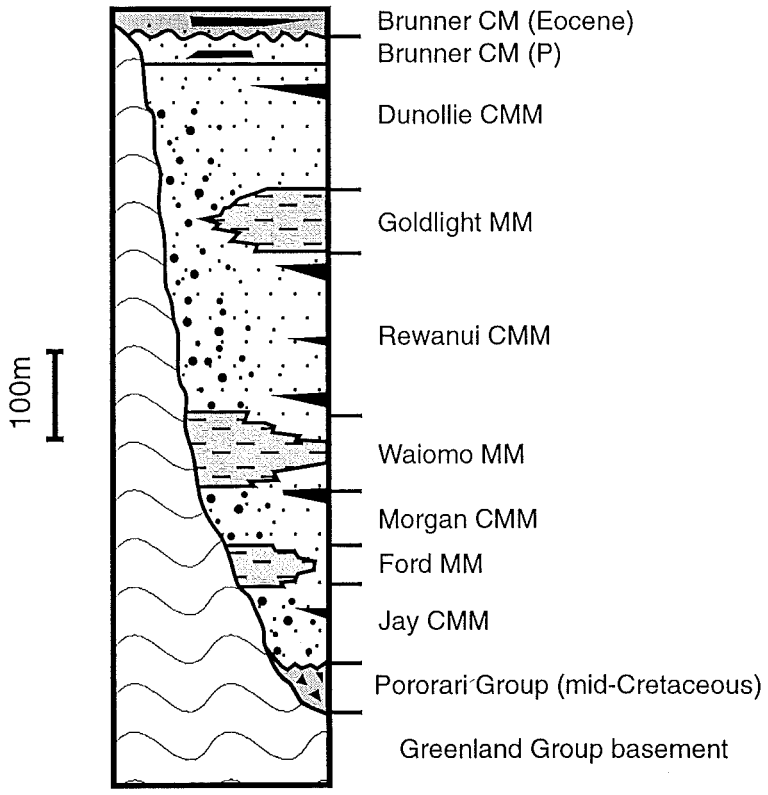

B. Newman & Newman (1992)

Figure 2.1 Existing lithotratigraphic nomenclature, Greymouth Coalfield
CM = Coal Measures, CMM = Coal Measure Member, MM = Mudstone Member
Brunner CM (P) = Paleocene Brunner CM

2.3 Lithological subdivision of the Paparoa Group

The most comprehensive source of information in Greymouth Coalfield for lithological subdivision of the Paparoa Group is the suite of geophysical logs, which are available for many recent drillholes. The log suite consists of natural gamma-ray measurements, two gamma–gamma density records (Long–Spacing Density, resolution = 48cm and Bed Resolution Density, resolution = 15cm) and drillhole diameter (caliper). Neutron and sonic logs are also available for selected drillholes. Many drillholes were uncored above coal-bearing target horizons, and selected drillholes were not cored, thus geophysical logs provide the only continuous record of Paparoa Group stratigraphy.

For many modern drillholes, core description was undertaken by numerous geologists (Bowman et al. 1984, p. 34), resulting in a substantial database of lithological descriptions. These lithological logs provide accurate descriptions of bed thickness and overall grainsize, and information on sediment composition and structural features present in the core. However, gradational trends (such as clay content and proportion of carbonaceous material) were not consistently recorded, and many non-coaly intervals were not described in detail. In addition, sedimentary structures are poorly developed in core from Greymouth Coalfield, thus the lithological database was of limited use for detailed facies analysis. In contrast, the geophysical log suite provides an objective record of the stratigraphy, with high quality data available for all intervals of all logged drillholes.

Interpretation of geophysical logs follows standard practice (e.g. BPB 1981; Schlumberger 1985). N. Newman (1988) demonstrated that Greymouth Coalfield "mudstones" are commonly quartz-rich siltstones with a high proportion of potassic minerals, notably illite and muscovite, which would provide the characteristic high gamma signature. Sandstones in the Mt. Davy sector, which contain abundant microcline feldspar and muscovite (Boyd & Lewis 1995), also have high natural gamma signatures. The gamma ray log character of some Greymouth Coalfield rocks therefore reflects compositional as well as size variation, and distinction of clay-rich sediments from sandstone on the basis of geophysical logs alone requires caution (e.g. Rider 1990).

Some uncored drillholes in the southern Mt. Davy Sector (e.g. DH620, DH625) were formerly interpreted (CRS) as comprising mudstone–dominated sequences, whereas strata are more probably dominated by sandstones which have a high gamma character. Neutron logs assisted in recognition of unit boundaries and high-gamma sandstone beds in these drillholes, though no drillholes in the southern Mt. Davy Sector were both fully cored and comprehensively logged to provide reliable calibration.

Stratigraphic columns were subdivided according to gross changes in geophysical log character. These subdivisions are "lithosomes", which are defined as "lithostratigraphic bodies which are mutually intertongued with one or more bodies of differing lithic constitution" (Wheeler & Mallory 1956). The lithosomes reflect fundamental differences in lithological character between the various units, and form the basis for recognition and description of lithostratigraphic units (formations, members) within the Paparoa Group.

Selected intervals of core were examined to test lithosome designations and contacts, and to check ambiguous or incomplete descriptions of sedimentary structures, textures or composition taken from existing geological logs. Structural disruption which may have influenced stratigraphy was also noted from geophysical logs (caliper) and core inspection. Relevant details are reported in Appendices 2 and 10. The three lithosome subdivisions are listed below and summarised in Figure 2.2.

1) Coal Measure lithosomes: Thick to thin–bedded (10m to 10cm) pebble–cobble conglomerate and poorly sorted very coarse to very fine sandstone, carbonaceous siltstone, bedded–laminated carbonaceous mudstone, (rare massive mudstone and siltstone) and coal lithofacies. Must contain carbonaceous material. Often contains multiple thick (>10m), clean (<5% ash) coal seams.
Key to geophysical log identification: dominance of irregular to fining upwards and blocky geophysical log motifs; carbonaceous beds and coal commonly indicated on long–spacing density log.
Interpreted environments: alluvial fan, alluvial plain, fluvial, floodplain, crevasse-splay, floodbasin and mire (may be raised).

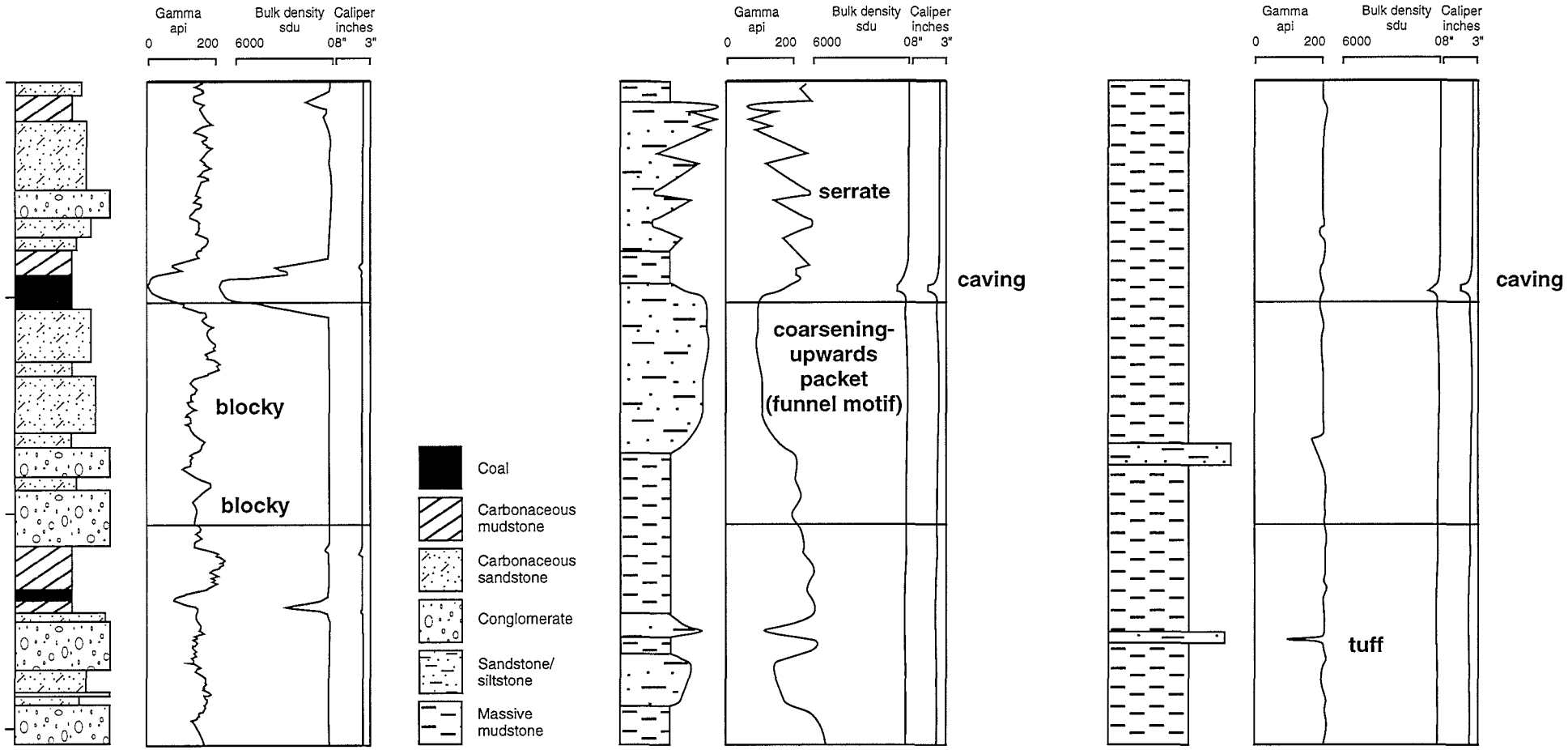

COAL MEASURE LITHOSOME

Note variability, common carbonaceous material, coal distinct on density log, blocky motif through conglomerate, sandstone.

TRANSITIONAL LITHOSOME

Note interbedded coarsening upwards siltstone and sandstone, no carbonaceous material, funnel or serrate log motifs typical.

MUDSTONE LITHOSOME

Note monotonous high-gamma character, no carbonaceous zones indicated on density log, thin sandstone or tuff interbeds.

Figure 2.2 Lithologic and geophysical character of the three lithosomes identified within the Paparoa Group.
Each section shows 30m.

2) Transitional lithosomes: Interbedded mudstones, siltstones and moderately sorted to sorted very fine to medium sandstones. Beds often thick (2–20m); soft sediment deformation (slumping, flame structures, chaotic bedding) common. Rare matrix-supported pebble conglomerate; may contain mudstone (rip-up) clasts. Fresh-water bivalve impressions may be present. Carbonaceous material limited to leaf fossils, fine detritus and rare thin carbonaceous mudstone beds.

Key to geophysical log identification: Coarsening-upwards packets, either thick with funnel-shaped log motif, or thinner and variable, with serrate log motif; often interbedded with massive mudstone (high gamma) beds, carbonaceous material rarely recorded on long spacing density log.

Interpreted environment: lacustrine delta (subaqueous, rarely emergent)

3) Mudstone lithosomes: Massive mudstone, muddy siltstone and siltstone. Rare matrix-supported conglomerates, slumping common. Well preserved leaf fossils and freshwater bivalve impressions may be present. Rare thin sandstone interbeds; tuffaceous beds (including volcanic breccia) may be common.

Key to geophysical log identification: thick, monotonous intervals with high gamma counts (c.120-150 api units). Interbedded tuffs have blocky, low-gamma log motif. Carbonaceous material not recorded on long spacing density log.

Interpreted environment: lacustrine

Interpretation of the depositional environments represented by the mudstone and coal measure lithosomes follows existing studies (Bowman et al. 1984; Newman 1985, 1987; Newman & Newman 1992; Ward 1995; Ward et al. 1995). Geophysical log character of the coal measure lithosomes is typical for fluvial environments (e.g Cant 1984, Figure 11; Schlumberger 1985), and consistent with existing environmental interpretations. Further detailed interpretation of fluvial environments was hampered by poor representation of sedimentary structures both in outcrop and in core.

Interpretation of transitional lithosomes as deposits of lacustrine deltas is based upon geophysical log character and lithofacies occurrence. Funnel-shaped gamma-ray profiles which are typical of the lithosome (Figure 2.2) are not a uniquely associated with deltaic deposits (Cant 1984, Figure 11). However, the intercalation of high-gamma intervals identical to those of the mudstone lithosomes indicates lateral equivalence to

lacustrine deposition, and suggests that a deltaic setting is most likely. Lithofacies of the transitional lithosomes are typically coarsening-upwards medium to very fine sandstone bodies intercalated with mudstone beds, and similar deposits from various settings and ages of strata have been interpreted to represent prograding mouth bar deposits in high-constructive lobate deltas (e.g. Farquharson 1982; Ayres 1986; Flint et al. 1989). Slumping and soft sediment deformation, which are common in transitional lithosomes at Greymouth Coalfield, are also common in some lacustrine delta facies associations (e.g. Flint et al. 1989; Anadón et al. 1991, Figure 15). Further discussion of the transitional lithosomes is presented in Section 7.8.2.

An example of recognition of the three lithosomes from geophysical log character throughout a typical Paparoa Group sequence is illustrated in Figure 2.3. Correlation between the lithosomes and lithostratigraphic subdivisions of DH645 is summarised in Table 2.1.

Member	CRS lithological log	Newman (1985)	this project	lithosomes
Dunollie CMM	0–48.0	0–48.0	0–20.0	coal measures
Goldlight MM	48.0–113.0	48.0–194.0	20.0–48.0 48.0–103.5 103.5–181.5	transitional mudstone transitional
Rewanui CMM	113.0–427.9	194.0–407.6	181.5–407.6	coal measures
Waiomo MM	427.9–476.9 (eoh)	407.6–eoh	407.6–427.9 427.9–eoh	transitional mudstone

Table 2.1 Present and former interpretations of lithostratigraphy, DH645. Member names follow existing nomenclature. All depths in metres. CRS lithological log by P. Caffyn, May–July 1981. Newman (1985) transferred 20m of basal Rewanui CMM to Waiomo MM.

All stratigraphic sections were subdivided into lithosomes, though assignment of lithosomes to lithological records from older drillholes, which lack geophysical log data, was based on lithological character, in particular carbonaceous content. Lithosomes were assigned to match overall lithological patterns where specific details were not recorded, and transitional lithosomes were often difficult to identify in older records. Uncertain lithosome identifications are noted in Appendix 10.

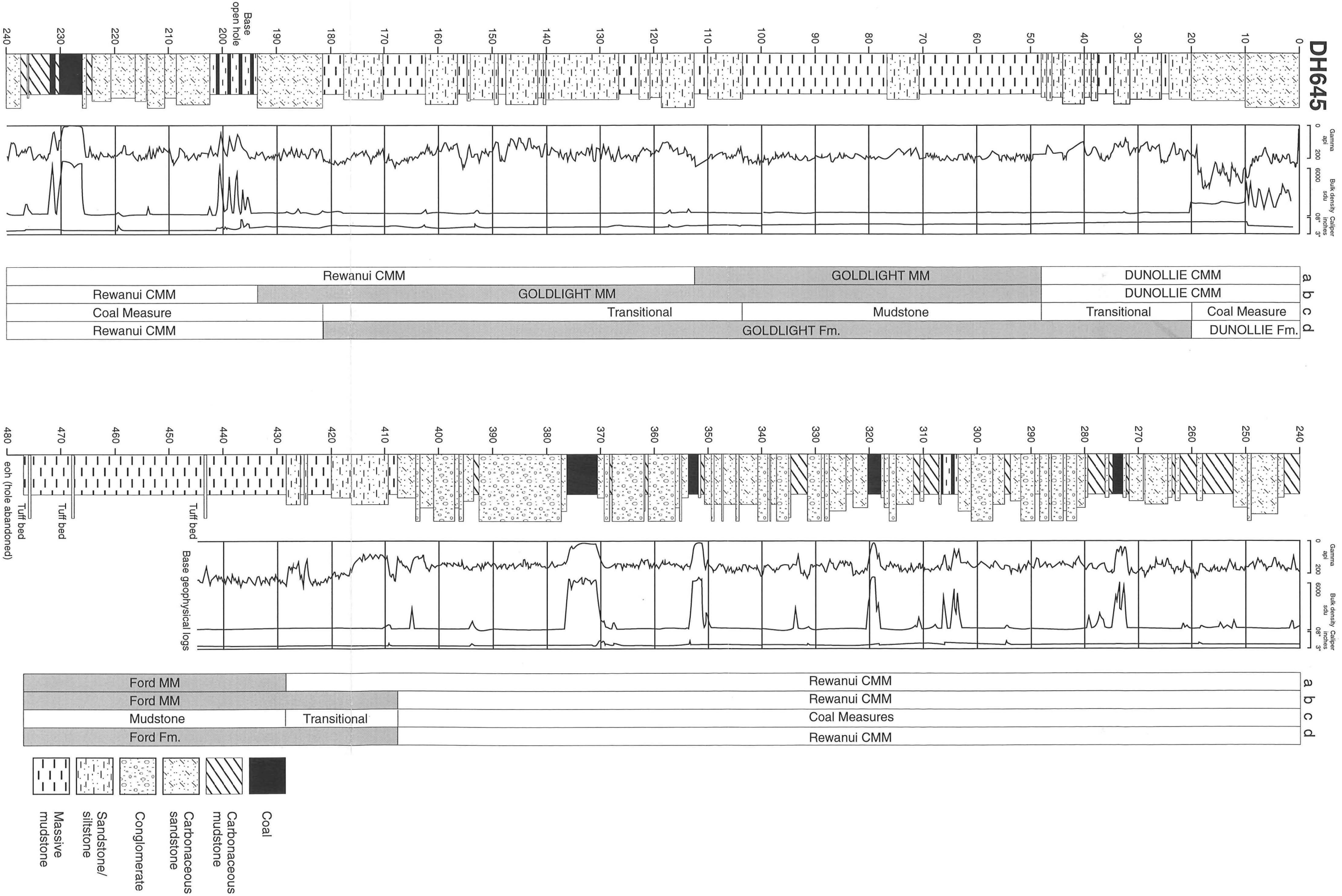

Figure 2.3 Lithostratigraphy of DH645. Stratigraphic subdivisions are a = CRS, b = Newman (1985), c = lithosomes, d = present project.

2.4 Relationship between lithosomes and lithostratigraphic units

In accordance with existing nomenclature (Appendix 1), the Paparoa Group was divided into coal-bearing and coal-free lithostratigraphic units. Coal-bearing units contain exclusively coal measure lithosomes. Coal-free (mudstone-dominated) units contain both mudstone and transitional lithosomes, which are laterally continuous. Thus, the Paparoa Group was subdivided into lithostratigraphic units which reflect alternation between subaerial and subaqueous depositional environments. The present recognition and stratigraphic grouping of lithosomes resolved many of the lithostratigraphic problems discussed above (Section 2.2). As illustrated for DH645 (Figure 2.3, Table 2.1), application of the new lithostratigraphic framework also resulted in significant revision of the placement of stratigraphic contacts.

2.5 Revised lithostratigraphic nomenclature

The fundamental unit of lithostratigraphy is the Formation, which is a body of rock identified by lithologic characteristics and stratigraphic position, and is mappable at the surface or traceable in the subsurface (NASC 1983, Article 24). In the present study, five Formations within a revised Paparoa Group are defined: Jay Formation, Ford Formation, Rewanui Formation, Goldlight Formation and Dunollie Formation. These definitions constitute a revision of the rank, lithological content and boundary positions of units previously defined by Gage (1952) and Nathan (1974, 1978) (see Appendix 1).

The revised stratigraphic nomenclature (listed below) is depicted schematically in Figure 2.4. Descriptions for all units are presented in Section 2.7, and thickness data are given in Appendix 10. Definition and regional correlation of the revised Paparoa Group is discussed in Section 2.8.

Jay Formation: Jay CMM is elevated to Formation status. Jay Formation comprises the Jay (ii) and Jay (iii) units of Gage (1952) (Figure A1.1A, B). These units are not assigned to members due to limited data, and are retained as informal subdivisions.

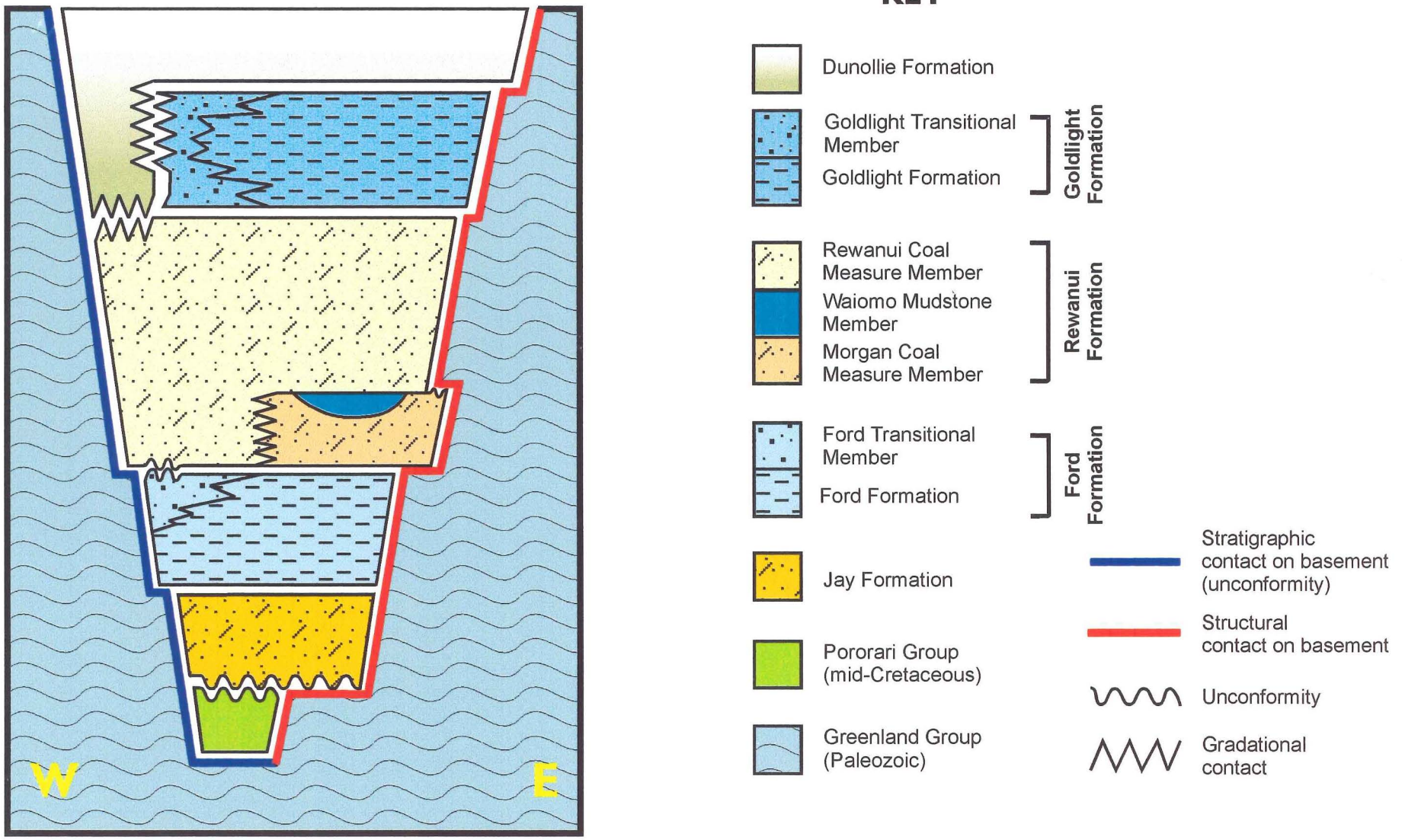

Figure 2.4 Lithostratigraphic summary diagram, Paparoa Group, Greymouth Coalfield.
Exploded view showing relationships between Formations and Members.
(not drawn to scale)

Ford Formation: Ford MM is elevated to Formation status, and now includes western strata previously placed in Waiomo MM. Transitional lithosomes within Ford Fm. are named the **Ford Transitional Member**. Volcaniclastic lithofacies within Ford Fm. have a discontinuous distribution, and are not assigned to a formal stratigraphic unit.

Morgan Coal Measure Member: Nomenclature for Morgan Coal Measure Member is unchanged, though the extent of the unit is redefined to only include strata present in the Mt. Davy Sector, and sediments formerly called Morgan CMM at Twelve Mile Beach are transferred to Jay Fm.

Waiomo Mudstone Member: Nomenclature for Waiomo Mudstone Member is unchanged. The extent of the unit is redefined to only include strata present in the Mt. Davy Sector.

Rewanui Coal Measure Member: The name Rewanui Coal Measure Member is retained for those strata previously thus named, but excluding any transitional lithosomes which were formerly incorporated in Rewanui CMM. Compositional suites are retained as informal stratigraphic subdivisions, but not distinguished as members.

Rewanui Formation: Rewanui Formation is redefined, and comprises three Members, Rewanui CMM, Waiomo MM and Morgan CMM. In the west of the coalfield, Rewanui CMM comprises the full thickness of the Rewanui Fm.

Goldlight Formation: The Goldlight Formation incorporates the previous Goldlight MM plus those transitional lithosomes now recognised to be laterally equivalent to Goldlight MM mudstone lithosomes. Transitional lithosomes represent mappable units of limited lateral and vertical extent, and are named the **Goldlight Transitional Member**. Where a thick mudstone lithosome separates transitional lithosomes, upper and lower subdivisions of the Member are informally recognised (Appendix 10.1).

Dunollie Formation: Dunollie CMM is elevated to Formation status. The basal contact is redefined as lying above transitional lithosomes. No further investigation of Dunollie Fm. was undertaken in the present project.

2.6 Recorrelation of units beneath Rewanui CMM

Significant changes in the definition, correlation and extent of both mudstone and coal measure units below Rewanui CMM are embodied in the revised stratigraphic nomenclature, and these changes are discussed below.

2.6.1 Revision of mudstone lithostratigraphy beneath Rewanui CMM

Recent field observations have shown that Waiomo MM does not thicken west of Spring Creek, as depicted by existing isopach maps (Figures A1.3D, A1.4A; Ward 1995), but rather the unit thins rapidly westwards in the vicinity of Spring Ck. (P. Caffyn, pers. comm. October 1995). Waiomo MM should therefore be regarded as only the relatively thin package (<c.60m) of dominantly massive mudstone found throughout the eastern half of the coalfield. Correlation of the great thickness of sandy/tuffaceous mudstone present throughout much of the Rapahoe Sector (e.g. in DH632, DH657; see also Ward 1995) must therefore be revised.

Existing observations, assisted by the present recognition of transitional lithosomes (Section 2.3), highlight greater lithological similarity between thick western Waiomo MM and typical Ford Fm. than between the former and typical Waiomo MM (Table 2.2). Indeed, Gage (1952, p. 30) observed that Waiomo MM in the northwestern corner of the coalfield "resembles the Ford beds", being lighter in colour than the typical dark-grey to brown-grey mudstone, and containing interbeds of siltstone and fine sandstone. Western Waiomo MM is now transferred to Ford Fm.

Lithological feature	Ford MM	Western Waiomo MM	Eastern Waiomo MM
Maximum thickness	c.150m	>150m	<c.60m
Strata beneath	coal measures or basement	coal measures or basement	coal measures
Lithology	grey to dark brown siltstone–mudstone, fine–coarse sandstone interbeds, rare plant frags. Soft-sediment deformation and ripup clasts present.	massive to interbedded grey–pale grey mudstone, siltstone and fine sandstone, increasing sand in NW	massive dark-grey to grey-brown mudstone, siltstone and rare sandstone.
Tuffaceous material	may be present	common, may include volcanic breccias	very rare (only in DH658)
Transitional lithosomes in upper part of unit	n/a	Common, includes siltstone to conglomerate	generally absent

Table 2.2 Summary of lithological features, previous correlations of mudstone units beneath Rewanui CMM.

Rewanui CMM was previously described as resting either conformably upon Waiomo MM, or unconformably on basement (Appendix 1.2.5). The present recorrelation of mudstone units indicates Rewanui CMM in the western Greymouth Coalfield lies conformably on Ford Fm. (where present), and the Rewanui / Ford contact is generally placed immediately above transitional lithosomes. In the northwest of the coalfield, at Twelve Mile Beach, large ripup clasts of mudstone and siltstone are present in basal Rewanui CMM (Figure 2.5A), indicating an erosional contact. Bowman et al. (1984, p. 43) and Newman (1985, p. 41) have demonstrated that northwestern Paparoa Group strata were deposited proximal to the margin of the basin, and gradation from conformable to unconformable contacts is commonplace at basin margins (NASC 1983, Article 58).

Angular–rounded coal clasts within lowermost Rewanui CMM and Ford Transitional Member are also present at Twelve Mile Beach, the head of Ten Mile Ck road (United Mine) and in DH708 and DH710 (Figure 2.5B). Lack of plastic deformation suggests these clasts were deposited as coal and not as peat, and were therefore coalified prior to erosion and redeposition. Burial of peat by >c.1km is necessary to induce significant coalification (Appendix 4.2.4), thus the source cannot have been pre-existing Paparoa Group, which had attained a maximum thickness of <200m in the northwestern area prior to Rewanui CMM deposition (Section 4.2.5).

A possible source for the coal clasts is erosion of mid-Cretaceous Pororari Group sediments, which are known to occur c.10km to the WNW of Greymouth Coalfield in the offshore Takutai half-graben (Bishop 1992; see also Section 2.8), and also in small areas of the Greymouth Coalfield (Figure 1.2). An erosional unconformity between syn-rift Pororari Group strata and thin Paparoa Group sediments was illustrated by Bishop (1992) on seismic profiles of the Takutai half-graben. Presently, coal is only known from the upper portion of outcropping Pororari Group (Laird 1988), however these strata may have formerly been thicker, as the upper contacts of all known sequences are eroded (Bishop 1992; Laird, pers. comm. 1996).

Figure 2.5A Siltstone and mudstone ripup clasts in basal Rewanui CMM, Twelve Mile Beach.

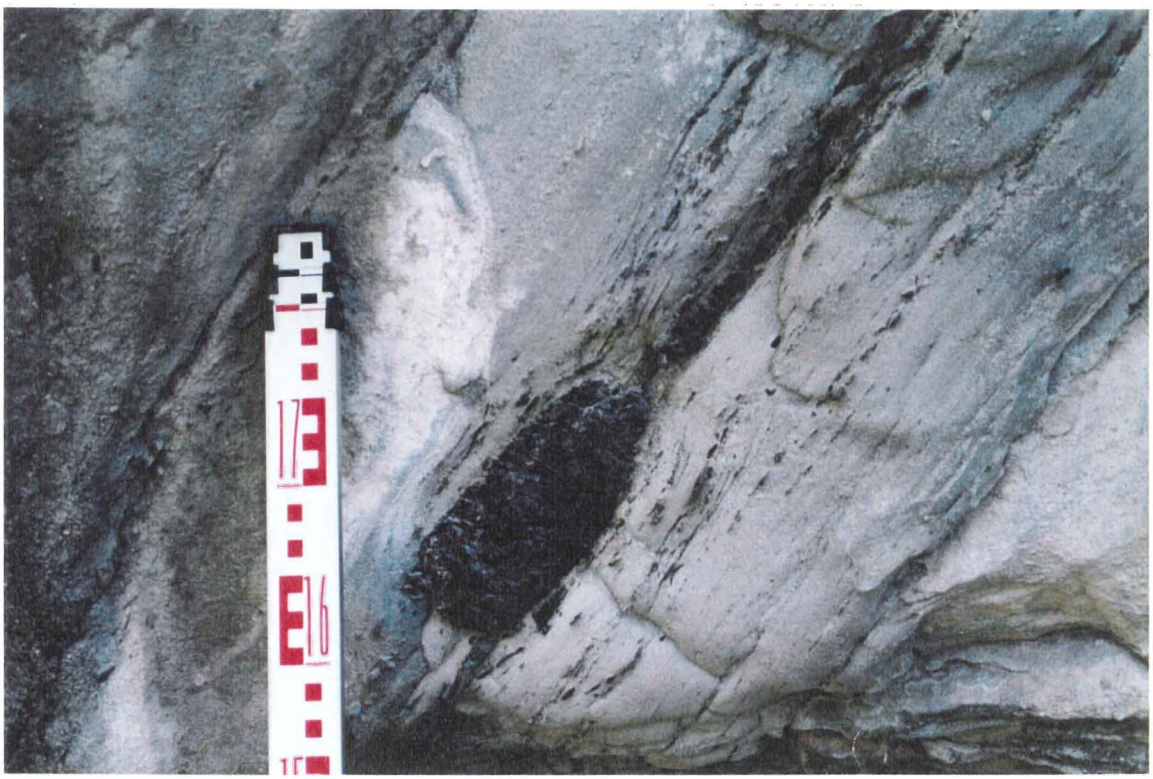

Figure 2.5B Angular coal clast in Ford Transitional Member, outcrop at head of Ten Mile Ck. road.

2.6.2 Revision of coal measure lithostratigraphy below Rewanui CMM

Recorrelation of the mudstone units beneath Rewanui CMM results in restriction of Morgan CMM to the eastern half of the coalfield. Morgan CMM was previously mapped continuously across the northern reaches of the coalfield (Gage 1952; Nathan 1978), and the western portion of this outcrop (from Trig "Z" to Twelve Mile Beach; see Figure 1.2) must now be transferred to Jay Fm., as it lies beneath Ford Fm.

Other adjustments to existing mapping of Jay Fm. occurrence were required in the far northeast of the coalfield, near Mt. Watson. The original stratigraphic interpretation of DH661 at Mt. Watson was consistent with mapping by Gage (1952) and Nathan (1978) of this locality, which indicated a thin sequence of Rewanui CMM, Waiomo MM and Morgan CMM resting on basement (Figure 1.2). Recent field investigations (P. Caffyn pers. comm. 1995) revealed that the units were interpreted incorrectly (Morgan CMM was called Rewanui CMM etc.), and the section in DH661 comprises Morgan CMM, Ford Fm. and Jay Fm. on basement. The mapping of Jay Fm. in the northeast requires revision, and the relationship between the area previously mapped as Morgan CMM and the nearest mapped Jay Fm. is unclear.

Morgan CMM is now largely enclosed within mudstone (rarely transitional) lithosomes, and only lies directly on basement in the extreme east of the coalfield (Gage 1952; Nathan 1978, recently remapped by Caffyn 1994). Morgan Volcanics, indicated by Gage (1952) and Nathan (1978) as being extensive in the east of the coalfield (Appendix 1.2.3, Figure 1.2), were not present in any drillholes used in this project, and no specific investigation of these strata was undertaken.

2.6.3 Compositional distinction of Jay Fm., Morgan CMM and Rewanui CMM

Previously, Rewanui CMM and Morgan CMM were distinguished on the basis of clast composition at Twelve Mile Beach (Newman 1985, Appendix 1), where abundant granite clasts first occur at the base of Rewanui CMM, but are absent from underlying conglomerates. Limited petrological data from Smale (1978) supported the compositional distinction of Rewanui CMM from Morgan CMM and Jay Fm., with only Rewanui CMM sandstones containing conspicuous feldspar or rock fragments.

Morgan CMM and thin Waiomo MM in DH266 and DH273 were transferred to Rewanui CMM on the grounds of abundant feldspar in the Morgan CMM sandstones (Appendix 1.2.3). However, mudstone lithosomes are excluded from Rewanui CMM, and conglomerates at Twelve Mile Beach are now placed in Jay Fm. (Section 2.5), therefore the compositional distinction of the coal measure units requires revision.

Inspection of core from Morgan CMM intervals in DH654, DH656 and DH658 revealed abundant quartzofeldspathic and micaceous sandstones, and rare fine pebble conglomerates containing granite and Greenland Group clasts with quartzofeldspathic sandstone matrix material (Appendix 10.4). Lithological logs for many older drillholes containing Morgan CMM (e.g. those numbered DH410–DH463) report the presence of "nearly white sandstone" in Morgan CMM, which is also probably quartzofeldspathic. Other Morgan CMM intervals (e.g. DH632) are exclusively of Greenland Group provenance. Morgan CMM is therefore composed of sediments of mixed or variable provenance, and includes strata which are compositionally similar to Rewanui CMM.

Clastic material may have been recycled from the Pororari Group into the Paparoa Group basin. Minor clast lithologies (e.g. rhyolite, angular coarse sandstone) present in the basal Paparoa Group conglomerates at Twelve Mile Beach, for which no source can be presently located, are probably recycled. However, the extent of recycling is difficult to determine, particularly as granite clasts are abundant within Pororari Group sediments in the southwestern Paparoa Range area (Topp 1996 p. 205), yet apparently absent from the sources (either primary or recycled) for basal Paparoa Group conglomerates.

2.6.4 Relationship between Morgan CMM, Waiomo MM and Rewanui CMM

Recorrelation of strata beneath Rewanui CMM, and recognition of similar provenance of Rewanui CMM and Morgan CMM, raises the possibility that Morgan CMM is stratigraphically continuous with Rewanui CMM. Comparison of two drillholes (DH631, DH632) which span the western limit of Morgan CMM and Waiomo MM occurrence revealed close stratigraphic similarity between the basal 60m of Rewanui CMM in DH631, and the Morgan CMM interval in DH632 (Figure 2.6). No interval corresponding to Waiomo MM is present in DH631. Morgan CMM is therefore inferred to be laterally equivalent to western basal Rewanui CMM. This correlation is supported by analysis of sediment transport patterns (Section 7.4).

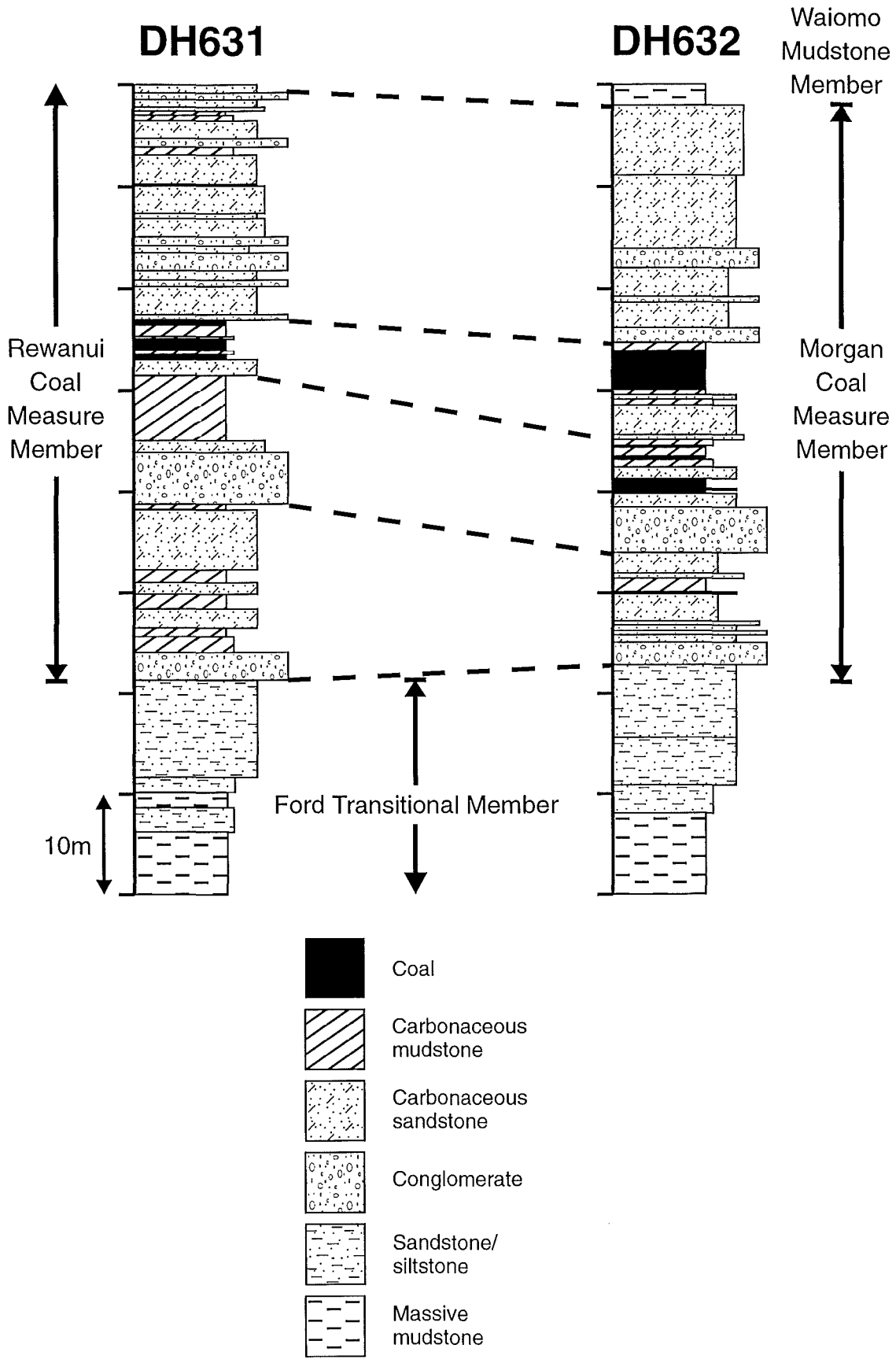

Figure 2.6 Correlation between basal Rewanui CMM in DH631 and Morgan CMM in DH632.
There is no interval corresponding to Waiomo MM in DH631.
Vertical units shown are true depth (dip corrected) down hole.
Top of section DH631 = 320m, DH632 = 440m.

2.7 Descriptions of lithostratigraphic units

This section presents specific lithological details for each of the units defined above, which highlight departures from the general descriptions implicit in the lithosome framework. Changes in definition of the units are discussed where applicable.

2.7.1 Jay Formation

The definition of Jay Fm. remains remain unchanged from previous descriptions (Appendix 1.2.1), however the extent of the formation has been expanded in this study. Jay Fm. comprises two distinct units, which correspond to Gage's (1952) Jay (ii) and Jay (iii) units (see Table A1.1). The upper Jay (iii) unit comprises typical coal measure lithosomes, with common carbonaceous mudstone but rare coal. Basal Jay (ii) is dominated by conglomerate (containing clasts of Greenland Group, hornfels, and rare rhyolite and quartzose sandstone but no granite), and contains little carbonaceous material. Quartzose sandstones are present in Jay Fm. in DH659 and DH661. Where determinable, thicknesses of the Jay (ii) and Jay (iii) are given in Appendix 10.6. Correlation of Jay (i) to Pororari Group (Nathan 1974, 1978) is retained.

2.7.2 Ford Formation

Ford Fm. comprises mudstone and transitional lithosomes, and interbedded tuffaceous material. Ford Fm. mudstone lithosomes are differentiated from other mudstone units by the presence of interbeds of siltstone and very fine sandstone, and debris-flow conglomerates in DH656 (37.7m thick), DH659 and DH719. Ford mudstone lithosomes vary from 0–128.3m (Appendix 10.5), whereas the Ford Transitional Member is up to c.60m thick (Appendix 10.5), and may comprise the full thickness of the Formation. (e.g. DH639, DH647, DH651).

Tuffaceous beds and volcanigenic material are present in at least 15 drillholes (Appendix 10.5). Beds vary from lapilli tuff to fine pebble volcanic breccias, present in DH631 and DH640, both of which contain a large amount of volcanigenic material. Tuffaceous beds are absent from Ford Fm. in nine drillholes, though six of these drillholes only partially intersect the unit. Tuffaceous beds are not unique to Ford Fm., however known occurrences in Waiomo MM (near Roa and in DH658) are very minor.

2.7.3 Morgan Coal Measure Member

Coal measure lithosomes of Morgan CMM (Appendix 10.4) comprise dominantly fine sandstone (rare medium–coarse sandstone and fine pebble conglomerate), carbonaceous mudstone and coal (0–10m, clean, split or dirty). The member is restricted to the eastern part of the coalfield, and is generally conformable with overlying Waiomo MM and underlying Ford MM, though Morgan CMM lies directly on basement in DH630 and along the rugged eastern flanks of Mt. Davy (Caffyn 1994). Morgan CMM may contain either granite-derived or Greenland Group derived detritus. Basaltic volcanic material, including pillow lavas, is intercalated with coal measure lithosomes in the east of the coalfield (Gage 1952; Nathan 1978).

2.7.4 Waiomo Mudstone Member

Waiomo MM is composed of dominantly mudstone lithosomes, and comprises <c.60m of dark-grey to grey-brown massive mudstone with rare sandstone and siltstone interbeds, and rare transitional lithosomes at the base or top (Appendix 10.3). Tuffaceous material is generally absent. Waiomo MM is conformable with overlying Rewanui CMM and underlying Morgan CMM, and is restricted to the eastern half of the coalfield. Many older drillholes in the Rewanui area probably contain thin transitional lithosomes between Waiomo MM and overlying Rewanui CMM, however drillhole records are poor and do not permit accurate recognition of these sediments.

2.7.5 Rewanui Coal Measure Member

The upper Rewanui CMM contact is generally marked by the abrupt change from carbonaceous mudstone or coal to mudstone or transitional lithosomes of the Goldlight Fm. The base of Rewanui CMM is either the contact with transitional lithosomes (western portion of coalfield), the contact with massive mudstone lithosomes (eastern portion of coalfield), or the contact with basement (southwestern portion of coalfield). A detailed discussion of the location of the upper and lower Rewanui CMM contacts, and calculation of Rewanui CMM thickness, is presented for each drillhole in Appendix 2. Previously unrecognised transitional lithosomes occur above and/or below Rewanui CMM in >30 drillholes. Major revisions of Rewanui CMM lithostratigraphy in DH632 and DH656 were necessary (Appendix 2, Table A2.1, A2.2), resulting in reduction of previous measurements of Rewanui CMM thickness by c.50% for both drillholes.

Along the western margin of Greymouth Coalfield, Goldlight Fm. is absent, and location of the upper Rewanui CMM contact is problematical. Previous workers placed the contact arbitrarily (Appendix 1.2.5). In four drillholes (DH634, DH637, DH639, DH710) in which Rewanui CMM and Dunollie Fm. are conformable, carbonaceous material is more common in Rewanui CMM than Dunollie Fm. Therefore, the upper Rewanui CMM contact in the west is placed at the upper limit of a conspicuously carbonaceous section indicated on the geophysical logs (Appendix 2). The use of palynostratigraphy and coal seam correlation in locating lithostratigraphic boundaries in the western Greymouth Coalfield is discussed in Section 6.4.

Coal measure lithosomes within Rewanui CMM comprise two distinct textural and compositional associations (Appendix 1.2.5). In the Western Compositional Suite (WCS), Rewanui CMM strata comprise grey/green, well indurated, massive to bedded (5m–0.1m scale), rounded to subrounded greywacke (minor granite) cobble to pebble conglomerate, and moderately to poorly sorted coarse to very fine sandstone, carbonaceous sandstone, siltstone, carbonaceous siltstone and mudstone, and coal (present in multiple widespread seams, generally clean and not split).

In the Eastern Compositional Suite (ECS), Rewanui CMM strata are predominantly white/yellow, well indurated, lenticular-bedded and planar crossbedded, poorly to moderately sorted, angular to subangular, quartzofeldspathic and micaceous, siderite and quartz-cemented, granule (rarely fine pebble) conglomerate to medium sandstone, with interbeds of quartzose fine sandstone fining upwards to carbonaceous mudstone and thin dirty coal, carbonaceous mudstone and siltstone (not part of fining-upwards packet) and coal (clean or dirty, seams often lenticular with rapid lateral thickness change).

There is a limited zone in which the two compositional suites are intermixed (Boyd & Lewis 1995, Figure 4), and a sharp boundary between the suites cannot be defined. Allocation of separate formal lithostratigraphic names to the compositional suites is therefore inappropriate.

2.7.6 Goldlight Formation

Stratigraphic definition of Goldlight Fm. was previously regarded as problematical (Appendix 1.2.6, Section 2.2). However, application of the lithosome framework allows Goldlight Fm. to be accurately defined in most drillholes. The base of overlying Dunollie Fm. is placed between the uppermost limit of upper Goldlight Transitional Member (where present) or mudstone lithosomes, and the lower limit of overlying coal measure lithosomes. Likewise, the base of Goldlight Fm. is defined by the contact between transitional or mudstone lithosomes and underlying coal measures. In the northwest, Goldlight Fm. grades (via transitional lithosomes) into Dunollie Fm. Goldlight Fm. does not overlie basement in any drillhole investigated for this study.

Goldlight Fm. comprises mudstone and transitional lithosomes (Appendix 10.1), though the latter, which are placed in the Goldlight Transitional Member, are restricted to the western part of the coalfield. Mudstone lithosomes comprise massive, dark grey brown silty mudstone, which is distinguished from other mudstone lithosomes by lack of variability over substantial thicknesses (>50m). Matrix-supported conglomerates and tuffaceous material are absent from Goldlight Fm. Along the western margin of Greymouth Coalfield, no distinct mudstone lithosome is present (Appendix 10.1) and Goldlight Fm. is entirely represented by transitional lithosomes.

An example of the effects of the present revision of Goldlight Fm. lithostratigraphy in DH645 is illustrated in Table 2.1 and Figure 2.3. Goldlight Fm. was previously interpreted to occur from 48.0–113.0m (CRS) or from 48.0–194.0m (Newman 1985), whereas the revised interval is 20.0–181.5m. Strata immediately above and below Goldlight Fm. in DH645 are carbonaceous, whereas no carbonaceous material is present within Goldlight Fm.

2.8 Definition of the Paparoa Group

Groups are defined to express the natural relationships of associated formations (NASC, 1983). The Formations and their component members present within Greymouth Coalfield occur together with well–defined inter–relationships (Figure 2.4). These Formations are here placed within the ***Paparoa Group***. Paparoa Group is used in preference to Paparoa Coal Measure Group, as Goldlight Fm., Waiomo MM and Ford

Fm. are not coal measure units. The use of Paparoa Group is consistent with historical precedence, and represents an affirmation of the usage of "Paparoa Beds" by Morgan (1911) and Lower, Middle and Upper Paparoa Group of Gage (1952) (Figure A1.1A) to encompass the coal measures and intercalated mudstone units found beneath the quartzose Brunner Coal Measures within Greymouth Coalfield.

The Paparoa Group includes correlative strata representing latest Cretaceous to early Tertiary terrestrial deposits (commonly coal-bearing) in the Westland area (Figure 2.7). The major Paparoa Group occurrence outside Greymouth Coalfield is at Pike River Coalfield (Raine 1984; Newman 1985; Ferguson 1993), in which various members are present (see Figure A1.1C). Probable Paparoa Group strata are present at Kowhiterangi Hill, and comprise a sequence similar to that of Greymouth Coalfield (Gage & Wellman 1944; Nathan 1974). Minor occurrences of coal measures in the upper Fox River and in Bullock Creek are correlated with Paparoa Group (Laird 1988).

Undifferentiated Paparoa Group strata are present in the on–shore petroleum exploration wells Arahura–1 (75m+), Aratika–2 (230m+) and Card Creek–1 (Raine 1984; Nathan et al. 1986; Czochanska et al. 1987). The subsurface continuity of the Paparoa Group in the lower Grey Valley area is unknown, and younger (Oligocene) strata are known to overlie basement in some drillholes (Matthews 1990). Paparoa Group strata are also inferred from seismic profiles to be present at the southwestern end of the off-shore Takutai half-graben (Bishop 1991, Figure 3).

Limited geochronology of intercalated basaltic rocks present at Pike River Coalfield, Kowhiterangi and Arahura–1 (Appendix 4.6) supports placement of of the various Late Cretaceous to early Tertiary terrestrial deposits present in the Westland area within the same Group.

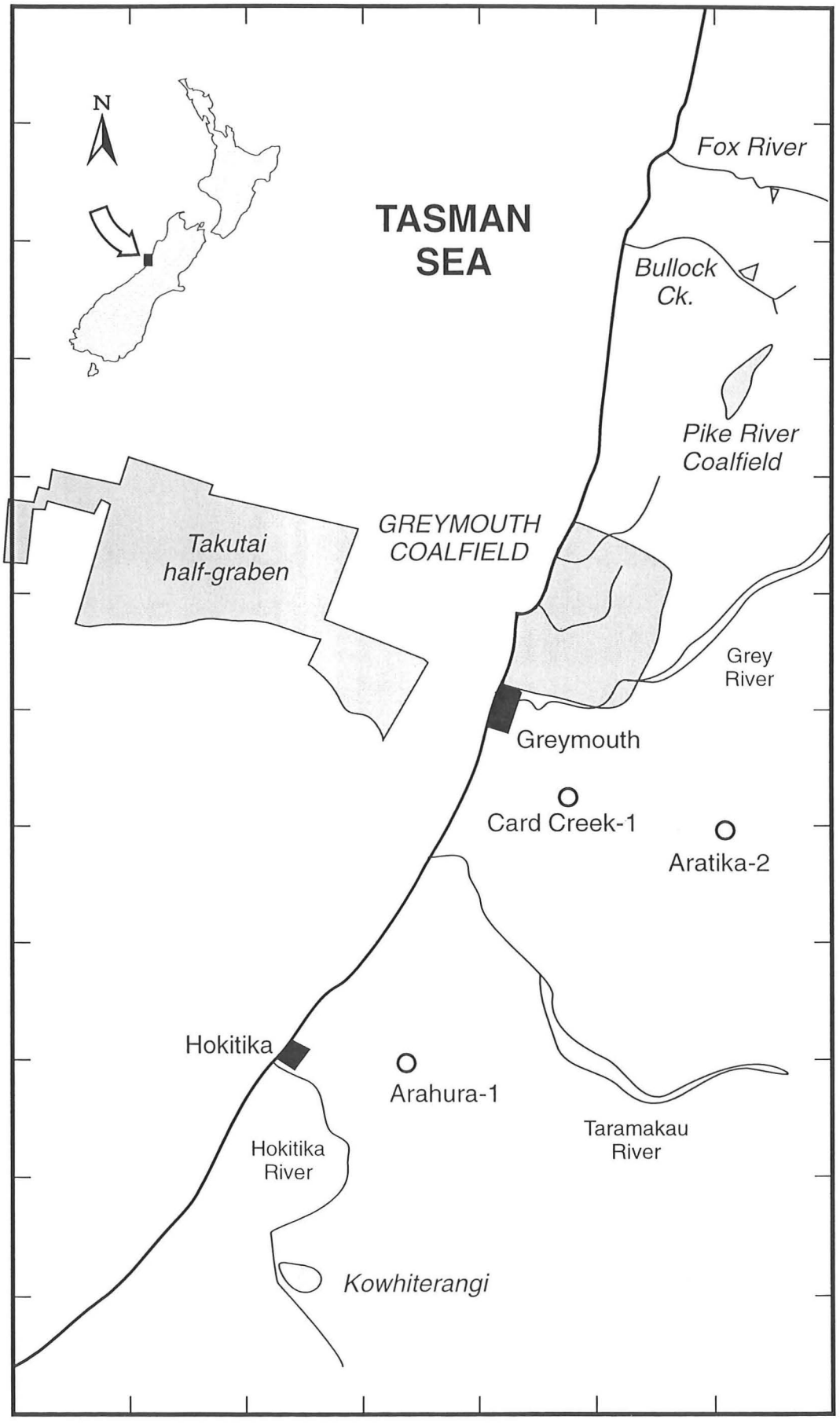

Figure 2.7 Distribution of Paparoa Group strata, central West Coast.
Grid ticks = 10km.

Chapter 3. Revision of isopach models

3.1 Introduction

Revision of isopach models for units present within the Paparoa Group is necessary to reflect changes to lithostratigraphy (Chapter 2), and to include data collected since previous isopach models (Figures A1.2 – A1.4) were constructed. Such data include recent drillhole information, and outcrop mapping which has redefined the extent of some units. All lithostratigraphic data collected prior to mid–1995 (Appendix 10) have been incorporated in the isopach models presented here.

3.2 Discussion of isopach modelling methods

Pre–existing isopach models (Figures A1.2–A1.4) were constructed by manual methods. However, availability of thickness data throughout Greymouth Coalfield for Goldlight Fm. and Rewanui CMM, plus accurate drillhole location data, facilitates numerical modelling techniques for the construction of isopach maps. Numerical modelling offers an objective method of depicting isopach patterns, and enables exploration of spatial variability and error within thickness data sets. Full details of numerical modelling of Goldlight Fm. and Rewanui CMM thickness data are given in Appendix 3.

Minimum curvature modelling is a simple technique which was suited to construction of initial unit thickness models (Figures A3.2, A3.5, A3.6). A degree of smoothing is inherent in the technique, and localised anomalies may be rapidly detected by comparing data with estimated values. Anomalies may result from errors in placements of stratigraphic contacts, or the effects of structural disruption. Minimum curvature modelling also provided a method for deciding whether thickness data should be included or excluded from the final data set. The greatest problem with minimum curvature modelling was poor representation of thickness patterns at basin margins.

Trend surface analysis revealed different basin orientations for the Goldlight Fm. and Rewanui CMM depocentres. The position of basin margins (i.e. zero isolines) was also estimated, and trend surface modelling indicated greater thickness variation near basin margins than in depocentres. Trend surfaces provided poor models for complex basins.

Geostatistical modelling was the most complex numerical technique applied in this study, though spurious edge effects are absent from the results of such modelling. There was good correspondence between Rewanui CMM thickness data and the resulting isopach model (Figure A3.12), and geostatistical modelling provided the basis for the construction of the final Rewanui CMM isopach model presented in this chapter.

Geological data (especially outcrop patterns) which are not present in the drillhole database must also be incorporated in final isopach models, using manual techniques. The critical outcrop constraint on the isopach pattern of all units is the eastern margin of the Paparoa Basin, which is defined by the occurrence of Brunner CM on Greenland Group basement to the east of the Roa–Hawera Fault (see Figure 1.2). Gage (1952, p. 28) concluded that there was "no reason to postulate a once greater extension eastwards" for the Morgan CMM. Onlap of Dunollie Fm. on basement near Mt. Buckley (Figure 1.2) also constrains the southeastern extent of lower units within the Paparoa Group.

Elsewhere in the coalfield, the position of zero isolines was generally determined from drillhole data, and from field evidence of unit boundaries. Evidence for erosion of or within the Paparoa Group (prior to basin inversion) is limited, suggesting that mapped zero isolines reflect true unit extents. Minor Morgan CMM volcanic clasts are reworked into Brunner CM near Roa (see Figure 1.2 for location; Gage 1952, p. 41), and there was minor erosion of Ford Fm. by Rewanui Fm. in the northwest (Section 2.6.1). Northward and southward extension of Rewanui Fm. and Goldlight Fm. isopach patterns depicted below is, however, hypothetical, and reasons for the illustrated unit geometries are discussed further below.

The isopach models presented in this chapter were therefore constructed using drillhole data, the results of numerical modelling (for Goldlight Fm. and Rewanui CMM), and relevant field information. Specific problems were the lack of fully drilled units in the north of the coalfield where erosion has removed relevant contacts, and the rapid thinning of units along the eastern basin margin, which is not reflected in the drillhole database. Drillhole data are concentrated in the southern Rapahoe Sector, and are sparse throughout the remainder of the coalfield. Thickness information from historic drillholes (pre–1979) could not always be reconciled with modern drillhole data, because of the uncertainties in assigning lithosome boundaries (Section 2.3).

3.3 Jay Formation isopach model

Jay Fm. is completely drilled in five drillholes and partially intersected in a further 12 drillholes (Appendix 10.6). In most of these drillholes, Jay (iii) coal measures and Jay (ii) conglomerate can be distinguished. Jay (iii) sandstones/carbonaceous mudstones vary from 0 to c.70m thick, and at least c.80m Jay (ii) conglomerate is present (DH656). Red staining was encountered in the lowermost conglomerates in DH658.

There is insufficient data to construct a reliable Jay Fm. isopach model, and an estimated (minimum) isopach model is presented in Figure 3.1. The depocentre is aligned approximately NW–SE, and comprises a broad (>4km) northern basin and a smaller southern basin. There is no evidence for the small central depocentre depicted beneath Mt. Davy by Gage (1952) (see Figure A1.2A). The southern depocentre depicted here is similar to that illustrated by Gage (1952), though there is no evidence to support the presence of 1500ft (460m) of Jay Fm. Both Jay (iii) and Jay (ii) thicken in a south-southwesterly direction in this depocentre.

The northern Jay CMM depocentre extends across the northern reaches of the coalfield, and is approximately aligned with the two areas of underlying Pororari Group (Figure 3.1). The northern margin lies north of Mt. Watson, and the western limit of Jay Fm. deposition is unknown. Jay (iii) strata in drillholes demonstrate a symmetrical thickening towards the basin axis, which is aligned similarly to that depicted by Gage (1952). Jay (iii) coal measures also thicken towards the western end of the Jay Fm. basin, suggesting enhanced subsidence in the northwest.

3.4 Ford Formation

Data for Ford Fm. isopach construction (Figure 3.2) comprises 23 drillholes where total thickness is known, 27 with minimum values and 28 drillholes in which the formation is stratigraphically absent (Appendix 10.5). Ford Fm. lies directly on basement in nine drillholes (coloured purple in Figure 3.2). Outcrop extents are taken from Figure 1.2, and were modified in accordance with the revision of lithostratigraphy in DH661 (Section 2.6.2), and recorrelation of western Waiomo MM to Ford Fm. (Section 2.6.1).

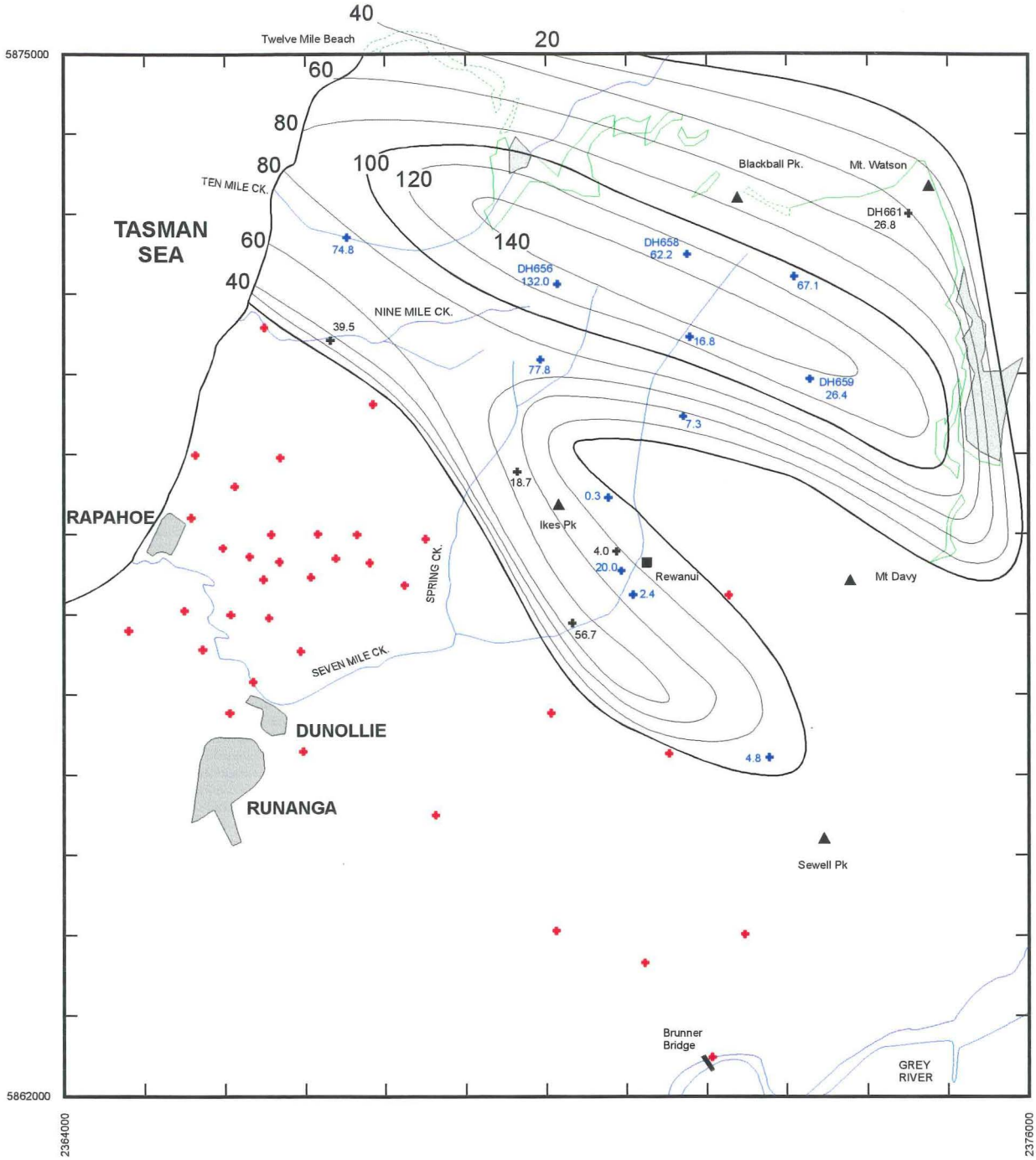

Figure 3.1 Isopach model, Jay Formation.
Isopach interval = 20m.
Numbered drillholes are discussed in text.

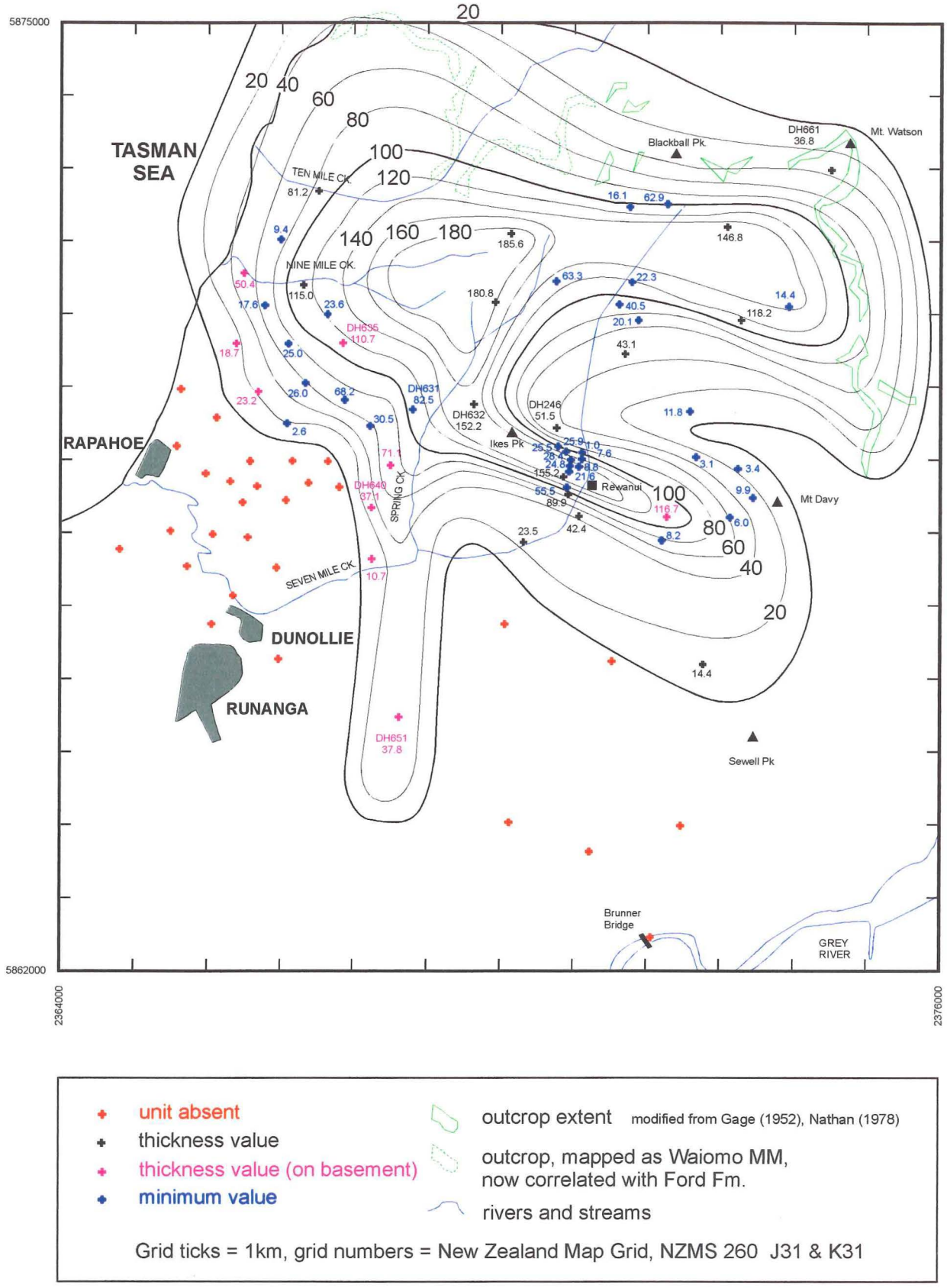

Figure 3.2 Isopach model, Ford Formation.
Isopach interval = 20m.
Numbered drillholes are discussed in text.

3.4.1 Ford Formation isopach model

The Ford Fm. isopach model presented here (Figure 3.2) is significantly different from previous models (Figures A1.2B, A1.3B) as a result of lithostratigraphic revision (Chapter 2). Ford Fm. occupies a broad, NW/SE oriented trough which divides eastward into two distinct depocentres, separated by a zone of thinning present beneath Mt. Davy. Gage (1952) presented a similar isopach model for eastern Ford Fm., though there is no evidence for the "central" basin beneath Mt. Davy (see Figure A1.2B). The narrow zone of Ford Fm. 2–3km east of Runanga is defined only by DH651. Occurrence of tuffaceous strata within Ford Fm. is reported in Appendix 10.5. Maximum occurrence of tuff is towards the Ford Fm. depocentre (e.g. DH631, DH632), suggesting the source was within the basin. A small dike intruding into the floor of the Ford lake is the likely source for volcaniclastic strata within Ford Fm.

3.4.2 Ford Transitional Member isopach model

Transitional lithosomes within the upper Ford Fm. are largely restricted to west of Seven Mile Ck., though they are also present in the vicinity of Blackball Pk (Figure 3.3). The Member is only depicted south of Ten Mile Ck. as there is no data on occurrence of transitional lithosomes further north. Transitional lithosomes are possibly indicated in the lithological logs for five drillholes in the Rewanui area (see Appendix 10.5). Consequently, the eastern limit of transitional lithosomes at Rewanui is poorly constrained. The southernmost occurrence is in DH651. Thickness trends within the Ford Transitional Member are similar to the total member isopach (Figure 3.2).

3.5 Morgan Coal Measure Member isopach model

The Morgan CMM isopach map (Figure 3.4) is constructed largely from subsurface (drillhole) data. Complete sections were intersected by 36 drillholes (DH's 266, 273, 625 and 630 on basement), and incomplete sections in 49 drillholes (Appendix 10.4). Morgan CMM is stratigraphically absent from 45 drillholes. Twelve drillholes with incomplete Morgan CMM sections which are close in thickness to the modelled isopach value are indicated in blue on Figure 3.4, and the remainder are omitted for clarity. In the Rewanui area, Morgan CMM thickness varies rapidly between closely spaced drillholes, and data have been smoothed in order to construct a sensible isopach pattern which reflects local trends.

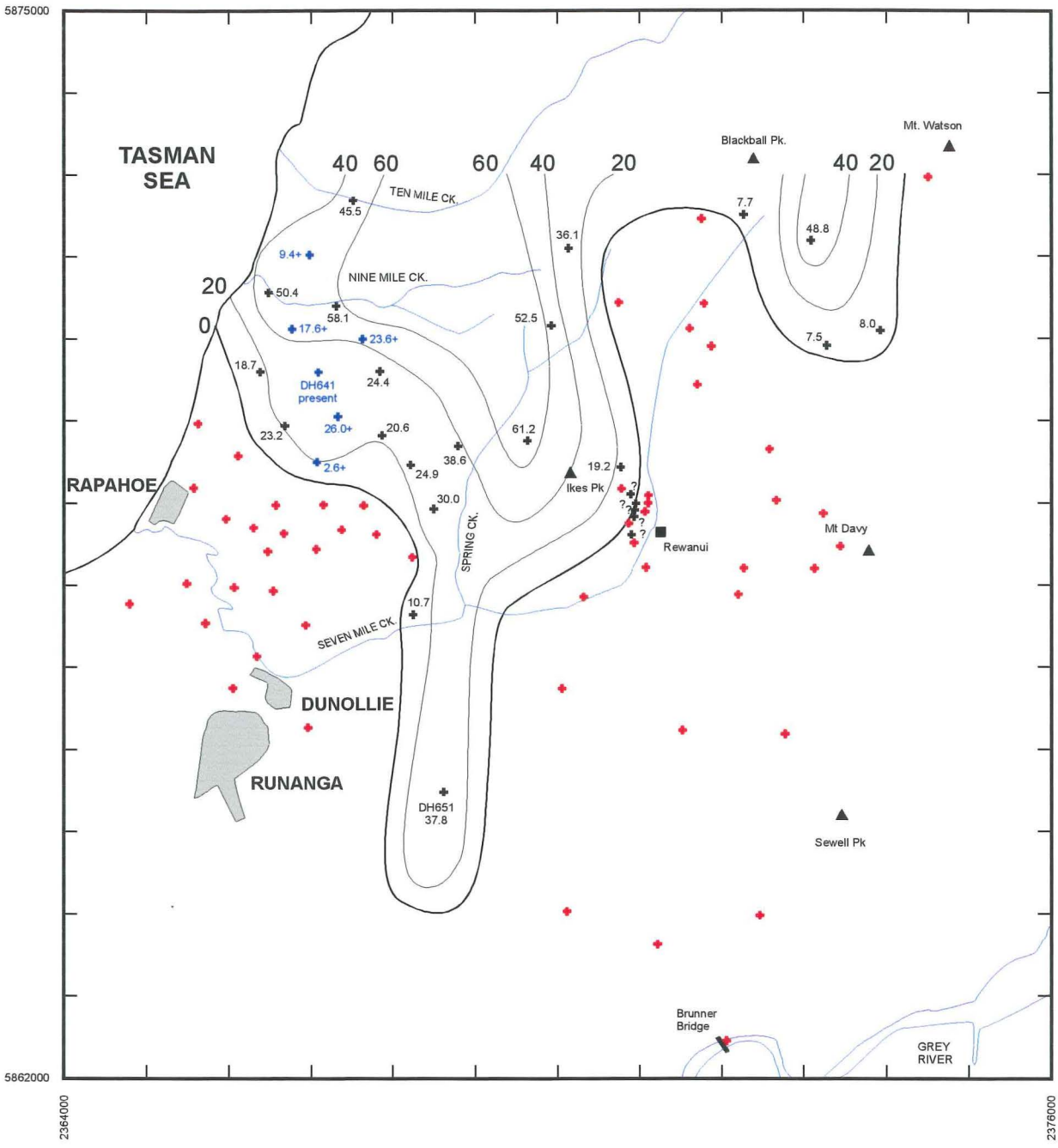

Figure 3.3 Isopach model, Ford Transitional Member.
Isopach interval = 10m.
Numbered drillholes are discussed in text.

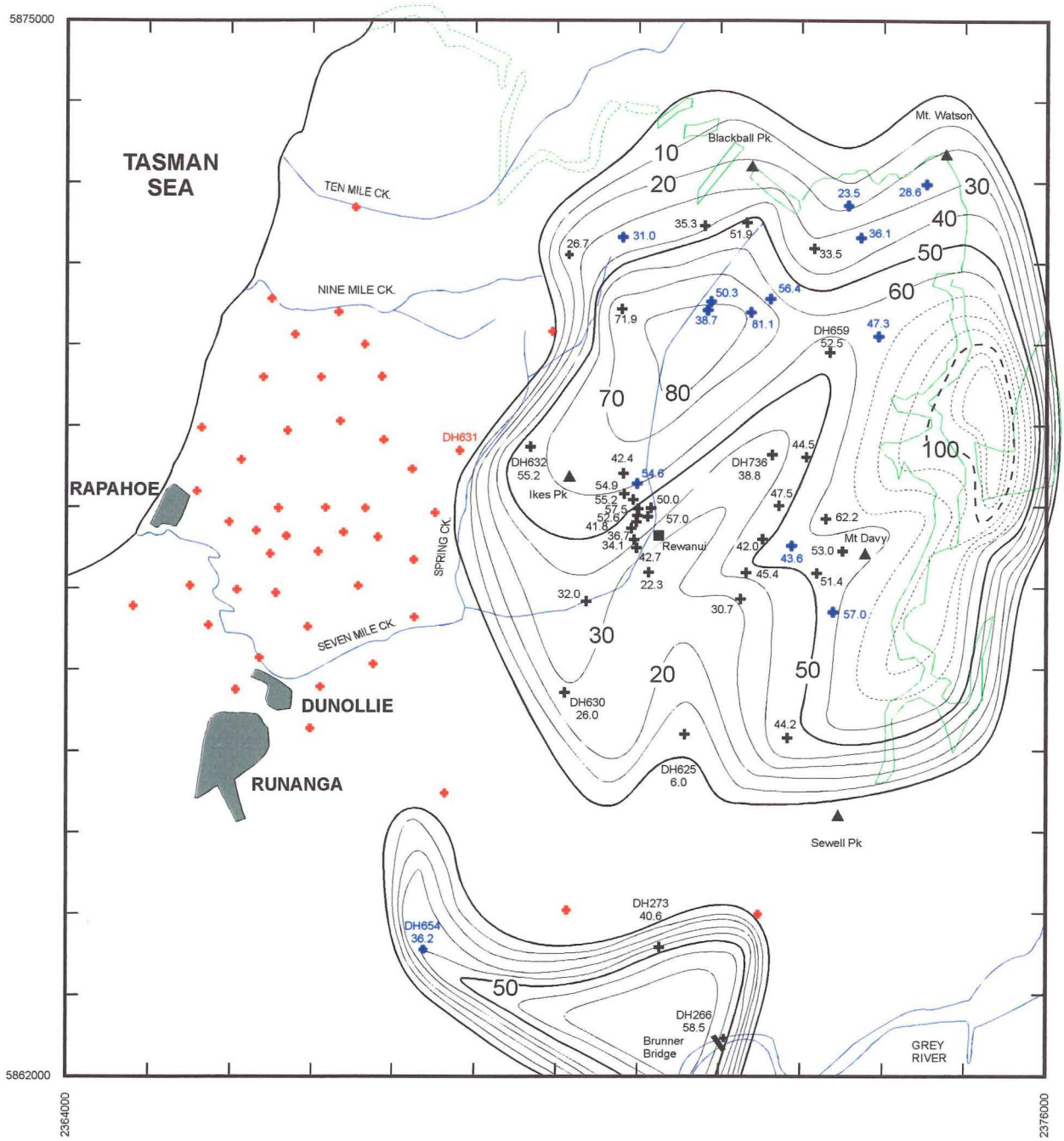

Figure 3.4 Isopach model, Morgan Coal Measure Member.
Isopach interval = 10m.
Dashed isolines correspond to thick volcanic facies reported by Gage (1952) but not intersected by any drillhole.
Numbered drillholes are discussed in text.

There is little outcrop information to constrain Morgan CMM occurrence. Caffyn (1994) indicated 60-70m of Morgan CMM (on basement) is present at the known southern limit of outcrop on the eastern flanks of Mt. Davy, and the present model is consistent with this. Gage (1952) indicated up to 1500ft/450m of Morgan CMM (notably volcanic facies) in the east (Figure A1.2C). Volcanic facies of Morgan CMM are poorly constrained stratigraphically (overlain unconformably by Brunner CM; Figure 1.2). Easterly thickening illustrated depicted in Figure 3.4 is speculative, and maximum thickness depicted (c.120m) is significantly less than indicated by Gage (1952).

Morgan CMM occurs in two parallel depocentres, one centered in the upper Seven Mile Ck. area, and the other in the vicinity of Mt. Davy, and also in a smaller southern basin (Figure 3.4). The western limit of Morgan CMM sedimentation is delineated by those drillholes in which Rewanui CMM lies directly on basement, or Rewanui CMM is conformable on Ford Fm. and intervening Waiomo MM and Morgan CMM are absent. Apparently rapid thinning along the western limit of Morgan CMM occurrence (e.g. DH632 = 55.2m, DH631 = 0m) reflects lateral continuity with basal Rewanui CMM (Section 2.6.4). The isopach pattern suggests the northern extent of Morgan CMM deposition was within 1km of the northern limits of present outcrop.

Separation of the western and eastern Morgan CMM depocentres is defined by DH736 and DH659, which together demonstrate an elongate zone of thinning oriented NNE/SSW from Rewanui. Previous interpretations of the stratigraphy of DH659 (CRS) indicate c.115m of Morgan CMM is present. However, examination of lithological and geophysical logs revealed repetition of 56.5m of Morgan CMM and Ford Fm., resulting from a reverse fault at c.325m. The correct thickness for Morgan CMM in DH659 is 55.4m when adjusted for dip (Appendix 10.4).

Three drillholes (DH266, DH273, DH654) indicate that Morgan CMM is present in the south of the coalfield (Brunner Bridge area). These occurrences of Morgan CMM are 2–3km from other drillholes containing Morgan CMM, and the relationship to the major depocentres is unclear. The sharp eastern margin of the southern depocentre reflects the mapped occurrence of Dunollie Fm. on basement at Mt. Buckley (Figure 1.2). However, recent observations suggest this mapping is incorrect (M. Cave, pers. comm. 1997), and Morgan CMM may extend further east than presently depicted.

3.6 Waiomo Mudstone Member isopach model

Total Waiomo MM thickness is constrained by 64 drillholes, in addition to 8 drillholes with minimum values (Appendix 10.3) and 44 drillholes in which the member is stratigraphically absent. Many closely adjacent drillholes in the Rewanui area have differing Waiomo MM isopach values, and isolines have been smoothed to reflect major thickness trends. Following recorrelation of western Waiomo MM to Ford Fm. (Section 2.6.1), the extent and thickness of Waiomo MM described here (Figure 3.5) is substantially reduced from previous models (Figures A1.2D, A1.3D, A1.4A).

Waiomo MM occurs in a broad, shallow, north-south oriented basin which lies west of Spring Ck, and also is found in a restricted area near Brunner Bridge. The eastern limit of Waiomo MM occurrence along the eastern flanks of Mt. Davy is poorly constrained. Previous mapping by Gage (1952) and Nathan (1978) was only approximate in this area. Some Goldlight Fm. was previously mapped as Waiomo MM, and present outcrop appears to be close to the eastern margin of Waiomo MM accumulation (Caffyn 1994). The northwestern limit of Waiomo MM occurrence is placed c.1km east of Ten Mile Ck., at the western edge of the westernmost fault-bounded block in which both Waiomo MM and Ford MM are mapped (Figure 1.2). All Waiomo MM indicated west of this fault-block is now correlated with Ford Fm (see outcrop pattern on Figure 3.5).

The southeastern limit of Waiomo MM occurrence is defined by the presence of Dunollie Fm. lying directly on basement south of Sewell Pk., and the zero isopach is constructed accordingly. However, confirmation of thin Waiomo MM in the Brunner Bridge area (Section 2.6.2) indicates the member is present southwest of Sewell Pk., and a minor depocentre is shown accordingly on Figure 3.5.

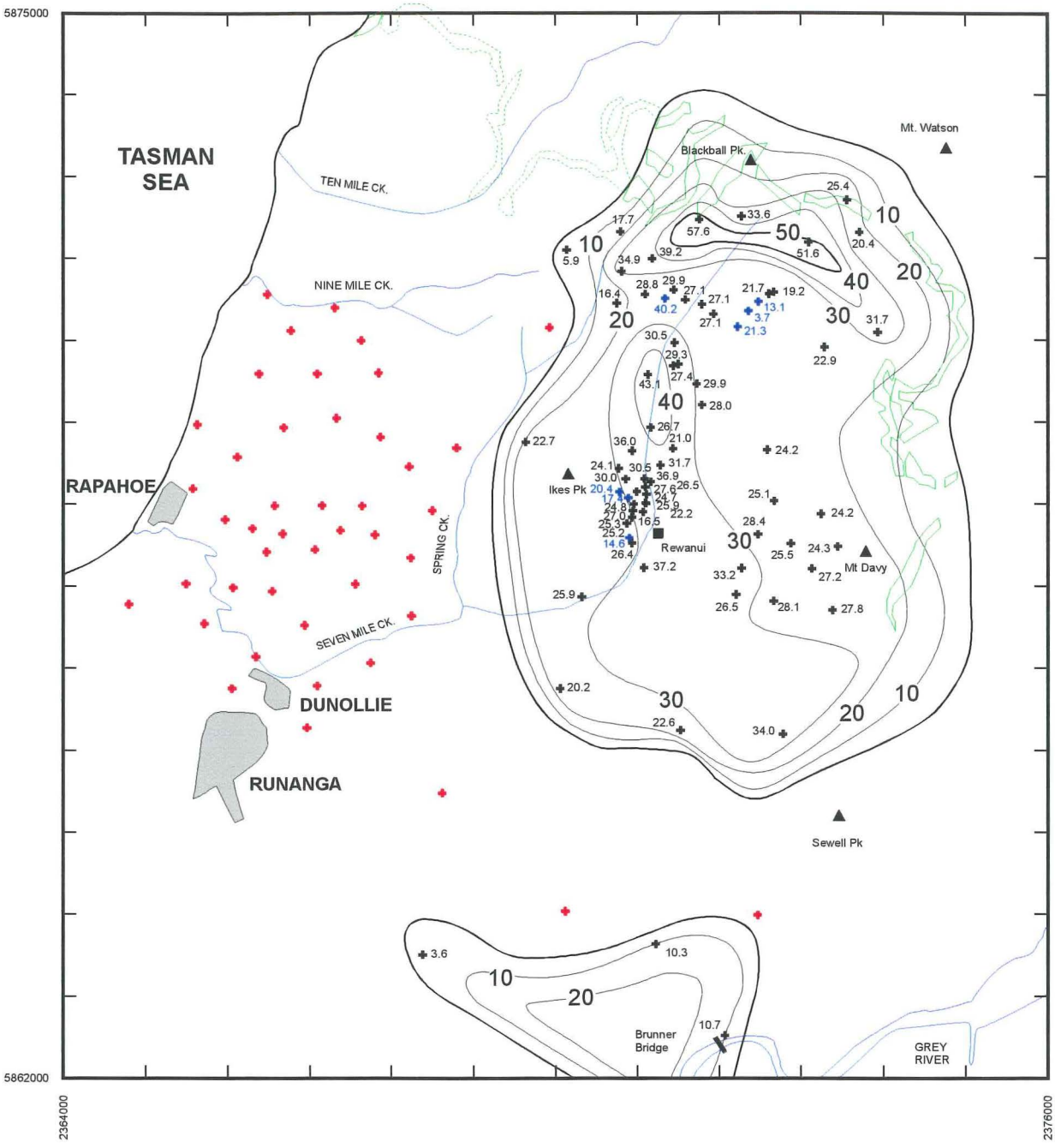

Figure 3.5 Isopach model, Waiomo Mudstone Member.
Isopach interval = 10m.

3.7 Rewanui Coal Measure Member isopach model

More than 200 drillholes intersect Rewanui CMM, though many were drilled in conjunction with mine development and intersect <50m of Rewanui CMM. Stratigraphic data (position of contacts, minimum or total thickness) for 156 drillholes are presented in Appendix 10.2. Holes drilled vertically upwards or at angles from underground workings have been excluded because of poor survey data and lack of stratigraphic contacts encountered. Some data for drillholes completed within the last five years (i.e. numbered > DH711) are presently confidential to the license operators (Coal Corporation of NZ Ltd., Greymouth Coal Operating Ltd.), and are presented as indicated in drillhole summary reports.

In the present project, particular attention has been placed on achieving the most accurate Rewanui CMM thickness data possible. Potential sources of error include the following factors, which are listed in order of significance:

- incorrect placement of contacts (i.e. lithostratigraphy)
- presence of structural disruption resulting in thinning or thickening of sections
- failure to correct to true stratigraphic thickness (especially where dip >20°)
- incorrect depth recording in lithological logs (resulting from core loss or spreading)

All drillholes contain minor structural disruption (bedding plane shearing is prevalent, jointing and crushing are common) thus true stratigraphic thicknesses may not be determinable. The methodology used for deriving input data for modelling of Rewanui CMM thickness is depicted in Figure 3.6. Details of data derivation for each drillhole (especially lithostratigraphic and structural problems) are discussed in Appendix 2, and intermediate numerical modelling steps are presented in detail in Appendix 3.

Minor adjustments to the Rewanui CMM outcrop pattern depicted in Figure 1.2 were incorporated to accommodate recent mapping and remove errors. The exact southern limit of Rewanui CMM outcrop occurrence east of Mt. Davy is presently unknown, though Caffyn (1994) states the member does not pinch out south of Dublin Ck. as depicted by Gage (1952) and Nathan (1978). Rewanui CMM is definitely absent in the vicinity of Sewell Pk. A simple geometrical calculation suggests Rewanui CMM outcropping along the coast south of Twelve Mile Beach is c.250m thick, however the

Raw data - drillhole logs from Gage (1952), SCM, CRS, GCOL, CCNZ

Locate contacts
- use criteria discussed in Section 2.3
- use geophysical logs where available
- use palynostratigraphy in NW (Section 6.4)
- inspect core where necessary

Identify structural features
- record dip throughout section
- identify shearing, gouge etc.
- use caliper logs where available
- inspect core where necessary

Correct for dip
- use average for each section
- dip often changes across faults

Estimate whether structure significant
- compare lithostratigraphy with all surrounding drillholes

Initial data values

Construct initial minimum curvature model
- identify anomalies
- reinspect stratigraphy/structure data to resolve problems
- transfer values to minimum if appropriate

Revised data values

Construct revised minimum curvature model
- resolve remaining anomalies

Final data values

Construct geostatistical isopach model
- see procedure in Table A3.4

Modify geostatistical isopach model to match all data
- incorporate field data and minimum values from drillholes

Construct final isopach model

Figure 3.6 Data preparation methodology, Rewanui CMM isopach construction. Steps listed are key tasks in an interative process.

Dunollie/Rewanui contact has not been adequately identified there (Appendix 1.2.5). Key outcrop information for constraining unit occurrence comes from the east of the coalfield, where mapping (e.g. Figure 1.2) illustrates Rewanui CMM is restricted to west of the Roa–Hawera Fault zone.

The Rewanui CMM isopach model presented in Figure 3.7 combines the results of numerical modelling with constraints from outcrop occurrence and drillhole data (i.e. minimum values) which are not reflected in the modelled drillhole data set. The fundamental isoline pattern was derived from geostatistical modelling (Figure A3.12). However, significant adjustments were required to fully accommodate available data. In the north of the coalfield where data are sparse, the general isoline pattern indicated by numerical modelling (Figure A3.6, A3.8, A3.12) was modified to depict a northwards opening to the basin (see below). Other manual modifications to modelled isoline patterns were made in the southeast where Rewanui CMM thins rapidly, in the vicinity of Sewell Pk., and south of DH654, where southward closure of isolines was indicated.

Rewanui CMM occurs in a broad (>10km) basin up to c.250m deep, of which the basin axis and complex southwestern and southern margins are preserved. The unit onlaps basement in the south and southeast of the coalfield, or rests conformably on Ford MM or Waiomo MM (where present). Two distinct orientations are present within the Rewanui CMM basin. The predominant basin axis is aligned NNE/SSW, and is defined by the steep eastern margin and the area near DH654. A secondary alignment of basin features, which is predominant in the Rapahoe Sector, follows a NW/SE orientation.

Textural trends of Rewanui CMM sediments indicate the NW basin margin lies close to the present outcrop limit at Twelve Mile Beach (Newman 1985, see also Appendix 4.4.1 and Section 7.6.1). Extension of the basin south of DH654 is conjectural, however this drillhole and DH266 (Brunner Bridge) contain a significant proportion of granite-derived coarse clastic strata, indicating continuing sediment transport through this region from the NNE (see further discussion in Section 7.6).

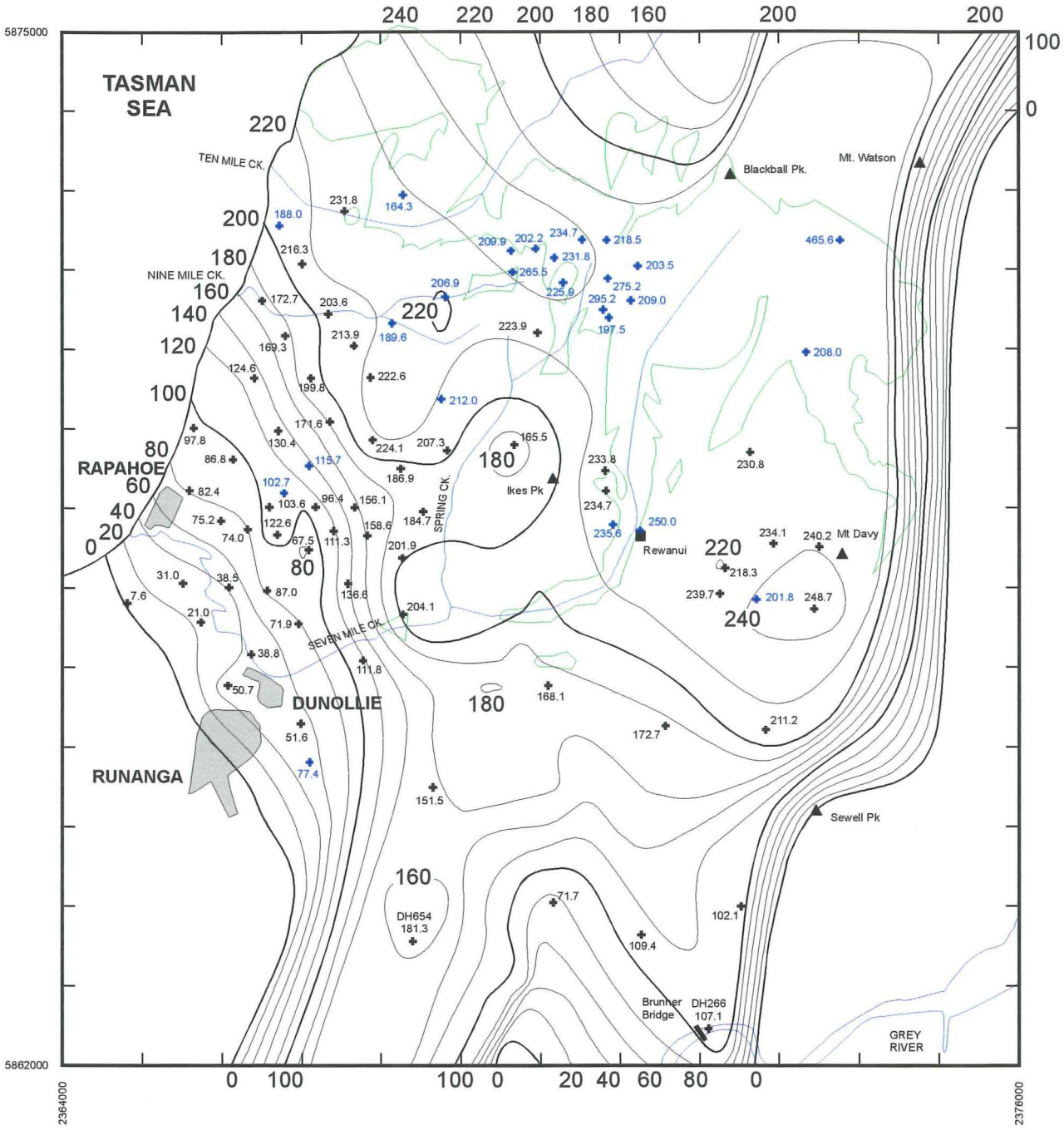

Figure 3.7 Final isopach model, Rewanui Coal Measure Member.
Isopach interval = 20m.
Numbered drillholes are discussed in text.
Selected minimum values are shown,
all minimum values are listed in Appendix 10.2.

Continuation of Rewanui CMM north from Mt. Watson and Blackball Pk. is suggested by paleocurrent analysis which indicates transport from the north in this area (Newman 1985), and textural trends within Rewanui CMM (Section 7.6.2). Correlation of Rewanui CMM with Member 4 at Pike River Coalfield (Figure A1.1C) also requires a physical connection between the two basins. However, no Paparoa Group strata are preserved between Greymouth Coalfield and Pike River Coalfield with which to conclusively demonstrate interconnection of the basins (Nathan 1978, Laird 1988).

3.8 Goldlight Formation

Total Goldlight Fm. thickness is intersected by 46 drillholes, and a further 58 partially intersect the member (Appendix 10.1). Goldlight Fm. is absent from three western drillholes in which Rewanui CMM and Dunollie Fm. are conformable (Section 2.7.5). Data points are concentrated in the Rapahoe Sector, with only sparse data east of Spring Ck. The southern pinchout of Goldlight Fm. immediately east of Sewell Pk., which is indicated on geological maps (e.g. Figure 1.2) but not reflected in the drillhole data set, is also incorporated, and other field observations of Goldlight Fm. occurrence are utilised where necessary.

3.8.1 Goldlight Formation isopach model

The Goldlight Formation isopach model presented in Figure 3.8 is based on the results of minimum curvature modelling and trend surface analysis, with necessary adjustments made to better reflect data values. Overall basin orientation corresponds with the second-order trend surface (Figure A3.4), and localised thickness variation generally follows the minimum curvature model (Figure A3.2). The isopach model defines a broad (c.9km wide), NNE/SSW oriented basin. Rapid thinning in the NW is due to lateral facies change (to Dunollie Fm.), whereas there is onlap onto basement at the steep southeastern margin. The depiction of the Goldlight Fm. basin as open to the northeast is hypothetical, and assumes that correlation of Goldlight Fm. with Member 5 at Pike River Coalfield (Figure A1.1C) implies connection between the basins.

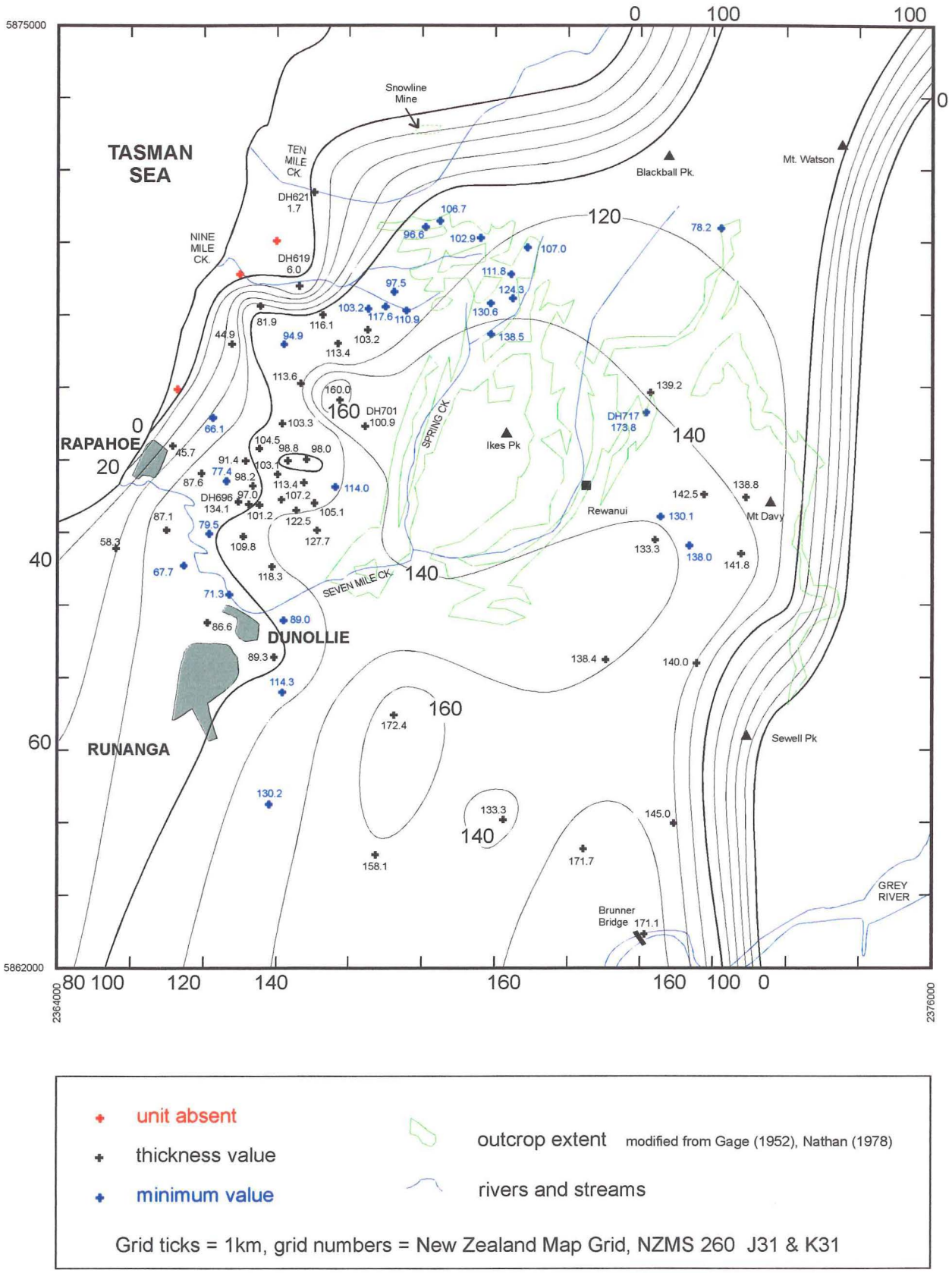

Figure 3.8 Final isopach model, Goldlight Formation.
Isopach interval = 20m
Numbered drillholes are discussed in text.
Note: continuation of basin to northeast is hypothetical.

Inclusion of transitional lithosomes in Goldlight Fm. (Section 2.4) has resulted in the unit extending further west than depicted by previous isopach models (Figure A1.2F, A1.3F, A1.4C) and mapping (green line, Figure 3.8; see also Figure 1.2). Also, thin Goldlight Fm. mudstone has not been previously recognised in DH619 or DH621 (Appendix 10.1). North of Ten Mile Ck., previously unmapped Goldlight Fm. occurs above the Snowline Mine (indicated on Figure 3.8).

Not all Goldlight Fm. thickness variation apparent in the data set could be accommodated by the final isopach model. Goldlight Fm. in DH696 (134.1m) is c.35m thicker than in surrounding drillholes (c.100m), whereas the unit in DH701 (100.9m) is c.30m less than indicated by the isopach model. DH717 (173.8m+), near Rewanui appears to contain at least 30m more Goldlight Fm. than predicted. All three drillholes may contain unrecognized structural features which have affected Goldlight Fm. thickness. The lack of marker horizons throughout the unit would make recognition of fault repetition or removal of strata difficult to detect.

Closed isopach lines, as depicted near Brunner Bridge in Figure 3.8, are generally discouraged on isopach maps (Lewis 1984, p. 208). Isopach patterns in the southern Greymouth Coalfield are probably a modelling artifact in response to the wide data point spacing (Krajewski & Gibbs 1994), though localised thickness variation may also reflect the effects of compaction on Goldlight Fm. thickness (discussed further in Section 4.2.7).

3.8.2 Goldlight Transitional Member isopach models

Transitional lithosomes of the Goldlight Transitional Member are restricted to the western and southern portions of the coalfield. Three components are recognised: a narrow western zone in which transitional lithosomes comprise the full thickness of the Goldlight Fm., an upper Goldlight Transitional Member which occurs between lacustrine lithosomes and Dunollie Fm., (Figure 3.9) and a lower Goldlight Transitional Member which occurs between lacustrine lithosomes and Rewanui CMM (Figure 3.10). Where lacustrine lithosomes are absent, the Goldlight Transitional Member thickens away from the basin margins, whereas the opposite thickening trend is evident in the upper and lower Goldlight Transitional Member packages where there are intervening lacustrine lithosomes.

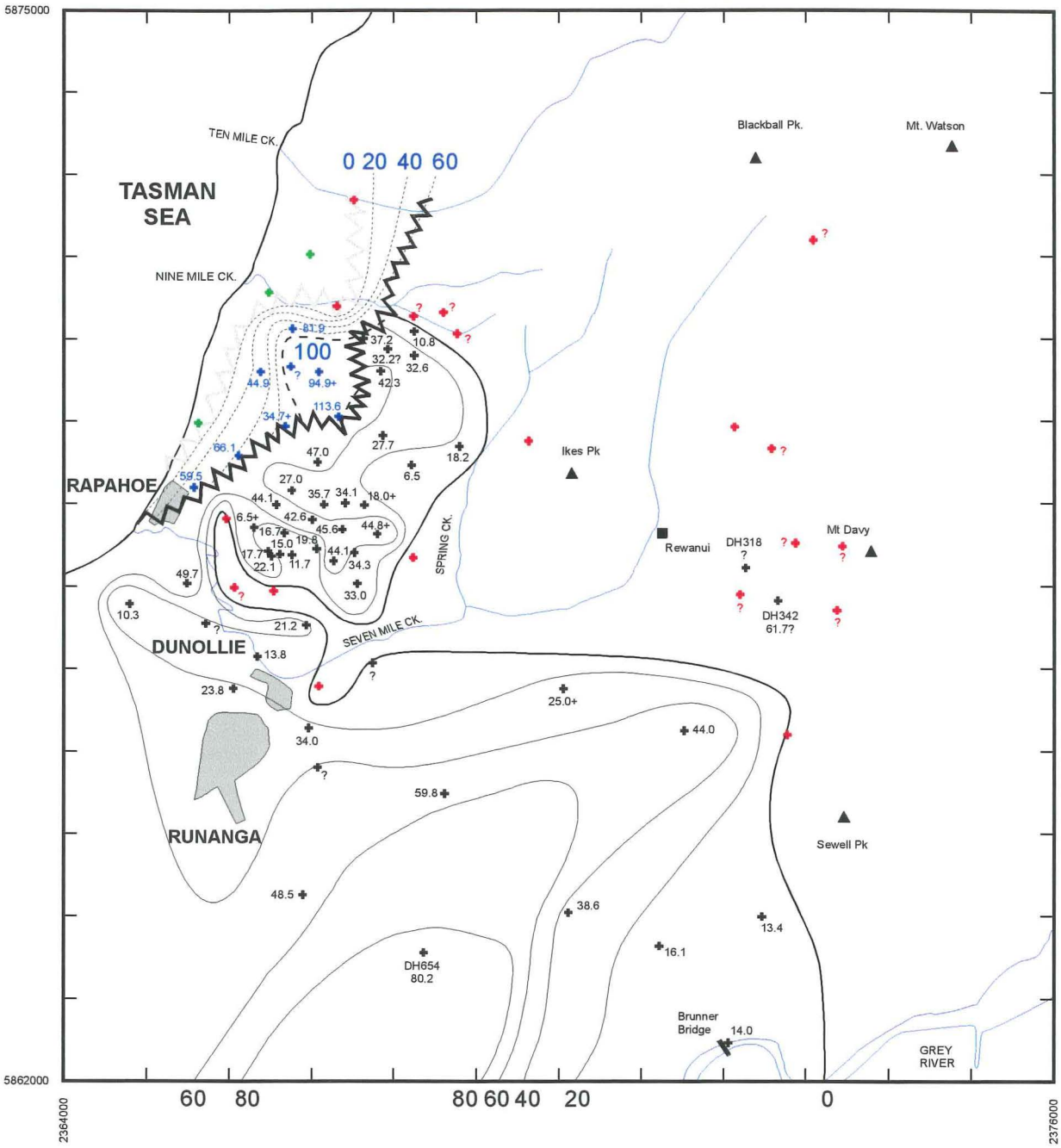

transitional lithosome absent (? = possibly)

transitional lithosome present (? = possibly)

all Goldlight Fm. transitional, thickness values shown in blue

gradation from Dunollie Fm. to Goldlight Fm.

western limit of Goldlight Fm. lacustrine lithosomes

Grid ticks = 1km, grid numbers = New Zealand Map Grid, NZMS 260 J31 & K31

Figure 3.9 Upper Goldlight Transitional Member isopach model.
Isopach inerval = 20m.
Numbered drillholes are discussed in text.

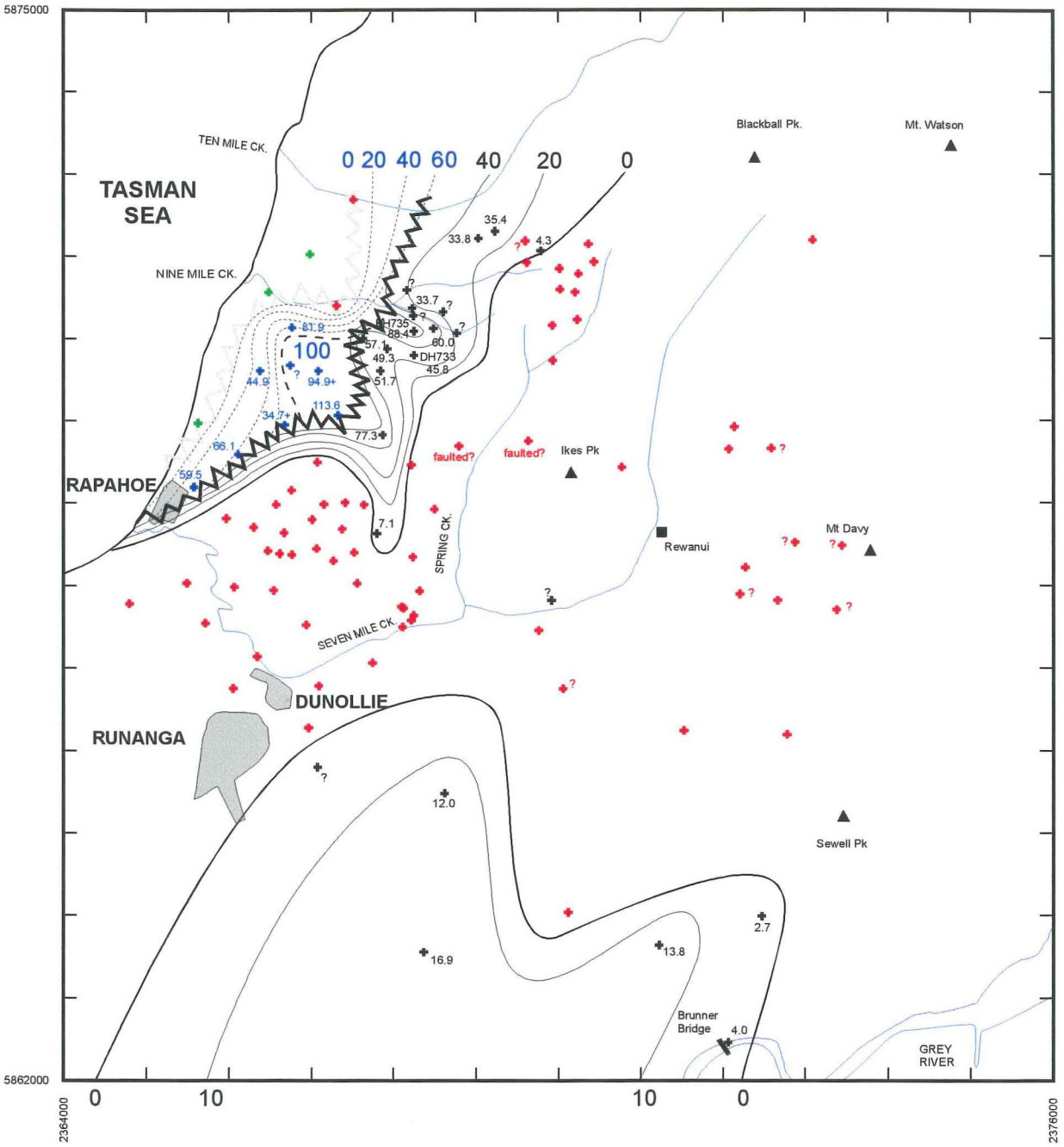

transitional lithosome absent (? = possibly)

transitional lithosome present (? = possibly)

all Goldlight Fm. transitional, thickness shown in blue

gradation from Dunollie Fm. to Goldlight Fm.

western limit of Goldlight Fm. lacustrine lithosomes

Grid ticks = 1km, grid numbers = New Zealand Map Grid, NZMS 260 J31 & K31

Figure 3.10 Lower Goldlight Transitional Member isopach model.
Isopach interval = 20m in north, 10m in south.
Numbered drillholes are discussed in text.

Presence of transitional lithosomes within Goldlight Fm. in some drillholes (e.g. DH318, DH342) is uncertain due to poor data quality. In particular, the lithological log of DH342 (near Mt. Davy) appears to indicate 61.7m of upper Goldlight Transitional Member, but the resultant Goldlight Fm. thickness would be greater than demonstrated by surrounding drillholes. Lower Goldlight Transitional Member strata occur in recent drillholes in the Strongman Mine area (e.g. DH733) but could not always be confirmed from poor quality lithological records for older drillholes nearby (Appendix 10.1).

Upper Goldlight Transitional Member strata are common in the Rapahoe Sector and occur throughout the area south and east of Dunollie (Figure 3.9). Near Rapahoe, these strata occur in a 2–3km wide zone which thins eastwards. Within this zone, there is a pronounced, narrow lobe of thicker strata east of Rapahoe. South of Seven Mile Ck., the upper Goldlight Transitional Member forms a broad zone (c.5km) which thins in a northeasterly direction. Maximum thickness occurs in DH654. Lower Goldlight Transitional Member strata have a similar but more restricted distribution (Figure 3.10), and are absent from the area between Rapahoe and Runanga. In contrast to the upper Goldlight Transitional Member, maximum thickness (DH735) is near Nine Mile Ck., and lower Goldlight Transitional Member strata are thin in the south (Runanga to Brunner Bridge).

3.9 Synopsis: Rewanui Formation and Paparoa Group distribution, Greymouth Coalfield

Use of computer techniques to represent isopach models (whether manually or numerically constructed) allows rapid construction of synoptic plots such as total unit thickness and cross-sections. All isopach models were digitised then gridded (250x250m cells) using the *TECHBASE POLYGRID* application, followed by manual editing to ensure the gridded models matched the manually-drawn isopach maps. Once gridded, isopach models could be easily combined to provide cumulative thickness maps, and cross-sections could be constructed. By adding individual isopach models, cumulative isopach plots (Figure 3.11, 3.12) and cross-sections (Figure 3.13) incorporate data from c.200 drillholes, in addition to outcrop information.

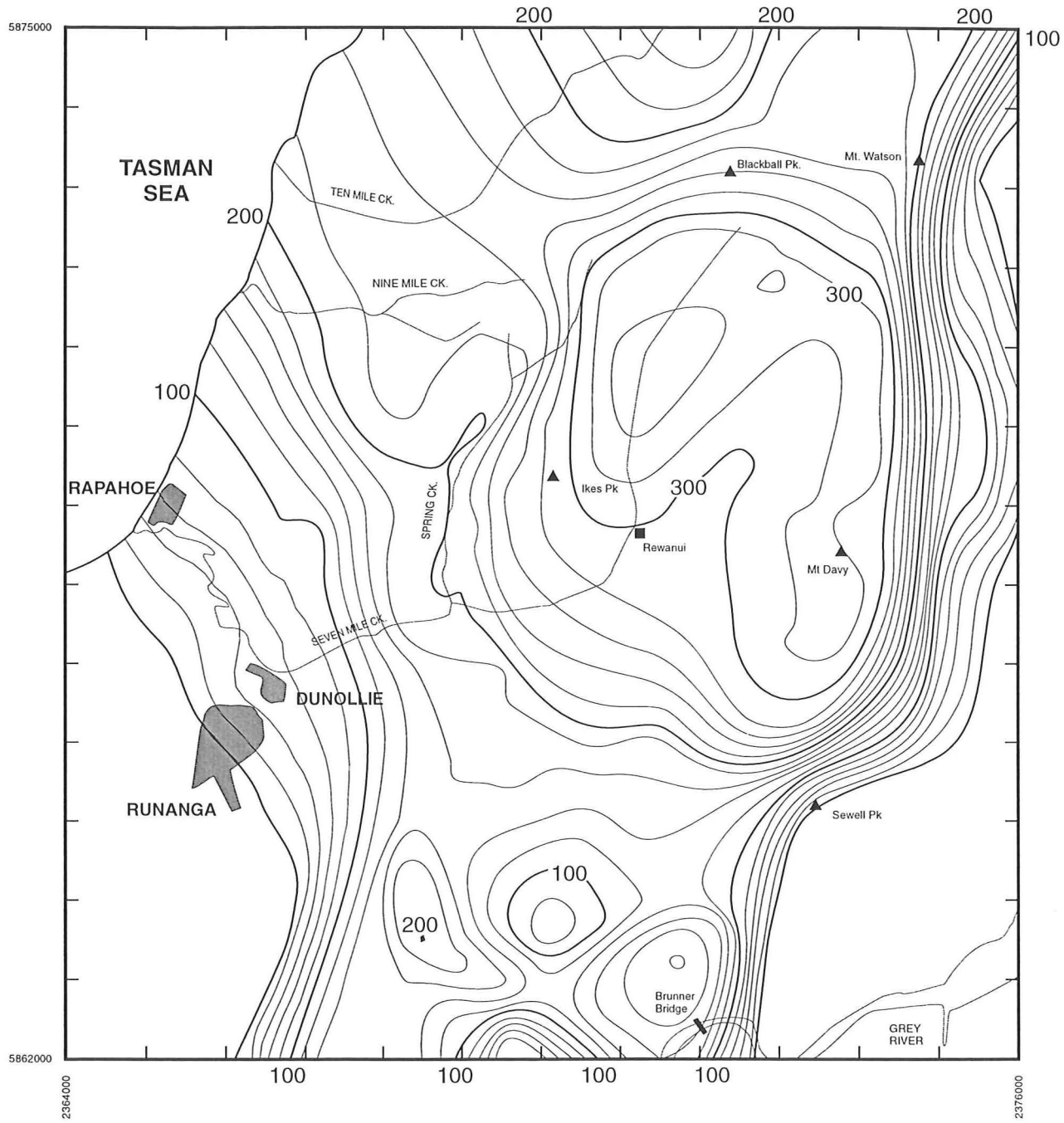

Figure 3.11 Isopach model, Rewanui Formation.
Model constructed by addition of Rewanui CMM, Waiomo MM and Morgan CMM isopach models.
Isopach interval = 20m.

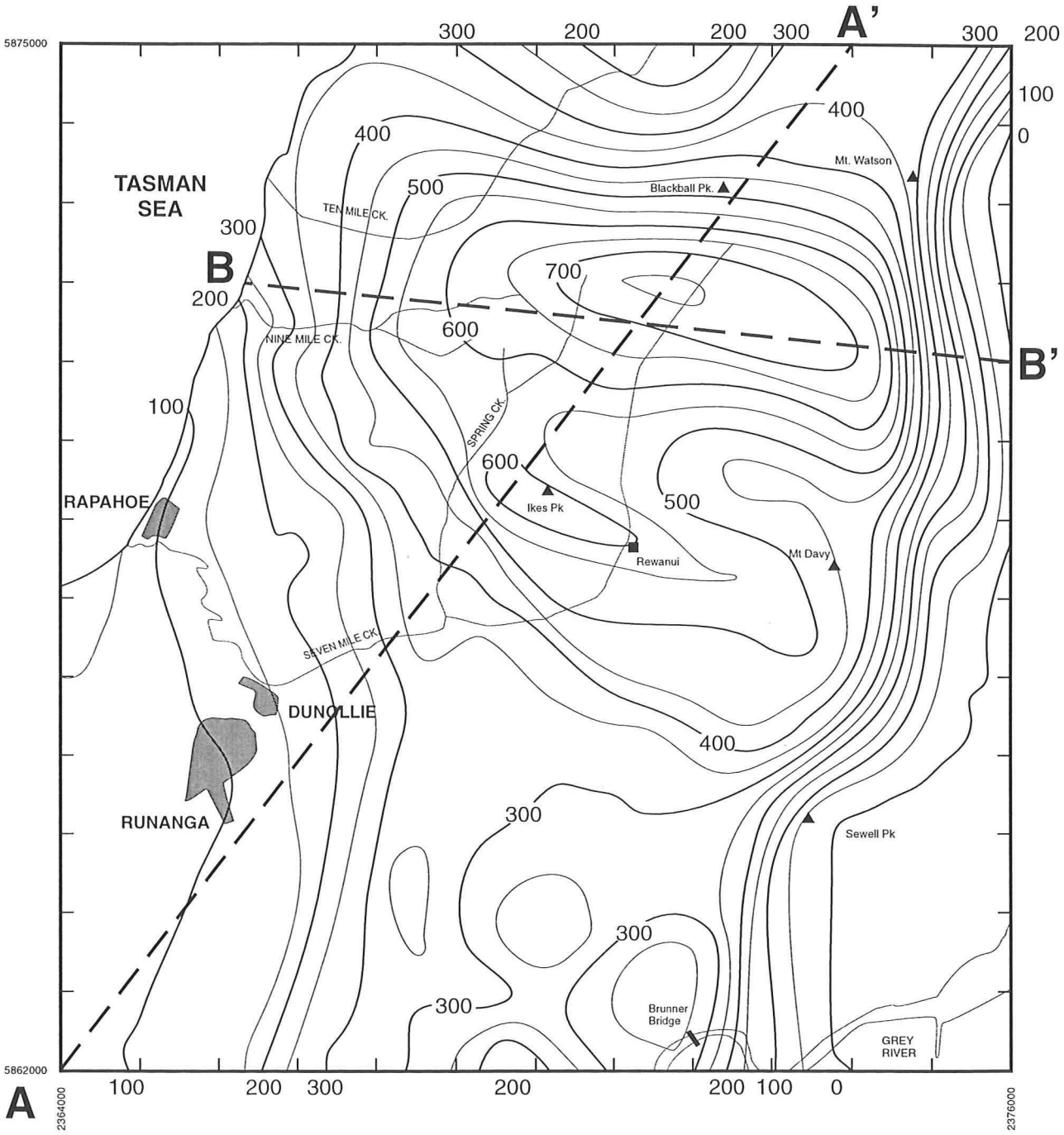

Figure 3.12 Isopach model of Paparoa Group
(excluding Dunollie Fm.)
Isopach interval = 50m.
Model constructed by addition of all
Formation and Member isopach models.
Locations of cross-sections in Figure 3.13 is indicated.

Rewanui Fm. comprises Rewanui CMM, Waiomo MM and Morgan CMM (Section 2.5), and the isopach model for the Formation (Figure 3.11) is the sum of the thickness of those three members (Figures 3.5, 3.6, 3.7). Rewanui Fm. occupies a complex basin which lies between basement highs in the southeast and southwest. The basin was open to the northeast, northwest and south. Maximum thickness of Rewanui Fm. strata (c.360m) occurs in the upper Seven Mile Ck. area, and the average thickness is 150m. Within the overall basin are a number of sub-basins, notably in the south where there is rapid thickness change over small distances (c.1km).

Total Paparoa Group thickness (excluding Dunollie Fm.) is illustrated in Figure 3.12. Maximum modelled thickness is 758.6m (headwaters of Seven Mile Ck. and Spring Ck.), and average thickness is c.290m. Overall thickness trends are similar to those exhibited by total Rewanui Fm. thickness (Figure 3.11), though the NW/SE alignment of basinal features is more apparent in the total Paparoa Group isoline pattern. The Paparoa Group basin is asymmetrical, with rapid thickness change along the eastern margin (up to 400m/km) and more gentle gradients elsewhere. Complex sub-basins are present in the south, whereas north of a line from Sewell Pk. to Rapahoe, Paparoa Group occurs in a broad, bifurcated, WNW/SSE oriented trough.

The vertical distribution of the various Paparoa Group Formations and Members is illustrated in cross-sections in Figure 3.13, which were plotted with the *TECHBASE SECTION* application. The Goldlight / Rewanui contact is used as the datum, following previous practice (e.g. Bowman et al. 1984).

Rapid easterly thinning of all units against basement is evident near B'. Successively younger formations onlap increasing areas of basement (illustrated in A–A'), and Goldlight Fm. blankets underlying strata. Northwesterly thinning of Goldlight Fm. (near B) reflects lateral facies change to Dunollie Fm. Lateral connectivity of Morgan CMM to (western) basal Rewanui CMM is illustrated in B–B', and the cross-section also shows continuity between the two units in the east where Waiomo MM is absent. Thus, thick eastern Morgan CMM (see Figure 3.7), which is the easternmost Paparoa Group unit, may be partially laterally equivalent to Rewanui CMM, though there are compositional differences between the units in the east of the coalfield (Chapter 7).

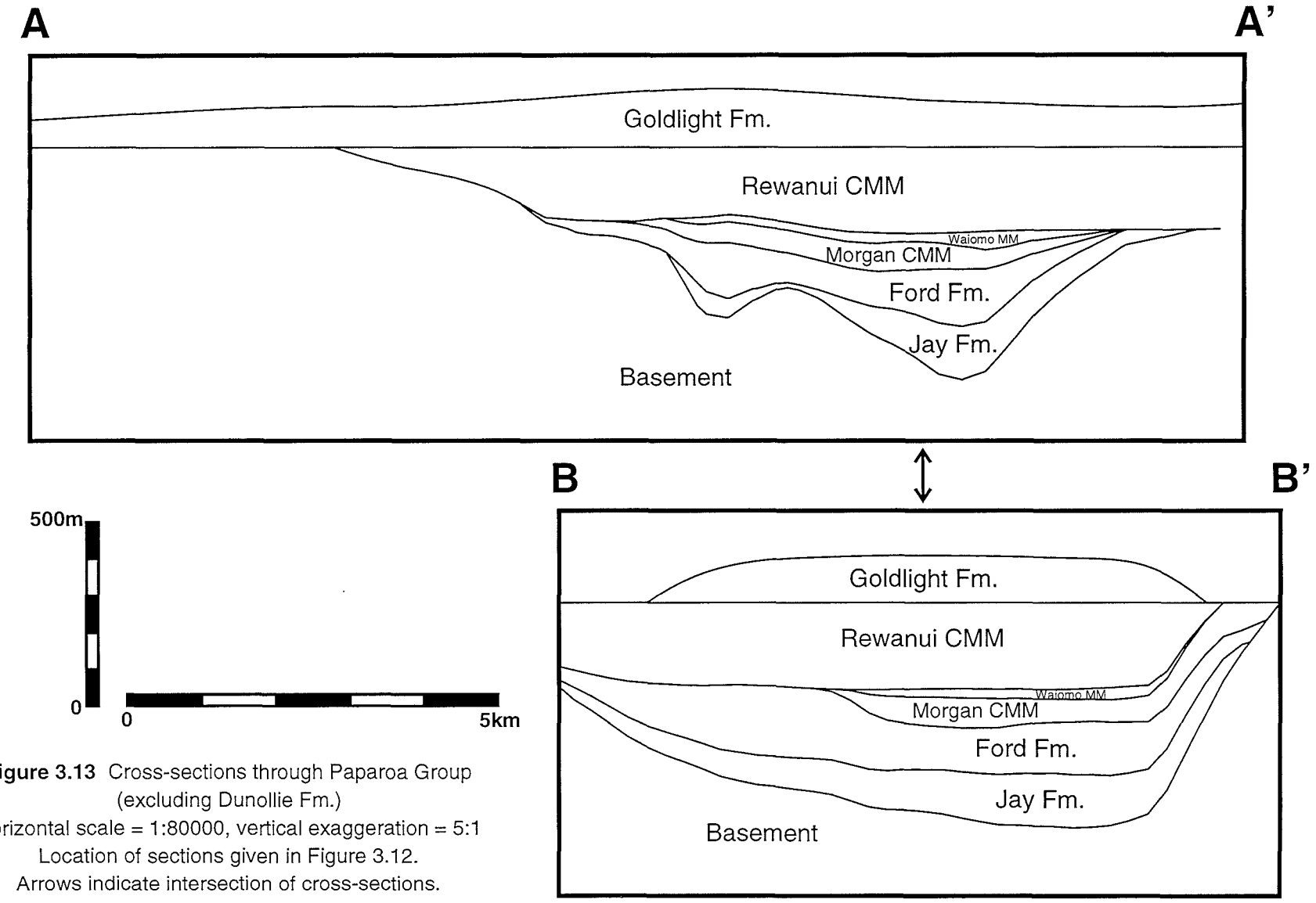

Figure 3.13 Cross-sections through Paparoa Group (excluding Dunollie Fm.)
Horizontal scale = 1:80000, vertical exaggeration = 5:1
Location of sections given in Figure 3.12.
Arrows indicate intersection of cross-sections.

Chapter 4. Decompacted isopach models and basin evolution

4.1 Introduction

The objectives of this chapter are to describe original thicknesses of the Paparoa Group members and formations, to determine the tectonic subsidence which was responsible for the deposition of those units, and to analyse how the basin evolved throughout Paparoa Group deposition. Decompaction was performed with a backstripping technique, which is fully described in Appendix 4. During backstripping, the effects of burial on Paparoa Group thickness were removed, which allowed the original basin configuration to be modelled. Full details of the decompaction analysis for 72 drillholes are given in Appendix 4, and input data and results are listed in Appendices 11 and 12.

In this project, tectonic subsidence was estimated from the decompacted thickness (listed in Appendix 12) of any unit within the sedimentary column, from which was subtracted any compaction of underlying strata (Appendix 4.7, example given in Figure 4.1). Isostatic subsidence from sediment and water loading on the crust was determined to be negligible in small basins such as the Paparoa Basin (Appendix 4.7). However, the assumption that all sedimentary space is due to tectonic movement or compaction of underlying strata is simplistic. The following additional factors may influence the thickness of a sedimentary package:

- compaction within units, especially of peat
- incomplete filling of basin during lacustrine intervals
- sediment accumulation above regional base level or basin floor
- erosion
- infilling of pre-existing topography

The role of these factors in determining decompacted isopach patterns and apparent basin configuration will be discussed below. Estimates of tectonic subsidence derived from decompacted unit thicknesses must be regarded as minimum values only, particularly for lacustrine units, for which the depositional water depths (which may reflect additional subsidence) are poorly constrained.

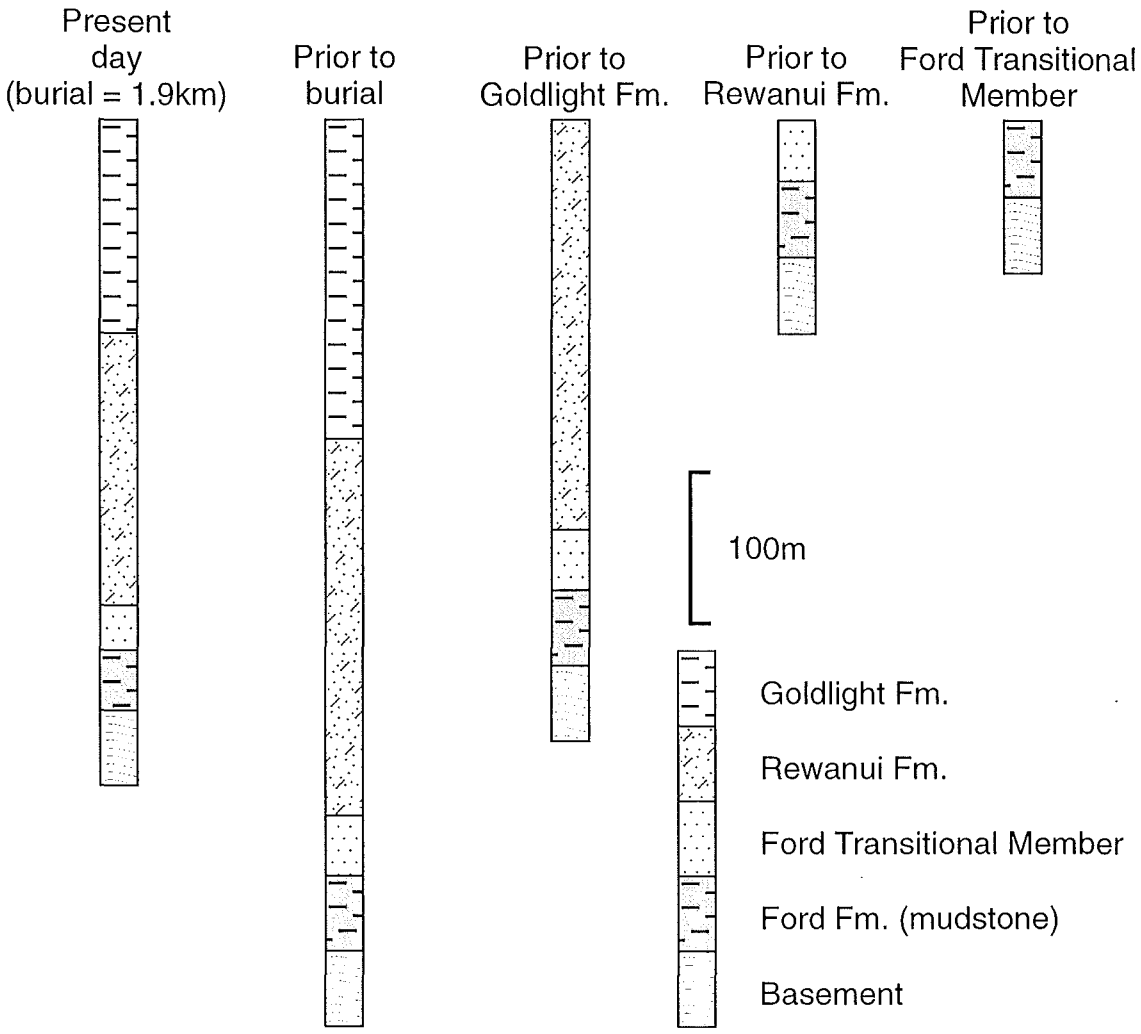

unit	initial thickness	tectonic subsidence	compaction beneath	present thickness	burial compaction
Goldlight Fm.	210	190	20	140	70
Rewanui Fm.	270	270	0	180	70
Ford Fm.	40	40	0	30	10
Ford Trans. Memb.	50	50	0	40	10

Figure 4.1A Evolution of sedimentary column, DH624, showing change in unit thicknesses with successive deposition. Details shown in table (all values in metres). Full data from *BASIN.XLS* spreadsheet (Larrieu 1995) shown in Figure 4.1B.

TABLE 1.1 - Data Entry - Lithologic

#	Unit Description	Top (km)	Base (km)	Thickness (km)	Depth Coefficient (1/km)	Surface Porosity
	Youngest					
5	cover	0	1.98	1.98	0.6	0.48
4	G	1.98	2.12	0.14	0.39	0.5
3	R	2.12	2.3	0.18	0.75	0.42
2	FTM	2.3	2.33	0.03	0.28	0.41
1	F mst	2.33	2.37	0.04	0.27	0.4
0						
	Oldest					

TABLE 2.1 - Solutions to Decompaction Equation

		Age (Ma)				
#	Unit	71	70	65	62	20
						0.00
5	cover				0.00	1.98
4	G			0.00	0.21	2.12
3	R		0.00	0.27	0.46	2.30
2	FTM	0.00	0.04	0.31	0.49	2.33
1	F mst	0.05	0.09	0.35	0.54	2.37

TABLE 2.2 - Decompaction Equations Approximated by Solver

		Age (Ma)				
#	Unit	71	70	65	62	20
5	cover					8.26E-08
4	G				2.61E-07	1.03E-07
3	R			-7.16E-07	-3.55E-07	9.97E-08
2	FTM		-1.72E-07	-4.24E-07	6.99E-07	2.76E-07
1	F mst	3.32E-07	3.05E-07	1.20E-08	6.42E-08	3.34E-07

TABLE 3.1 - Thicknesses of Decompacted Units

		Age (Ma)				
#	Unit	71	70	65	62	20
5	cover					1.98
4	G				0.21	0.14
3	R			0.27	0.25	0.18
2	FTM		0.04	0.04	0.04	0.03
1	F mst	0.05	0.05	0.05	0.05	0.04

TABLE 3.2 - Porosities of backstripped units

		Age (Ma)				
#	Unit	71	70	65	62	20
5	cover					0.28
4	G				0.48	0.22
3	R			0.38	0.33	0.08
2	FTM		0.41	0.38	0.36	0.21
1	F mst	0.40	0.39	0.37	0.35	0.21

TABLE 3.3 - Bulk densities of backstripped units

		Age (Ma)				
#	Unit	71	70	65	62	20
5	cover					2202.17
4	G				1872.10	2285.82
3	R			1940.55	2017.99	2382.22
2	FTM		1989.49	2036.96	2068.27	2302.63
1	F mst	2006.55	2013.40	2057.25	2086.28	2306.43

TABLE 4.0 - Paleobathymetry + Eustatic Sea-Level

		Age (Ma)				
#	Unit	71	70	65	62	20
	Paleobathymetry	0	0	0	0	0
	Eustatic Sea Level	0	0	0	0	0

TABLE 4.1 - Total Subsidence (km)

		Age (Ma)				
#	Unit	71	70	65	62	20
	TOTAL SUBSIDENCE	0.05	0.09	0.35	0.54	2.37
	Corrected for Paleo-bathymetry and Eustatic	0.05	0.09	0.35	0.54	2.37

Figure 4.1B Decompaction results, DH624.

4.2 Decompacted isopach models and tectonic subsidence, Paparoa Group units

Decompacted isopach and tectonic subsidence models were manually constructed from the data presented in Appendix 12 for the 72 modelled drillholes, and were drawn to conform with the present-day isopach models presented in Chapter 3. The resulting isopach maps were remodelled as surfaces into a *TECHBASE* cell table (48x52 cells, each 250m^2), which facilitates cross-section construction and addition or subtraction of surfaces. All surfaces were constructed using the *TECHBASE POLYGRID* application to generate models from isopach drawings, and cell table entries were carefully edited to remove spurious values. Small-scale features present in some decompacted isopach maps are not resolved in the gridded models, and therefore are not apparent in cross-sections which are plotted from those models.

4.2.1 Jay Formation

Jay Formation strata comprise mostly conglomerate (Section 2.7.1), and mechanical compaction was limited. Maximum compaction (40m) occurred in DH621, and five drillholes in the southern sub-basin (marked with circles on Figure 4.2) experienced no compaction during burial. Most compaction of Jay Fm. was due to cover deposition rather than burial by overlying Paparoa Group units. The method employed in the present study assigned all subsidence during Jay Fm. deposition to tectonic effects.

The Jay Fm. basin is oriented sub-parallel to known fold axes within Greenland Group (Figure 1.2), and appears to align with restricted occurrences of underlying Pororari Group (Figure 3.1). This latter alignment may be coincidental, as up to 30Ma is represented by the unconformity between Pororari Group and Paparoa Group strata (Raine 1984; Laird 1988). Terrestrial sedimentation was unlikely to have commenced on an initially flat surface, and the presence of paleotopography (i.e. a broad valley) was likely. However, eastward truncation of the Jay Fm., and asymmetry along the southwestern basin margin, suggest partial tectonic controls on basin geometry. Decollement and Neogene deformation have obscured the sedimentary basement/cover relationships, and the pre-Paparoa Group basement surface cannot be readily reconstructed (Gage 1952, p. 22).

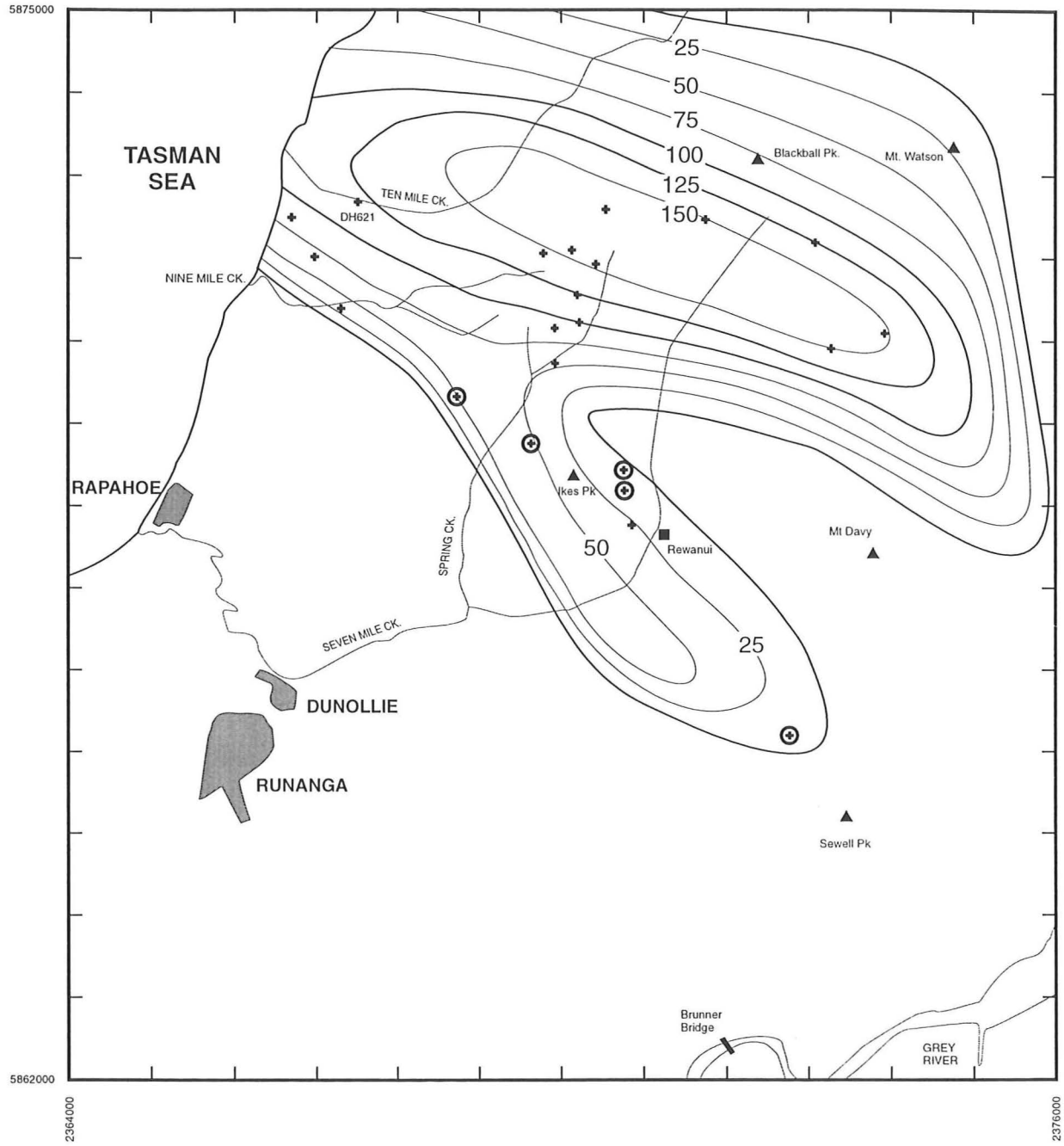

Figure 4.2 Decompacted isopach model, Jay Formation.
Isopach interval = 25m.
Numbered drillholes are discussed in text.

4.2.2 Ford Formation

Ford Fm. strata were compacted up to 100m (DH665, DH668) by burial beneath overlying Paparoa Group units and cover strata (Figure 4.3). Ford Transitional Member strata were compacted by 30m or less, and decompacted and present-day isopach patterns are similar. Ford Fm. deposition resulted in 10m of compaction of Jay Fm. in DH665, otherwise all subsidence is ascribed to tectonic effects. Localised thickness variation near DH645 and DH707 (Figure 4.3) may indicate paleotopography of the basement block on which Ford Fm. was onlapping to the southwest.

A combined decompacted isopach model for Jay Fm. and Ford Fm. is shown in Figure 4.4, and in cross-sections in Figure 4.5. The basin enlarged during Ford Fm. deposition, notably in the southwest and near Mt. Davy. Overall coincidence of Ford Fm. and Jay Fm. isopach patterns in the Mt. Davy Sector indicates a common control on basin geometry (Figure 4.4). The persistent region of limited or no deposition running NW from Mt. Davy represents a topographic high which restricted sedimentation (Figure 4.5, Section B–B'). Maximum decompacted thickness of Jay Fm. and Ford Fm. south of the basement high (in the Rewanui area) is not coincident, and Jay Fm. strata were tilted as the Ford Fm. depocentre migrated northwards (Figure 4.5, Section B–B', left-hand end).

The thin finger of Ford Fm. sediment extending south from the main basin (as indicated by DH651) defines a N/S depositional pattern not evident elsewhere during Ford Fm. or Jay Fm. accumulation. These sediments may represent infilling of a pre-existing shallow valley, the floor of which lay above the Jay Fm. depositional surface, hence absence of this feature from the Jay Fm. basin (Figure 4.2). However, alignment with the maximum extent of tuffaceous strata within Ford Fm. along Spring Ck. (Section 3.4.1), and coincidence with overlying features in both the Morgan CMM and Rewanui CMM (see below) indicates the likely cause for the formation of this sub-basin is a N/S oriented fault or fault zone which initiated during Ford Fm. deposition.

The combined Jay / Ford isopach model (Figure 4.4) is taken as an estimate of tectonic subsidence during the early stages of Paparoa Group deposition. However, some strata may have been eroded by Rewanui CMM deposition (see below), and an unknown amount of additional tectonic subsidence may have been required to generate the relative rise in base level necessary for creation of the Ford Fm. lake.

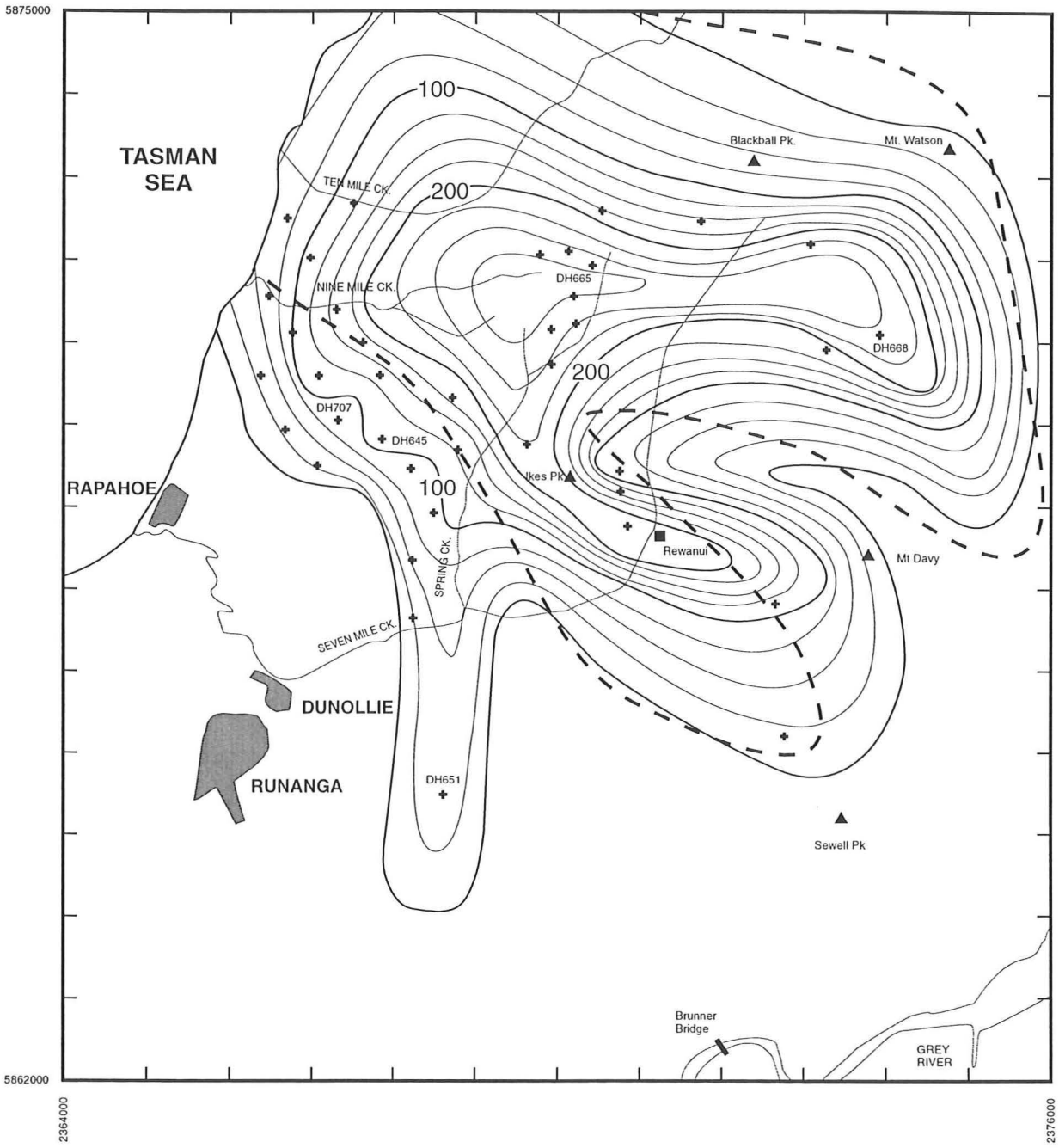

Figure 4.3 Decompacted isopach model, Ford Formation.
Isopach interval = 25m.
Numbered drillholes are discussed in text.

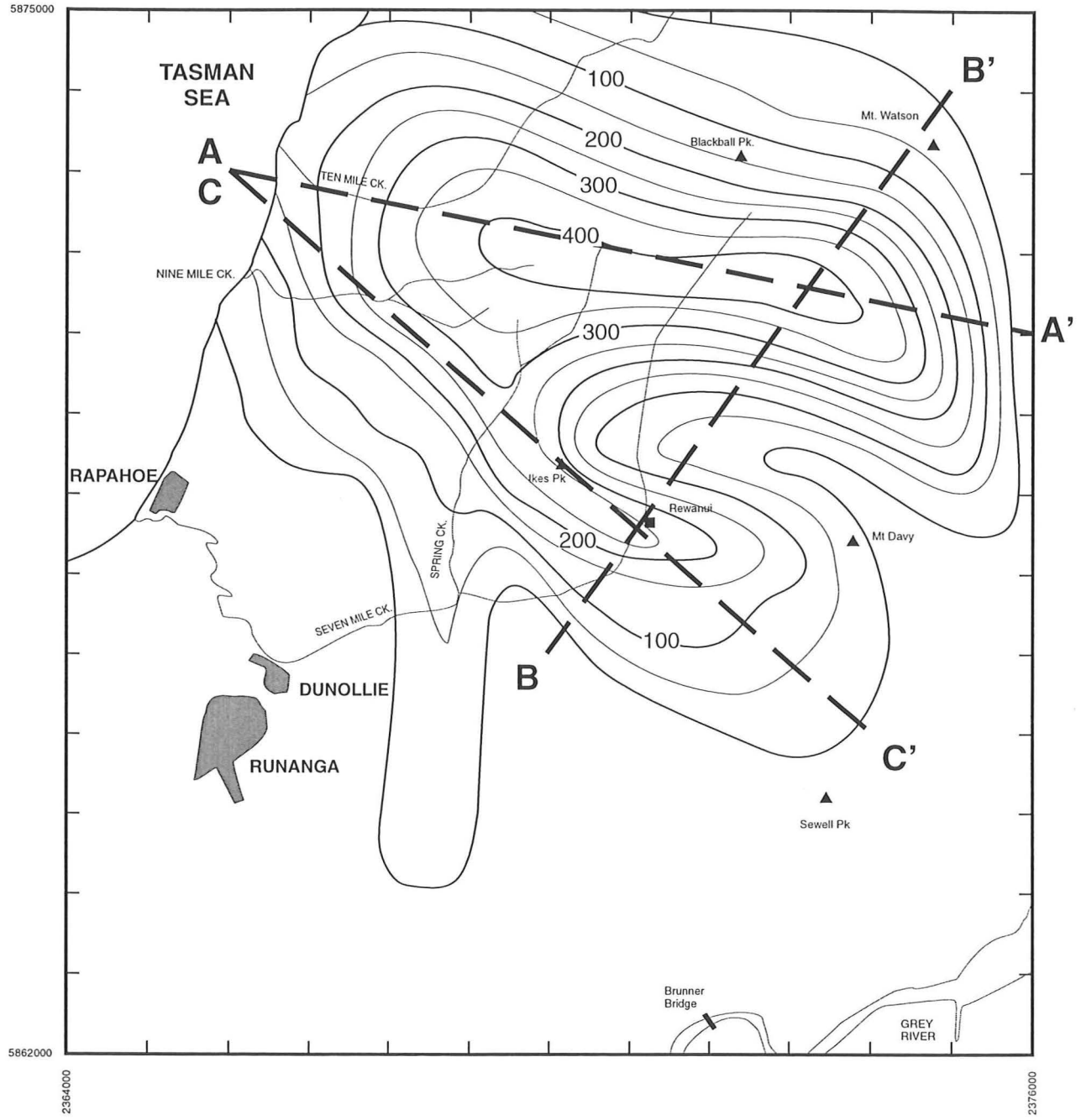

Figure 4.4 Combined decompacted isopach model, Jay Formation and Ford Formation. Isopach interval = 50m.

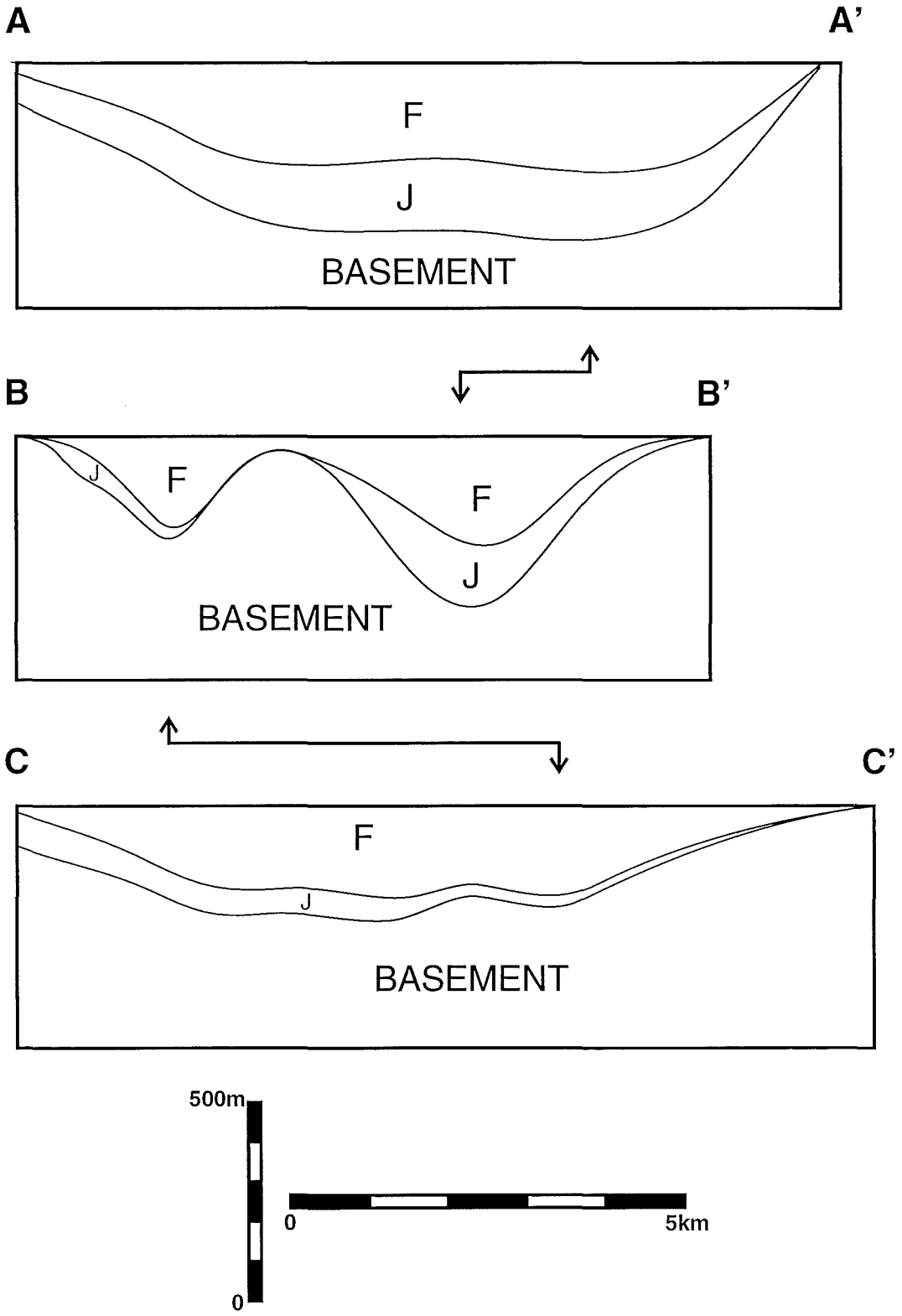

Figure 4.5 Cross-sections through decompacted Jay Formation (J) and Ford Formation (F) basin.
Horizontal scale = 1:80000, vertical exaggeration = 5:1
Location of sections given in Figure 4.4.
Arrows indicate intersection of cross-sections.

4.2.3 Morgan Coal Measure Member

Compaction of Morgan CMM strata by burial varies from nil (DH625, DH664) to 70m (DH668). Initial thicknesses of twice present-day are modelled for DH246, DH266 and DH668. The decompacted isopach model (Figure 4.6) differs from the present-day model (Figure 3.4) in the Ikes Pk./Rewanui/Mt. Davy area, though the overall pattern of a bifurcated main depocentre and a southern outlier remains. Maximum decompacted Morgan CMM thickness (c.200m) northeast of Mt. Davy is conjectural. Strata beneath Morgan CMM were compacted by 10m (circled on Figure 4.6), and some Jay Fm. may have been eroded by Morgan CMM deposition (Figure 4.7, C–C'). All other subsidence during Morgan CMM deposition is attributed to tectonic movements.

Morgan CMM was deposited mostly within the area of the eastern Jay Fm. and Ford Fm. basin, though Morgan CMM extends c.0.5–1.0km further south and east than underlying strata. The western Morgan CMM depocentre coincides approximately with the Jay / Ford depocentre, whereas the eastern Morgan CMM depocentre overlies an area of rapid easterly thinning of underlying strata (Figure 4.7, Section A–A'). The southeastern basement high extending into the Jay and Ford basins was covered by Morgan CMM strata, and differential subsidence evident in the Rewanui area exhibited by Ford Fm. and Jay Fm. was subdued during Morgan CMM deposition (Figure 4.7, Section B–B'). The "finger" of Ford Fm. extending south links up with the small southern Morgan CMM sub-basin (Figure 4.6), and this linkage may be interpreted as a conduit through which granite-derived sediment (Section 2.6.3) was transported into the Brunner Bridge depocentre.

Bowman et al. (1984 p. 47) attributed thickening of Morgan CMM in the central and northeast areas of Greymouth Coalfield to compaction of underlying thick Ford Fm. mudstones. However, this study demonstrates that both decompacted and present-day isopach patterns for Morgan CMM are discordant with Jay Fm. and Ford Fm. thickness trends. Topographic features within the Jay / Ford basin were largely buried during Ford Fm. deposition, and had little influence on Morgan CMM isopach patterns. During Morgan CMM deposition, the basin evolved further and new structural controls emerged, with the first appearance of the NNE/SSW trend evident in overlying units.

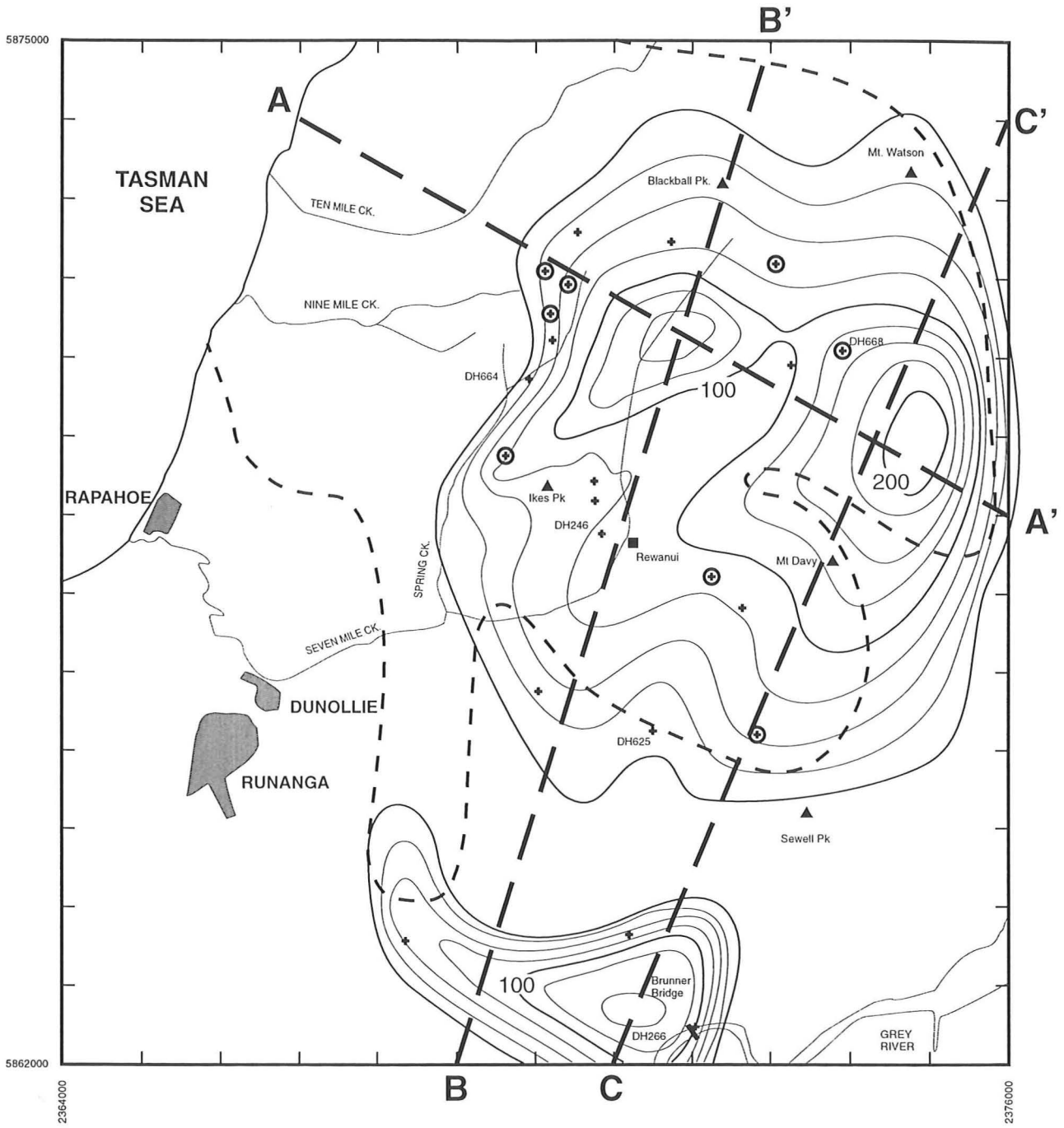

Figure 4.6 Decompacted isopach model, Morgan CMM.
Isopach interval = 25m.
Numbered drillholes are discussed in text.

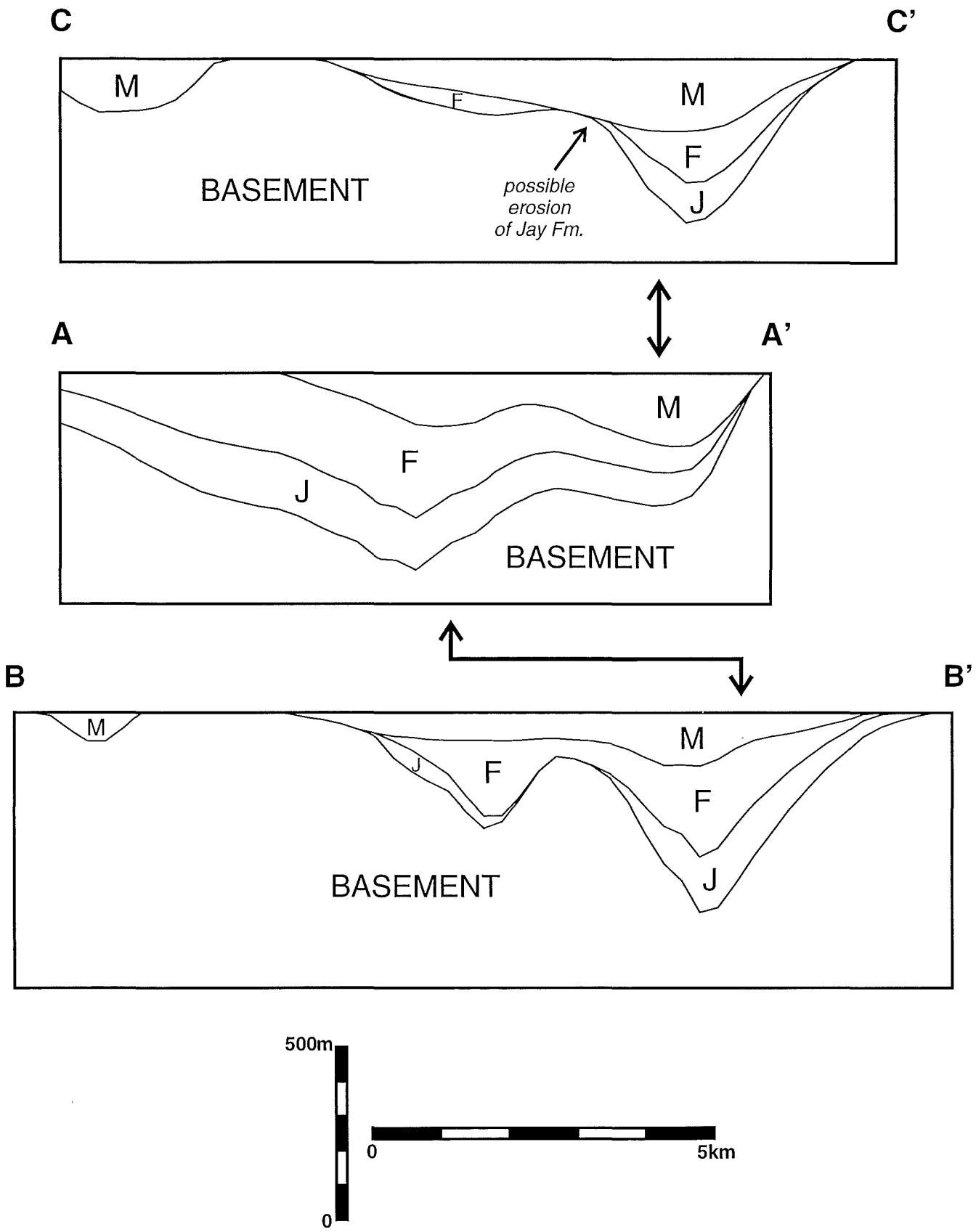

Figure 4.7 Cross-sections through decompacted Morgan CMM (M), Ford Fm. (F) and Jay Fm. (J)
Horizontal scale = 1:80000, vertical exaggeration = 5:1
Location of sections given in Figure 4.6.
Arrows indicate intersection of cross-sections.

Morgan CMM strata are laterally equivalent to western basal Rewanui CMM (Section 2.6.4), and the western limit of Morgan CMM (Figure 4.7, Section A–A') is due to thinning by lateral gradation and not a reduction of tectonic subsidence.

4.2.4 Waiomo Mudstone Member

Burial compaction of Waiomo MM (Figure 4.8) varied from zero to 30m (DH658, DH660). Waiomo MM deposition resulted in compaction of Morgan CMM by 10m in DH246, DH620 and DH668, and Ford Fm. by 10m in DH658. In all other modelled drillholes, there was no compaction of strata beneath Waiomo MM.

Maximum decompacted Waiomo MM thickness coincides approximately with underlying Jay / Ford basin (Figure 4.4), and Bowman et al. (1984, p. 52) attributed Waiomo MM thickness in the northern depocentre to compaction of Ford Fm. mudstone. The present analysis suggests such compaction beneath Waiomo MM was limited to c.10m. Correlation of Waiomo MM with Morgan CMM isopach trends (other than overall occurrence) is poor, suggesting different controls on intrabasin geometry. The eastern limit of Waiomo MM overlies the thickest area of Morgan CMM, and Waiomo MM may onlap Morgan CMM to the east, which would suggest a palegeographic rather than paleotectonic control on the eastern margin of Waiomo MM.

No lateral equivalent to Waiomo MM within lower Rewanui CMM to the west can be recognised (Section 2.6.4, Figure 2.6), and tectonic subsidence of the Waiomo MM basin must have declined rapidly westwards. Waiomo MM records a period of subsidence which was restricted to the Mt. Davy Sector, indicating structural partitioning of the basin into distinct depocentres with independent subsidence histories.

4.2.5 Rewanui Coal Measure Member

Rewanui CMM was compacted by between 20m and 130m by deposition of Goldlight Fm. and cover strata. Decompacted thickness ranges from 30m (DH653) to 350m (DH342), and preburial Rewanui CMM in DH633, DH646, DH648 and DH653 is equal to or greater than double present-day thickness. The decompacted Rewanui CMM thickness model is illustrated in Figure 4.9, and cross-sections illustrating Rewanui CMM and underlying basin geometry are shown in Figure 4.10A–C (cross-sections A–A' through J–J').

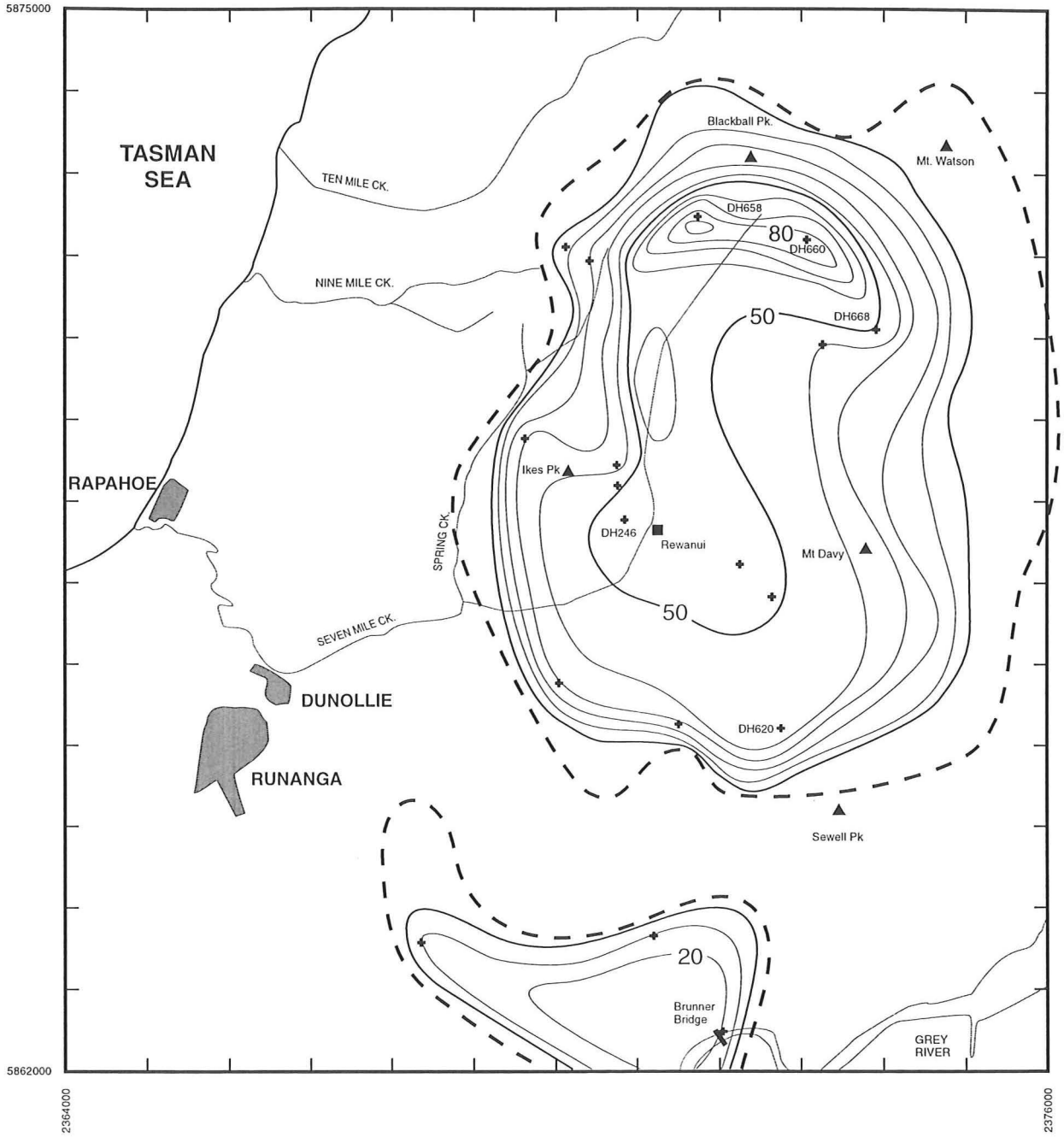

Figure 4.8 Decompacted isopach model, Waiomo MM.
Isopach interval = 10m.
Numbered drillholes are discussed in text.

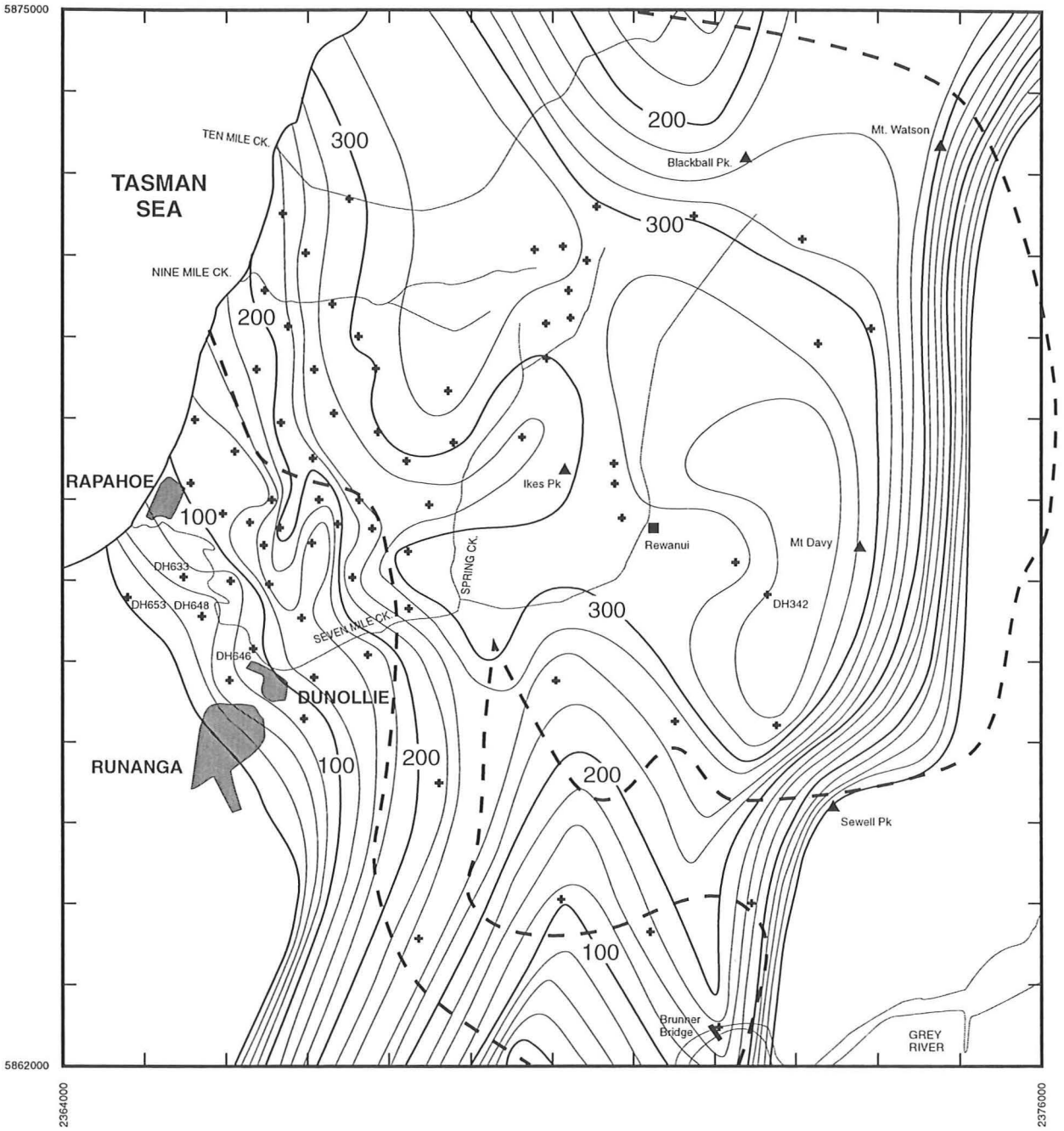

Figure 4.9 Decompacted isopach model, Rewanui CMM.
Isopach interval = 25m.
Numbered drillholes are discussed in text.

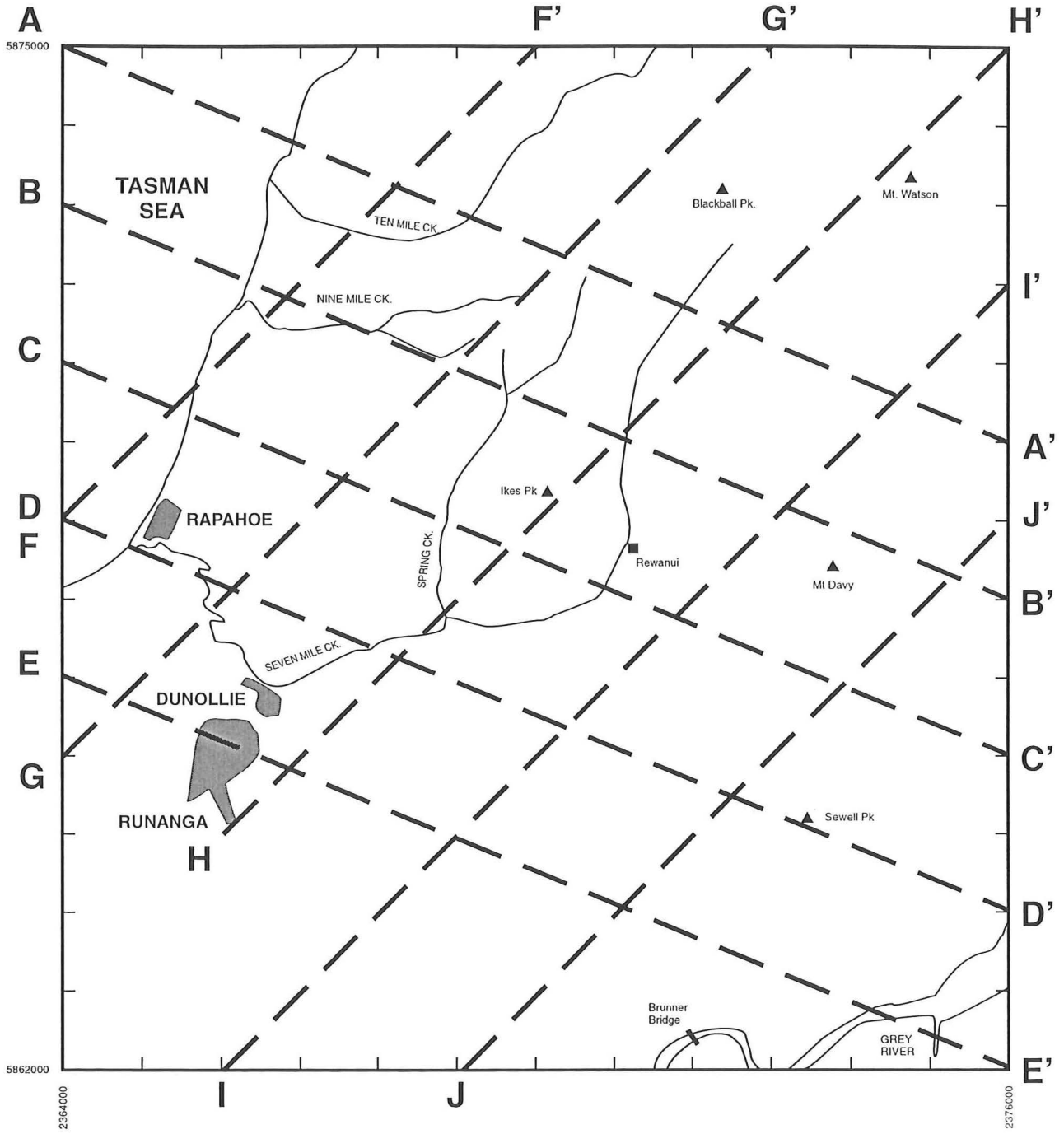

Figure 4.10A Location of section lines shown in Figure 4.10B and 4.10C.

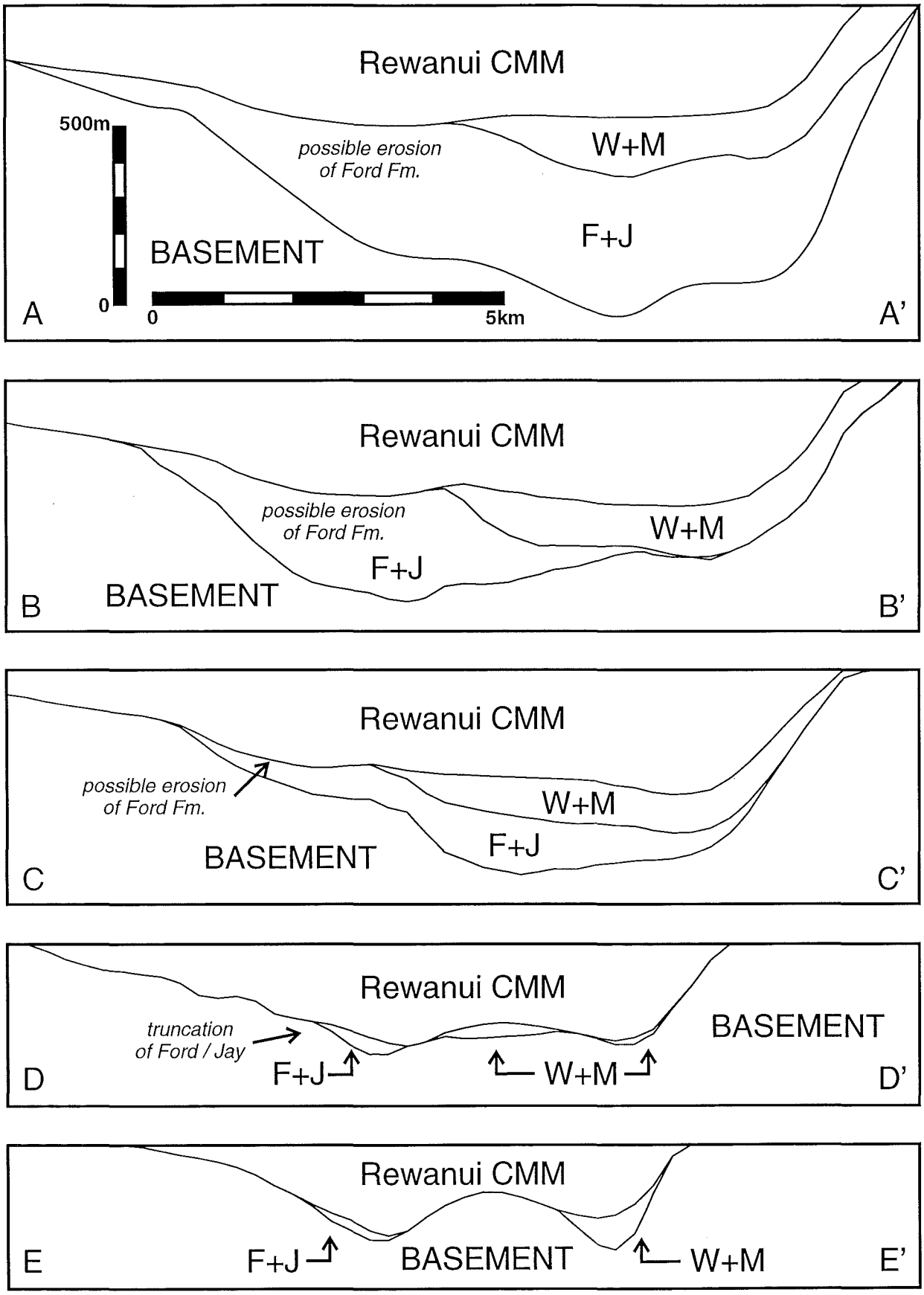

Figure 4.10B Cross-sections through Paparoa Basin
at end of Rewanui CMM deposition.
W+M = Waiomo MM and Morgan CMM, J+F = Jay Fm. and Ford Fm.
Horizontal scale = 1:80000, vertical exaggeration = 5:1
Location of sections given in Figure 4.10A.

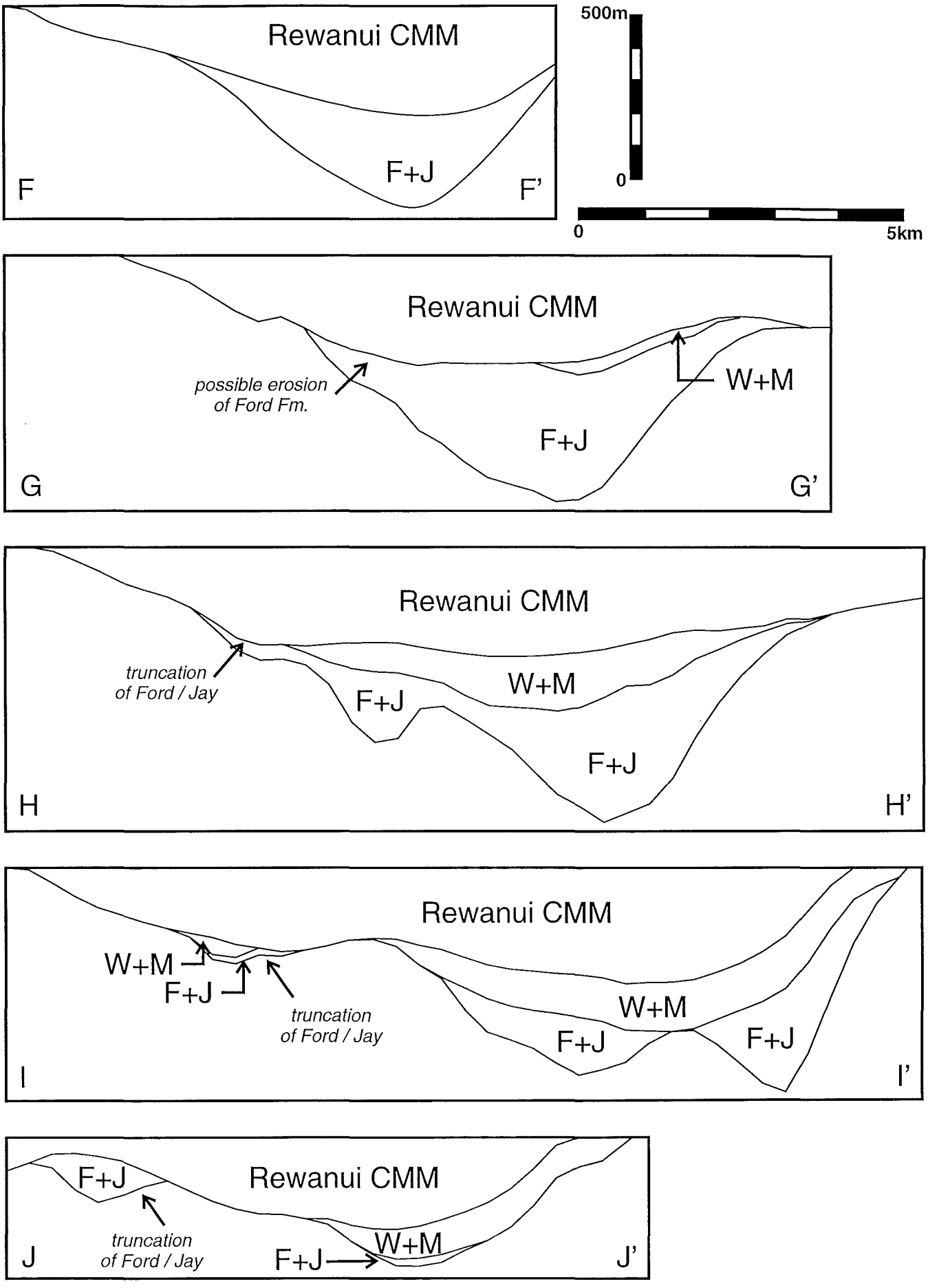

Figure 4.10C SW-NE cross-sections. Details as for Figure 4.10B, See Figure 4.10A for locations.

Correspondence between the Rewanui CMM basin and underlying strata thickness is poor (dashed line in Figure 4.9, see also Figure 4.10, Sections B–B', H–H', I–I', J–J'). However, the NW/SE aligned basin defined by Jay Fm. and Ford Fm. remains evident in the northwest (e.g. Figure 4.10, Section A–A', F–F'). Minor sub-basins containing Morgan CMM and Waiomo MM in the Brunner Bridge area enlarged to contain thick sections of Rewanui CMM (Figure 4.10, Sections D–D', E–E' I–I', J–J') and a new basin geometry developed in the southern portion of the study area. The N/S oriented southern extension of Ford Fm. enlarged to become a 3km-wide trough which continued to the south of the study area. A similar trough extended to the NNE, between Blackball Pk. and Mt. Watson.

Erosion of Ford Fm. and Jay Fm. beneath Rewanui CMM is suggested by the concave basal contact of the Rewanui CMM evident in cross-sections A–A', B–B', C-C' and G–G', and apparent truncation of Ford/Jay depicted in cross-sections D–D', H–H', I–I' and J–J'. Up to 50m of strata may have been removed. Basal Rewanui CMM contacts in drillholes near the intersection of Sections C–C' and G–G' (DH's 635, 645, 704, 707, 708) are scoured, and erosion of Ford Fm. by Rewanui CMM also occurred in the northwest of the coalfield (Section 2.6.1).

Rewanui CMM sediments covered basement areas west of Sewell Pk. and in the southern Rapahoe Sector, indicating continued expansion of the basin. Rapid variation in decompacted Rewanui CMM thickness 2km east of Rapahoe is not evident in Ford Fm. deposited slightly to the north (Figure 4.3), suggesting that previously limited basement topography was enhanced by small-scale faulting.

Rewanui CMM sedimentation resulted in compaction of underlying strata by amounts varying between 10m and 50m in 30 drillholes (Table 4.1), indicating that not all subsidence can be attributed to tectonic movements. Initial estimates by Ward (1995, Table 1) suggested compaction of mudstones beneath Rewanui CMM may be a significant source of subsidence in the Strongman Mine area. However, the present study indicates that compaction of Ford Fm. by Rewanui CMM, though common, is limited 20m or less in all but one modelled drillhole (Table 4.1).

Amount of compaction beneath Rewanui CMM	Waiomo MM	Morgan CMM	Ford Fm.	Jay Fm.
10m	246, 265, 659, 660, 665	246, 262, 265, 342, 632, 658, 659, 665	262, 265, 318, 342, 621, 631, 632, 634, 635, 640, 645, 656, 658, 660, 663, 667, 708, 709, 710	246, 634, 659, 662, 666, 710
20m		266, 318, 660	246, 446, 619, 659, 662, 664, 665, 666, 668	621
30m		668	657	

Table 4.1 Summary of compaction of strata (listed by Member or Formation) beneath Rewanui CMM by Rewanui CMM deposition.

A scatter plot of decompacted Rewanui CMM thickness vs. compaction beneath Rewanui CMM (Figure 4.11) illustrates that, though compaction of underlying strata occurred where Rewanui CMM is >160m, and >20m of compaction is restricted to drillholes with >260m Rewanui CMM, there is no strong correlation between the amount of compaction beneath Rewanui CMM and resultant Rewanui CMM thickness.

The tectonic subsidence map, constructed by subtracting compaction from decompacted Rewanui CMM thickness (Figure 4.9), is shown in Figure 4.12. Differences from the decompacted Rewanui CMM isopach pattern (Figure 4.9) are most evident where tectonic subsidence is >c.300m. Two major depocentres are evident, one in the northwest (middle reaches of Ten Mile Ck.), and another in the Mt. Davy area. The depocentres are separated by a subtle c.1–2km wide northeast-oriented ridge along Spring Ck., across which subsidence was c.25–50m less than in the depocentres to either side. Subsidence in the Rapahoe/Runanga area is all tectonic, and the isotect pattern indicates both tilting and localised N/S oriented faulting of the basement block.

4.2.6 Rewanui Formation

Decompacted thickness of Rewanui Fm. (Rewanui CMM, Waiomo MM and Morgan CMM) is shown in Figure 4.13, and maximum initial thickness exceeds 500m. Corrections for compaction within those three units (i.e. Rewanui CMM compacting Waiomo MM and Morgan CMM, and Waiomo MM compacting Morgan CMM) have been made in 12 modelled drillholes. Rewanui Fm. sedimentation caused compaction of underlying strata by up to 40m in 30 of the 72 modelled drillholes.

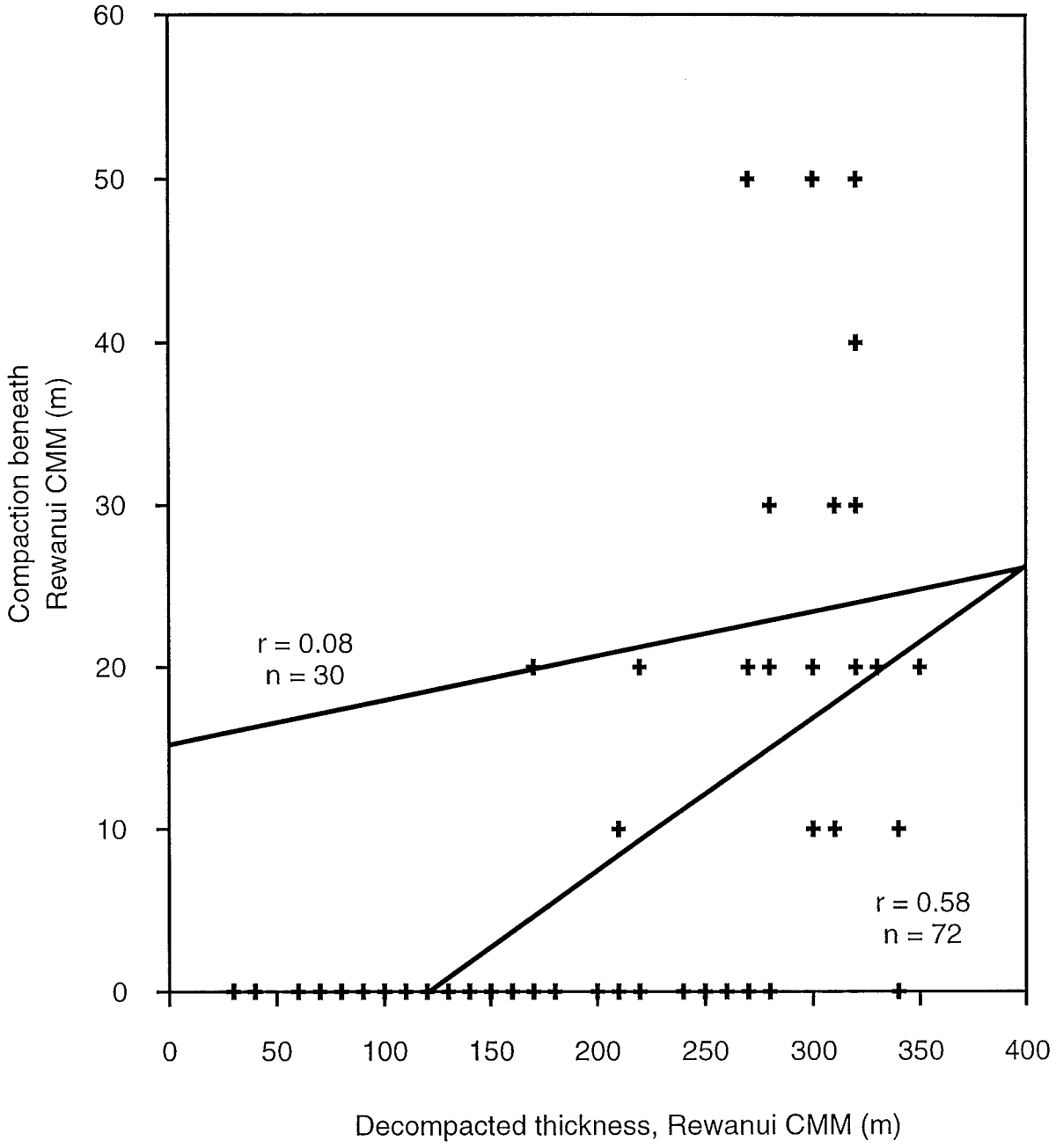

Figure 4.11 Correlation between decompacted Rewanui CMM thickness and compaction of strata beneath Rewanui CMM.
Lower correlation line is for all modelled drillholes,
Upper correlation line is for 30 drillholes with compaction beneath Rewanui CMM.
Note: some sample points represent > 1 data pair.

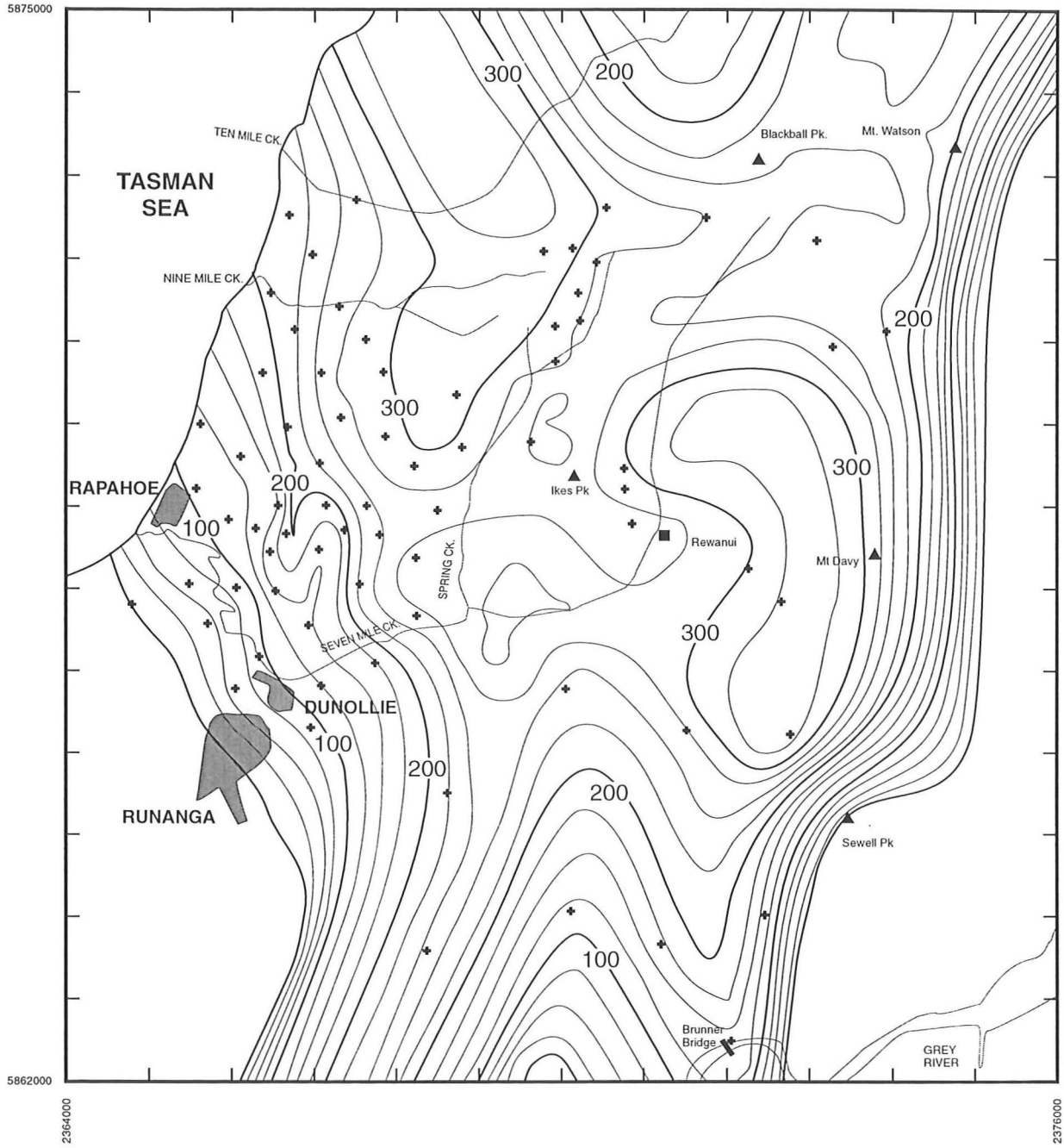

Figure 4.12 Map of tectonic subsidence, Rewanui CMM.
Isotect interval = 25m.

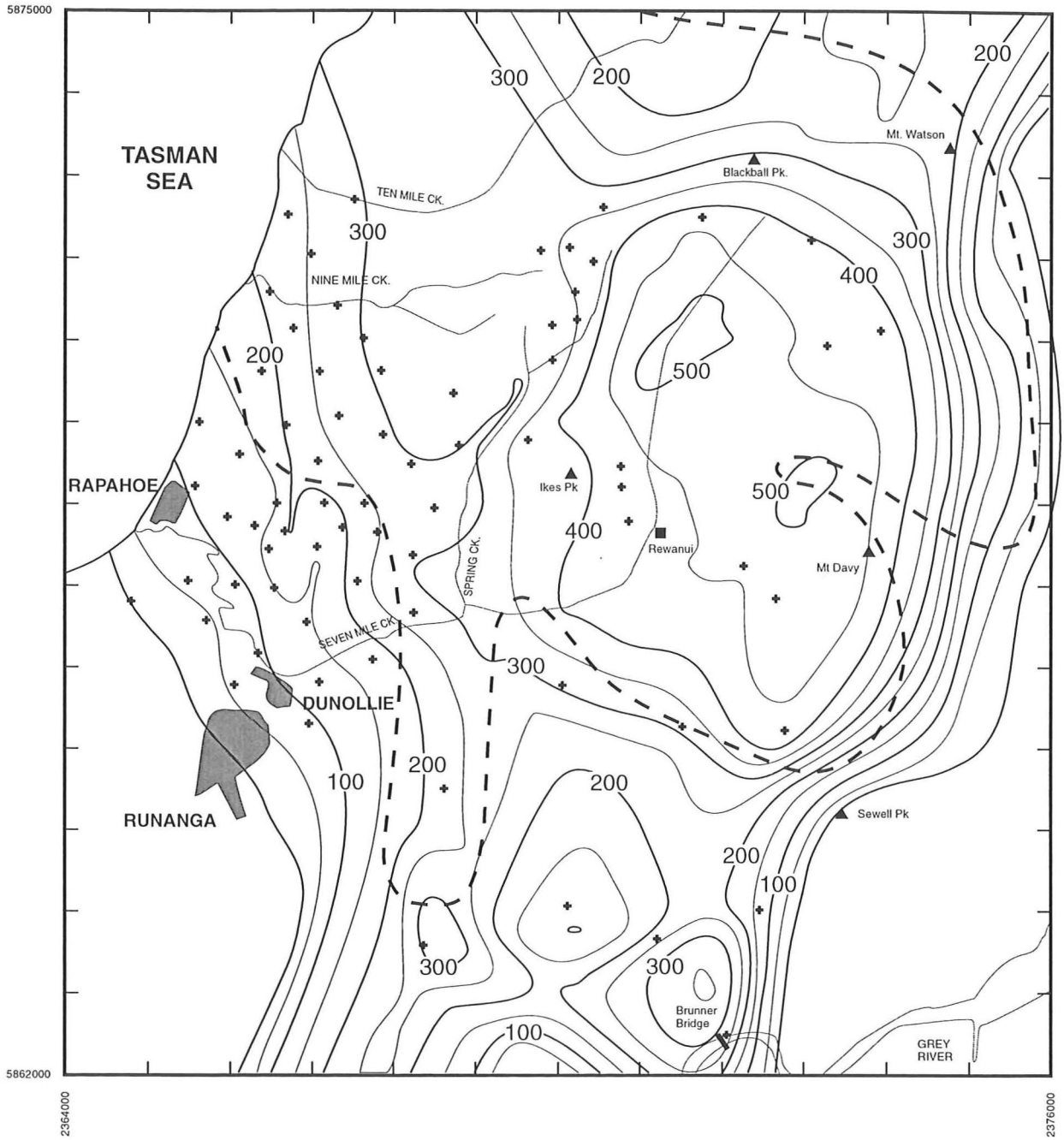

Figure 4.13 Decompacted thickness, Rewanui Formation (comprising Rewanui CMM, Waiomo MM and Morgan CMM). Isopach interval = 50m.

Cumulative tectonic subsidence during Rewanui Fm. deposition is depicted in Figure 4.14. Maximum tectonic subsidence (c.500m) in the Mt. Davy area directly overlay the prominent ridge in the Jay/Ford basin (Figure 4.4). Into this 6km by 4km depocentre fed a broad trough from the northwest, on the southwestern flank of which a platform-like area developed in the Nine Mile Ck./Strongman Mine area. Tectonic subsidence in the eastern depocentre was c.100–150m greater than in northwestern trough. Complex subsidence patterns in the south suggest smaller-scale (1–2km) basement faulting was active, whereas in the southwest a 3km wide basement block tilted to the north, with only minor faulting.

4.2.7 Goldlight Formation

Compaction of Goldlight Fm. by burial varies from 10m (DH619, 621, 622) to 100m (DH266). The decompacted isopach model (Figure 4.15) shows a broad depocentre in the Rewanui–Mt. Davy area in which c.200m ±20m of Goldlight Fm. accumulated, and minor thickening to >250m in the Brunner Bridge area. Rapid localised thickness variation 2–3km east of Rapahoe evident in the present-day Goldlight Fm. isopach model (Figure 3.8) persisted during the decompaction exercise, suggesting that such anomalies did not result from differential compaction. Anomalies in initial Rewanui CMM thickness occur in the same area (Figure 4.9), but at different orientations.

Burial compaction of Goldlight Transitional Member was limited (up to 40m), and decompacted thickness patterns are little different from present-day thickness (Figure 3.9, 3.10). In three drillholes (DH273, DH635 and DH704) there was compaction within Goldlight Fm. during deposition, which is incorporated in Figure 4.15. For example, in DH273, Goldlight Fm. mudstone lithosomes (initially 230m) compacted underlying lower Goldlight Transitional Member (initially 20m) by 10m, and were themselves compacted 10m by overlying upper Goldlight Transitional Member.

Goldlight Fm. deposition resulted in compaction of underlying strata in 57 of the modelled drillholes. Most compaction (c.70%) occurred within Rewanui CMM, a further c.10% in Waiomo MM and Morgan CMM, and the remainder in Ford Fm. Compaction of Rewanui CMM in drillholes dominated by fine sediment (coarse:fine ratio <1.00; see Appendix 4.4.1) varied from zero to 30m.

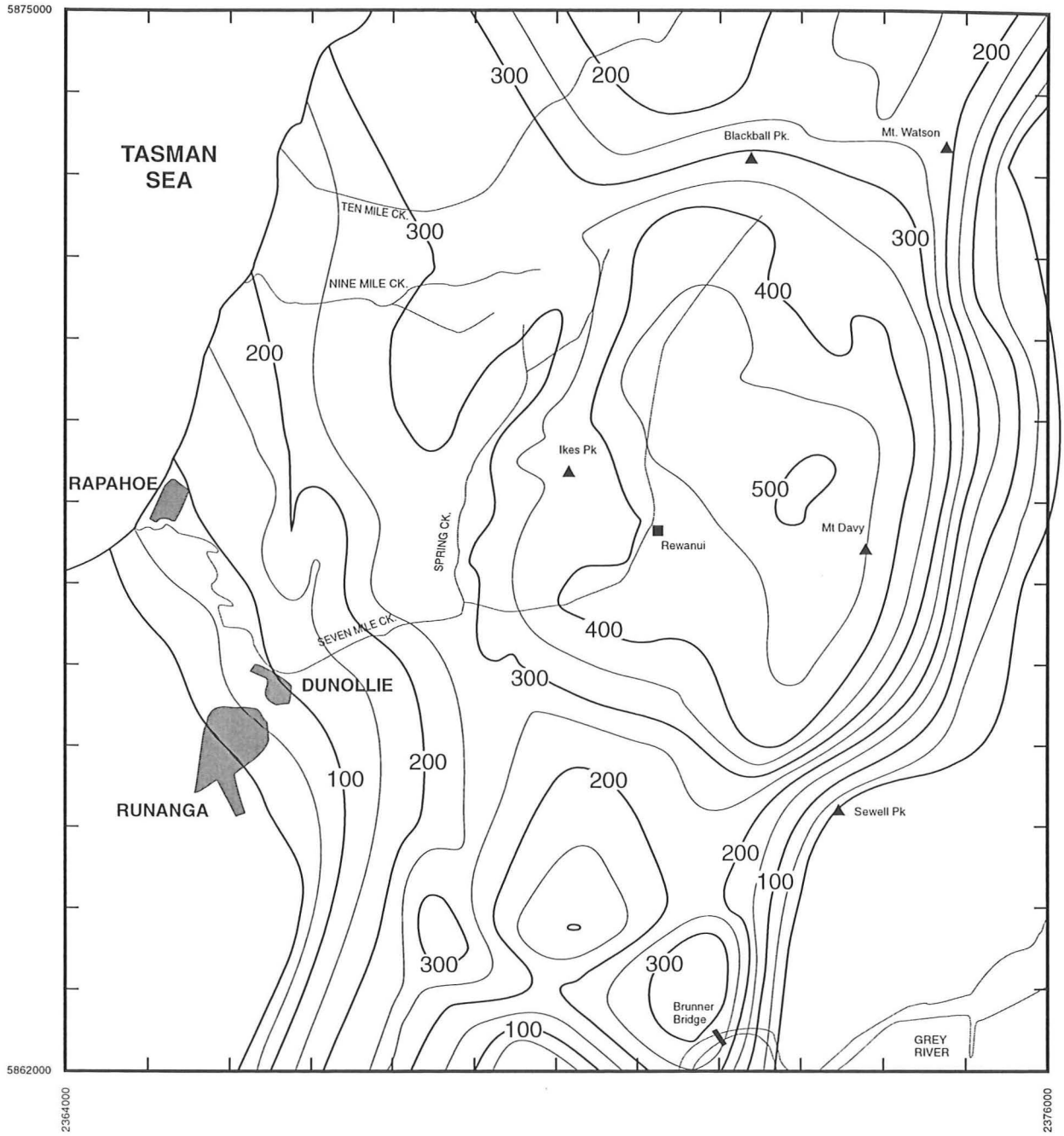

Grid ticks = 1km, grid numbers = New Zealand Map Grid, NZMS 260 J31 & K31

Figure 4.14 Tectonic subsidence map, Rewanui Formation
(Rewanui CMM, Waiomo MM, Morgan CMM)
Isotect interval = 50m.

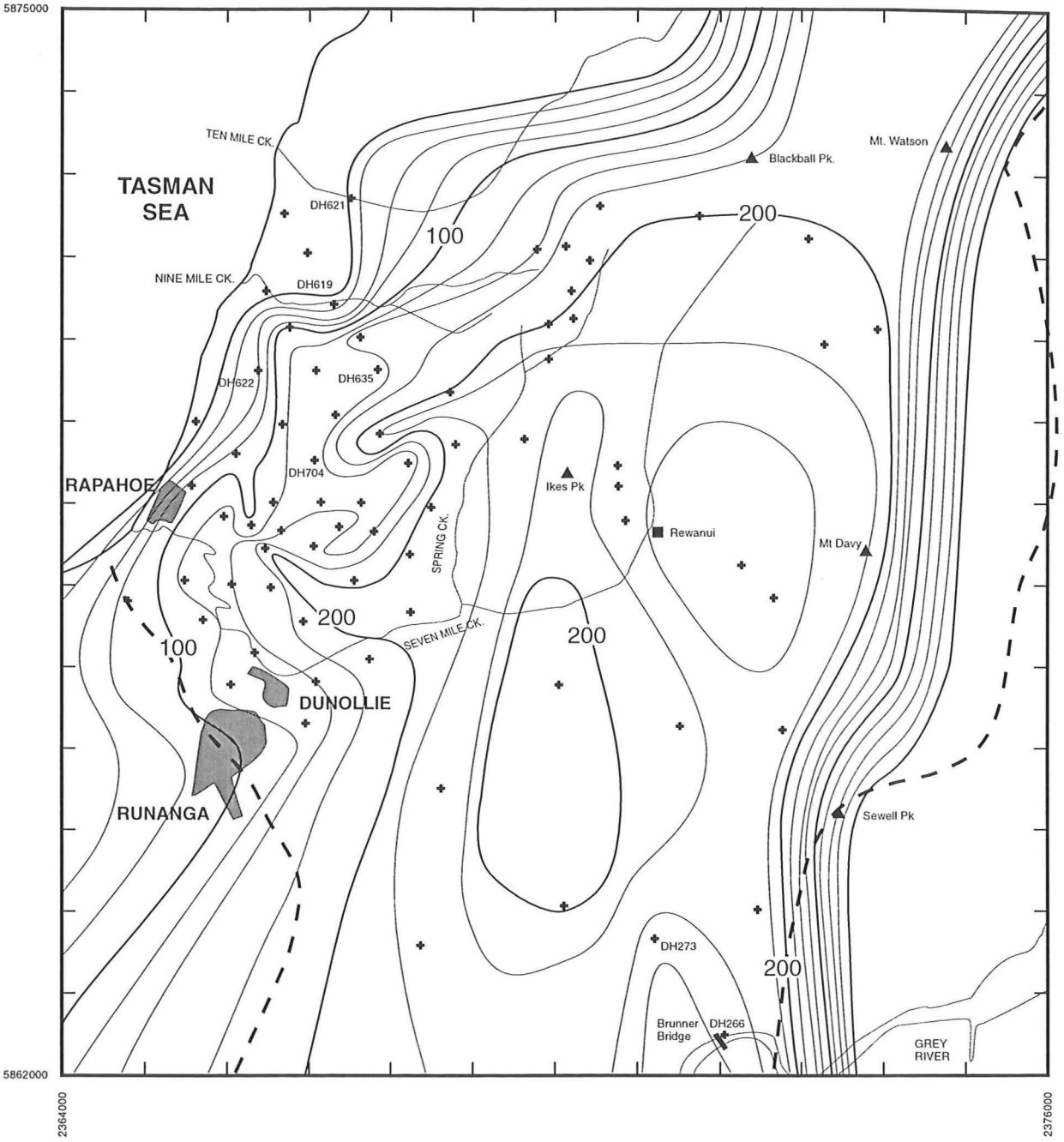

Figure 4.15 Decompacted isopach model, Goldlight Formation.
Isopach interval = 25m.
Numbered drillholes are discussed in text.

Thick Goldlight Fm. in the southwest Rapahoe Sector was previously attributed to compaction of underlying peats within Rewanui CMM (Bowman et al. 1984, p. 58). Compaction of Rewanui CMM beneath Goldlight Fm. is a function of decompacted Goldlight Fm. thickness, proportion of compactible, fine sediment (including coal) within Rewanui CMM, and the decompacted thickness of Rewanui CMM. Analysis of the decompacted results for all 72 modelled drillholes shows a positive correlation ($r = 0.56$) between decompacted Goldlight Fm. thickness and compaction within Rewanui CMM, though correlation with coal percentage within Rewanui CMM is less significant ($r = 0.39$). However, there is a strong correlation between Rewanui CMM compaction beneath Goldlight Fm. and thickness of coal within all modelled drillholes ($r = 0.72$).

Accurate estimates of initial peat thickness within Rewanui CMM, with which to fully test Bowman's hypothesis, cannot be derived from present data. However, peat bodies within upper Rewanui CMM in the Rapahoe Sector would have been buried by c.100–200m at the end of Goldlight Fm. deposition, and the peat compaction regime applied in the present study (Appendix 4.3.4) supports significant compaction (up to c.60%) throughout these shallow burial depths.

Modelled tectonic subsidence (decompacted thickness less compaction beneath Goldlight Fm.) is depicted in Figure 4.16. The NNE/SSW alignment of the basin in which Goldlight Fm. accumulated was previously highlighted by trend surface analysis (Appendix 3.3) and this pattern is reinforced in Figure 4.16. Goldlight Fm. occupies a southward-broadening, 5–11km wide trough with a steep eastern margin and a complex western margin. The underlying NW/SE pattern evident in western Rewanui Fm. (Figure 4.9), and Jay/Ford basins (Figure 4.4) appears to be absent. Goldlight Fm. isotects (Figure 4.16) in the northwest of Greymouth Coalfield are at right angles to Rewanui Fm. isotects (Figure 4.12).

The complex isotect pattern demonstrated in the Rapahoe Sector (Figure 4.16) suggests factors other than tectonics influenced Goldlight Fm. thickness. In the west, tectonic subsidence patterns exhibit similar trends to isopach models of the upper and lower Goldlight Transitional Members (Figure 3.9 and 3.10). Coincidence of paleogeographic features with subsidence patterns suggests either tectonic control on the location of those paleogeographic features, or the superimposition of a depositional environment

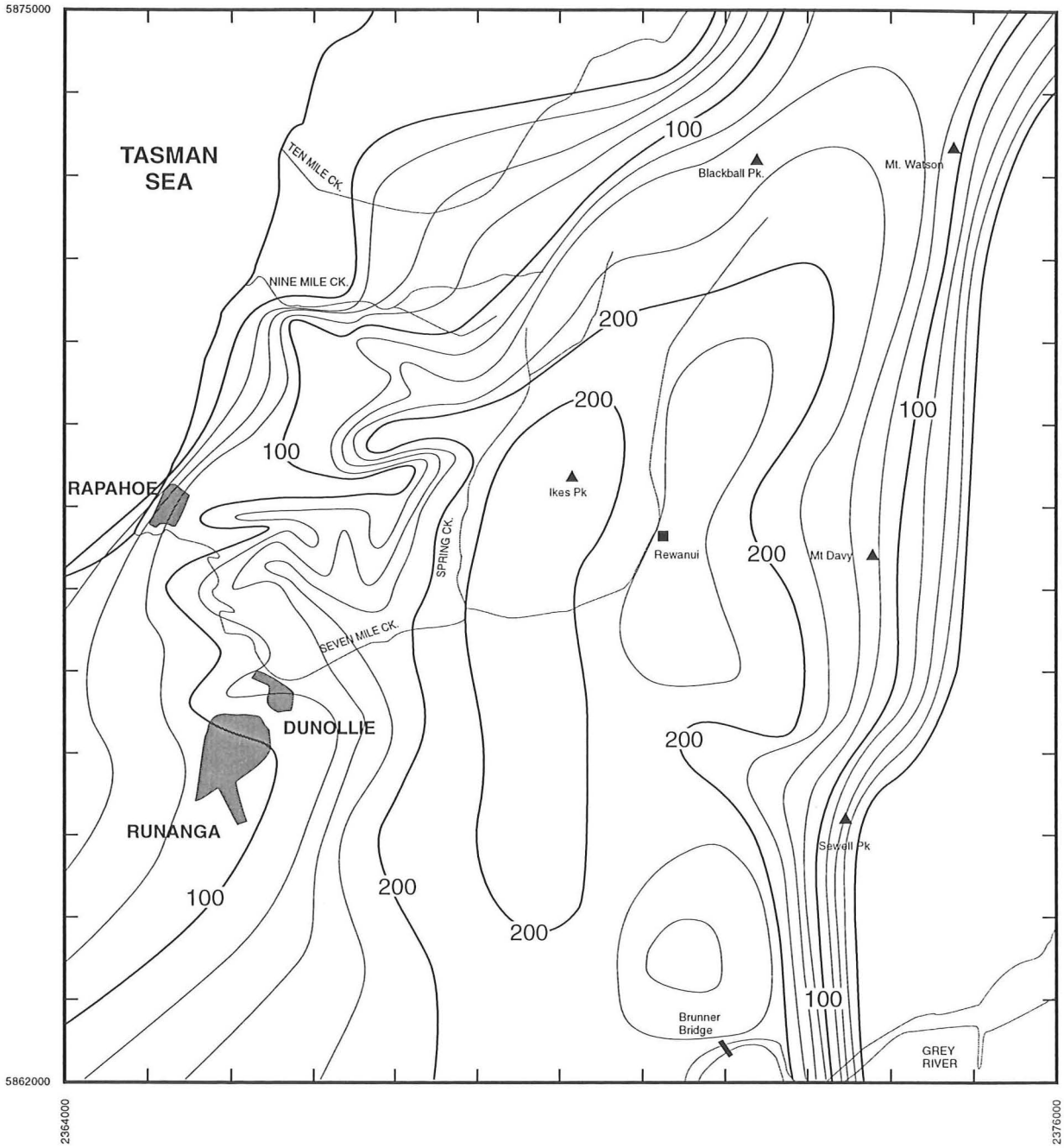

Grid ticks = 1km, grid numbers = New Zealand Map Grid, NZMS 260 J31 & K31

Figure 4.16 Tectonic subsidence map, Goldlight Formation.
Isotect interval = 25m.

signal on the tectonic subsidence trends. In the latter case, coarse-grained sediment supplied from the basin margins built up above the basin floor as deltaic wedges, resulting in greater sediment accumulation and greater apparent tectonic subsidence in comparison to laterally adjacent areas, where only fine-grained lacustrine sedimentation persisted.

Goldlight Fm. is defined in the west and south by complex lateral/vertical relationships especially with the overlying and laterally equivalent Dunollie Fm. (Section 2.7.6). The base of Goldlight Fm. is approximately isochronous (Section 5.5.4), however the upper contact may involve significant diachroneity, hence unit thickness may not reflect an equal duration of tectonic subsidence events throughout the basin.

4.3 Paparoa Group configuration, pre-burial

Total Paparoa Group thickness (excluding Dunollie Fm.) prior to burial is depicted in Figure 4.17, and in cross-sections in Figure 4.18. Initial thickness exceeded 1000m at the deepest point (1060m is greatest depth in the model), whereas the present day maximum thickness is 760m (Figure 3.12). Overall, the Paparoa Group experienced c.27% thickness reduction during burial. The dominant trend of depocentre alignment depicted by Figure 4.17 is NNE/SSW, with subsidiary trends aligned NW/SE and E/W.

Cumulative Paparoa Group compaction resulting from cover deposition ranges from 20m (DH637) to 290m (DH668) (Appendix 12). Where present, Goldlight Fm. was compacted by 10–100m, with minimum compaction experienced in the northwest (DH619, 621, 622) and maximum in the Mt. Davy–Brunner area (DH266, 318, 342). Rewanui CMM was compacted in all 72 modelled drillholes by amounts varying from 10m to 110m, and the average thickness reduction was 25%. Waiomo MM compacted by 10 or 20m in 13 out of 18 drillholes and Morgan CMM compacted 10–70m in all but 2 drillholes. Ford Fm. compacted by 10–70m in 34 out of 40 drillholes and Jay Fm. compacted by 10–20m in 16 out of 22 drillholes. In general, absence of modelled compaction by cover deposition occurred in thin units (<30m), and compaction was probably less than the precision of the method employed (±5m, see Appendix 4.4.1).

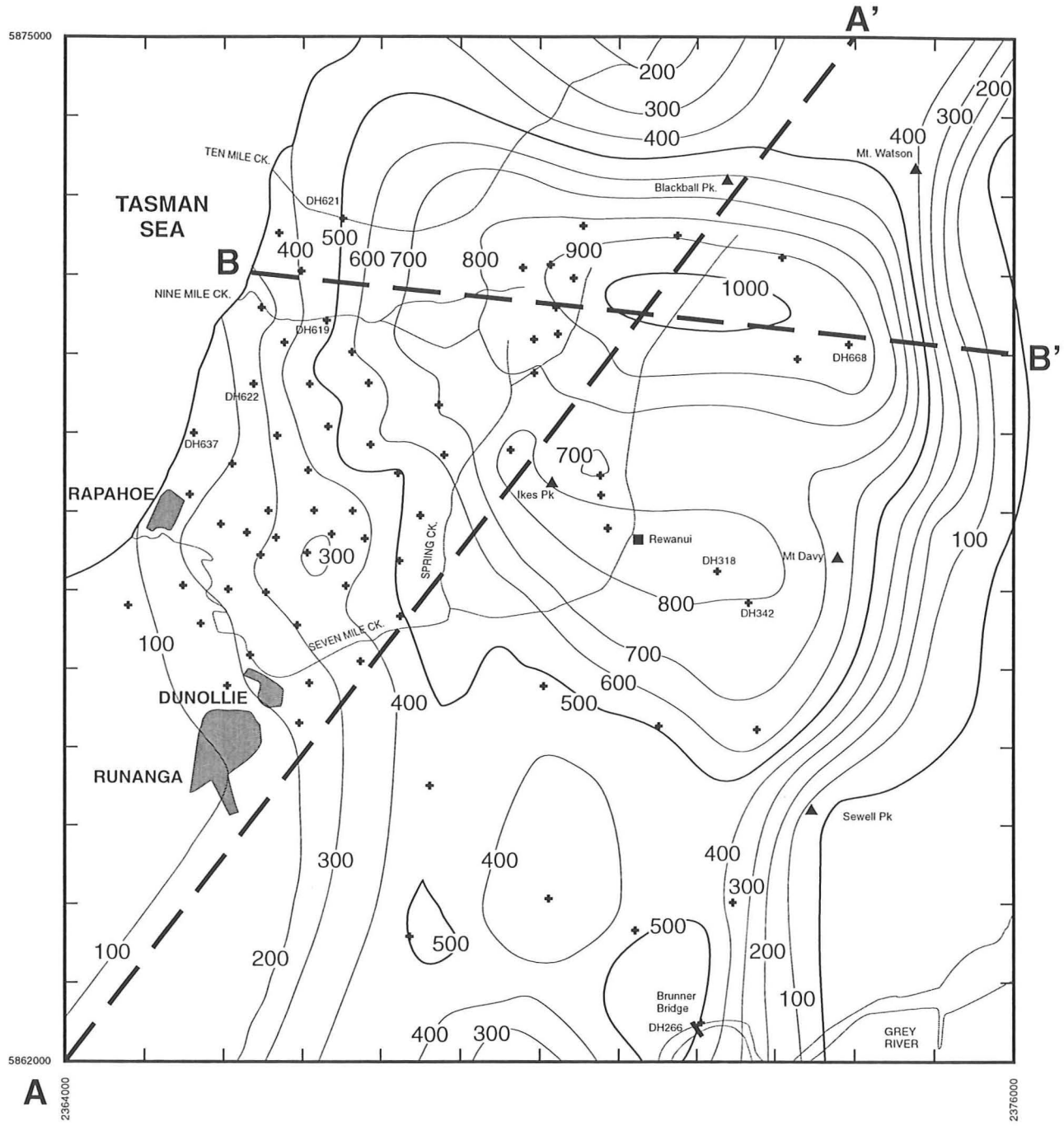

Figure 4.17 Total thickness of Paparoa Group strata (excluding Dunollie Fm.) prior to burial. Isopach interval = 100m, 500m and 1000m highlighted. Numbered drillholes are discussed in text.

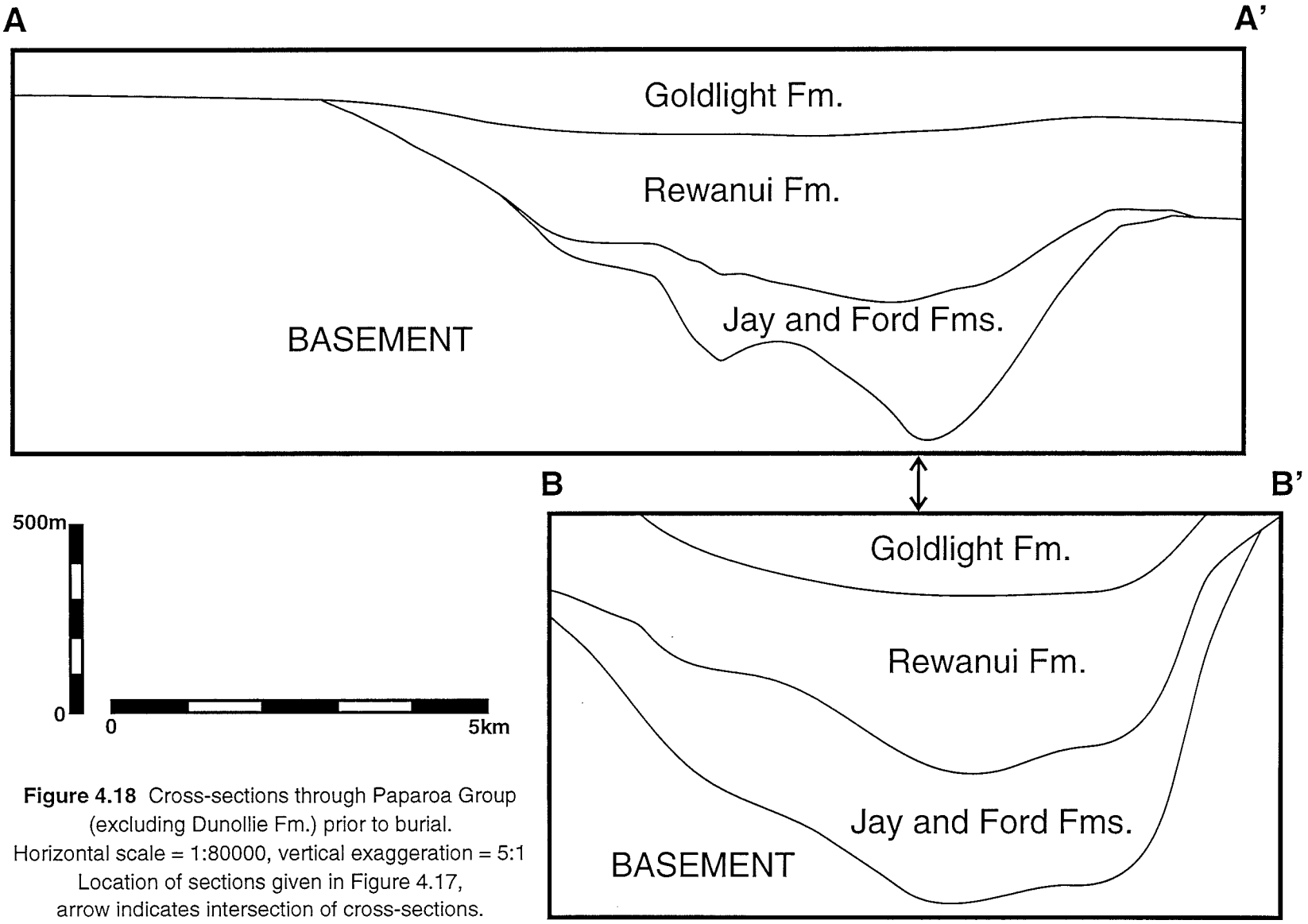

Figure 4.18 Cross-sections through Paparoa Group (excluding Dunollie Fm.) prior to burial.
Horizontal scale = 1:80000, vertical exaggeration = 5:1
Location of sections given in Figure 4.17,
arrow indicates intersection of cross-sections.

Compactional effects of cover deposition were greater than compaction during Paparoa Group accumulation within Rewanui CMM, Waiomo MM, Jay Fm. and most drillholes containing Ford Fm. Morgan CMM was compacted more by overlying Paparoa Group strata than by cover in six drillholes. These results conform to the compactional models described in Appendix 4.3.5, which depict compaction of clastic sediments generally occurring beneath >1km of strata. The more rapid rate of coal (peat) compaction during burial has had a lesser effect on present-day isopach patterns than the effects of burial beneath a thick sequence of cover strata.

4.4 Summary and discussion

Backstripping studies reported in the literature (e.g. Steckler & Watts 1978; Bond & Kominz 1984) typically involve analysis of a small number of drillholes, and report the tectonic history of single localities within a basin (typically continental margin basins). Other studies analyse drillholes from throughout a basin, in order to determine regional tectonic parameters such as β (stretching factor) (e.g. Gumati & Nairn 1991). Yet another approach is to undertake detailed analysis of the differential compaction experienced by varied lithologies within a sedimentary system, and to relate paleogeographic controls to such compaction (e.g. Brown 1975).

This exercise falls within the latter two approaches, but lack of chronostratigraphic control precluded construction of geohistory plots which are the typical outcome of the first type of decompaction study. Key applications of decompaction of Paparoa Group strata are the identification and quantification of tectonic subsidence which contributed to basin formation, and the assessment of the relative roles of tectonic subsidence and differential compaction during burial in the creation of observed unit thickness patterns.

Determination of decompacted unit thicknesses documents the position of various depocentres which developed during Paparoa Group deposition (Figure 4.19). Depocentres overlap in two areas: Jay Fm., Ford Fm. and Rewanui Fm. depocentres are present in the northwest, and depocentres of all units overlap in the northern Mt. Davy Sector. The only significant depocentres outside these two areas are the Morgan CMM outlier near Brunner Bridge, and the Goldlight Fm. depocentre which extends southwards from the Ikes Pk./Sewell Pk. area. The N/S oriented thin finger of Goldlight

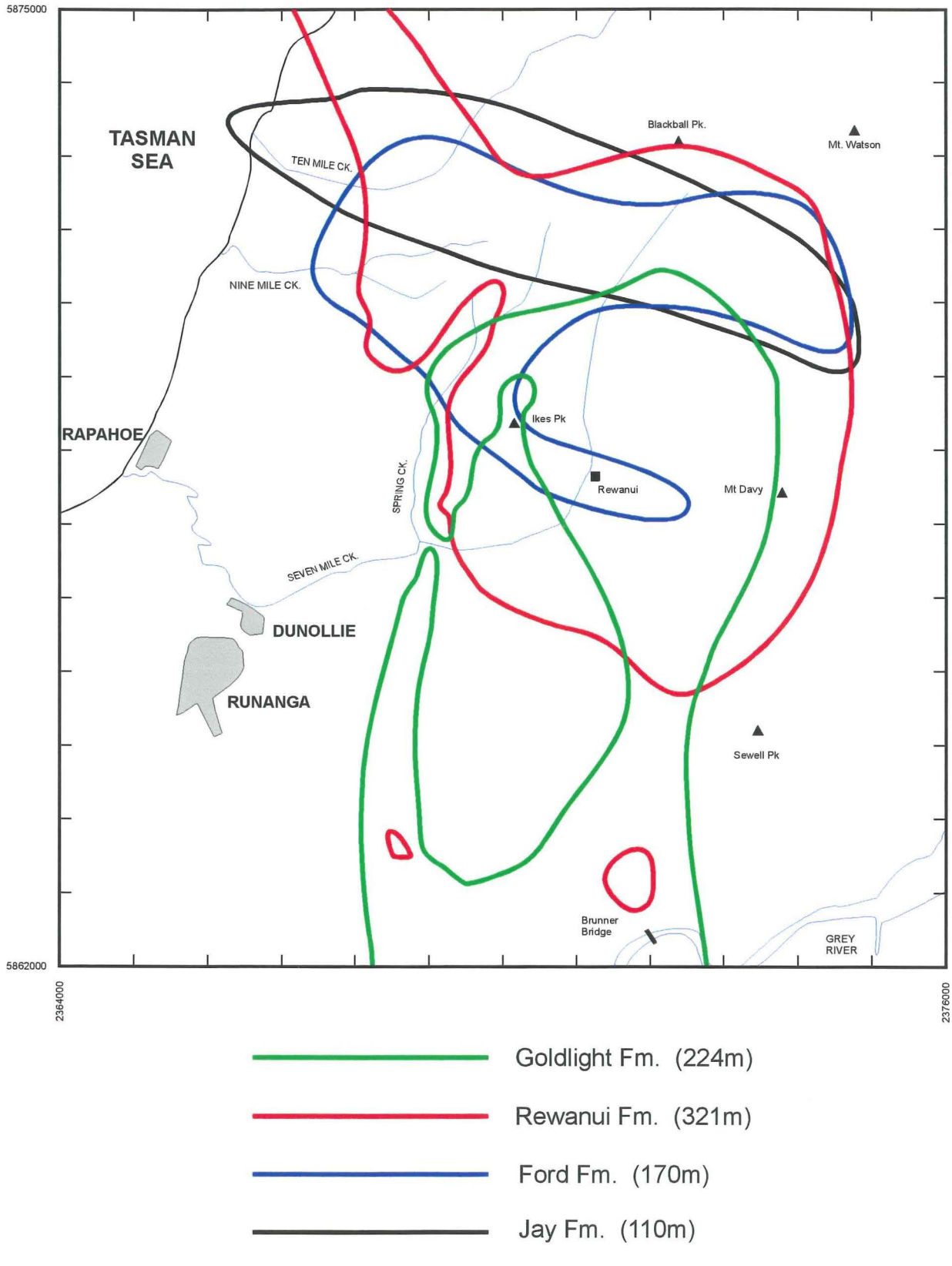

Figure 4.19 Depocentres of the Paparoa Group Formations, Greymouth Coalfield. Depocentres are delineated by the upper quartile (thickest 25%) decompacted thickness for each unit. Key and quartile values are shown above.

Fm. which aligns with Spring Ck. is coincident with the thin southern extension of the Ford Fm. basin (Figure 4.3) and the corresponding portion of the Brunner Bridge Morgan CMM depocentre (Figure 4.6).

In the above analysis, subsidence was partitioned between a tectonic component and compaction within the sediment pile. However, factors such as paleotopography (Jay Fm. and Ford Fm.), erosion (Rewanui Fm.) and paleogeography (Goldlight Fm.). influenced unit thickness, particularly in lacustrine units where sediment thickness is less than total tectonic subsidence. Where there are gradational contacts between units (e.g. Morgan CMM with Rewanui CMM, Goldlight Fm. with Dunollie Fm.), isopach patterns, and consequently modelled tectonic subsidence, will reflect those lateral changes but will not represent true tectonic features. Thus, the decompacted isopach models and tectonic subsidence models presented in this chapter offer a general guide for tectonic interpretation (Chapter 8), but specific details may not be resolved.

Differences between decompacted unit thicknesses, modelled tectonic subsidence and present-day thicknesses are summarised in Table 4.2. Estimates of the magnitude of tectonic subsidence are closer to decompacted thickness than present-day thickness, which indicates that decompaction should be performed if tectonic subsidence histories are to be derived from stratigraphic databases. Successive formations overlap greater areas of basement, indicating continued basin growth during Paparoa Group deposition.

unit	area km^2	decompacted thickness		tectonic subsidence		present day thickness	
		average	maximum	average	maximum	average	maximum
Goldlight Fm.	117.9	170.8	288.8	147.9	255.3	113.5	177.5
Rewanui CMM	125.0	219.8	363.4	209.5	344.9	161.5	274.4
Waiomo MM	46.3	32.7	89.3			21.1	51.1
Morgan CMM	57.6	77.1	216.5			46.0	122.4
Ford Fm.	68.8	107.1	286.5			66.4	193.7
Jay Fm.	58.1	73.8	173.9			64.2	146.3

Table 4.2 Summary of unit area and decompacted and present-day unit thicknesses and tectonic subsidence (where available). All values in metres.

Chapter 5. Cretaceous–Tertiary Boundary palynostratigraphy, Rapahoe Sector

5.1 Palynostratigraphy of the Rapahoe Sector: present objectives

The use of lithostratigraphic member or formation boundaries within the Paparoa Group as generally basin-wide correlation datum surfaces, which can be recognised both in outcrop and in drillholes, is well established, and discussed in detail elsewhere (Chapters 2, 3). However, absence of the lithostratigraphically important Goldlight Fm. mudstone marker horizon in the northwest of the study area (Section 3.8.1), and consequent difficulty in identifying the upper contact of Rewanui CMM, has resulted in stratigraphic uncertainty.

Potential (or likely) diachroneity of the contacts between formations and/or members must also be considered. Newman (1987, Figs. 29–32) proposed alternative correlation models for coal seams in the southern Rapahoe Sector, which depend on the degree of diachroneity of the Goldlight / Rewanui contact. However, at that time there was no means of assessing which of the various correlation models was valid, and wide drillhole spacings (often c.1km) precluded establishment of reliable seam correlation criteria for the southern Rapahoe Sector.

Correlation of coal seams within the Strongman Mine area was achieved by using the Goldlight / Rewanui contact as a datum, as documented by Thorburn (1981a). However, transferral of some strata from Rewanui CMM to lower Goldlight Transitional Member in that area (Section 3.8.2) involved repositioning of the Goldlight / Rewanui contact, and existing seam correlation models may now be invalid. The relationship between the coal seams in the Strongman area and those of the southern Rapahoe Sector is poorly understood, because of coal-poor zones within intervening drillholes (e.g. DH635).

Limited palynostratigraphy demonstrated that the Cretaceous–Tertiary Boundary (KTB) was preserved within Greymouth Coalfield, near the top of the Rewanui CMM (Raine 1981, 1984, 1990b, 1994a). The KTB represents a synchronous surface which potentially could provide a correlatable datum across the coalfield. Location of the KTB with palynology offers a means of testing the various stratigraphic and seam correlation models, and provides an alternative to lithostratigraphic correlation.

The objective of this study was to locate the KTB at a reconnaissance level throughout the Rapahoe Sector. Drillholes were chosen for analysis to incorporate existing sampling (4 drillholes), to encircle the former Strongman Mine workings, and to provide a network of sample sites throughout the southern Rapahoe Sector (Figure 5.1A). Further details of sampling procedures and processing are presented in Appendix 5.1 and Appendix 13.

5.2 Summary of palynological zonation criteria

Palynological criteria for assigning ages to Greymouth Coalfield palynofloras are discussed in detail in Appendix 5.4. The KTB corresponds to the boundary between pollen Zones PM2 (Haumurian/Late Cretaceous) and PM3 (Teurian/Paleocene) of Raine (1984) (Figure 5.1B). Palynostratigraphic zones are defined by the occurrence or abundance of certain taxa, and in particular angiosperm pollen taxa. All samples with adequate palynofloras were grouped by occurrences of key taxa, and assigned to Pollen Zones PM2 or PM3 (Appendix 5.4.3). Groupings and corresponding ages are summarised in Table 5.1. Five angiosperm pollen taxa were found to be significant for age diagnosis, whereas the occurrences of many diagnostic angiosperm and spore taxa used by previous workers (Appendix 5.4.2) were inconclusive, and could not be used to support age assignments.

Group	Zone	*Tricolpites lilliei*	*Nothofagidites kaitangataensis*	*Beauprea -idites*	*Triorites minor*	*Tricolpites secarius*	others
1	PM2	yes	rare	rare	rare	no	
2	PM3	no			mod–high %	yes	*Malvacipollis* sp., *Triorites minisculus*, *Myrtaceidites*
3	PM2	no	yes	rare	very rare	no	*Trilites morleyi*, *Trilites ohaiensis*, *Malvacipollis* sp.,
4	PM3		rare		high %	no	*Trilites morleyi*, *Trilites ohaiensis*
5	PM3	no	no	no	low %	yes	*Malvacipollis* sp., *Triorites minisculus*
6	PM2	yes	rare	rare	rare	rare	*Gambierina rudata*
7	PM2 ?	–	–	–	rare	–	–

Table 5.1 Summary of palynological groups and assigned pollen zones.

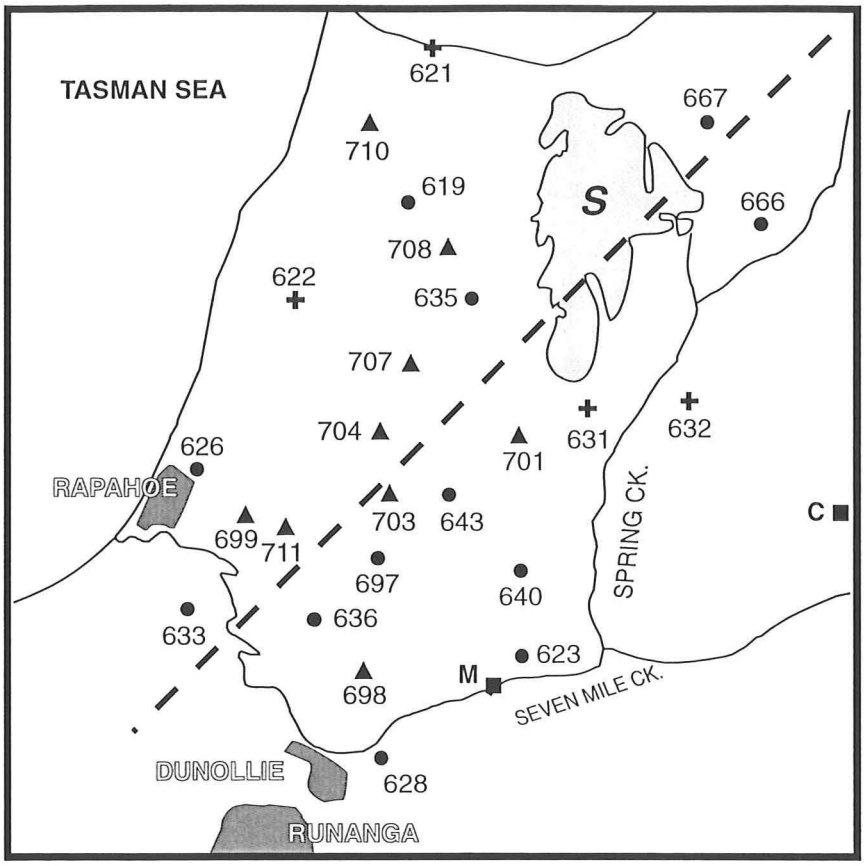

● Drillholes investigated in this study
✚ Drillholes investigated by previous workers
▲ Drillholes sampled by D.I. MacKinnon, limited results
■ Outcrop sections, M = Moody Ck., C = Compressor Ck.

Figure 5.1A Location of drillholes and outcrops in the Rapahoe Sector investigated for the KTB. Dashed line indicates location of cross-section shown in Figure 5.4. S = Strongman State Mine

	NZ stage	Ma	NZ palynology	
			assemblage	zone
PALEOCENE	TEURIAN (Dt)	60	*Phyllocladidites mawsonii (PM)*	PM3
		65		
CRETACEOUS	HAUMURIAN (Mh)	70		PM2
		75		

Figure 5.1B Simplified New Zealand biostratigraphic nomenclature and palynological zonation. After Raine (1984). For further details, see Figure A5.1.

All studied samples which yielded sufficient palynofloras could be dated by application of the criteria given in Table 5.1, though five study samples lacked indicator species and could not be assigned to a pollen zone (Appendix 5.4.3). Occurrences of diagnostic taxa in the study samples are reviewed in Table A5.2. Ecological and environmental factors affecting the presence of key taxa listed in Table 5.1 are discussed in Appendix 5.5, and all palynofloras are described in detail in Appendix 6.

5.3 Location of the Cretaceous–Tertiary Boundary in the study drillholes

Key objectives of this study were (a) to locate the KTB in the study drillholes, and (b) to determine the relationship between the palynostratigraphic and lithostratigraphic datum surfaces. The position of the KTB was determined by applying the palynostratigraphic criteria reviewed above (Table 5.1). Lithostratigraphic definition of the upper contact of the Rewanui CMM is discussed in Chapter 2 and Appendix 2, and contact positions are listed in Appendix 10.2. Drillhole locations are indicated in Figure 5.1A, and lithostratigraphy, geophysical logs, sample locations and age assignments are presented for each drillhole in Figure 5.2 (in the map pocket).

DH619: The upper 4 samples from DH619 are Zone PM3, however assignment of 619/5 and 619/6 to Zone PM2 is tentative due to insufficient occurrence of key taxa (Group 7). The PM2/3 boundary is located below 254.75m, and possibly above c.260m. The upper Rewanui CMM contact is located at 241.8m, which is between 12.8 and c.17.9m above the KTB when the dip of 10° is corrected for.

DH623: All but one of the samples from DH623 have been confidently assigned to Zone PM2. The age of the remaining sample, 623/3 (Group 7), is confirmed by its stratigraphic position. The Goldlight / Rewanui contact is at 45.6m, thus the KTB is no more than 1.4m (true thickness) below the lithological contact. Minor structural disruption over the interval 46.4–54.0m is unlikely to have affected biostratigraphy.

DH626: The PM2/3 boundary in DH626 can be confidently placed between 301.8m and 310.61m. The Goldlight / Rewanui contact is at 302.4m, thus the KTB is located in an interval from 0.6m above to 7.9m below the lithological contact.

DH628: Eight samples were analysed from DH628, six of which yielded useful palynofloras to which ages were assigned (Groups 1–3). Palynostratigraphy confirms the presence of fault-repetition of strata in this drillhole (Appendix 2). Structural complexity and prevalence of sheared and faulted contacts between the various packets of strata in DH628 prevents determination of the true relationship between the KTB and the Goldlight / Rewanui contact. However, available sampling confirms that Goldlight Fm. and Rewanui CMM are of different ages in DH628.

DH633: All samples from DH633 are assigned to PM2 using the criteria discussed above (Groups 1, 3 and 6). The KTB lies above 380.16m, close to the Goldlight / Rewanui contact which is located at 378.0m. Fracturing and shearing in the vicinity of the lithostratigraphic contact may indicate faulting, though there is no evidence from surrounding drillholes that strata are absent from Rewanui CMM in DH633 (Appendix 2).

DH635: The PM2/3 boundary in DH635 lies between 394.3m (635/2) and 400.0m (635/5). No useful taxa were observed in 635/4 (399.7m) and determination of 635/5 (a coal) is tentative, but is supported by sparse data from the sample below (635/6) which is consistent with PM2. The Goldlight / Rewanui contact is located at 379.2m, and the KTB lies within 14.6m and 20.1m below this when correction is made for the average 15° dip. No significant structural disruption is present.

DH636: Two samples were analysed from DH636, the upper (636/1, 302.0m) yielding a PM3 flora and the lower (636/2, 306.4m) PM2. The KTB is therefore constrained to lie between the Goldlight / Rewanui contact, located at 302.0m, and 4.4m below the contact. However, a fault lies between the two sample positions (Appendix 2), and Cretaceous and Tertiary strata are in structural, rather than stratigraphic, contact.

DH640: The two samples from DH640 are coals which yielded assemblages which are interpreted as PM3 (Group 5). The KTB is located at least 2.0m below the Goldlight / Rewanui contact at 187.0m.

DH643: Initial sampling of DH643 comprised two sediment samples (643/1, 643/2) which yielded PM3 floras (Group 2), and two coal samples (643/3, 643/4), which yielded PM2 floras with age-diagnostic taxa consistent with Group 3. In order to test the

hypothesis that the apparent age differences between the two pairs of samples reflected facies control on flora, two additional samples (643/5, 643/6) were prepared from sediments at or near the floor of the seam. These samples are assigned to Zone PM2 (Groups 1, 6). The KTB in DH643 is therefore located approximately at the roof of the coal seam, between 1.5 and 1.7m below the Goldlight / Rewanui contact at 281.2m.

DH666: The upper two samples from DH666 (666/1, 666/2) contain Teurian floras (Group 2). As discussed above, 666/3, at 165.37m contains a mixed assemblage which is assigned to Zone PM3 (Group 2). No useful material was recovered from 666/4 (166.0m), and 666/5 (167.6m) is assigned to Zone PM2. The Goldlight / Rewanui contact is located at 146.5m, thus the KTB is located between 16.3m and 18.2m below the lithological contact when the dip of 30° is corrected for.

DH667: Poor yields were obtained from two of the samples from DH667, while the remaining two samples were very poor with almost no pollen recovered. 667/1 (102.2m) and 667/3 (120.5m) both yielded assemblages consistent with PM3. These indicate the KTB is located at least 16.0m below the Goldlight / Rewanui contact at 104.5m, when correction is made for the shallow (10°) dip.

DH697: DH697 was sampled in 1988 by D.I. MacKinnon (UoC) and investigated by M.D. Warnes (unpublished Canterbury Coal Research Group data, 1992), who suggested sample 697/8, from within Goldlight Fm. at 283.3m, should be assigned to Zone PM2. A reassessment (Table A5.2) revealed an assemblage consistent with Group 2, indicating the sample should be assigned to Zone PM3. A further sample from 292.25m (697/9) yielded a poor assemblage containing 2.5% *T. minor* and no age-diagnostic taxa, which was tentatively assigned to Zone PM2 (Group 7). The KTB is therefore located between 3.3m above and 5.5m below the Goldlight / Rewanui contact, which is at 286.6m. Dip is low (12°) and there are no structural complications. Three samples (697/5–7) from Goldlight Fm. yielded PM3 floras (Groups 2 and 4).

5.4 Location of the Cretaceous–Tertiary Boundary in other drillholes and sections at Greymouth Coalfield

The KTB has been investigated by previous workers at six localities in Greymouth Coalfield, namely DH621 & 622 and DH631 & 632, and outcrop sections at Moody Ck. and Compressor Ck. (Raine 1994a). Data sources and zonation details for DH621 & 622 and DH631 & 632 are discussed in Appendix 5.4.2 and summarised in Table A5.1. Further sampling of DH631 & 632 was undertaken by J.I. Raine in March 1994 (Raine pers. comm. 1994), however results are not yet available. Preliminary results are also available for a number of southern Rapahoe Sector drillholes (Figure 5.1).

DH621: Raine (1981) located the KTB in DH621 between 81.35m and 94.35m. The KTB therefore lies within an interval of approx. 18–30m below the upper Rewanui CMM contact, which is located at 64.3m. The interval between the KTB and the lithostratigraphic contact is reduced to 16.4–27.2m when correction is made for the average dip of 25°.

DH622: Widely spaced samples indicate the KTB is located between 257.46m and 286.5m in DH622 (Raine 1981). The Goldlight / Rewanui contact is at 268.5m, though the presence of shearing suggests intact upper Rewanui CMM stratigraphy may not be preserved (Appendix 2).

DH631: A preliminary pollen diagram for DH631 (Raine 1990b) indicated the KTB is located between 155.4m and 164.4m, with the upper sample containing *T. secarius*, and the lower sample containing *T. lilliei* and lacking Cenozoic index taxa. In contrast, Warnes (pers. comm. 1992) reported abundant *T. minor* with *Myrtaceidites* sp. and *T. secarius* from 164.4m (UCP1220), and assigned this sample to Zone PM3, thereby placing the KTB between 164.4 and. 175.45m. Both workers reported similar abundances of gymnosperm and pteridophyte taxa at 164.4m, and the representation of small angiosperm taxa in this sample is crucial to age determination. In the present study, Warnes' location for the KTB in DH631 is retained, as his processing methods were identical to those of the present study (Appendix 5.1.2).

Strata throughout the lower Goldlight Fm. and upper Rewanui CMM in DH631 are disrupted by faulting (Appendix 2), and other, more competent, KTB sections are now receiving greater attention (Raine 1994a).

DH632: A PM3 flora was recovered from 258.2m (UCP1250), and samples from 270.3m (L13590, UCP1224) yielded PM2 assemblages (Table A5.1). Intervening samples from 261.0m and 262.3m yielded assemblages dominated by conifer pollen and pteridophyte spores with few age-diagnostic taxa. Warnes observed 1 specimen of *Myrtaceidites* and other Teurian taxa from UCP1251 (at 261.0m), and assigned this sample to Zone PM3 (Table A5.1). Presence of *Densoisporites microrugulatus* in a spore-dominated assemblage was sufficient for both Raine and Warnes to assign samples at 262.3m to Zone PM2. However, tentative Cenozoic taxa are also present at 262.3m (Table A5.1), and the assigned age is not reliable. The lowermost samples (270.3m) were confidently assigned to Zone PM2. Therefore, the KTB is reinterpreted to fall between 261.0m and 270.3m. The Goldlight / Rewanui contact is at 250.9m, dip is low (10°) and the palynostratigraphic boundary lies between 10.1m and 19.4m below the lithostratigraphic contact.

Southern Rapahoe Sector drillholes: In addition to DH697 (Section 5.3), nine drillholes from the southern Rapahoe Sector were sampled in November 1988 by D.I. MacKinnon for determination of the KTB position (Figure 5.1, Table 5.2). At that time, the exact position of the KTB was poorly defined (Raine 1984), and only Goldlight Fm. was sampled. The lowermost samples from each drillhole, which range from 0.0–6.0m above Rewanui CMM, were rescanned for key taxa and yielded Zone PM3 palynofloras.

DH	UCP	Depth	Lithology	*T. secarius*	*T. minor*	Group	Zone
698	1674	270.2	siltstone	*	H	2	PM3
699	1675	319.4	silty mudstone	*	H	2	PM3
701	1676	166.4	silty mudstone	*	H	2	PM3
703	1677	262.1	silty mudstone		H	4	PM3
704	1678	296.0	silty mudstone	*	H	2	PM3
707	1679	324.7	fine sandstone	*	H	2	PM3
708	1680	199.4	fine sandstone		H	4	PM3
710	1681	253.4	sandy siltstone		H	4	PM3
711	1682	207.9	silty mudstone		M	4	PM3

Table 5.2 Palynological data, southern Rapahoe Sector drillholes, Goldlight Fm. samples. 15 tracks on all samples were scanned. **H** = highly abundant, **M** = moderate abundance. Palynological groups are explained in Table 5.1.

Outcrop sections: J.I. Raine (IGNS) is presently undertaking a detailed analysis of palynofloral change across the KTB at Moody Ck. and Compressor Ck. (Figure 5.1). Preliminary results (Raine 1994a) indicate the KTB is located approx 1m below the top of the Rewanui CMM at Moody Ck., within a clastic parting in the uppermost Rewanui CMM coal seam. Results are not yet available for the Compressor Ck. site. A number of samples (UCP1292–1299) were collected from outcrop in the northwest of the coalfield, however all were in weathered lithologies and no useful palynomorph assemblages have been produced (Appendix 13).

5.5 Analysis of the Cretaceous–Tertiary Boundary position, Rapahoe Sector

The KTB in the Rapahoe Sector of Greymouth Coalfield has been located in 10 drillholes. In six other drillholes, the upper or lower limits of the KTB position can be constrained, though structural complications are present in four of those drillholes. A summary of lithostratigraphic and palynostratigraphic data for each drillhole is presented in Table 5.3.

DH	G-R	lowest PM3	highest PM2	min	max	dip °	min (corr)	max (corr)
619	241.8	254.8	260.0	13.0	18.2	10	12.8	17.9
621	64.3	82.4	94.4	18.1	30.1	25	16.4	27.2
622	268.5	257.5	286.5	-11.0	18.0	15F	-10.7	17.4
623	45.6	n/a	47.1	–	1.5	18	–	1.4
626	302.4	301.8	310.6	-0.6	8.2	15	-0.6	7.9
628	274.4?	274.2	275.0	-0.2	0.6	10F	-0.2	0.6
631	148.5	164.4	175.5	15.9	27.0	var. F	11.6	21.6
632	250.9	261.0	270.3	10.1	19.4	10	10.0	19.1
633	378.0	n/a	380.2	–	2.2	10	–	2.1
635	379.2	394.3	400.0	15.1	20.8	15	14.6	20.1
636	302.0	302.0	306.4	0.0	–	15 F	0.0	–
640	187.0	189.0	n/a	2.0	–	5–10	2.0	–
643	281.2	282.7	282.9	1.5	1.7	5	1.5	1.7
666	146.5	165.4	167.6	18.8	21.1	30	16.3	18.2
667	104.5	120.5	n/a	16.0	–	10	16.0	–
697	286.6	283.3	292.3	-3.4	5.6	12	-3.3	5.5

Table 5.3 Summary of lithostratigraphic and palynostratigraphic data.
G-R = depth of Goldlight / Rewanui contact (see Appendix 10.2).
"F" in the "dip" column indicates the section is faulted, "var." = variable dip.
The "min (corr.)" and "max (corr.)" indicate upper and lower range of KTB location when corrected for dip. Negative values indicate above the upper Rewanui CMM contact, positive values are below.

5.5.1 Precision and accuracy of the Cretaceous–Tertiary Boundary location

The precision with which the KTB can be located varies from ± 0.1m (DH643) to ± 14.5m (DH622), and is a function of sampling interval. The average sample spacing across the KTB is 7.35m, and such sampling reflects the reconnaissance nature of this study. Results from DH643 indicate the KTB can be precisely located where closely spaced samples are available, and suggest that further sampling would be worthwhile.

Postdepositional structural disruption of strata in four drillholes (DH622, 628, 631 & 636) influences the reliability of KTB location, and the juxtaposition of Haumurian and Teurian strata in these drillholes may be a structural, rather than a stratigraphic, phenomenon. Stratigraphic modelling techniques (Appendix 3.2, 3.4) enable removal or repetition of strata by significant structural disruption to be recognised. However, small scale (<c.5m) structural thickening or thinning, which would be significant for location of the KTB, but insignificant for assessing total unit thickness, would be difficult to identify.

The position of the KTB in most study drillholes (where present) is constrained by samples from Groups 1–3 (Table 5.1), to which pollen zones are reliably assigned. In contrast, the uppermost PM2 sample in DH619 (619/5) is identified by the least reliable zonation category (Group 7), which is characterised by the absence of age-diagnostic taxa (Appendix 5.4.3). However, another Group 7 sample (DH623/3) occurs in stratigraphic sequence between confident Zone PM2 samples (Group 1), indicating that assignment of a PM2 age to Group 7 samples is justified (Appendix 5.4.3).

In the present project, the KTB has been identified by changes in palynofloras (Appendix 6.4) which occur in samples of various lithologies and are believed to represent synchronous floral change which correlates with the KTB. As discussed elsewhere (Appendix 5.5.5), occurrences of some key stratigraphic index taxa (e.g. *T. secarius*) at Greymouth Coalfield are inconsistent with reported regional occurrences (Raine 1984, see also Appendix 5.4.1). In addition, there is no independent evidence for the position of the KTB at Greymouth Coalfield, such as siderophile element anomalies or correlative change in marine microfossil floras and faunas (Appendix 5.3).

Thus, there is no conclusive evidence that the floral change recorded in Greymouth Coalfield correlates with the KTB. However, a review of other Southern Hemisphere palynofloras which span the KTB (Appendix 7) indicated the floral events which defined the KTB at Greymouth Coalfield (notably extinction of ornamented proteaceous taxa and increase in *T. minor* abundance) also occurred elsewhere, giving confidence that the KTB at Greymouth Coalfield has been correctly identified.

5.5.2 Location of the Cretaceous–Tertiary Boundary in the Rapahoe Sector

Present results (summarised in Table 5.3) indicate the KTB occurs within an interval ranging from 10.7m above to 27.2m below the Goldlight (or Dunollie) / Rewanui contact. However, all dated samples from Goldlight Fm. or Dunollie Fm. are PM3 (Table 5.2), suggesting that the KTB always lies within Rewanui CMM.

The upper and lower limits for the location of the KTB in each drillhole (excluding DH628, 631 and 636 which are faulted) are plotted relative to the upper Rewanui CMM contact in Figure 5.3. If the midpoint between the highest PM2 and lowest PM3 samples is assumed to approximate the true position of the KTB (the "average" positions in Figure 5.3), two clusters of KTB locations are evident, one at 1.8m and another at 17m below the upper Rewanui CMM contact. The constrained positions of the KTB (maximum or minimum) in DH623, 633, 640 and 667, also plot within the clusters of average KTB positions. These data indicate that the position of the KTB in the Rapahoe Sector is not continuously variable with respect to the lithostratigraphic datum of the upper Rewanui CMM contact, as would be expected if the contact was significantly diachronous.

5.5.3 Spatial variation of the Cretaceous–Tertiary Boundary position

Inclusion of the geographic locations of the KTB data reveals the true relationship between the KTB and the upper Rewanui CMM lithological datum. This relationship is demonstrated by projecting palynostratigraphic data onto a SW/NE cross-section which bisects the Rapahoe Sector at 45° (Figure 5.4, location of cross-section indicated in Figure 5.1). In the south and west of the Rapahoe Sector, the interval between the KTB and the upper Rewanui CMM contact is small (<4m), whereas in the north and east, the corresponding interval is c.17m. The Rapahoe Sector may therefore be divided into two distinct palynostratigraphic domains, and the interface between the domains lies approximately NW/SE between DH641 and DH643 (Figure 5.5).

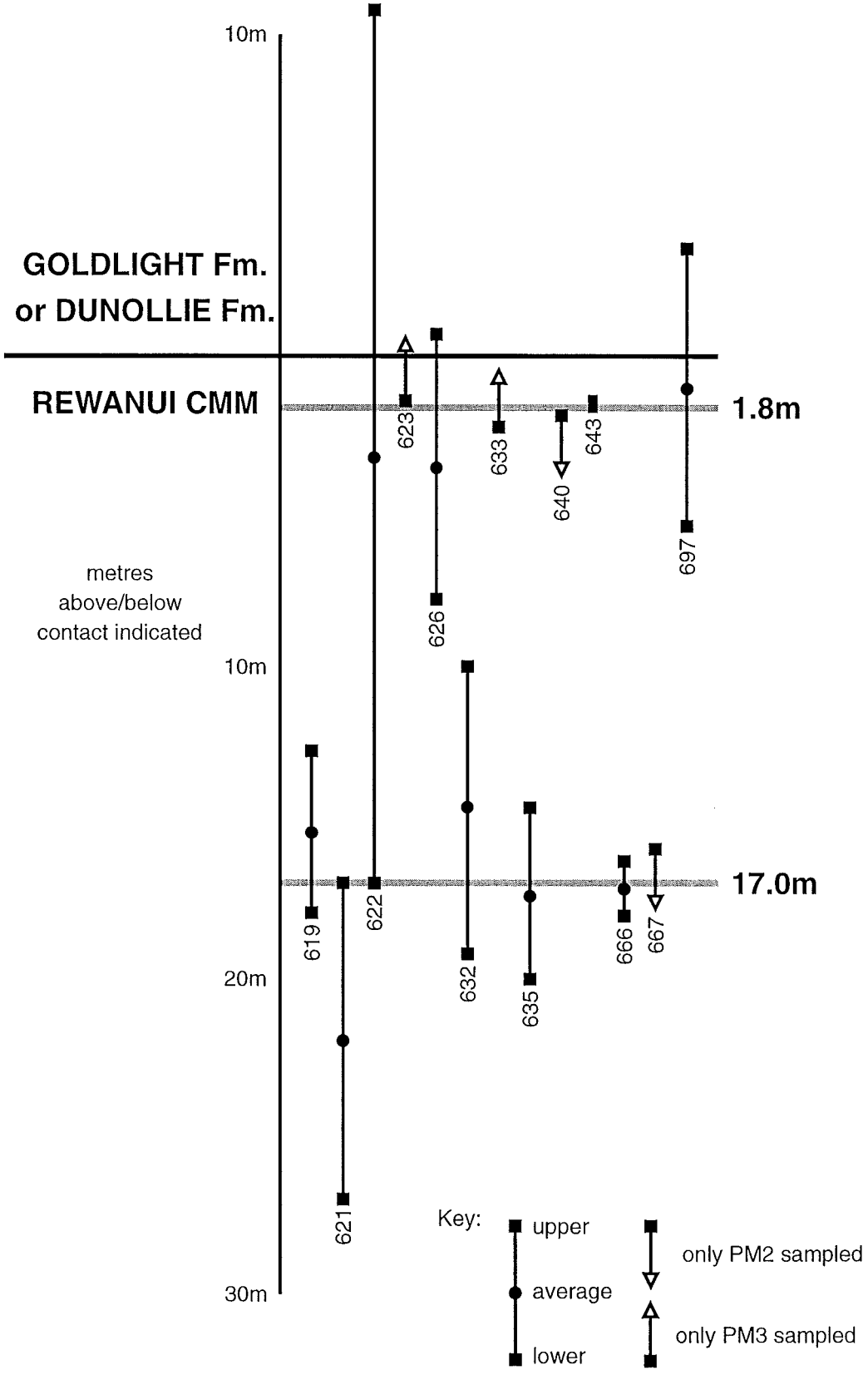

Figure 5.3 Upper and lower limits of KTB position in sampled drillholes, plotted relative to upper Rewanui contact. No horizontal scale implied.

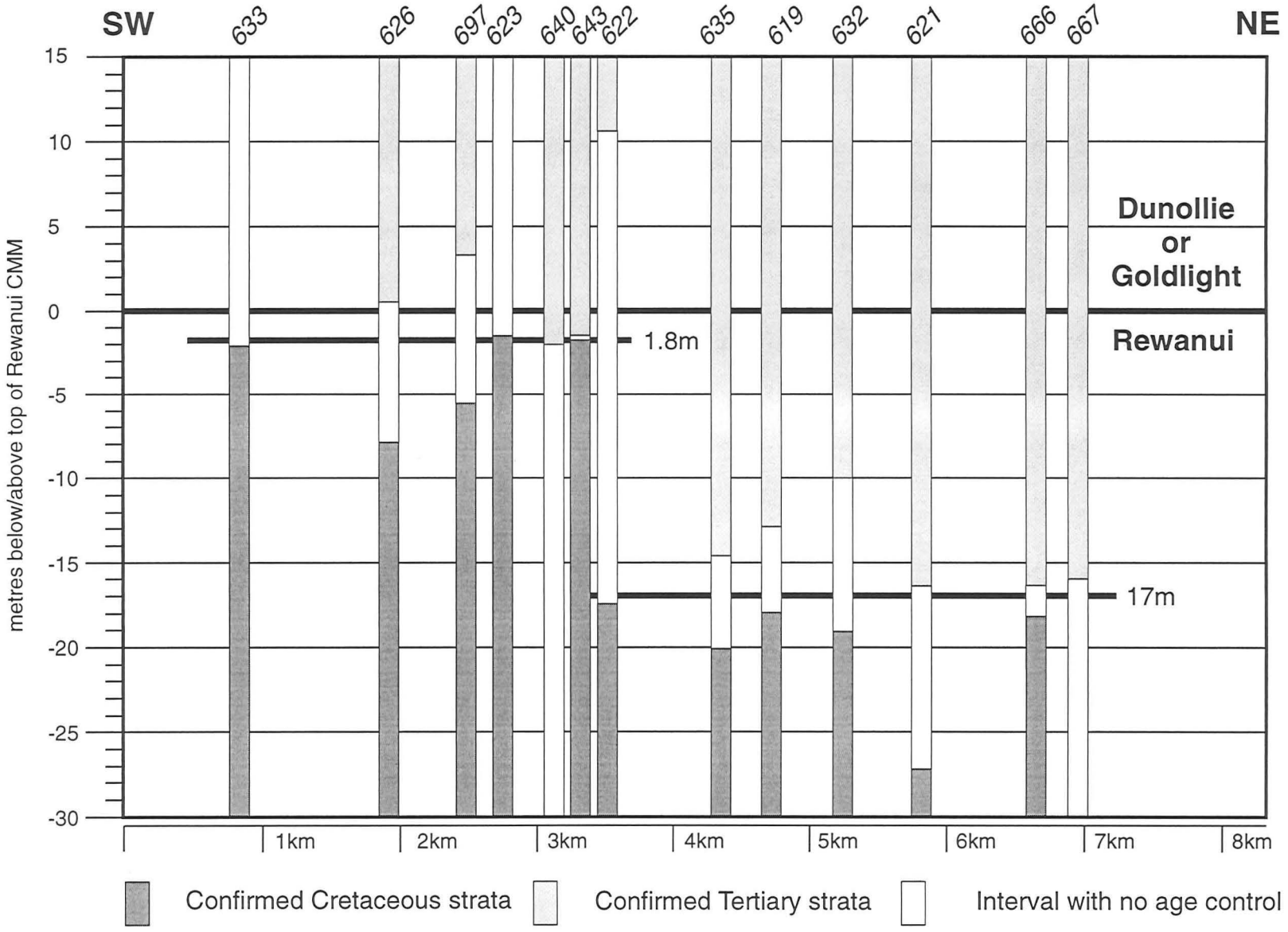

Figure 5.4 Drillholes containing KTB projected on to SW-NE cross-section of Rapahoe Sector. Datum is Rewanui/Goldlight (or Dunollie) contact. Drillhole and section locations given in Figure 5.1. Faulted drillholes are not shown.

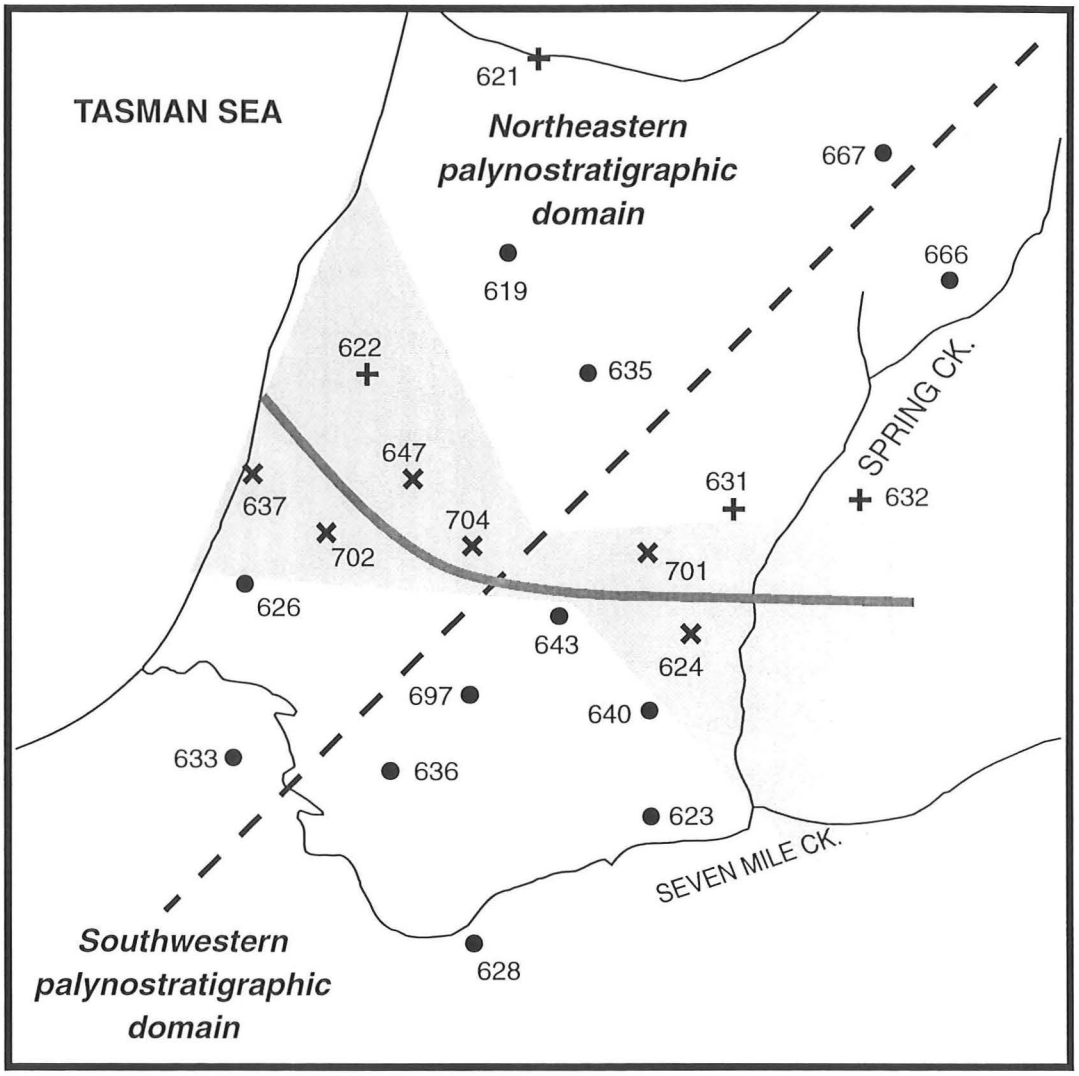

Figure 5.5 Location of palynostratigraphic domain interface, Rapahoe Sector.
Dashed line indicates location of cross-section shown in Figure 5.4.

Poor precision of the KTB location in DH622 allows this drillhole to be placed in either palynostratigraphic domain, however lithostratigraphy of DH622 is more similar to DH619 & DH635 than DH626 or DH643, suggesting that DH622 lies to the north of the interface. Use of lithostratigraphic patterns to estimate the position of the palyno-stratigraphic domain interface can be extended to all those drillholes which fall within the stippled area of Figure 5.5 (Ward 1996, Table 2). The resulting position of the interface (Figure 5.5, heavy grey line) defines an arc which is oriented NW/SE to the west of DH704, and E/W to the east of DH704. Presently there are no data for the position of the KTB east of Spring Ck., and continuation of the palynostratigraphic domains into the Mt. Davy Sector is unknown.

5.5.4 Diachroneity of the upper Rewanui Coal Measure Member contact

In the southwestern palynostratigraphic domain, the position of the KTB is tightly constrained to lie between 1.5m and 2.2m (average = 1.8m) below the Goldlight / Rewanui contact. The lithological datum therefore closely approximates an isochronous surface, and the transition from Rewanui CMM to Goldlight Fm. occurred at approximately the same time throughout the domain (as suggested by Bowman et al. 1984, p. 58). Minor variation of KTB position with respect to the Goldlight / Rewanui contact can be attributed to sample spacing, topography within the depositional environment, or differential compaction of lithologies during burial (Appendix 4.3).

In the northeastern palynostratigraphic domain, the KTB is located at 17±1m below the upper Rewanui CMM contact in all sections, and that contact can also be regarded as an approximately isochronous surface. The three lithosomes recognised in the present study (coal measure, transitional and mudstone; see Section 2.3) all lie above the upper Rewanui CMM contact in the northeastern palynostratigraphic domain (see e.g. Figure 3.10). Zone PM3 floras have been recovered from all three lithosomes (Appendix 5.5.3), confirming the described pattern of lateral continuity of those lithosomes from western fluvial Dunollie Fm. to eastern lacustrine Goldlight Fm.

5.6 Summary

The Cretaceous–Tertiary Boundary has been identified or constrained in 16 drillholes in the western Greymouth Coalfield. Key palynological events defining the KTB are the extinction of *Tricolpites lilliei* at the end of the Cretaceous, and the rise in abundance of *Triorites minor* in the early Paleocene. There was no mass extinction event recorded in the terrestrial palynofloras from Greymouth Coalfield at the KTB (Appendix 6.5). Many stratigraphically significant angiosperm taxa are rare or absent from Greymouth Coalfield palynofloras, and the occurrence of some taxa is not consistent with reported age ranges. Occurrence of age-diagnostic taxa was influenced by facies, flora and age (Appendix 5.5). However, similar floral change was observed at other localities with independent evidence for the position of the KTB (Appendix 7.6), thus the dominant control of sample age on Greymouth Coalfield palynofloras has been distinguished from the effects of flora and facies, and the KTB at Greymouth Coalfield has been accurately located.

The stratigraphic relationship between the KTB and the Rewanui CMM / Goldlight Fm. contact was variable, enabling the Rapahoe Sector to be subdivided into two palynostratigraphic domains. In the southwest, the KTB lies c.1.8m below the upper Rewanui CMM contact, whereas in the northeast, the corresponding interval is c.17m. In either domain, the upper Rewanui CMM contact is approximately isochronous. The interface between the two domains is arcuate, and is oriented NW/SE west of DH704, and E/W east of DH704.

Chapter 6. Applications of palynostratigraphy and palynology to basin analysis

6.1 Introduction

Identification of two palynostratigraphic domains (Section 5.5.3) offers a predictive tool for estimating the position of the KTB throughout the Rapahoe Sector, which can be used as an independent datum for stratigraphic and paleogeographic investigations. Three specific stratigraphic applications of the KTB are discussed here, namely paleogeography at the time of the KTB, use of the KTB in resolving lithostratigraphic problems in the NW of the coalfield, and coal seam correlation. Mechanisms responsible for the observed relationship between the KTB and the Goldlight / Rewanui contact are discussed in Section 6.5. The relevance of results from other palynological studies (Appendix 6, 7 & 8) to basin analysis within Greymouth Coalfield is presented in Section 6.6.

6.2 Paleogeography of the Cretaceous–Tertiary Boundary

The KTB represents a synchronous surface which provides a time slice through the rock record. Paleogeography of the Greymouth Coalfield depositional environment at the time of the KTB can be reconstructed by estimating the position of the KTB in all drillholes, and determining which lithofacies occur at that stratigraphic position. The position of the KTB can be estimated by subtracting 1.8m (southwestern palynostratigraphic domain) or 17.0m (northeastern palynostratigraphic domain) from the elevation of the upper Rewanui CMM contact (Appendix 10.2), and making allowance for dip (Table 6.1).

In the study drillholes, use of the estimated position for the KTB removes the uncertainty in KTB position arising from variable sampling interval (Section 5.5.1), and increases the potential accuracy of stratigraphic interpretations. Within these drillholes, the estimated position of the KTB generally falls within a coal seam or carbonaceous interval (indicated on respective columns, Figure 5.2). The exceptions are DH621, where the KTB is in conglomerate, and DH635, where the KTB is in mudstone. The estimated KTB position in DH632, is also within a coal seam interval, suggesting that the present revision of the palynostratigraphy (Section 5.4) is correct.

DH	Upper Rewanui CMM contact	palynostratigraphic domain	estimated KTB position	Lithology at estimated depth
619	241.8	NE	259.1	coal
621	64.3	NE	83.1	pebble conglomerate
622	268.5	NE	286.1	carbonaceous mudstone
623	45.6	SW	47.6	coaly mudstone
626	302.4	SW	304.3	carbonaceous mudstone
632	250.9	NE	268.2	carbonaceous mudstone
633	378.0	SW	379.9	carbonaceous mudstone
635	379.2	NE	396.8	mudstone
640	187.0	SW	188.9	carbonaceous mudstone
643	281.2	SW	283.1	coal
666	146.5	NE	166.1	carbonaceous mudstone
667	104.5	NE	121.8	coal
697	286.7	SW	288.6	carbonaceous mudstone

Table 6.1 Estimated positions of the KTB and corresponding lithologies, study drillholes. Faulted drillholes (DH628, 631, 636) are omitted.

Various lithofacies, ranging from conglomerate to coal, are present at the estimated KTB position in other drillholes throughout the Rapahoe Sector (Table 6.2). Drillhole locations are indicated in Figure 1.3 (map pocket).

DH	estimated KTB	lithology	DH	estimated KTB	lithology	DH	estimated KTB	lithology
433	188.9	sandstone	653	559.1	coal	708	221.3	muddy sst
624	54.0	sandstone	657	211.2	coal	709	326.4	coaly mst
634	337.1	conglomerate	662	139.6	sandstone	710	281.7	conglomerate
637	253.9	carb mudstone	664	178.1	sandstone	711	21.8	coaly mst
638	219.7	carb mudstone	665	143.2	sandstone	712	352.5	carb mudstone
639	290.4	carb mudstone	696	282.5	carb mudstone	713	190.5	dirty coal
641	357.2	mudstone	699	328.9	coaly mst	714	311.9	dirty coal
642	283.1	coal	700	124.3	mudstone	715	300.1	coaly mst
644	459.7	siltstone	701	186.6	coaly mst	716	276.6	carb mudstone
645	198.8	coaly mst	702	256.7	carb mudstone	725	319.0	coaly mst
646	339.9	sandstone	703	267.7	coaly mst	726	306.8	carb mudstone
647	301.5	coal	704	314.2	carb mudstone	728	90.5	mudstone
648	309.9	sandstone	705	299.1	coaly mst	731	285.1	carb sandstone
649	327.2	mudstone	706	285.0	carb mudstone	733	281.1	cse sandstone
650	267.4	sandstone	707	346.9	coaly mst	735	201.2	fine sandstone

Table 6.2 Estimated positions of the KTB, other Rapahoe Sector drillholes.

A paleogeographic reconstruction of the Rapahoe Sector at the time of the KTB (Figure 6.1) was constructed from the data presented in Tables 6.1 and 6.2. The dominant depositional environment was a low-relief, vegetated floodplain on which carbonaceous mud accumulated by vertical accretion. In places, silt and mud was deposited by settling of suspended sediment in lakes and ponded areas on the floodplain. Small areas ($<0.5km^2$) of clean peat formation, probably in domed mires, occurred throughout the area, and low-lying (minerotrophic) mires, which were regularly inundated, were common in the central Rapahoe Sector. Dirty peat and organic-rich muds accumulated in the latter mire type, which supported a moisture-loving plant community (see below).

Bisecting the floodplain in the north was a sandy river which flowed from the toe of Greenland Group-derived alluvial fans in the northwest. A sandy crevasse splay of ECS affinities entered the area from the northeast, eroding underlying peat (as indicated by a washout in the roof of the uppermost coal seam in DH662). Sandstone units at the modelled position of the KTB in DH433 and DH624 (eastern Rapahoe Sector) have no obvious western (WCS) source and may also represent minor crevasses splays of axial (ECS) derivation. In the southwest, sediment derived from the adjacent basement block was carried by streams into an area of mire deposition, resulting in a split in the southwestern coal seam (Ward 1995, Figure 10).

During the majority of Rewanui CMM deposition in the Rapahoe Sector, a NW–derived fluvial system bisected the Rapahoe Sector at approximately the location of the palynostratigraphic domain interface (Ward 1996). However, at the time of the KTB, this fluvial system had migrated c.1–2km to the north, and raised or low-lying mires occupied the position of the former channel belt. The western fringe of alluvial fans retreated to the northwest of the area, and much of the western margin of the Rapahoe Sector was occupied by low-relief vegetated floodplain. Reduction in coarse sediment supply marked the first phase of transition from coal measure (Rewanui CMM) to lacustrine (Goldlight Fm.) sedimentation in the Rapahoe Sector.

Previous paleogeographic reconstructions of the Rapahoe Sector (e.g. Bowman et al. 1984, Figure 12; Newman 1987, Figures 27 & 28; Ward 1996, Figure 6) have emphasised general patterns of sediment transport and deposition. In contrast, the KTB time slice reconstruction illustrates specific sedimentological and paleoenvironmental features, and

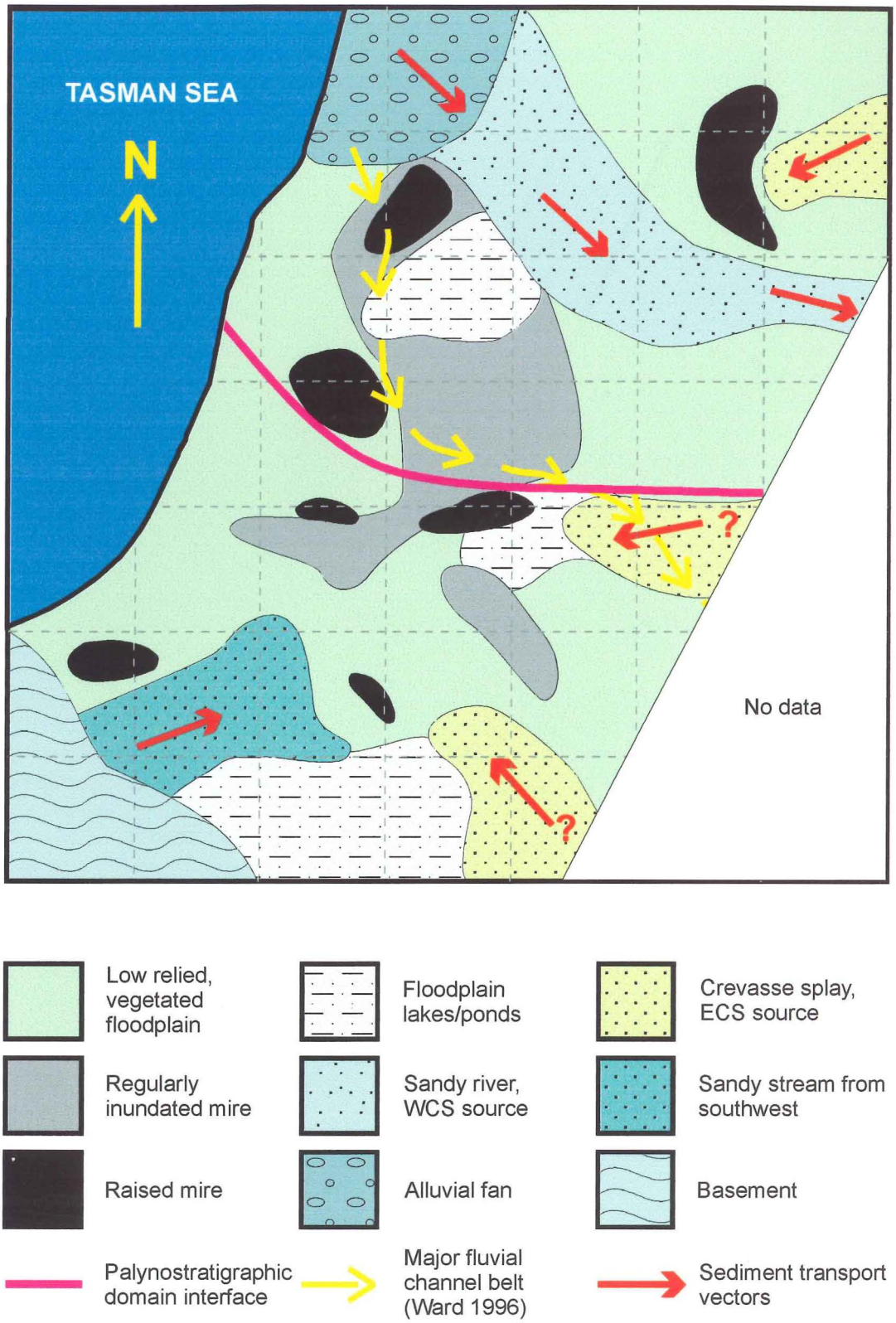

Figure 6.1 Paleogeographic reconstruction of the Rapahoe Sector at the time of the KTB (65Ma). Map area is the same as shown in Figure 5.5, grid square = 1km. Yellow arrows indicate position of fluvial axis which bisected the Rapahoe Sector for much of Rewanui CMM deposition (Ward 1996), note that fluvial deposition moved northwards c.2km at time of KTB.

demonstrates the complexity present within the basin at a given time. The contribution of this reconstruction to the understanding of sediment transport within Greymouth Coalfield is discussed in Section 7.6.1.

The influence of lithofacies on the occurrence of age-diagnostic palynomorphs is discussed in Appendix 5.5. Occurrence of four of the five taxa listed in Table 5.1 (*T. lilliei*, *T. minor*, *Beaupreaidites* sp., *Tricolpites* sp. F) is generally restricted to clastic rather than organic lithologies. The paleogeographic reconstruction presented in Figure 6.1 shows large areas of mire deposits in the central Rapahoe Sector, and future palynostratigraphic studies of the KTB may be hampered by the absence of suitable age-diagnostic taxa from these areas.

6.3 Seam correlation in the Rapahoe Sector

Correlation of coal seams throughout the Rapahoe Sector is difficult (Section 5.1). Traditionally, the Goldlight / Rewanui contact has been used as the correlation datum (e.g. Thorburn 1981a; Bowman et al. 1984; Newman 1987). Confirmation that this contact is generally isochronous (Section 5.5.4) increases confidence in correlation models, however subdivision of the study area into two palynostratigraphic domains (Section 5.5.3) is an added complication which must be incorporated in any new seam correlation model.

The KTB offers an alternative datum for seam correlation models (Ward 1996). Correlation of seams in drillholes which span the palynostratigraphic domain interface can be achieved by using either the known (e.g. DH643) or estimated (e.g. DH701) positions of the KTB to define the correlation datum (Figure 6.2). The palynostratigraphic correlation highlights that previous correlation models for the central Rapahoe Sector which used the Goldlight / Rewanui contact as a datum were incorrect.

Further development of the palynostratigraphic seam correlation model was discussed in Ward (1996). A key finding was that major seams tended to occur at similar intervals below the KTB throughout the Rapahoe Sector. The Upper seam occurs close to the KTB, the Main seam at c.35m below the KTB and the Submain seam at c.60m below the KTB. Carbonaceous "barren" zones which are laterally equivalent to seams could also be correlated with this framework.

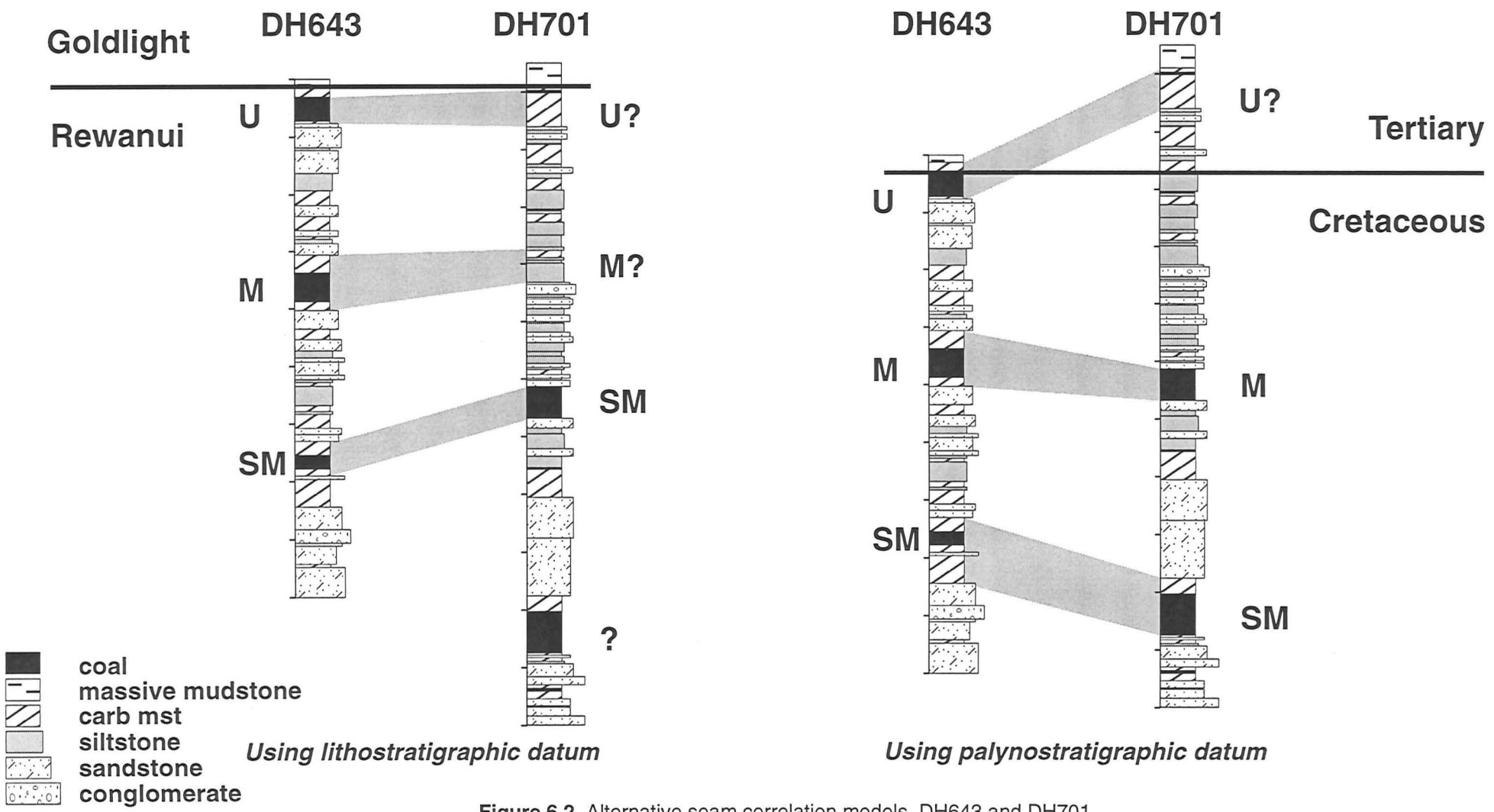

Figure 6.2 Alternative seam correlation models, DH643 and DH701.
Seams are marked as follows: U = Upper, M = Main, SM = Submain.

The Submain Seam of the southern Rapahoe Sector was correlated through a barren zone in the vicinity of DH635 to the "C" Seam of the Strongman Mine area, whereas other southern Rapahoe Sector seams are absent from the Strongman area. The "D" and "E" seams at Strongman Mine are also absent further south (Ward 1996).

From the correlation models, a map of seam extents was constructed (Ward 1996, Figure 12). A revised version of this map, which incorporates known seam extents in the Strongman Mine area (taken from Thorburn 1981) is presented in Figure 6.3. This map shows the maximum extent of each seam (where >1m thick), but not internal details such as splitting or barren zones, which intersect most seams in the Rapahoe Sector.

The seam correlation framework offers an additional means of assessing stratigraphic completeness of upper Rewanui CMM sections where faulting is present (Appendix 2). In DH631 and DH636, seam intervals occur 13–20m above where expected (Ward 1995, 1996), suggesting removal of upper Rewanui CMM strata by faulting. These findings are corroborated by minimum curvature modelling (Appendix 3.4). Seam correlation and modelling also indicate c.35m of Rewanui CMM are missing in DH696 (Ward 1995), whereas the same methods confirmed that structural disruption in DH698 did not adversely affect stratigraphy (Appendix 2). Faulting in DH628 was also confirmed by palynostratigraphy (Section 5.3, Figure 5.2), and the position of the Main seam in this drillhole indicates c.10–20m of strata is missing from the Rewanui CMM.

Recent detailed analyses of coal seam palynomorph abundance profiles (N. Moore 1996a, b) and vitrain banding profiles (T. Moore 1996) for the central, thickest part of the Main seam of the Rapahoe Sector have supported the palynostratigraphic seam correlation model presented above. However, these other studies have concentrated on the area with the greatest density of drillhole data, whereas the present correlation model may be applied throughout the Rapahoe Sector.

6.4 Resolving the upper Rewanui CMM contact in the northwest

Palynological results presented in Chapter 5 and Appendix 5.5.3 provided confirmation that transitional lithosomes of the lower Goldlight Transitional Member, and coal measure lithosomes of the Dunollie Fm., which occur above Rewanui CMM in the northwest of the

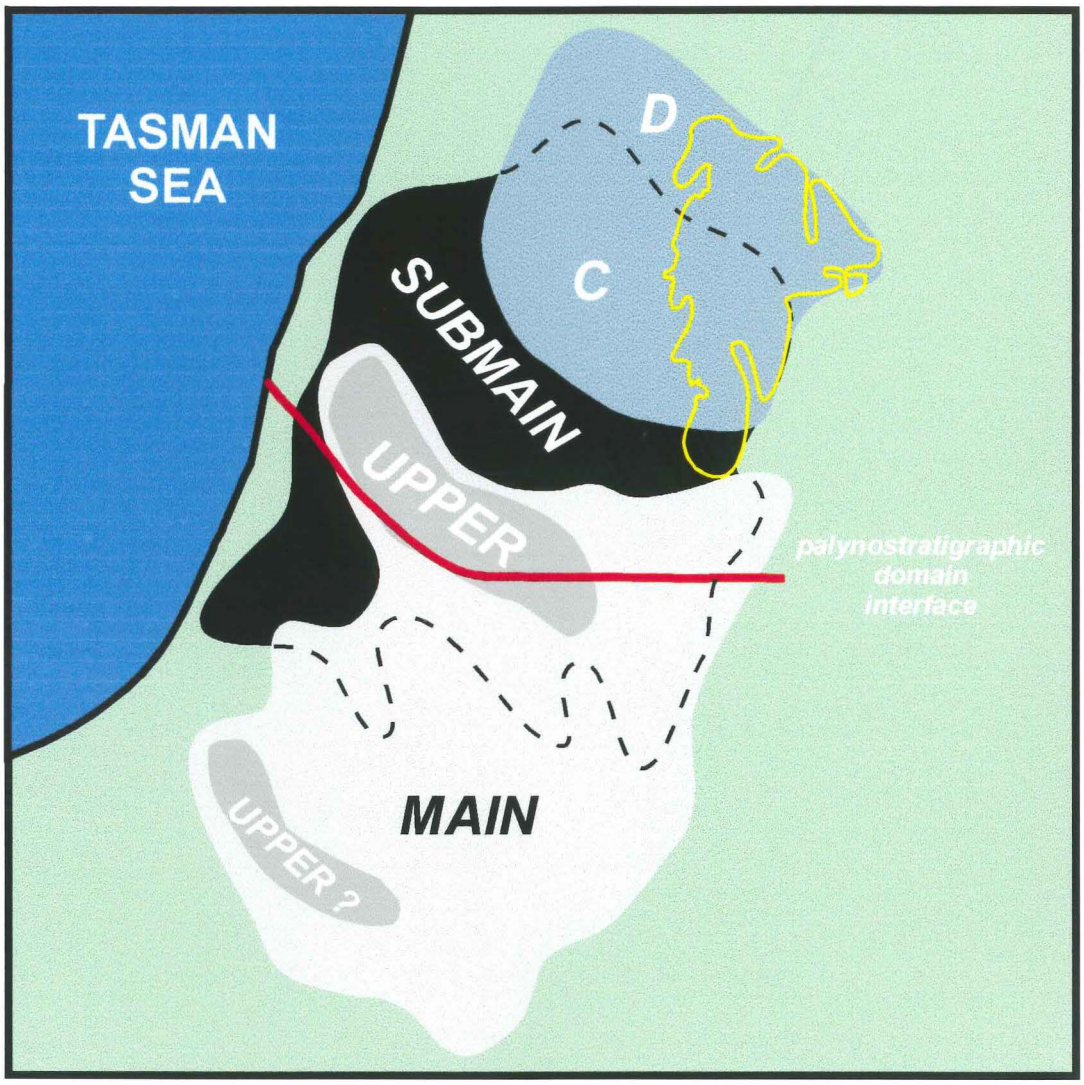

Figure 6.3 Distribution of major coal seams, Rapahoe Sector, derived from palynostratigraphic correlation model (Figure 6.2). Note that D seam lies above C seam. Barren or splitting zones within seam intervals are not shown.

study area, are time-equivalent to lacustrine Goldlight Fm. strata. Location of the KTB and the Main seam in some northwestern drillholes provides a stratigraphic framework for testing the position of the upper Rewanui CMM contact where Goldlight Fm. is absent.

Palynostratigraphic data are available for three drillholes (DH619, DH621, DH622) in the northwest of the coalfield (Sections 5.3, 5.4). In DH622, the upper Rewanui CMM contact was placed on lithostratigraphic grounds beneath transitional lithosomes within the Goldlight Fm. (Appendix 2), and a coaly interval is present at the estimated KTB location, suggesting the contact is correctly located. In DH619 and DH621, lithostratigraphy is less certain, and recognition of a thin Goldlight Fm. interval was tentative (Appendix 2). There is a carbonaceous interval at the estimated KTB position in DH619 (Figure 5.2), whereas in DH621, the top-most coaly interval is at 90.6–95.0m, and the estimated KTB position lies within conglomerate (Figure 5.2). The lowermost Zone PM3 (Teurian) sample in DH621 is at 82.4m, 0.7m above the estimated KTB position (83.1m).

If the coaly horizon at 90.6–95.0m in DH621 correlates to coaly intervals at or near the KTB elsewhere (e.g. Tables 6.1, 6.2), lithostratigraphic boundary placement in DH621 is inconsistent with the palynostratigraphy. However, conglomerate deposition is widespread in the northwestern Greymouth Coalfield (Appendix 4.4.1), and carbonaceous strata are not the norm. In the paleogeographic reconstruction for the KTB (Figure 6.1), conglomerate deposition is therefore depicted as continuing across the KTB in the northwest, reflecting the continuous outcrop of such strata at Twelve Mile Beach.

Four further drillholes (DH634, 637, 639, 710) lie within the area where Rewanui CMM and Dunollie Fm. are conformable (Figure 6.4). There are no palynostratigraphic data for these drillholes, therefore the estimated position of the KTB (Table 6.2) must be used as a correlation datum. DH637 is in the southwestern palynostratigraphic domain (Ward 1996, Table 2), and the estimated KTB position is within the uppermost 2m of Rewanui CMM carbonaceous mudstone (Figure 6.4). Lack of coal development at the estimated KTB in DH637 is consistent with proximity to the NW basin margin where coal formation was limited (Ward 1995).

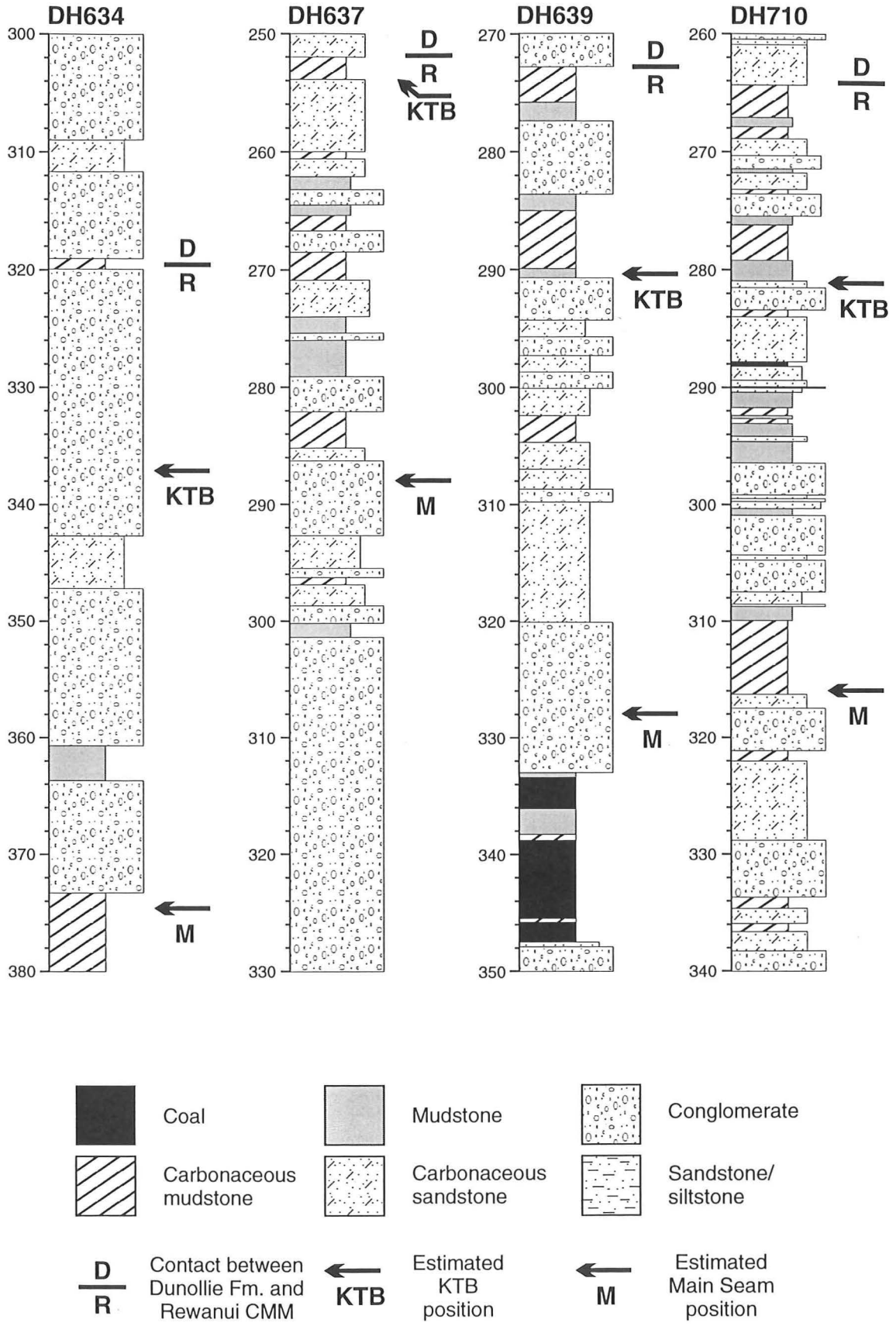

Figure 6.4 Lithostratigraphy and estimated palynostratigraphy of northwestern drillholes in which Goldlight Fm. is absent, and Dunollie Fm. is in conformable contact with Rewanui CMM.

Lithostratigraphic correlation of DH639 and DH710 to surrounding drillholes is difficult, however carbonaceous intervals are present at approximately the depths indicated by the estimated KTB locations (Figure 6.4), suggesting that the lithostratigraphic contacts are correctly placed. No correlatable carbonaceous intervals are present near the estimated KTB position in DH634, which is dominated by conglomerates (Figure 6.4).

Further support for stratigraphic boundary placements within the northwestern drillholes comes from the seam correlation model discussed above. In DH619, DH621 and DH622 (Figure 5.2), there is a split to dirty coal horizon at the estimated position of the Main seam (c.35m below the KTB). Carbonaceous intervals are present at the appropriate depths in DH634 and DH710, whereas the positions are occupied by conglomerate in DH637 and DH639 (Figure 6.4). However, in the latter drillholes, coaly intervals are present within 3–6m of the estimated Main seam positions, and minor stratigraphic variation of seam position is typical (Ward 1996, Figures 11, 13). Correlation of the Main seam and its lateral (dirty) equivalents in the northwest is therefore consistent with occurrence of the seam throughout the Rapahoe Sector (Figure 6.3), indicating that the upper Rewanui CMM lithostratigraphic contact is correctly placed in those drillholes where Goldlight Fm. is absent.

6.5 The origin of the two palynostratigraphic domains in the Rapahoe Sector

Proximity of the KTB and the upper Rewanui CMM contact in the southwestern palynostratigraphic domain indicates very little sedimentation between the two "events", whereas some 17m of strata was deposited in the northeastern domain. However, the KTB and upper Rewanui CMM contact remain approximately parallel throughout both palynostratigraphic domains, despite total Rewanui CMM thickness varying from c.10m to >220m (Figure 3.7). Strongly differential subsidence, which resulted in variable Rewanui CMM thickness, appears to have ceased, yet there is no evidence for a break in deposition in the southwestern domain.

The likely control, given the distinct domains produced and the need for a (geologically) discrete subsidence event, is a normal fault oriented along the interface of the two palynostratigraphic domains, and downthrown to the north by c.15m (and probably more prior to compaction). The fault had an arcuate surface trace, which was at least 3km long.

The position of the fault is approximately coincident with the southwestern margin of the underlying lacustrine Ford Fm. basin (Figure 3.2), which suggests the fault may have existed prior to Rewanui CMM deposition.

Maximum subsidence along the fault at the time of the KTB occurred in the vicinity of DH647 and DH704, where there is greatest development of the "Upper" seam (Ward 1996, Figure 11). Enhanced subsidence persisted during early Goldlight Fm. deposition, restricting thick lower Goldlight Transitional Member strata (Figure 3.10) to immediately north of the fault (Ward 1996). The northwestern end of the fault trace would have offered an erodible zone in basement through which the rivers feeding the Goldlight Transitional Member delta could pass (Section 7.8.2). The significance of structurally controlled sediment sources is discussed further in Section 8.3.2.

6.6 Applications of other palynological studies to basin analysis

Palynological and paleobotanical studies presented elsewhere in this thesis (Appendices 5–8; Ward et al. 1995) provide useful evidence about aspects of the Greymouth Coalfield paleoenvironment and basin history that cannot be directly established from lithostratigraphy and palynostratigraphy.

During deposition of coal measure units within Paparoa Group strata, Greymouth Coalfield was covered by dense rainforest vegetation (Appendix 6; Ward et al. 1995), dominated conifers and the ferns Gleicheniaceae (in mires) or Sphagnaceae and Cyatheaceae (in clastic depositional environments). The climate was wet, cool temperate, with temperature ranging from 0–10° in winter and averaging 10–14° annually (Appendix 8.1.4). Comparisons with palynofloras from other localities (Appendix 7) indicate conditions at Greymouth Coalfield were generally cooler than experienced elsewhere, possibly because of increased distance from the coast (Appendix 8.1.5). Late Cretaceous climatic seasonality at Greymouth Coalfield is indicated by the presence of growth rings within gymnosperm wood (Ward et al. 1995, Figure 10).

The predominance of *Phyllocladidites mawsonii,* Sphagnaceae and Cyatheaceae in most palynofloras supports the paleogeographic reconstruction for the Rapahoe Sector at the time of the KTB depicted in Figure 6.1. The probable parent plant of the palynomorph

P. mawsonii (*Lagarostrobos franklinii*) can reproduce vegetatively, and survives in regularly inundated floodplain or mire environments (see Ward et al. 1995 for further discussion). Modern Cyatheaceae (tree ferns) fill gaps in the tree canopy on better drained soils developed on river flats (Duncan et al. 1990), and were restricted to sites without permanent wetness (e.g. Wardle 1991, p. 118), whereas modern Sphagnaceae occupy permanently wet places such as wet forest floors and small depressions (Wardle 1991, p. 322).

Palynofloras present in the environments where clean coal was deposited support previous suggestions (Newman 1987; Ward 1995) that some mires were raised (Appendix 6.3.2, 7.2; Ward et al. 1995). Increases in abundance of Gleicheniaceae spores towards the roof of both the Strongman area "D" seam and the central Rapahoe Sector Main seam (Ward et al. 1995; Moore 1996a, b) represented increasing acidity as the domed mires developed above local base level. In the Main Seam, the increasing proportion of Gleicheniaceae spores is accompanied by a decline in ash proportions and volatile matter, suggestive of reduced clastic influx and slight reduction in saturation (Moore 1996b). These observations provide further evidence for the existence of raised mire profiles in the Rapahoe Sector.

The final aspect of basin analysis which benefits from palynological input is interpretation of the cause of basinwide change from fluvial sedimentation of the Rewanui CMM, to lacustrine deposition of the Goldlight Fm. This event is generally marked by the rapid reduction in carbonaceous material and a change from floodplain to lacustrine or transitional lithosomes (Section 2.7.5), though fluvial sedimentation persisted in the northwest of the area (Figure 3.10).

The palynostratigraphic domain model (Section 5.5.3, Figure 5.5) suggests the depositional surface during uppermost Rewanui CMM deposition was essentially planar, and the basin was not subjected to strongly differential subsidence (though minor faulting continued). This setting would have permitted a rapid lacustrine transgression for a small rise in relative base level. The paleogeographic reconstruction for the KTB timeslice (Figure 6.1) also suggests there was a reduction in supply of coarse clastic sediment from the northwest (see above), which would have prevented the newly-formed lake from filling with sediment.

Transgression of the Goldlight lake throughout the Paparoa Basin might be expected to have influenced the paleovegetation. However, floral change which occurred at the KTB was not coincident with change in depositional environment, and the same patterns of floral change are evident in all lithosomes (Section 5.5.4).

Floral change at the KTB probably reflects climatic change (Appendix 8.3), however there is no evidence for an increase in precipitation in Greymouth Coalfield which could account for the rapid lacustrine transgression. Indeed, the reduction in total spore proportion across the KTB (Table A6.11) could be interpreted as indicating lower precipitation in the earliest Paleocene. Increased rainfall in the hinterland would enhance source-area erosion and sediment transport, whereas the Goldlight Fm. is dominated by very fine clastic strata with limited coarse sediment influx (Section 2.7.6).

The regional trend of climate change from the Haumurian to Teurian is for reduction in precipitation (Appendix 8.2), and increased precipitation is an unlikely cause for the lacustrine transgression. Furthermore, older lacustrine deposits within Greymouth Coalfield (Ford Fm., Waiomo MM) indicate such sedimentation is not atypical. Climatic variation cannot account for Waiomo MM occurrence, as this unit is restricted to only the eastern half of the coalfield (Section 3.6). Mechanisms other than climate must therefore be responsible for the lacustrine events during Paparoa Group deposition.

6.7 Summary

The position of the KTB throughout the Rapahoe Sector can be estimated using the palynostratigraphic domain model, and the paleogeography at the time of the KTB reconstructed. The relationship between the KTB and the position of coal seams and coaly intervals throughout upper Rewanui CMM in the Rapahoe Sector is predictable, resulting in enhanced understanding of the distribution of coal seams in the area. The same predictive stratigraphic framework can be applied to assist in the resolution of lithostratigraphic problems, and to provide details about subsidence and sediment transport patterns within the basin. In conjunction with other palynofloral evidence, increased precipitation is ruled out as a potential mechanism for the evolution of the sedimentary system from fluvial to lacustrine immediately after the KTB.

Chapter 7. Evolution of sediment transport within the Paparoa Basin

7.1 Introduction

Information with which to determine sediment transport history within the Paparoa Basin can be derived from many sources. Previous studies (e.g. Newman 1985, Boyd & Lewis 1995) have highlighted compositional variation within and between the various units, and have also addressed textural variation within the Rewanui CMM (Appendix 1.2, Figure A4.11). These studies indicated the presence of two sediment compositions within the Paparoa Basin, termed the Eastern Compositional Suite (ECS) and the Western Compositional Suite (WCS) (Appendix 1.2.5).

This chapter primarily addresses the relative roles of the eastern/northern (ECS) and western (WCS) sediment sources in supplying sediment to each unit. Textural variation within the coal measure units is also discussed, and the implications for source area evolution are evaluated. Sedimentary dynamics of the transitional lithosomes, which have not previously been defined, are discussed in detail.

7.2 Jay Formation

Clasts within Jay Fm. conglomerates (= Jay (ii) unit, Figure A1.1B) were generally derived from Greenland Group, and pebble sizes range from 20cm in the northwest (DH621) to typically <6cm in the Rewanui area. Subangular fine pebbles to granules of quartz are a rare component of Jay Fm. conglomerates throughout the coalfield. Clasts were transported from the northwest along the axis of the Jay Fm. depocentre, and into the southern depocentre near Rewanui (Figure 3.1).

Jay (iii) sandstones are typically grey-green and also derived from Greenland Group. However, in DH661 (near Mt. Watson), a 30cm bed of quartzose medium sandstone with scattered fine quartz pebbles which resembles ECS Rewanui CMM sandstones is present, and conglomerates contain up to 10% quartz. Coarse quartzose sandstone was reported from DH226 (Gage 1952), and sandstones of mixed provenance (including scattered quartz pebbles) are also present in DH659.

The presence of quartz-rich sandstones within Jay Fm. in the northeast of the coalfield suggests that the northern (granitic) sediment source was supplying sediment during initial sedimentation in the Paparoa Basin. An alternative explanation is that a quartz-rich lag developed from weathering of Greenland Group, which is highly quartzose (Laird 1972), was transported into the Paparoa Basin when sedimentation commenced. The latter scenario accounts for the presence of rare quartz in Greenland Group-dominated conglomerates, however the former scenario best explains the coincidence of quartz sandstone occurrence in Jay Fm. with that of overlying units (see below), and is the preferred explanation.

7.3 Ford Formation

Information on sediment transport during Ford Fm. deposition (excluding volcaniclastic sediments) is derived from thickness trends and compositional and textural variation within the Ford Transitional Member, and the composition of sandstone beds within Ford Fm. lacustrine lithosomes. Ford Transitional Member thickness trends (Figure 3.3) suggest a major coarse sediment source north of Ten Mile Ck. (c.2km inland from the present coastline), and a minor source between Blackball Pk. and Mt. Watson.

Sandstones of ECS composition occur within transitional lithosomes and as thin interbeds in the uppermost lacustrine lithosomes in DH660, indicating a granitic input into the eastern minor lobe of Ford Transitional Member sediments. Pebbles within northeastern conglomerates are generally Greenland Group, and coarse sediment elsewhere within the Ford Transitional Member is of Greenland Group (WCS) provenance, with minor amount of quartz pebbles and granules as observed in Jay Fm. However, rare granite clasts are present in Ford Fm. in DH656 and DH657.

The distribution of coarse sediment within the Ford Transitional Member (Figure 7.1) confirms the presence of two principal sediment sources as suggested by the isopach model. The coarsest pebbles are generally found in the north, in the vicinity of Ten Mile Ck. Abundant debris flow conglomerates within Ford Fm. lacustrine lithosomes are also found in the north, in DH657. Further evidence for a northern sediment source comes from the distribution of coal clasts within the Ford Transitional Member, which is highlighted by stipple in Figure 7.1. Coal clasts observed in drillholes occur around

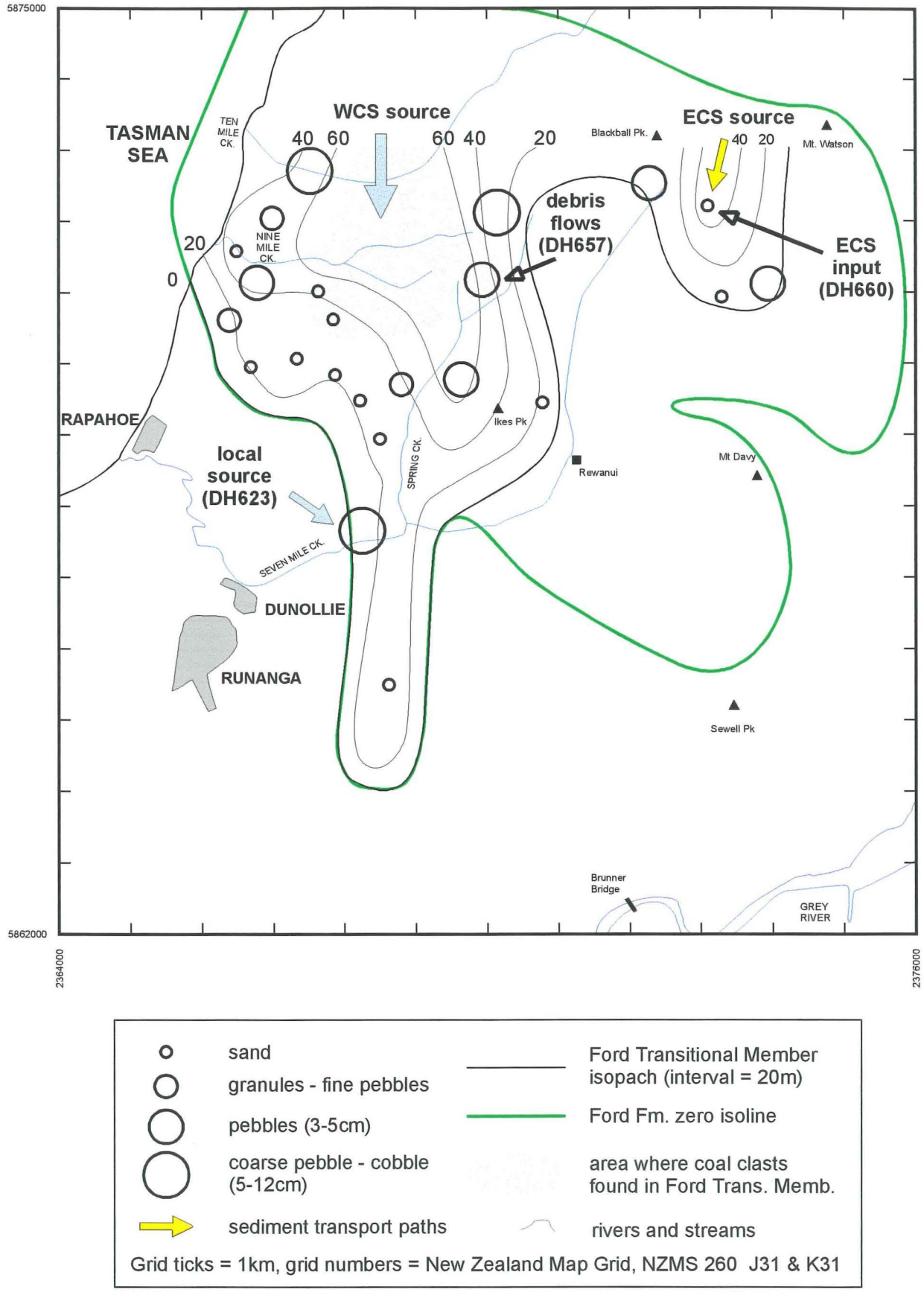

Figure 7.1 Sediment transport patterns, Ford Transitional Member. Circles represent coarsest grain size present in drillholes.

the upper reaches of Nine Mile Ck., and none are present in drillholes to the west. Similar coal clasts within probable Ford Transitional Member are present due north at the Ten Mile Ck. roadend (Figure 2.5b). An additional, southwestern source of coarse (cobble) material is indicated by DH623, though this occurrence is a thin basal conglomerate which was rapidly deposited at the onset of Ford Fm. deposition.

Sediment transport paths within the Ford Fm. basin are shown on Figure 7.1. Most coarse sediment, irrespective of provenance, was derived from the north, and other inputs were minimal. ECS sandstones in the northeastern lobe of Ford Transitional Member indicate that two distinct source areas were feeding into the basin. However, at this time, the northeastern sediment flux comprised both ECS and WCS material.

7.4 Morgan Coal Measure Member

Variation in Morgan CMM texture (Figure A4.14) does not provide conclusive evidence for sediment transport directions within the Morgan CMM depocentres, and further detailed information (notably composition) is required. Most drillholes which intersect Morgan CMM contain ECS sandstones. The exceptions are DH625, DH630 and DH632, which are located in the southwest of the major Morgan CMM depocentre (Figure 3.4), and contain only WCS sandstones, and DH620, DH656 and DH658 in which there is mixed ECS and WCS sandstone provenance. Greenland Group clasts are present in conglomerates in DH630, DH632 and DH656 (located along the western margin of Morgan CMM occurrence), and in basal Morgan CMM conglomerates in DH659 and DH661. WCS sediment is absent from the Brunner Bridge depocentre.

The observed pattern of sediment composition within Morgan CMM requires a complex explanation (Figure 7.2). Initial sedimentation comprised a fringe of WCS material (continuous with western basal Rewanui CMM) along the southwestern margin of the Morgan CMM basin, and contemporaneous ECS sedimentation in the north of the basin (with westward or southwestwards transport resulting in mixed provenance in DH656 and DH658). Seam isopachs and splitting trends indicate sediment fed into the Rewanui area from the northwest throughout Morgan CMM deposition (Thorburn 1981b). The western Morgan CMM depocentre only received very fine sediment.

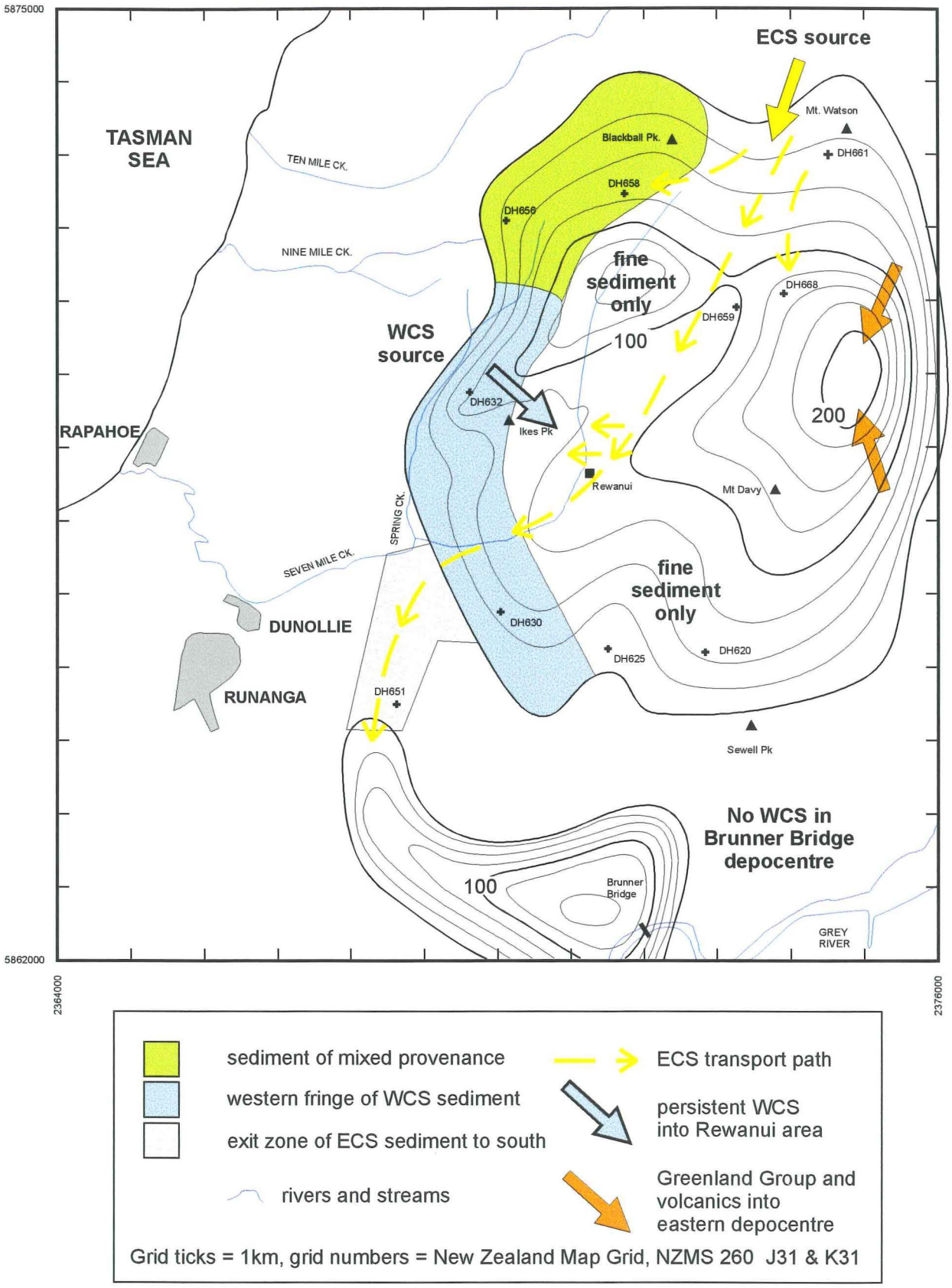

Figure 7.2 Sediment transport patterns, Morgan CMM.
Decompacted isopach model shown, interval = 25m.
Numbered drillholes are discussed in text.

ECS sediments prograded southwards, along a transport system which coincided with the intrabasin ridge separating the main Morgan CMM depocentres (Figure 7.2). Intermittent floods from this river disrupted WCS sedimentation in the Rewanui area as overbank material. Eventually ECS sediment was transported southwards from the main Morgan CMM depocentre through a poorly-defined exit between DH630 and Spring Ck., via a zone of bypass (indicated by absence of Morgan CMM from DH651), and eventually into the Brunner Bridge depocentre.

ECS material was not deposited in thin Morgan CMM sequences in southern drillholes (e.g. DH625, DH630), and may have been absent from the eastern depocentre south of DH658 and DH659. Gage (1952, p. 28) states that Morgan volcanics are laterally gradational to, and interbedded with, conglomerates containing Greenland Group clasts, and that Morgan CMM conglomerates coarsen eastwards, suggesting an eastern source. Such a source may have supplied the rare Greenland Group clasts encountered in basal Morgan CMM in DH659 and DH661, which are c.3km further east than other occurrences of Greenland Group pebbles. However, the above discussion for Ford Fm. indicates Greenland Group material was being transported from the northeastern source area, and this may have continued until the early phases of Morgan CMM deposition. An eastern Greenland Group source therefore only contributed sediment to the eastern Morgan CMM depocentre, which also trapped all volcaniclastic material.

7.5 Waiomo Mudstone Member

Specific information about coarse sediment transport into the Waiomo MM basin is derived from the limited occurrences of transitional lithosomes (Figure 7.3). ECS sediment is present (up to granule size) in thin transitional lithosomes in DH656, DH660 and DH719. In DH632, which lies close to the western limit of Waiomo MM, there is sequence of mixed provenance which includes thin conglomerates (Greenland Group and rare granite and quartz pebbles up to 3cm). In the southern (Brunner Bridge) depocentre, Waiomo MM contains very fine to medium sandy interbeds, and thin sandstones in DH654 are quartz-rich.

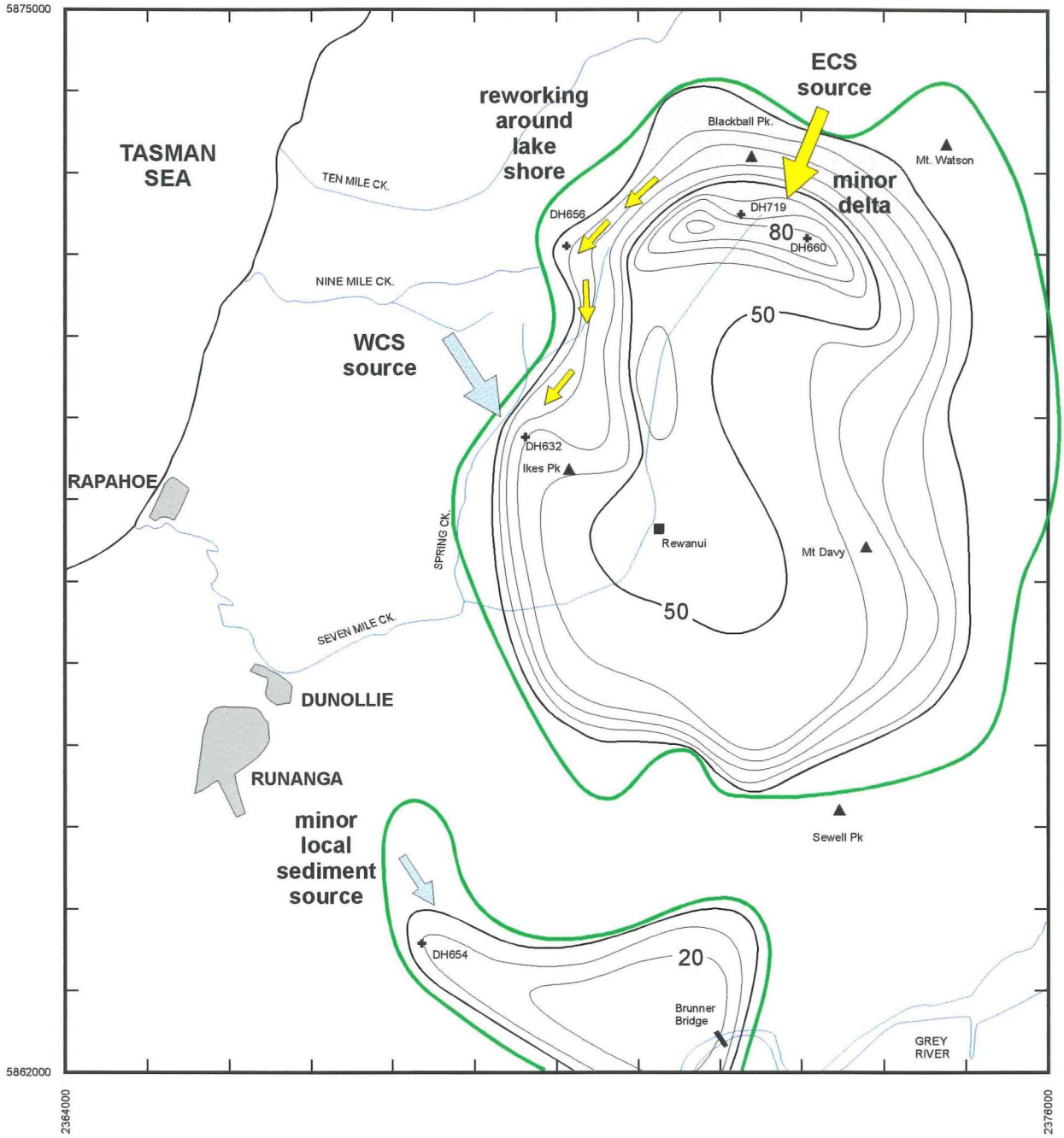

Figure 7.3 Sediment transport patterns, Waiomo MM.
Decompacted isopach model shown, interval = 10m.
Numbered drillholes are discussed in text.

Coarse sediment influx from the northeast continued during Waiomo MM deposition, whereas transport from the west was restricted to near DH632. Coarse sediment in the southern depocentre may have been derived or reworked from the surrounding area of Greenland Group basement, and the small extent of this basin plus the limited thickness suggests little influx from outside the Paparoa Basin would have been necessary.

7.6 Rewanui Coal Measure Member

Methods for determining sediment transport patterns within Rewanui CMM included textural analysis (Figure A4.13), petrological studies (Appendix 1.2.5, Boyd & Lewis 1995) and observations of composition from core and outcrop samples. These data distinguish the compositional suites, and delineate general sediment transport trends. Additional information about specific sediment transport events can be derived from paleogeographic reconstructions of the Rewanui basin (e.g. Newman 1987; Ward 1995, 1996) or selected time intervals (e.g. the KTB, Figure 6.1).

7.6.1 Rapahoe Sector

Coarse, Greenland Group derived sediment (WCS) is dominant in the west of the coalfield (along the present-day coastline), where the ratio of coarse to fine sediment exceeds 4 (e.g. DH634; see also Figure 6.4). The coarse:fine ratio reduces rapidly eastwards, and is c.1.0 throughout much of the Rapahoe Sector (Figure 7.4). There is also a rapid southwards decline in coarse proportion near Rapahoe, reflecting proximity to the basin margin.

Coal seam correlation and paleogeographic models (e.g. Bowman et al. 1984, p. 112–115; Ward 1995, 1996) highlight the general subdivision of Rewanui CMM in the Rapahoe sector into a lower, coarse sediment (conglomerate) dominated portion with thin, discontinuous coal seams, and an upper, fine sediment dominated portion, with thick, extensive coal seams (e.g. Figures 6.2, 6.3). The coarse:fine sediment ratio for the Rapahoe Sector is therefore mostly a function of the thickness of fine sediment (including coal) which developed above lower Rewanui CMM conglomerates. Low energy depositional environments (including mires) generally did not encroach to the northwest, suggesting greater depositional slope in that direction. Increased clast size to the northwest (Figure A4.11) supports this conclusion.

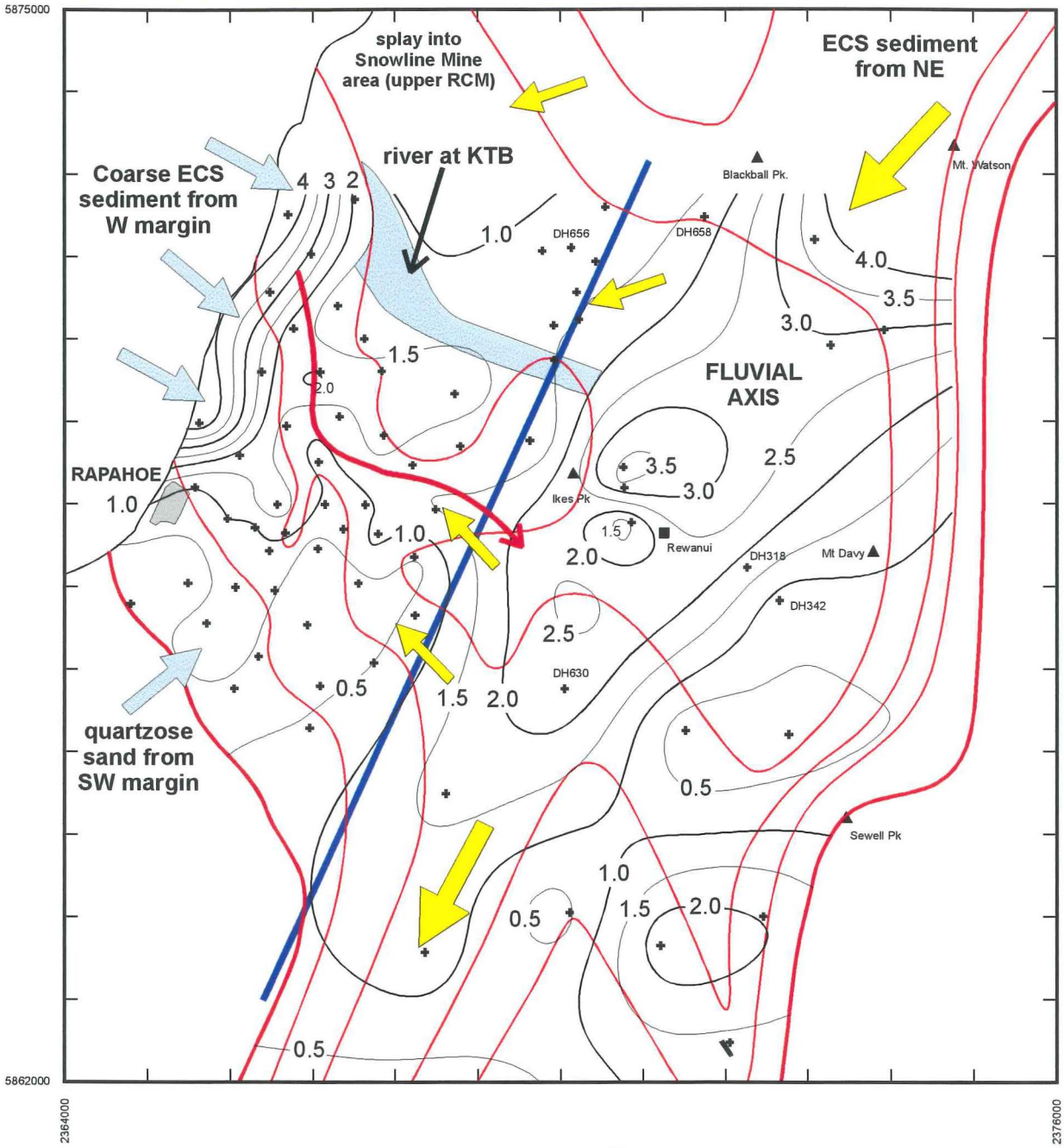

Figure 7.4 Sediment transport patterns, Rewanui CMM. Numbered drillholes are discussed in text.

Specific sources of coarse sediment which fed into the Rapahoe Sector are indicated by paleogeographic reconstructions. Quartz-rich sand from weathered Greenland Group basement entered the Rewanui CMM basin from the southwestern margin, resulting in seam splitting (Ward 1995; Figure 6.1). This event is reflected in the textural variation model (Figure 7.4), with anomalous coarsening indicated immediately northeast of Dunollie. In contrast, the fluvial system which bisected the central Rapahoe Sector throughout much of Rewanui CMM deposition (Ward 1995), and the locus of coarse sedimentation at the time of the KTB (Figure 6.1), are not clearly represented in the textural variation model (Figure 7.4). The likely reason is limited lateral migration of those fluvial systems, such that any given drillhole within the fluvial corridors will contain both coarse and fine sediment, and coal (Ward 1995, Figure 10).

7.6.2 Mt. Davy Sector

Throughout the Mt. Davy Sector, Rewanui CMM sediments are quartzofeldspathic (ECS of Boyd & Lewis 1995), and comprise the axial fluvial system of Newman (1985, 1987). Textural variation within Rewanui CMM defines an elongate lobe of coarse sediment which is sourced from the northeast, and fines southwest and laterally away from the axis of deposition (Figure 7.4). Localised variation in the proportion of coarse sediment in the Rewanui area represents small-scale paleoenvironmental control of overall sediment texture. Sediment also moved laterally from the axial system into the Brunner Bridge depocentre (Figure 7.4). In contrast to underlying units, no Greenland Group-derived clasts entered the Rewanui CMM basin from the northeast or east.

In the Mt. Davy Sector, thick, extensive coal seams are restricted to the lower Rewanui CMM, where they are interbedded with lenticular beds of coarse (often granular) sandstone (Thorburn 1981b) in fining-upwards cycles of 5–20m (Bowman et al. 1984, p. 107). Splitting and thinning trends in the most widespread lower Rewanui CMM seam show a distinct NNE/SSW trend (Bowman et al. 1984, p. 107), and are parallel to sediment texture trends (Figure 7.4). In the Rewanui area, splitting trends within lower Rewanui CMM seams have variable orientation (Thorburn 1981b), and textural patterns are also complex (see above). Middle and upper Rewanui CMM seams in the Mt. Davy Sector are thin and discontinuous, and occur within medium to fine quartzofeldspathic sandstones and mudstone (Bowman et al. 1984, p. 110–112).

Little information about upper Rewanui CMM sediment texture in the Mt. Davy Sector is available. Upper Rewanui CMM in older drillholes DH318 and DH342 comprises abundant fine carbonaceous sandstone and thin beds of coarse ECS sandstone and dirty coal. In contrast, the corresponding interval in DH630, which lies within the axis of ECS sediment distribution (Figure 7.4), is dominated by coarse ECS sandstones. Newman (1987, Figure 33) illustrated an outcrop sequence of upper Rewanui CMM lenticular bedded sandstones overlain by tabular bedded sandstones near Rewanui, and attributed the change in sedimentary architecture to a shift from braided to meandering deposition. However, meandering streams did not reach DH318 or DH342, and coarse sediment deposition remained within the previous axial channel belt.

7.6.3 The compositional interface

The interface between the ECS and WCS sediments throughout most of Rewanui CMM deposition, as delineated by the textural patterns, occurs approximately along Spring Ck. (Figure 7.4). This position is coincident with the narrow zone of mixed composition described by Bowman et al. (1984, p. 56) and Boyd & Lewis (1995), which occurs between DH656 and DH658. Westward migration of the axial fluvial system into the Rapahoe Sector during late Rewanui CMM deposition is well documented, and was attributed to declining depositional gradient following the cessation of conglomerate deposition in the Rapahoe Sector, accompanied by the change from braided to meandering deposition in the Mt. Davy Sector (Newman 1985, 1987; Newman & Newman 1992).

The KTB paleogeographic reconstruction (Figure 6.1) demonstrated that minor amounts of ECS sediment crossed the Spring Ck. area and were deposited as crevasse splays in the eastern Rapahoe Sector. ECS sediments also migrated in isolated channels into the northern Rapahoe Sector (Snowline Mine area) near the end of Rewanui CMM deposition (Figure 7.4). Low depositional gradients within the Rapahoe Sector are supported by the KTB timeslice reconstruction (Figure 6.1), in which floodplain facies are dominant.

7.7 Goldlight Formation

Sediment transport paths into the Goldlight Fm. basin (Figure 7.5) are indicated by thickness trends within the upper and lower Goldlight Transitional Members (Figure 3.9, 3.10) and limited sandstone compositional information. The western zone, in which Goldlight Fm. comprises only transitional lithosomes, is adjacent to the area of rapid Rewanui CMM coarsening (Figure 7.4), indicating a common and persistent sediment source. In the north, where fluvial activity was concentrated at the time of the KTB (Figure 6.1), the western limit of Goldlight Fm. was pushed c.1km to the east, indicating that the fluvial system persisted after the KTB.

Further south, a broad apron of transitional lithosomes was deposited in the same locality as the persistent Rapahoe Sector river system (Figure 7.5). However, the transitional lithosomes are dominated by very fine to medium sandstone, and coarse sandstone and granules were not carried into the lake basin. In contrast to Ford Fm., pebbles and cobbles are absent from Goldlight Fm.

Two sediment transport patterns are evident within the areas in which upper and lower Goldlight Transitional Members are distinguished (Figure 7.5). North of Dunollie, elongate zones of thickening within both upper and lower transitional lithosomes indicate persistent point sources of sediment feeding from the western basin margin (Figures 3.9, 3.10). In the lower Goldlight Transitional Member, a northern delta lobe overlies the northern (KTB) Rapahoe Sector river system, and a southern lobe matches the position of the major fluvial system which bisected the Rapahoe Sector (Figure 7.3). A new sediment source, near Rapahoe, fed an elongate zone of transitional lithosomes in the upper Goldlight Transitional Member.

In contrast, upper and lower Goldlight Transitional Members in the south of the coalfield cover broad areas, which exhibit gradational thickness reduction from south to north (Figure 3.9, 3.10). These thickness trends suggest sediment was sourced from the south (Figure 7.5), however Goldlight Transitional Member in DH654 and DH655 has ECS composition, which normally indicates a northeastern source. No other ECS material is present within Goldlight Transitional Member, though erosion has removed any deposits which may have been present in the northern Mt. Davy Sector.

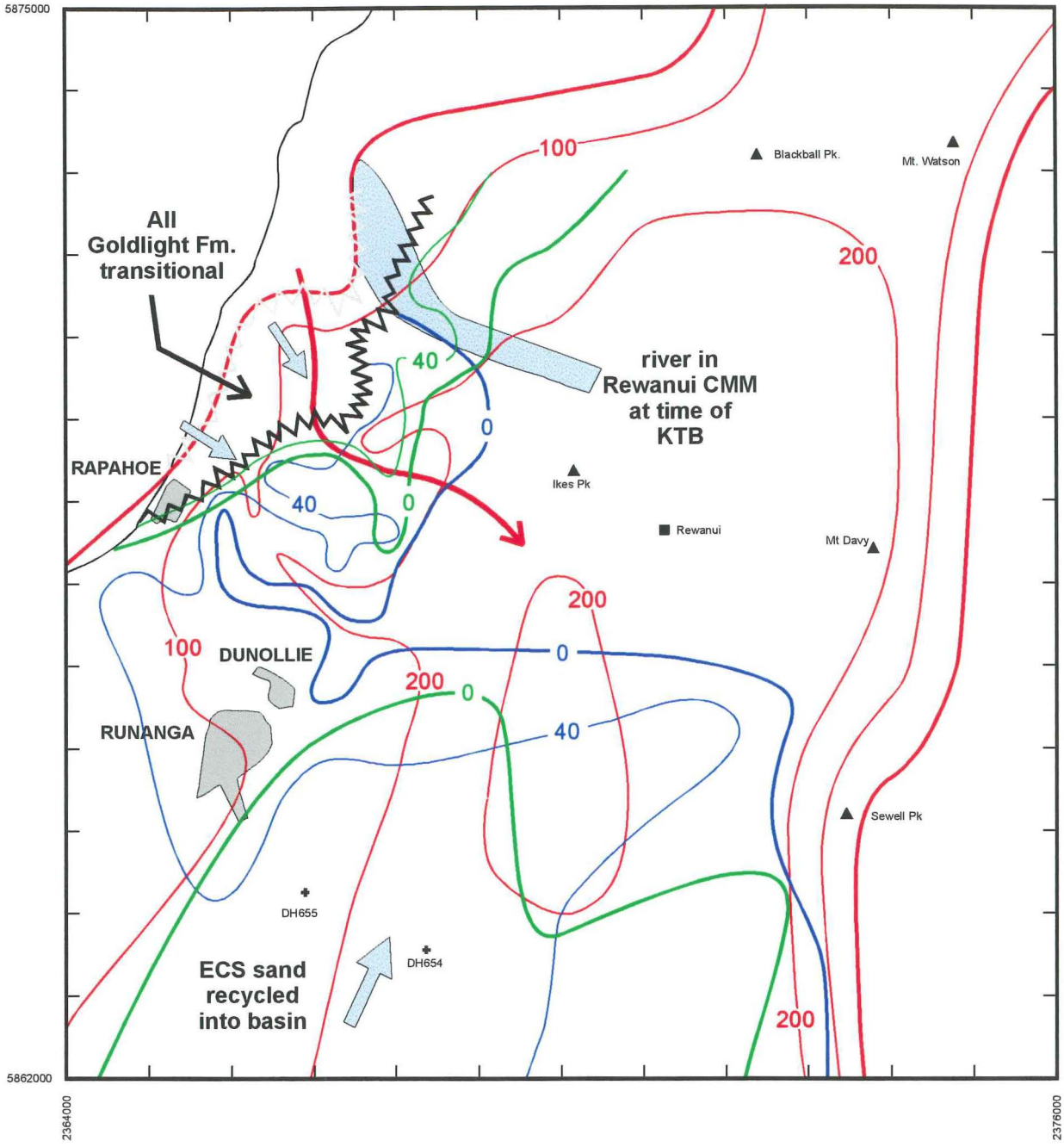

Figure 7.5 Sediment transport patterns, Goldlight Formation.
Numbered drillholes are discussed in text.
Full details of Goldlight Transitional Member
distribution given in Figures 3.9 and 3.10.

The apparent centre of the southern Goldlight Transitional Member sediment source is coincident with the southern trough which formed the exit for the axial fluvial system in the Rewanui Fm. basin (Figure 7.4). There was a reversal in sedimentary dynamics between Rewanui Fm. and Goldlight Fm. deposition, and ECS material previously deposited in the south of the coalfield was reworked northwards. There was probably no ECS material entering the basin from the northeast during Goldlight Fm. deposition.

7.8 Summary and discussion

Sources for coarse clastic sediment in the Paparoa Basin are summarised in Table 7.1.

Unit	WCS	ECS	other
Goldlight Fm.	point sources in NW	nil	minor reworking of ECS material northwards from S of basin
Rewanui CMM	conglomerate fringe in W, major point sources feeding rivers	major point source in NE	minor source from SW (WCS material)
Waiomo MM	very limited	minor source	minor reworking into Brunner Bridge depocentre
Morgan CMM	active in W of basin, persistent in Rewanui area	initially in N, prograded S along intrabasin ridge, eventually into Brunner Bridge depocentre	eastern source for Greenland Group and volcanics
Ford Fm.	major source of pebbles and sand, to N of basin	minor lobe in NE, mixed	minor WCS source in SW, volcaniclastic source in S of lake
Jay Fm.	major source in NW	possible source, mixed	

Table 7.1 Summary of sediment source evolution during Paparoa Group deposition. WCS = Western Compositional Suite, derived from west or northwest of coalfield. ECS = Eastern Compositional Suite, derived from northeast of coalfield. All other sources are listed in the "other" column.

All units within the Paparoa Group at Greymouth Coalfield contain sediment derived from more than one source area. The granitic source area to the northeast was supplying sediment into the basin during Ford Fm. deposition, and possibly during Jay Fm. accumulation. Minor Greenland Group-derived material was also supplied from the northeast, and this continued until basal Morgan CMM deposition. At all times, Greenland Group-derived sediment entered the basin from various points along the northwestern basin margins, though this flux was very limited during Waiomo MM deposition. Localised sources, or minor reworking of sediment already within the Paparoa Basin, contributed the remainder of the sediment supply.

During periods of lacustrine deposition, there was a reduced influx of coarse sediment into the basin. However, many sources remained active, resulting in deposition of transitional lithosomes and debris flow conglomerates within the lakes. The exception is the northeastern ECS source, which appears to have been quiescent during Goldlight Fm. deposition. Fine sediment supply must have remained abundant during lacustrine deposition, and was transported into the lake basins as suspended load.

7.4.1 Implications for source areas

Change in clast composition between the coal measure units (Section 2.6.3) was previously interpreted as indicating progressive unroofing within the source area(s) (Newman 1985). The present analysis indicates that there is a complex history of sediment flux into the Paparoa Basin, however source area composition remained relatively constant, and sediment composition within the basin reflects mainly the proportion of sediment delivered by the various source areas.

Hornfels, quartzose sandstone and rhyolite clasts (Jay Fm.; Section 2.7.1), and large granite boulders (Rewanui CMM; Section 2.7.5) are restricted in occurrence to the far northwest of the coalfield (Twelve Mile Beach). These are regarded as exotic material, which was probably reworked from Pororari Group strata, or from unknown and now eroded sediments or basement rocks.

There were two basement lithologies which contributed sediment to the Paparoa Basin: Paleozoic Greenland Group and Mesozoic granite. In general, Greenland Group detritus was derived from the west or northwest, whereas granite detritus was derived from the northeast. Minor amounts of Greenland Group clasts also entered the basin from its southwest and eastern margins. As indicated above, during lower Paparoa Group deposition, Greenland Group clasts were also derived from the northeast.

Basement north of Greymouth Coalfield comprises Greenland Group and granite (Figure 1.2; Laird 1988). Both lithologies were exposed by tectonic unroofing during extension around c.100Ma (Tulloch & Kimbrough 1989; Laird 1993), and contributed clasts to the Pororari Group (Laird 1988; Topp 1996). Thus, change in clast composition during Paparoa Group deposition does not represent unroofing in the source area, but rather, records evolution of the sediment transport system. The river

system to the northeast of Greymouth Coalfield must have initially flowed across both basement lithologies, and as that system extended northwards, it intersected more granite within its catchment. Decline in Greenland Group supply from the northeast reflects sediment bypass between the granite source terrain and Greymouth Coalfield.

Absence of axially derived ECS material from Goldlight Fm. may be related to the reversal of sediment transport observed in the south of the coalfield, or alternatively, elevated base level would have shifted the locus of coarse clastic deposition upstream (northwards). Equivalent strata at Pike River Coalfield (Member 5; see Figure A1.1C), which comprise interbedded sandstone, siltstone and mudstone, and were deposited in a fluvial environment (Newman & Newman 1992), support the latter hypothesis.

7.8.2 Discussion of deltaic sequences

Coal measure lithosome depositional environments in Greymouth Coalfield have received much attention (e.g. Gage 1952; Bowman et al. 1984; Newman 1987; Ward 1995). However, lacustrine depositional environments have attracted less discussion, and deltaic subenvironments within Greymouth Coalfield have not been systematically described prior to this project. Facies associations (Section 2.3) and unit geometry (Section 3.8.2) clearly indicate that transitional lithosomes within lacustrine units are deltaic deposits, which represent limited transport of coarse clastic sediment (sand to cobbles) into the Ford, Waiomo and Goldlight lakes. There are differences between the deltaic units (Table 7.2), which reflect the nature of the various sediment sources, and differences in sedimentary process between the delta complexes.

Delta system	Geometry	Coarse clastics	Thickness/number of coarsening upwards packets	carbonaceous material at top
Western Goldlight Transitional Member	narrow apron plus lobes	mostly very fine-medium, up to granule	varies 1–25m, multiple packets	minor roots, rare carb. mst
Southern Goldlight Transitional Member	broad apron	mostly fine, up to very coarse	3-5m, multiple packets	not recorded
Waiomo MM	limited area in north, and along W margin of lake	up to very coarse	up to 12m, only 1–2 packets present	not recorded
Ford Transitional Member	broad fan	pebbles up to 12cm	up to 37m, often 10–20m, 1–4 packets present	thin carb. mst at tops of sequences

Table 7.2 Summary of deltaic sequences, Greymouth Coalfield

Coarsening upwards packets, which characterise transitional lithosomes within Greymouth Coalfield (Figure 2.2), are the product of repeated progradation of distributary mouth bars into shallow (<25m), non-stratified lakes (e.g. Hyne et al. 1979; Farquharson 1982; Flint et al. 1989; Tye & Coleman 1989; Postma 1990). Absence of Gilbert-type or gravelly fan deltas with steep foreset beds (e.g. Dunne & Hempton 1984), and rarity/absence of turbidite sandstones in distal parts of the various lakes (Postma 1990), supports the conclusion that lakes in the Paparoa Basin were shallow.

Shallow-water sandy lacustrine deltas comprise a delta plain, a gently inclined delta front (dominated by coarse sediment deposition), and a prodelta, which is dominated by hemipelagic deposition (Postma 1990). In the delta front, bar finger sand bodies, oriented perpendicular to the shoreline, are deposited, resulting in a lobate or birdsfoot delta (e.g. Hyne et al. 1979; Ayres 1986; Flint et al. 1989). Levees, which constrain distributary channel position and result in elongate delta morphologies, are poorly developed in such systems (Flint et al. 1989).

Upper Goldlight Transitional Member lithosomes in the west of Greymouth Coalfield are the most variable of the deltaic deposits, with individual coarsening-upwards packets ranging in thickness from 1m to 16m (Table 7.2). The intercalated mudstone beds are thin in the west, where no lacustrine lithosome has been recognised (Figure 3.9, 3.10), whereas sand bodies become thinner and less frequent offshore (to the east). Bar-finger to lobate sand bodies indicate stability of the sediment sources during deposition. Plugging of channels by sediment diverted sand into interdistributary bay areas, resulting in rapid lateral changes in sand body frequency and thickness.

One feature of many upper Goldlight Transitional Member sequences in the west is the upwards transition from typical coarsening upwards cycles with funnel-shaped log patterns (Figure 2.2) to thinner-bedded cycles resulting in a serrate log pattern (Figure 7.6A). This represents reduction in depositional water depth as the delta prograded, though lack of carbonaceous sediment suggests much of the delta plain remained submerged. Thin mudstone beds within conglomeratic strata which are correlated with Goldlight Fm. in DH619 and DH621 (Appendix 2, Section 6.3) represent minor transgressions of the lake onto the upper (fluvial) delta plain.

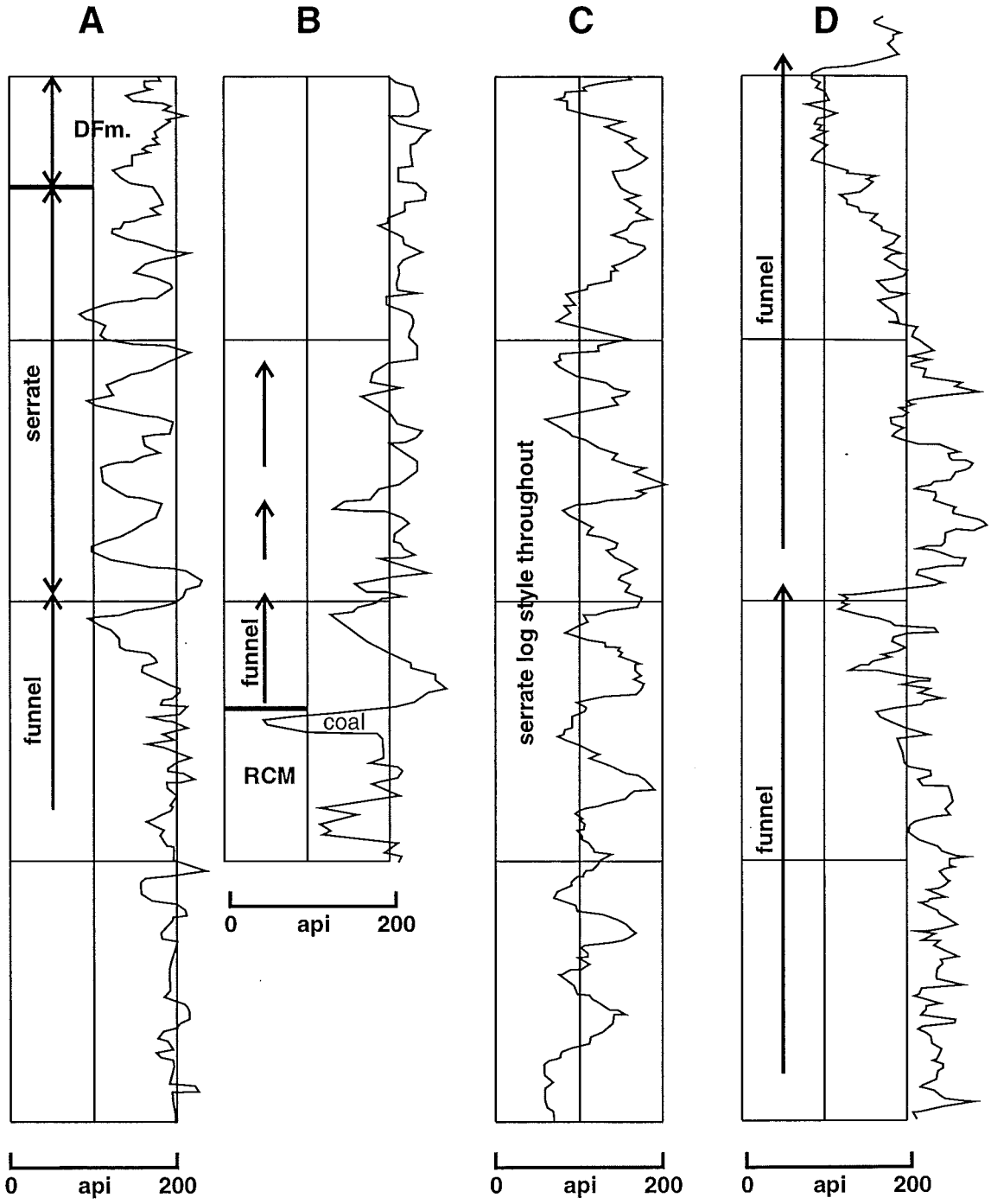

Figure 7.6 Selected geophysical (gamma-ray) logs for transitional lithosomes, Greymouth Coalfield.
A = western upper Goldlight Transitional Member (DH696, 140-180m)
B = southern lower Goldlight Transitional Member (DH651, 470-500m)
C = southern upper Goldlight Transitional Member (DH654, 460-500m)
D = Ford Transitional Member (DH624, 238-280m)

DFm. = Dunollie Fm., RCM = Rewanui CMM

The southern Goldlight Transitional Member, Ford Transitional Member and minor Waiomo MM delta complexes represent variations on the shallow lacustrine delta environment described above. Low sediment supply in the northeast during Waiomo MM and Ford Fm. deposition resulted in minor deltas. The isolated occurrence of mixed ECS and WCS transitional lithosomes in the west of the Waiomo MM basin (DH632, DH656) suggests movement of ECS sediment southwards around the lake shore. Goldlight Transitional Member in the south of the coalfield occurs in a widespread apron, and individual lobes cannot be recognised (Figure 3.9, 3.10). Limited data for the southern lower Goldlight Transitional Member delta (5 drillholes, only 2 with geophysical logs) suggests that only three pulses of coarse sediment entered the basin from the south. The first of these pulses prograded across uppermost Rewanui CMM peats in DH651 (Figure 7.6B).

In the southern upper Goldlight Transitional Member, coarsening upwards cycles are generally only 3–5m thick, resulting in serrate log patterns with many superimposed prodelta to mouth-bar packets (Figure 7.6C). Thin beds may reflect lower sediment supply in the south, or lack of persistence of individual channel systems. Flint et al. (1989) attributed areally extensive deltaic sand bodies (as opposed to bar-finger sands) to complex splitting of delta channels due to high sediment load and highly variable discharge rate, resulting in a broad, lobate delta. Limited data precludes correlation of individual mouth-bar sand bodies in the southern upper Goldlight Transitional Member, and continuity of sand deposition between drillholes cannot be confirmed. However, coarse sediment penetrated c.6km into the lake, suggesting the transport system was persistent.

A possible explanation for the southern upper Goldlight Transitional Member delta morphology is that coarse sediment would not have been fed from a point source (as depicted by Flint et al. 1989), but rather from a broad zone comprising the distal end of the former axial fluvial system, in which transport was now reversed (see above). As sand prograded into the shallow lake basin from multiple streams, an apron of coalesced mouth-bar deposits would have accumulated. Such a scenario was demonstrated in the axial fluvial system of a pull-apart basin by Dunne & Hempton (1984), and corresponds to the braid deltas depicted by McPherson et al. (1987).

The final delta system requiring discussion is the main Ford Transitional Member delta complex, which is distinguished from other delta systems by the overall coarse grainsize, presence of coal clasts, broad fan-like geometry, and the limited number of thick, coarsening upwards packets (Table 7.2, Figure 7.6D). Another feature of the Ford Transitional Member is that it overlies a thick (>100m in places) mudstone unit in the depocentre, but also overlies basement in the southwest, indicating enlargement of the basin during upper Ford Fm. deposition.

Initiation of Ford Transitional Member deposition was accompanied by an influx of coarse (gravelly) sediment into the Ford lake basin, as indicated by debris flow deposits in DH657. Basal coarsening upwards packets are up to 22m thick, and thin southwards from the depocentre towards the basin margin. The thickness of these units may be taken as an approximate estimate of water depth.

In order for the basin to enlarge, relative lake level would have risen, resulting in a transgression of c.1km in the southwest. Very thick coarsening upwards packets (up to 37m in DH656) occur in the upper part of the unit in the depocentre, which suggests at least c.40m of water was present in the lake. A similar thickness of Ford Transitional Member overlies basement in DH651 (37.8m), and the similarity of unit thickness in the depocentre and at the basin margin suggests the relative lake level rose c.40m towards the end of Ford Transitional Member deposition.

An absolute (regional) rise in lake level would have moved the locus of coarse clastic deposition up the depositional slope towards the source area in the northwest. However, coarse sediment continued to be supplied to the delta front environment, suggesting that change in base level was restricted to the lake basin. The likely control was a tectonic subsidence event, during which the lake basin and the southwestern basement block subsided about 40m. A broad delta complex prograded southwards into the enlarged lake, indicating that coarse sediment load remained high (as for the southern upper Goldlight Transitional Member). Deeper lake water resulted in deposition of thicker coarsening-upwards lithosomes than observed in other delta complexes (Table 7.2).

7.9 Conclusion

Sediment transport patterns within Greymouth Coalfield are delineated by unit geometry, textural variation, composition (especially of coarse clastics) and coal seam distribution. Throughout deposition within the Paparoa Basin, there was an interplay of two source areas, which supplied different textures and compositions of detritus into the basin. The northeast (axial) source area evolved from being insignificant during deposition of lower units, to providing a large sediment flux during Rewanui CMM deposition, and then declining during Goldlight Fm. accumulation. The northwest source area shed similar material into the basin at all times, with the addition of some reworked material during early Paparoa Group deposition. Some sediment was also derived from the immediate basin margins, though local sources were only significant during Morgan CMM deposition.

Recognition of deltaic deposits provides an additional tool for understanding sediment dynamics within the Paparoa Basin. Deltaic sediments record the entry of coarse sediment into the basin when fine sediment was predominant, and specific sediment sources can be identified from unit geometry, texture and composition. Differences between the various deltaic complexes can be attributed to variation in water depth, sediment supply, tectonic subsidence and source character (linear vs. point sources). However, all deltaic deposits were the result of progradation of distributary channels into shallow lakes.

Sources of coarse clastic sediment during deltaic deposition were often coincident with sediment transport features present during fluvial sedimentation, suggesting a common control. The role of tectonics in controlling basin geometry and sedimentary dynamics is highlighted in the next chapter.

Chapter 8. Tectonic evolution of the Paparoa Basin

8.1 Introduction

The objective of this chapter is to reconstruct the tectonic setting of the Late Cretaceous to early Tertiary Paparoa Basin at Greymouth Coalfield. Previous studies (see below) have demonstrated that the Paparoa Basin was extensional. Development of a tectonic model requires integration of observed geology into the general structural framework for extensional basins. The task is complicated by deformation associated with basin inversion, and tectonic features must generally be inferred from the results of basin analysis (e.g. Leeder & Gawthorpe 1987; Frostick & Steel 1993a).

Understanding of rift basins has increased markedly in the last c.15 years, which may partially be attributed to the increased resolution of seismic methods (e.g. McWhorter & Torguson 1995). Knowledge of rift basins can be broadly subdivided into geodynamics, i.e. the crustal mechanisms of rifting (e.g. Olsen & Morgan 1995), and structural details within rift systems (e.g. Morley 1995). A third significant advance is the understanding of tectonic controls on basin fill patterns and depositional environments, following the seminal paper of Leeder & Gawthorpe (1987).

8.2 Overview of existing tectonic models for Greymouth Coalfield and environs

The role of Late Cretaceous to early Tertiary extensional tectonics as a primary control on basin formation and sedimentation within the Paparoa Group, and throughout the West Coast region, has been emphasised by previous workers. A schematic block model for basement faulting within the Paparoa Basin developed by Bowman et al. (1984) divided the basin into depocentres separated by more stable areas (Figure 8.1). This model emphasised NNE/SSW trending structures which were functional from Rewanui CMM deposition onwards (especially the basin margin faults), and did not include the WNW/ESE trending structures evident during Jay Fm. and Ford Fm. deposition. Bowman et al. (1984, p. 73) stated that the latter structures had little influence on Morgan CMM or younger sedimentation.

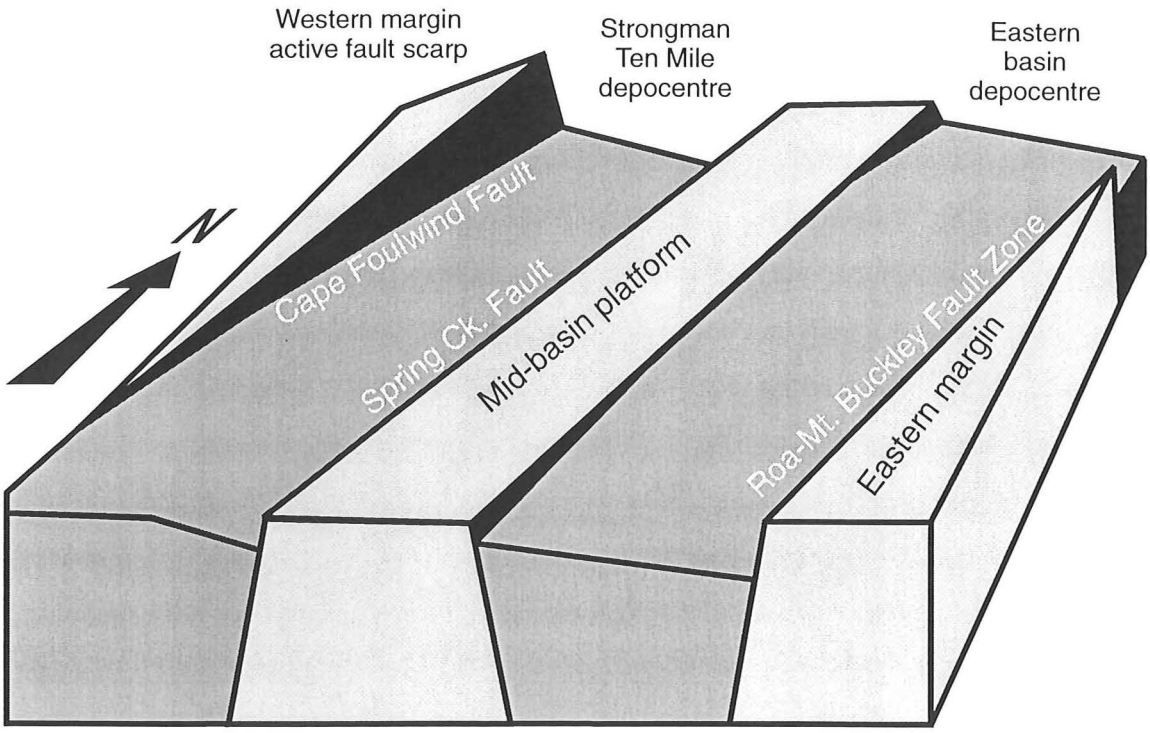

Figure 8.1 Schematic tectonic model for Paparoa Group, Greymouth Coalfield, after Bowman et al. (1984, Figure 18).

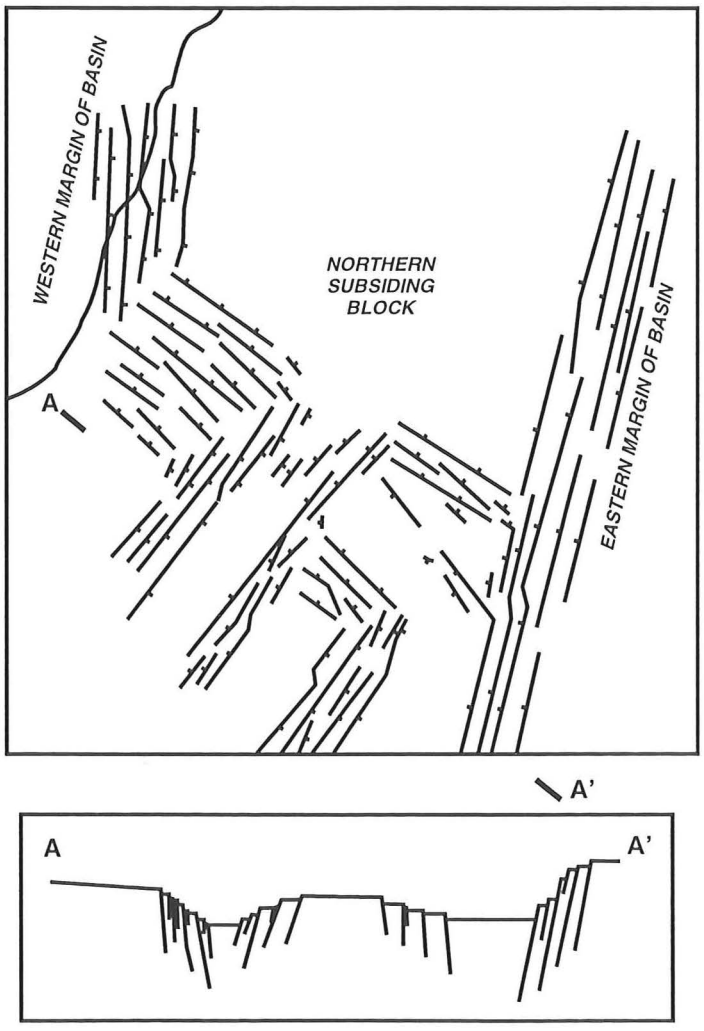

Figure 8.2 Schematic structural model for Paparoa Group, Greymouth Coalfield. From Newman (1981).

A more complex model for basin structure was presented by Newman (1981), which incorporated both NNE/SSW and WNW/ESE structural trends (Figure 8.2). Important features of this model are the lack of structure depicted within the northern subsiding block, and the bifurcation of the basin south of Rewanui into two troughs through which coarse (ECS) clastic sediment was transported southwards. The model also suggested a southern continuation of the basin in the Brunner Bridge area.

Both the structural models discussed above described similar structural elements, but the relative role of the two structural orientations received different emphasis. Both models are most relevant to basin development during Rewanui CMM deposition, and neither accounts for changes in basin geometry during filling of the basin. The models provide a conceptual framework for interpreting the tectonic history of the Paparoa Basin, however neither is consistent with current structural models for rift basins.

Regional geology illustrates that Late Cretaceous and early Tertiary extension occurred throughout the West Coast area (e.g. Laird 1968, 1993; Nathan et al. 1986). Cretaceous-age normal faults with a WNW extension direction are present at Twelve Mile Beach (D.U. Wise pers. comm. 1993). Morgan CMM volcanics at Pike River Coalfield posses continental rift-like geochemistry (McDougall 1993), and correlative rocks elsewhere in the region (Appendix 4.6) indicate widespread Late Cretaceous extension.

The presence of two fault and basin orientations at Greymouth Coalfield has been interpreted as the product of rotation of the extension direction from NNE to WNW at c.70Ma, between Jay Fm. and Morgan CMM deposition (Laird 1993, 1994, 1996), or oblique extension (Bishop 1991, 1992). A Late Cretaceous strike component of movement has not been interpreted for any faults in the Westland region (D.U. Wise, pers. comm. 1993; McDougall 1993; McNee 1997). However, younger overprinting and fault reactivation during Neogene basin inversion (Bishop & Buchanan 1995), and the effects of erosion, may have obscured or destroyed primary movement indicators on faults which were present in the Cretaceous.

8.3 Input data for reconstruction of tectonic setting

The primary sources of information for tectonic reconstruction of the Paparoa Basin are the decompacted isopach maps and tectonic subsidence maps presented in Chapter 4. Isopach or isotect patterns and the KTB timeslice map (Figure 6.1) indicate the location of specific faults. Less direct evidence for fault location comes from basin geometry, the coincidence of basinal features, and from sediment source locations (Chapter 7). Regional geology also assists in the location of major faults.

8.3.1 Isopach models

Basin-floor geometry in rift basins can be depicted with structure contour maps, sonic travel-time maps, bathymetric maps and isopach maps of the synrift sequence (e.g. numerous papers within Keller & Cather (1994) and Lambiase (1995)). In the present study, decompacted isopach maps and tectonic subsidence maps (Chapter 4) define the geometry of the basin during the deposition of each unit, and may be used as an approximation for structure contour maps for basin floor geometry. As discussed in Section 4.4, the decompacted isopach patterns were influenced by more factors than tectonic subsidence alone (e.g. paleotopography, paleogeography, depositional water depth, erosion), and are probably minimum estimates for true tectonic subsidence. However, recognition that the various lacustrine deposits were deposited in shallow lakes (Section 7.4.2) reduces one potential source of underestimation of tectonic subsidence from the respective isopach or isotect patterns.

Maximum subsidence in rift basins occurs adjacent to the largest (often basin-bounding) faults (e.g. Schlische 1991). The deepest part of an extensional basin lies at the intersection of the basin bounding fault with the basin floor (Figure 8.3A), and will migrate with time (Schlische & Anders 1996). Direct measurement of cumulative fault displacement (e.g. Nicol et al. 1996) confirms that maximum displacement occurs in the centre of individual faults. Furthermore, there is a scaling relationship between fault length and total displacement over at least 8 orders of magnitude (Figure 8.3B), though the exact nature of the relationship is the subject of debate (e.g. Schlische & Anders 1996; Schlische et al. 1996; Nicol et al. 1996). Minimum subsidence within half-graben rift basins occurs above the flexural margin (Figure 8.3A), along which there is only limited extension on many minor faults (Morley 1995, Table 1).

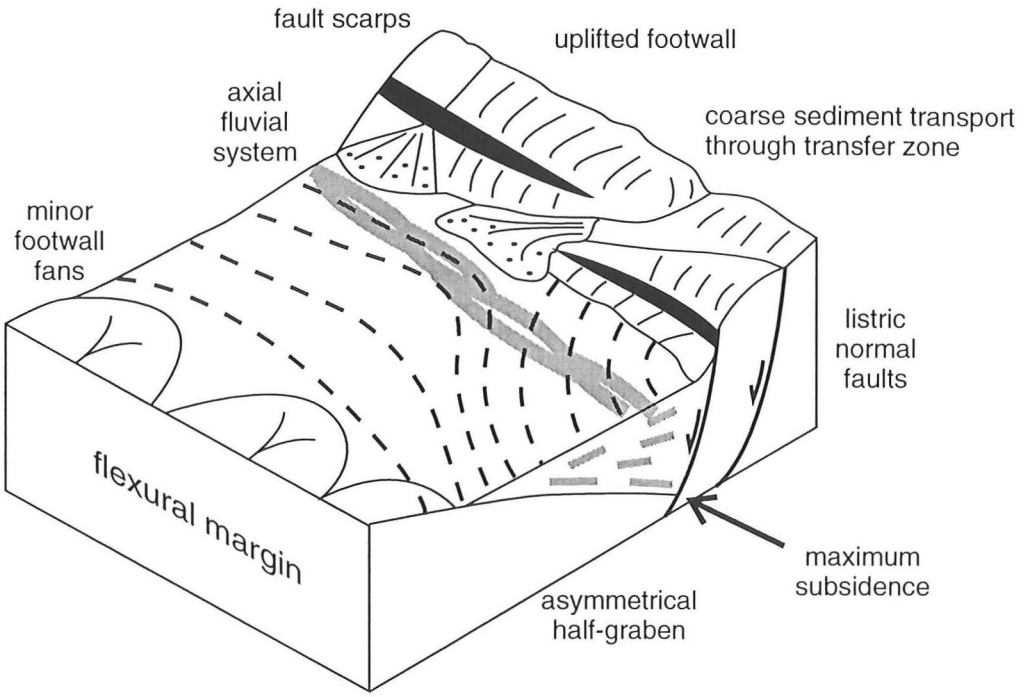

A. Generalised model for continental half-graben with axial through drainage. Modified from Leeder & Gawthorpe (1987). Dashed lines are isopach pattern of synrift sediments.

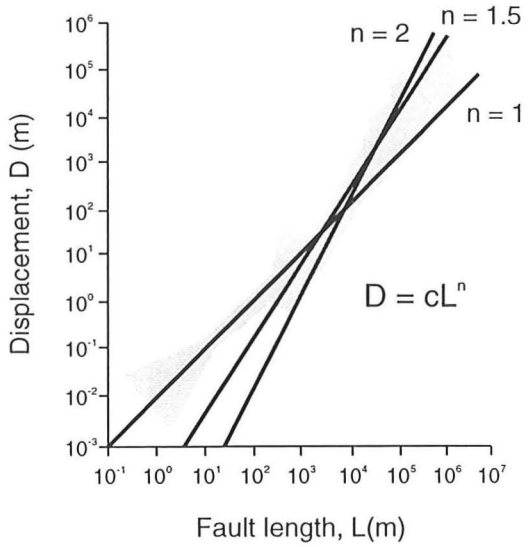

B. Log-log plot of fault length vs. displacement. Scaling law and proposed values for n are indicated. c = a constant related to rock properties. From Schlische & Anders 1996, Figure 2. Stipple is area of data points on original plot.

Figure 8.3 Elements of the conceptual framework for interpretation of tectonic setting of the Paparoa Basin, Greymouth Coalfield.

The relationship between depocentre location and causative structures enables structural parameters (e.g. fault length, displacement and dip) to be estimated from isopach models. Maximum pre-burial basin-fill thickness adjacent to the eastern basin margin was c.1000m (Figure 4.18, B–B'), and the fault throw vs. length relationships shown in Figure 8.3B suggest that the eastern basin bounding fault was c.20–30km long. Such a fault is consistent with the present-day dimensions of the basin (>13km north–south).

Use of point data (e.g. drillholes) for mapping of smaller scale features in rift basins, such as intrabasin faults and transfer zones, is difficult (Peacock and Sanderson 1994), because of smoothing inherent in the isopach construction techniques (e.g. Appendix 3). Isopach lines in a sub-basin or basin are not necessarily parallel to the adjacent major faults. They may be oblique or perpendicular to structural trends, and are commonly truncated against the fault plane (e.g. Peacock & Sanderson 1994, Figure 7; Morley 1995, Figure 10). In the present study, isolines depicted in Chapters 3 and 4 are not truncated, but are generally smoothed. Thus, individual sub-basins adjacent to discrete faults cannot always be identified with certainty.

8.3.2 Location of faults

Previous chapters have identified minor faults within Greymouth Coalfield from stratigraphic evidence, isopach models and tectonic subsidence estimates. A NNE/SSW oriented fault aligned approximately along Spring Ck. is interpreted as controlling the distribution of tuffaceous material within Ford Fm. (Section 4.2.2). Small-scale faulting is also interpreted within the southwestern basement block during Rewanui CMM deposition (Section 4.2.5, Figure 4.12). Palynostratigraphy enables recognition of an arcuate fault in the central Rapahoe Sector which influenced uppermost Rewanui CMM and lower Goldlight Fm. sedimentation (Section 6.5).

Less direct evidence for fault location comes from identification of sediment transport paths, which were persistent during deposition of many units (Chapter 7). The entry point of the axial (ECS) fluvial system into the Paparoa Basin was persistent, and was probably structurally controlled. At the intrabasin scale, sediment sources along the southern and western basin margins (Section 7.8) provide evidence for the location of smaller structural features. Persistent coarse sediment influx typically occurs at transfer zones between individual extensional faults (Gawthorpe & Hurst 1993; Morley 1995).

Transfer zones along the margins of the Paparoa Basin were probably small-scale transfer faults or relay ramps, along which foot-wall derived sediment passed (Gawthorpe & Hurst 1993). Southwestern sediment sources (Chapter 7) represent streams flowing across the flexural basin margin (e.g. Figure 8.3A).

8.3.3 Relationship between present-day and basin forming faults

Greymouth Coalfield is an inverted basin, and movement on Late Cretaceous and early Tertiary faults, which controlled rift basin sedimentation, was reversed by Neogene to recent compressional tectonics (Bishop & Buchanan 1995). The NNE/SSW oriented faults depicted by Bowman et al. (1984) as controlling Rewanui CMM sedimentation (Figure 8.1) correspond with zones of present-day structural disruption within the coalfield. In particular, the Roa–Hawera Fault (Figure 1.2) provides a structural link between Greymouth Coalfield and Pike River Coalfield to the NNE, and represents the reactivated Late Cretaceous basin-bounding fault zone.

8.3.4 Summary of tectonic elements

Regional geology and stratigraphic evidence indicates the Paparoa Group in Greymouth Coalfield was deposited in a predominantly NNE/SSW oriented rift basin. The Paparoa Basin was bounded by normal faults in the east and a corresponding flexural and faulted margin in the west. Persistence of coarse sediment supply from the western basin margin (Section 7.9) is inconsistent with the general model for continental half-graben fill (Leeder & Gawthorpe 1987; Figure 8.3A). However, the elements of that model, in particular controls on basin asymmetry and sediment input, remain valid and are used as a general framework for tectonic interpretation of the Paparoa Basin. Tectonostratigraphic models for extensional basins are discussed further in Section 9.3.

Faults in the tectonic models discussed below are shown schematically as having arcuate surface traces, which is consistent with some observations (e.g. Figure 6.1). However, this depiction may not be realistic, and listric faults which are curved in cross-section can have straight traces (Morley 1995). Fault dips were estimated from the cross-sections presented in Chapter 4, making allowance for vertical exaggeration.

8.4 Tectonic evolution of the Jay and Ford Formation basin

8.4.1 Jay Formation

Jay Fm. represents the commencement of sedimentation in the Paparoa Basin, hence there is likely to have been some control (probably tectonic) to initiate subsidence and basin formation. Previous discussions (Section 4.2.1) suggested the presence of paleotopography, and this probably comprised a c.100m deep valley eroded into Pororari Group, an associated WNW/ESE oriented basin-bounding fault zone, and surrounding basement. At the initiation of sedimentation, the valley floor subsided along paired N/S to NNE/SSW oriented normal fault zones at either end of the basin (Figure 8.4). Transfer zones along the northwest margin provided sites of sediment influx (Section 7.2), and the southeast end was dammed by westwards-dipping fault scarps. Thickening of Jay (iii) coal measures to the northwest (Section 3.3) indicates tilting of the basin floor in that direction towards the end of Jay Fm. deposition.

A secondary, fault-controlled basin developed to the south of the main depocentre (Figure 3.1, 4.2). The southern margin was probably controlled by en echelon small normal faults oriented approximately NW/SE (Figure 8.4). Similar faulting may have also occurred on the flanks of the paleogeographic high beneath Mt. Davy, and across the northern limit of Jay Fm. occurrence. Evidence for active faulting within the main Jay depocentre is poor, though reactivation of pre-existing WNW/ESE oriented structures was likely.

8.4.2 Ford Formation

Previous analysis (Section 4.2.2, Figure 4.5) indicated that Ford Fm. was deposited in a similar basin to the Jay Fm. Coarse sediment fed into the basin from the northwest during upper Ford Fm. deposition, indicating persistent structural movement (Figure 8.4). Rare debris flows in the Ford Fm. (e.g. DH656; Section 2.7.2) may have been triggered by seismic activity on the northern basin-bounding faults. Subsidence along the southwestern margin of the Jay Fm. basin persisted during Ford. Fm. deposition, resulting in relatively rapid thickness increase across this area on the combined Jay/Ford isopach model (Figure 4.4). Rapid eastward thinning of Ford Fm. (Figure 4.5, A–A') suggests the eastern basin-bounding fault, which probably initiated Jay Fm. deposition, remained active.

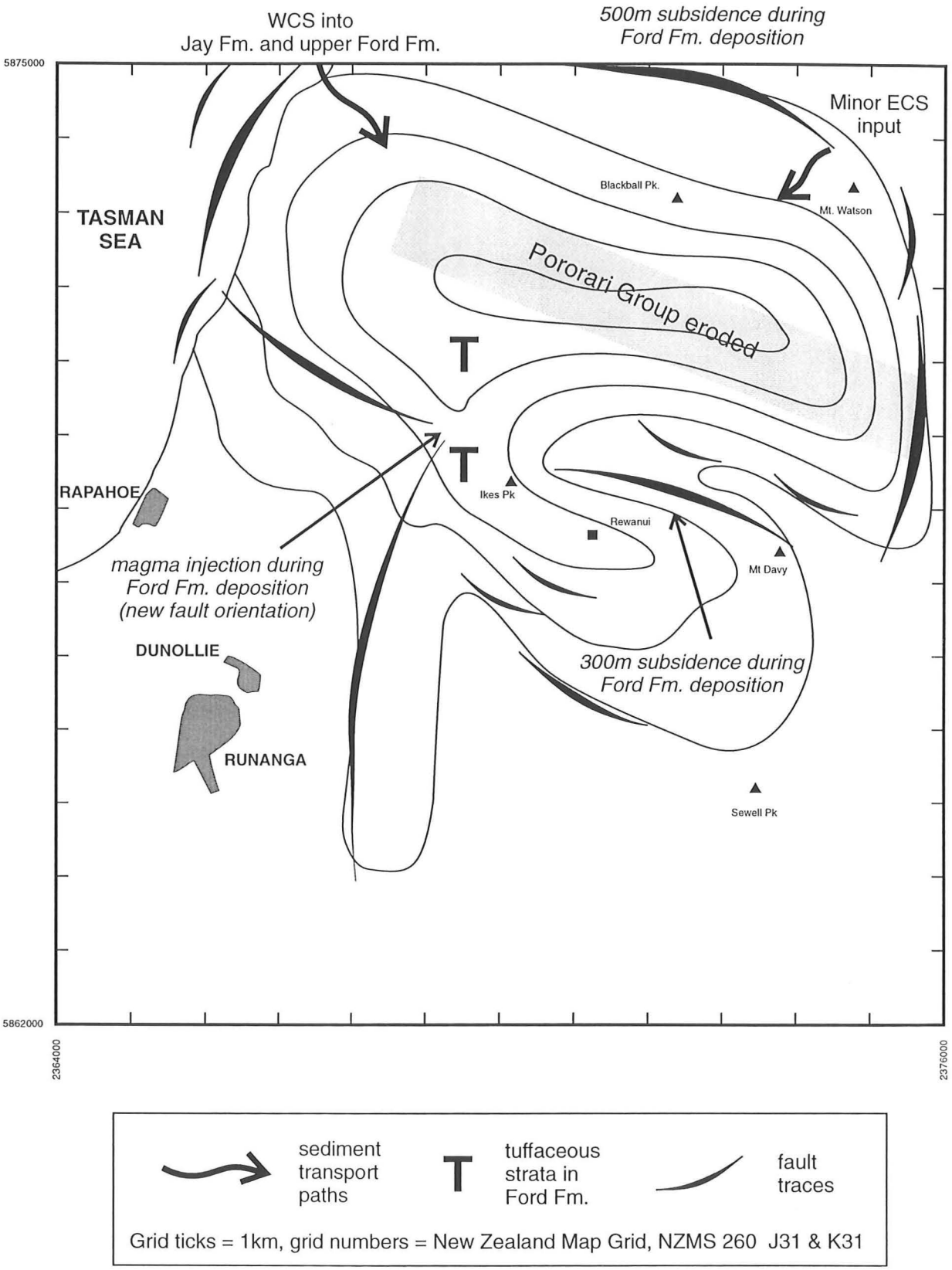

Figure 8.4 Summary of tectonic controls and sediment transport paths, Jay Fm. and Ford Fm. The combined Jay/Ford isopach pattern is shown, isopach interval = 100m.

During Ford Fm. deposition, the intrabasin high running NW from Mt. Davy became a prominent feature, with c. 400m maximum basin floor relief (Figure 4.5). The basins on either side of this ridge were slightly asymmetrical, and were controlled by southwesterly dipping shallow (c.15°) normal faults (Figure 8.4). Displacement on the faults was c.300m (southern) and c.500m (northern), which corresponds to trace lengths of 5–10km (Figure 8.3B). These estimates agree with basin dimensions (Figure 4.3).

Tuffaceous strata within the Ford Fm. were interpreted to have resulted from dike injection along a NNE/SSW oriented fault (Section 3.4.1, 4.2.2). The same fault was responsible for the thin southern extension of the Ford Fm. basin (Section 3.4.1). This fault may also have limited westwards propagation of the fault which formed the southern side of the topographic high, with the two structures intersecting near DH632. Magma injection accompanied the initiation of the NNE/SSW fault trend, and the corresponding fault was the earliest expression of the Spring Creek Fault Zone.

Towards the end of Ford Fm. deposition, the basin enlarged, as a result of relative base level rise of c.40m (Section 7.8.2). This event was controlled by subsidence of both the basin floor, and the adjacent basement blocks to the southwest and east, and is indicated by deltaic deposition over basement (Section 7.8.2) and overtopping of the intrabasin high (Figures 4.5). Subsidence of structurally controlled areas of emergence suggests that movement on those structures was not responsible for the basin-wide subsidence event. A probable cause was renewed movement of the NNE/SSW oriented fault set, accompanied by reduced differential subsidence within the basin.

8.5 Tectonic evolution of the Rewanui Formation basin

The primary source of information for reconstruction of tectonic events active during Rewanui Fm. deposition is the tectonic subsidence map presented in Figure 4.14. Summation of subsidence components for all Members of the Rewanui Fm. overcomes the complications of non-tectonic influences on member thickness within the Rewanui Fm., such as lateral equivalence between basal Rewanui CMM and western Morgan CMM. However, structural details also can be interpreted from Morgan CMM and Waiomo MM isopach patterns, which provide an insight into tectonic evolution of the Mt. Davy Sector during early Rewanui Fm. accumulation.

8.5.1 Morgan Coal Measure Member

Three depocentres are present within Morgan CMM (Section 3.5). The western depocentre was bounded to the west by a new fault which extended the Spring Creek Fault zone northwards. Correspondence of Morgan CMM in the western depocentre to the underlying Jay/Ford depocentre (Section 4.2.3, Figure 4.7) suggests that minor subsidence on the WNW/ESE oriented fault at the north of the basin continued (Figure 8.5). However, there is no evidence for the basement high within the Morgan CMM basin, and strongly differential subsidence in the Rewanui area had ceased.

The eastern Morgan CMM depocentre represented a new locus of subsidence, overlying an area where underlying strata are thinning(Section 4.2.3). This sub-basin is further east than other Paparoa Group occurrences (Section 3.5), and was partially filled with volcaniclastic strata. Sediment transport patterns (Section 7.4) indicate this area did not receive ECS material from the northeast. The depocentre can be attributed to fault development in the footwall of the previous eastern basin margin, creating a basin and providing a conduit for magma injection. Greenland Group-derived sediment, sourced locally on the footwall, would have entered this basin around the ends of the eastern basin-bounding fault (Figure 8.5).

Bowman et al. (1984, p. 74) considered that the location of the Morgan CMM volcanics may be explained by the intersection of the WNW and ENE fault trends. While the volcanics are adjacent to Pororari Group sediments (Figure 1.2), this study indicates there was minimal subsidence on the WNW-oriented faults during Morgan CMM deposition.

Separating the eastern and western Morgan CMM depocentres was a NE/SW aligned ridge, and sediment transport patterns (Section 7.4) suggest this ridge was a west-facing fault scarp, or perhaps a series of scarps. There was a minor basin on the western side of this fault system (Figure 8.5), along which ECS sediment passed from the NE source into the southern depocentre. The southern Morgan CMM depocentre, near Brunner Bridge, represented another new locus of subsidence, controlled by a small normal fault at its eastern end (Figure 8.5).

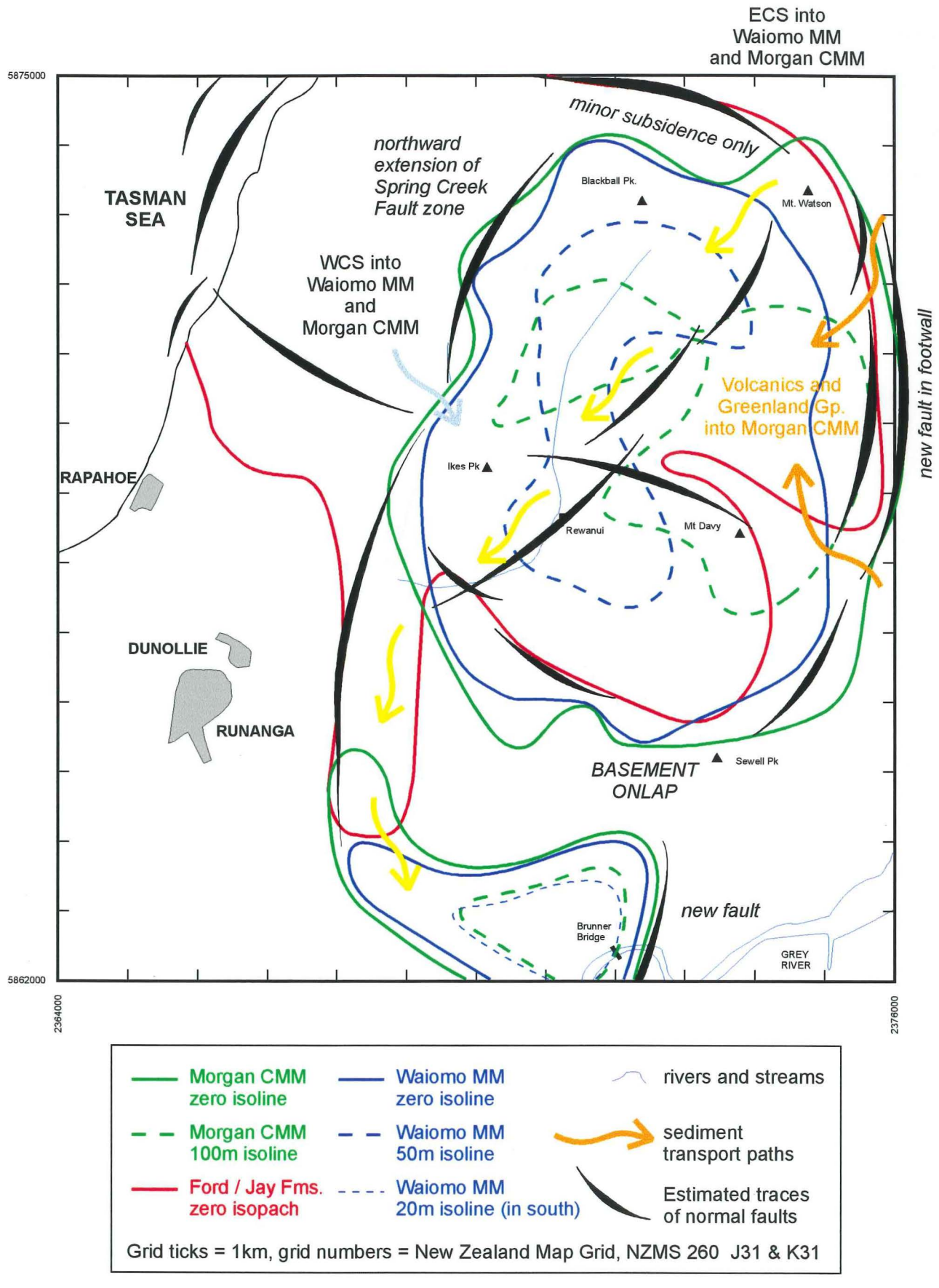

Figure 8.5 Summary of tectonic controls and sediment transport paths, Waiomo MM and Morgan CMM.

Data are sparse for interpretation of tectonic controls on Morgan CMM distribution in the southeast of the coalfield, and isopach patterns (Figure 4.6) suggest there was onlap onto basement around the southeastern part of the eastern Morgan CMM depocentre (Figure 8.5). A ridge of basement separated the main Morgan CMM depocentres from the minor Brunner Bridge depocentre, suggesting persistent topography in the area.

8.5.2 Waiomo Mudstone Member

Limited tectonic information can be interpreted from the decompacted Waiomo MM isopach pattern (Figure 4.8). The thickest occurrence in the north indicates persistent (but minor) subsidence on the WNW/ESE trending structures which dominated during deposition in the Jay/Ford basin (Figure 8.5). Though overall occurrence of Waiomo MM and Morgan CMM is similar, isopach patterns are discordant (Section 3.6), suggesting that subsidence on some faults which controlled Morgan CMM deposition (e.g. the central ridge and eastern depocentre) declined during Waiomo MM deposition. Thickness variation within the Waiomo MM basin therefore reflected subtle influences of pre-existing structures rather than strongly differential subsidence.

There is no equivalent to Waiomo MM in the Rapahoe Sector (Section 2.6.4), thus Waiomo MM deposition must have resulted from a discrete subsidence event which influenced only the Mt. Davy Sector (Section 4.2.4). This event resulted in a relative base level rise by at least 25m throughout the Mt. Davy Sector, probably controlled by synchronous subsidence along the Spring Creek Fault zone and the eastern basin-bounding fault zone.

8.5.3 Rewanui Coal Measure Member

Previous analysis demonstrated that maximum Rewanui CMM thickness prior to burial was in two depocentres, in the northern Rapahoe Sector and throughout the Mt. Davy Sector (Figure 4.9). Basin expansion during Rewanui CMM deposition resulted in an isopach pattern which was discordant with underlying basins (Section 4.2.5). However, this need not imply development of new tectonic trends. Rather, Rewanui CMM deposition was accompanied with reinforcement of some existing trends, and waning of activity on other fault orientations (Figure 8.6).

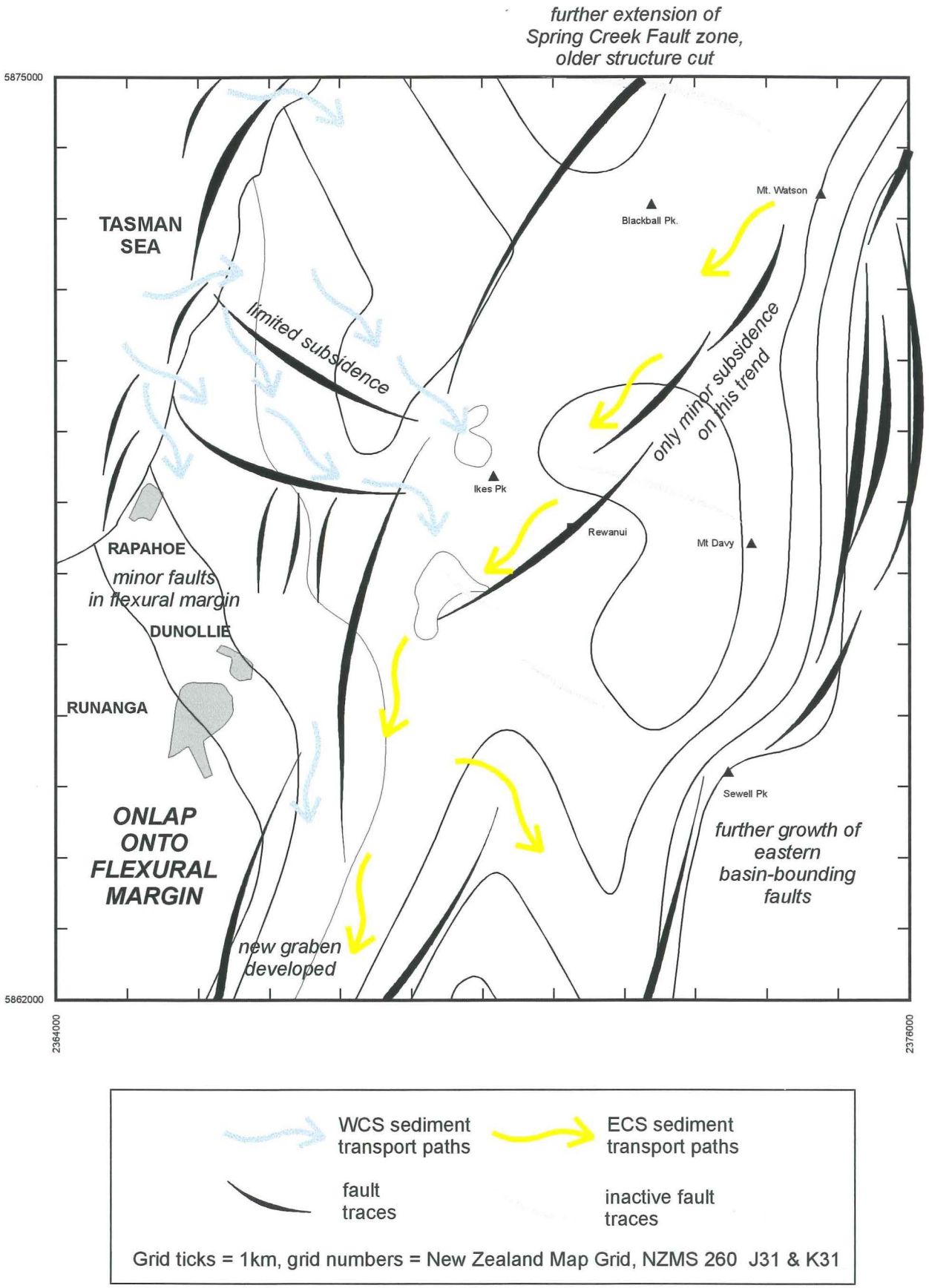

Figure 8.6 Summary of tectonic controls and sediment transport paths, Rewanui CMM. Tectonic subsidence map shown for reference, isotect interval = 100m.

In the Mt. Davy Sector, existing NNE/SSW trending faults enlarged and additional faults developed along the eastern basin margin. Movement ceased on the WNW/ESE trending structures which strongly influenced Ford and Jay deposition and were modestly active during Morgan CMM and Waiomo MM deposition. The northernmost WNW/ESE fault plane was probably bisected by northwards extension of the Spring Ck. Fault zone (Figure 8.6). In the southern Mt. Davy Sector (Brunner Bridge area), previously minor basins expanded and the paleogeographic high west of Sewell Pk. (Figure 8.5) was covered. The southern conduit which directed sediment into the Brunner Bridge depocentre expanded (Section 4.2.5), and was bounded by paired normal faults forming a small graben.

Major basin expansion occurred in the Rapahoe Sector during Rewanui CMM deposition, with strata onlapping a large area of basement (Section 3.7). The basement block was a flexural margin, cut only by small-scale faulting east of Rapahoe (Section 4.2.5). The fault which influenced sedimentation spanning the KTB (Section 6.5) was subparallel to an earlier WNW-trending fault to the north (Figure 8.6). The "KTB" fault position is also approximately coincident with the southwestern margin of the Jay/Ford basin (Figure 8.4), suggesting that the fault was in existence prior to Rewanui CMM deposition (Ward 1995). However, offset on WNW/ESE faults is not evident in cross-sections (Figure 4.10) or the tectonic subsidence model (Figure 4.12), indicating that the effects of these faults, though measurable with detailed stratigraphic studies (e.g. Section 6.4), were minimal in comparison to total unit thickness.

Sediment transport patterns (Figure 7.4) provide support for the Rewanui CMM tectonic model presented in Figure 8.6. In the Rapahoe Sector, coarse sediment entered the basin along the length of the western basin-bounding fault zone. Transport paths in the central Rapahoe Sector flowed across the Spring Ck. Fault zone 1km west of Ikes Pk., through the same transfer zone which fed ECS sediment into the Morgan CMM and Waiomo MM basins (Figure 8.5). Coal seam trends (Ward 1995, Figure 10) suggest some sediment was also diverted southwards along the footwall of the southern Spring Ck. Fault, emerging through the fault zone southeast of Dunollie (Figure 8.6).

In the Mt. Davy Sector, ECS sediment feeding from the northeast followed the line of faults which had separated the eastern and western Morgan CMM depocentres (Figure 8.6), though there was no additional subsidence along these faults during Rewanui CMM deposition. Subsidence along the Spring Ck. Fault zone prevented ECS sediment from entering the Rapahoe Sector, though minor splays in the uppermost Rewanui CMM which crossed the fault zone (Figure 7.4) indicate subsidence in the Mt. Davy Sector declined during upper Rewanui CMM deposition. Faulting near Brunner Bridge created a sub-basin into which ECS material moved southeastwards, and the earlier path which fed sediment into the Brunner Bridge depocentre (Figure 8.5) ceased to function.

8.5.4 Summary of structural controls, Rewanui Formation

All tectonic elements identified within the Paparoa Basin during Rewanui Fm. deposition are illustrated in Figure 8.7. Throughout this period, NNE/SSW oriented faulting was the dominant control on sediment transport and accumulation, though minor subsidence along WNW/ESE oriented structures continued in the Rapahoe Sector. Intrabasinal faults had only a small influence on total subsidence, though sediment transport tended to follow existing structures within the basin. Onlap onto basement in the southwest, and lengthening of the eastern basin-bounding fault zone to both the south and north indicates Rewanui Fm. deposition accompanied a period of basin expansion. However, basin fill was largely influenced by existing basin geometry and controlling structures.

8.6 Tectonic evolution of the Goldlight Formation basin

Goldlight Fm. was deposited in a broadly asymmetrical basin controlled by NNE/SSW oriented structures, with continued onlap to the southwest (Figure 8.8). Thickness variation in the Rapahoe Sector can be largely attributed to paleogeographic influences (i.e. delta progradation; Section 4.2.7), however the coincidence of thickness anomalies with the location of existing faults suggests the locus of deltaic sedimentation was controlled by tectonic subsidence. Continued influx of coarse clastic sediment into the Goldlight Fm. lake, and lateral transition to Dunollie Fm. in the west of the basin, indicates persistent activity along the western basin-bounding fault complex, with sediment feeding through transfer zones, as discussed above.

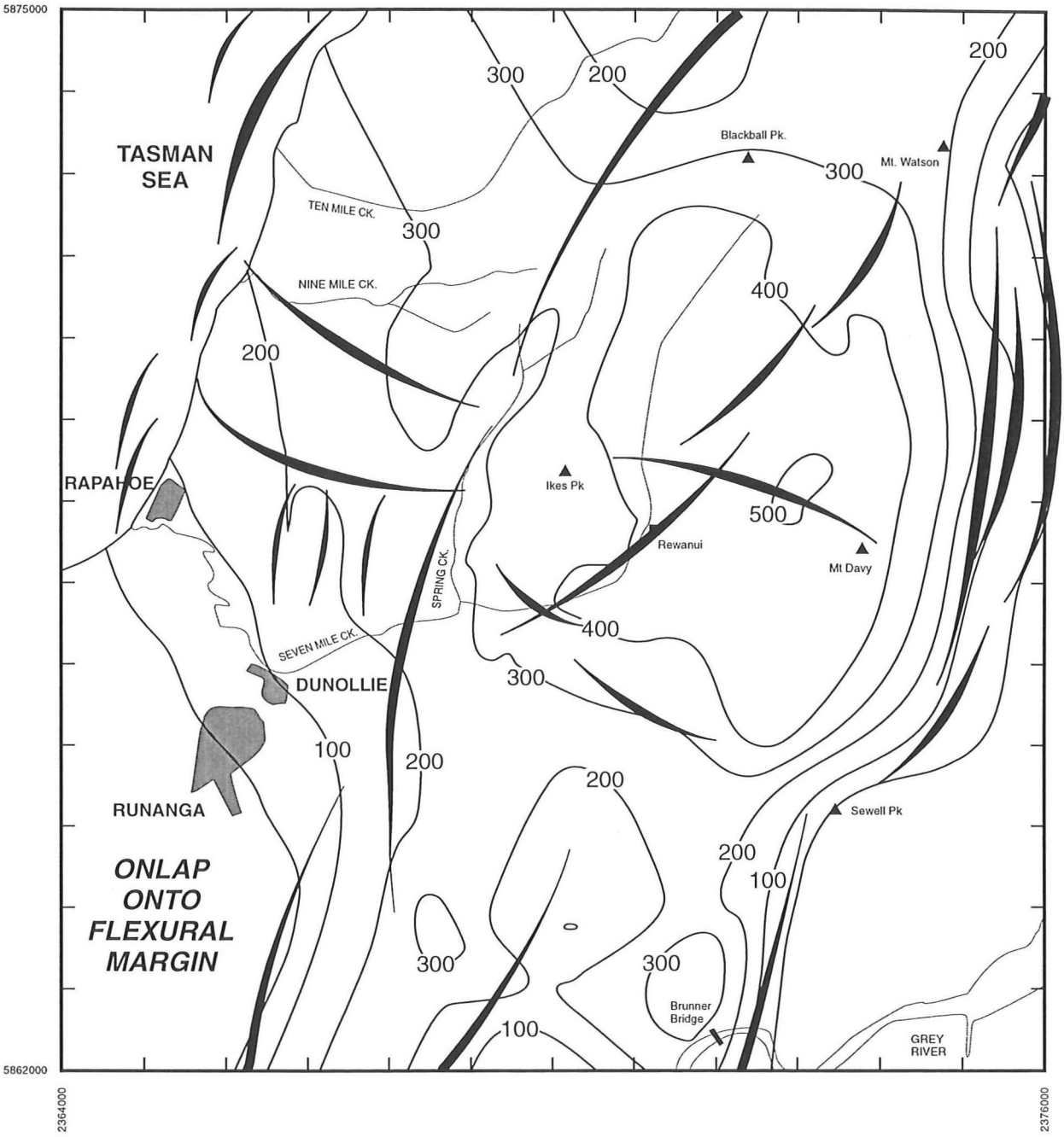

Figure 8.7 Summary of tectonic features, Rewanui Formation (Rewanui CMM, Waiomo MM, Morgan CMM). Total tectonic subsidence map shown for reference, isotect interval = 100m.

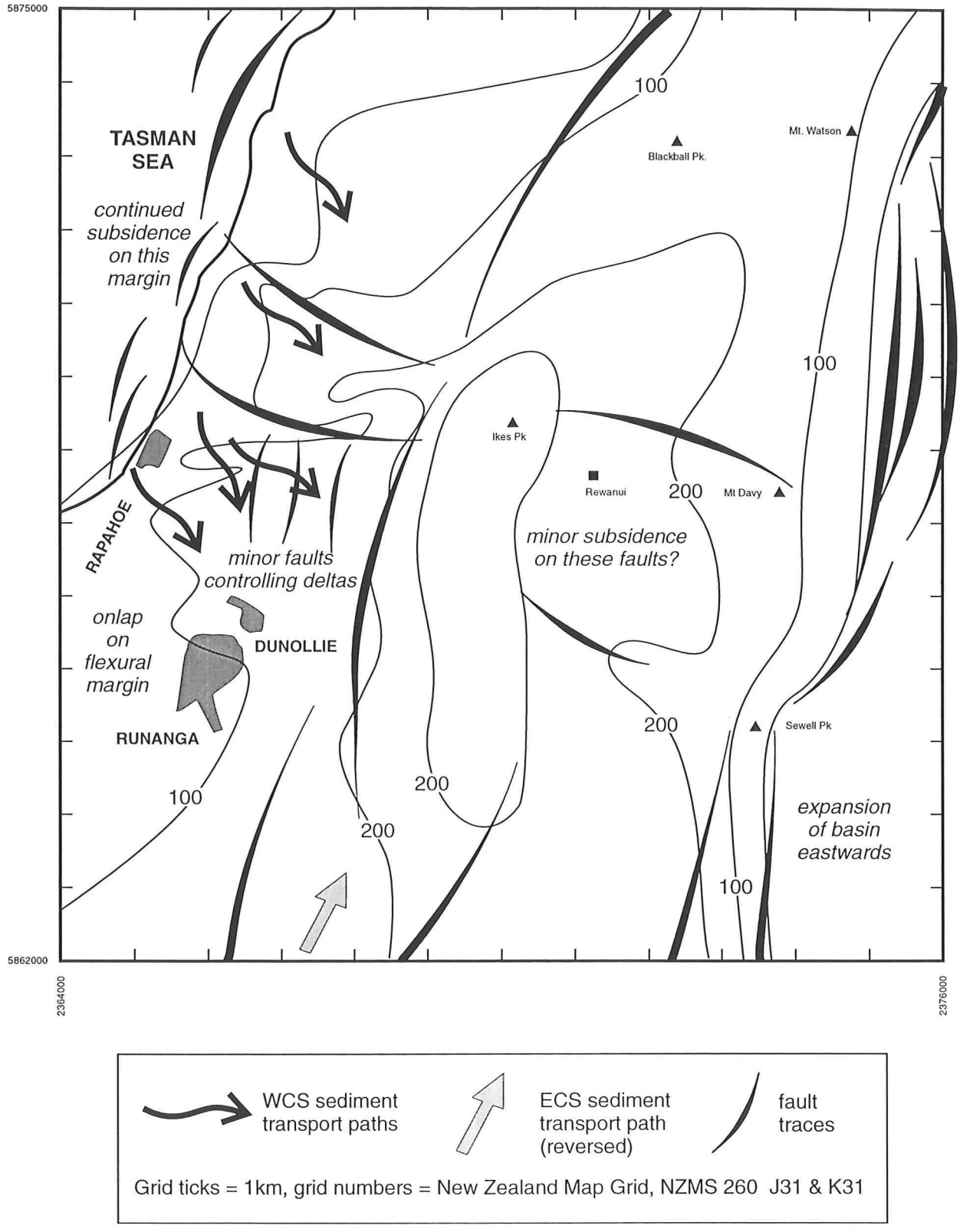

Figure 8.8 Summary of tectonic controls and sediment transport, Goldlight Formation.
Tectonic subsidence pattern shown for reference, isotect interval = 100m.

In the south of the Goldlight basin, sediment entered along the graben which developed during Rewanui CMM deposition (Figure 8.7), though flow had reversed (Section 7.8.2). The eastern basin margin was controlled by pre-existing structures (notably those active during Rewanui CMM deposition), though expansion of the Brunner Bridge depocentre eastwards by c.1km indicates continued evolution of the basin margin. There was little intrabasinal faulting in the Mt. Davy Sector, though zones of lower subsidence immediately west of Sewell Pk. and Mt. Davy were coincident with the location of WNW/ESE oriented faults active during Ford Fm. deposition (Figure 8.4).

8.7 Summary: tectonic model for Paparoa basin development

Basin-floor geometry of the Paparoa Basin was complex (Figure 8.9), because of the influence of two orientations of structures. However, a generalised structural model (Figure 8.10) shows that the basin is best characterised as a half-graben which deepened eastwards, with a faulted eastern margin, comprising three overlapping, curved fault planes, and a western margin along which there was relatively minor but locally important faulting, and flexure in the southwest. Prominent cross-basin ridges, representing subsidence along inherited structures, were present in the centre of the basin, and these controlled segmentation of the eastern basin margin (Figure 8.9).

The eastern fault zone dipped westwards at c.30° (Figure 8.10). This value may be too low, as low-angle normal faults typically dip 30–40° (Morley 1995). Dip estimation is very dependent on the location of the zero contour lines for the various units, and these are estimated from known outcrop positions (Chapter 3). Structural disruption and poor access has limited accurate mapping of the eastern limits of the Paparoa Group at Greymouth Coalfield (e.g. Caffyn 1994), and the eastern basin boundary was probably steeper than presently estimated.

Along the western edge of the Paparoa Basin, a zig-zag fault pattern developed (Figure 8.10), resulting in rhomb blocks around which sediment was transported (cf. Morley 1995, Figures 15, 16). Overall extension in the west was low, and the southwestern basin margin remained flexural, with only minor intrabasin faulting. Minor grabens developed in the northeast and south of the coalfield, providing the locus of entry and exit for the axial fluvial system.

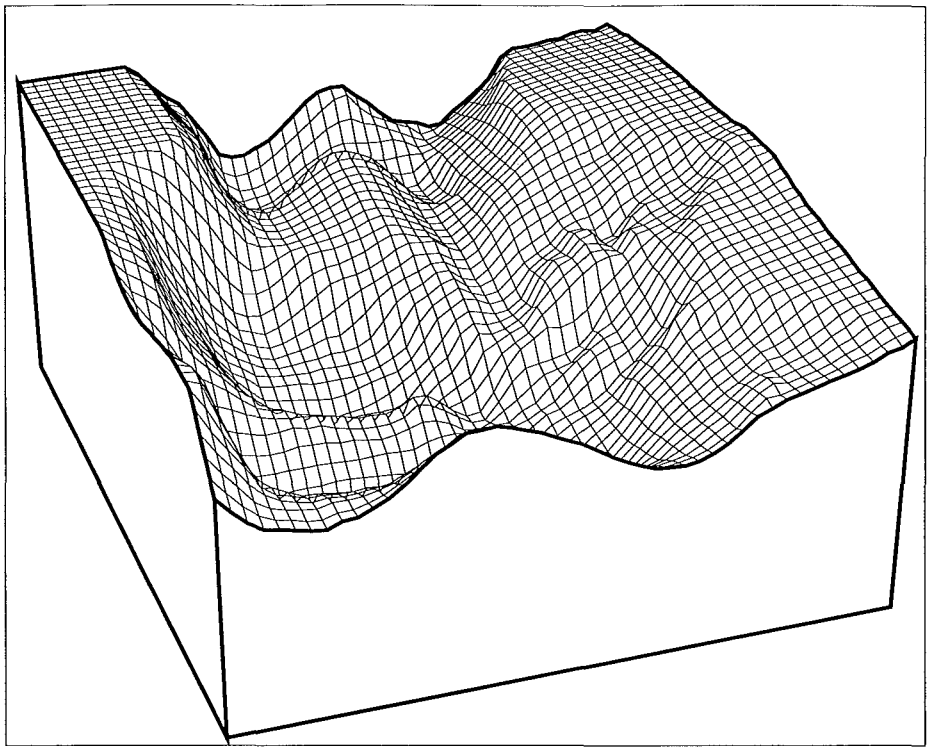

A. View along basin axis, looking SSW

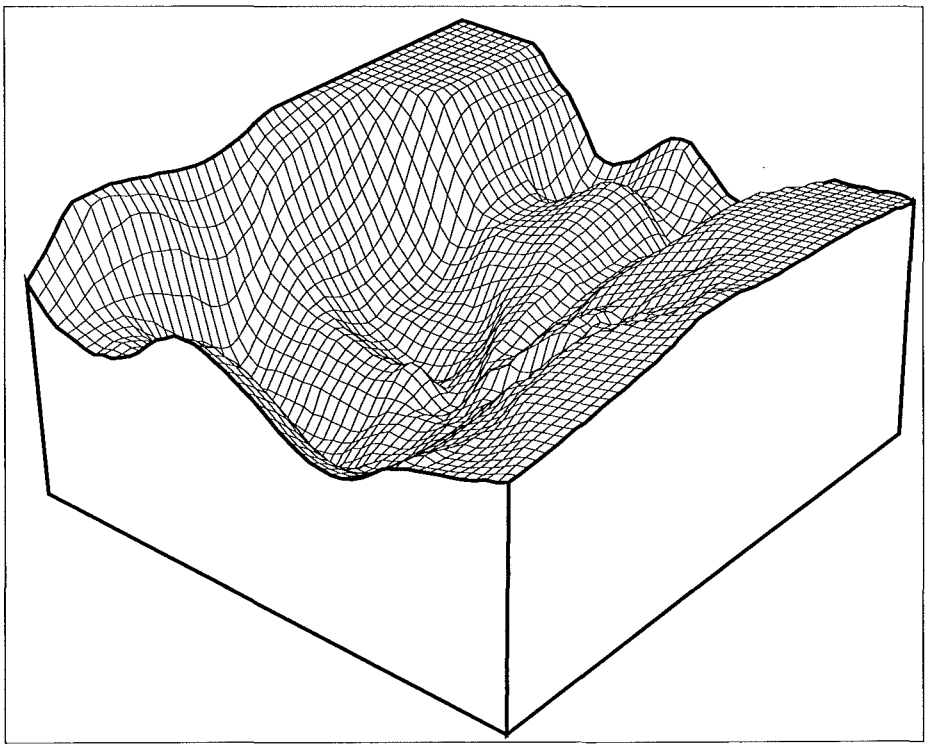

B. View from the NW, looking towards SW basin margin

Figure 8.9 Isometric models of the Paparoa Basin floor.
Datum is top of Goldlight Fm., vertical exaggeration = 5x.
Viewpoints for models are
A: azimuth 200°, dip 30°, distance to eye 50km
B: azimuth 140°, dip 30°, distance to eye 50km

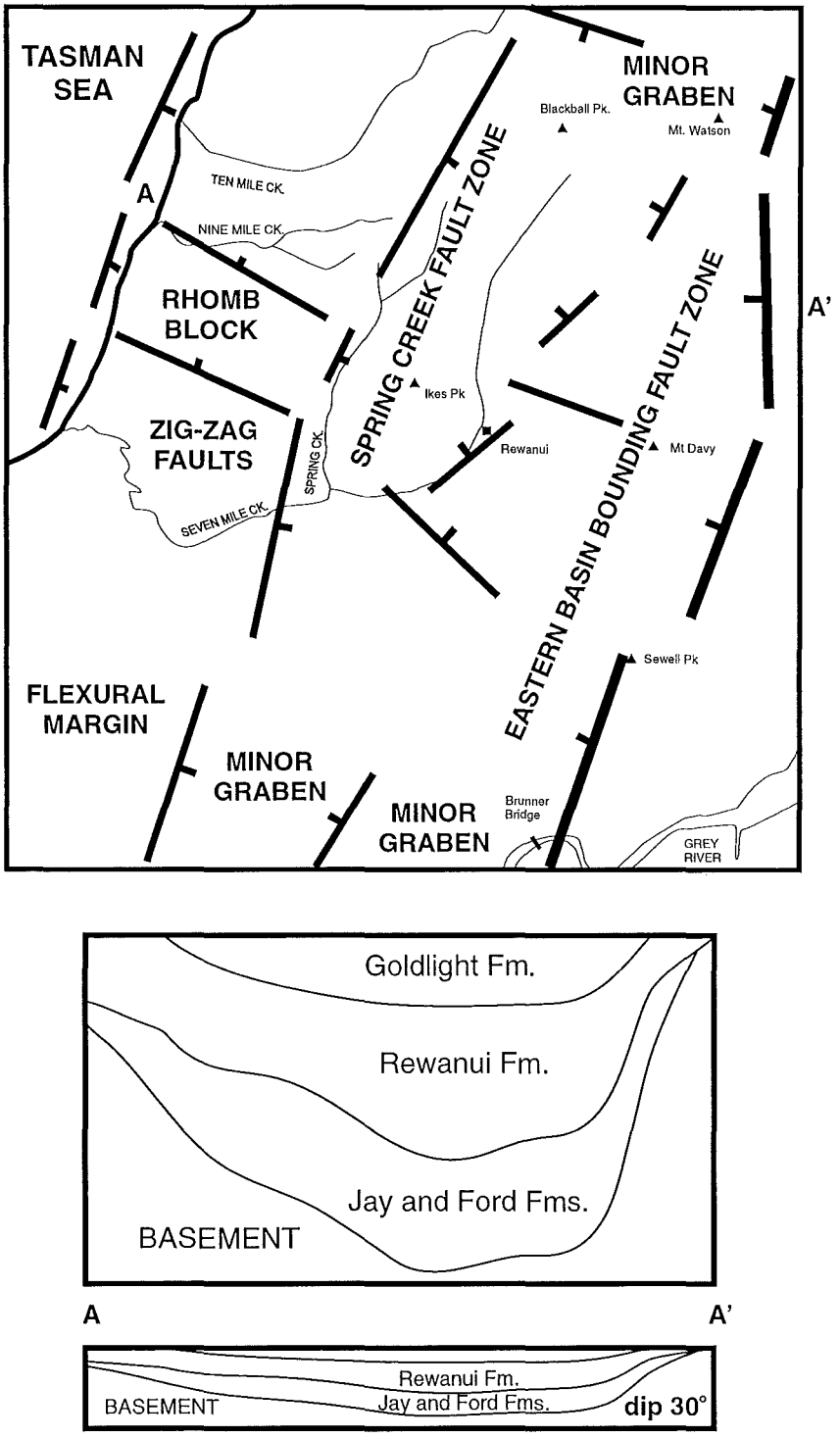

Figure 8.10 Generalised structural model for the Paparoa Basin.
Ticks on faults indicate downthrown side.
Upper cross-section from Figure 4.18, 5x vertical exaggeration.
Lower cross-section at true scale.

During Paparoa Group deposition, four trends in basin development emerged:

1) with deposition of each formation, the basin expanded, and new strata overlapped increasing areas of basement, and intrabasin highs.

2) successively younger units occupied simpler basins as early-formed faults (many of which were reactivated mid-Cretaceous structures) became less active.

3) length and displacement of the basin-bounding faults increased with time.

4) sediment transport patterns were governed by the interaction of NNE/SSW and WNW/ESE faults, and remained persistent throughout deposition of the sequence.

At all times, subsidence in the basin was differential, and even during Goldlight Fm. deposition, during which the southwestern basin margin was blanketed in sediment, movement continued on the eastern boundary faults. At certain times (e.g. Morgan CMM, Waiomo MM deposition), subsidence was strongly partitioned by the major intrabasin fault zone along Spring Creek, which was initiated during Ford Fm. deposition and continued to be significant throughout the sequence.

8.8 Discussion

The present description of the tectonic history of the Paparoa Basin at Greymouth Coalfield is significant in three contexts. Firstly, the structures which defined the basin provide a means of determining the causal tectonic regime. Secondly, this study offers a means of interpreting regional tectonics, i.e. the tectonics of related basins within the Paparoa Group (Section 2.8). Finally, regional tectonic history provides clues about the timing and nature of plate tectonic activity in the New Zealand region.

8.8.1 Tectonics of the Paparoa Basin

The presence of two depocentre orientations, and two interpreted fault trends, was previously interpreted as indicating oblique extension or a change in extension direction during Paparoa Group deposition (Section 8.2). In the present study, the WNW/ESE trend is interpreted as reactivation of structures which formed in association with mid–Cretaceous Pororari Group deposition, whereas the ENE/SSW normal fault trend is believed to have initiated at the commencement of sedimentation (Section 8.4.1).

Pre-existing basement fabrics are known to control rift basin fault geometry (Nelson et al. 1992). Extension occurs in a low mean stress environment, and mechanical anisotropies oriented up to 60° to the extension direction are commonly reactivated (e.g. Morley 1995). However, steep transfer faults, which are oriented at 90° to the extension direction, are kinematically stable during orthogonal reactivation, and suppress oblique or strike movement on abutting normal faults during oblique-slip reactivation (Etheridge 1986).

Late Cretaceous extension which created the Paparoa Basin was interpreted by Laird (1993, 1994) to have occurred along transfer faults related to the mid–Cretaceous extensional regime. NNE/SSW oriented transfer faults sub-divided the offshore Takutai Half-graben into discrete fault-blocks (Bishop 1991; see Figure 2.7), and this pattern may have continued onshore in the Greymouth Coalfield region. A small rotation in the mid-Cretaceous (NNE/SSW) extension direction could have initiated reactivation of transfer faults and related structures (Bishop 1992), however the above discussion suggests that transfers would not be a favoured site for reactivation.

At Greymouth Coalfield, the angle between the reactivated (i.e. mid–Cretaceous) and newly extensional (Late Cretaceous) structures is c.90° (Figure 8.10). Fault patterns depicted in the present study (Figures 8.4–8.8) suggest oblique extension oriented 310–340° would allow all structures to remain kinematically functional (assuming those structures are at a maximum of 60° from the extension direction). By comparison, the regional extension direction, estimated from the NNE/SSW oriented basin-bounding faults was c.290°. Declining subsidence along WNW/ESE faults during deposition (Section 8.6) indicates slight anticlockwise rotation of the extension direction with time, as suggested by Bishop (1992).

The Paparoa Basin therefore formed in response to northwest oriented oblique extension, which reactivated WNW/ESE oriented mid–Cretaceous normal faults and initiated new subsidence along a NNE/SSW trend. Though the NNE/SSW oriented structures probably represent an existing anisotropy within the basement, reactivation of transfer faults generated during earlier crustal extension was unlikely.

8.8.2 Regional tectonics – the West Coast Rift System

An important geological feature of the West Coast region is the NNE/SSW alignment of Paparoa Group occurrences at Pike River, Greymouth Coalfield and Kowhiterangi (Figure 2.7). The alignment of the basins is parallel to the major basin-bounding faults, and Laird (1981) proposed that the various basins and faults comprised the West Coast Rift System, which extended from the southern West Coast to Taranaki Basin.

The West Coast Rift System enlarged during the early Tertiary to form the 200km - long Paparoa Tectonic Zone (Laird 1968, 1981), in which >3km of Late Cretaceous to Oligocene sediment accumulated in two c.80km long depocentres (Nathan et al. 1986, Map 9). Locally, burial estimates at Greymouth Coalfield indicate >4km of strata was present adjacent to the eastern basin margin (Appendix 4.2). However, much of the Tertiary "cover" sequence has been eroded by Neogene basin inversion, and the general trend of maximum inversion where previously there was maximum subsidence (Laird 1968; Nathan 1978; Bishop & Buchanan 1995) could be interpreted as indicating that former depocentres have been inverted and now completely eroded. Observed Paparoa Group occurrences may therefore be the remnants of a once more extensive deposit.

Tectonic subsidence estimates indicate maximum subsidence of c.1000m within the Paparoa Basin, which corresponds to a basin-bounding fault length of c.20–30km (Figure 8.3B). This is approximately the known strike dimension of Greymouth Coalfield (Section 8.3.1). Basin geometry therefore suggests that the Paparoa Basin could not have been significantly more extensive in the past. In contrast, the maximum burial estimate of c.4km corresponds to a basin of c.100km length, which agrees with the dimensions of the regional depocentres (see above). Subsidence within the Paparoa Tectonic Zone therefore commenced in isolated basins of the West Coast Rift System, which subsequently expanded in the early Tertiary.

The West Coast Rift System can be interpreted as colinear, segmented rift (Figure 8.11) along which individual grabens or half-grabens are separated by "gaps" where there was limited extension and sedimentation (Nelson et al. 1992). Gaps between rift segments are typically occupied by sandy axial fluvial systems (Morley 1995). The persistent axial fluvial system, which brought coarse clastic sediment into the Paparoa Basin from the NNE (Section 7.8), flowed through the rift gap which separated Pike River Coalfield

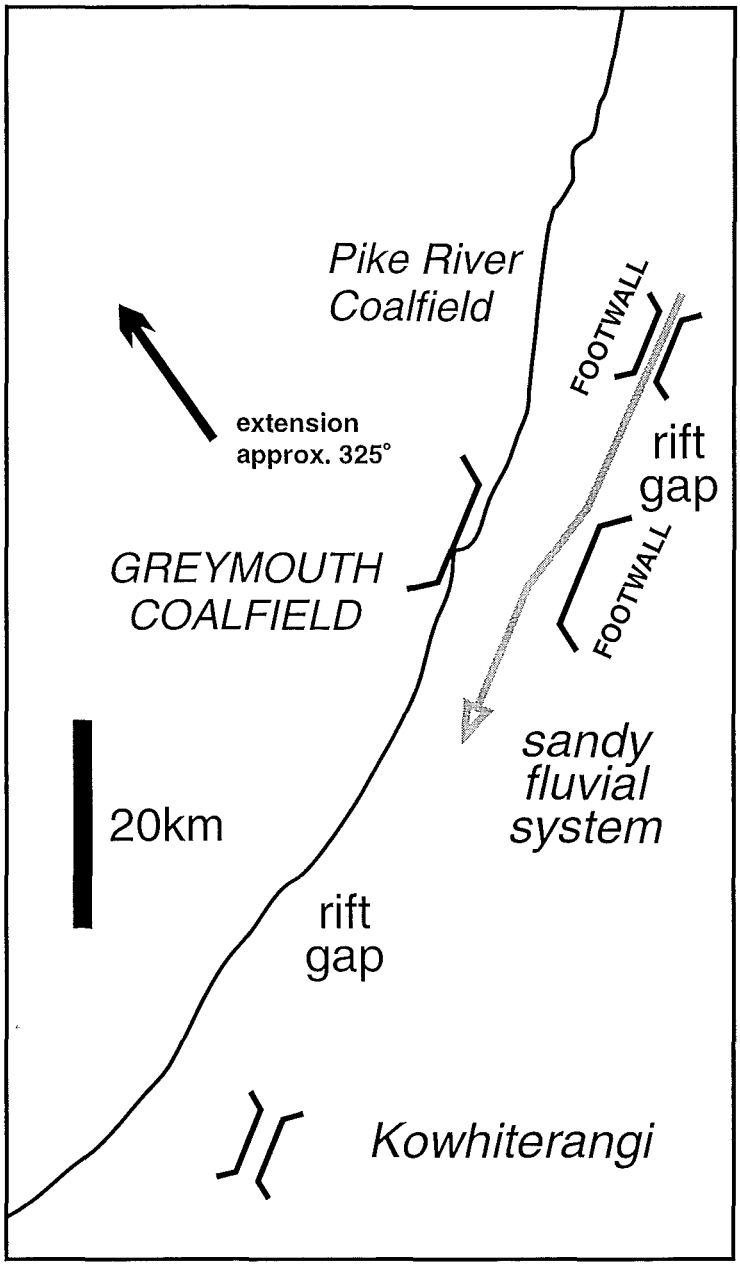

Figure 8.11 Generalised map of the West Coast Rift System, showing main basins, rift gaps, and fluvial axis.
Note reversal of basin polarity between Pike River and Greymouth.

and Greymouth Coalfield (Figure 8.11). Basin-bounding fault polarity reversed between Pike River and Greymouth Coalfield (Ferguson 1993), and such reversals are typical of elongate rift systems (Gawthorpe & Colella 1990).

The basins of the West Coast Rift are not offset in an en echelon manner, as would be expected during oblique extension, which may be explained by the role of basement fabrics in determining locations of the rift segments (Nelson et al. 1992), the overall low proportion of extension (<5%; Bishop & Buchanan 1995) and the small degree of obliquity (c.30°). Lack of evidence for Late Cretaceous strike movement (Section 8.2) probably reflects the same factors, though analogue modelling suggests that oblique extension does not generate strike-slip and oblique-slip faults (McClay & White 1995).

All Paparoa Group occurrences were coeval, as indicated by lithostratigraphy (Section 2.8), limited geochronological data (Laird 1996) and palynostratigraphy (Appendix 7.5.1). Deposition of the Paparoa Group at Greymouth Coalfield probably commenced slightly earlier than 71±1.3Ma, the age of Member 2 volcanic rocks at Pike River Coalfield (Laird 1996), which are regarded as equivalent to Morgan CMM volcanic rocks at Greymouth Coalfield (Newman 1985). This date provides a lower limit for the initiation of Late Cretaceous oblique extension in the central Westland area.

Previously, Paparoa Group sedimentation was believed to have commenced during the Campanian, at c.80Ma (Bishop 1992, Figure 10; Laird 1993, 1994). Were this the case, there would be a c.10Ma unconformity between the Ford Fm. and overlying strata (basal Rewanui CMM or Morgan CMM). Though there is a slight erosional unconformity in some parts of the basin (Section 2.6.1, 4.2.5), the intimate relationship between lacustrine and succeeding fluvial sedimentation indicated by the Ford Transitional Member (Section 7.8.2) suggests there was no major break in sedimentation.

Rotation of depocentres throughout Paparoa Group deposition in Greymouth Coalfield (Figure 4.19) reflects evolution of the basin-bounding faults which were initiated at c.71Ma, as the axis of extension rotated slightly to the south (Section 8.8.1). There was no orthogonal change in extension direction at c.70Ma, as previously postulated (Laird 1993, 1994; Section 8.2).

8.8.3 Regional tectonic implications

Oblique rifting and basin formation in the West Coast Rift System occurred c.11My after the initiation of sea-floor spreading in the Tasman Sea at 82Ma (Weissel & Hayes 1977), suggesting that the two events not directly related (Laird 1996; King & Thrasher 1996). Sea-floor spreading was continuing at the time of initial Paparoa Group deposition (anomaly 32, c.72Ma; Kamp 1986, Figure 5), and sedimentation was widespread in the New Zealand region at this time (e.g. Figure A7.3).

The presently favoured Late Cretaceous tectonic setting for the West Coast Region (including Taranaki) is one of oblique extension between the present-day New Zealand land mass and the Challenger Plateau, across the Taranaki Rift, which may have been related to opening of the New Caledonia Basin (Thrasher 1990; Bishop 1992; Laird 1993, 1994; King & Thrasher 1996). However, recent work has demonstrated the presence of thick synrift strata of Ngaterian to Haumurian age (Taniwha Fm.) in offshore Northland basins, suggesting an earlier (early Late Cretaceous) initiation of rifting in the New Caledonia and Northland Basins (Isaac et al. 1994, Laird 1996).

The West Coast Rift System provided a structural link between the southern end of Tasman Sea spreading and the Taranaki Rift (Bishop 1992; Laird 1993, 1994, 1996), though whether the initiation of rifting was coeval in both Taranaki and the West Coast Rift System, as proposed by Laird (1996), is not certain. Two distinct units are generally present beneath the KTB in the Taranaki and Northland Basins (Schmidt & Robinson 1990; King & Thrasher 1996). The older unit corresponds to the Haumurian non-marine Rakopi Fm. (King & Thrasher 1996), and may incorporate the Taniwha Fm. in Northland (Isaac et al. 1993). Overlying the Rakopi Fm. in Taranaki and probably Northland is the marine North Cape Fm., which contains latest Haumurian dinoflagellates (Wizevich et al. 1992; Isaac et al. 1994; King & Thrasher 1996).

Poor palynostratigraphic resolution (Raine 1984) and lack of sampling prevents precise determination of the age of the base of the Rakopi Fm., and the recent revision of the base Haumurian to 81Ma (Crampton et al. 1995) or 84Ma (Crampton 1995) increases uncertainty on the age of initial rifting in the Taranaki Basin. More precise dating of the North Cape Fm. suggests that this unit is coeval with the latest Cretaceous Paparoa Group, which was deposited c.150–200km south of the Taranaki Basin.

Initiation of oblique extension in the West Coast Rift System, which gave rise to deposition of the Paparoa Group, occurred at c.70Ma. This system, and minor extensional basins elsewhere in the South Island region (e.g. Nicol 1993), indicate a new tectonic regime, which postdated initiation of Tasman Sea spreading by c.10My. Initiation of rifting in the West Coast Rift System possibly occurred up to 10My after other Late Cretaceous extensional basins such as the Taranaki Basin (see above) and Ohai Coalfield (Appendix 8.1) began to form. Improved resolution of terrestrial palynostratigraphy for the Haumurian is required to provide more accurate dates for initiation of rifting throughout western New Zealand.

Chapter 9. Summary, discussion and conclusions

This thesis presents the results of basin analysis of the Paparoa Group at Greymouth Coalfield. Research was founded upon the stratigraphic record contained in numerous drillholes, and basin analysis involved collection of new data, greater utilisation of existing data, and the application of quantitative stratigraphic methods. New insights into Greymouth Coalfield geology are summarised below.

Lithostratigraphic analysis, basin modelling and palynostratigraphy enabled reconstruction of the sediment transport systems and tectonic setting of the Paparoa Basin. The interplay between tectonics and sedimentation determined the lithological character of the Paparoa Group, and a model for basin evolution is presented below. The conclusion presents a review of the major findings of this thesis, and highlights the enhanced understanding of the Paparoa Basin achieved by this study.

9.1 Summary of methods and results

The purpose of this summary is to review the contribution of the various basin analysis techniques employed in this project to meeting the themes and objectives stated in Chapter 1. Particular emphasis is placed on methods which have not previously been applied in Greymouth Coalfield.

9.1.1 Lithostratigraphy

The first theme pursued in the thesis was lithostratigraphy. Many problems were identified with the existing lithostratigraphic nomenclature and its application, ranging from the lithological content of individual Members to definition of Groups (Appendix 1, Section 2.2). Revision of lithostratigraphic definitions was clearly warranted, to account for variability within the stratigraphic units, apparent complexity of contacts, and regional geology.

In this project, strata within the Paparoa Group at Greymouth Coalfield were subdivided into three lithosomes, representing coal forming, deltaic and lacustrine environments (Section 2.3). Geophysical logs (natural gamma, density and caliper) were found to be ideal for identification of lithosomes, because of availability through many uncored

intervals, and resolution of gradational units which were poorly described in lithology (core) logs. New criteria for unit boundary placements are implicit in the lithosome framework. Coal-bearing units contain exclusively coal measure lithosomes, whereas mudstone units contain both mudstone and transitional lithosomes (Section 2.4). Recognition of lithosomes facilitated accurate identification of stratigraphic contacts, and application of the objective criteria developed for lithosome recognition resolved many of the known lithostratigraphic problems.

Lithostratigraphic nomenclature was revised to accommodate the lithosome framework, and subsequent recorrelations of units to conform to that framework. Five Formations within a re-instated Paparoa Group were defined (Section 2.5). Particular attention was given to description and definition of the economically important Rewanui CMM. Correlation of the coal measure and mudstone units beneath Rewanui CMM was also revised, resulting in new patterns of unit extent. Major changes were made to Morgan CMM and Waiomo MM definition, and these units are now restricted to the Mt. Davy Sector. The Rewanui Fm. now rests on Ford Fm. in the Rapahoe Sector. Isopach models therefore also needed revision, and use of lithosomes to locate unit boundaries increased the accuracy of unit thickness estimates in many drillholes. The revised lithostratigraphic framework formed the basis for all subsequent basin analysis.

The final benefit derived from the lithosome framework was the recognition of deltaic sequences within Greymouth Coalfield (Section 2.3). Two new lithostratigraphic units, the Goldlight Transitional Member and the Ford Transitional Member, were erected to represent the deltaic portions of the Goldlight and Ford Formations, respectively (Sections 2.7.2, 2.7.6). Recognition of deltaic strata (Chapter 7) demonstrated the points of coarse sediment supply into the basin.

9.1.2 Basin modelling

Suites of isopach models were constructed for the present-day (Chapter 3) and pre-burial thickness (Chapter 4) of the Paparoa Group units. The former models were derived directly from stratigraphic data, whereas the latter models, and the interpreted tectonic subsidence maps, were adjusted for the effects of burial compaction on unit thicknesses (Appendix 4).

Accurate lithostratigraphic contact placements were determined with the lithostratigraphic criteria discussed above, however other factors, especially structural disruption, influenced unit thickness (Section 3.7). An iterative methodology was applied to Rewanui CMM thickness measurements in order to achieve the most accurate data set for isopach construction (Figure 3.6). An important component of this methodology was the use of computer modelling techniques (in particular, minimum curvature models) as a means of testing local variation in unit thickness and identifying anomalies resulting from incorrect lithostratigraphy, faulting or errors in the data set (Appendix 2, 3). Other stratigraphic methods, particularly palynostratigraphy and seam correlation (see below) also assisted in recognition of missing or repeated strata. Revised isopach patterns for all units (Chapter 3) incorporate stratigraphic revision, and correction for previously unrecognised faulting in some drillholes.

Numerical modelling methods were used as a basis for construction of Goldlight Fm. and Rewanui CMM isopach models (Appendix 3). Trend surface analysis delineated orthogonal depocentre orientations between Rewanui CMM and Goldlight Fm. Geostatistical modelling of Rewanui CMM isopach data highlighted complex thickness variation within that basin. However, the benefits of numerical modelling were found to be limited by irregular drillhole spacing and coverage, and the absence of critical information, such as basin margin sequences, from the drillhole data set. Outcrop extents from existing mapping were needed to constrain isopach models, however revision of map patterns was required to conform to new lithostratigraphic correlations. Further mapping is needed to verify these revisions.

Computer representations of all present-day isopach models were generated to facilitate addition of unit thicknesses and cross-section construction (Section 3.9). This technique did not improve the accuracy of individual isopach models, however few drillholes penetrated all units (Appendix 9), and numerical summation of the models ensured the maximum amount of drillhole data was incorporated in summary plots (e.g. total Paparoa Group thickness).

Determination of the pre-burial thickness, and associated tectonic subsidence of Paparoa Group units (Chapter 4) was the most complex basin modelling exercise undertaken in this project. An unconventional approach to backstripping and tectonic subsidence estimation was required (Appendix 4) to account for the setting of Greymouth Coalfield, which is a small, eroded, inverted basin comprising wholly continental strata (in the interval of interest).

Burial of the Paparoa Group was estimated from basin-wide vitrinite reflectance (VR) data (Appendix 4.2). Such data are influenced by many variables, and all measurements were normalised to one stratigraphic level (the Goldlight / Rewanui contact) and corrections were made for coal type and measurement technique (Appendix 4.2.2). A simple relationship between VR and burial depth was used, assuming constant down-hole rank change. However, limited data indicated that assumption was not always valid, and steeper rank gradients were detected in the east and south of the coalfield.

Lithological proportions were determined for all units in the 72 modelled drillholes (Appendix 4.4). For lacustrine units, geophysical logs were used to estimate sand proportion. Sediment proportions in coal measure units were derived from the drillhole database, and anomalous coarse to fine sediment ratios in selected drillholes were detected with minimum curvature modelling. Where necessary, unit thicknesses were estimated from the isopach models presented in Chapter 3. Cover strata parameters were estimated from the burial model and regional stratigraphic information (Appendix 4.5). Decompaction profiles for each lithology were estimated from limited petrological data and comparative studies (Appendix 4.3), and a customised decompaction regime for each unit in each drillhole was calculated.

Burial resulted in c.27% average compaction of Paparoa Group strata, and total pre-burial thickness was c.1000m. Thickness of the Rewanui Fm. exceeded 500m prior to burial. Compactional effects of cover deposition were greater than compaction within the sedimentary pile during Paparoa Group sedimentation, and Morgan CMM and Rewanui CMM thickness was reduced by >=50% in some drillholes (Chapter 4.3).

One objective of the decompaction analysis was to test previous hypotheses about the role of mudstone and peat compaction in determining unit thicknesses (Bowman et al. 1984; Ward 1995). Compaction of thick Ford Fm. mudstone beneath Morgan CMM was found to be minimal, and there was a poor correlation between Rewanui CMM thickness and compaction of Ford Fm. in the northern Rapahoe Sector. Mudstone compaction was therefore previously over-estimated. Deposition of Goldlight Fm. resulted in compaction of underlying strata in 57 of the 72 modelled drillholes, 75% of which occurred within Rewanui CMM. Total coal thickness was the most significant factor in determining the amount of Rewanui CMM compaction beneath Goldlight Fm., though pre-burial peat thickness, which is probably the controlling factor, could not be determined by the present methods (Section 4.2.7).

Removal of the effects of compaction from the stratigraphic column enabled tectonic subsidence to be estimated, and isotect maps formed the basis of subsequent tectonic interpretations. However, isotect patterns were influenced by non-tectonic factors such as paleotopography, paleogeography, lateral gradation between units, and erosion, particularly in the Ford and Goldlight Formations (Section 4.4).

9.1.3 Palynology

The third theme of investigation pursued in this study was palynology, which addressed both palynostratigraphy of the Cretaceous–Tertiary Boundary (Appendix 5, Chapter 6) and analysis of Haumurian and Teurian paleovegetation (Appendix 6). In order to fully interpret palynological results from Greymouth Coalfield, an extensive review of correlative material from elsewhere in New Zealand and the Southern Hemisphere was undertaken (Appendix 7). One feature of this review was the quantitative comparison of palynofloras using ternary diagrams, which clearly illustrated variation within the major floral components. The proportion of angiosperm pollen in Greymouth Coalfield palynofloras was found to be lower than in other Late Cretaceous to early Tertiary floras, and this was interpreted as indicating an inland, cool, humid setting (Chapter 6.6, Appendix 8.1.5).

The KTB in the Rapahoe Sector was identified palynologically with the occurrence and/or abundance of selected angiosperm pollen taxa. Regional criteria for palynological zonation were found to be inconsistent with the study sample suite, because of the influences of paleovegetation and lithology on the occurrence of diagnostic taxa (Appendix 5.5). However, those factors were accommodated, and zonation criteria were developed which allowed ages to be assigned to all study samples (where sufficient palynomorphs were recovered) without recourse to stratigraphic position (Appendix 5.4.3).

No independent criteria (e.g. marine microfossils, siderophile element anomalies) for recognition of the KTB at Greymouth Coalfield are available, however trends in floral change across the KTB are comparable to floral change elsewhere in the Southern Hemisphere (Appendix 7.5). There was no mass extinction of terrestrial plant ecosystems at the KTB in Greymouth Coalfield, though angiosperm and gymnosperm diversity declined immediately above the KTB (Appendix 6.4). Floral change at the KTB was probably controlled by climate change (Appendix 8.3).

The KTB in the Rapahoe Sector lies in the uppermost Rewanui CMM, and the relationship between the KTB position and the top contact of the Rewanui CMM was found to be predictable. Two palynostratigraphic domains were recognised (Section 5.5.3), with the KTB lying c.1.8m below the top Rewanui CMM contact in the southwest and c.17m below the contact in the northeast. Syndepositional normal faulting was the probable control on the two domains (Section 6.5).

The palynostratigraphic domain model allowed the position of the KTB to be estimated throughout the Rapahoe Sector, thus providing a time plane which can be used as a datum surface for paleogeographic reconstruction, seam correlation and resolution of litho-stratigraphic problems (Chapter 6). At the time of the KTB, the Rapahoe Sector was dominated by low relief floodplain, with minor lakes and small raised mires (Figure 6.1). Paleovegetation (Appendix 7, Ward et al. 1995) was consistent with this setting. Coarse sediment was transported across the area in a river which flowed from the toe of a northwestern alluvial fan, and splays carried sand into the area from the northeast and southwest.

Coal seams in the Rapahoe Sector (and laterally equivalent barren intervals) were found to occur at predictable intervals beneath the KTB (Ward 1996), therefore previous correlation models which used the upper Rewanui CMM contact as a datum were incorrect. The revised correlation model enabled seam extents throughout the Rapahoe Sector to be mapped, and seams in the northern (Strongman Mine) area could be correlated with those in presently un-mined areas to the south (Section 6.3). The seam correlation framework also provided a means of estimating structural removal or repetition of strata, which assisted in assembly of accurate Rewanui CMM thickness data for isopach modelling.

The final application of palynostratigraphy was resolution of the contact between Rewanui CMM and Dunollie Fm. in the northwest, where Goldlight Fm. is absent (Section 6.4). The estimated positions of the KTB and the Main seam were used as marker horizons to verify the approximate location of the upper Rewanui CMM contact where conventional lithostratigraphic criteria for contact placement were inapplicable.

9.2. Controls on fluvial and lacustrine deposition

The recognition of an alternating sequence of coal-bearing and mudstone strata within the Paparoa Group was a primary achievement of early workers at Greymouth Coalfield (Morgan 1911; Gage 1952). This stratigraphic signature remains a characteristic of Greymouth Coalfield which is not present in other Late Cretaceous to early Tertiary basins in New Zealand (Appendix 8.1). Previous interpretations have suggested that deposition of coarse units was initiated by rapid source area uplift, followed by reduction in source area relief and sediment supply, and quiescent deposition as lakes migrated into the basin, possibly as a result of accelerated subsidence (Gage 1952; Bowman et al. 1984).

The present project provides information about basin geometry, tectonic subsidence, depositional gradients, sediment supply and climate, all of which could influence the initiation of lacustrine sedimentation (Table 9.1).

Controlling factors	Ford Fm.	Waiomo MM	Goldlight Fm.
setting prior to transgression	Jay Fm. finer at top, probably low depositional gradient	Morgan CMM generally fine, low sediment supply	reduction in depositional gradient/sed. supply in west, fluvial axis in east still active
initiation	rapid - no deltas at base in Jay depocentre	probably single subsidence event	rapid transgression over floodplain
tectonic subsidence	enhancement of Jay basin, much differential subsidence on WNW/ESE faults, new fault trend with magma injection.	tectonic event restricted to Mt. Davy Sector, faults controlling Morgan CMM declined though NNE/SSW trend active	dominant subsidence on NNE/SSW faults, little intrabasin faulting, onlap over flexural margin in SW
sediment supply	initially quiescent, then coarse sediment (up to cobbles) from NW, minor from NE	minor from existing NE and W sources	persistent sand sources in W (no gravel), new source in south with reversal of transport
delta style	large delta complex in NW, deeper water	minor in NE, shallow water	elongate to lobate, restricted in west, broad in south
climate	unknown	no influence likely	no influence likely
cessation of lacustrine depositon	regional subsidence, basin enlargement, then rapid gravel encroachment in W, some erosion.	rapid filling of basin with coarse sand from NE	influx of sand from NW and NW (Bowman et al. 1984)

Table 9.1 Summary of factors influencing lacustrine sedimentation, Greymouth Coalfield. Information is taken from Chapters 4–8.

Three features are common to all lacustrine units. Lacustrine transgressions were initiated rapidly, following a reduction (but not always complete cessation) of coarse sediment supply. Continued tectonic activity is associated with all lacustrine intervals, though significant intrabasin fault activity is only present during Ford Fm. deposition. Finally, lacustrine sedimentation ceases at the commencement of a new phase of coarse clastic input. However, differences between the lacustrine intervals are apparent.

The Ford Fm. represents initial passive fill of a pre-existing (and still-developing) basin, into which coarse sediment supply temporarily ceased. Commencement of Ford Transitional Member deposition, which occurred after c.100m of mudstone had accumulated in the depocentre, represented the initiation of the succeeding coarse-clastic aggradational phase in the Rapahoe Sector (Rewanui CMM). This event was accompanied by basin-wide tectonic subsidence, and the related faulting in the western basin margin may have initiated coarse sediment supply. In the Mt. Davy Sector, filling of the Ford basin was less energetic, and fine clastic lithologies and coal dominate Morgan CMM (Appendix 4.4.1). The abundance of coal in Morgan CMM, in comparison to western basal Rewanui CMM, suggests higher water tables persisted in the Mt. Davy Sector during Morgan CMM deposition.

Deposition of Waiomo MM can be attributed to a discrete subsidence event in the Mt. Davy Sector, coupled with almost complete cessation in coarse sediment supply. However, this lacustrine event was rapidly terminated by progradation of ECS sand from the NE, which initiated Rewanui CMM deposition in the Mt. Davy Sector. Increase in sediment supply from the NE represented extrabasinal evolution of the rift-gap river system (Section 7.8.1, Figure 8.11). Loss of Greenland Group material from the ECS at this time was interpreted as indicating sediment bypass (Section 7.8.1). A probable mechanism which accounts for source area evolution, sediment bypass and deposition of thick Rewanui CMM in the Paparoa Basin is an enhanced period of tectonic subsidence throughout the West Coast Rift System.

Goldlight Formation deposition commenced synchronously throughout the coalfield, and was initiated by an orthogonal phase of extension, during which intrabasin faulting declined and previously emergent basement in the SW was covered. Coarse sediment supply in the NW persisted, and the lake was fringed by a western alluvial apron. However, only sand entered the lake, suggesting a period of relative quiescence in the NW source area. Deposition of sand in the NE was shifted northwards towards Pike River Coalfield as a result of rising base level (Section 7.8.1), and there was a reversal of axial sediment transport in the south of the basin (Table 7.1). Goldlight Fm. deposition was coincident with regional subsidence and basin-floor tilting, which was controlled by the now-dominant NNE/SSW trending basin-bounding fault zones.

Various explanations have been proposed for fluvial-lacustrine transitions in rift basins. Blair & Bilodeau (1988) suggested that, contrary to commonly held beliefs that progradation of coarse clastic sediment indicates increased tectonic activity, lacustrine deposition was typical of periods of high subsidence rate during basin evolution. During periods of enhanced subsidence, accommodation exceeds sediment supply, coarse clastic sediments are unable to penetrate into the depocentres, and basins become starved (Lambiase, 1990; Frostick & Steel 1993a). Schlische (1991) proposed an alternative explanation for the transition from fluvial to lacustrine sedimentation in rift basins. As basin-bounding fault segments propagate, for a constant subsidence rate and sediment supply, the capacity of the basin will exceed the ability of inflowing sediment to fill available space, resulting in a change to lacustrine conditions.

Elements of the above models may be identified within the Paparoa Group. Basin expansion and rapid subsidence was associated with Ford Fm. deposition, and the Paparoa Basin also expanded during Goldlight Fm. accumulation, resulting in a reversal of axial drainage patterns. Supply of coarse sediment into all lacustrine basins was limited.

Gross sedimentary character of the Paparoa Group therefore reflects a combination of intrabasin subsidence, regional subsidence and the interplay of sediment sources. However, fluvial and lacustrine events can both be related to phases of enhanced subsidence, and the alternating fluvial/lacustrine character of the basin fill was determined largely by sediment supply, which was influenced by tectonic activity of the West Coast Rift System beyond the Paparoa Basin itself.

9.3 Tectonostratigraphic evolution of the Paparoa Basin

The intimate interaction between tectonics and sedimentation is inherent in the structural model presented for the Paparoa Basin and its regional setting (Figure 8.10, 8.11). Whereas reconstruction of rift basin geometry is generally achieved by direct observations of tectonic features, in the present project, the structural setting was interpreted from the results of basin analysis, which identified consistent patterns in sedimentation (e.g. Frostick & Steel 1993a).

Tectonostratigraphic evolution of the Paparoa Basin and its fill was controlled by four factors: NNE/SSW and WNW/ESE fault orientations (Figure 8.10), and northwestern and northeastern sediment sources (Section 7.9). The relative roles of these controls throughout Paparoa Group deposition is reviewed in Figure 9.1, and the net effect on Paparoa Basin fill is a poor correlation between some observed stratal patterns with aspects of conventional tectonostratigraphic models for rift basins (Section 8.3.4, Figure 8.3A), though other features of the Paparoa Basin are consistent with such models (Table 9.2).

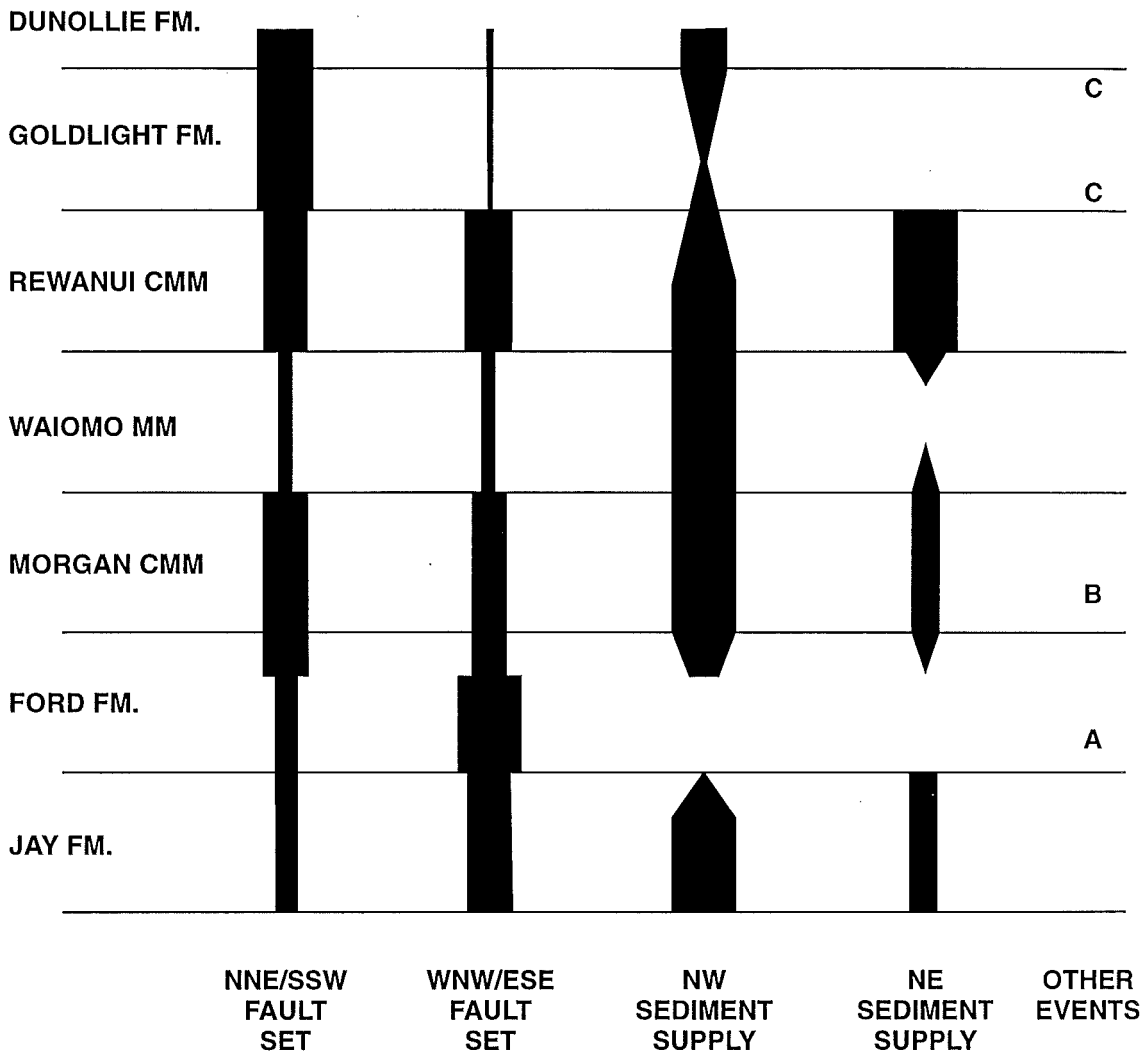

Figure 9.1 Summary diagram showing relative magnitude of major controls on Paparoa Basin formation and fill. Note that differences between the Rapahoe Sector and Mt. Davy Sector are simplified. Other significant events in Paparoa Basin history are:
A - initiation of Spring Creek Fault Zone and magma injection
B - Morgan Volcanics along eastern margin
C - reversal of axial sediment transport direction

Source	features of rift basin	Paparoa Basin compliance
L&G, T&N	alluvial braidplains derived from footwall dominate syntectonic deposits, hanging-wall fans limited	no – only footwall (eastern) source present in Morgan volcanics.
L&G, A&L	axial system displaced to above bounding fault by basin-floor tilting	no – axial system follows intrabasin fault trend
L&G	hanging-wall dip-slope coal seams which thicken towards basin axis	no, but thickest coal on flexural margin block
G&C	footwall coarse-grained deltas, fringe of finer deltas on hangingwall, deltas sourced through transfer zones or from axial system	yes – though footwall deltas absent, and flow in axial system reversed.
S, S&A	basin fill follows fluvial / deep lacustrine / shallow lacustrine / fluvial pattern	no – more lacustrine events and none deep
S, T&N, S&A	upsection units become more symmetrical, onlap other basin fill and basement	yes – all units formations cover larger area
P, T&N	initial units in restricted basins, axial drainage from adjacent mature areas	yes, but sediment in Jay Fm. not sandy, axis of basins orthogonal to main trend
S	basal unconformity	yes

Table 9.2 Selected features of continental extensional basin fill sequences, and presence of those features in the Paparoa Basin. Sources are as follows: A&L = Alexander & Leeder 1987; G&C = Gawthorpe & Colella (1990); L&G = Leeder & Gawthorpe (1987); P = Prosser (1993); S = Schlische (1991); S&A = Schlische & Anders 1996; T&N = Travis & Nunn 1994.

Maximum departure from predicted basin fill patterns occurred during deposition of the Rewanui Fm., as a result of continued oblique extension, and the interaction between sediment sources and fault block subsidence (Figure 9.2). Footwall sediment supply from the east was restricted to a minor footwall sub-basin which trapped Greenland Group and volcanic sediment (Section 7.4), and there was no footwall input during Rewanui CMM deposition. Frostick & Steel (1993b) stated that, with the exception of basins adjacent to readily erodible hinterlands, the volume of footwall derived sediments was commonly overestimated. There was persistent subsidence along the eastern basin boundary fault zone (Figure 9.1), and the suggestion that coarse-grained sediment may indicate tectonic quiescence (Blair & Bilodeau 1988) could explain the general absence of footwall derived material from the Paparoa Basin.

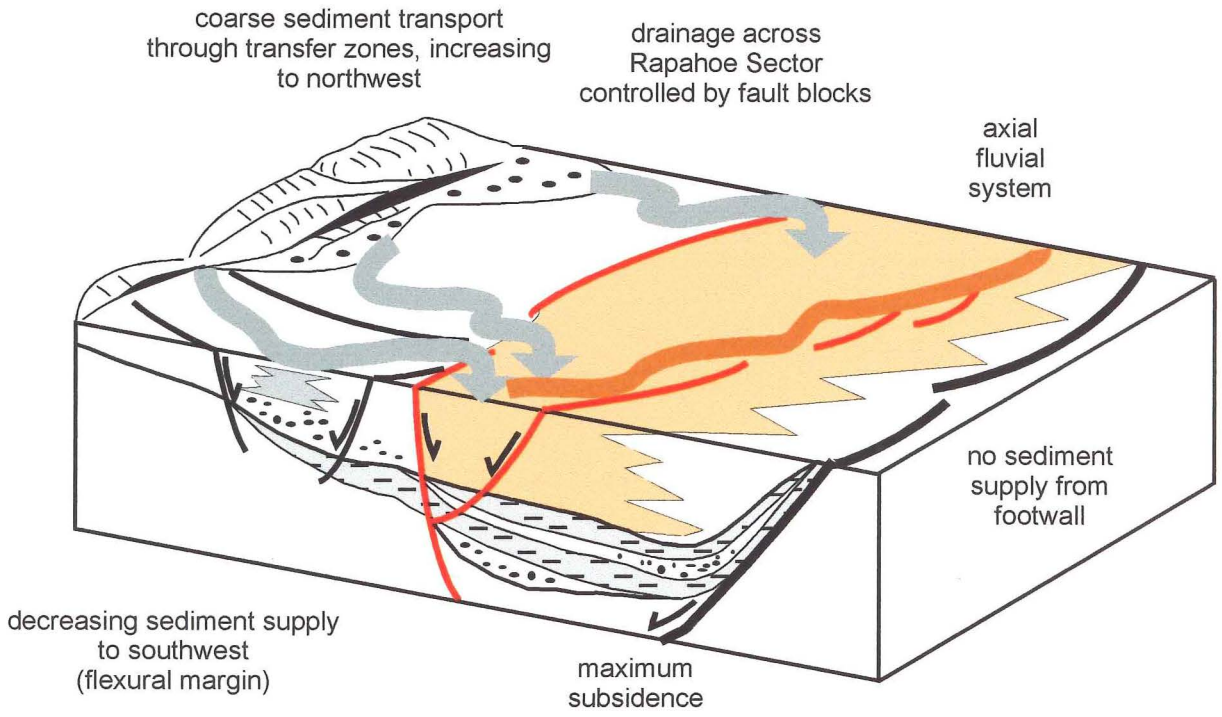

Figure 9.2 Tectonostratigraphic model for Rewanui Formation.
Compare with Figure 8.3A (Leeder & Gawthorpe 1987).
Axial fluvial system is entrained by intrabasin faults (red).
Front face of block diagram equates to Figure 4.10, C-C'.
View is to northwest.

The western margin of the Paparoa Basin was a persistent source of coarse sediment, resulting in braidplain deposition throughout the Rewanui Fm. and succeeding units. Coarse sediment entered the basin via transfer zones, and was carried down the depositional slope towards the central Spring Creek Fault Zone. Minor faulting within the Rapahoe Sector controlled the location of fluvial channels in the upper Rewanui CMM. In the southwest, Rewanui CMM onlapped onto basement, and sand was carried into the basin across the flexural margin.

In the Mt. Davy Sector, the sandy axial fluvial system dominated sedimentation. The fluvial axis was not constrained to lie adjacent to the basement bounding fault as predicted by basin-fill models (e.g. Leeder & Gawthorpe 1987), nor was its position constrained by adjacent alluvial fan deposition (Table 9.2). Rather, the fluvial axis followed a structural lineament which developed during Morgan CMM deposition (Figure 8.5), and paired subsidence along the Spring Creek Fault Zone and the eastern boundary fault (Roa–Hawera Fault Zone) controlled lateral migration of the axial river throughout Rewanui CMM deposition. Minor movement on the Spring Creek Fault Zone prevented the axial fluvial system from entering into the Rapahoe Sector until the uppermost Rewanui CMM.

Within the context of persistent sediment supply into the Paparoa Basin during Rewanui Fm. deposition, there was extensive growth of peat bodies, both within the fluvial axis, and adjacent to the western and southwestern sediment sources. Analysis of paleovegetation and paleoclimate indicates that conditions were ideal for coal accumulation (Ward et al. 1995; Chapter 6). Maximum coal development was in the southern Rapahoe Sector (Ward 1995, Figure 10; Ward 1996, Figure 5), above the northerly sloping flexural basin margin block. Faulting in the central Rapahoe Sector prevented influx of clastic sediment into the southwestern area. The net result was accumulation of extensive, thick clean coal.

The Paparoa Basin was not a simple, asymmetrical half-graben, as depicted by available tectonostratigraphic models (Table 9.2), but rather a complex basin which formed as a result of oblique continental extension. The basin was filled by a non-marine sequence of alternating fluvial and lacustrine/deltaic sediments, and all sedimentation was influenced by the interaction of two orientations of basement faults and two principal

sediment sources. The resulting stratigraphic succession is complex, and differs from typical rift basin sequences. Simplistic tectonostratigraphic models failed to account for the observed features of the Paparoa Group. Enhancement of models, to incorporate the controls exerted on sedimentary patterns by oblique extension, intrabasin faulting and limited footwall sediment supply, is required for those models to gain predictive ability for stratigraphic successions in complex rift basins. However, many components of existing rift-basin models were found to be applicable to the Paparoa Group, and these were used to interpret the tectonic history of the basin from its sedimentary fill.

9.4 Conclusions

Reconstruction of the Paparoa Basin and its fill, the Late Cretaceous to early Tertiary Paparoa Group of the Greymouth Coalfield, was achieved from drillhole data by the integration of lithostratigraphy, basin modelling and palynostratigraphy. The Paparoa Basin and related basins within the West Coast Rift System were formed by NW-oriented oblique extension in the last c.6My of the Cretaceous, and represent a discrete phase of extension of the New Zealand continent which was not directly related to earlier Cretaceous events such as spreading within the Tasman Sea.

Formation of the Paparoa Basin was initiated by development of NNE/SSW oriented low-angle basin-bounding normal faults and the reactivation of existing WNW/ESE oriented structures. During basin development, the NNE/SSW fault trend became dominant, and the extension direction rotated slightly to the WNW in the earliest Tertiary. Depocentre orientations rotated during Paparoa Gp. accumulation, in response to evolution of the basin-bounding faults and cessation of activity on intrabasin faults.

Sedimentation within the Paparoa Basin was controlled by the interplay of two dominant sediment sources, which were texturally and compositionally distinct. Locally derived coarse clastic material entered the basin throughout Paparoa Group deposition from the northwest. Sand from a granitic source area further north within the West Coast Rift System entered the basin from the northeast. This source was initially minor, but became significant as the source area evolved. Minor sources of clastic and volcaniclastic sediment also entered the basin, but little sediment was derived from the eastern basin margin.

Subdivision of the Paparoa Group into fluvial and lacustrine intervals reflected changes in subsidence rate and sediment supply. Periods of greater subsidence and reduced supply resulted in underfilling of the basin and rapid lacustrine transgression. Deltaic deposits, comprising coalesced mouth bar complexes, prograded into the shallow lakes. The locations of deltas were structurally controlled, and persistent sediment influx resulted in elongate to lobate delta forms. Sediment transport patterns reversed during the final lacustrine episode, with sand entering the basin in the south (forming a braid delta), and the northeastern axial system was displaced upslope, so that no coarse sediment entered the basin.

Within coal measure units, sedimentary patterns were determined by syndepositional subsidence on intrabasin faults. The eastern axial fluvial system was constrained within a shallow graben which bisected the coalfield, preventing lateral migration. Sediment was transported to the southwest along the axial river system, which exited the basin to the south via a small graben. In the west of the coalfield, a braidplain carried gravelly sediment from the western margin into the basin. Towards the end of coal measure deposition, coarse sediment was confined to structurally controlled river channels, and extensive mires developed on the floodplain, particularly above the southwestern flexural margin of the basin.

The climatic setting of the Paparoa Basin was cool, seasonal and humid, and the basin was vegetated by rainforest and mires occupied by moisture-loving plants. Vegetation was dominated by conifers, tree ferns and mosses, and flowering plants were rare. Raised mires, which supported limited conifer, fern and moss floras, were common throughout the west of the Paparoa Basin. Prior to the final lacustrine transgression, floras were disrupted by the Cretaceous – Tertiary Boundary event. Some flowering plants became extinct at this time, and for a brief period floral diversity declined. Other flowering plant taxa became abundant, though the dominant conifer and fern forms were unaffected. Decline in the spore floras suggests the climate may have become drier at this time.

The Paparoa Basin was subsequently compacted and buried by up to 4km of Paleogene sediment which accumulated in an expanded, regional rift basin. As a result of Neogene compressional tectonics, the basin was inverted and structurally disrupted, and eroded. Those events superimposed further complexity on the geology of Greymouth Coalfield. However, that complexity was identified and accounted for in this thesis, to reveal the primary sedimentary and tectonic character of the Paparoa Basin.

9.5 Suggestions for future work

The following additional investigations of the Paparoa Group are warranted to further refine basinal, sedimentological and floral history of the Paparoa Basin and West Coast Rift System:

- incorporation of post-1995 drillhole and exploration data, which could lead to further refinement of basin geometry and coal seam correlation models
- limited remapping where lithostratigraphy has changed, especially in the north of the coalfield
- lithological and geophysical definition of the Dunollie Fm. / Brunner CM contact
- comprehensive petrological/petrophysical analysis of compositional variation within the Paparoa Group, especially focussing on the ECS/WCS interface within the Rewanui CMM
- analysis of vitrinite reflectance trends and mapping of regional changes in vertical rank gradient, explanation of why some areas (e.g. Brunner Bridge) have a higher apparent gradient
- expansion of the KTB palynostratigraphy eastwards into the Mt. Davy Sector
- location of Iridium anomalies and related features at the KTB
- further determination of palynofloral change throughout all formations
- improvement of the resolution of the palynological zonation scheme, in light of recent revisions of the New Zealand biostratigraphic framework

References

Adams, C.J.; Raine, J.I., 1988: Age of Cretaceous silicic volcanism at Kyeburn, Central Otago, and Palmerston, eastern Otago, South Island, New Zealand. *New Zealand Journal of Geology and Geophysics 31*: 471–475.

Addis, M.A.; Jones, M.E. 1985: Volume changes during diagenesis. *Marine and Petroleum Geology 2*: 241–246.

Alexander, J.; Leeder, M.R., 1987: Active tectonic control on fluvial architecture. In Ethridge, F.G.; Flores, R.M.; Harvey, M.D. (eds). **Recent developments in fluvial sedimentology.** *SEPM Special Publication no. 39*, pp. 243–266.

Allen, P.A.; Allen, J.R. 1990: **Basin Analysis: Principles and Applications**. Blackwell Scientific Publications, 451pp.

Alvarez, L.W.; Alvarez, W.; Asaro, F.; Michel, H.V. 1980: Extraterrestrial cause for the Cretaceous/Tertiary extinction. *Science 208*: 1095–1108

Anadón, P.; Cabrera, Ll.; Julià, R.; Marzo, M. 1991: Sequential arrangement and asymmetrical fill in the Miocene Rubielos de Mora Basin (northeast Spain). In Anadón, P.; Cabrera, Ll.; Kelts, K. (eds.) **Lacustrine facies analysis**. *Special Publication No. 13, International Association of Sedimentologists,* pp. 257–275.

Anderson, H.J. 1981: Densities of Tertiary rocks, West Coast, South Island, New Zealand. *New Zealand Journal of Geology and Geophysics 24*: 545–553.

Artemjev, M.E.; Kaban, M.K.; Kucherinenko, V.A.; Demyanov, G.V.; Taranov, V.A. 1994: Subcrustal density inhomogeneities of Northern Eurasia as derived from the gravity data and isostatic models of the lithosphere. *Tectonophysics 240*: 249–280.

Askin, R.A. 1989: Endemism and heterochroneity in the Late Cretaceous (Campanian) to Paleocene palynofloras of Seymour Island, Antarctica: implications for origins, dispersal and paleoclimates of southern floras. In Crame, J.A. (ed.) **Origins and Evolution of the Antactic Biota**. *Geological Society Special Publication 47*, pp. 107–119.

Askin, R.A. 1990: Campanian to Paleocene spore and pollen assemblages of Seymour Island, Antarctica. *Review of Palaeobotany and Palynology 65*: 105–113.

Askin, R.A. 1992: Late Cretaceous-Early Tertiary Antarctic outcrop evidence for past vegetation and climates. In Kennett, J.P.; Warnke, D.A. (eds.) **The Antarctic paleoenvironment: a perspective on global change**. *Antarctic Research Series 56*: 61–73.

Askin, R. A.; Jacobson, S.R. 1996: Palynological changes across the Cretaceous – Tertiary Boundary on Seymour island, Antarctica: environmental and depositional factors. In MacLeod, N. & Keller, G. (eds.) **Cretaceous – Tertiary mass extinctions: biotic and environmental changes**. W.W. Norton & Coy, pp. 7–25.

Askin, R.A.; Spicer, R.A. 1995: The Late Cretaceous and Cenozoic history of vegetation and climate at northern and southern high latitudes: a comparison. In National Research Coucil (U.S.) Board on Earth Sciences and Resources: **Effects of past global change on life**. Studies in Geophysics, National Academy Press, Washington DC, pp. 156–173.

Ayres, J.B. (Jr.) 1986: Lacustrine and fluvial-deltaic depositionial systems, Fort Union Formation (Paleocene), Powder River Basin, Wyoming and Montana. *American Association of Petroleum Geologists Bulletin 70*: 1651–1673.

Bal, A.A. 1992: Estuarine to fluvial transition: the Cretaceous/Tertiary "Puponga" Coal Measures in the Pakawau Group, northwest Nelson. Unpublished B.Sc.(Hons.) thesis, University of Canterbury. 67pp.

Bal, A.A. 1994: Disparate hydrocarbon generation potential and maturation profiles of Pakawau Group source coals: implications for Taranaki Basin exploration. *Proceedings, 1994 N. Z. Petroleum Expl. Conf.*, pp. 322–337.

Bal, A.; Lewis. D.W., 1994: A Cretaceous–early Tertiary macrotidal estuarine–fluvial succession: Puponga Coal Measures in Whanganui Inlet, onshore Pakawau Sub-basin, northwest Nelson, New Zealand. *New Zealand Journal of Geology and Geophysics 37*: 287–307.

Baldwin, B.; Butler, C.O. 1985: Compaction curves. *American Association of Petroleum Geologists Bulletin 69*: 622–626.

Barker, C.E.; Goldstein, R.H. 1990: Fluid-inclusion technique for determining maximum temperature in calcite and its comparison to the vitrinite reflectance geothermometer. *Geology 18*: 1003–1006.

Barker, C.E.; Pawlewicz, M.J. 1986: The correlation of vitrinite reflectance with maximum temperature in humic organic matter. In Buntebarth, G. & Stegena, L. (eds.) **Paleogeothermics: Evaluation of geothermal conditions in the geological past.** *Lecture Notes in Earth Sciences 5*. Springer-Verlag, pp. 79–93.

Barrera, E. 1994: Global environmental changes preceding the Cretaceous–Tertiary boundary: Early–late Maastrichtian transition. *Geology 22*: 877–880.

Barrera, E.; Keller, G. 1994: Productivity across the Cretaceous/Tertiary boundary in high latitudes. *Geological Society of America Bulletin 106*: 1254–1266.

Barry, J.M.; Duff, S.W.; MacFarlan, D.A. 1994: **Coal resources of New Zealand.** *Resource Information Report 16*, Energy and Resources Division, Ministry of Commerce, New Zealand. 73pp.

Beard, D.C.; Weyl, P.K. 1973: Influence of texture on porosity and permeability of unconsolidated sand. *American Association of Petroleum Geologists Bulletin 57*: 349–369.

Bishop, D.G. 1994: Geology of the Milton area. Scale 1:50000. *Institute of Geological and Nuclear Sciences Geological Map 9.*

Bishop, D.J. 1991: Cretaceous and Cenozoic tectonics of the West Coast region of the South Island. *Proceedings, 1991 N. Z. Oil Exploration Conf.,* pp. 122–133.

Bishop, D.J. 1992: Extensional tectonism and magmatism during the middle Cretaceous to Paleocene, North Westland, New Zealand. *New Zealand Journal of Geology and Geophysics 35*: 81–91.

Bishop, D.J.; Buchanan, P.G. 1995: Development of structurally inverted basins: a case study from the West Coast, South Island, New Zealand. In Buchanan, J.G. & Buchanan, P.G. (eds.) **Basin Inversion**. *Geological Society Special Publication No. 88*, pp. 549–585.

Blair, T.C.; Bilodeau, W.L. 1988: Development of tectonic cyclothems in rift, pull-apart and foreland basins: Sedimentary response to episodic tectonism. *Geology 16*: 517–520.

Blair, T.C.; McPherson, J.G. 1994: Alluvial fnas and their natural distinction from rivers based on morphology, hydraulic processes, sedimentary processes and facies assemblages. *Journal of Sedimentary Research A64*: 450–489.

Boggs, s. (Jr.) 1987: **Principles of sedimentology and stratigraphy.** Merrill Publishing Company, 784pp.

Bond, G.C.; Kominz, M.A. 1984: Construction of tectonic subsidence curves for the early Paleozoic miogeocline, southern Canadian Rocky Mountains: implications for subsidence mechanisms, age of breakup and crustal thinning. *Geological Society of America Bulletin 95*: 155–173.

Bowen, F.E. 1964: Geology of Ohai Coalfield. *New Zealand Geological Survey Bulletin 51*: 203pp.

Bowman, R.G. 1982: **The Rapahoe Sector of the Greymouth Coalfield.** New Zealand Coal Resources Survey Report, Ministry of Energy, Wellington, New Zealand. 84pp.

Bowman, R.G.; Caffyn, P.; Duff, S.W. 1984: **Greymouth Coalfield**. New Zealand Coal Resources Survey Report, Ministry of Energy, Wellington, New Zealand. Part 1, 211pp.

Boyd, R.J. 1993: Progressive diagenetic changes calibrated with temperature and depth from vitinitre reflectance and fission track data – an assessment of the usefulness of inorganic diagenesis as a paleoburial indicator. Unpublished M.Sc. thesis, University of Canterbury. 163pp.

Boyd, R.J.; Lewis, D.W. 1995: Sandstone diagenesis relating to varying burial depth and temperature in Greymouth Coalfiled, South Island, New Zealand. *New Zealand Journal of Geology and Geophysics 38*: 333–348.

BPB 1981: **Coal Interpretation Manual**. BPB Instruments Ltd., 100pp.

Broadbent, M.; Callender, P.F. 1991: A resistivity survey near Waimakariri River, Canterbury Plains, to improve understanding of local groundwater flow and of the capabilities of the survey method. *New Zealand Journal of Geology and Geophysics 34*: 441–453.

Brooks, R.R.; Reeves, R.D.; Yang, X.-H.; Ryan, D.E.; Holzbecher, J.; Collen, J.D.; Neall, V.E.; Lee, J. 1984: Elemental anomalies at the Cretaceous–Tertiary boundary, Woodside Creek, New Zealand. *Science 226*: 539–542.

Brooks, R.R.; Hoek, P.L.; Reeves, R.D.; Strong, P.C. 1986a: Geochemical delineation of the Cretaceous/Tertiary boundary in some New Zealand rock sequences. *New Zealand Journal of Geology and Geophysics 29*: 1–8.

Brooks, R.R.; Strong, C.P.; Lee, J.; Orth, C.J.; Gilmore, J.S.; Ryan, D.E.; Holzbecher, J. 1986b: Stratigraphic occurrences of iridium anomalies at four Cretaceous/Tertiary boundary sites in New Zealand. *Geology 14*: 727–729.

Brown, L.F. (Jr.) 1975: Role of sediment compaction in determining geometry and distribution of fluvial and deltaic sandstones. In Chilingarian, G.V. & Wolf, K.H. (eds.) **Compaction of coarse-grained sediments, I**. *Developments in Sedimentology 18A*. Elsevier, pp. 247–292.

Browne, K.W. 1986a: A palynological study of drillholes 380 and 354, Ohai Coalfield. Unpublished report, September 1986, 17pp.

Browne, K.W. 1986b: The Palynology of the Kaitangata Coalfield, southeast Otago. Unpublished M.Sc. thesis, University of Canterbury. 144pp.

Browne, K.W. 1987: Reconnaissance palynological investigation of the Kaitangata Sector, Kaitangata Coalfield. Unpublished report produced for Resource Management and Mining Group, Ministry of Energy.

Browne, K.W.; MacKinnon, D.I. 1989: Palynological correlations at Kaitangata Coalfield. Report RD8819, Ministry of Energy, Wellington. 43pp.

Burnham, A.K.; Sweeney, J.J. 1989: A chemical kinetic model of vitrinite maturation and reflectance. *Geochimica et Cosmochimica Acta 53*: 2649–2657.

Caffyn, P. 1994: Mt. Davy East: summary report of geological mapping. Unpublished Coal Corporation of New Zealand Ltd. report.

Cant, D.J. 1984: Subsurface facies analysis. In Walker, R.G. (ed.) **Facies Models (Second Edition)**. *Geoscience Canada, Reprint Series* 1, pp. 297–310.

Cave, M.P.; Newman, J. 1995: Vitrinite reflectance variations between Brunner and Paparoa coal measure sequences in the Greymouth Coalfield and the inplications for petroleum source rock maturation; some initial results. *Proceedings, 6th N. Z. Coal Conf.*, pp. 3–14.

Christophel, D.C. 1995: The impact of climate changes on the development of the Australian flora. In National Research Coucil (U.S.) Board on Earth Sciences and Resources: **Effects of past global change on life**. Studies in Geophysics, National Academy Press, Washington DC, pp. 174–183.

Couper, R.A. 1953: Upper Mesozoic and Cainozoic spores and pollen grains of New Zealand. *New Zealand Geological Survey Paleontological Bulletin 22*: 77pp.

Couper, R.A. 1960: New Zealand Mesozoic and Cainozoic plant microfossils. *New Zealand Geological Survey Paleontological Bulletin 32*: 87pp.

Crampton, J.S.; Beu, A.G.; Campbell, H.J.; Cooper, R.A.; Morgans, H.E.G.; Raine, J.I.; Scott, G.H.; Stevens, G.R.; Strong, C.P.; Wilson, G.J. 1995: An interim New Zealand geological time scale. *Institute of Geological and Nuclear Sciences Science Report 95/9*: 5pp.

Crampton, J.S. 1995: Revised inoceramid bivalve zonation and correlations for the Cenomanian to Santonian stages (Late Cretaceous) in New Zealand. In **The Cretaceous system in east and south Asia. Research summary 1995.** *IGCP 350, Newsletter special issue 2*: 49–59.

Crouch, E.M. 1994: Kaitangata Coalfield samples for palynological assessment (FRST contract DON301). Unpub. Institute of Geological and Nuclear Sciences report EMC 2/94.

Czochznska, Z.; Sheppard, C.M.; Weston, R.J.; Woolhouse, A.D. 1987: A biological marker study of oils and sediments from the West Coast, South Island, New Zealand. *New Zealand Journal of Geology and Geophysics 30*: 1–17.

Daniel, I.L.; Lovis, John D. 1988: The mid-Cretaceous megaflora of the Clarence Valley, New Zealand. *Abstracts - International Organization of Palaeobotany Conference 3*, p.7.

Diessel, C.F.K. 1992: **Coal-Bearing Depositional Systems**. Springer-Verlag, 721 pp.

Dettmann, M.E.; Playford, G. 1968: Taxonomy of some Cretaceous spores and pollen grains from eastern Australia. *Proceedings of the Royal Society of Victoria 81, Part 2*: 69–94.

Dettmann, M.E.; Jarzen, D.M. 1988: Angiosperm pollen from uppermost Cretaceous strata of southeastern Australia and the Antarctic Peninsula. *Memoir of the Association of Australasian Paleontologists 5*: 217–237.

Dettmann, M.E.; Jarzen, D.M. 1991: Pollen evidence for Late Cretaceous differentiation of Proteaceae in southern polar forests. *Canadian Journal of Botany 69*: 901–906.

Dettmann, M.E.; Pocknall, D.T.; Romero, E.J.; Zamaloa, M. del C. 1990: *Nothofagidites* Erdtman ex Potonié, 1960; a catalogue of species with notes on the paleogeographic distribution of *Nothofagus* Bl. (Southern Beech). *New Zealand Geological Survey Paleontological Bulletin 60*: 79pp.

Dubrule, O. 1994: Estimating or choosing a geostatistical model. In Dimitrakopoulos, R. (ed.) **Geostatistics for the next century**. Kluwer Academic Publishers, pp. 3–14.

Duff, S.W. 1988: Greymouth Project Feasability Study Volume 2: Geology. Unpublished Greymouth Coal Ltd. report.

Duncan, R.P.; Norton, D.A.; Woolmore, C.B. 1990: The lowland vegetation pattern, south Westland, New Zealand. 2. Ohinemaka forest. *New Zealand Journal of Botany 28*: 131–140.

Dunne, L.A.; Hempton, M.R. 1984: Deltaic sedimentation in the Lake Hazar pull-apart basin, southeastern Turkey. *Sedimentology 31*: 115–132.

Edwards, A.R.; Hornibrook, N.de B.; Raine, J.I.; Scott, G.H.; Stevens, G.R.; Strong, C.P.; Wilson, G.J. 1988: A New Zealand Cretaceous-Cenozoic time scale. *New Zealand Geological Survey Record 35*: 135–149

Elliot, D.H.; Askin, R.A.; Kyte, F.T.; Zinsmeister, W.J. 1994: Iridium and dinocysts at the Cretaceous-Tertiary boundary on Seymour Island, Antarctica: implications for the K–T event. *Geology 22*: 675–678.

Etheridge, M.A. 1986: On the reactivation of extensional fault systems. *Philosophical Transactions of the Royal Society of London A317*: 179–194.

Falvey, D.A.; Deighton, I. 1982: Recent advances in burial and thermal geohistory analysis. *APEA Journal 22, pt. 1*: 65–81.

Farabee, M.J.; Canright, J.E. 1986: Stratigraphic palynology of the lower part of the Lance Formation (Maestrichtian) of Wyoming. *Palaeontographica Abt. B 199*: 1–89.

Farquharson, G.W. 1982: Lacustrine deltas in a Mesozoic alluvial sequence from Camp Hill, Antarctica. *Sedimentology 29*: 717–725.

Ferguson, R.J. 1993: Tectonic controls on basin development, fluvial architecture and coal occurrence in the Paparoa coal measures at the Pike River coalfield, West Coast of the South Island. Unpublished M.Sc. thesis, University of Canterbury. 131pp.

Field, B.D.; Odin, G.S. 1981: K-Ar dating of Paleocene glaucony from North Canterbury, New Zealand. *New Zealand Geological Survey Report G45*, 16pp.

Flint, S.; Stewart, D.J.; van Riessen, E.D. 1989: Reservoir geology of the Sirikit oilfield, Thailand: lacustrine deltaic sedimentation in a Tertiary intermontane basin. In Whateley, M.K.G.; Pickering, K.T. (eds.) **Deltas: Sites and Traps for Fossil Fuels**. *Geological Society Special Publication No. 31*, pp. 223–237.

Francis, J.E. 1986: Growth rings in Cretaceous and Tertiary wood from Antarctica and their paleoclimatic implications. *Palaeontology 29*: 665–684.

Frostick, L.E.; Steel, R.J. 1993a: Tectonic signatures in sedimentary basin fills: an overview. In Frostick, L.E.; Steel, R.J. (eds.) **Tectonic controls and signatures in sedimentary successions.** *Special Publication No. 20 of the International Association of Sedimentologists*, pp. 1–9.

Frostick, L.E.; Steel, R.J., 1993b: Sedimentation in divergent plate-margin basins. In Frostick, L.E.; Steel, R.J. (eds.) **Tectonic controls and signatures in sedimentary successions.** *Special Publication No. 20 of the International Association of Sedimentologists*, pp. 111–128.

Gage, M. 1952: **The Greymouth coalfield**. *New Zealand Geological Survey bulletin 45*. 232p.

Gage, M.; Wellman, H.W. 1944: The geology of Koiterangi Hill, Westland. *Transactions of the Royal Society of New Zealand 73*: 351–364

Gallagher, K.; Lambeck, K. 1992: Subsidence, sedimentation and sea-level changes in the Eromanga Basin, Australia. *Basin Research 2*: 115–131.

Gawthorpe, R.L.; Colella, A., 1990: Tectonic controls on coarse-grained delta depositional systems in rift basins. In Colella, A.; Prior, D.B., (eds.) **Coarse–Grained Deltas.** *Special Publication No. 10 of the International Association of Sedimentologists*, pp. 113–127.

Gawthorpe, R. L.; Hurst, J.M. 1993: Transfer zones in extensional basins: their structural style and influence on drainage development and stratigraphy. *Journal of the Geological Society, London 150*: 1137–1152.

Gradstein, F.M.; Agterberg, F.P.; Ogg, J.G.; Hardenbol. J.G.; van Veen, P.; Thierry, J.; Huang, Z. 1994: A Mesozoic time scale. *Journal of Geophysical Research 99 (B12)*: 24051–24074.

Green, P.F.; Duddy. I.R.; Gleadow, A.J.W.; Lovering, J.F. 1989: Apatite fission track analysis as a palotemperature indicator for hydrocarbon exploration. In Naeser, N.D. & McCulloh, T. (eds.) **Thermal history of sedimentary basins: methods and case histories**. Springer-Verlag, pp. 181–195.

Gumati, Y.D.; Nairn, A.E.M. 1991: Tectonic subsidence of the Sirte Basin, Libya. *Journal of Petroleum Geology 14*: 93–102.

Hails, J.R. 1976: Compaction and diagenesis of very coarse-grained sediments. In Chilingarian, G.V. & Wolf, K.H. (eds.) **Compaction of coarse-grained sediments, II.** *Developments in Sedimentology 18B*. Elsevier, pp. 445–473.

Helby, R.; Morgan, R.; Partridge, A.D. 1987: A palynological zonation of the Australian Mesozoic. In Jell, P.A. (ed.) **Studies in Australian Mesozoic Palynology.** *Memoirs Assoc. Australasian Palaeontologists 4*: 1–94.

Hornibrook, N. de B. 1962: The Cretaceous–Tertiary boundary in New Zealand. *New Zealand Journal of Geology and Geophysics 5*: 295–303.

Hornibrook, N. de B.; Brazier, R.C.; Stong, C.P. 1989: Manual of New Zealand Permian to Pleistocene foraminiferal biostratigraphy. *New Zealand Geological Survey Paleontological Bulletin 56*: 175pp.

Houlding, S. 1994: **3D geoscience modelling: computer techniques for geological characterization**. Springer-Verlag, 309pp.

Houseknecht, D.W. 1987: Assessing the realtive importance of compaction processes and cementation to reduction of porosity in sandstones. *American Association of Petroleum Geologists Bulletin 71*: 633–342.

Hower, J.C.; Rathbone, R.F.; Wild, G.D.; Davis, A. 1994: Observations on the use of vitrinite maximum reflectance versus vitrininte random reflectance for high volatile bituminous coals. *Journal of Coal Quality, July–Dec. 1994*: 71–76.

Hyne, N.J.; Cooper, W.A.; Dickey, P.A. 1979: Stratigraphy of intermontane, lacustrine delta, Catatumbo River, Lake Maracaibo, Venezuela. *American Association of Petroleum Geologists Bulletin 63*: 2042–2057.

Ian R. Brown Associates Ltd. 1992: Greymouth Coalfield drillhole database: conversion from GEODAS to TECHBASE. Unpublished report for Resource Information Unit, Energy & Resources Division, Ministry of Commerce, 23pp.

Isaacs, E.H.; Srivastava, R.M. 1989: **Applied geostatistics**. Oxford University Press, 561pp.

Johnson, K.R. 1992a: Megafloral biostratigraphy of the Cretaceous–Tertiary boundary: Great Plains, USA and South Island, New Zealand. *International Organisation of Paleobotany Conference, Paris*: p. 82.

Johnson, K.R. 1992b: High latitude deciduous vegetation and muted floral response to the Cretaceous–Tertiary boundary event in New Zealand. *Abstracts with programs, 1992 Annual meeting, Geological Society of America 24(7)*: A–333.

Johnson, K.R.; Greenwood, D. 1993: High-latitude deciduous forests and the Cretaceous–Tertiary boundary in New Zealand. *Abstracts with programs, 1993 Annual meeting, Geological Society of America 25(6)*: A–295.

Johnson, K.R; Raine, J.I. 1991: A southern hemisphere terrestrial Cretaceous/Tertiary boundary section: Macro- and microfloral record from the Paparoa Trough, South Island, New Zealand. *Abstr. with prog, 1991 Annual mtg, Geological Soc. of America 23(5)*: 358.

Kamp, P.J.J. 1986: Late Cretaceous – Cenozoic tectonic development of the southwest Pacific region. *Tectonophysics 121*: 225–251.

Kamp, P.J.J.; Whitehouse, I.W.S.; Newman, J. 1992: Thermotectonic history and hydrocarbon prospectivity of the Greymouth Coalfield, Westland, assessed by apatite fission track analysis. *Proceedings, 1991 N.Z. Oil Expl. conf.,* pp. 321–335.

Karner, G.D.; Egan, S.S.; Weissel, J.K. 1992: Modelling the tectonic development of the Tucano and Sergipe–Alagoas rift basins, Brazil. *Tectonophysics 215*: 133–160.

Kear, D. 1994: Major economic geology successes in New Zealand since the Second World War. *Geological Society of New Zealand Newsletter 103*: 30–48.

Keller, G. 1993: The Cretaceous–Tertiary boundary transition in the Antarctic Ocean and its global implications. *Marine Micropaleontology 21*: 1–45.

Keller, G.R.; Cather, S.M. (eds.) 1994: **Basins of the Rio Grande Rift: Structure, stratigraphy and tectonic setting.** *Geological Soc. of America Special Paper 291*, 304pp.

Kennedy, E.M. 1993: Palaeoenvironment of an Haumurian palnt fossil locality within the Pakawau Group, North West Nelson, New Zealand. Unpublished M.Sc. thesis, University of Canterbury. 201pp.

Kennett, J.P.; Barker, P.F. 1990: Latest Cretaceous to Cenozoic climate change and oceanographic developments in the Weddell Sea, Antarctica: an ocean-drilling perspective. *Proceedings of the Ocean Drilling Program, Scientific Results 113*: 937.

King, P.R.; Thrasher, G.P. 1996: Cretaceous–Cenozoic geology and petroleum systems of the Taranaki Basin, New Zealand. *Institute of Geological and Nuclear Sciences monograph 13*, 243pp.

Krajewski, S.A.; Gibbs, B.L. 1994: Computer contouring generates artifacts. *Geotimes, April 1994*: 15–19.

Kusznir, N.J.; Karner, G.D.; Egan, S.S. 1987: Geometric, thermal and isostatic consequences of detachments in continental lithosphere extension and basin formation. In Beaumont, C. & Tankard, A.J. (eds.) **Sedimentary Basins and Basin-forming Mechanisms**. *Canadian Society of Petroleum Geologists Memoir 12*, pp. 185–203.

Kusznir, N.J.; Ziegler, P.A 1992: The mechanics of continental extension and sedimentary basin formation: a simple-shear / pure-shear flexural cantilever model. *Tectonophysics 215*: 117–131.

Laird, M.G. 1968: The Paparoa Tectonic Zone. *New Zealand Journal of Geology and Geophysics 11*: 435–454.

Laird, M.G. 1972: Sedimentology of the Greenland Group in the Paparoa Range, West Coast, South Island. *New Zealand Journal of Geology and Geophysics 15*: 372–393.

Laird, M.G. 1981: The Late Mesozoic fragmentation of the New Zealand segment of Gondwana. In Cresswell, M.M.; Vella, P. (eds.) **Gondwana Five.** *Proceedings of the 5th International Gondwana Symposium, Wellington, 1980.* A.A. Balkema, pp. 311–318.

Laird, M.G. 1988: Geological map of New Zealand 1:63360 Sheet S37 **Punakaiki**. Wellington, New Zealand Geological Survey, 48pp.

Laird, M.G. 1993: Cretaceous continental rifts: New Zealand region. In Ballance, P.F. (ed.) **South Pacific Sedimentary Basins.** *Sedimentary Basins of the World, 2.* Elsevier, pp. 37–49.

Laird, M.G. 1994: Geological aspects of the opening of the Tasman Sea. In Van der Lingen, G.J., Swanson, K.M., Muir, R.J. (eds.) **Evolution of the Tasman Sea Basin.** A.A.Balkema, Rotterdam, pp. 1–17.

Laird, M.G. 1996: What plate rearrangement at ~70Ma initiated the West Coast–Taranaki Rift System? In Wood, R., Herzer, R.H., Sutherland, R., Edbrooke, S., Uruski, C. Plate reconstruction workshop proceedings. *Institute of Geological and Nuclear Sciences science report 96/35*, pp. 15–19.

Lambiase, J.J. 1990: A model for tectonic control of lacustrine stratigraphic sequences in continental rift basins. In Katz, B.J. (ed.) **Lacustrine Basin Exploration: Case Studies and Modern Analogs.** *AAPG Memoir 50*, pp. 265–276.

Lambiase, J.J. (ed.) 1995: **Hydrocarbon habitat in rift basins.** *Geological Society Special Publication No. 80*, 381pp.

Larrieu, T. L. 1995: Basin analysis with a spreadsheet. *Journal of Geological Education 43*: 107–113.

Larter, S. 1989: Chemical models of vitrinite evolution. *Geologische Rundschau 78*: 349–359.

Lawver, L.A.; Gahagan, L.M.; Coffin, M.F., 1992: The development of paleoseaways around Antarctica. In Kennett, J.P. & Warnke, D.A. (eds) **The Antarctic paleoenvironment: a perspective on global change.** *Antarctic Research Series 56*: 7–30.

Leeder, M.R.; Gawthorpe, R.L., 1987: Sedimentary models for extensional tilt-block/half graben basins. In Coward, M.P.; Dewey, J.F.; Hancock, P.L. (eds.) **Continental extensional tectonics.** *Geological Society Special Publication No. 28*, pp. 139–152.

Lerche, I.; Yarzab, R.F.; Kendall. C.G.St.C 1984: Deteremination of paleoheat flux from vitrtinite reflectance data. *American Association of Petroleum Geologists Bulletin 68*: 1704–1717

le Roux, J.P. 1994: The use of trend surfaces in paleoenvironmental reconstructions. *Palaeogeography, Palaeoclimatology, Palaeoecology 111*: 185–190

Lewis, D.W. 1984: **Practical Sedimentology.** Hutchinson Ross, 229pp.

Lindqvist, J.K. 1995: Wangaloa and Abbotsford Formations: Measly Beach drillhole, South Otago, New Zealand. *Institute of Geological and Nuclear Sciences Science Report 95/12*: 44pp.

Lister, G.S.; Etheridge, M.A.; Symonds, P.A., 1986: Detachment faulting and the evolution of passive continental margins. *Geology 14*: 246-250.

Macphail, M.K. 1994: Impact of the K/T event on the southeast Australian flora and vegetation: mass extinction, niche disruption or nil? *Palaeoaustral (PPAA Newsletter) 1994, No. 1*: 9–13.

Martin, A.R.H. 1995: Palaeogene proteaceous pollen and phylogeny. *Alcheringa 19*: 27–40.

Matthews, E.R. 1990: Exploration in the on-shore Westland Basin. *Proceedings, 1989 New Zealand Petroleum Exploration Conference*, pp. 62–69.

McClay, K.R.; White, M.J. 1995: Analogue modelling of orthogonal and oblique rifting. *Marine and Petroleum Geology 12*: 137–151.

McDougall, A.J. 1993: Investigation of geological structure, coal optical fabrics, and basin evolution at Pike River Coalfield, West Coast, South Island. Unpublished M.Sc. thesis, University of Canterbry. 208pp.

McIntyre, D.J. 1964: Report on pollen floras in Arahura–1. Unpublished report, New Zealand Geological Survey.

McIntyre, D.J. 1965: Some new pollen species from New Zealand Tertiary deposits. *New Zealand Journal of Botany 3*: 204–214.

McKellar, I.C. 1990: Southwest Dunedin urban area. *Miscellaneous series, map 22.* New Zealand Geological Survey.

McKenzie, D.P. 1978: Some remarks on the development of sedimentary basins. *Earth and Planetary Science Letters 40*: 25–32.

McMillan, S.G. 1995: Report of the Fairfield Estate drillhole (FE1) near Dunedin, Otago. *Institute of Geological and Nuclear Sciences Science Report 95/17*: 20pp.

McNee, J. 1997: Structural geology of the Rapahoe Sector, Greymouth Coalfield, New Zealand. Unpublished M.Sc. thesis, University of Canterbry. 108pp.

McPherson, J.G.; Shanmugam, G.; Moiola, R.J. 1987: Fan-deltas and braid deltas: Varieties of coarse-grained deltas. *Geological Society of America Bulletin 99*: 331–340.

McWhorter, R.; Torguson, W. 1995: Palacios Field: a 3-D case history. *The Leading Edge, December 1995*: 1225–1230.

Miall, A.D. 1990: **Principles of Sedimentary Basin Analysis**. Springer-Verlag, 668pp.

Mildenhall, D.C., 1980: New Zealand Late Cretaceous and Cenozoic plant biogeography; a contribution. *Palaeogeography, Palaeoclimatology, Palaeoecology 31*: 197–233.

Mildenhall, D.C. 1994: Palynological reconnaissance of Early Cretaceous to Holocene sediments, Chatham Islands, New Zealand. *New Zealand Geological Survey Paleontological Bulletin 67 / Institute of Geological and Nuclear Sciences Monograph 7*: 206pp.

MINEsoft, Ltd. 1996: *TECHBASE* ® Reference manual. Version 2.40.

Moore, N.A. 1996a: Palynology and coal petrography of Rewanui Member seams in the Rapahoe Sector, Greymouth Coalfield. Unpublished M.Sc. thesis, University of Canterbury. 130pp.

Moore, N.A. 1996b: Seam identification, correlation and coal quality prediction using in-seam variations in key palynomorph abundances. *Proceedings, Australasian Institute of Mining and Metallurgy, New Zealand Branch annual conference, Greymouth*, pp. 228–246.

Moore, T.A. 1996: Rock and coal type distribution in the Greymouth area: applications for mining. *Proceedings, Australasian Institute of Mining and Metallurgy, New Zealand Branch annual conference, Greymouth*, pp. 200–227.

Moore, T.A.; Hilbert, R.E. 1992: Petrographic and anatomical characteristics of plant material from two peat deposits of Holocene and Miocene age, Kalimantan, Indonesia. *Review of Palynology and Paleobotany 72*: 199–227.

Morgan, P.G. 1911: The geology of the Greymouth subdivision, North Westland. *New Zealand Geological Survey Bulletin 13*, 159pp.

Morley, C.K. 1995: Developments in the structural geology of rifts over the last decade and their impact on hydrocarbon generation. In Lambiase, J.J. (ed.) **Hydrocarbon habitat in rift basins.** *Geological Society Special Publication No. 80*, pp. 1–32.

NASC 1983: **North American Stratigraphic Code**. *American Association of Petroleum Geologists Bulletin 67*: 841–875.

Nathan, S. 1974: Stratigraphic nomenclature for the Cretaceous–Lower Quaternary rocks of Buller and North Westland, West Coast, South Island, New Zealand. *New Zealand Journal of Geology and Geophysics 17*: 423–445.

Nathan, S. 1978: Geological map of New Zealand 1:63360 Sheet S44 **Greymouth**. Wellington, New Zealand Geological Survey, 36pp.

Nathan, S.; Anderson, H.J.; Cook, R.A.; Herzer, R.H.; Hoskins, R.H.; Raine, J.I.; Smale, D. 1986: Cretaceous and Cenozoic sedimentary basins of the West Coast region, South Island, New Zealand. *New Zealand Geological Survey Basin Studies 1*, 90pp.

Nelson, R.A.; Patton, T.L.; Morley, C.K. 1992: Rift-segment interaction and its relation to hydrocarbon exploration in continental rift systems. *American Association of Petroleum Geologists Bulletin 76*: 1153–1169.

Newman, J. 1981: Development of the Late Cretaceous–Paleocene Paparoa Coal Measure Basin at Greymouth. The interrelationship of differential subsidence, sedimentary facies, coal seam distribution and coal seam character. Report to Lime and Marble Ltd. for Mines Division, Ministry of Energy. 15pp.

Newman, J. 1985: Paleoenvironments, coal properties, and their inter–relationships in Paparoa and selected Brunner Coal Measures on the West Coast of the South Island. Unpublished Ph.D. thesis, University of Canterbury. 269pp.

Newman, J. 1987: Coal type and paleoenvironments in the Rapahoe Sector, Greymouth Coalfield. *Resource Management and Mining Coal Geology Technical Report 3*: 28pp.

Newman, J. 1994: Climate controls on New Zealand coal measures. *Coal Research Newsletter, December 1994.*

Newman, J. 1995: Relationship between quantitative vitrinite fluorescence and the chemistry and industrial properties of West Coast coals. *Proceedings, 6th N.Z. Coal Conf.*, pp. 15–22.

Newman, J. 1997: New approaches to detection and correction of suppressed vitrinite reflectance. *APPEA Journal 1997*: 524–535.

Newman, J.; Newman, N.A., 1982: Reflectance anomalies in Pike River coals: evidence of variability in vitrinite type, with implications for maturation studies and 'Suggate rank'. *New Zealand Journal of Geology and Geophysics 25*: 469–476.

Newman, J.; Johnston, J.H.; Lake, P.J. 1992: The influence of isorank variations in vitrinite chemistry on vitrinite reflectance and some sterane and triterpane maturation indicators. *Proceedings, 1991 N. Z. Petroleum Expl. Conf.*, pp. 336–350.

Newman, J.; Newman, N.A., 1992: Tectonic and paleoenvironmental controls on the distribution and properties of Upper Cretaceous coals on the west Coast of the South island, New Zealand. In McCabe, P.J. & Parrish, J.T. (eds.) **Controls on the distribution and quality of Cretaceous coals**. *Geological Soc. of America Special paper 267*, pp. 347–368.

Newman, J.; Kennedy, E.M.; Daniel, I.L.; Warnes, M.D. 1993: Paleofloral and paleoclimatic influences on the properties of Cretaceous and Eocene New Zealand coals. *10th Annual Meeting for the Society for Organic Petrology*, pp. 31–34.

Newman, J.; Price, L.C.; Johnston, J.H. 1994: Variations in source potential and maturation of New Zealand coals. *Proceedings, 1994 N. Z. Petroleum Expl. Conf.*, pp. 370–384.

Newman, J.; Price, L.C.; Johnston, J.H. 1997: Vitrinite source potential and maturation in Eocene age New Zealand coals: Insights from traditional coal analyses, and *Rock-Eval* and biomarker studies. *Journal of Petroleum Geology 20*: 137–163.

Newman, J.; Ward, S.D. 1996: Combined vitrinite reflectance and fluorescence: a new method for improving reflectance measurement. *Programme and Abstracts, Geological Society of New Zealand Miscellaneous publication 91A*: 134.

Newman, N. 1988: Mineral matter in coals of the West Coast, South Island, New Zealand. Unpublished Ph.D. thesis, University of Canterbury. 293pp.

Nichols, D.J.; Fleming, R.F. 1990: Plant microfossil record of the terminal Cretaceous event in the western United States and Canada. In Sharpton, V.L.; Ward, P.D. (eds.) **Global catastrophes in earth history; an interdisciplinary conference on impacts, volcanism and mass mortality.** *Geological Society of America Special Paper 247*, pp. 445–455.

Nicol, A. 1993: Haumurian (c.66–80Ma) half-graben development and deformation, mid-Waipara, North Canterbury, New Zealand. *New Zealand Journal of Geology and Geophysics 36*: 127–130.

Nicol, A.; Walsh, J.J., Watterson, J.; Gillespie, P.A. 1996: Fault size distributions – are they really power law? *Journal of Structural Geology 18*: 191–197.

Officers of the Geological Survey 1974: Outline of the paleontology of the Greymouth District. *New Zealand Geological Survey Report 67*: 61pp.

Olsen, K.H.; Morgan, P. (1995) Introduction: Progress in understanding continental rifts. In Olsen, K.H. (ed.) **Continental rifts: evolution, structure, tectonics.** *Developments in Geotectonics 25*, pp. 3–26.

Peacock, D.C.; Sanderson, D.J. 1994: Geometry and development of relay ramps in normal fault systems. *American Association of Petroleum Geologists Bulletin 78*: 147–165.

Pocknall, D.T.; Crosbie, Y.M. 1988: Pollen morphology of *Beauprea* (Proteaceae): modern and fossil. *Review of Paleobotany and Palynology 53*: 305–327.

Postma, G. 1990: Depositional architecture and facies of river and fan deltas: a synthesis. In Colella, A.; Prior, D.B. (eds.) **Coarse-Grained Deltas**. *Special Publication No. 10, International Association of Sedimentologists*, pp. 13–27.

Prosser, S. 1993: Rift-related linked depositional systems and their seismic expression. In Williams, G.D.; Dobb, A. (eds.) **Tectonics and seismic sequence stratigraphy.** *Geological Society Special Publication No. 71*, pp. 35–66.

Quick, J.C. 1994: Isorank variation of vitrinite reflectance and fluorescence intensity. In Mukhopadhyay, P.K. & Dow, W.G. (eds.): **Vitrinite reflectance as a maturity parameter: applications and limitations**. *American Chemical Society Symposium Series 570*: 65–75.

Raine, J. I 1979: Palynological dating of Teurian samples associated with glauconie K/Ar dating, Grey River, North Canterbury (M34/f30-34). *Unpublished NZGS report JIR 22/79*, 4pp.

Raine, J.I. 1981: Palynological correlation of the Dunollie/Rewanui Member boundary in drillholes 621 and 622, Greymouth Coalfield. *New Zealand Geological Survey Report PAL47*, 10pp.

Raine, J.I. 1984: Outline of a palynological zonation of Cretaceous to Paleogene terrestrial sediments in West Coast region, South Island, New Zealand. *New Zealand Geological Survey Report 109*, 82pp.

Raine, J.I. 1986: Palynological samples, Ohai Coalfield. Unpublished Palynology Section, NZGS report JIR4/86, 4pp.

Raine, J.I. 1989: Palynology of outcrop upper Pakawau Group, northwest Nelson, New Zealand. New Zealand Geological Survey Report PAL148, 18pp.

Raine, J.I. 1990a: Nonmarine Cretaceous correlations. *Geological Society of New Zealand Miscellaneous publication 50A (GSNZ 1990 Annual conf., prog. & abst.)*: 112–113.

Raine, J.I. 1990b: K/T boundary in New Zealand terrestrial sequences. *Geological Society of New Zealand Miscellaneous publication 50A (GSNZ 1990 Annual conf., prog. & abst.)*: 110.

Raine, J.I. 1994a: Terrestrial K/T boundary studies in New Zealand. *Palaeoaustral (PPAA Newsletter), December 1994*: 9–12.

Raine, J.I. 1994b: Palynology of Kaitangata outcrop samples - a preliminary report. Unpublished Institute of Geological and Nuclear Sciences report JIR 1/94.

Raine, J.I.; Wilson, G.J. 1988: Palynology of the Mt. Somers (South Island, New Zealand) early Cenozoic sequence (note). *New Zealand Journal of Geology and Geophysics 31*: 385–390.

Raine, J.I.; Strong, C.P.; Wilson, G.J. 1993: Biostratigraphic revision of petroleum exploration wells, Great South Basin, New Zealand. *Institute of Geological and Nuclear Sciences Science Report 93/32,* 146pp.

Raine, J.I.; Strong, C.P.; Wilson, G.J.; Pocknall, D.T. 1994: Biostratigraphic revision of the Late Cretaceous to Early Eocene in selected offshore exploration wells, south Canterbury Bight, New Zealand. *Institute of Geological and Nuclear Sciences Science Report 94/30,* 98pp.

Rider, M.H. 1990: Gamma-ray log shape used as a facies indicator: critical analysis of an oversimplified methodology. In Hurst, A.; Lovell, M.A.; Morton, A.C. (eds.) **Geological applications of wireline logs**. *Geological Society Special Publication No. 48*, pp. 27–37.

Robert, P. 1988: **Organic metamorphism and geothermal history: microscopic study of organic matter and thermal evolution of sedimentary basins**. D. Reidel, 311pp.

Roder, G.H.; Suggate R.P. 1990: Geological map of New Zealand 1:50000 Sheet L29 BD **Upper Buller Gorge**. Wellington, New Zealand Geological Survey. 51pp.

Ryer, T.A.; Langer, A.W. 1980: Thickness change involved in the peat-to-coal transformation for a bituminous coal of Cretaceous age in central Utah. *Journal of Sedimentary Petrology 50*: 987–992.

Schlische, R.W. 1991: Half-graben basin filling models: new constraints on continental extensional basin development. *Basin Research 3*: 123–141.

Schlische, R.W.; Anders, M.H. 1996: Stratigraphic effects and tectonic implications of the growth of normal faults and extensional basins. In Beratan, K.K. (ed.) **Reconstructing the history of Basin and Range extension using sedimentology and stratigraphy.** *Geological Society of America Special Paper 103*, pp. 183–203.

Schlische, R.W.; Young, S.S.; Ackerman, R.V.; Gupta, A. 1996: Geometry and scaling relations of a population of very small rift-related normal faults. *Geology 24*: 683–686.

Schlumberger 1985: **Sedimentary environments from wireline logs**. O. Serra (ed.) 211pp.

Schmidt, D.S.; Robinson, P.H. 1990: The structural setting and depositional history for the Kupe South field, Taranaki Basin. *Proceedings, 1989 N.Z. Oil Exploration Conf.*, pp. 151–172.

Sclater, J.G.; Christie, P.A.F. 1980: Continental stretching: an explanation of the post-mid-Cretaceous subsidence of the central North Sea Basin. *Journal of Geophysical Research 85 B7*: 3711–3739.

Sewell, R.J.; Nathan, S.; Adams, C.J. 1988: Geochemistry of Late Cretaceous basaltic rocks from north Westland. *New Zealand Geological Survey Record 35:* 113–121

Shaw, C.A.; Hay, W.W. 1989: Mass-balanced paleogeographic maps: modelling program and results. In Cross, T.A. (ed.) **Quantitative dynamic stratigraphy**. Prentice Hall, pp. 277–291.

Shearer, J.C. 1992: The sedimentology, coal chemistry and petrography of the Morley and Beaumont Coal Measures, Ohai Coalfield. Unpublished Ph.D. thesis, University of Canterbury. 377pp.

Shearer, J.C. 1995: Tectonic controls on styles of sediment accumulation in the Late Cretaceous Morley Coal Measures of Ohai Coalfield, New Zealand. *Cretaceous Research 16*: 367–384.

Shearer, J.C.; Moore, T.A., 1994: Botanical control on banding chracter in two New Zealand coal beds. *Palaeogeography, Palaeoclimatology, Palaeoecology 110*: 11–27.

Shearer, J.C.; Moore, T.A. 1996: Effects of experimental coalification on texture, composition and compaction in Indonesian peat and wood. *Organic Geochemistry 24*: 127–140.

Sleep, N.H. 1971: Thermal effects of the formation of Atlantic continental margins by continental breakup. *Geophysical Journal of the Royal Astronomical Society 24*: 325–350.

Smale, D. 1978: Petrology of some Mawheranui Group rocks. *New Zealand Geological Survey Report G25*, 9pp.

Stach, E.; Mackowsky, M.-Th.; Teichmüller, M; Taylor, G.H.; Chandra, D.; Teichmüller, R. 1982: **Stach's textbook of coal petrology** (3rd edition). Gebrüder Borntraeger, 535pp.

Stam, B.; Gradstein, F.M.; Lloyd, P.; Gillis, D. 1987: Algorithms for porosity and subsidence history. *Computers & Geosciences 13*: 317–349.

Stark, C.J. 1996: Interpretation of Paleocene fluvial sediments from upper Pakawau and Kapuni Groups, Pakawau Sub-basin, North-West Nelson. Unpublished M.Sc. thesis, University of Canterbury. 220pp.

Steckler, M.S.; Watts, A.B. 1978: Subsidence of the Atlantic-type continental margin off New York. *Earth and Planetary Science Letters 41*: 1–13.

Stover, L.E.; Evans, P.R. 1973: Upper-Cretaceous–Eocene spore-pollen zonation, offshore Gippsland Basin, Australia. *Special Publication, Geological Society of Australia 4*: 55–72.

Stover, L.E.; Partridge, A.D. 1973: Tertiary and Late Cretaceous spores and pollen from the Gippsland Basin, southeastern Australia. *Proceedings of the Royal Society of Victoria 85*: 237–286.

Strong, C.P.; Brooks, R.R.; Wilson, S.M.; Reeves, R.D.; Orth, C.J.; Mao, X.-Y.; Quintana, L.R.; Anders, E. 1987: A new Cretaceous–Tertiary boundary site at Flaxbourne River, New Zealand: biostratigraphy and geochemistry. *Geochimica et Cosmochimica Acta 51*: 2769–2777.

Suggate, R.P. 1959: New Zealand coals. Their geological setting and its influence on their properties. *DSIR Research Bulletin 134*, 113pp.

Suggate, R.P. 1974: Coal ranks in relations to depth and temperature in Austrailan and New Zealand oil and gas wells. *New Zealand Journal of Geology and Geophysics 17*: 149–167.

Suggate, R.P. 1984: Geological map of New Zealand 1:50000 Sheet M29 AC **Mangles Valley**. Wellington, New Zealand Geological Survey, 39pp.

Swan, A.R.H.; Sandilands, M. 1995: **Introduction to geological data analysis**. Blackwell Science, 446pp.

Sweeney, J.J.; Burnham, A.K. 1990: Evaluation of a simple model of vitrinite reflectance based on chemical kinetics. *American Association of Petroleum Geologists Bulletin 74*: 1559–1570.

Sweet, A.R.; Braman, D.R.; Lerbekmo, J.F. 1990: Palynofloral response to K/T boundary events; a transitory interruption within a dynamic system. In Sharpton, V.L.; Ward, P.D. (eds.) **Global catastrophes in earth history; an interdisciplinary conference on impacts, volcanism and mass mortality.** *Geological Society of America Special Paper 247*, pp. 457–469.

Taggart, R.E.; Cross, A.T. 1995: The use of three-axis (ternary) diagrams in stratigraphic palynology. *Palynology 19:* 250 (abstract only).

TECHBASE 1992: *TECHBASE* tips. Techbase Australasia Pty Ltd.

TECHBASE 1996: *TECHBASE*® reference manual, Version 2.40. Lakewood, Colorado, MINEsoft Ltd.

Technote 1991: *TECHBASE* Technote, November 1991.

Thorburn, D. F. 1981a: Geology of the Strongman State Coal Mine and environs, Greymouth coalfield, New Zealand. Unpublished New Zealand State Coal Mines report, 15pp.

Thorburn, D. F. 1981b: Geology of the Liverpool No. 3 State Coal Mine and environs. Unpublished New Zealand State Coal Mines report, 15pp.

Thrasher, G.P. 1990: Tectonics of the Taranaki Rift. *Proceedings, 1989 N. Z. Oil Exploration Conf.*, pp. 124–133.

Topp, R.A. 1996: Petrology and provenance of lower Pororari Group clast lithologies, Buller – North Westland, New Zealand. Unpublished M.Sc. thesis, University of Canterbury. 266pp.

Travis, C.J.; Nunn, J.A. 1994: Stratigraphic arechitecture of extensional basins: Insights from a numerical modelling of sedimentation in evolving half grabens. *Journal of Geophysical Research 99, B8*: 15653–15666.

Tulloch, A.J.; Kimbrough, D.L., 1989: The Paparoa metamorphic core complex, New Zealand: Cretaceous extension associated with the fragmentation of the Pacific margin of Gondwana. *Tectonics 8*: 1217–1234.

Tye, R.S.; Coleman, J.M. 1989: Evolution of Atchafalaya lacustrine deltas, south-central Louisiana. *Sedimentary Geology 65*: 95–112.

Ward, S.D. 1990: A palynological investigation of 11 boreholes in the Ohai Coalfield, Southland, with a note on the Haumurian *Nothofagidites* flora. Unpublished B.Sc.(Hons.) project, University of Canterbury. 33pp.

Ward, S.D. 1995: Controls on sedimentology and coal occurrence in the Rewanui Coal Measure Member, western Greymouth Coalfield (Rapahoe Sector). *Proceedings, 6th New Zealand Coal Conference,* pp. 151–161.

Ward, S.D. 1996: Application of lithostratigraphic and chronostratigraphic analysis to seam modelling in the Rapahoe Sector, western Greymouth Coalfield. *Proceedings, Australasian Institute of Mining and Metallurgy, New Zealand Branch annual conference, Greymouth,* pp. 173–199.

Ward, S.D.; Moore, T.A.; Newman, J. 1995: Floral assemblage of the "D" coal seam (Cretaceous): Implications for banding characteristics in New Zealand coal seams. *New Zealand Journal of Geology and Geophysics 38*: 283–297.

Wardle, P.A. 1991: **Vegetation of New Zealand.** Cambridge University Press, 672pp.

Warnes, M.D. 1988: The palynology of Ohai Coalfield, Southland. Unpublished M.Sc. thesis, University of Canterbury. 131pp.

Warnes, M.D. 1992: Palynological investigation of coal forming vegetation in the latest Cretaceous sub-situminous Morley Coal Measures, New Zealand. Unpublished Coal Research Group report, University of Canterbury, 87pp.

Watts, A.B.; Torné, M. 1992: Subsidence history, crustal structure and thermal evolution of the Valencia Trough: a young extensional basin in the Western Mediterranean. *Journal of Geophysical Research B 13*: 20021–20041.

Weissel, J.K.; Hayes, D.E. 1977: Evolution of the Tasman Sea reappraised. *Earth and Planetary Science Letters 36*: 77–84.

Wellman, H.W. 1950: Paparoa–Brunner unconformity near Greymouth. *New Zealand Journal of Science and Technology (Section B) 32*: 84–95.

Wernicke, B. 1981: Low-angle normal faults in the Basin and Range province: nappe tectonics in an extending orogen. *Nature 291*: 645–648.

Wheeler, H.E.; Mallory, V.S. 1956: Factors in lithostratigraphy. *American Association of Petroleum Geologists Bulletin 40*: 2711–2723.

Wilson, G.J. 1978: The dinoflagellate species *Isabelia druggii* (Stover) and *I. seelandica* (Lange): their association in the Teurian of Woodside Creek, Marlborough, New Zealand. *New Zealand Journal of Geology and Geophysics 21*: 75–80.

Wilson, G.J. 1994: Palynological Cretaceous-Tertiary boundary sites in New Zealand marine sequences. *Geological Society of New Zealand Miscellaneous publication 80A (Annual conference, programme and abstracts)*: 190.

Wizevich, M.C.; Thrasher, G.P.; Bussell, M.R.; Wilson, G.J.; Collen, J.D. 1992: Evidence for marine deposition in the Late Cretaceous Pakawau Group, northwest Nelson. *New Zealand Journal of Geology and Geophysics 35*: 363–369.

Wolff, M. 1993: Discussion: initial results of VR round robin analysis. *The Society for Organic Petrology newsletter 10*: 5.

Part 2.

Appendices 1 – 8

Appendix 1. Review of existing lithostratigraphic nomenclature and isopach models, Greymouth Coalfield

A1.1 Historical background

Morgan (1911), in defining the Paparoa Beds, recognised a sequence comprising basal conglomerate, succeeded by Lower Paparoa Beds (sandstones and shales), Middle Paparoa Beds (sandstones with minor shales) and Upper Paparoa Beds (sandstones and shales). Stratigraphy of the Paparoa Coal Measures became a major focus of the investigations reported by Gage (1952), who identified an essentially conformable sequence of "four coal-bearing parts and three intervening barren parts", resting unconformably on Paleozoic Greenland Group basement. The seven Formations of the Paparoa Group, which were formally defined by reference to lithology and relationships to underlying and overlying strata (Gage 1952, pp. 20–39), are summarised in Table A1.1 and Figure A1.1A.

Formation	Lithology	Relationship to underlying beds
Dunollie	Mostly tabular sandstones with interbedded siltstone, mudstone and thin carbonaceous mudstone and coals. Conglomerate in NW.	Usually transitional with Goldlight. On basement near Sewell Pk. and Mt Buckley.
Goldlight	Massive dark brown to brown-grey micaceous mudstone. Sandstone bands in NW, dark siltstone and fine sandstone in SE. Leaf fossils. Grades laterally into coal measures in NW.	Conformable on Rewanui, brief transition may be present
Rewanui	Lensoidal bodies of medium to coarse white and yellow quartz-mica sandstone separated by comparatively thin layers of dark-brown or grey carbonaceous mudstone and coal seams. Pebble and cobble conglomerates in the NW.	Conformable upon Waiomo.
Waiomo	Massive dark brown to brown-grey micaceous mudstone, occasional fine sandstone.	Conformable on uppermost Morgan carbonaceous mudstone or coals.
Morgan	(a) lensoidal conglomerate, sandstone, siltstone and coal in upper part, minor interbedded lavas (b) igneous conglomerate (basalt, lamprophyres) and tuff	Conformable on Jay or Ford, or unconformable on basement.
Ford	Dark brown or brown-grey micaceous siltstone with thin interbeds of light grey fine sandstone, rare lenses of conglomerate, tuff	Conformable with Jay or thin basal conglomerate on basement.
Jay	(iii) sandstone, shale, coal and minor conglomerate (ii) conglomerate, minor sandstone (i) red-coloured breccia, conglomerate	Jay (i) in fault-contact with basement, Jay (ii) unconformable, sedimentary contact with basement

Table A1.1 Definitions of stratigraphic units, Paparoa Coal Measures, Greymouth Coalfield, after Gage (1952). Lower Paparoa Group = Jay, Ford, Morgan and Waiomo Formations; Middle Paparoa Group = Rewanui Formation; Upper Paparoa Group = Goldlight, Dunollie Formations.

Group	Formation
Brunner	Brunner
Upper Paparoa	Dunollie
	Goldlight
Middle Paparoa	Rewanui
Lower Paparoa	Waiomo
	Morgan
	Ford
	Jay ii, iii
	Jay i

A. Gage (1952)

Group	Formation	Member
Mawheranui	Brunner CM	
	Paparoa CM	Dunollie CMM
		Goldlight MM
		Rewanui CMM
		Waiomo MM
		Morgan CMM
		Ford MM
		Jay CMM
Pororari	Hawks Crag Breccia	

B. Nathan (1974, 1978)

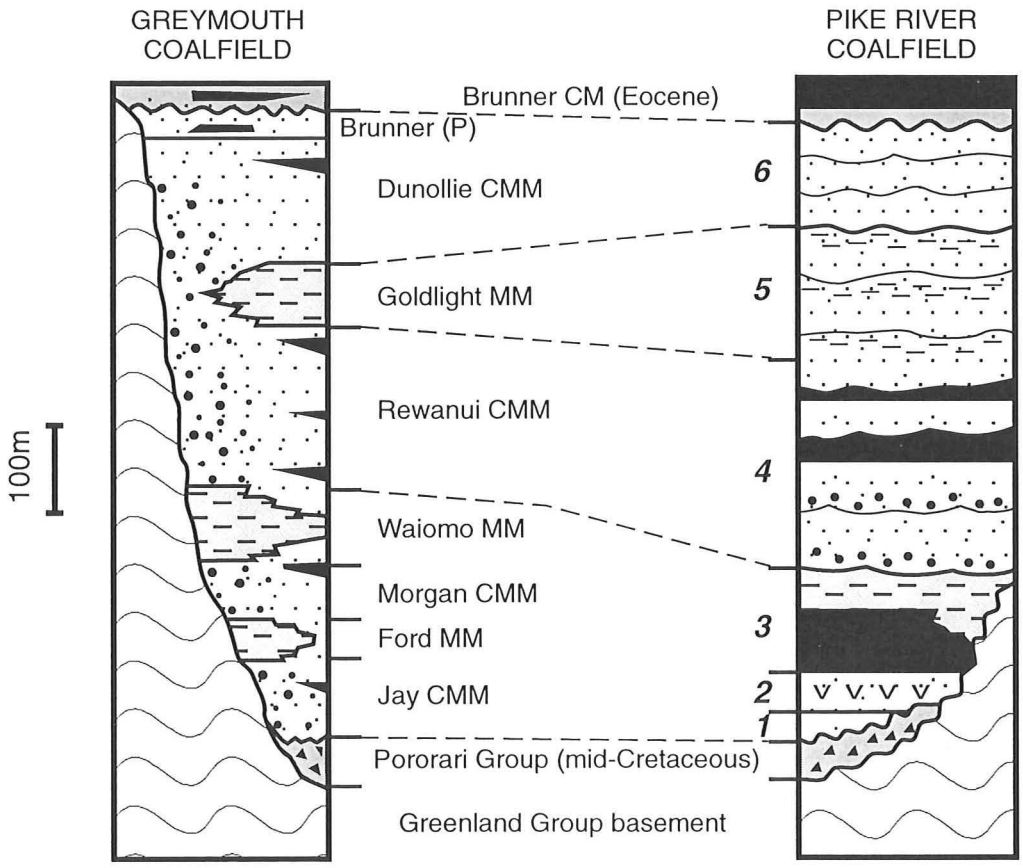

C. Newman & Newman (1992)

Figure A1.1 Stratigraphic nomenclature, Greymouth Coalfield
CM = Coal Measures, CMM = Coal Measure Member, MM = Mudstone Member
Brunner (P) = Paleocene Brunner CM

Nathan (1974, 1978) reassigned (on lithological evidence) the lowermost portion of the Jay Formation to the mid-Cretaceous Hawks Crag Breccia (Pororari Group), and relegated the remaining formations to the status of Member (Figure A1.1B). The reason given for changing stratigraphic status was the localized extent of Gage's Formations, which could not be recognised outside Greymouth Coalfield. Gage's Lower, Middle and Upper Paparoa Groups were abandoned, and Paparoa Coal Measures were combined with the overlying Brunner Coal Measures to form the Mawheranui Group.

Newman (1985) established the presence of both Paleocene and Eocene Brunner CM at Greymouth Coalfield, and correlated the various Members of the Paparoa Coal Measures at Greymouth Coalfield to un–named but numbered Members present in equivalent strata at Pike River Coalfield (Figure A1.1C).

The Mawheranui Group was rejected by Laird (1988), citing the generally unconformable nature of the Paparoa CM – Brunner CM contact, and the different tectonic setting of the two formations. However, neither the Paparoa CM or Brunner CM has been formally reassigned to a Group. Bishop (1991, Table 3) informally included Paparoa CM in the Pakawau Group of NW Nelson–Taranaki, and Brunner CM in the Rapahoe Group, which includes those formations overlying Brunner CM (Nathan 1974, 1978).

Neither reassignment is satisfactory. Pakawau Group strata are lithologically distinct from Paparoa CM (e.g. Bal & Lewis 1994) and there is no evidence for connectivity between the two basins. Brunner CM are more widespread than other formations in the Rapahoe Group (Nathan 1986), yet were accorded Member status in the Maruia Formation of the Murchison Basin by Suggate (1984) and Roder & Suggate (1990), who made no attempt to assign Maruia Formation to a Group. Thus there are inconsistencies in the application of lithostratigraphic nomenclature for West Coast Late Cretaceous and early Tertiary strata, and full revision, which is beyond the scope of this thesis, is required.

A1.2 Distribution of lithostratigraphic units: existing models

The distribution of Greymouth Coalfield stratigraphic units has previously been depicted by Gage (1952), Bowman et al. (1984) and Newman (1985). Isopach models of Gage (1952) were largely constructed from outcrop data, whereas later studies have relied on

drillhole data. Low economic potential of the lower Paparoa CM units led to a low priority for drilling or mapping activities, and only four drillholes drilled between 1945 and 1979 intersected basement. One stipulation of CRS drilling contracts was that drillholes were to reach basement wherever possible (Bowman et al. 1984, p. 22, 41), which was achieved for 28 of the 49 drillholes. Consequently, basin models developed after CRS drilling provide a better representation of overall stratigraphy.

Differences between the various existing isopach models (see Figures A1.2–A1.4) which reflect input data, the choice of contact placement and lithological content of each unit as used by the various authors, are discussed below.

A1.2.1 Jay CMM

Gage (1952) described three units within Jay CMM (see Table A1.1, FigureA1.1A). Most thickness variation is attributed to units (i) and (ii), with unit (iii) always being <50' (15m) thick (Gage 1952, p. 21). Gage (1952) and Bowman et al. (1984) correlated basal conglomerates at Twelve Mile Beach with Jay CMM. Nathan (1974, 1978) recorrelated Jay CMM on the Twelve Mile Beach coastal platform to Morgan CMM, and transferred Jay (i) conglomerates to mid–Cretaceous Hawks Crag Breccia (Pororari Group: see Figure A1.1B).

Newman (1985, p. 32 and Figure 13) considered that rapid eastwards thinning of Jay CMM depicted by Gage (1952) (see Figure A1.2A) was the result of recent erosion of the flanks of Mt. Davy, rather than denudation along the Roa–Mt. Buckley Fault Zone prior to Brunner CM deposition, as argued by Gage (1952, p. 18). No intact eastern limit of Paparoa CM is preserved, though all members are absent to the east (near Blackball), where Brunner CM lie directly on Greenland Group basement (Figure 1.2).

A1.2.2 Ford MM

Ford MM strata were distinguished from younger mudstone members by the abundance of fine to coarse sandstone beds, interpreted as sublacustrine turbidites or debris flow deposits by Bowman et al. (1984, p. 46). Gage (1952) and Bowman et al. (1984) depicted similar Ford MM isopach maps (Figure A1.2B, A1.3B), though the latter shows truncation the unit to the northwest. Ford MM onlaps onto basement along its northern and southern margins.

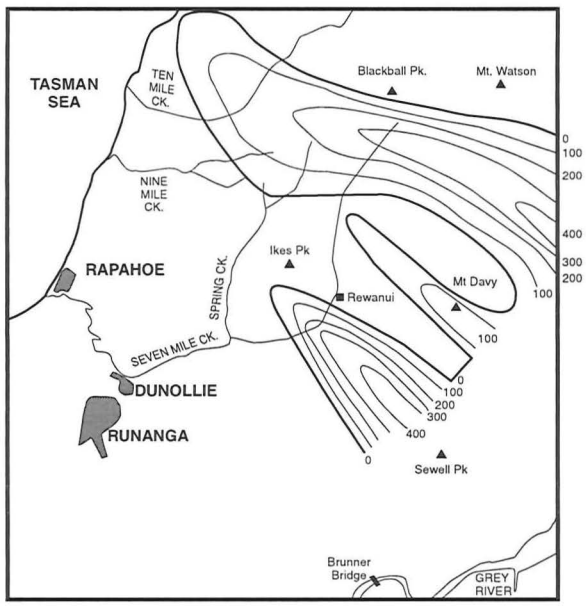

A. Isopach model, Jay Formation.
Interval = 100m

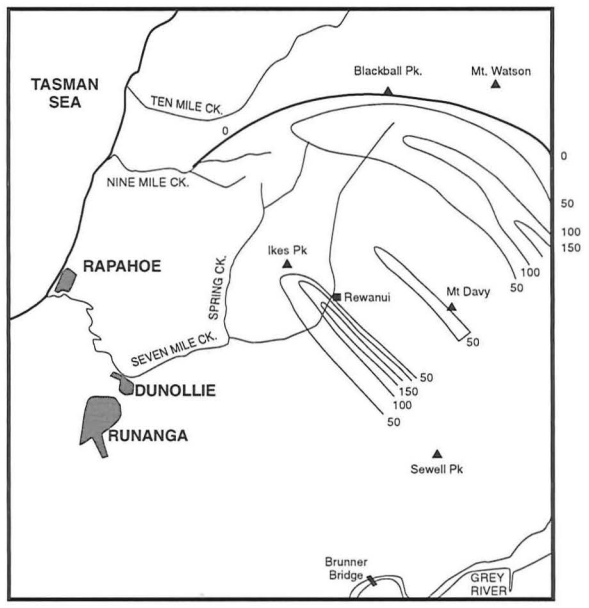

B. Isopach model, Ford Fm.
Interval = 50m

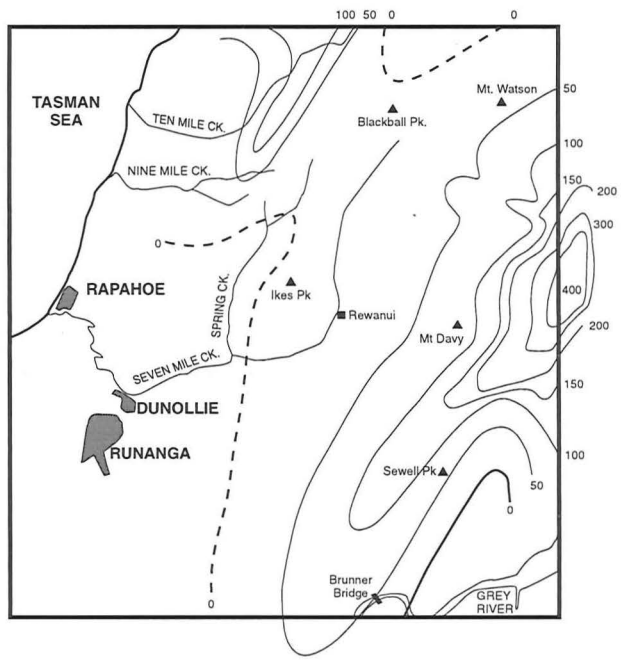

C. Isopach model, Morgan Fm.
Interval = 50m below 200m, 100m above 200m.
Dashed zero lines as depicted by Gage (1952).

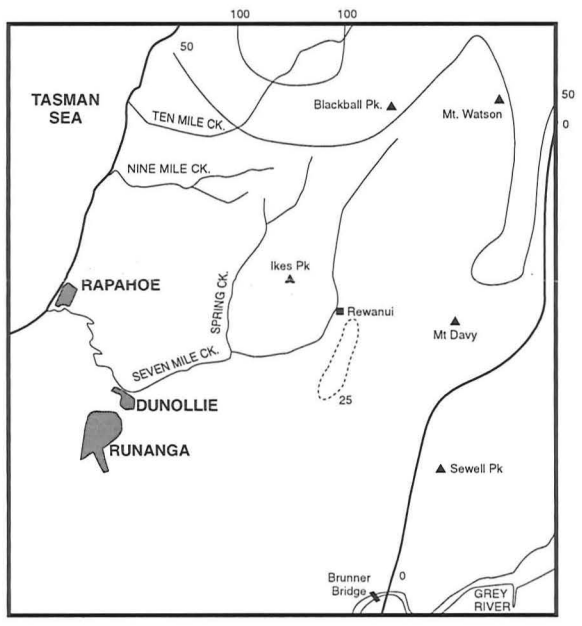

D. Isopach model, Waiomo Fm.
Isopach interval 50m, 25m line interpolated

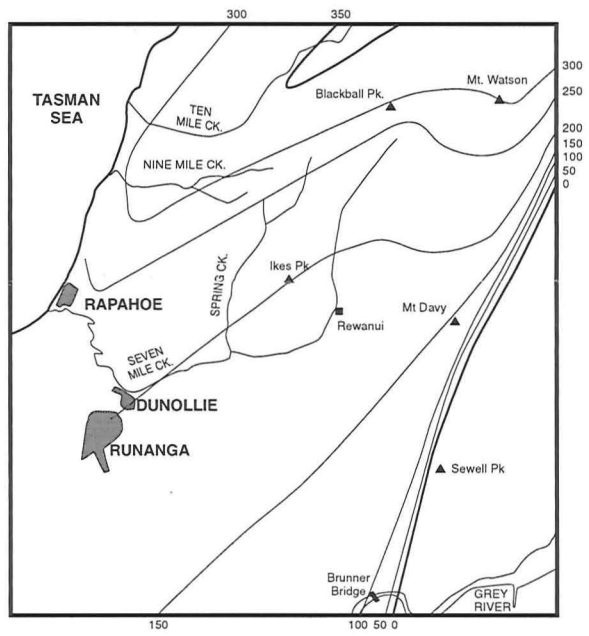

E. Isopach model, Rewanui Fm.
Interval = 50m

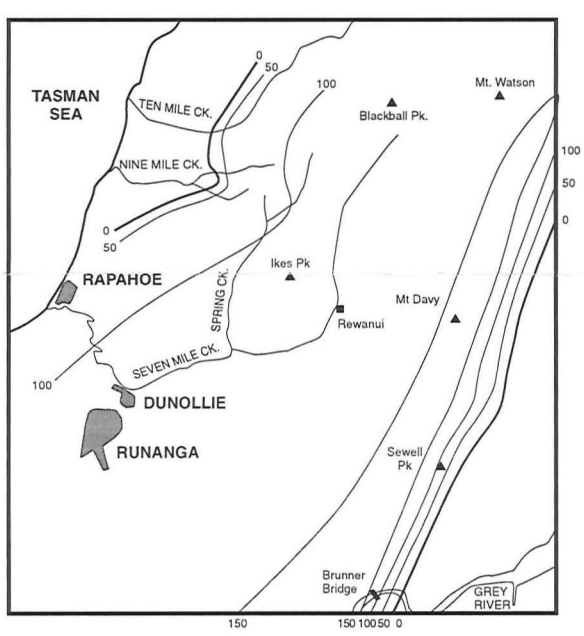

F. Isopach model, Goldlight Fm.
Interval = 50m

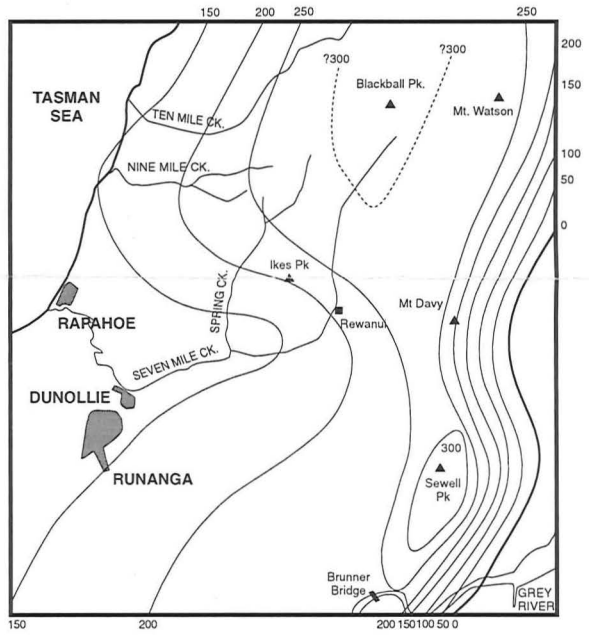

G. Isopach model, Dunollie Fm.
Interval = 50m
300m isopach line in north estimated

0 5km

Figure A1.2 Isopach models for Paparoa Group Formations,
Gage (1952).
All isolines redrawn to metric values by interpolation.

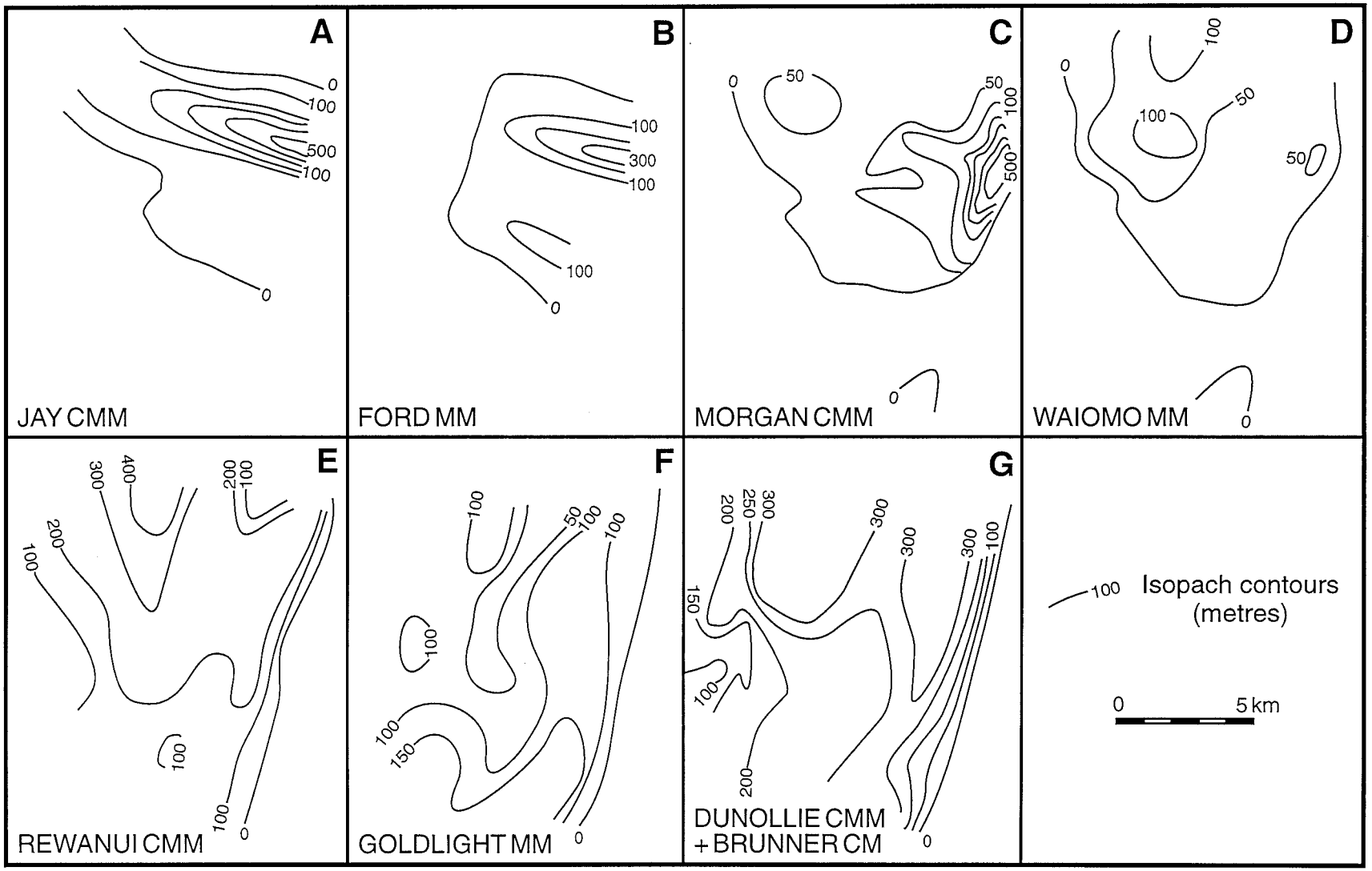

Figure A1.3 Coal Resources Survey isopach models.
From Bowman et al. 1984 (Figure 16 and Volume 1, Plans 20-26).

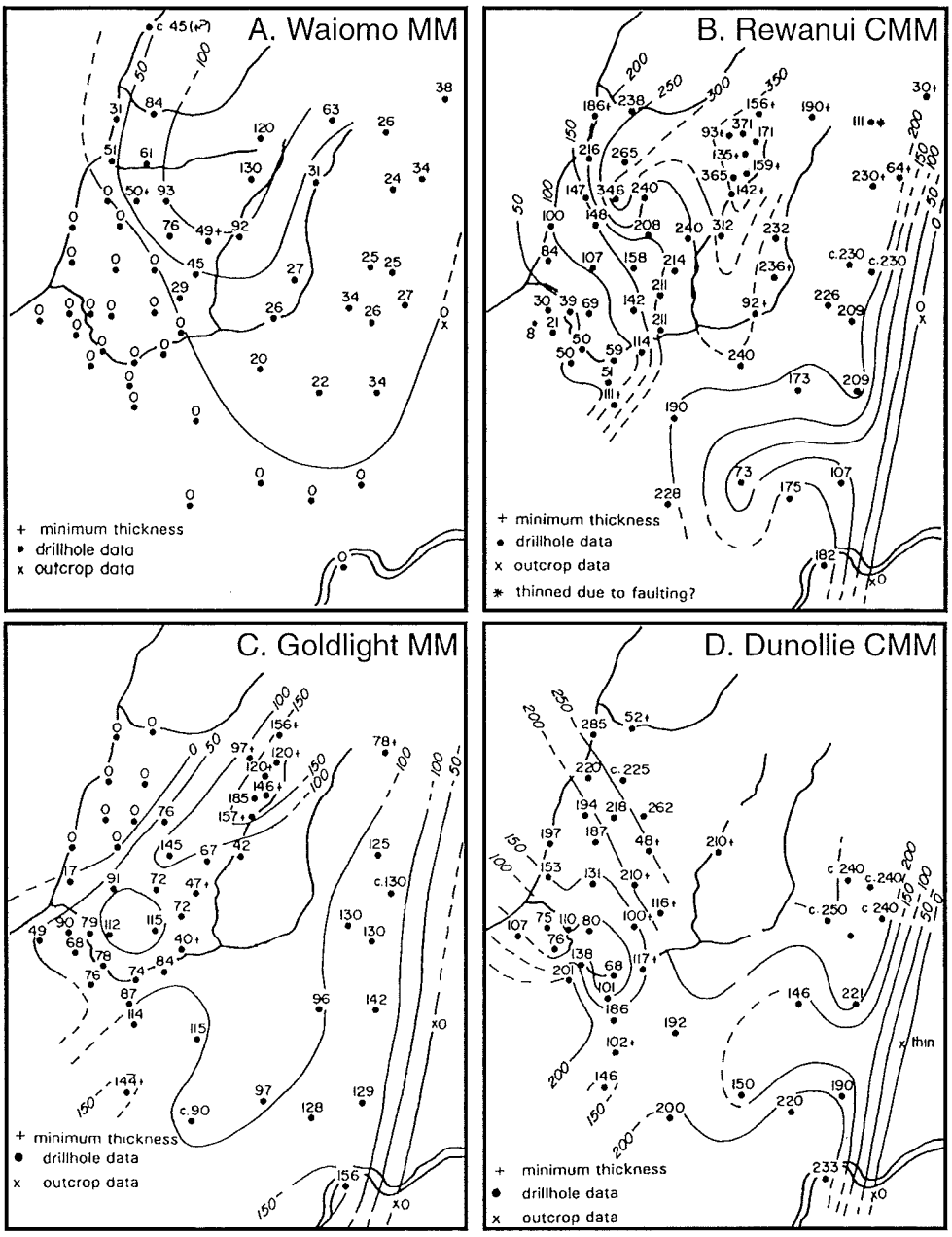

Figure A1.4 Isopach models from Newman (1985) and Newman & Newman (1992).

A1.2.3 Morgan CMM

Gage (1952) and Bowman et al. (1984) presented similar isopach models for Morgan CMM (Figure A1.2C, A1.3C), in which the dominant feature is the restricted extent of thick Morgan CMM (volcanic facies) in the east. The southern limit of Morgan CMM deposition depicted by Gage (1952) and Bowman et al. (1984) reflects initial interpretations of the stratigraphy of DH266 (at Brunner Bridge), in which a sequence comprising Rewanui CMM, thin Waiomo MM and Morgan CMM on basement was intersected. This drillhole was subsequently reinterpreted by Newman (1985, p. 39 and Appendix 4) as containing Rewanui CMM on basement, citing compositional similarity between Morgan CMM sandstones in DH266 and Rewanui CMM sandstones in nearby DH273. Recorrelation of DH266 suggests existing isopach models for Morgan CMM require revision.

A1.2.4 Waiomo MM

Differences between isopach models for Waiomo MM presented by Gage (1952) (Figure A1.2D) and more recent models (Figure A1.3D, A1.4A) reflect increased data availability from deep drilling in the Rapahoe Sector. Bowman et al. (1984) and Newman (1985) present a revised isopach pattern, showing an extensive eastern area of thin Waiomo MM and thickening in the western half of the coalfield. The southern outlier depicted by Bowman et al. (1984) represents DH266, which Newman (1985) reinterpreted as containing no Morgan CMM (see above).

A1.2.5 Rewanui CMM and contacts

Lower contact of Rewanui CMM: Gage (1952) placed the base of Rewanui CMM at the conformable contact between lensoidal quartz-mica sandstones (or conglomerate in the northwest) and massive mudstones of Waiomo MM (Table A1.1). This description reflects the stratigraphic interpretation of 18 drillholes in the Rewanui area (Liverpool Mine), which intersect the lower Rewanui CMM contact, and mapping of outcrop in the upper Seven Mile Ck. catchment, across the northern and eastern reaches of the coalfield, and at Twelve Mile Beach. CRS drilling subsequently demonstrated that Rewanui CMM lies directly on basement in the southern Rapahoe Sector (Bowman et al. 1984; Newman 1985).

Recent drilling has also revealed that up to 70m of interbedded sandstone (locally conglomerate) and thick mudstone occurs between typical Rewanui CMM and underlying massive mudstone in some drillholes. Bowman et al. (1984) interpreted these sediments as marking the commencement of Rewanui CMM deposition, whereas Newman (1985, Figure 18 and Appendix 4) included them in Waiomo MM, citing the predominance of muddy sediments and the presence of tuffaceous beds.

Rewanui CMM: All previous isopach models for Rewanui CMM (Figure A1.2E, A1.3E, A1.4B) depict a broad basin oriented NNE/SSW with maximum unit thickness in the north of the coalfield. Complex isopach patterns in the south and southwest depicted in Figure A1.4B (Newman 1985) were only revealed by CRS drilling.

Rewanui CMM as defined by Gage (1952) comprises predominantly quartz–mica sandstone with pebble to cobble conglomerates in the northwest (Table A1.1). Subsequent work has revealed the presence of two compositional suites within Rewanui CMM; a western compositional suite (**WCS**), dominated by Paleozoic Greenland Group derived sandstone and conglomerate, and the eastern compositional suite (**ECS**), which is predominantly of granitic provenance (Bowman et al. 1984, p. 53; Newman 1985, p. 50; Boyd & Lewis 1995). Limited interfingering of the two compositional suites indicates both were coeval (Boyd & Lewis 1995), thus the definition of Rewanui CMM requires modification to accommodate compositional variation.

Upper contact of Rewanui CMM: The contact between Rewanui CMM and overlying Goldlight MM has been described as "usually abrupt" (Gage 1952, p. 35), and "very sharp over practically the whole basin" (Bowman et al. 1984, p. 58). The exception is the northwestern area where massive Goldlight MM mudstone is absent, due to lateral gradation to sandstone and conglomerate of either Rewanui CMM or Dunollie CMM (Newman 1985). In this area, the Rewanui CMM / Dunollie CMM contact was arbitrarily placed at 200ft (61m) above the uppermost Rewanui CMM coal horizon by Gage (1952, p. 35), or, more recently (CRS), immediately above the last carbonaceous horizon within Rewanui CMM (Newman 1985).

A1.2.6 Goldlight MM and contacts

Gage (1952 p. 38) described the relationship between Dunollie CMM and Goldlight MM as "one of transition and complete conformity", and only included massive mudstone in the Goldlight MM (Figure 2.2G). Alternating mudstone and sandstone in the northwest of the coalfield were placed in the Dunollie CMM. The Dunollie / Goldlight contact is not specifically discussed by Bowman et al. (1984), though lateral relationships between northwestern "massive to weakly bedded sandy mudstones" (placed in Dunollie CMM) and Goldlight MM strata are acknowledged. Bowman et al. (1984, p. 57) also expanded the definition of Goldlight MM to incorporate strata with up to 50% interbedded sandstone lithofacies. Newman (1985, p. 40) described the contact as characterised by intercalated mudstones and sandstones, and its position to be "somewhat arbitrary", resulting in complex isopach patterns (Figure A1.4C).

Despite differences in the lithological content and location of the upper contact, the three existing isopach models for Goldlight MM (Figure A1.2F, A1.3F, A1.4C) depict a similar broad trough elongate to the NNE/SSW.

A1.2.7 Brunner CM, Dunollie CMM

Gage (1952) included northwestern greywacke conglomerates in Brunner CM, but noted (p. 41) that Wellman (1950) had proposed that Brunner CM be restricted to quartzose conglomerate and sandstone plus coal. Subsequent workers (Nathan 1978; Newman 1985) included the northwestern conglomerates in Dunollie CMM. Bowman et al. (1984 p. 61) considered the contact between Dunollie CMM and overlying Brunner CM to be difficult to define, and presented a combined isopach of the two units (see Figure A1.3G). Aspects of Brunner CM stratigraphy and chronology are discussed in detail by Newman (1985, pp. 15–21), and are not covered in the present study.

A1.3 Conclusion

Despite all previous studies applying the similar lithostratigraphic definitions, there is uncertainty about the lithological content of each unit, and therefore the correct placement of contacts, and the construction of accurate isopach models. Specific lithostratigraphic problems, and a means of resolution, are presented in Chapter 2.

Appendix 2. Discussion of structural/stratigraphic problems in Rewanui CMM, and derivation of input data for isopach modelling

Notes: Drillholes with useful Rewanui CMM thickness data are discussed here. Stratigraphic columns for selected intervals of drillholes with palynostratigraphy (marked *) are presented in Figure 5.2 (map pocket). Locations for all drillholes are shown in Figure 1.3 (map pocket), and contact depths and thickness data are summarised in Appendix 10.2.

DH205: DH205 is the deepest hole of a series (DH201–215) drilled in the 1930's during exploration for the former Strongman State Mine. The base Goldlight Fm. was formerly placed at 16.5m (Gage 1952), at the first occurrence of sandy beds below shale. Transitional lithosomes lie above Rewanui CMM throughout the western Strongman Mine area (Section 3.8.2 and Figure 3.10), and the Goldlight / Rewanui contact is better placed at the first appearance of carbonaceous beds at 55.2m. The resulting minimum Rewanui CMM thickness is 206.9m (previously 245.7m).

DH246: At least 228.6m Rewanui CMM is present in DH246. The revised minimum curvature model (Figure A3.6) suggests this represents nearly the full Rewanui CMM thickness, and the thickness is similar to nearby drillholes DH262 and DH265.

DH262 & DH265: Existing lithostratigraphy is retained.

DH266 & DH273: Basal sandstones, mudstone and coal measures formerly attributed to Waiomo MM and Morgan CMM were included in Rewanui CMM by Newman (1985), however original correlations have been retained here (Appendix 1.2.3, 1.2.4).

DH289, DH318, DH342, DH433: Existing stratigraphy is retained. Modelling (Figure A3.6) suggests the thickness for DH342 (201.8m) is c.38m too low.

DH446 & DH449: These drillholes are included to provide stratigraphic control in the southern Strongman Mine area. Both were drilled from mine workings. DH446 was drilled underground from "C" seam, and encountered 157.6m of Rewanui CMM, plus 25.3m of non-carbonaceous, sandy strata (cuttings data only), which may represent conglomerates (present in basal Rewanui CMM in nearby DH631), or Ford Transitional Member. CRS sections (Bowman et al. 1984, Volume 1, Plan 33, Section 5) indicate 54m of Rewanui CMM is present above collar height. The thickness of Rewanui CMM in DH446 is therefore 212.0m if Ford Fm. is present, and >237.3m if the eoh is in Rewanui CMM. 212.0m is used as a minimum value for stratigraphic modelling.

DH449 was drilled underground from "D" seam. The Rewanui CMM interval above the collar is estimated from Bowman et al. (1984, Volume 1, Plan 32, Section 3). At least 251.2m Rewanui CMM may be present, assuming Ford Fm. was not intersected, or 174.0m if basal non-carbonaceous sandstones are Ford Transitional Member. 174.0m is used as a minimum value for stratigraphic modelling.

DH619*: Previous work (CRS) located the Goldlight / Rewanui contact at 236.0m, coincident with apparently carbonaceous material on the density log. However, the caliper log indicates caving at this position, suggesting a sheared interval which would account for the density signature. Immediately below (237.5–241.8m) is a mudstone unit containing

well-preserved leaf and stem fossils, which resembles Goldlight Fm. lacustrine lithosomes, below which are fining-upwards sandstone packets with carbonaceous material, typical of Rewanui CMM sediments. The lower contact is placed above transitional lithosomes, resulting in a lesser thickness (203.6m) than previously used (CRS, 263.1m).

DH620: Rewanui CMM in DH620 was not cored, and contacts are located from geophysical logs. The top contact is indicated by the density log which indicates carbonaceous material, and the lower contact is placed 7m below the lowermost carbonaceous unit at a distinct break on the gamma and neutron logs.

DH621*: This drillhole, and DH622, is located in the northwest of the coalfield where lacustrine Goldlight Fm. is absent, and previous placements of the top Rewanui CMM are arbitrary (Appendix 1.2.5). The lithological boundary in DH621 was previously placed at 61.5m (CRS), at the first occurrence of coaly traces in the core. However, disseminated carbonaceous material is present throughout the interval 50–90m, and is therefore not a reliable guide to stratigraphy. The contact is now placed at 64.3m, beneath a fractured non-carbonaceous siltstone/mudstone interval at 62.6–64.3m which is correlated with Goldlight Transitional Member. The lower Rewanui CMM contact (311.0m) is placed above transitional lithosomes, in accordance with Newman (1985).

DH622*: The top Rewanui CMM contact was formerly placed at 265.1m (CRS), however the first indication of carbonaceous material in core and on the long spacing density log is at 268.5m, below coarsening upwards packets now interpreted as Goldlight Transitional Member. Shearing and caving indicate structural disturbance from 268–270m.

The lower Rewanui CMM contact is either basement, or above a thin packet of transitional/lacustrine strata below 397.5m correlated with Ford Fm. The former interpretation produces a Rewanui CMM thickness (142.7m) which conforms to the initial minimum curvature model (c.150m; Figure A3.5), whereas the latter interpretation is consistent with nearby drillholes DH641 and DH647, in which Ford Fm. is present. Inspection of the core from 397.5m–416.2m indicates bedding is diffuse, and basal conglomerates are matrix-supported (i.e. debris flow origin). Coarsening-upwards geophysical log motifs below 400m support a subaqueous origin (Section 2.3) . A thin carbonaceous bed at 412.0m contains predominantly detrital (woody) material, and does not represent *in situ* plant accumulation. The base of Rewanui CMM is therefore placed at 397.5m, and the thickness is 124.6m.

DH623*: Previous interpretations of DH623 (CRS) indicated 214.6m of Rewanui CMM on basement. A thin, predominantly coarsening-upwards sequence of siltstone, muddy sandstone and minor tuffaceous sandstone is now correlated with Ford Fm., and the base Rewanui CMM is now placed at 252.8m. The resulting thickness (204.1m) is closer to the value predicted by the minimum curvature model (Figure A3.6) than the previous value. Dip increases from 18° to 45° over the interval 46.4m (where coring commenced) to 54.0m, and there is crushing and shearing present at 54.0m and 57–59m, indicating a minor fault is present. Thin gouge is also present at 180.0m. The stratigraphic effects appear to be minor, and comparison with adjacent drillholes suggests no significant faulting is present.

DH624: The lower Rewanui CMM contact is placed above transitional lithosomes, resulting in a lesser thickness (184.7m) than previously used (CRS, 215.2m).

DH625: DH625 was not cored, and caving indicated on the caliper log at 442–444m suggests the upper Rewanui CMM contact may be faulted. The thickness (172.7m) is consistent with the revised minimum curvature model (Figure A3.6), thus faulting effects appear to be negligible.

DH626*: The upper Rewanui CMM contact (302.4m) is placed beneath transitional lithosomes, and lacustrine Goldlight Fm. is absent. Dip is variable (average 15°), and there are no structural complications.

DH627: Lithostratigraphy of DH627 is unchanged from previous descriptions.

DH628*: The lithological log for DH628 (Chapter 5) indicates a thin section of coaly mudstone and sandstone separated from a thicker carbonaceous and sandy section by 15.6m of mudstone. This stratigraphy was initially interpreted as indicating interfingering between Goldlight Fm. and Rewanui CMM (Bowman et al. 1984; Newman 1985, 1987), though a later analysis (Duff 1988) recognised the presence of fault repetition.

Fault gouge is present at the top and base of the upper coal measure section, and all non-sandy lithologies from 251.4–258.6m are sheared. Gouge is also present at the top of the lower coal measure section, and fracturing is intense throughout the upper 10m, and moderate within the thick seam. The mudstone section between the coal measure packets is mostly intact.

Various interpretations of the structure are possible. Simplistically, the interval between the upper (251.4m) and lower (274.4m) Goldlight / Rewanui contacts would suggest a repetition of 23.0m of strata. However, the stratigraphy of the upper intersection of Rewanui CMM is unlike that at the top of the lower intersection, but is more similar to the interval at the base of the main seam (approx. 298m). The upper intersection of Rewanui CMM may therefore be interpreted as a thin sliver of strata from the base of the seam, inserted higher in the stratigraphy by thrust faulting. However, a thin (<5m) packet of incompetent carbonaceous lithologies is unlikely to survive severe lateral and vertical translation, and a more reasonable interpretation is infaulting of the Goldlight Fm. interval between the carbonaceous units, with subsequent structural disruption above and below.

The minimum Rewanui CMM thickness (43.4m) is the aggregate of the two fault-bounded sections of coal measures, and conforms to the initial minimum curvature model (Figure A3.5). However, the revised minimum curvature model (Figure A3.6) indicates a greater thickness (c.55m) should be present, and geostatistical modelling indicates there should be c.70m of Rewanui CMM in DH628 (Figure A3.12).

DH629: DH629 was not part of the CRS drilling programme.

DH630: Correlation of the topmost 73m of DH630 is uncertain (CRS). Geophysical logging (through casing) indicates an absence of carbonaceous beds, and this section is correlated with Goldlight Fm.

DH631*: Previous work (CRS) placed the Goldlight / Rewanui contact at 147.5m, and adjustment was necessary to ensure the contact corresponded to the first occurrence of

carbonaceous sediment below the Goldlight Fm. interval, at 148.5m. The lithological log also indicates shearing, and abrupt dip increase from 5° to 45° at 148.5m. Steep dips persist downhole to 164.2m, where there is a thin (10cm) recemented fault gouge, below which the dip changes to 25°. There is further fault gouge at 177.4–178.1m. Stratigraphic modelling (Appendix 3.4) and seam correlations (Ward 1996) indicate c.13–20m of strata are absent from the upper Rewanui CMM. Recognition of transitional lithosomes below Rewanui CMM has reduced the thickness (207.3m) from those of previous analyses (CRS = 281.7m, Newman (1985) = c.240m).

DH632*: Initial (CRS) and alternative lithostratigraphic correlations for DH632 are listed in Table A2.1. Correlation SDW (1) reflects transferral of transitional lithosomes from Rewanui CMM to Waiomo MM, and this thickness (244.5m) was used in the construction of the initial minimum curvature model (Figure A3.5). Correlation SDW (2) incorporates the recorrelation of sub-Rewanui CMM mudstone units (Section 2.6.1), and the assignment of a thin transitional/mudstone sequence which was previously unrecognized as a member to Waiomo MM. The resulting thickness (165.5m) is significantly less than previously used (CRS, 310.4m), and strata beneath Rewanui CMM have been recorrelated accordingly.

Member/horizon	CRS	SDW (1)	SDW (2)
base Goldlight Fm	250.9	250.9	250.9
Rewanui CMM	310.4	244.5	165.5
base Rewanui CMM	561.3	499.2	419.0
Waiomo MM	92.4	152.2	22.7
Morgan CMM	19.4	18.7	55.2
Ford Fm	–	–	152.2
Jay Fm	–	–	18.7

Table A2.1 Previous and present stratigraphic interpretations, DH632.

A caved interval on the caliper log at 251.0–251.4m corresponds to gamma and density signatures typical of a dirty coal rather than a faulted interval, and no significant structural disturbance is recorded in the lithological log.

DH633*: Lithostratigraphy of DH633 is unchanged from previous descriptions. Shearing at the Goldlight / Rewanui contact does not represent significant faulting.

DH634: Lithostratigraphy for DH634 is poorly constrained. Goldlight Fm. is absent, and Dunollie Fm. and Rewanui CMM are dominated by conglomerates which lack correlateable carbonaceous horizons. The top contact of Rewanui CMM is estimated to lie at 319.0m (carbonaceous bed on density log), and the base is a probable fault at 513.0m, at the top of a transitional lithosome c.38m thick (containing coarsening-upwards packets and convoluted bedding). The resulting minimum Rewanui CMM thickness is c.188m, which is less than predicted by the minimum curvature model (c.215m; Figure A3.5, A3.6). Below 544.3m is conglomerate in which numerous pebble long-axes lie sub-parallel to the core orientation, indicating structural complication.

DH635*: The lower Rewanui CMM contact (605.2m) is now placed above transitional lithosomes, resulting in a lesser thickness (222.6m) than previously used (CRS = 269.5m; Newman 1985 = 239.5m).

DH636*: A 0.7m gouge zone and corresponding caliper and density log profiles indicates the presence of a major fault at 305.8–306.5m. Minimum curvature isopach modelling (Appendix 3.4) and seam correlation (Ward 1995) indicates c.20m of Rewanui CMM is missing. The listed thickness (87.0m) is adjusted accordingly.

DH637: Goldlight Fm. is absent from DH637, and the upper Rewanui CMM contact is placed at the first recorded carbonaceous mudstone beneath a thick sequence of v.fine–medium sandstone which is now correlated with Dunollie Fm. Basal conglomerates are correlated with Rewanui CMM, in accordance with Newman (1985, Appendix 4).

DH638: The top Rewanui CMM contact has been moved slightly from 215.1m (CRS) to 217.7m, at the first carbonaceous unit beneath massive mudstone and siltstone. This adjustment also accounts for a c.1.6m discrepancy between the geophysical and lithological logs. The interval from 230–260m is fractured, though no significant faulting is present.

DH639: Goldlight Fm. is absent from DH639, and interpretation of the upper Rewanui CMM contact is complicated by the lack of core. The upper Rewanui CMM contact was previously (CRS) placed at the first indication of carbonaceous material on the density log at 244.1m. However, the caliper log at this location indicates a heavily caved interval which would influence the density log response, and the contact is now placed at the first confirmed (cored) carbonaceous interval at 272.8m.

Basal Rewanui CMM in DH639 was correlated with Waiomo MM by Newman (1985), and is now placed in Ford Fm. The resulting Rewanui CMM thickness is 172.7m, which is consistent with the minimum curvature model (Figure A3.6). Structural disruption between 433m and 453m does not appear to have affected the stratigraphy.

DH640*: Existing lithostratigraphy for DH640 is valid, and the thickness (201.9m) accounts for dip, which was not corrected for previously. Caliper increase and shearing indicates a fault at approx. 183m, within Goldlight Fm. There is minor structural disruption between 260m and 290m which has not affected Rewanui CMM stratigraphy.

DH641: The initial minimum curvature model (Figure A3.5) indicates c.205m of Rewanui CMM should be present in DH641, however the initial thickness is 230.2m, and the 200m isopach line is perturbed around this point. The numerical model could not accommodate all the variation, which suggests the thickness value is anomalously high. The lower Rewanui CMM contact was previously (CRS) placed at 578.5m, at the contact between sandstone/conglomerate and massive siltstone. There is no geophysical log data available for >535m, and inspection of core reveals numerous sheared/faulted intervals between 540m and 580m. Dip increases abruptly from c.25° to 45° at 540m, and further increases to c.80° below 570m.

The most likely location of the base Rewanui CMM is 547.0m, at a thin carbonaceous unit overlying coarsening upwards siltstone–sandstone. The conglomerate and sandtone beds below this depth are probably Rewanui CMM infaulted into the section, and a major fault is located at a highly weathered and disrupted section at 562–564m. The resulting Rewanui CMM thickness is 199.8m.

DH642, DH643*, DH644: Minor adjustments for dip have been made to existing data.

DH645: Transitional lithosomes above and below Rewanui CMM have been transferred to Goldlight Fm. and Ford Fm., respectively.

DH646: The Rewanui CMM thickness is corrected for a dip of 40°.

DH647: The upper Rewanui CMM contact is difficult to locate as the section is uncored and the caliper log indicates caving throughout the interval 80–290m. By reference to DH622, the contact is placed at 284.2m, beneath lower Goldlight Transisitonal Member. The lower Rewanui CMM contact is placed above tuffaceous Ford Transitional Member strata which lie on basement.

DH648–DH650: Existing lithostratigraphy is retained.

DH651: Basal sandstones, mudstones and minor breccia are transferred to Ford Transitional Member, and the Rewanui CMM thickness (151.5m) is less than previously used (CRS = 188.9m). The lower Rewanui CMM contact is sheared, though no significant faulting is indicated.

DH652: Only drilled into Brunner CM.

DH653: Existing lithostratigraphy is retained.

DH654: The lower Rewanui CMM contact in DH654 is poorly defined. Initial interpretations (CRS) tentatively correlated thin sandstones and mudstones from 860.2m–863.8m to Waiomo MM and all strata below (to eoh at 900.0m) to Morgan CMM. Newman (1985, Appendix 4) transferred these units to Rewanui CMM, which is consistent with the correlations of DH273 and DH266. Inspection of the core indicated that many of the sandstone beds below 860.2m contain quartz, weathered feldspar and abundant muscovite, which are typical of ECS Rewanui CMM, though now also recognised within Morgan CMM (Section 2.6.3). The mudstone packet from 860.2m–863.8m has close affinities to Waiomo MM (dark grey, massive, scattered plant fragments, possible fresh-water mollusc impressions). Therefore, the CRS stratigraphy is retained in this project.

DH655: Only drilled to Goldlight Fm.

DH656: DH656 is drilled from upper Rewanui CMM, thus only a minimum thickness can be determined. However, the initial Rewanui CMM thickness (273.7m+) derived in the present project was much greater than the minimum curvature models (Figures A3.5, A3.6) suggested (c.210m). Location of the basal Rewanui CMM contact in this drillhole is difficult, and is strongly influenced by interpretation of the sub-Rewanui CMM stratigraphy. Various interpretations are summarised in Table A2.2.

unit	CRS	Newman (1985)	SDW (1)	SDW (2)	SDW (3)
Rewanui CMM	427.1+	371.1+	273.3+	273.7+	231.8+
Waiomo MM	64.1	120.1	c.150	39.1	5.9
Morgan CMM	c.51.3	c.51.3	c.49.6	35.2	26.7
Ford Fm.	–	–	–	111.5	185.6
Jay Fm.	83.38+	83.38+	80.5+	132+	132+

Table A2.2 Stratigraphic interpretations, DH656.

Original logging (CRS) placed the lower Rewanui CMM contact at 427.1m, at the lowermost occurrence of conglomerates and above massive mudstone. Newman (1985) transferred the sequence from 370.0–427.1m, which is predominantly muddy but contains thin conglomerates, to Waiomo MM. At 332.8–370.0m is a fault-bounded packet of conglomerate. In column SDW (1), this packet is considered to be infaulted into Waiomo MM, the top of which coarsens upwards to 292.1m where the first carbonaceous material appears. Column SDW (2) incorporates the correlation of western Waiomo MM to eastern Ford Fm., and the "infaulted" conglomerate is correlated with Morgan CMM.

The final interpretation (SDW 3) was made after inspecting the core, which revealed a coarsening upwards packet from 246.7–253.5m, which has strong affinities to transitional lithosomes (e.g. mud-rich at base, convoluted bedding), and is interpreted to represent thin Waiomo MM. The "infaulted" conglomerate, though bounded by shearing and fracturing, comprises debris flow units with extensive soft-sediment deformation, and is now interpreted to lie conformably within Ford Fm. The result is a minimum Rewanui CMM thickness (231.8m+) which is close to the value predicted by the revised minimum curvature model (c.210m; Figure A3.6).

DH657: The interval from 187–440m is extensively fractured and sheared, and at least 2 faults are present (405m, 436m). The listed thickness is the aggregate of the true stratigraphic thickness of Rewanui CMM within each fault-bounded section. The stratigraphic effects of the faulting are unknown. Ford Transitional Member strata (which includes minor conglomerate and coal clasts at c.506–510m) were previously correlated (CRS) with Rewanui CMM, therefore the thickness reported here (223.9m) is less than that of earlier interpretations (c.360m).

DH658 & DH659: Only minimum thicknesses were obtained from these drillholes.

DH660: Both upper and lower Rewanui CMM contacts are present in DH660, however there is substantial structural disruption throughout the drillhole and the thickness (c.90m) is substantially less than indicated by minimum curvature modelling (c.150m). The basal contact (178.7m) is placed at the lowermost carbonaceous bed above a coarsening-upwards package. DH660 was drilled from a fault-bounded block (mapped by Gage 1952), and intact stratigraphy is not likely to be present.

DH661: Recorrelation of DH661 (Section 2.6.2) indicates Rewanui CMM is not present in this drillhole.

DH662–DH665: These drillholes only partially penetrate Rewanui CMM.

DH666*: Bedding plane shear and minor crushing is common throughout the upper 35m of Rewanui CMM in DH666, but no major faults are evident in the lithologic log.

DH667*: A thin section of siltstone and coarsening upwards sandstone from 100.1–104.5m has been transferred to Goldlight Fm., and the top of Rewanui CMM is now placed at the first occurrence of carbonaceous mudstone.

DH668, DH686–DH694: These drillholes only partially penetrate Rewanui CMM.

DH695: Hole only drilled into Goldlight Fm.

DH696: At least two faults (at 305.4m, 314.3m), and possibly two more faults (at 292.4m and 320.2m) are present in DH696. The minimum curvature model (Figure A3.6) indicates c.75m of Rewanui CMM at this locality, whereas only 38.2m is present.

DH697*: Existing lithostratigraphy is retained.

DH698: The upper Rewanui CMM contact in DH698 lies 0.3m above a 0.6m fault gouge at the roof of a coal seam (271.2m–274.2m). Comparison with adjacent drillholes is not helpful due to faulting elsewhere (e.g. DH628, DH636) and rapid Rewanui CMM thickness change. The present thickness (71.9m) is consistent with the revised minimum curvature model (Figure A3.6), and seam correlations (e.g. Ward 1995, Figure 11C) suggest little strata is absent.

DH699: Existing lithostratigraphy is retained.

DH700: The upper Rewanui CMM contact in DH700 is placed beneath a coarsening-upwards mudstone-sandstone packet which was formerly (GCL) included in Rewanui CMM but is now correlated with Goldlight Transitional Member. The interval between 130m and 224m is structurally disrupted, and a fault is likely between 220m and 224m. Stratigraphic effects are unknown, however comparison with adjacent drillholes and the revised minimum curvature model (Figure A3.6) suggests the Rewanui CMM thickness is close to the true thickness.

DH701: The lower Rewanui CMM contact in DH701 is placed at 362.5m, above a packet of coarsening-upwards muddy sandstone and sandstone correlated with Ford Transitional Member. Previous interpretations (GCL) placed this contact at 376.1m.

DH702: Existing lithostratigraphy is retained. The interval 257–308m is structurally disrupted, though comparison with surrounding drillholes and the revised minimum curvature model (Figure A3.6) indicates the stratigraphic effects are negligible.

DH703: Existing lithostratigraphy is retained.

DH704: DH704 was abandoned in probable Ford Transitional Member strata at 415.9m (well sorted sandstone beneath conglomerate) because of a strong artesian. Correlation of this unit with Ford Fm. is supported by reference to nearby drillholes DH647 and DH707, in both of which the basal Rewanui CMM contact is placed between conglomerate and transitional sandstones. There is structural disruption in carbonaceous intervals between 317.5m and 327.5m, and the revised minimum curvature model (Figure A3.6) indicates c.10m of Rewanui CMM is absent.

DH705: The Rewanui CMM thickness (122.6m) for DH705 is c.23m greater than predicted by the revised minimum curvature model (Figure A3.6). There is shearing and crushing associated with a coal seam between 340m to 368m, though comparison with surrounding drillholes does not suggest strata are absent or repeated.

DH706: A fault is reported from 283m to 286m in the uppermost Rewanui CMM (top contact at 283.0m). Comparison with surrounding drillholes, and the revised minimum curvature model (Figure A3.6), indicates the stratigraphic effects are negligible.

DH707: The interval 390–404m is structurally disturbed, and strike-slip and normal faulting are reported in the lithological log (GCL). Comparison with nearby drillholes and the revised Rewanui CMM minimum curvature model (Figure A3.6) indicates the stratigraphic effects are negligible. The basal Rewanui CMM contact has been shifted slightly to carbonaceous mudstone above a coarsening-upwards package.

DH708: The basal Rewanui CMM contact has been shifted up section slightly to a granule conglomerate above a coarsening-upwards sandstone package. A fault is present at the roof of the coal seam at 395.3–398.9m, indicated by high-angle juxtaposition of fine sandstone and coal. The stratigraphic effects are not significant.

DH709: Shearing and possible faulting are present at six depths between 374m and 482m. The stratigraphic effects are negligible. The base of Rewanui CMM has been reinterpreted from geophysical logs to lie above thin Ford Transitional Member.

DH710: Goldlight Fm. is absent from DH710, and the contact between Dunollie Fm. and Rewanui CMM is placed at the first occurrence of carbonaceous material indicated in the lithological log. The basal Rewanui CMM contact has been adjusted and now lies below carbonaceous sandstones at 484.0m, above Ford Fm. This contact is structurally disrupted, however comparison with adjacent drillholes shows the effects are minimal.

DH711: Existing lithostratigraphy is retained.

Recent drillholes: The majority of drillholes numbered >711 only partially penetrate Rewanui CMM, and are not discussed in detail. Data are summarised in Appendix 10.2. Total Rewanui CMM thicknesses are known from five recent drillholes in the Mt. Davy area. Data was obtained (with permission) from drillhole summary sheets, however logs were not inspected and no corrections have been made for dip or other structural complications, and stratigraphy remains unverified.

Appendix 3. Numerical modelling of Goldlight Formation and Rewanui CMM thickness data

A3.1 Introduction to numerical modelling methods

Numerical modelling techniques estimate unit thickness values at centroids of cells within a user-defined grid, by application of algorithms which interpolate between known data points to calculate the corresponding value in all cells. Values from the cells ("gridded" data) can then be contoured to construct isopach models. For numerical modelling of Greymouth Coalfield data, a grid of 250m x 250m cells was constructed, covering an area of 11km x 11km (total 1936 cells). This area is smaller than the total study area, but encloses all available drillhole data (Figure A3.1).

The *TECHBASE®* software package (version 2.4, ©MINEsoft, 1996) offers 6 numerical modelling tools, which differ in their ability to interpolate or extrapolate data, and the degree to which data points are honoured by the model (Technote 1991). Three tools were used to investigate spatial variability within isopach data sets: minimum curvature modelling, trend surface analysis, and geostatistics.

Minimum curvature modelling (*TECHBASE MINQ* application) uses a bi-harmonic spline function, which may be likened to fitting a flexible metal sheet through the data points, in order to interpolate grid values from the raw data (TECHBASE, 1992). Data values are generally honoured, though anomalously low or high values will exceed the model's ability to bend the "metal sheet", and are truncated by the model. This feature of minimum curvature models enables anomalies in thickness data to be identified.

Trend surfaces are a means of numerically detecting regional variation of various geological parameters (le Roux 1994). First order trend surfaces are always planar, and are the three-dimensional equivalent of regression lines. Second order trend surfaces are described by quadratic polynomial equations, and third order by cubic polynomial equations. With reference to isopach modelling, a first order trend surface will indicate the general pattern of unit thickening, whereas second or third order trend surfaces defines the geometry of a basin (Swan & Sandilands 1995, p. 292).

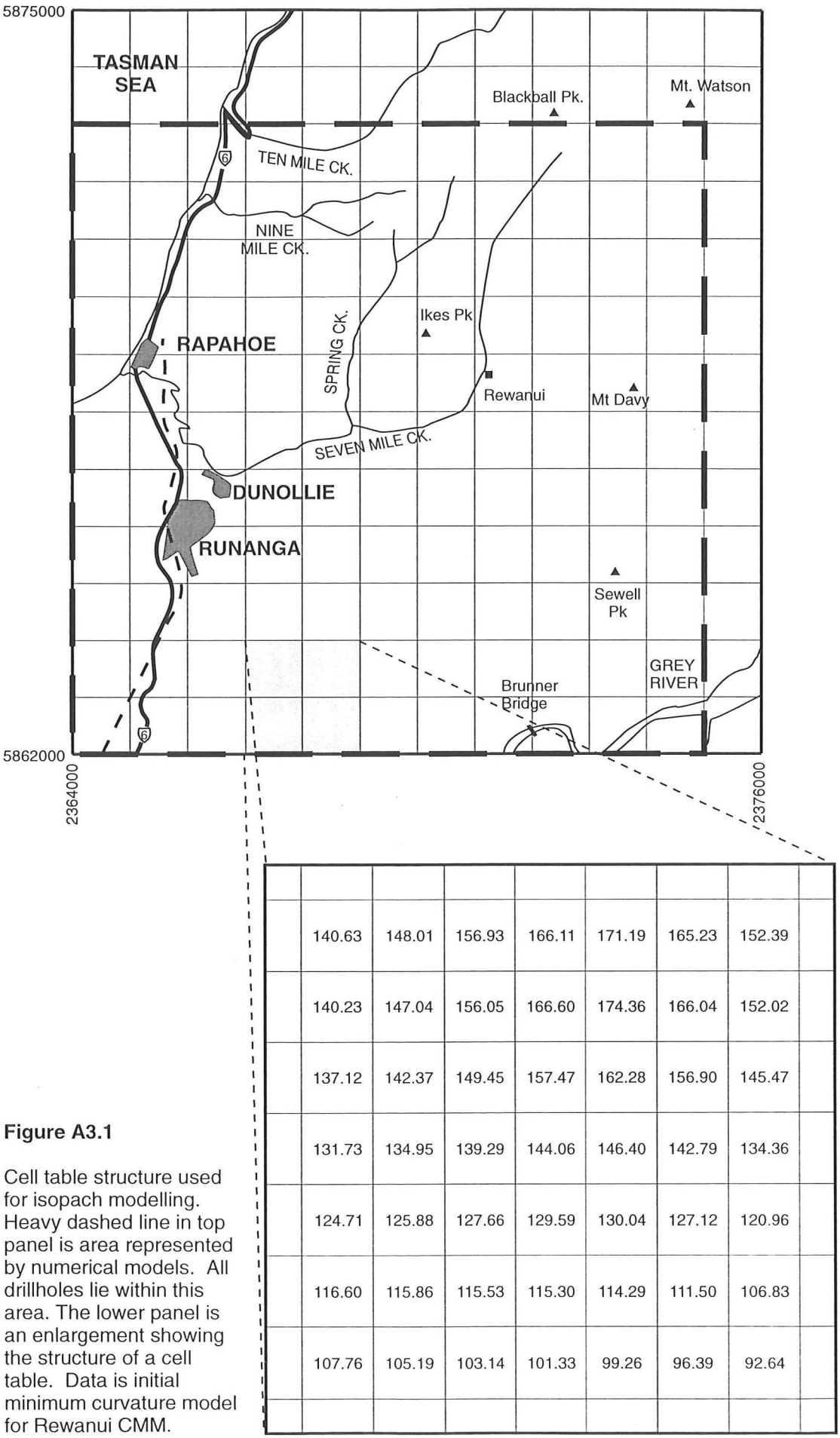

Figure A3.1

Cell table structure used for isopach modelling. Heavy dashed line in top panel is area represented by numerical models. All drillholes lie within this area. The lower panel is an enlargement showing the structure of a cell table. Data is initial minimum curvature model for Rewanui CMM.

A data value may be broken down into a "regional" trend component (as defined by the polynomial) and "local" residual component, being the difference between the trend value and the data point. For any order trend surface, the mean of residuals is zero, and the variance defines the degree to which the model describes the data set. The calculations generate "goodness of fit" values, and f-values which may be tested for significance with the Poisson distribution for the appropriate degrees of freedom. In practice, orders of trend surface above 4 are not used, as the goodness of fit and significance decline, and such equations are unlikely to be relevant in describing the causative geological processes (Swan & Sandilands 1995, p. 299).

The final numerical modelling technique applied in the present study is geostatistics (kriging), which is used for construction of an isopach model for Rewanui CMM. Geostatistical techniques enable interpolation of data values to be customised to match the spatial structure of the data (e.g. Swan & Sandilands 1995, p. 318). Of the various numerical modelling techniques commonly used, kriging provides the best correlation between estimated and true data values (Isaacs & Srivastava 1989, p. 318).

A3.2 Goldlight Formation minimum curvature model

The minimum curvature isopach model for Goldlight Fm. is presented in Figure A3.2. Initial models included thickness values for DH650 and DH711, however the value for both drillholes was >10m lower than predicted by the model. Re-inspection of the lithological and geophysical logs for DH711 revealed that the upper Goldlight Fm. contact was sheared, crushed and caved, indicating the presence of faulting. Hence, the thickness for both drillholes has been transferred to a minimum value.

Correspondence between data and the minimum curvature model for the western limit of Goldlight Fm. occurrence is poor. There is no Goldlight Fm. present in DH637, yet the model predicts c.15m. Similarly, Goldlight Fm. in DH619 is thin (6.0m) yet c.25m is predicted. DH653, SW of Rapahoe, also appears to be anomalously thin with respect to the model. Lateral facies equivalence to Dunollie Fm. explains the apparent thickness anomalies (Section 2.7.6).

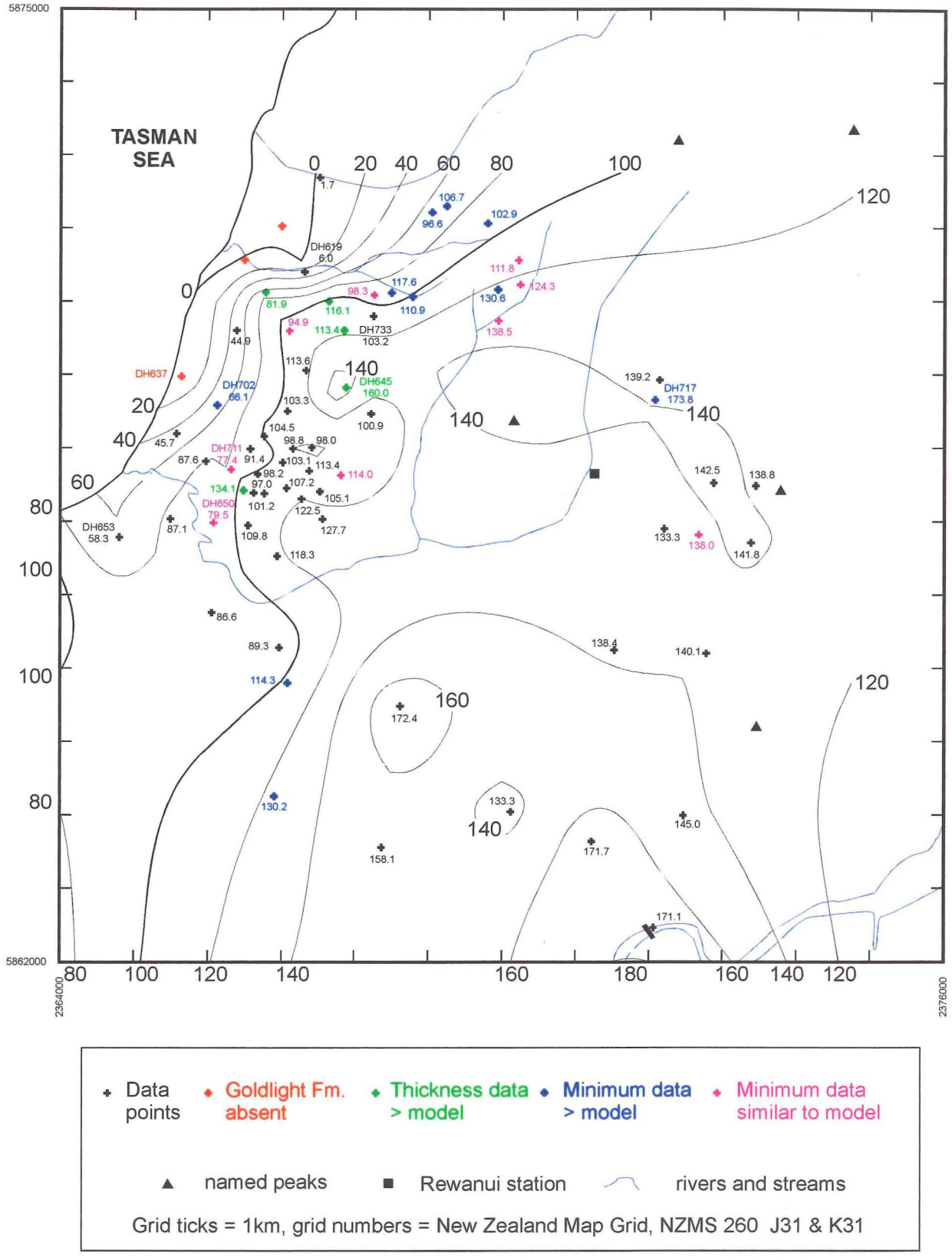

Figure A3.2 Minimum curvature isopach model,
Goldlight Formation.
Isopach interval = 20m.
Numbered drillholes are discussed in text.

Five drillholes have Goldlight Fm. thickness values >10m above the minimum curvature model surface (in green on Figure A3.2). Most notable is DH645, which produces a positive "bullseye" anomaly in the model. This modelled anomaly is still c.20m below the data value, reinforcing the inability of a minimum curvature model to respond to extreme data values.

Minimum value data from sites where Goldlight Fm. was incompletely drilled may be compared with the minimum curvature model to locate those points which should be accounted for in the final isopach model. Minimum Goldlight Fm. thickness in nine drillholes is close to the predicted isopach value (plotted in purple on Figure A3.2), and ten drillholes have minimum Goldlight Fm. thicknesses greater than the minimum curvature model predicts (plotted in blue on Figure A3.2). Six of these are located in the upper reaches of Nine Mile Ck. and Spring Ck., where the model is only controlled by one data point (DH733, 103.2m). The minimum Goldlight Fm. thickness in DH702 is slightly greater than predicted, despite being disrupted by faulting. DH717 has a minimum isopach value of 173.8m, c.34m higher than predicted, though data is poor, and no correction for dip has been made.

Overall, minimum curvature modelling of Goldlight Fm. thickness does not honour all data values. The likely cause is the lack of control points, especially in the southwest and northwest of the coalfield. Minimum values from drillholes in the northwest strongly suggest thickness change along the western margin of Goldlight Fm. is more rapid than presently modelled.

A3.3 Goldlight Formation trend surface analysis

First to Fourth order trend surfaces and relevant statistics for Goldlight Fm. are illustrated in Figure A3.3A–D. The First order trend surface suggests Goldlight Fm. thickens from the northwest to the southeast of the coalfield, but this surface only accounts for c.57% of variation in unit thickness. Second to Fourth order surfaces generated similar patterns with similar goodness of fit values, though the f-value declines with increasing order as degrees of freedom decreases. All that is gained from Second to Fourth order is decreasing significance of the trend (high f-value = more significant), therefore the best trend surface to illustrate overall Goldlight Fm. thickness

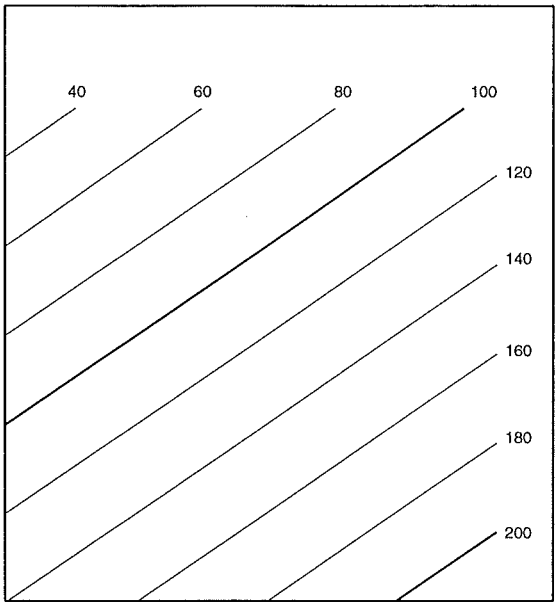

A. First order

Goodness of fit = 56.76%
Correlation coefficient = 0.75
f = 30.2

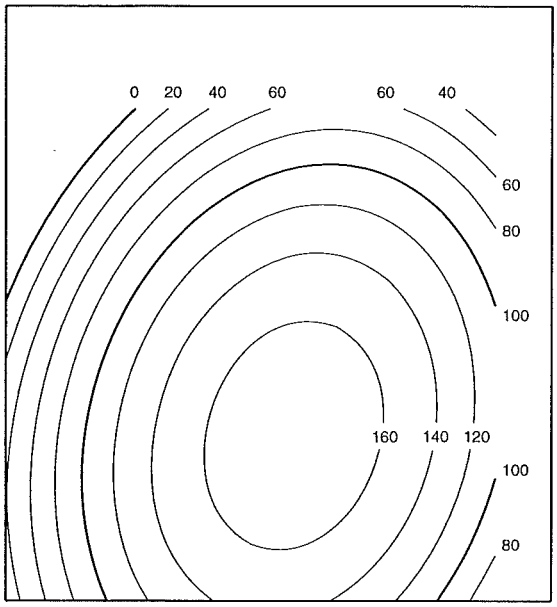

B. Second order

Goodness of fit = 76.11%
Correlation coefficient = 0.87
f = 27.4

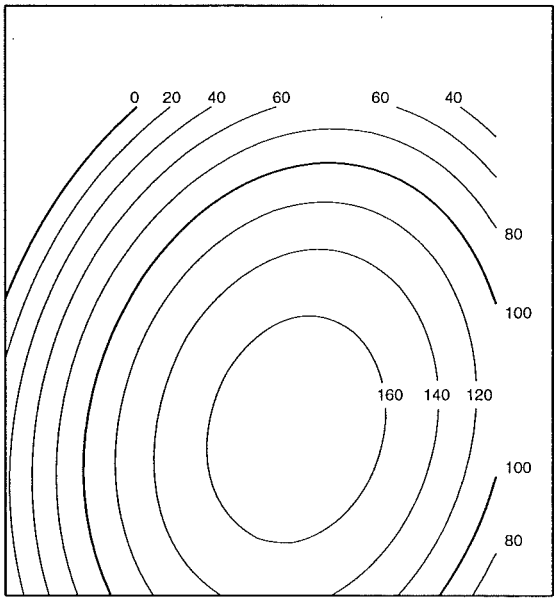

C. Third order

Goodness of fit = 76.00%
Correlation coefficient = 0.87
f = 13.7

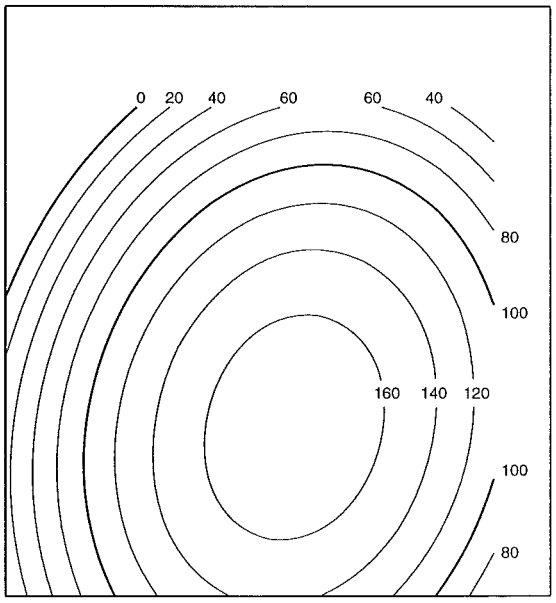

D. Fourth order

Goodness of fit = 76.50%
Correlation coefficient = 0.87
f = 7.9

Figure A3.3 Goldlight Formation trend surface analysis
Area of each map is study area, as in Figure A3.1.

patterns is the Second order (cubic) surface. This was confirmed by ANOVA comparison (Swan and Sandilands 1995, p. 296) of the results of each trend surface analysis (Table A3.1), which demonstrated that the Second order trend surface accounts for significantly more variation (at $\alpha = 0.05$) in the data set than the First order trend surface, whereas there is no significant improvement in Third or Fourth order analyses.

Order	f-value (calculated)	degrees of freedom	f-value (critical)	result
Second over First	11.61	(3,46)	2.81	reject null hypothesis
Third over Second	-0.04	(4,39)	2.61	accept null hypothesis
Fourth over Third	0.14	(5,34)	2.49	accept null hypothesis

Table A3.1 Results of ANOVA test, Goldlight Fm. trend surface analysis. F–distribution table used from Swan and Sandilands (1995, Appendix 2.5).

Trend surface analysis suggests that the basin in which Goldlight Fm. accumulated was elliptical (long:short axis ≈1.4), and oriented NNE–SSW (Figure A3.3B). The basin margins were probably within 2km of the modelled area to the north and east, and may extend up to 6km south of the present coalfield limits.

Although the Second order trend surface provides the best description of trends in Goldlight Fm. thickness, only c.76% of variation is accounted for. Examination of the residuals from the Second order trend surface (Figure A3.4) assists in explaining the remaining variation. Residuals vary from -48.57m (DH619) to +54.63m (DH645), and are generally low (within ±15m) where maximum data density occurs. The exception is DH696 (+38.68m), which has a higher residual than other adjacent drillholes. This drillhole is also anomalous when compared to the minimum curvature model (see above). Trend values are greater than data values (i.e. positive residuals) for the five drillholes in which Goldlight Fm. is thin (<10m) or absent.

Drillholes near the modelled depocentre (DH625, DH627) have negative residuals, and there is a gradient towards positive residual in both a northeasterly and southeasterly direction from these drillholes, indicative of a local trend which is not accommodated by the Second order trend surface. The locus of maximum thickness indicated by the second order trend surface is therefore not truly representative of the data.

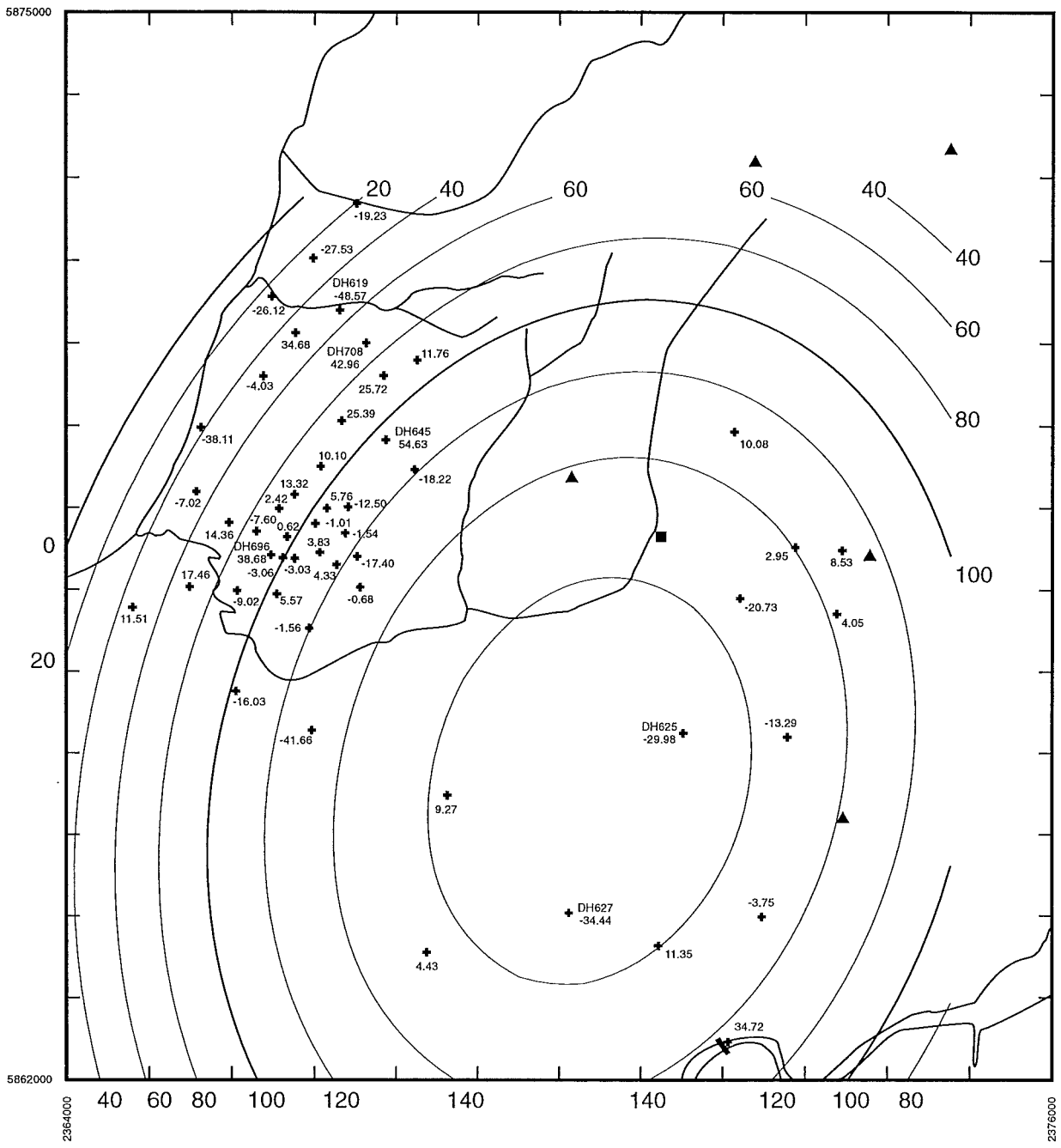

Figure A3.4 Second order trend surface and residuals,
Goldlight Formation.
All values in metres.
Numbered drillholes are discussed in text.

The patterns depicted by trend surface analysis of Goldlight Fm. are strongly influenced by uneven data point distribution, and there are localized trends within domains which are poorly accounted for by the Second order model. Although the Second order surface provides the best fit to the data, higher order surfaces may account better for rapid thinning of Goldlight Fm. in the west, as these produce steep gradients at the edge of data sets ("edge effects"; Swan & Sandilands 1995, p. 299).

A3.4 Rewanui CMM minimum curvature models

Two minimum curvature models for Rewanui CMM are presented here. Figure A3.5 was constructed from a preliminary compilation of Rewanui CMM thickness data, and Figure A3.6 is the model generated after revision of that data set. Both models illustrate similar isopach patterns, with major differences present in the Spring Ck. and Brunner Bridge areas, reflecting modification to previous correlations of drillholes in these locations (DH632, DH266, DH273: see Appendix 2).

Use of minimum curvature modelling of Rewanui CMM thickness values permitted resolution of many of the potential error sources discussed in Section 3.7. The various applications of the models, and corresponding drillholes in which each application contributed to more reliable Rewanui CMM thickness values, are summarised in Table A3.2, and resulting adjustments to thickness values are noted in Appendix 2.

Application of minimum curvature modelling	Drillholes
confirmation of lithostratigraphy	318, 623, 639, 641, 656
confirmation of faulting	628, 631, 636, 660, 696, 704
confirmation that structural problems are minor	625, 698, 702, 706, 707
confirmation of minimum thickness	342, 634
minimum values close to full thickness	246, 659, 693, 700, 726, 743, 749
minimum values > modelled thickness	656, 687, 691, 746, 750
minimum value excessive	745
models do not match isopach data	697, 703, 705

Table A3.2 Applications of minimum curvature modelling and corresponding drillholes where applications useful, Rewanui CMM isopach data.

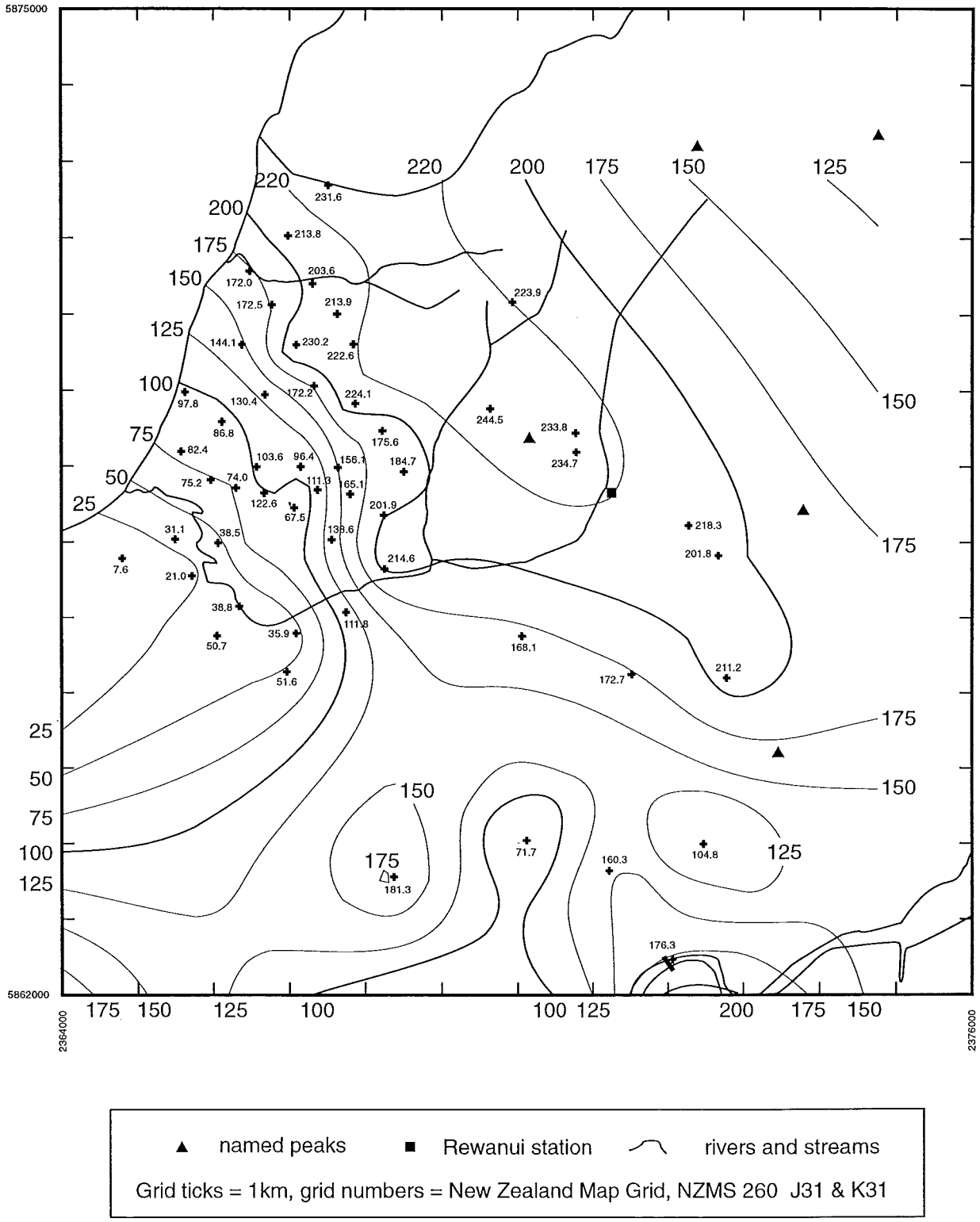

Figure A3.5 Initial minimum curvature isopach model,
Rewanui Coal Measure Member.
Isopach interval = 25m.

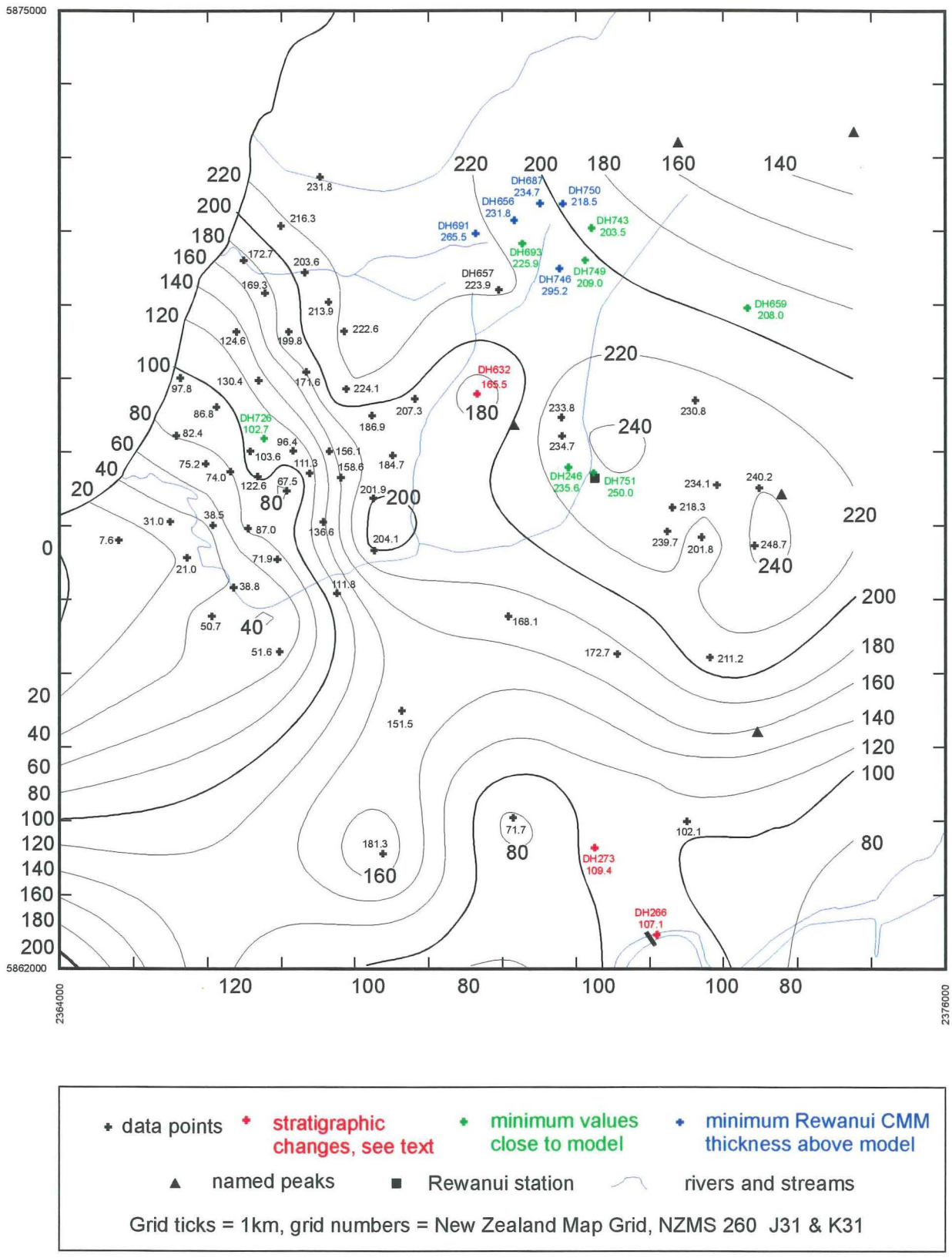

Figure A3.6 Revised minimum curvature isopach model,
Rewanui Coal Measure Member.
Isopach interval = 20m.
Numbered drillholes are referred to in text.

In the north of the coalfield, the minimum curvature isopach pattern is poorly constrained (Figure A3.6), with no total Rewanui CMM values known east of DH657. Minimum values from four drillholes (DH659, DH693, DH743, DH749) lie close to the revised modelled isopach value, suggesting that the 200m isoline in this area is correctly placed. Conversely, five minimum values from drillholes in the headwaters of Spring Ck. (DH656, DH687, DH691, DH746, DH750) are greater than indicated by the revised model (Figure A3.6), perhaps reflecting lack of correction of input values for structural problems or dip.

Overall, the minimum curvature models for Rewanui CMM honour data values. The exception occurs in the vicinity of DH726, where there is rapid variation in Rewanui CMM thickness in closely spaced drillholes, which cannot be accommodated by the minimum curvature models. Extrapolation beyond data points (e.g. in southwest) also produces spurious isoline patterns which have no geological meaning.

A3.5 Rewanui CMM trend surface analysis

First to Fourth order trend surfaces for Rewanui CMM thickness (Figure A3.7A–D) were constructed from 59 data points. Statistical variance between the models is summarised in Table A3.3.

Order	f-value (calculated)	degrees of freedom	f-value (critical)	result
Second over First	9.43	(3,56)	2.77	reject null hypothesis
Third over Second	1.83	(4,49)	2.56	accept null hypothesis
Fourth over Third	-1.20	(5,44)	2.42	accept null hypothesis

Table A3.3 Results of ANOVA test, Rewanui MM trend surface analysis. F–distribution table used from Swan and Sandilands (1995, Appendix 2.5).

Despite there being no statistically significant improvement (at $\alpha = 0.05$) from Second to Third order, the Third order surface (Figure A3.7C) is chosen as the best model because of the highest goodness of fit (85.5%), and because it defines a basin which has similar geometry to that demonstrated by the revised minimum curvature model (Figure A3.6), and does not extrapolate maximum Rewanui CMM thickness beyond the known maximum value (DH730, 248.7m). Residuals from the Third order surface are plotted in Figure A3.8.

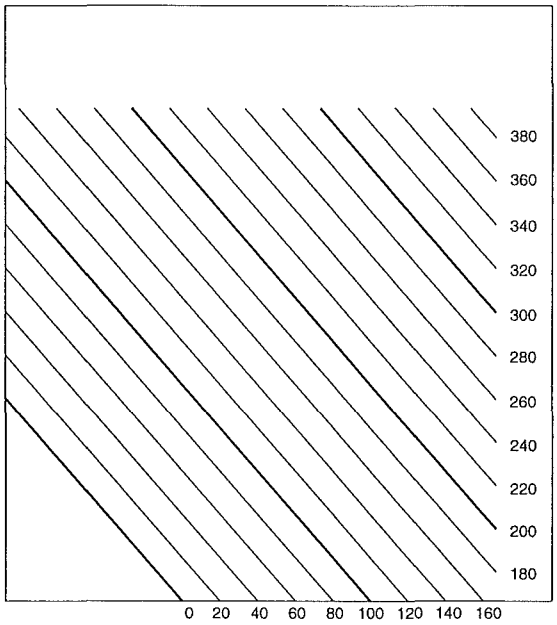

A. First order

Goodness of fit = 74.41%
Correlation coefficient = 0.86
f = 81.4

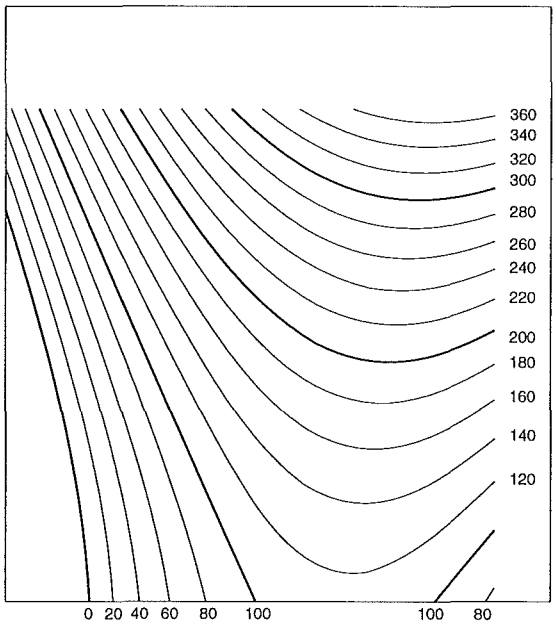

B. Second order

Goodness of fit = 83.31%
Correlation coefficient = 0.91
f = 52.9

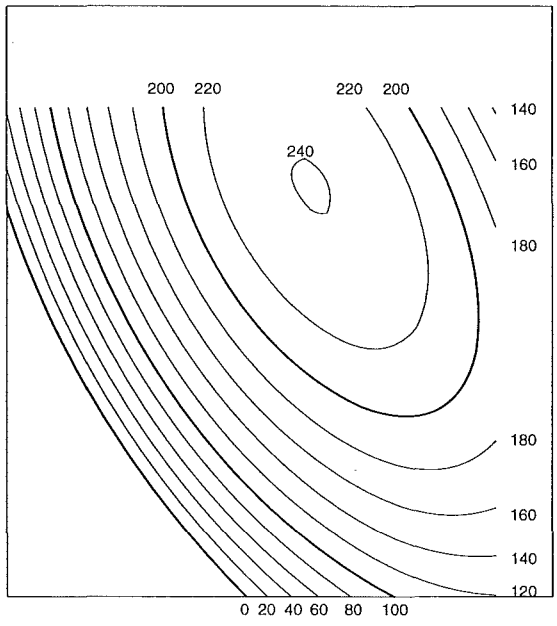

C. Third order

Goodness of fit = 85.48%
Correlation coefficient = 0.92
f = 32.0

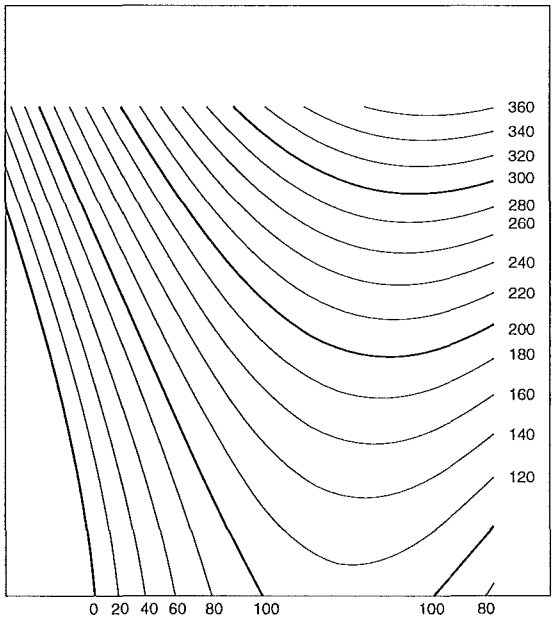

D. Fourth order

Goodness of fit = 83.19%
Correlation coefficient = 0.91
f = 15.6

Figure A3.7 Rewanui Coal Measure Member trend surface analysis
Area of each map is study area, as in Figure A3.1.

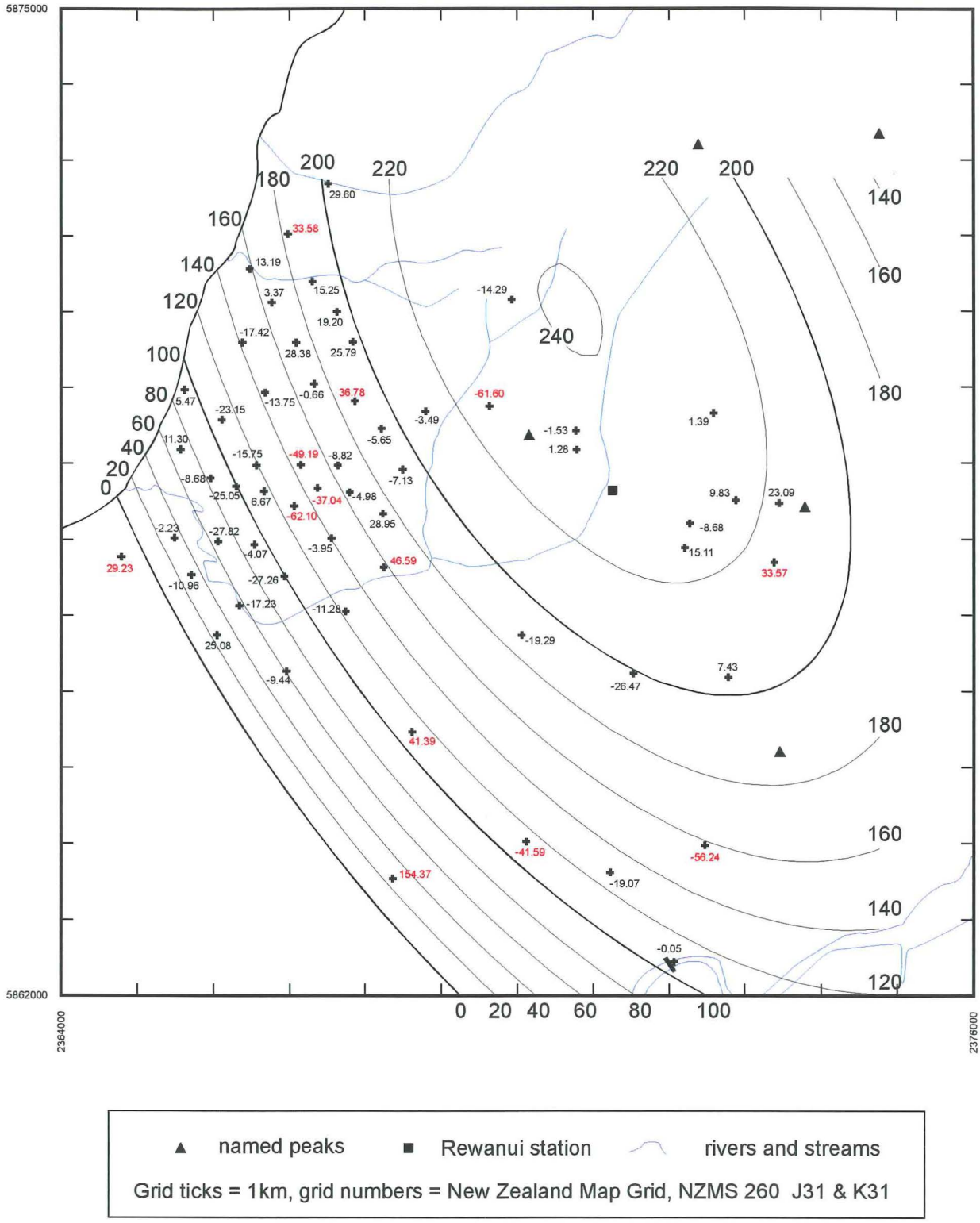

Figure A3.8 Third order trend surface and residuals,
Rewanui Coal Measure Member.
All values in metres.
High magnitude residuals highlighted in red.

High magnitude residuals (±30m or greater) occur in the south of the coalfield, notably DH654 (+154.37m), and also DH289, DH627 and DH651. The area 2km east of Rapahoe is poorly accounted for by the trend surface (e.g. DH697, DH703, DH706), and large residuals are also present in DH710, DH632 and DH730. Rewanui CMM thickness in DH653 is modelled as -21.63m, whereas the true isopach value is 7.6m. Residuals within the depocentre depicted in Figure A3.7C are generally low, which indicates less variable thickness patterns. As with trend surface models for Goldlight Fm. (Figure 3.4), there is more thickness variability near the basin margins than in the depocentre.

A3.6 Geostatistical analysis of Rewanui CMM thickness data

Geostatistical analysis, using the kriging technique, provides the most accurate method for modelling of spatially distributed data (Isaacs & Srivastava 1989, p. 318; Houlding 1994, p. 34). A key requirement is that the data set be stationary, i.e. non-random trends or drift in the data must be removed (Swan & Sandilands 1995, p. 317). Stationarity within the Rewanui CMM thickness data is achieved by using results of trend surface analysis as input. The Third order trend surface for Rewanui CMM (Figure A3.8) accounts for c.85% of unit thickness variability, and the remaining variation, which is the residual values, was modelled geostatistically. The final isopach model was constructed by summation of the modelled (kriged) residual values and the corresponding trend surface values (Isaacs & Srivastava 1989, p. 532; Swan & Sandilands 1995, p. 321).

The various steps in constructing a geostatistical model are outlined in Table A3.4 and illustrated in associated figures (Figures A3.9–A3.11). Sources for the methodology include Isaaks & Srivastava (1989), Houlding (1994), Swan & Sandilands (1995), and *TECHBASE* documentation. There is no definitive method for the construction of geostatistical models (e.g. Dubrule 1994), and many iterations (e.g. of semivariogram construction) are commonly needed before data structure is revealed (Isaaks & Srivastava 1989, p. 145). Contour patterns generated by a robust geostatistical model should be free from computer-generated artifacts (e.g. Krajewski & Gibbs 1994) and deliver geologically plausible results.

Step	Requirement	Result	Action
1) selection of grid parameters	Grid should be 2–5x less than average sample spacing	Using technique in Technote (1991), average spacing is 0.7km. Distribution of sample spacing shown in Figure A3.9	Existing 250m x 250m grid is adequate
2) detection of trend	data should be stationary	see Appendix 3.5	Residuals of third order trend surface will be modelled
3) description of spatial structure of data	Experimental semivariogram construction	See Figure A3.10 for all directions. Best fit is lag = 600m, number = 15	Model is Spherical with range of 5500m and sill (γ) of 1400
4) detection of anisotropy	Must find directions of greatest and least variance	Directional variograms illustrated in Figure A3.11. Tolerance for each direction is ±60° in order to obtain sufficient pairs (>30 desirable). Maximum semivariance evident at 22.5°, minimum semivariance at 90° See discussion below.	Chosen variogram model (Figure A3.11) is spherical, sill (γ) = 750, range = 2000 at 90°
5) development of search strategy	reflect anisotropy in data structure (need not be same as variogram anisotropy)	See discussion below.	search ellipse set as: u = 3500m at 22.5° v = 1500m variogram model isotropic, sill (γ) = 750, range = 2000
6) compute model	various inputs as given above: using ordinary kriging, other inputs are defaults		
7) generate isopach map	add modelled residuals to Third order trend, use *GRIDCONT* to construct map	see Figure A3.12	

Table A3.4 Summary of development of geostatistical model for Rewanui CMM isopach values. note: (γ) = semivariance; at the sill, semivariance = variance.

Analysis of experimental variogram anisotropy reveals that over short distances (i.e. <c.3km) there is no significant anisotropy (Figure A3.11). A tolerance of ±60° was used to ensure sufficient sample pairs for each variogram, and the number of lag steps was reduced to 13 in order to remove points with fewer than c.25 pairs. As the objective was to model small-scale variation (the larger scale variation having been largely accommodated by the Third order trend surface), a variogram model was chosen to reflect short-distance variation. A spherical model with sill = 750 and range = 2000m can be fitted to the 90° variogram (Figure A3.11), and this model adequately describes the behaviour of other directions of variogram near the origin. Continued increase of gamma with distance evident in the 45° variogram suggests some trend elements are still present in the data set.

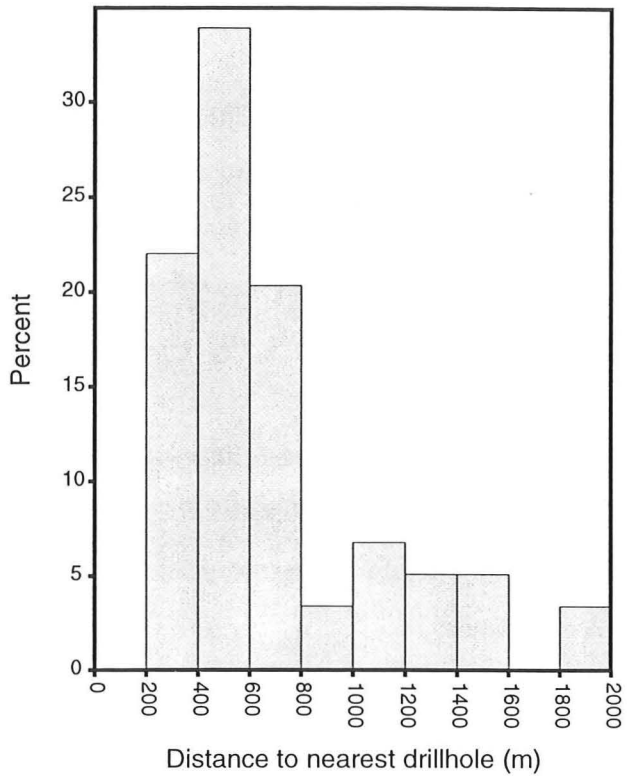

Figure A3.9

Histogram showing spacing of drillholes with Rewanui CMM thickness data. Determined by inverse distance method described in Technote (1991). Average drillhole spacing is 700m.

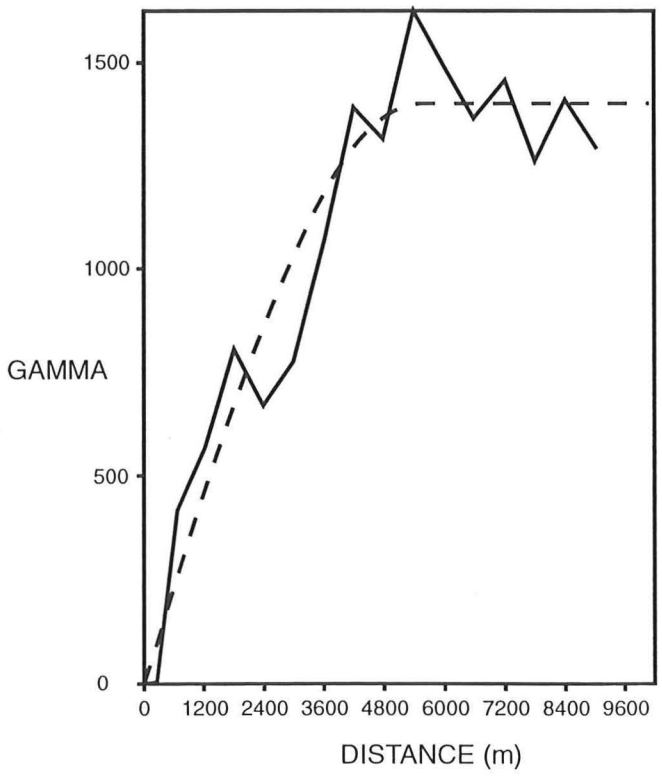

Figure A3.10

Experimental variogram, Third order residuals of Rewanui CMM thickness. Isotropic (i.e. all directions included), lag distance = 600m, number = 15 (i.e. 9000m covered). Sold line is data, dashed line is model, shperical, sill = 1400, range = 5500.

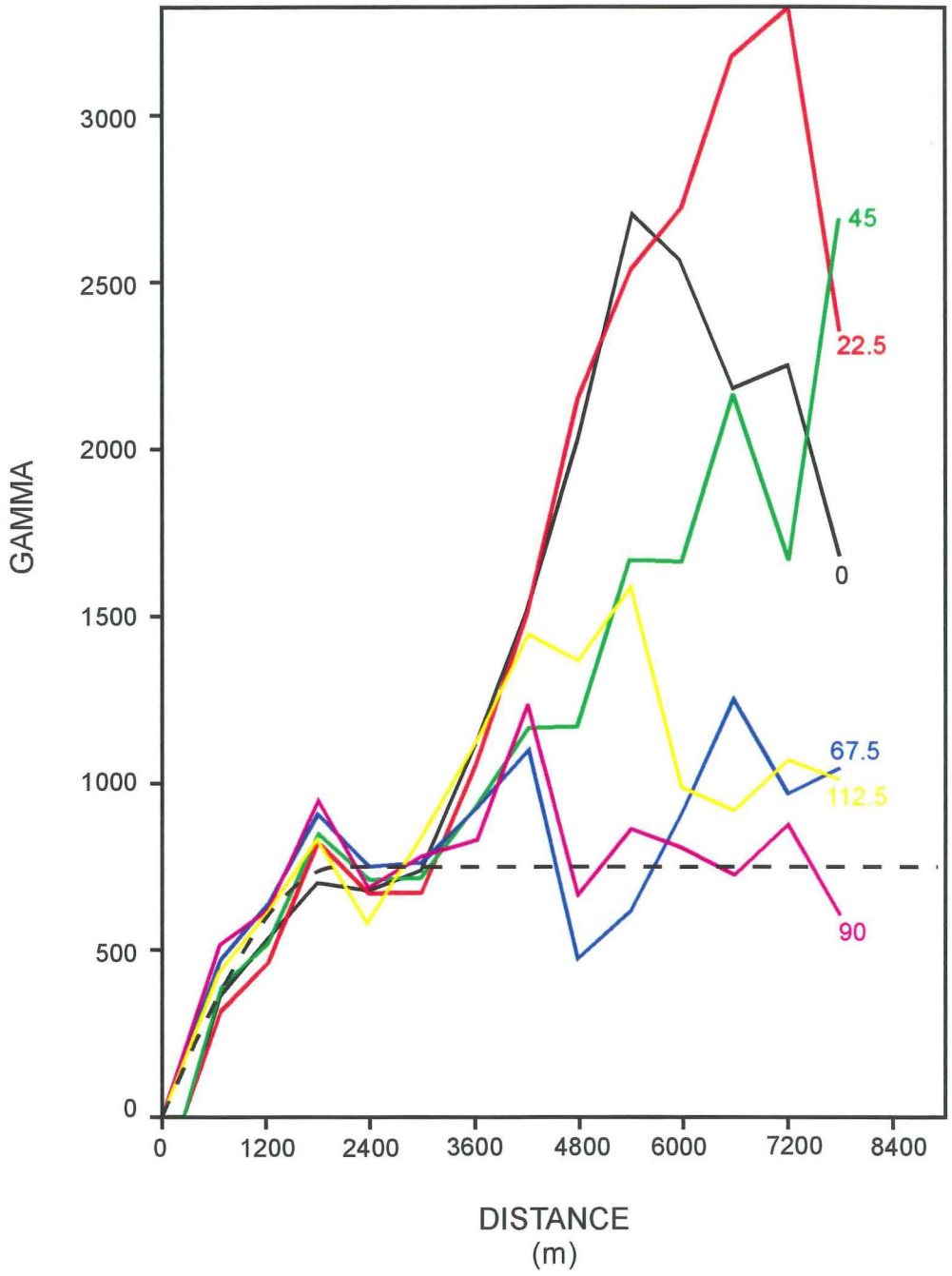

Figure A3.11 Directional variograms (22.5° increments),
Rewanui CMM Third order residuals.
Variation isotropic below c. 3km.
Lag distance = 600m, n = 13.
Model (dashed line) is fitted to 90° variogram:
spherical, sill = 750, range = 2000m.

Careful selection of kriging search strategy parameters enables the resulting isopach model to be optimised. An initial search ellipse of u = 3000m, v = 1000m oriented at 22.5° (orientation of maximum variance) produced a noisy result, and the final parameters (u = 3500m, v = 1500m) were selected by trial and error to produce an acceptably smooth model, and also to permit estimation of more grid cells. Estimates generated using larger search areas or the isotropic variogram produced similar isopach patterns to the final model discussed below, with significant differences between the models occurring only in the south and north where there are few data points.

The resulting geostatistical model of Rewanui CMM thickness (Figure A3.12) closely resembles the corresponding minimum curvature model (Figure A3.6) though without the extrapolation in the southwest. In general, the geostatistical model honours the data values (within ±10m). The exceptions are DH697 (data c.15m below model) and DH705 (data c.20m above model), which are also poorly accommodated by the minimum curvature models (see above), and DH632 (data c.10m below model) and DH654 (data c.20m above model). The Rewanui CMM thickness in DH289 appears to be lower than the model, however the 110m isopach (not shown) passes to the north of the data point.

Minimum Rewanui CMM thickness values which are close to or greater than predicted by the geostatistical model are present in drillholes in the northern reaches of the coalfield and near Rewanui (indicated in green on Figure A3.12). Modelled isolines in the northern portion of the coalfield are jagged, which reflects lack of control points, and Rewanui CMM could be thicker than presently indicated. Isolines in the south are fragmented because no data points lay within the search area for certain cells, thus no value was estimated.

A3.7 Conclusion

Numerical modelling enhances understanding of a data set and the reliability with which data values may be used. These modelling exercises provide geologically meaningful results, and contour plots are generally devoid of many the artifacts that may be generated by poor modelling technique or inadequate data preparation (Krajewski & Gibbs 1994). Applications of the modelling exercise to construction of final isopach models are discussed in the relevant sections of Chapter 3.

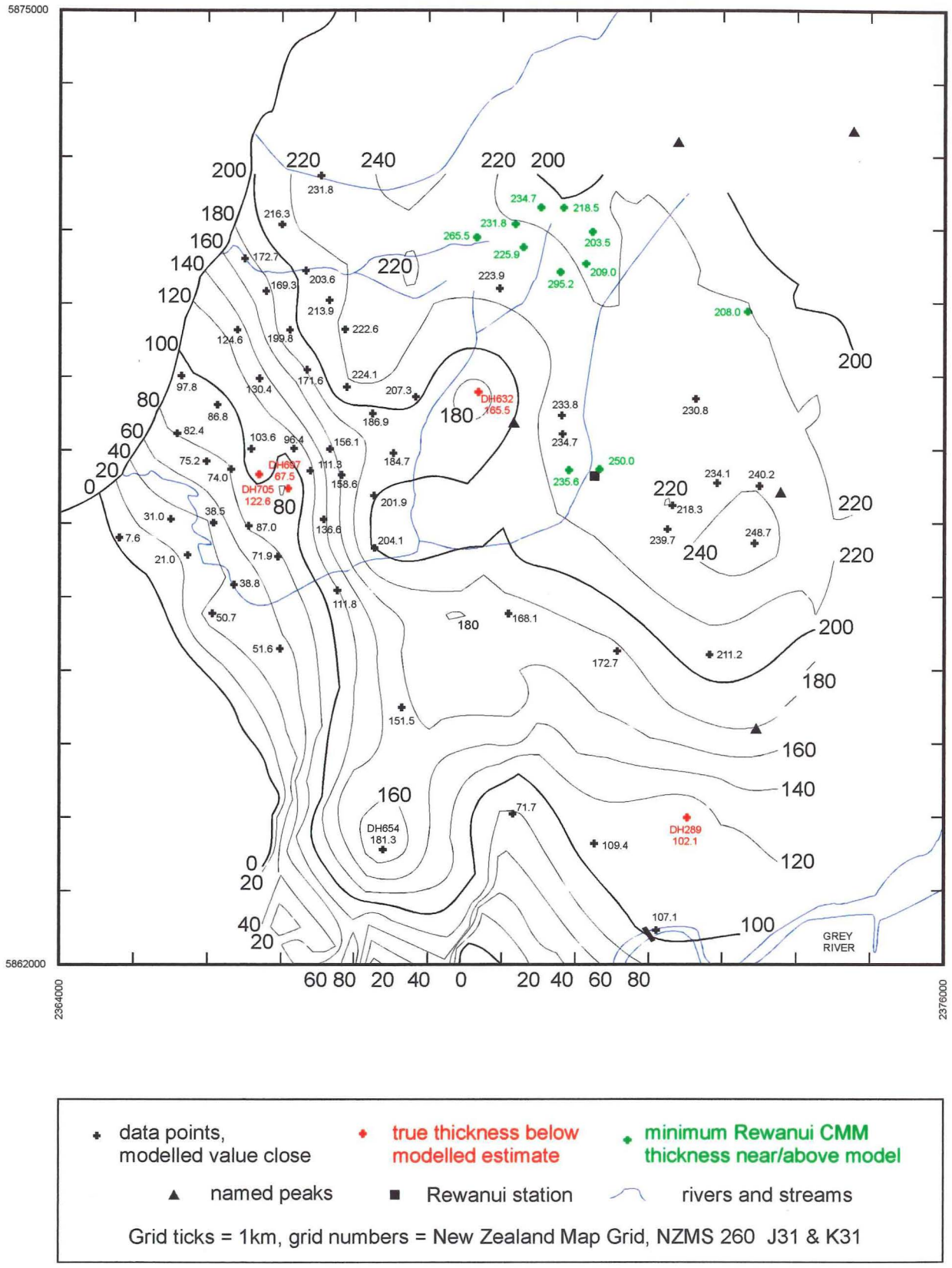

Figure A3.12 Geostatistical isopach model of Rewanui Coal Measure Member. Model comprises Third order trend surface (Figure A3.8) plus kriged residuals. Isolines shown are as reported by modelling with no smoothing.

Numbered drillholes are discussed in text.

Appendix 4. Data preparation for decompaction of Paparoa Group, and modelling of tectonic subsidence

A4.1 Introduction

The thickness of strata within a basin (as indicated by isopach patterns) is influenced by tectonic subsidence, effects of compaction by overlying strata, and isostatic effects (i.e. load on crust) of the sedimentary pile plus the water in which it was deposited (Miall 1990 p. 420). Computation of these parameters is achieved with the technique of backstripping (Sleep 1971), which determines the elevation of basement relative to present-day sea level during the history of a sedimentary basin. Backstripping is commonly applied to drillhole records from continental margin sequences (e.g. Steckler & Watts 1978; Sclater & Christie 1980; Bond & Kominz 1984). The input for backstripping is a stratigraphic column, and comprises the following information:

unit thickness
lithology of unit
initial porosities for various lithologies
porosity/depth relationships for various lithologies
depositional water depth
eustatic sea level changes
age of unit

Burial history curves, showing progressive changes in the elevation of basement with time, are the conventional means of reporting the results of backstripping.

An unconventional approach to backstripping is required for the strata present in Greymouth Coalfield. The objective of the backstripping exercise is to determine pre-burial thickness of the Paparoa Group units, and the distribution of tectonic subsidence within the basin. The compaction effects of deposition of the "cover" sequence must be corrected for, however much of the cover sequence has been eroded during basin inversion, and its thickness may only be estimated by indirect means. While Late Cretaceous–early Tertiary lithostratigraphy is well defined (Chapter 2), chronostratigraphic control is poor and construction of conventional burial history plots is not possible. Evolution of the basin in which the cover sequence was deposited was not investigated.

The focus of this appendix is the assembly of all necessary input data with which to undertake backstripping analysis. Unit thicknesses are taken from Appendix 10 (where known) or estimated from isopach models presented in Chapter 3. Other necessary information required as inputs are a description of Paparoa Group burial, knowledge of how porosity of the various units changes with depth, and proportions of the various lithologies within each unit. Results of the backstripping analysis are presented in Appendix 12 and discussed in Chapter 4.

A4.2 Modelling of Paparoa Group burial

A4.2.1 Introduction

Initial recognition of variable Paparoa Group burial was demonstrated from coal-rank trends by Wellman (in Gage 1952, p. 94). Extrapolation of outcrop thicknesses of Cenozoic strata preserved south of Greymouth Coalfield indicated that > c.3300m of strata have been eroded from the axis of the Brunner-Mt. Davy anticline (Figure 1.2). Vitrinite reflectance (VR) data (e.g. Suggate 1959; Bowman et al. 1984; Newman 1987; Cave & Newman 1995) also indicated that former burial of Paparoa Group across Greymouth Coalfield is non-uniform.

A4.2.2 Data collection and verification

Vitrinite reflectance (VR) is primarily a function of thermal history (Barker & Pawlewicz 1986). In order to estimate Paparoa Group paleoburial from VR data, VR data should ideally respond only to lateral variation in burial depth. Available VR data come from many stratigraphic intervals, and existing VR models (Bowman et al. 1984, Newman 1987) suggest the influence of variables other than burial depth (Figure A4.1, A4.2). Principal sources of VR data include CRS VR measurements, Bowman et al. (1984, Part I, Plan 45) and data from Newman (1987, Figure 4b). Additional data were obtained from Boyd (1993), Cave & Newman (1995) and unpublished CRL measurements. J. Newman (pers. comm. 1996) collected new data for DH266, DH273 and DH659. Corrections applied to the VR data are summarised in Table A4.1 and discussed further below.

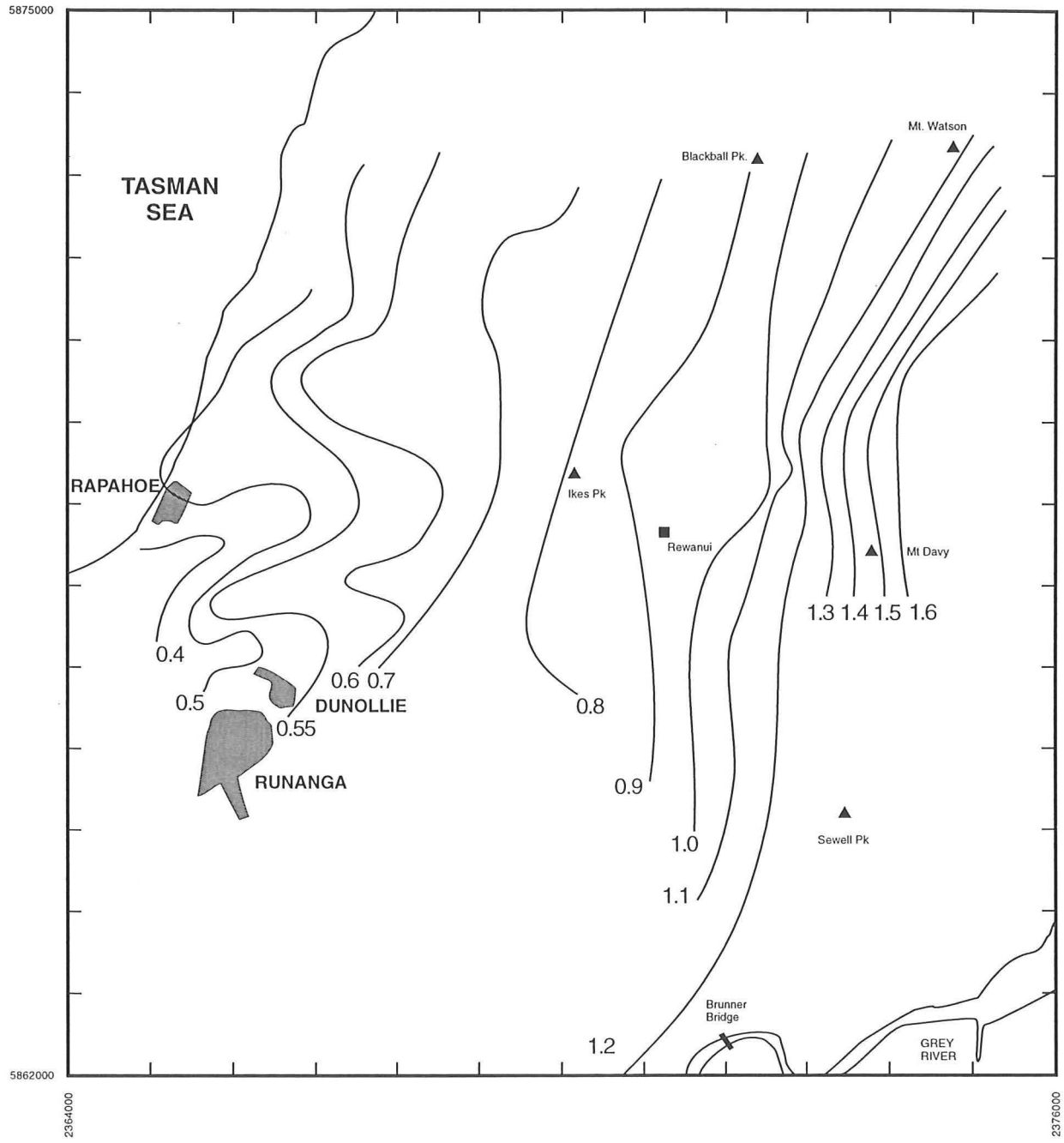

Grid ticks = 1km, grid numbers = New Zealand Map Grid, NZMS 260 J31 & K31

Figure A4.1 Vitrinite reflectance model, Coal Resources Survey, from Bowman et al. (1984, Part I, Plan 45).

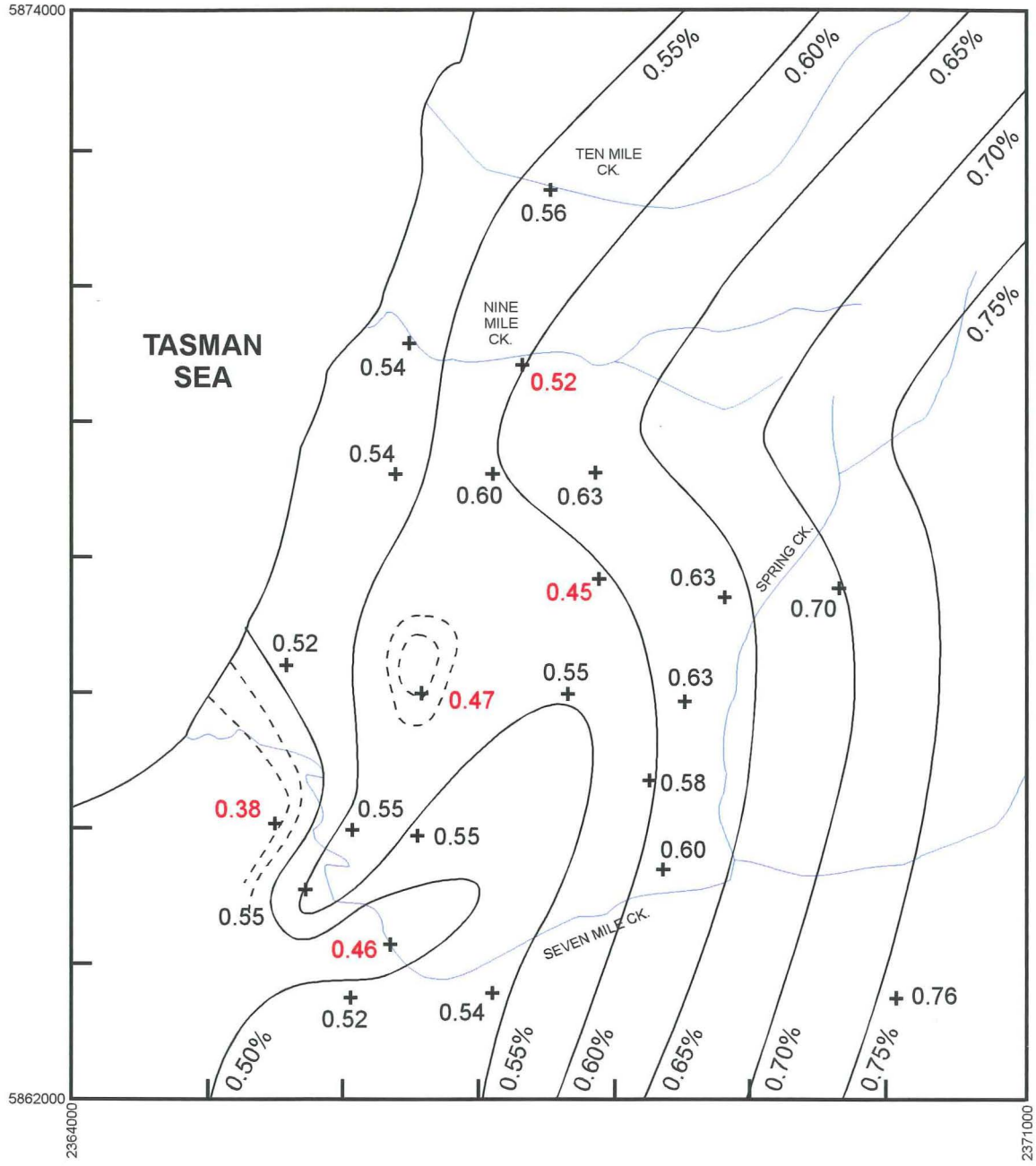

Grid ticks = 1km, grid numbers = New Zealand Map Grid, NZMS 260 J31 & K31

Figure A4.2 Vitrinite reflectance map, Rapahoe Sector, Greymouth Coalfield. From Newman (1987). Values in red cause perturbations of the VR model.

variable	problem	correction applied	references
coal type	VR suppression in perhydrous vitrinite	normalisation to "average type" volatile matter for given rank	Newman (1997)
depth of sample	increasing VR with depth	adjust VR up or down using appropriate gradient to normalise to Goldlight / Rewanui contact	Boyd (1993), Boyd & Lewis (1995)
measurement technique	optical anisotropy of VR	apply correction factor to convert Ro (random) to Ro max	Hower et al. (1994)
VR measurement from sediments	maceral identification in sediments - inertinite measured as vitrinite	use of VRF technique to derive "correct" measurements	Newman (1995, 1997), Newman & Ward (1996)

Table A4.1 Major variables influencing VR measurements, and corrections applied.

Type correction: Coal type (in the sense of vitrinite chemistry) variation is due to variable original floral composition and the effects of biochemical alteration prior to burial, and vitrinite which is high in hydrogen (perhydrous) has suppressed VR and high volatile matter relative to vitrinite of normal chemistry for a given rank (Suggate 1974; Newman & Newman 1982; Newman et al. 1997). Techniques for correction of type influences on rank measurement are well established for New Zealand coals. New Zealand coals of "average" chemistry exhibit a "normal" coalification path (Figure A4.3A, dashed line) whereas samples with elevated hydrogen lie along isorank paths oblique to the "average type" line (solid lines, Figure A4.3A) (Suggate 1959; Newman & Newman 1992). Corrected VR values are obtained from the known VR/VM relationship for the "average" type line (Figure 4.3B, after Newman et al. 1992). Type corrections by this method are not possible at high rank (Ro max > c.0.9%), because type and rank effects become indistinguishable (left-hand end of Figure A4.3B).

Rewanui Fm. coals used in this study generally lie a small to moderate distance from the "average type" line (Figure A4.4A), indicating slightly to moderately suppressed VR values. Corrected VR values are obtained by moving the samples along isorank lines to meet the "average" type VM / VR curve (Figure A4.4B). Suppression in Greymouth Coalfield coals is believed to result from the effects of bacterial alteration on peat accumulated in anoxic environments (Newman 1987). Much of the "noise" evident in existing isorank plots (Figures A4.1, A4.2), and the anomalous values highlighted in red in Figure A4.2, can be accounted for by undertaking correction for VR suppression.

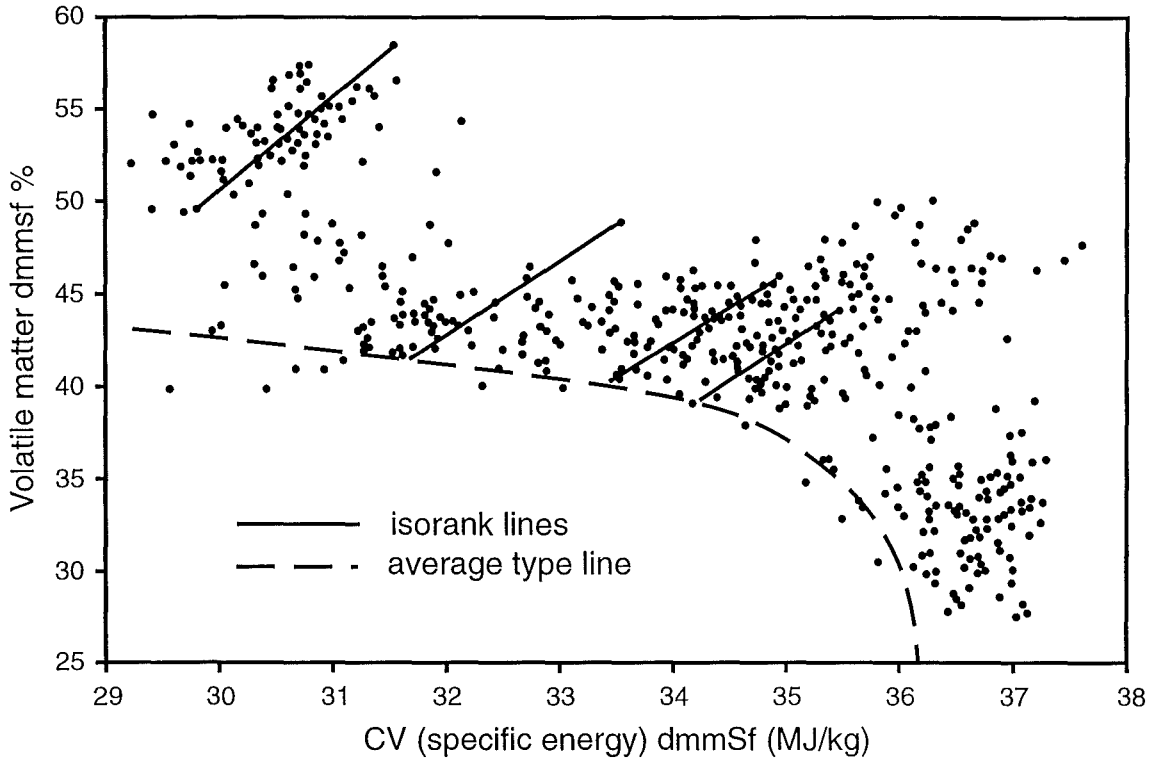

Figure A4.3A Specific energy / volatile matter relationship for Late Cretaceous to Miocene West Coast coals. From Newman & Newman 1992 (Figure 16). dmmSf = dry, mineral matter, sulphur free

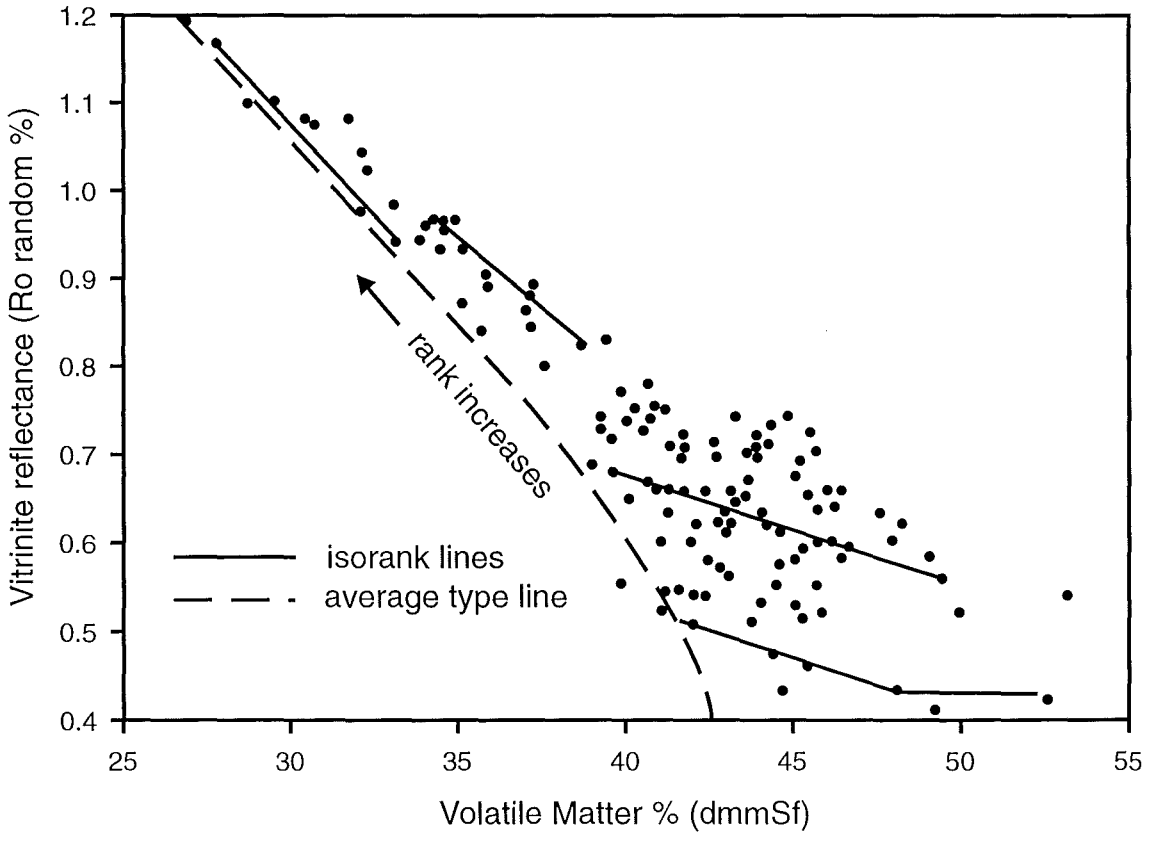

Figure A4.3B Volatile matter / vitrinite reflectance relationship for West Coast coals. From Newman et al. 1992 (Figure 6).

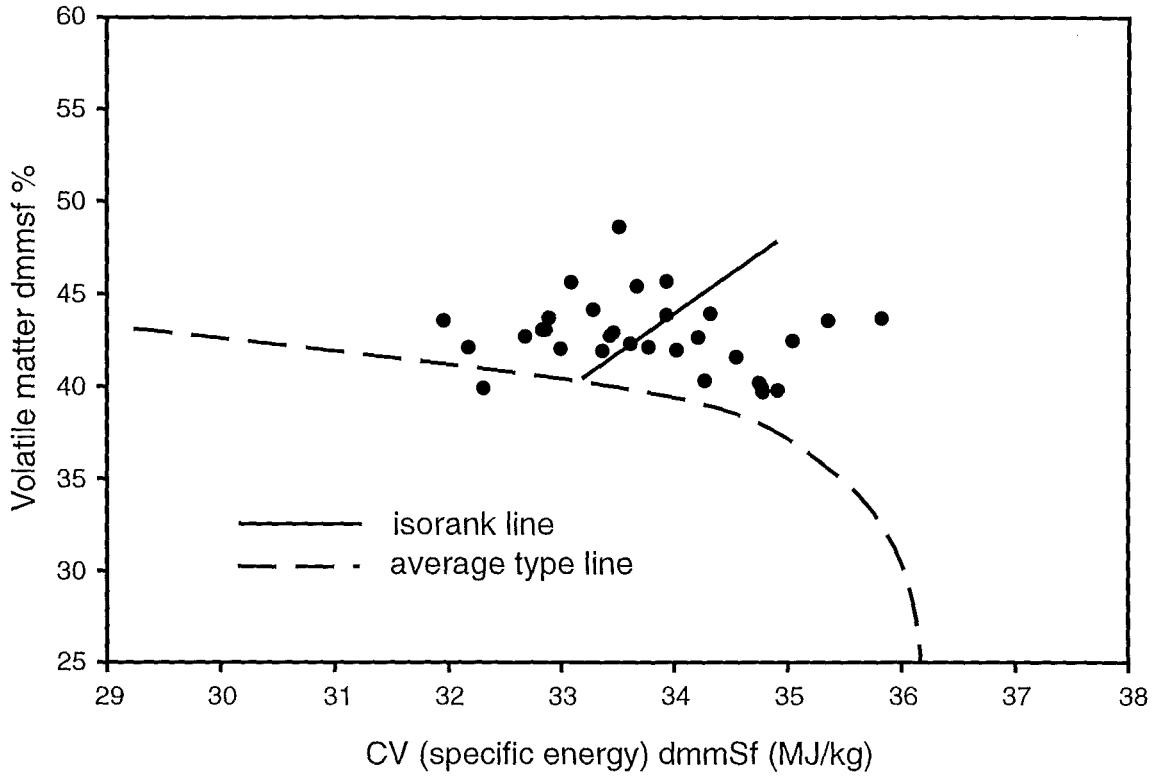

Figure A4.4A Specific energy / volatile matter relationship for Greymouth Paparoa Group coals. Data sources given in Appendix 11.1. dmmSf = dry, mineral matter, sulphur free

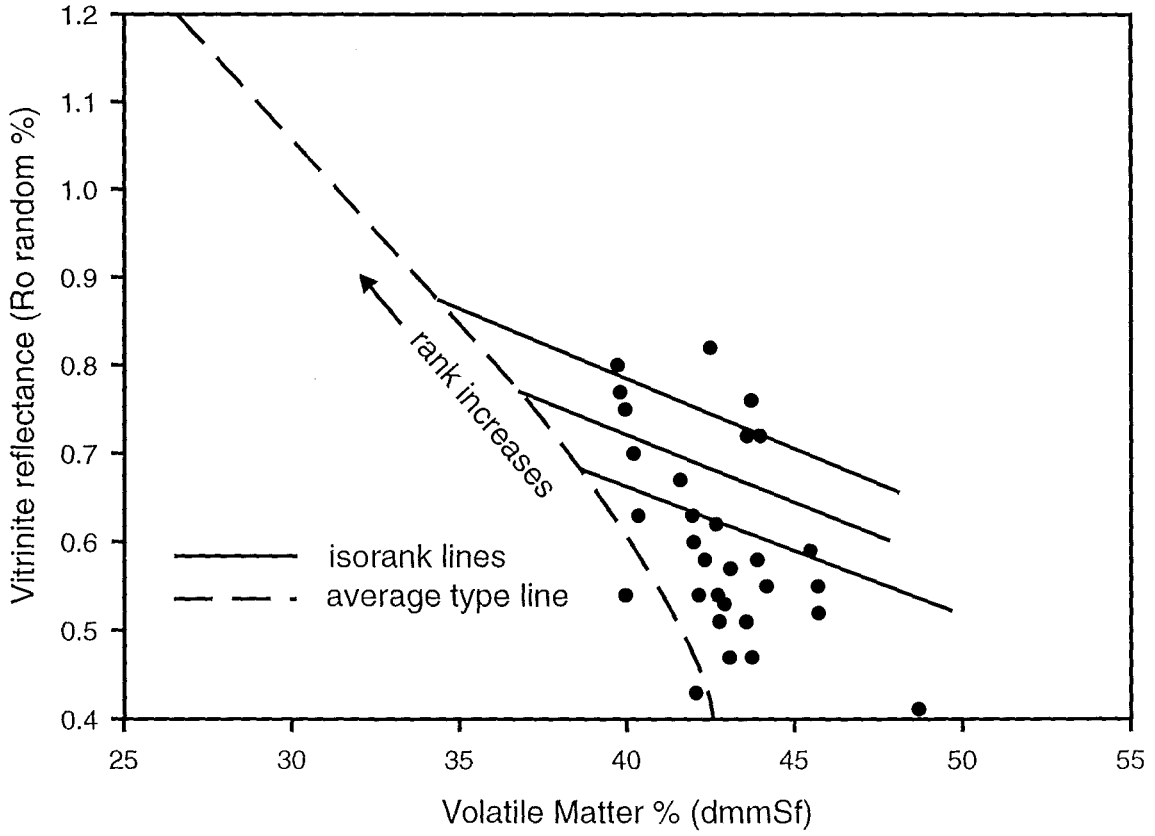

Figure A4.4B Volatile matter / vitrinite reflectance relationship for Greymouth Paparoa Group coals. Data sources given in Appendix 11.1

Depth corrections: Boyd (1993) (also Boyd & Lewis 1995) investigated coal rank trends along a transect across northern Greymouth Coalfield, comprising DH's 621, 635, 656, 658, 659 and 660. An average downhole rank gradient of 0.32 Ro max km^{-1} was found to explain most downhole variation present where Ro max is <1.10%. Boyd & Lewis (1995) suggested that this gradient is a minimum as drillholes are not perpendicular to isorank surfaces (Figure A4.5), however the angle is <10° and the difference between true and apparent rank gradient will be <2%. In the present study, sample depths (in km) above or below the Rewanui/Goldlight contact were determined from stratigraphic data given in Appendix 10.2, and VR data were normalised to that contact by applying the Boyd & Lewis (1995) gradient.

Thirteen VR measurements in the Mt. Davy Sector were obtained from lower Rewanui CMM or Morgan CMM, in which Ro max exceeds 1.10%. Many authors (e.g. Stach et al. 1982 p. 383; Larter 1989) illustrate exponential increase of VR with depth, therefore depth-corrected VR values may be slightly high as result of using the Boyd & Lewis (1995) linear VR/depth model.

Measurement technique: Vitrinite exhibits uniaxial anisotropic reflectance, and maximum reflectance is attained along bedding planes, perpendicular to the axis of burial stress (Stach et al. 1982 p. 98). Laterally imposed tectonic stress may generate biaxial reflectance anisotropy (Hower et al. 1994). Ro max data is available for the majority of samples (51/58), however Ro random was measured for the remaining 7 samples. While anistropy is present in all coal with sub-bituminous or greater rank (Stach et al. 1982, p. 98), various authors debate the necessity or possibility of differentiating Ro max from Ro random at VR values of <1.0% (e.g. Wolff 1993 *cited in* Hower et al. 1994) or <2.0% (e.g. Robert 1985). Hower et al. (1994) suggest the following relationship:

$$\textbf{Ro max} = 1.06 \pm 0.1 \times \textbf{Ro random} \qquad \textit{Equation A4.1}$$

as a universal formula for high volatile bituminous coals (Ro = 0.5%–1.0%). Diessel (1992, p. 79) cites other similar conversion factors. In this study, the correction factor given in Equation A4.1 is applied to all Ro random values.

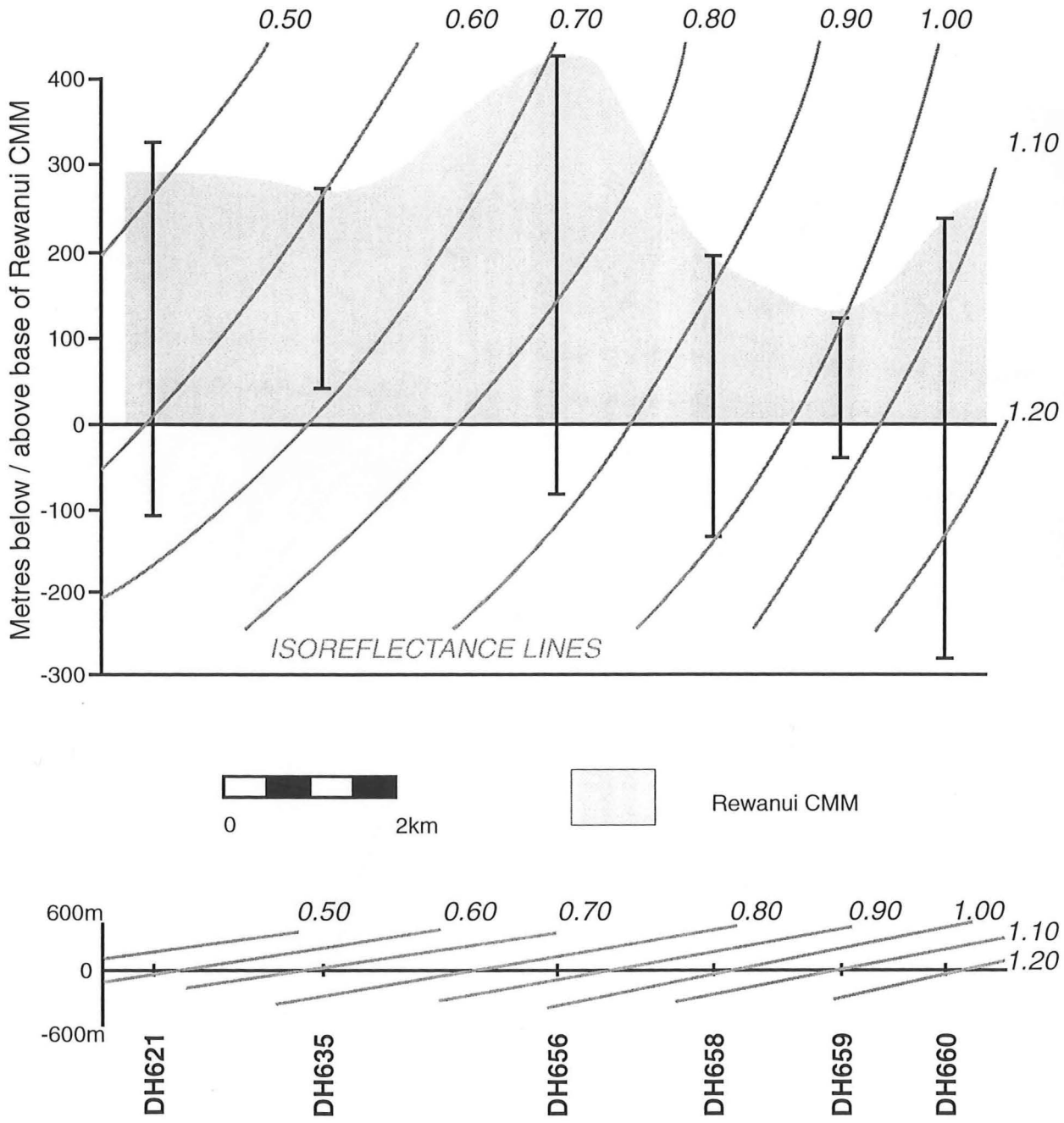

Figure A4.5 Diagrammatic reflectance profile across Greymouth Coalfield, from Boyd (1993) and Boyd & Lewis (1995).
Datum is base of Rewanui CMM (stratigraphy according to CRS).
Vertical exaggeration of upper diagram = 10:1,
no vertical exaggeration in lower diagram.
All reflectance values are Ro max.

VR measurements from dispersed organic matter: Isorank plots (e.g. Figure A4.1) indicate reflectance increases rapidly in the east of Greymouth Coalfield, (VR > c.1.00%), relative to the Rapahoe Sector. Downhole data from DH266 (Brunner Bridge) also demonstrate rapid increase in reflectance above 1.00% (Cave & Newman 1995). Measurements of 0.93 % Ro max at 135.0m (Dunollie Fm.) and 1.38 % Ro max at 560.8m (Morgan CMM) indicate a rank gradient of 1.10% Ro max km^{-1}. However, VR measurements in DH266 are from dispersed organic matter (DOM), and elevated VR values may result from measurement being made on inertinite rather than vitrinite.

The VRF technique (Vitrinite Reflectance and Fluorescence) permits differentiation of vitrinite (both suppressed and normal) from inertinite where measurement is made from DOM (Newman 1995; Newman & Ward 1996; Newman 1997). Reflectance and fluorescence measurements are made from discrete organic particles within a polished sediment sample. A nitrogen atmosphere is used during fluorescence recording to eliminate the effects of alteration (Quick 1994). Cross-plots of reflectance and fluorescence enable identification of the true normal vitrinite population, from which a correct mean reflectance is calculated.

Results from VRF analysis for four depths in DH266 are shown in Table 4.2 and Figure A4.6. The resulting corrected downhole rank gradient in DH266 is 0.91 Ro max km^{-1}, and there is no evidence for a logarithmic relationship between VR and depth.

Depth (m)	Formation/Member	Ro random %
137	mid - Dunollie Fm.	0.83
295	upper Goldlight Fm.	0.99
517	lower Rewanui CMM	1.18
566	upper Morgan CMM	1.22

Table A4.2 Vitrinite reflectance data from sediment samples, DH266. Measured by the VRF technique (Newman 1997).

Results from DH266 confirm that the rapid increase in rank observed in the east of Greymouth Coalfield is due to a greater rate of VR increase with depth, rather than significantly greater burial.

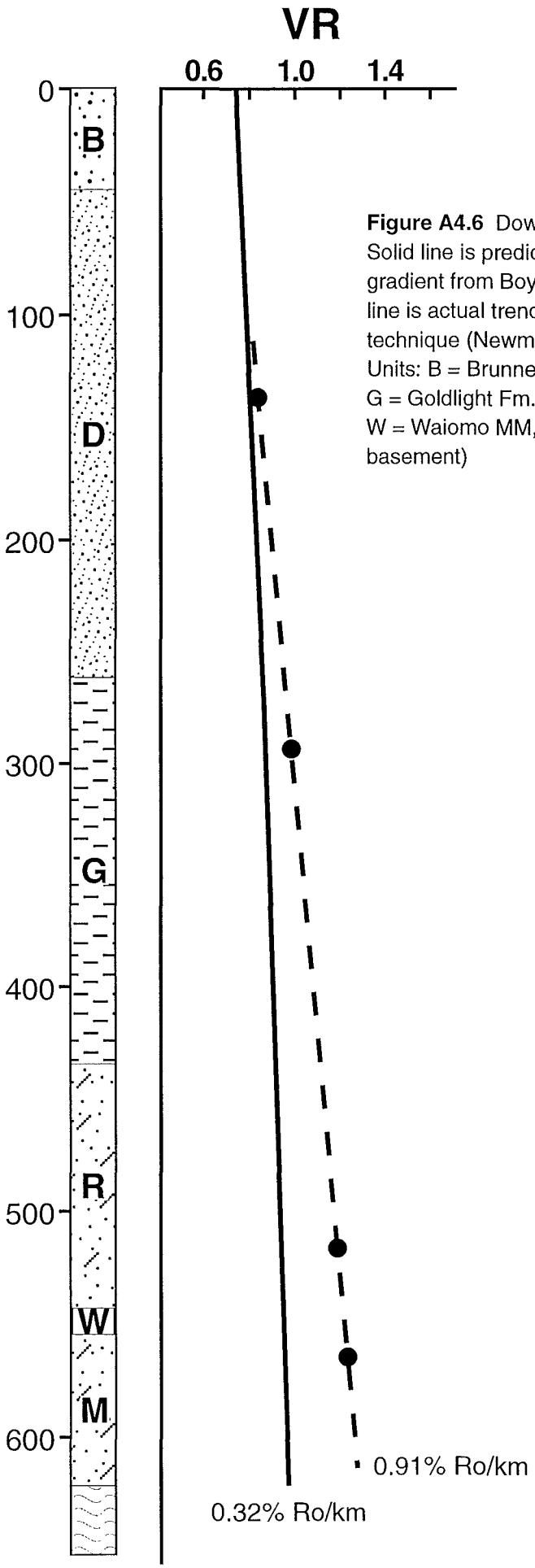

Figure A4.6 Downhole rank trends, DH266. Solid line is predicted trend using downhole gradient from Boyd & Lewis (1995). Dashed line is actual trend, measured with VRF technique (Newman 1997).
Units: B = Brunner CM, D = Dunollie Fm., G = Goldlight Fm., R = Rewanui CMM, W = Waiomo MM, M = Morgan CMM (on basement)

A4.2.3 Construction of a VR model

Once the various corrections were applied to the VR measurements, a data set showing lateral variation in VR of the Rewanui / Goldlight contact was obtained. All inputs, corrections and final data are summarised in Appendix 11.1. An isorank plot, constructed with the *TECHBASE MINQ* modelling application, is presented in Figure A4.7. This isorank model presents a straightforward pattern of rank change across the coalfield, and does not contain the anomalies depicted in Figures A4.1 or A4.2.

While VR at the Goldlight / Rewanui contact clearly increases eastwards, the pattern of increase is not linear. In the Rapahoe Sector, VR increases slowly from c.0.55% at the coastline to c.0.70% in the vicinity of Spring Ck., whereas the increase in VR eastwards from Spring Ck. (0.70% to 1.30%) is more rapid. This pattern is consistent with increased downhole rank gradient observed in DH266 (Figure A4.6).

Declining VR values in the southeast corner of the coalfield are an artifact of the modelling algorithm (there are no data points in this area). However, VR measurements from Brunner Coal Measures do decrease eastwards across the axis of basin inversion (Brunner-Mt. Davy Anticline) which passes through the Brunner area (Nathan et al. 1986, Figure 3.18; Cave & Newman 1995), hence the modelled pattern may be realistic. The depicted VR pattern in the southwest of the study area is also unconstrained by data.

A4.2.4 Estimation of burial depth from Vitrinite Reflectance

Numerous methodologies for interpretation of burial depth or paleotemperature from VR data are described in the literature. Direct determination of paleotemperature from VR using chemical kinetic equations is described by Lerche et al. (1984), Larter (1989), Burnham & Sweeney (1989) and Sweeney & Burnham (1990). Other workers use correlations with alternative paleothermometers (e.g. apatite fission track analysis (AFTA), fluid inclusions) to determine paleotemperature from VR data (e.g. Barker & Goldstein 1990; Green et al. 1989).

Boyd & Lewis (1995) concluded that AFTA thermometry from Greymouth Coalfield (Kamp et al. 1992) provided the most useful estimate of paleotemperature. However, there are no reliable direct temperature measurements (e.g. geothermal gradient measurements, bottom-hole temperatures) for Greymouth Coalfield with which to

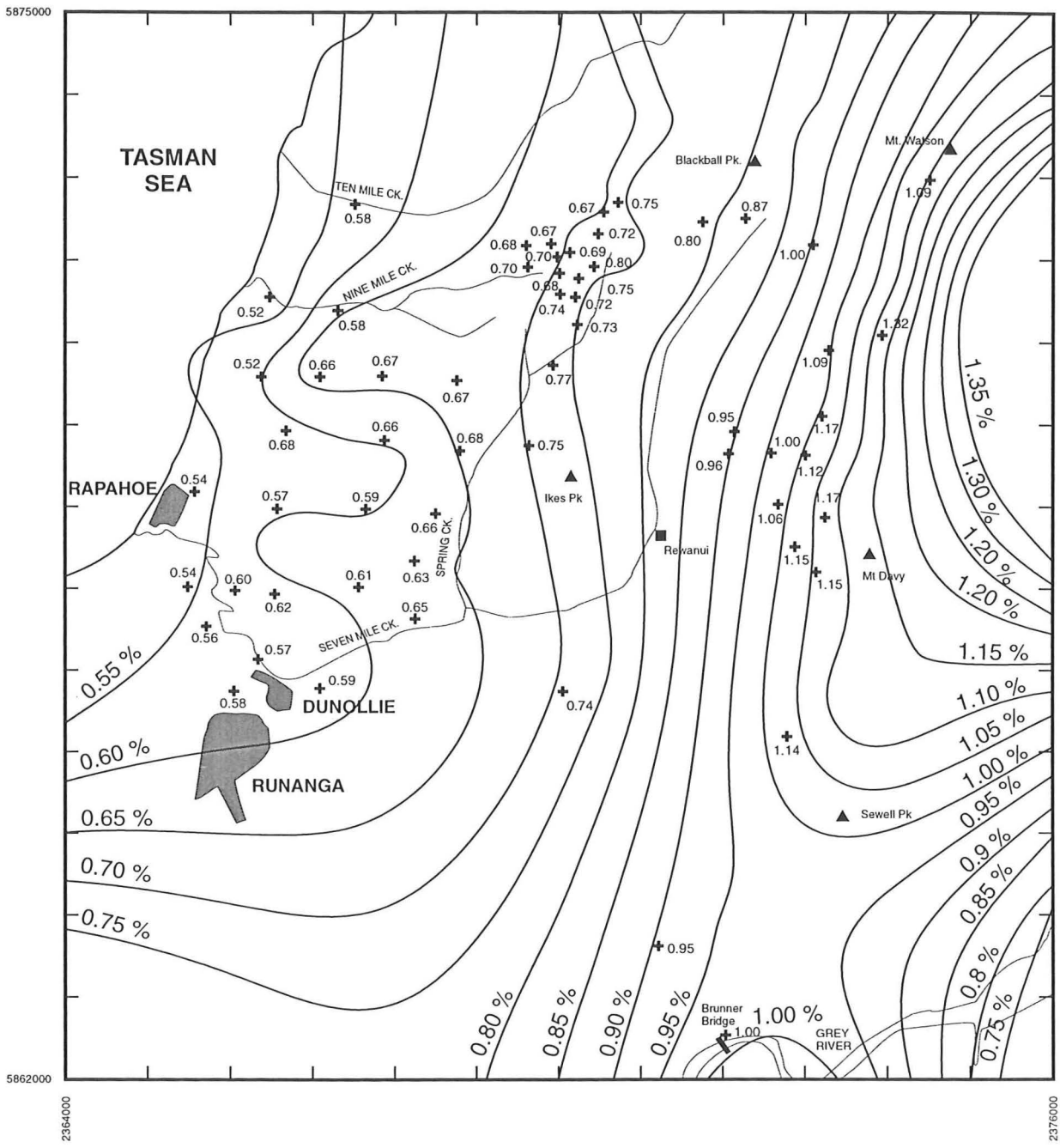

Figure A4.7 Virinite reflectance map, Greymouth Coalfield.
Data modelled with *TECHBASE MINQ* (minimum curvature) application.
Isoline interval = 0.05% Ro max.

convert paleotemperature estimates to burial depth. Kamp et al. (1992) and Kamp (pers. comm. ms. 1993) assume a gradient of 29°/km for Greymouth Coalfield, taken from Taranaki Basin drillholes, in order to convert paleotemperatures to burial depth.

A simpler approach is to calculate paleoburial directly from known downhole VR gradients, thereby avoiding the need to estimate paleogeothermal gradient or initial basin temperatures. Burial may be approximated by the following equation:

$$\textbf{depth} = [\textbf{VR} - \textbf{VR (init)} / \textbf{0.32}] + \textbf{1.0} \qquad \textit{Equation A4.2}$$

where **VR (init)** = initial vitrinite reflectance (estimated to be 0.3%)
0.32 = gradient (%Ro max km^{-1}) from Boyd & Lewis (1995)
1.0 = 1km, the interval over which initial VR does not change

The two critical assumptions made are initial vitrinite reflectance, and the depth at which VR becomes sensitive to burial. Many authors (e.g. Stach et al. 1982; Lerche et al. 1984; Sweeney & Burnham 1990) illustrate minimum VR values of 0.2%–0.3%, and such reflectances are commonly exhibited by vitrinite maceral precursors in modern peats (Shearer & Moore 1996). The principal coalification effect during early burial is porosity reduction (expulsion of water), and physico-chemical coalification generally does not occur at burial depths <1km (Stach et al. 1982, Fig 22A). A depth of 1km is therefore taken in this study as the onset of coalification.

Burial depth for the Rewanui / Goldlight contact was calculated from VR data using Equation A4.2 (results reported in Appendix 11.1), and modelled with the *TECHBASE MINQ* application (Figure A4.8). Burial trends mimic VR isograd patterns exactly, as a result of the linear relationship between VR and depth used in this study. In the east of Greymouth Coalfield, burial will be overestimated if the true rank gradient, as indicated by VRF data, is higher than was used for modelling.

A4.2.5 Discussion of VR and burial model

Independent estimates of paleoburial of Greymouth Coalfield strata have been derived from geological mapping (Nathan 1978), regional synthesis of basin history (Nathan et al. 1986), studies of diagenetic mineralogy (Boyd 1993; Boyd & Lewis 1995), and apatite fission track analysis (AFTA) (Kamp et al. 1992; Kamp pers. comm. ms. 1993).

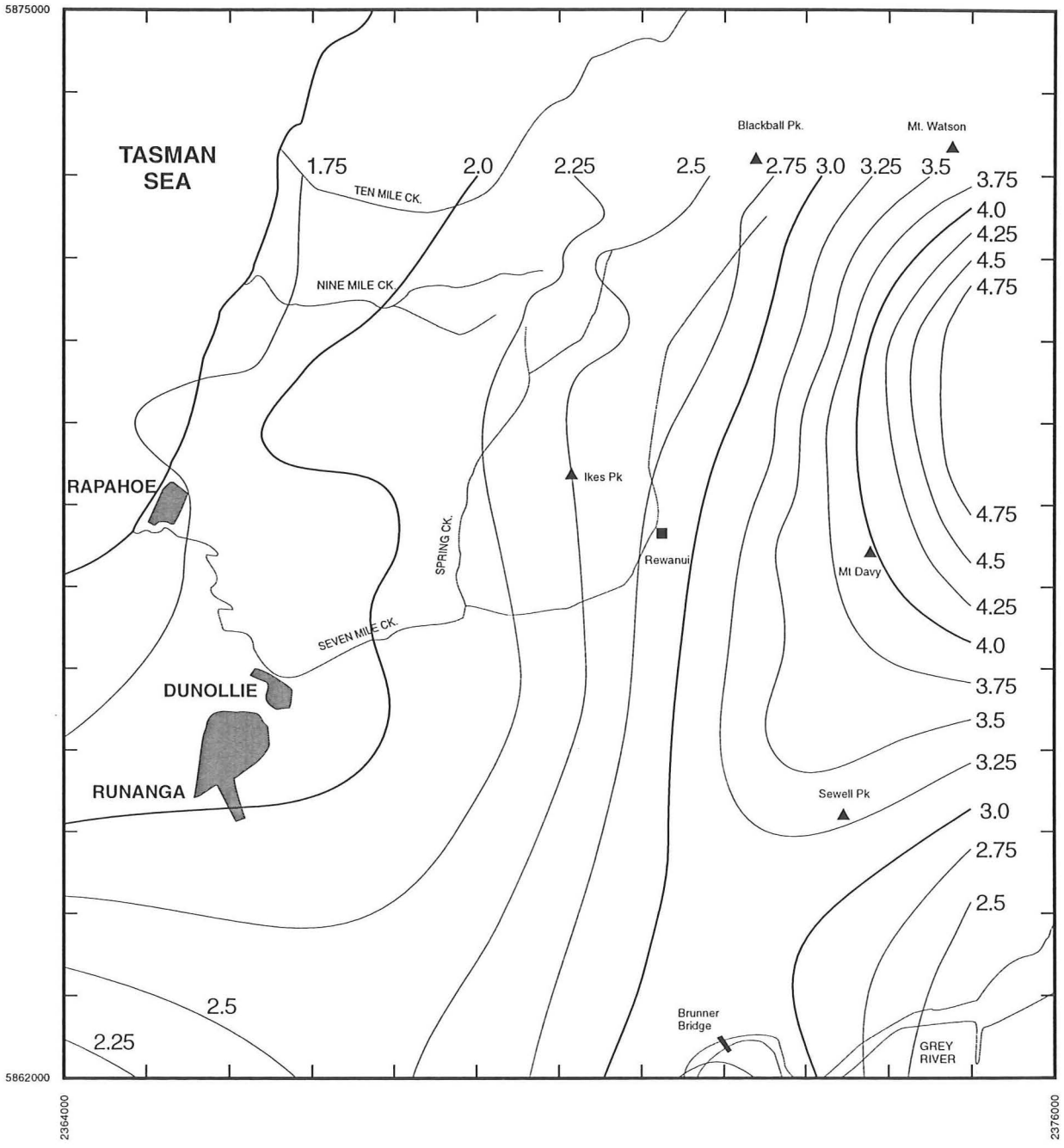

Figure A4.8 Burial model for Rewanui CMM / Goldlight Fm. contact.
Depths in km, interval = 250m.
Calculated from vitrinite reflectance model (Figure A4.7).

Burial estimates derived from regional isopachs for the entire Late Cretaceous to Oligocene sequence in the Greymouth area (Nathan et al. 1986, Figure 3.8 & 3.13, Maps 12–14) closely match present estimates. Nathan et al. (1986) depicted in excess of 4300m of strata adjacent to the Roa-Hawera Fault Zone, and c. 1600m at the present-day coastline near Runanga, and both values are similar to corresponding burial estimates shown in Figure A4.8. However, burial estimates derived from diagenetic mineralogy and AFTA are c.20–40% higher than estimates determined from VR alone, possibly because of incorrect assumptions about paleogeothermal gradient used by Kamp et al. (1992) and Boyd (1993) to convert VR via paleotemperature to burial depth.

The above discussion highlights that VR varies both vertically and laterally throughout Greymouth Coalfield. The relationship between VR and paleoburial is also potentially variable, dependent upon rank and location within the basin. The Boyd & Lewis (1995) relationship is preferred because it represents actual measurements, at least in the area of their sampled transect (Figure A4.5), and computation of burial depth is straightforward. Despite clear departures from this simple relationship, the modelled burial was reliably estimated throughout the area of the coalfield where the majority of drillholes in which compaction was estimated lie. The only drillhole with Ro max significantly greater than 1.00% which was used for decompaction modelling was DH668 (buried c.4.2km). However, compaction parameters (see below) at corresponding burial depths are not sensitive to small depth changes, and errors resulting from decompaction are small.

A4.3 Estimation of compaction parameters

Compaction of sediments during burial has been modelled using exponential equations (e.g. Sclater & Christie 1980), power-law equations (e.g. Baldwin & Butler 1985) or linear equations (e.g. Stam et al. 1987), and different relationships may be required for different lithologies (e.g. Baldwin & Butler 1985; Stam et al. 1987). The combined role of mechanical compaction and diagenesis in porosity reduction is highlighted by Bond & Kominz (1984) and Addis & Jones (1985), and modelling a complex process by a simple continuous numerical function may be inappropriate, despite being commonplace.

In this exercise, decompaction was performed using *BASIN.XLS*, a spreadsheet–based application which operates under *MICROSOFT EXCEL®* (Larrieu 1995). *BASIN.XLS* solves the decompaction equation using iterative numerical techniques, and applies an exponential decompaction model:

$$\phi = \phi_0 \, e^{-cy} \qquad \textit{Equation A4.3}$$

where ϕ_0 = initial porosity
c = lithology-dependent compaction coefficient
y = depth (km)

Baldwin and Butler (1985) demonstrate that exponential compaction models are inappropriate for mudstones, whereas power-law equations can easily account for porosity changes in mudrocks over 0.4m–5km. They also illustrate (their Figure 3) that the exponential equations from Sclater and Christie (1980) allow for no compaction of sandstone between 0 and c.100m. Exponential decompaction models may therefore be appropriate for decompaction of thick sedimentary sections (few km scale) but less appropriate for modelling shallow (few 100's of metres) compaction. Both scales are relevant to this study. However, no choice of decompaction model is offered by *BASIN.XLS*, whereas other routines offer alternative regimes (e.g. Stam et al. 1987).

Paparoa Group strata are lithologically heterogeneous, and a wide range of textures is present, ranging from pebble-cobble conglomerate to mudstone and coal (Chapter 2). Thus, an appropriate decompaction regime is required for both clastic and organic strata.

A4.3.1 Conglomerate

Reduction of conglomerate porosity by compaction can only be achieved when pressure is sufficiently great so as to cause crushing of framework clasts, thus compaction of conglomerates after deposition is a relatively unimportant process (Hails 1976 p. 450). Initial packing density of gravels is dependent on depositional environment (Hails 1976 p. 469), and an initial porosity of c.30% is a reasonable estimate for fluvial gravels (e.g. Broadbent & Callender 1991). A compaction coefficient of 0.05 allows for minor compaction resulting from the presence of thin sandy and muddy interbeds and compactible organic material (e.g. logs). The resulting compaction curve is illustrated in purple in Figure A4.9. Porosity reduction is approximately linear and final porosity at 6km burial depth is c.22%, however such porosity is unlikely to survive due to cementation in pore spaces.

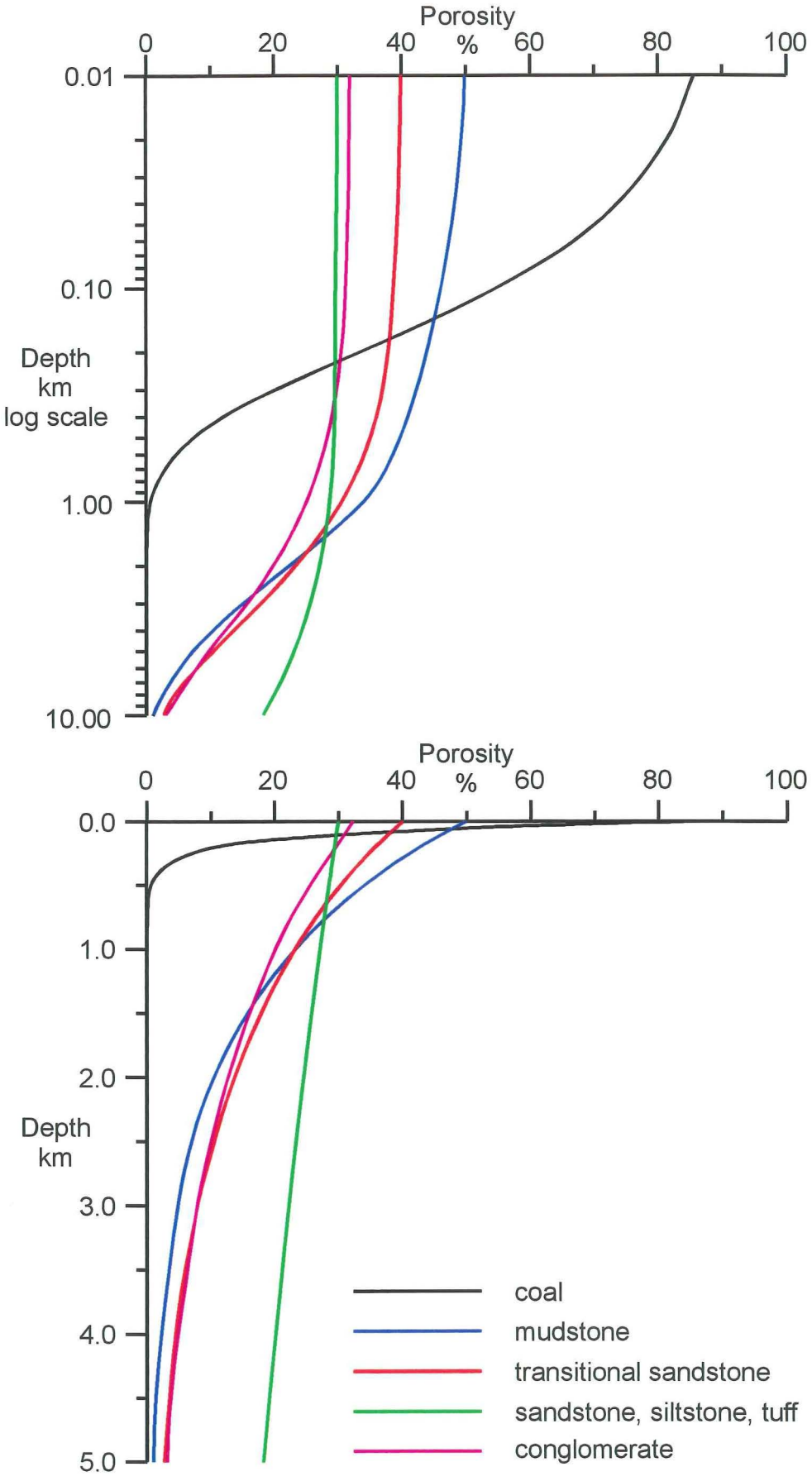

Figure A4.9 Decompaction models, showing exponential decrease in porosity with depth. Upper plot shows logarithmic depth scale, lower plot shows linear depth scale.

A4.3.2 Sandstone

Sclater & Christie (1980) use an initial porosity of 49% and a compaction coefficient of 0.27 for North Sea sands, and 56% and 0.39 respectively for shaley sand (reflecting a higher proportion of compactible mud). Initial sand porosity is largely controlled by sorting (Beard & Weyl 1973; Houseknecht 1987). Rewanui Fm. sandstones are moderately to poorly sorted (Boyd & Lewis 1995), and finer sandstones are commonly silty. Diagenetic siderite within ECS sandstones (up to 30%) indicates the presence of significant initial porosity (Boyd & Lewis 1995). Corresponding porosity values reported by Beard & Weyl (1973) for artificially mixed sands are 34.0% (moderately sorted) and 30.7% (poorly sorted). A value of 32% was used in the present analysis.

Boyd & Lewis (1995) indicated porosity survived to >2km, below which pseudomatrix (WCS) and coarse siderite (ECS) formed, resulting in porosity reduction. Compaction of ECS sandstones was limited by presence of quartz grains and strong metamorphic rock fragments. In ECS sandstones, total kaolinite plus siderite is typically c.20% (Boyd 1993, Appendix 1). These data indicate porosity reduction within Rewanui Fm. sandstones occured by means other than mechanical compaction, particularly at depths >2km, and that a conservative mechanical compaction regime was functional.

Baldwin & Butler (1985) stated that texturally or mineralogically immature sandstones will have greater solidity (i.e. less porosity) than those described by the Sclater & Christie (1980) parameters, and a compaction coefficient of 0.24 (which would give c.20% porosity at 2km) was selected (green line, Figure A4.9). This value was also used for siltstones, though these sediments are relatively rare (Section 2.3). Tuffaceous beds within Ford Fm. are generally sandy, and compaction was modelled with the same parameters as sandstones.

Transitional lithosomes contain sorted to well sorted very fine-fine sandstones with rare medium–very coarse sandstone and conglomerate (Section 2.3). A suitable value for initial porosity is 40% (Beard & Weyl 1983; Houseknecht 1987), and the compaction coefficient of 0.27, which was determined by Sclater & Christie (1980) for marine (subaqueously deposited) sands, was used (red line, Figure A4.9).

A4.3.3 Mudstone

Mudstone constitutes a large proportion of the strata in many Greymouth Coalfield drillholes. Mudstones of the Goldlight Fm. and Waiomo MM typically have high gamma log signatures (Section 2.3) which generally indicate high clay contents (BPB 1981). However, N. Newman (1988) demonstrated elevated gamma output from these mudstones was caused by high potassium content from illite and muscovite, and there is very little montmorillonite or other hydrated clay present. These sediments are not shales or claystones and initial porosities were moderate rather than high. Ford Fm. is also dominated by muddy siltstone and very fine sandstone (Section 2.7.2), and claystone is absent. The other occurrence of fine-grained sediments within Paparoa Group strata is carbonaceous mudstones within coal measure lithosomes.

Shale has initial porosities of >60%: Baldwin & Butler (1985) report c.78%, Sclater & Christie (1980) use 63%, and Falvey and Deighton (1982) use 70%. These values are too high for Greymouth Coalfield sediments, and in the absence of any specific data for porosity/depth relationships, the Sclater & Christie (1980) "shaley sand" values (ϕ_o = 56%, c = 0.39) were used (blue line, Figure A4.9). Organic matter within carbonaceous mudstones and siltstones may result in greater compaction during early burial than is modelled by the chosen parameters. Conversely, authigenic kaolinite, which is present in organic matter in sandstones (Boyd & Lewis 1995), could inhibit compaction.

A4.3.4 Coal

Compaction of peat to form coal has been the subject of numerous studies, and compaction ratios ranging from 1.4:1 to 30:1 have been determined (Ryer & Langer 1980, Table 1). Peat compaction occurs by organic mass loss, compaction of plant material and loss of pore space (Shearer & Moore 1996), and is the result of continuing peat accumulation ("autocompaction") and burial by younger strata. Reduction of pore space accounted for 45% of total compaction (72%) generated in artificial coalification studies of Indonesian peat (Shearer & Moore 1996), and compaction of plant material was found to be minimal when comparing peat with lignite (Moore & Hilbert 1992). Both these studies describe loss of pore space of c.50% during the transition from peat to lignite. Compaction of coal by reduction of pore space is believed to be negligible once sub-bituminous rank is reached (Stach et al. 1982, p. 40).

A selection of compaction curves illustrating rapid porosity reduction from $\phi_0 = 90\%$ is presented in Figure A4.10. The significant differences between the curves are the rate of initial porosity decline (in the first 100m) and the depth at which total porosity reaches zero. The thermal regime described above for Greymouth Coalfield would require c.1km of burial to achieve sub-bituminous rank, at which depth porosity in peat is destroyed. The appropriate compaction coefficient is therefore **c** = 5, which corresponds to a compaction ratio of 10:1 (black line, Figure A4.9).

A4.3.5 Summary of compaction input parameters

Input parameters derived above for decompaction of Greymouth Coalfield sediments are summarised in Table A4.3. Grain density values for siliciclastic sediments and coal, which are required as inputs for *BASIN.XLS*, are also included in Table A4.3.

Lithology	Initial porosity %	Compaction coefficient	Grain density kg/m^3
Conglomerate	30	0.05	2650
Sandstone (include tuffs)	32	0.24	2650
Transitional sandstone	40	0.27	2650
Siltstone	32	0.24	2650
Mudstone	50	0.39	2650
Coal	90	5.00	1200

Table A4.3 Summary of compaction input parameters for Paparoa Group sediments.

A4.4 Derivation of lithological proportion data

For the backstripping exercise, the proportion of each lithology within all units is required in order to generate a customised compaction profile for each interval. Drillholes chosen were those with complete or mostly complete Rewanui CMM thickness data, and a total of 72 drillholes were modelled.

Newman (1985) (see also Newman & Newman 1992, Figure 6) presented an analysis of textural trends within the Rewanui CMM, derived from manual summation of lithological log data (Figure A4.11). Revision of Rewanui CMM lithostratigraphy (Chapter 2), coupled with data from recent drillholes and the availability of geophysical logs and a comprehensive lithology database (Section 1.7), provided the impetus to revise and expand Newman's analysis.

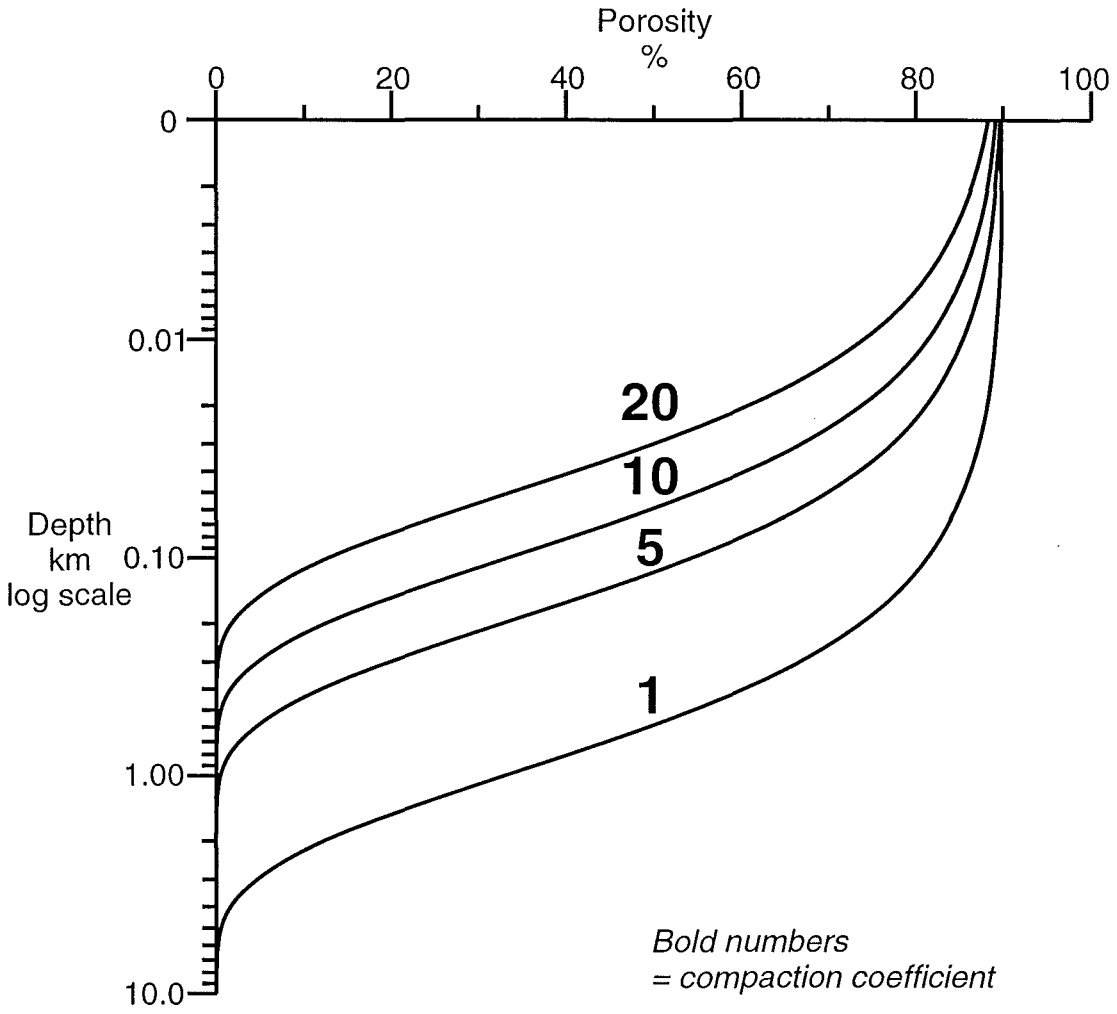

Figure A4.10 Exponential compaction curves for coal, initial porosity = 90%.
Porosity is lost over c.300m for compaction coefficient = 20,
c.600m for compaction coefficient = 10,
c.1km for compaction coefficent = 5,
and c.5km for compaction coefficient = 1.

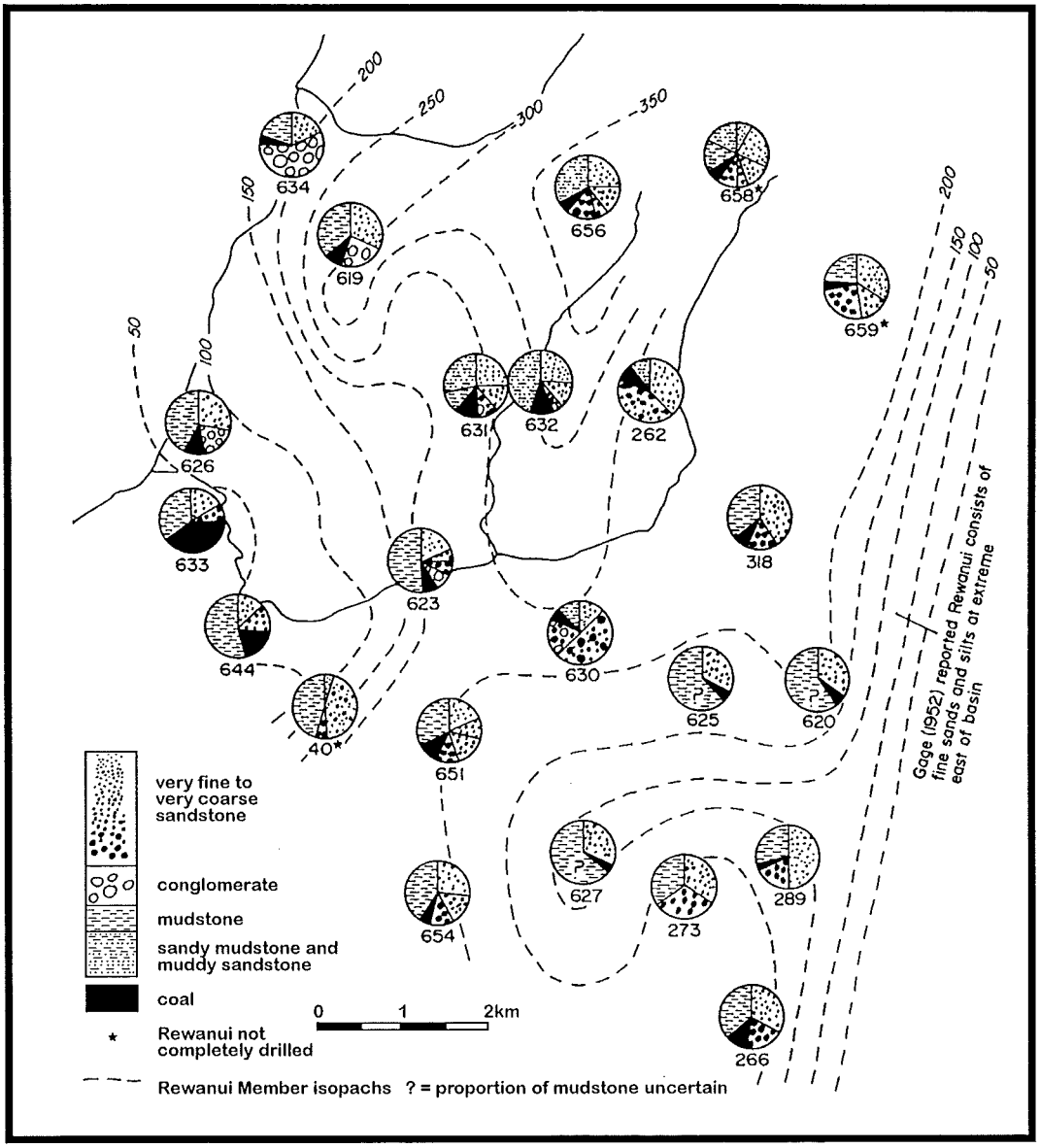

Figure A4.11 Textural variation of Rewanui CMM sediments.
From Newman & Newman (1992, Figure 6).

A4.4.1. Lithological proportions, coal measure lithosomes

For coal measure units (Rewanui CMM, 72 drillholes; Morgan CMM, 22 drillholes; Jay Fm., 22 drillholes) with many individual beds, *TECHBASE* functionalities were applied to sort and sum the occurrence of lithologies within each drillhole (Table A4.4A). Lithologies are divided into five textural classes, plus a class for miscellaneous codes which are not required (Table A4.4B). *TECHBASE* lithology data are entered in two fields (one for lithology, one for grain size), thus only major lithological groupings can be extracted in this manner. Textural trends within the sand-size fraction, as illustrated in Figure A4.11, could not be derived by this routine.

	Step	action required
1	enter correct lithological and depth data	8122 records
2	assign integer values to lithology codes	use *MEASURED FIELD* to assign integer values 0–5
3	determine thickness of all beds	define *CALCULATED FIELD*
4	select required depth interval	set *FILTERS* for depth range
5	select lithologies 1 – 5	set *FILTER* for lithology integer
6	report out total thickness for each lithology	use *REPORT* total function
7	enter data into table, calculate %	use *CALCULATED FIELD*
8	determine porosity, compaction, density	use *CALCULATED FIELD*, weighted average
9	report values	use *REPORT*

Table A4.4A Procedure for extracting lithological proportion data from *TECHBASE* lithology database. Note that steps 4–6 are performed with an automated *TECHNICN* routine which only requires stratigraphic range to be entered.

Integer	class	Lithology codes
0	not required	AR, BA, CV, DI, GL, GO, GV, GW, IG, LM, NL, NS, PU, QU, SK, SL, SO, TU, UN, XX
1	coal	C1, C2, C3, C4, C5, C6, C7, CO, CQ, CX
2	mudstone	CC, CH, CL, CM, CW, CY, HC, MS, MU, SH
3	siltstone	CT, ST, ZS
4	sandstone	CS, CU, SA, SC, SN, SS
5	conglomerate	BR, CG, GC, GT, PC

Table A4.4B Lithology codes and classes assigned by *TECHBASE MEASURED FIELD*. A measured field reads the two letter lithology code for each record and assigns a corresponding integer integer value stored in a lookup text file. Two-letter codes are explained in Table A4.4C.

Lithology code	Lithology	Lithology code	Lithology	Lithology code	Lithology
AR	argillite	C2	high ash coal	NL	no log
BA	basement	C3	coal-bright	NS	no sample
BR	breccia	C4	coal-bright, dull bands	PC	pebble conglomerate
CC	carb claystone	C5	coal-bright, dull bands	PU	pug
CG	conglomerate	C6	coal-dull	QU	quartz
CH	highly carb mudstone	C7	coal-heat altered	SA	sand
CL	clay	DI	diorite	SC	sandstone to carb mst
CM	carb mudstone	GC	granule conglomerate	SH	shale
CO	coal	GL	glauconite	SK	silcrete
CQ	high ash coal	GO	gouge	SL	slate
CS	carb sandstone	GT	grit	SN	sandstone
CT	high ash coal	GV	gravel	SO	soil
CU	carb mudstone to sst	GW	greywacke	SS	sandstone
CV	colluvium	HC	coaly mudstone	ST	siltstone
CW	sl carb mudstone	IG	igneous	TU	tuff
CX	dirty coal	LM	limestone	UN	unknown
CY	claystone	MS	mudstone	XX	no sample
C1	clean coal	MU	mud	ZS	siltstone

Table A4.4C Two-letter lithology codes and corresponding lithologies, Greymouth Coalfield drillhole database (Ian R. Brown Associates Ltd. 1992).

For those drillholes where complete lithology data for each coal measure unit was absent, estimates of lithological proportions were made from nearby complete drillholes, or in some instances from interpreted cross-sections. Where total unit thicknesses are unknown, estimates were made from isopach models presented in Chapter 3. All unit thicknesses are rounded to the nearest 10m (0.01km), to match the input requirements of *BASIN.XLS*. Proportions of each textural class for all coal measure intervals, and full details of input estimation, are given in Appendix 11.2.

In order to verify estimated lithological proportions within Rewanui CMM, the ratio of coarse to fine sediment (i.e. % sandstone plus % conglomerate vs. % coal plus % mudstone plus % siltstone) was determined and modelled using the minimum curvature modelling (see Appendix 3.1 for explanation). Lithological proportions for specific drillholes were assessed in relation to local trends, and the preliminary model (Figure A4.12) indicated some estimates of lithological proportions were anomalous.

Coarse strata were over-represented in DH446, and lithological proportions within the unknown section above collar height (Appendix 2) were re-estimated to be dominantly fine strata, thereby reducing the coarse:fine ratio from 4.88 to 1.92. Only 63.0m of Rewanui CMM strata were drilled in DH668, and lithological proportions were estimated from the more complete section obtained in DH659. DH704 is faulted (Appendix 2), and addition of 15m of mostly coarse strata increased the coarse:fine ratio

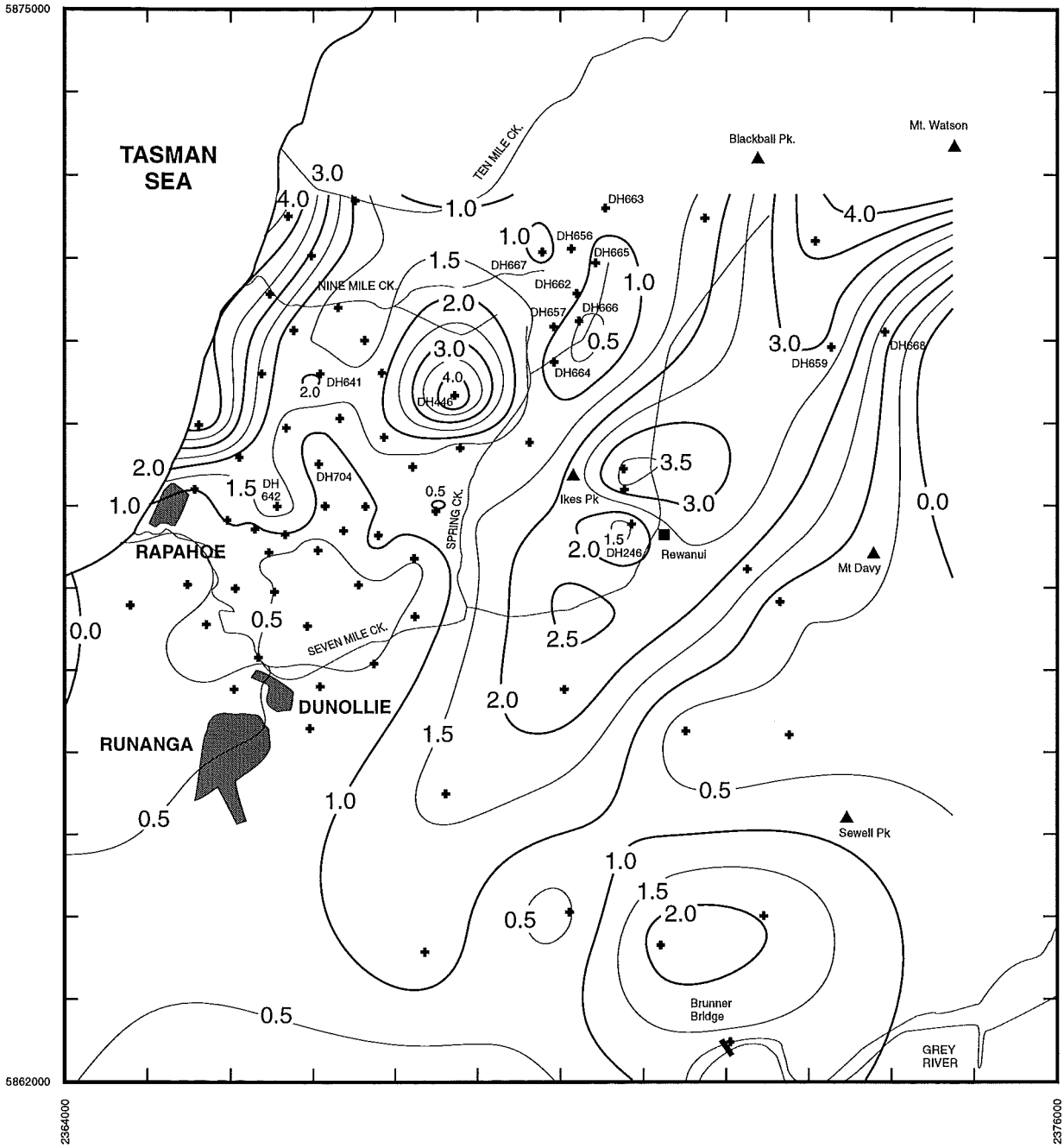

Figure A4.12 Initial (minimum curvature) model of coarse:fine ratio, Rewanui CMM sediments.
Isoline interval = 0.5.
Numbered drillholes are discussed in text.

from 0.76 to 0.91. Faulting may also account for the slightly high coarse:fine ratio present in DH641 (Appendix 2). Coarse:fine ratios of DH662–667 in the Doherty Block are lower than indicated by the two nearby drillholes with complete Rewanui CMM sections, DH656 and DH657 (Figure A4.12). DH662–667 did not fully intersect lower Rewanui CMM coarse clastic strata, resulting in over-estimation of the proportion of fine strata. Compaction parameters for incomplete Rewanui CMM sections were therefore estimated from nearby complete sections. Other drillholes with apparent textural anomalies include DH642 (coarse:fine ratio too high), and DH246 (coarse:fine ratio too low). These two drillholes contain complete and undisrupted Rewanui CMM sections, and anomalies probably reflect localised variations in paleogeography.

The final textural model for Rewanui CMM is presented in Figure A4.13. The textural model for Morgan CMM, which is based on drillholes in which Morgan CMM sections are generally complete, is indicated in Figure A4.14. Jay Fm. textures were mostly estimated from a small number of drillholes which penetrated the unit, and formation thickness was estimated for 18 of the 22 modelled drillholes. Given the limited stratigraphic or textural data, no map of textural variation for Jay Fm. was constructed.

A4.4.2 Transitional and lacustrine lithosomes

Lithological proportions for mudstone-dominated units were estimated from geophysical logs (where available), and CRS and GCOL lithological logs. Distinction was made between mudstone, siltstone/sandstone and tuffaceous sandstone/volcanic conglomerate, particularly within transitional lithosomes. Where necessary, unit thicknesses were obtained from isopach models presented in Chapter 3. Data for transitional and lacustrine members was entered as separate units in order to retain sensitivity to facies variation within Ford Fm. and Goldlight Fm.

A4.5 Estimation of cover parameters

Cover comprises all strata deposited above Goldlight Fm. prior to the commencement of basin inversion in the Miocene (Nathan 1978; Nathan et al. 1986; Kamp et al. 1992). Units include Dunollie Fm. (uppermost unit of the Paparoa Group), Brunner CM, Island Sandstone, Kaiata Fm., and Nile Group. Cover thickness for each drillhole was calculated as burial depth of the Goldlight / Rewanui contact (Section A4.2.4), less the thickness of any Goldlight Fm. strata present.

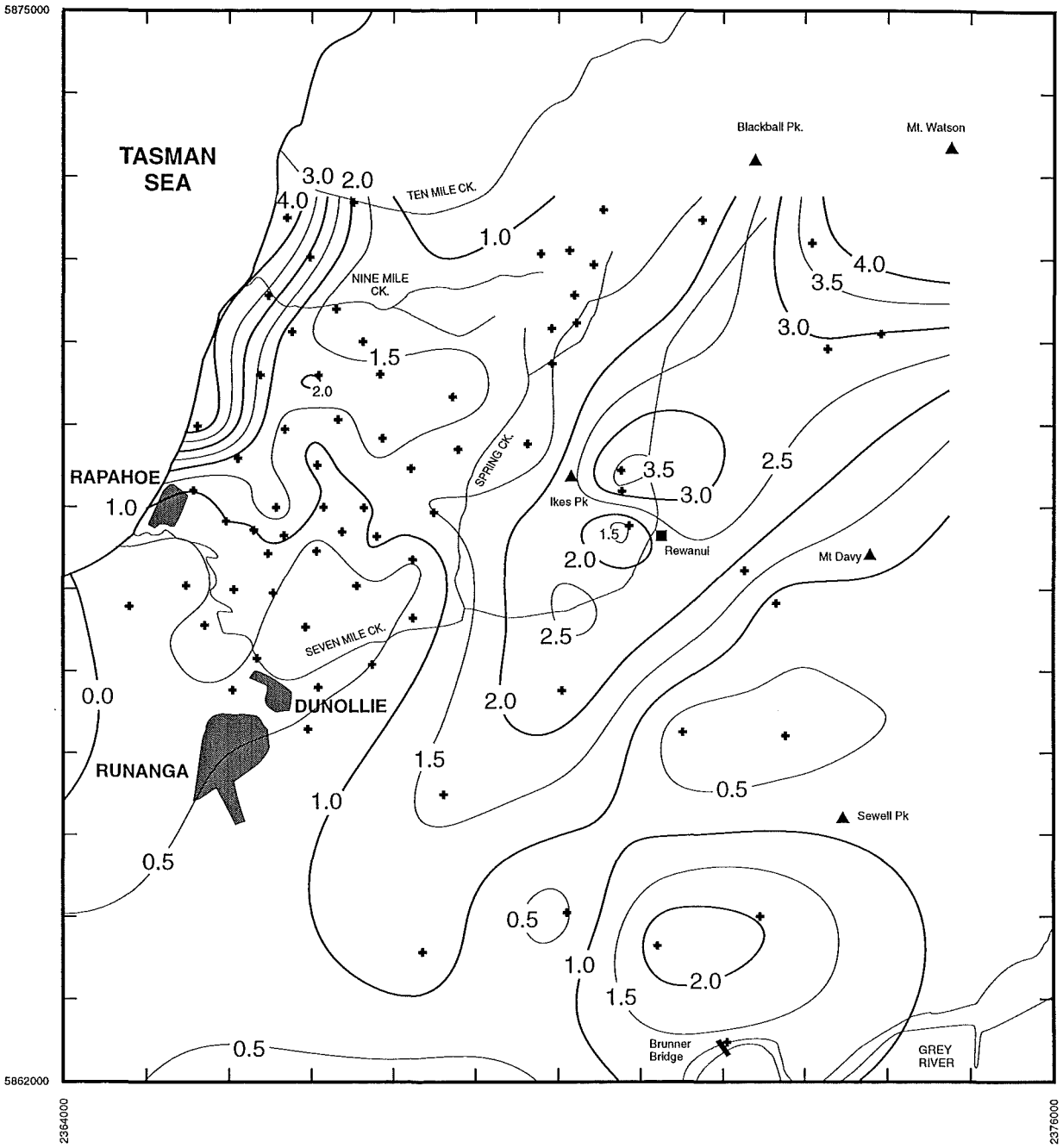

Figure A4.13 Final (minimum curvature) model of ratio of coarse to fine sediments, Rewanui CMM. Isoline interval = 0.5.

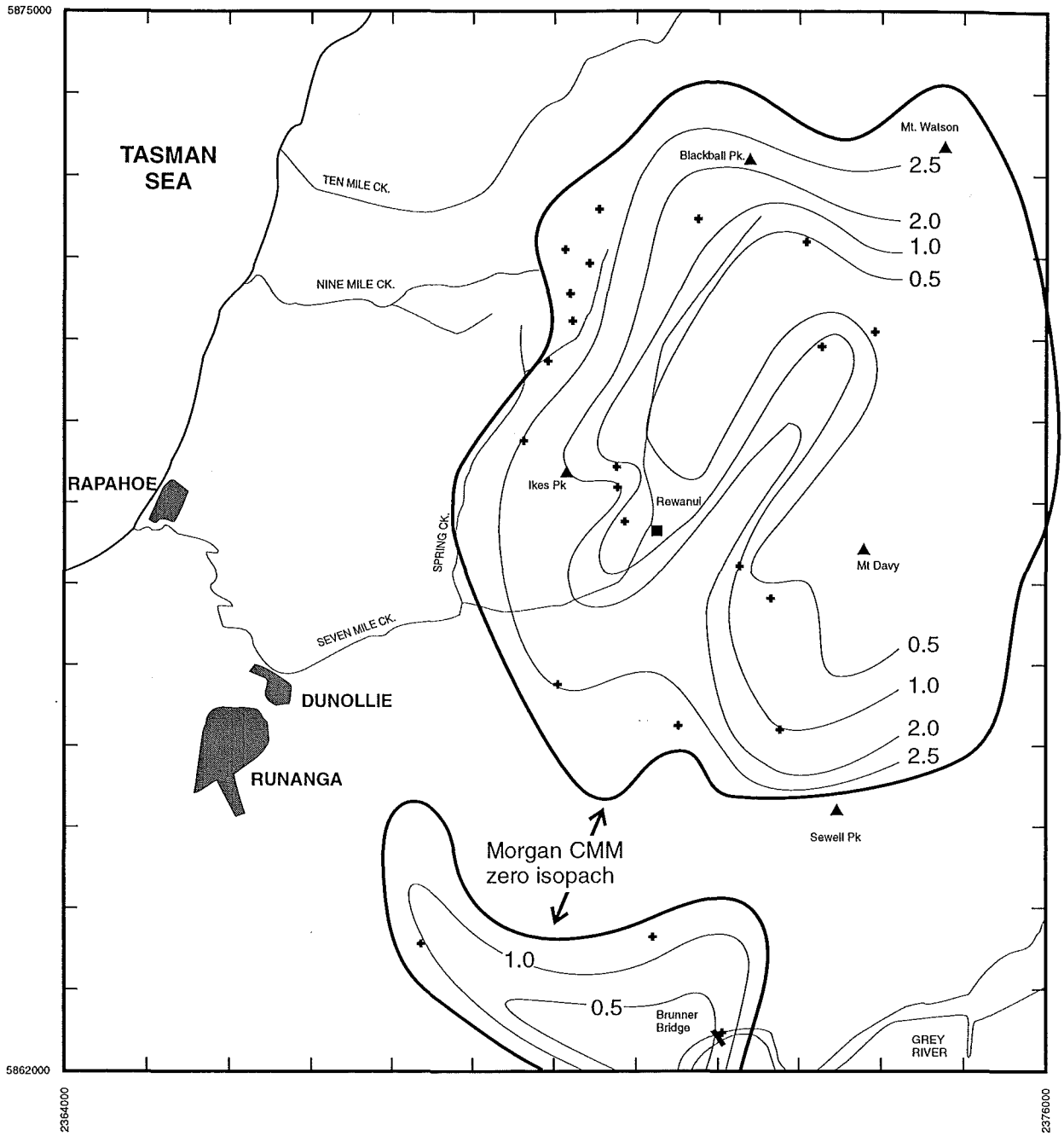

Figure A4.14 Model of ratio of coarse to fine sediments, Morgan CMM.
Zero isopach line (from Figure 3.4) shown for reference.
No data are available east of Mt. Davy.
Isoline interval = 0.5.

Grain density and porosity/depth relationships for Kaiata Fm. and Nile Group strata were taken or estimated from Anderson (1981), and are summarised in Table A4.5. An exponential compaction curve was modelled to match the porosity/density relationship for Kaiata Fm. presented by Anderson (1981, Figure 4), which was extrapolated to give an initial porosity of 50%. Porosity in Nile Group strata was destroyed by cementation during the first kilometre of burial, thereby limiting mechanical compaction, and initial porosity of Nile Group sediments was assumed to be equal to that of Kaiata Fm.

Dunollie Fm., Brunner Fm. and Island Sandstone are dominantly sandy units with minor coal and conglomerate (Gage, 1952; Nathan 1978; Bowman et al. 1984). The three units, generalised to comprise 95% sandstone and 5% coal, were combined for inclusion in the cover sequence (Table A4.5), and compaction parameters used values given above for Paparoa Group (Table A4.3). Formations or Groups within the cover sequence were assumed to remain at the same relative proportion throughout the coalfield. Small-scale thickness variations within Dunollie Fm. or Brunner Fm. (e.g. Bowman et al. 1984, see Figure A1.3G) was not incorporated within this model. Proportions of the units were estimated from Nathan (1978), and cover is dominated by Kaiata Fm. strata (Table A4.5). Final values for the cover strata are the weighted average of the three components.

Unit	Lithology	proportion of total cover %	compaction coefficient	initial porosity %	density kg/m^3
Nile Group	marl and limestone	20	1.0	50	2670
Kaiata Fm.	calcareous mudstone	70	0.5	50	2670
Island, Brunner, Dunollie	sandstone plus 5% coal	10	0.48	35	2570
Total cover	all above	100	0.60	0.48	2660

Table A4.5 Summary of decompaction parameters for units comprising cover strata.

A4.6 Estimation of age

The only reliable chronostratigraphic information for Paparoa Group comes from the Cretaceous–Tertiary Boundary (= 65Ma) which lies close to the Goldlight / Rewanui contact (Section 5.5). No age control from palynomorphs is possible in the Late Cretaceous portion of Paparoa Group because of lack of evolutionary floral change throughout the corresponding pollen zone (Raine 1984). Morgan Volcanics (Figure 1.2) correlate to basalts in Paparoa Group strata at Pike River Coalfield, Kowhiterangi and the Arahura–1 exploration well, which are dated at 68–71Ma (Sewell et al. 1988; Ferguson 1993; McDougall 1993). Lack of age control within Paparoa Group does not present a problem, as the present objective is to determine pre-burial unit thickness rather than to construct basin history curves.

A4.7 Calculation of tectonic subsidence

Previous studies of the tectonic setting of Greymouth Coalfield and the West Coast area demonstrated an extensional tectonic setting during the Late Cretaceous and early Tertiary (e.g. Bowman et al. 1984; Nathan et al. 1986, see Section 8.2 for full discussion). Vertical movements of the lithosphere at divergent plate boundaries involve both uplift and subsidence, and are the result of loading or buoyancy forces within the mantle, crust or sedimentary cover (Table A4.6).

type	effect	load
tectonic	+ve	thinning of crust by pure shear and replacement by denser mantle
tectonic	-ve	thinning of upper crust by faulting
tectonic	-ve	syn-rift increase in geothermal gradient
tectonic	+ve	post-rift cooling of lithosphere
isostatic	+ve	loading by water on crust, including eustatic sea level changes
isostatic	+ve	syn-rift and post-rift sedimentation
isostatic	-ve	syn-rift and post-rift erosion

Table A4.6 Vertical loads on the lithosphere during a rifting event.
Positive (+ve) loads are sinking, negative (-ve) loads are buoyancy.
Modified from Kusznir & Ziegler (1992).

Two principal components of subsidence are recognised: isostatic (Airy) subsidence, due to the effects of adding sediment and water loads to the crust, and tectonic subsidence, which results from plate tectonic forces (Table A4.6). The proportion of

subsidence attributable to isostatic effects is a function of the relative density of the sediment pile compared to the water it replaces and the mantle displaced beneath (Allen & Allen 1990, p. 264).

Backstripping procedures determine subsidence from decompacted stratigraphic columns, and the calculation of tectonic subsidence is described by Steckler & Watts (1978) and Bond & Kominz (1984) with the following equation:

$$\mathbf{Y} = \Phi\mathbf{S}^*(\rho_m - \rho_s) / (\rho_m - \rho_w) + \mathbf{Wd} - \Delta\mathbf{SL}(\rho_w / \rho_m - \rho_w) \qquad \textit{Equation A4.4}$$

where $\mathbf{Y}$ = tectonic subsidence, Φ is a basement response factor, $\mathbf{S}^*$ = decompacted sedimentary section, ρ_s = mean bulk density of that section, ρ_m = mantle density, ρ_w = water density, $\mathbf{Wd}$ = water depth and $\Delta\mathbf{SL}$ = sea level relative to present day.

The *BASIN.XLS* spreadsheet (Larrieu 1995) uses a simplified form of Equation A4.4:

$$\mathbf{Y} = \mathbf{S}^*(\rho_m - \rho_s) / (\rho_m - \rho_w) \qquad \textit{Equation A4.5}$$

to determine the proportion of Airy subsidence, with no account being made for the isostatic effects of water loading. Values for ρ_m and ρ_w may be entered during the setup procedure, and ρ_s is determined from the calculated decompacted sedimentary sections.

Paparoa Group comprises dominantly terrestrial strata deposited directly on basement (Chapter 2), and sediment is not replacing water as would occur during marine sedimentation. Backstripping of subaerially deposited sediments therefore requires accounting for both solid-phase (i.e. sediment grains) and pore-fluid masses as layers of sediment are removed from the stratigraphic column, because the space occupied by pore fluid is replaced by air (Shaw & Hay 1989). If the crust was not loaded by water prior to deposition, an appropriate equation for tectonic subsidence would be:

$$\mathbf{Y} = \Phi\ \mathbf{S}^*(\rho_m - \rho_s) / \rho_m \qquad \textit{Equation A4.6}$$

When Equation A4.6 is applied, the Airy component of subsidence increases, and correspondingly the tectonic component decreases. Tectonic subsidence values calculated for Paparoa Group strata using Equation A4.5, which is appropriate for marine strata will therefore be overestimated.

The most significant variable in determining the accuracy of tectonic subsidence estimates is the basement response factor (Φ). If crustal rigidity is assumed to be zero, all strata are in (Airy) isostatic equilibrium (i.e. locally compensated) with the crust and mantle, and Φ is equal to one. If the crust has a finite flexural rigidity and supports sediment loading by long-wavelength bending (Allen & Allen 1990, p. 272–274), the system is not behaving in an Airy manner, Φ will be <1 and the proportion of subsidence attributed to tectonic effects will increase.

The pure shear model of extension (McKenzie 1978) assumes Airy isostasy. Numerous backstripping studies of large-scale (>100km) continental margin sedimentary systems (e.g. Steckler & Watts 1978; Bond & Kominz 1984; Sclater & Christie 1980) follow this assumption, and tectonic subsidence is modelled as being much less than total subsidence. However, alternative models for extensional dynamics (e.g. Wernicke 1981; Lister et al. 1986; Kusznir et al. 1987; Watts & Torne 1992; Kusznir & Ziegler 1992) require the crust to retain finite rigidity.

Flexural subsidence is believed to approximate Airy subsidence for sediment loads of >100–300km radius (e.g Gallagher & Lambeck 1992; Artemjev et al. 1994). In contrast, for smaller sedimentary loads such as may be present in tectonically active areas, the lithosphere remains sufficiently strong to support the load and the system will not be in isostatic equilibrium (e.g. Allen & Allen 1990, p. 273; Karner et al. 1992; Artemjev et al. 1994). Paparoa Group strata were deposited in a small basin (radius < 10km), and the above discussion suggests that local (Airy) isostatic compensation would not have been a significant factor during deposition.

Tectonic subsidence during Paparoa Group deposition was therefore estimated directly from decompacted section thickness (reported in Appendix 12). Subsidence during deposition of any unit was assigned to either tectonic movement or to compaction of underlying strata (where present). No attempt was made to estimate tectonic or isostatic subsidence during deposition of the cover sequence, though the compactional effects of cover upon Paparoa Group were removed during the backstripping exercise.

Appendix 5. Palynological sampling and zonation

This Appendix presents all necessary material on the collection of palynological data, and on the derivation of the palynological zonation scheme with which ages are assigned to samples collected in the present study. The appendix concludes with a discussion of facies and floral control on the occurrence of age-diagnostic taxa.

A5.1 Sampling and methods

A5.1.1 Material

The primary source of samples was core from drillholes of the Coal Resources Survey (CRS) program (Bowman et al. 1984). Criteria for selecting drillholes also included completeness of core through the desired interval, presence of suitable lithologies, relatively low (<20°) dips, and absence of severe fracturing (where possible). Cores were initially sampled at c.10m intervals, with additional samples added to improve stratigraphic resolution. Some material (e.g. DH697-711, miscellaneous coals) was obtained from UoC collections, and a small number of outcrop samples were collected. Four coal samples, from Tiller, Snowline and Kiwi mines, and the Goldlight seam exposed near the Moody Ck. Mine, were analysed to increase available reference data for coal palynofloras. A total of 62 new samples from 12 drillholes plus four additional coal samples have been analysed, and existing material has been revised. Details of sample locations and lithologies are presented in Appendix 13.

A5.1.2 Processing

Palynological processing followed conventional techniques, and information for each sample is summarised in Appendix 13. Sediment samples were crushed to <5mm then macerated in cold HF for 3-6 days, followed by concentrated HCl washing to remove reaction products. Moderate oxidation was found to be necessary to remove coaly material, and coarse organic particles were removed by passing material through a 0.1mm sieve. Unwanted fine material was removed by light oxidation in a 10% solution of domestic bleach (sodium hypochlorite) and "short centrifuging" (whereby samples were accelerated from 0–2000rpm over 30sec.). Both these steps were repeated as necessary (Appendix 13) until adequate results were obtained.

Coals were ground and sieved to <1.5ϕ, and processed by the wet Schulze method, with 10-15mins oxidation being necessary. Further processing details are given in Ward et al. (1995). Heavy minerals were removed by ZnBr separation (S.G. 2.0), and all material was mounted in glycerine jelly and sealed with nail varnish. All samples were allocated UCP (University of Canterbury Palynology) numbers (Appendix 13), and samples, residues and slides are housed in the Department of Geological Sciences, University of Canterbury.

A5.1.3 Data collection

Slides were examined using Zeiss Photomicroscope III and Zeiss KM microscopes at 200x and 312x respectively. Higher magnifications were used where necessary to confirm identifications. Where possible, 250 grains were recorded for each sample. This was generally achieved from one slide, though additional slides were prepared if required. Where a count was completed from a portion of a slide, an additional 10 tracks were scanned for the presence of key taxa. Eight additional samples yielded poorly preserved, sparse assemblages, which were unable to be counted, but these were still scanned for the presence of key taxa. Count or scan data for 66 samples are presented in Appendix 14.

Pollen and spore recovery was generally good to excellent from coal samples, but poor to moderate from clastic samples due to the presence of dark woody material (?semifusinite) which proved difficult to remove. Organic material was sparse or absent in some fine and very fine sandstone samples. Palynomorph preservation was similarly variable, though adequate for reliable identification of taxa.

A5.2 The Cretaceous–Tertiary Boundary in New Zealand

Sedimentary sequences spanning the Cretaceous-Tertiary Boundary (KTB) are preserved in the New Zealand region as a consequence of mid-Cretaceous–Paleogene sea-floor spreading, continental extension and thermal subsidence. The KTB is located at the boundary between the local Haumurian (Mh, Mata Series) and Teurian (Dt, Dannevirke Series) Stages (Figure A5.1), (Hornibrook 1962). Correlation with the international Maastrichtian–Danian boundary is based on dinoflagellates, foraminifera, and nanofossils (Wilson 1978, 1994; Edwards et al. 1988; Hornibrook et al. 1989), and the boundary is presently dated as 65.0 ± 0.1Ma (Gradstein et al. 1994).

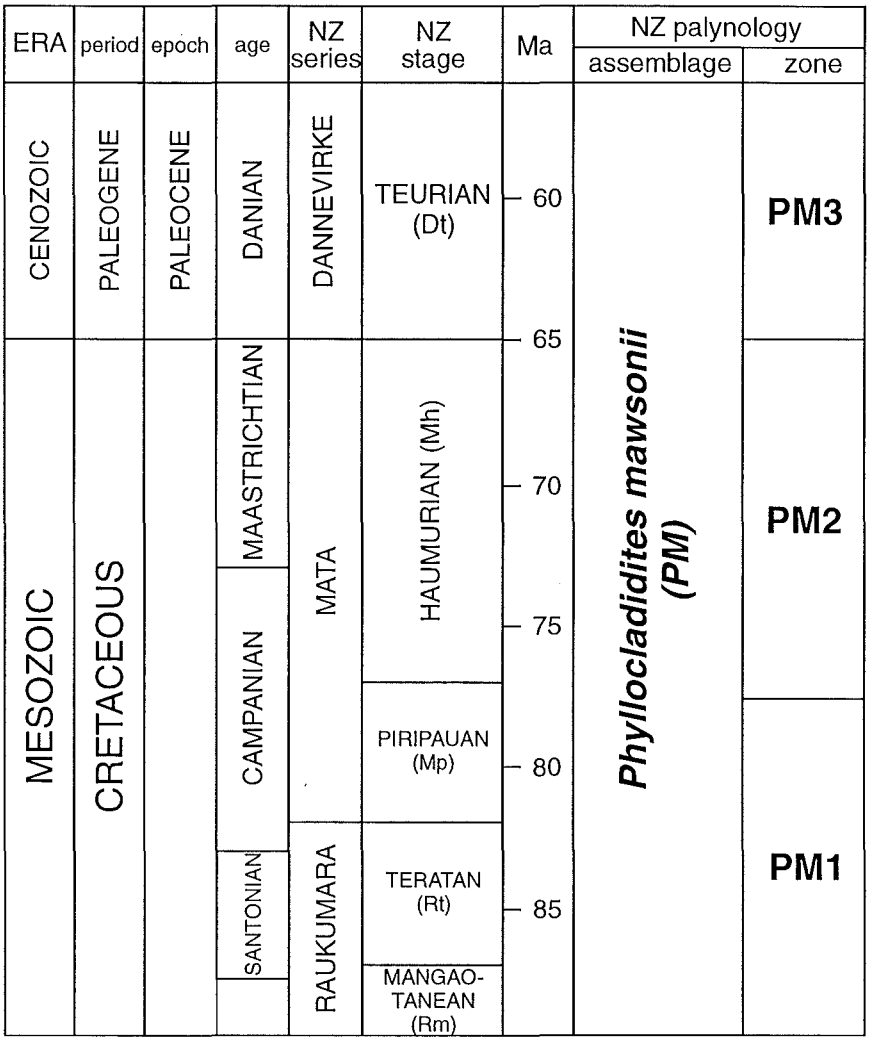

Figure A5.1 Comparison of international and New Zealand biostratigraphic nomenclature and New Zealand palynological zonation. After Raine (1984). Note: more recent studies (e.g. Edwards et al. 1988, Gradstein et al. 1994) cite different chronostratigraphic correlations. New Zealand Stages are presently under revision (Crampton et al. 1995). The base Haumurian is now tentatively placed at c.81Ma, and the base Piripauan at c.85Ma. Palynological zonation is yet to be revised accordingly, and the existing scheme is retained in this study.

Microfossil biostratigraphy has identified numerous KTB sections within marine strata in the northeastern South Island and eastern North Island. Recognition of an iridium anomaly at Woodside Creek in Marlborough (Alvarez et al. 1980; Brooks et al. 1984) established international interest in New Zealand's KTB sites, and geochemical research has identified iridium and other elemental anomalies at 7 further localities (Brooks et al. 1984, 1986a, 1986b; Strong et al. 1987). Terrestrial KTB sections are known from the Paparoa, Kaitangata and Pakawau Basins (Raine 1994a) and the Tara–1 exploration hole in the Great South Basin (Raine et al. 1993) (see also Appendix 7.5.4).

The terrestrial Cretaceous-Tertiary boundary in New Zealand is recognised biostratigraphically by change in spore and pollen assemblages. The KTB is located at the boundary between pollen Zones PM2 and PM3 (Figure A5.1) which are subdivisions of the Mangaotanean–Teurian *Phyllocladidites mawsonii* assemblage of Raine (1984). Validity of the Cretaceous miospore zonation is confirmed by correlation with marine dinoflagellate floras and foraminifera (e.g. Raine & Wilson 1988; Raine 1990a; Raine et al. 1993, 1994), by comparison with correlative Australian sequences (Helby et al. 1987), and radiometric dating (e.g. Raine 1981; Adams & Raine 1988; Edwards et al. 1988).

A5.3 Establishment of the Cretaceous–Tertiary Boundary in Greymouth Coalfield

Preliminary palynological and palynostratigraphic investigations of the Paparoa Coal Measures in Greymouth Coalfield were reported by Couper (1953, 1960), who assigned a small number of samples from various members to the Raukumara Series (Figure A5.1). Raine (1981) demonstrated the presence of a boundary between two distinct biostratigraphic zones in DH621 and DH622 (Figure A5.2), which was tentatively correlated with the KTB. Subsequently, Raine (1984) established a KTB (= PM2/PM3) boundary reference section in the upper Rewanui CMM and lower Goldlight Fm. sequence between Moody Ck. Mine and Dunollie (Figure 5.2). KTB intervals have also been recognised previously in DH631 and 632 (e.g. Raine 1990b).

Other research on the Greymouth Coalfield KTB has concentrated on contrasting megafloral and microfloral events with those from Northern Hemisphere boundary sequences (Johnson & Raine 1991; Johnson 1992a,b; Johnson & Greenwood 1993), and improving the definition of the KTB in sections at Moody Ck., Compressor Ck. and

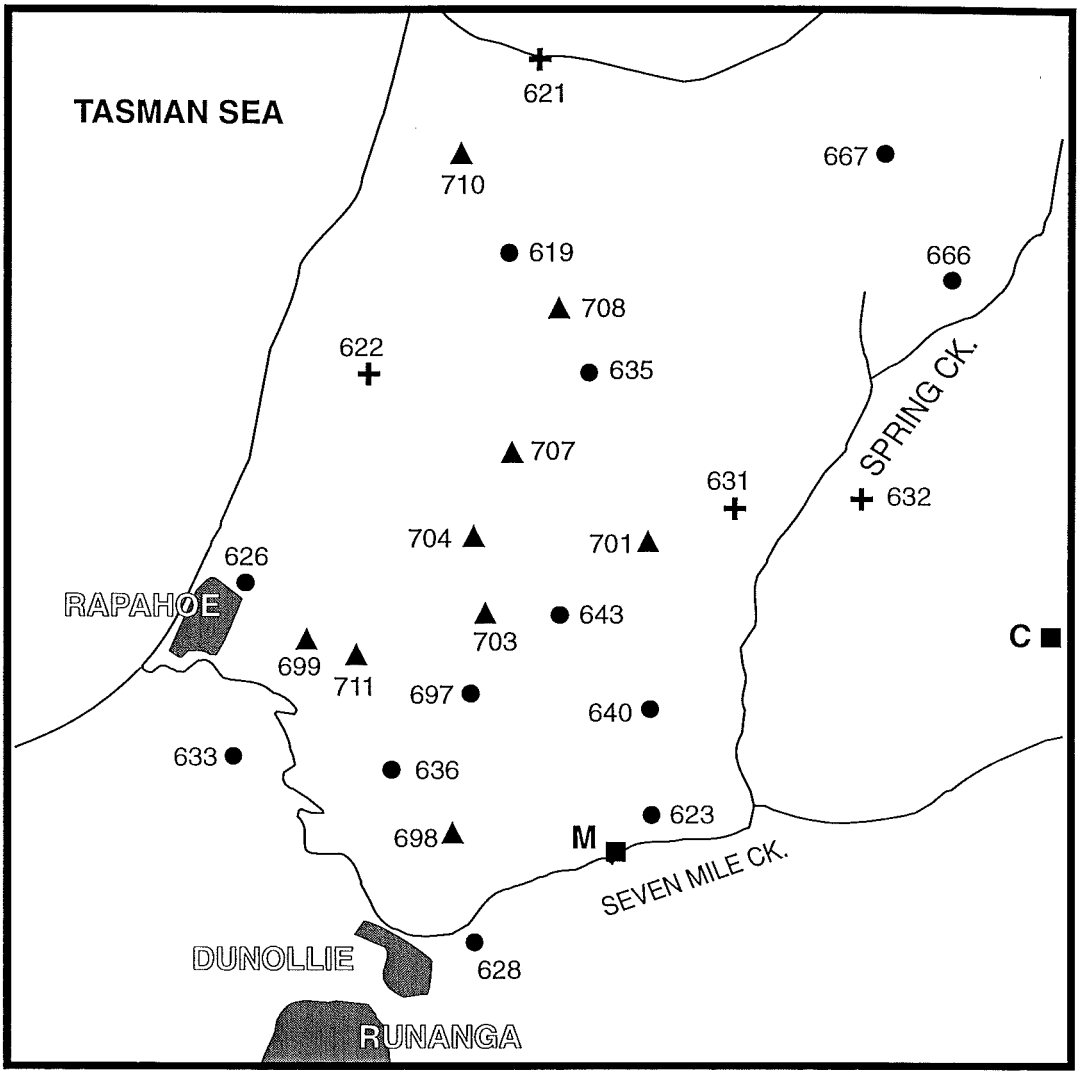

Figure A5.2 Location of drillholes and outcrop investigated for KTB reconaissance study, Rapahoe Sector.

- ● Drillholes investigated in this study
- \+ Drillholes investigated by previous workers
- ▲ Drillholes sampled by D.I. MacKinnon, limited results
- ■ Outcrop sections, M = Moody Ck., C = Compressor Ck.

DH632 (Raine 1994a). Preliminary attempts at paleomagnetic analysis have proved unsuccessful, and analyses for iridium anomalies are still awaited (Raine 1994a). Brooks et al. (1986a) investigated chemical anomalies at a suspected KTB site within the Goldlight Fm. near Rewanui. The site was selected on the basis of (unpublished) palynology, which indicated the KTB lay within a 4m interval near the middle Goldlight Fm. However, palynology within the 4m interval was inconclusive, and subsequent results (e.g. Raine 1990b) indicate the placement of the KTB was erroneous.

A5.4 Palynological zonation and age determination

A5.4.1 Regional criteria for pollen zone determination

Couper (1960) provided the first palynological identification of the Haumurian/Teurian boundary at the marine Middle Waipara section (location shown on Figure A8.3), on the basis of the presence or absence of 38 pollen and spore taxa. Raine (1981) later reported the ranges of 10 zonally useful taxa from DH621 & 622 in Greymouth Coalfield. Only one of Raine's taxa (*Tricolpites lilliei*), was included in Couper's listing, because many of those taxa considered by Couper (1960) to be Haumurian were not useful due to rarity or uncertain taxonomic status (Raine 1981). Also, new biostratigraphically useful taxa had been discovered. Some of Couper's observations were subsequently confirmed with development of a regional palynological zonation scheme for terrestrial deposits (Raine 1984, 1990b), though age ranges of some of Couper's taxa were extended.

Floral change across the KTB is expressed regionally by the last appearance of 28 taxa, the first appearance of 38 taxa, and changes in the abundance of other taxa (Raine 1984, 1990b). However, some 48 taxa are reported to have ranges which span the PM2/PM3 boundary, thus microfloral change at the KTB is subdued in comparison to other New Zealand miospore zonal boundaries (e.g. mid-Cretaceous and Paleocene/Eocene: Raine 1990b), and Northern Hemisphere KTB sections (Johnson and Raine 1991).

The principal bioevents which delineate the KTB (Raine 1984, Fig. 2 and p. 22) are the last appearance of the angiosperm *Tricolpites lilliei* Couper, which is the index taxon for Zone PM2, and the first appearance of the small angiosperm *Tricolpites secarius* McIntyre. The occurrence of *T. secarius* and *T. lilliei* is reported to be mutually exclusive, except from within a short section of strata immediately above the KTB, at the Moody Ck.

/ Dunollie KTB reference section (Raine 1984) and at Middle Waipara (Helby et al. 1987). Short-term survival of *T. lilliei* across the KTB, or reworking, were invoked to explain the coincidence of the two taxa (Raine 1994a).

(Taxonomic note: *Tricolpites lilliei* was originally described by Couper (1953), and was transferred to the form-genus *Tricolporites* by Stover and Evans (1973) to incorporate forms with tricolporate apertures. Farabee & Canright (1986) transferred North American specimens of *"lilliei"* to *Tubulifloridites*, which includes tricolpate, echinate pollen with conspicuous apertures. Dettmann & Jarzen (1988) concluded that *Tricolporites* was an inappropriate form-genus, and *Tubulifloridites* was used with reservation. Mildenhall (1994, p. 89) rejected *Tubulifloridites,* citing morphological dissimilarity between type material of that genus and *T. lilliei,* and reverted to the original form-genus *Tricolpites.*)

A5.4.2 Palynological zonation, Greymouth Coalfield: previous studies

Occurrence data for key palynomorphs, are available for previous studies of four drillholes in Greymouth Coalfield, namely DH621 & 622, and DH631 & 632 (Table A5.1). No detailed palynological data is available for samples from the Moody Ck. KTB reference section proposed by Raine (1984).

DH621 & 622: Key index taxa from DH621 and 622 (Raine 1981) are *T. lilliei* (PM2) and *T. secarius* (PM3), which have mutually exclusive occurrences in these drillholes. Other biostratigraphically useful taxa reported by Raine (1981) include *Beaupreaidites* n.sp., *Quadraplanus brossus*, and *Triporoletes reticulatus* (PM2), and *Matonisporites ornamentalis*, *Peromonolites densus* and *Tricolpites phillipsii* (PM3).

DH631 & 632: 25 samples spanning the PM2-3 boundary in DH631 & 632 were analysed by Raine (pers. comm., 1988 & 1989; 1990b), and Warnes (pers. comm. 1992). Warnes duplicated six of Raine's samples, and prepared new material. One additional sample (DH631, 130.0m, IGNS lab no. L12372/1) was scanned for key taxa, but not counted because of poor preservation. Occurrences of stratigraphically significant taxa in these samples are summarised in Table A5.1. Taxa included are those mentioned specifically by Raine and Warnes, and three forms (*Trilites ohaiensis*, *Trilites morleyi*, *Triorites minisculus*) which have potentially useful stratigraphic ranges, as reported by Couper (1960) and Raine (1984).

Depth	lithology	source	sample no.	taxa	TO	BE	DM	GR	NK	QB	TL	TMo	TR	PD	TM	MO	NW	PcT	TS	TP	MH	MY	RM	Tm
				range	PM1-PM2	PM2	PM2	PM2	PM2	PM2	PM2	PM2	PM2	PM2-MH2	PM2-NM	PM3	PM3	PM3-MH1	PM3-MH2	PM3-MH2	PM3-NM	PM3-NM	PM3-NM	PM3-NM
631				zone																				
100.2	mudstone	**R**	L13569	PM3										*	3	*								
120.0	mudstone	**R**	L13571	PM3										*	0.5	*				*	*			
130.0	mudstone	**SW**	L12372	PM3											*						*		*	
140.0	mudstone	**R**	L13575	PM3										*	9.5	*			*	*				
148.0	mudstone	**R**	L13576	PM3										*	7.5	*		*		*				
148.6	carb mst	**W**	UCP 1218	PM3		*									26		*		*		*	*	*	
155.4	carb mst	**R**	L13577	PM3						*				*	7	*	*		*		*			*
155.4	carb mst	**W**	UCP 1219	PM3											31				*	*			*	
164.4	muddy sst	**R**	L13578	PM2				*			*			*	1.5									
164.4	muddy sst	**W**	UCP 1220	PM3											16		*		*					
175.5	carb mst	**R**	L13580	PM2										*	2								*	
179.4	muddy sst	**W**	UCP 1233	PM2					*		*	*			1									
181.1	coal	**W**	UCP 1246	PM2	*						*	*			*									
188.0	carb mst	**R**	L13583	PM2		*			*		*			*										
188.0	carb mst	**W**	UCP 1221	PM2		*			*		*				7				*					*
632																								
240.0	mudstone	**R**	L13587	PM3				*	*										*					
250.0	mudstone	**R**	L13588	PM3					*				*	*	*	*			*					
250.0	mudstone	**W**	UCP 1222	PM3											26				*			*	*	
251.0	carb mst	**W**	UCP 1247	PM3											12				*		*	*		
258.2	muddy sst	**W**	UCP 1250	PM3											19				*			*	*	
261.0	muddy sst	**W**	UCP 1251	PM3											2							*	*	*
262.3	muddy sst	**R**	L13589	PM2			*	*	*					*									*	*
262.3	muddy sst	**W**	UCP 1223	PM2			*								0.5									*
270.3	carb mst	**R**	L13590	PM2		*			*		*													
270.3	carb mst	**W**	UCP 1224	PM2		*			*		*													

Table A5.1 Occurrence of stratigraphically significant taxa in DH631 & 632. Data sources: **R** = J.I. Raine (IGNS, pers. comm. 1988, 1989; 1990b); **W** = M.D. Warnes (Coal Research Group, University of Canterbury, pers. comm. 1992); **SW** = author. IGNS samples designated "L", DH631 is Fossil Record File no. J31/f160, DH632 is J31/f159. University of Canterbury samples are designated "UCP".
Age ranges: *Nothofagidites* spp. from Dettmann et al. (1990); *Trilites ohaiensis* from Couper (1960); all others from Raine (1984).
Assigned sample ages are as designated by Raine or Warnes. * = taxon present. Taxa are as follows:

TO	Trilites ohaiensis	TM	Triorites minor (% total)
BE	Beaupreaidites sp.	MO	Matonisporites ornamentalis
DM	Densoisporites microrugulatus	NW	Nothofagidites waipawaensis
GR	Gambierina rudata	PcT	Proteacidites cf. tuberculatus
NK	Nothofagidites kaitangataensis	TS	Tricolpites secarius
QB	Quadraplanus brossus	TP	Tricolpites phillipsii
TL	Tricolpites lilliei	MH	Myricipites harrisii
TMo	Trilites morleyi	MY	Myrtaceidites sp.
TR	Triporoletes reticulatus	RM	Rugulatisporites mallatus
PD	Peromonolites densus	Tm	Triorites minisculus

T. lilliei is present in 7 samples, in which it occurs with *Nothofagidites kaitangataensis*, *Beaupreaidites* n.sp. and rare *T. ohaiensis* and *T. morleyi*. *Triorites minor* is rare and *T. secarius* is absent from samples containing *T. lilliei*, with the exception of one sample (DH631, 188.0m) which contains *T. minor* (7%), *T. secarius* and *T. minisculus* (all typical PM3 taxa). This sample occurs below samples with typical PM2 floras, and is notable for a comparatively high proportion (36%) of angiosperm pollen.

T. secarius occurs in 11 samples, in conjunction with both Haumurian and Teurian taxa (as defined by Raine 1984). Haumurian taxa include *Beaupreaidites* n.sp., *T. lilliei, Gambierina rudata* and *N. kaitangataensis*. Teurian taxa include *Peromonolites densus*, *Matonisporites ornamentalis*, *Nothofagidites waipawaensis*, *Tricolpites phillipsii*, *Myricipites harrisii, Myrtaceidites* sp., and *Rugulatisporites mallatus*.

The abundance of *T. minor* provides additional evidence for the recognition of Zone PM3. Those samples which contain *T. secarius* generally contain moderate–high (up to 30%) abundances of *T. minor*. Where Raine's samples were duplicated by Warnes, the latter material generally contained higher proportions of *T. minor*. This may be attributed to differences in processing technique, whereby small angiosperm pollen grains are unintentionally eliminated from IGNS samples. As a consequence, different ages were assigned to the two samples from DH631 at 164.4m (Table A5.1), which alters the location of the KTB in this drillhole (see also Section 5.4).

The following criteria for zonal determination can be established:

PM3: *T. secarius*, usually with moderate-high abundances of *T. minor*. May include *M. harrisii, Myrtaceidites sp., M. ornamentalis, T. phillipsii* and *N. waipawaensis*. Without *T. lilliei*.

PM2: *T. lilliei*, commonly with *N. kaitangatensis* and *Beaupreaidites n.sp.* Rare *T. minor*, *T. secarius* and other Teurian forms absent.

These criteria, which encompass the zonal index taxa and the most common occurrences within the sample suite, are applicable to 15 of the 25 samples from DH631 & 632. Five samples designated PM3 lack *T. secarius* but contain other taxa listed as Teurian or younger (e.g. *M. harrisii*, *Myrtaceidites*, *M. ornamentalis*, *T. phillipsii*, *N. waipawaensis* and *P. cf. tuberculatus*). Occurrences of these taxa in DH631 & 632 are consistent with reported age ranges, however *R. mallatus* and *T. minisculus*, listed as PM3 or younger, both occur in samples assigned to Zone PM2. Raine (pers. comm. 1989) assigned the uppermost sample from DH631 (100.2m) to Zone PM3 on the basis of its stratigraphic position, and the presence of *M. ornamentalis* confirms a Teurian age.

Both samples from DH632 at 262.3m lack *T. lilliei* but contain *Densoisporites microrugulatus*, which indicates Zone PM2. The occurrence of *G. rudata* (PM2) in DH631 at 164.4m is an unreliable indicator of Zone PM2, as this species also occurs in the sample at 240.0m in DH632, which is PM3. There are also occurrences of Haumurian *N. kaitangataensis* in Teurian samples (DH632, 240.0m and 250.0m). The reported presence of *Beaupreaidites* n.sp. in a Teurian sample (DH631, 148.6m; Warnes pers. comm. 1992) could not be confirmed upon further inspection, and this species may be restricted to Zone PM2, as indicated by Raine (pers. comm. 1989). The occurrences of *T. morleyi*, *T. ohaiensis* and *P. densus* are consistent with their reported age ranges, whereas *Q. brossus* and *T. reticulatus* both occur in Zone PM3 samples but have a reported range of PM2.

As indicated above, the sample from DH631, 188.0m contains both Haumurian and Teurian elements, but is assigned to Zone PM2 because of stratigraphic position. The remaining sample (DH631, 175.45m), which Raine (pers. comm. 1989) assigned to Zone PM2 on the basis of stratigraphic position, lacks key taxa but contains *P. densus* and possible *R. mallatus*, neither of which are reliable zonal indicators.

Conclusions: Robust criteria which are consistent with the key bioevents of the regional zonation scheme (Raine 1984) apply to only 60% of the samples from DH631 & 632. Key "regional" taxa (*T. lilliei*, *T. secarius*) may be absent, and overlap of these taxa is possible. Ages were assigned to the remaining samples using the occurrence of other pollen taxa. However, the reported ranges of some taxa are not reliable over the geological interval being investigated and useful taxa are rare. Some samples could not be confidently dated by reference to the palynoflora alone.

A5.4.3 Palynological zonation and age assignment, study sample suite

Occurrences of stratigraphically significant taxa in the study sample suite are summarised in Table A5.2, and summary data for the miscellaneous coals are presented in Table A5.3. Many of the taxa discussed above were not recorded in the study samples, and others (*M. harrisii*, *Myrtaceidites*, *G. rudata*) are very rare (i.e. only one specimen of each). An additional form, *Malvacipollis* sp., was observed and is listed in Table A5.2.

Coal	UCP	TL	TMo	TS	Tm	MH	Zone
Tiller	1306			*	*		PM3
Goldlight	1307		*			*	PM3?
Kiwi	1278	*	*				PM2
Snowline	1279	*	*				PM2

Table A5.3 Occurrence of stratigraphically significant taxa, miscellaneous coal samples. Abbreviations as in Table A5.2, full data given in Appendix 14.

In order to assign ages to all samples on the basis of palynoflora (where possible), samples with similar occurrences of key taxa were grouped and the age for each group interpreted. Zonal criteria developed above allowed ages to be assigned to 28 of the 62 samples (45%). Of the remaining 34 samples, 23 contained age-diagnostic taxa inconsistent with the zonation criteria, 6 samples had moderate–abundant palynomorphs but lacked age-diagnostic taxa and 5 samples yielded insufficient pollen assemblages. Sample groups and interpreted ages are given for each sample in Table A5.2.

Group 1: Eleven samples, containing *T. lilliei*, are consistent with the criteria given above for recognition of Zone PM2. *N. kaitangataensis*, *Beaupreaidites* and *T. minor* are minor components, and *T. secarius* is absent. *Malvacipollis* sp. is present in 2 samples (626/3, 626/4) and other diagnostic taxa are absent.

Group 2: Seventeen samples contain *T. secarius* and moderate to abundant *T. minor* (4.8–34.6%, average = 20.7%), and are consistent with Zone PM3. *Malvacipollis* sp. is present in 6 of these samples, *T. minisculus* in 5 samples, *Myrtaceidites* in 2 samples and *M. harrisii* in 1 sample. Three Group 2 samples contain *T. morleyi,* and 1 contains *T. ohaiensis*. The occurrence of *T. lilliei* and *T. morleyi* in 628/3 is likely to reflect reworking, as these specimens are damaged and darker in colour than the remaining

DH	UCP	Depth	Unit	Lithology	Count	TL	NK	GR	TO	TMo	BE	TS	TM	Tm	MY	MA	MH	Group	Age
619 /1	1266	241.5	G	lam zst/mst	169								28.4					4	**PM3**
/2	1300	250.6	R	vfsst	254							*	34.6					2	**PM3**
/3	1267	251.1	R	vfsst-zst	141							*	23.4				*	2	**PM3**
/4	1301	254.75	R	carb zst	259							*	25.5					2	**PM3**
/5	1280	c.260	R	coal	254													7	**PM2**
/6	1268	262.7	R	coaly mst	s		*											3	**PM2**
623 /1	1316	47.1	R	coaly mst	249	*	*											1	**PM2**
/2	1317	48.5	R	dirty coal	257	*	*						*					1	**PM2**
/3	1318	54.0	R	dirty coal	250													7	**PM2**
/4	1319	61.27	R	dirty coal	270	*							*					1	**PM2**
/5	1320	62.36	R	carb zst	250		*				*			*		*		3	**PM2**
/6	1321	68.1	R	carb zst	s		*				*					*		3	**PM2**
/7	1322	76.55	R	coal	250					*								3	**PM2**
626 /1	1323	301.8	Gt	carb zst	253							*	21.7			*		2	**PM3**
/3	1325	310.61	R	coaly mst	249	*					*		*			*		1	**PM2**
/4	1326	320.68	R	dirty coal	250	*										*		1	**PM2**
/5	1327	331.84	R	carb vfsst	s														**n/d**
628 /1	1329	252.64	R	coal	260	*												1	**PM2**
/2	1330	257.5	R	dirty coal	251					*								3	**PM2**
/3	1331	259.59	G	mst	250	*r				*r		*	17.6	*		*		2	**PM3**
/4	1332	274.2	G	mst	257							*	14.8	*				2	**PM3**
/5	1333	275.0	R	coal	261													7	**PM2**
/6	1334	280.24	R	coal	306													7	**PM2**
/8	1312	291.75	R	coal	268	*							*					1	**PM2**
/9	1313	297.0	R	coal	250				*									3	**PM2**
633 /1	1336	380.16	R	carb mst	246	*				*		*	*					6	**PM2**
/2	1337	384.36	R	coaly mst	250	*	*	*				*		*				6	**PM2**
/3	1338	387.76	R	zst	267	*					*	*						6	**PM2**
/4	1339	391.19	R	carb mst	266	*						*						6	**PM2**
/5	1314	394.3	R	coal	255	*												1	**PM2**
/6	1315	400.0	R	coal	250		*			*				*				3	**PM2**
635 /1	1270	380.25	R	vfsst-zst	203							*	9.9		*			2	**PM3**
/2	1271	390.7	R	carb f-vfsst	207				*	*			32.9					4	**PM3**
/3	1302	394.27	R	carb vfsst	254				*			*	22.4			*		2	**PM3**
/4	1272	399.7	R	coaly vfsst	s								*						**n/d**
/5	1304	400.0	R	coal	245					*			*					3	**PM2**
/6	1273	410.52	R	fsst/carbzst	s	*												1	**PM2**
636 /1	1340	302.0	R	coaly mst	255							*	3.1	*		*		5	**PM3**
/2	1341	306.40	R	coaly vfsst	251								*					7	**PM2**
640 /1	1342	188.2	R	coal	250							*	*	*				5	**PM3**
/2	1343	189.0	R	coal	262							*	*	*		*		5	**PM3**
643 /1	1362	281.5	R	mst	253							*	13.8					2	**PM3**
/2	1363	282.7	R	carb mst	250							*	21.6					2	**PM3**
/3	1344	282.9	R	coal	250					*				*		*		3	**PM2**
/4	1345	283.2	R	coal	250		*			*								3	**PM2**
/5	1364	287.5	R	carb zst	253	*					*							1	**PM2**
/6	1365	288.2	R	carb zst	250	*					*	*	1.2					6	**PM2**
666 /1	1274	146.8	R	carb mst	191					*		*	17.3			*		2	**PM3**
/2	1275	156.0	R	carb vfsst	184					*		*	19.6			*		2	**PM3**
/3	1303	165.37	R	fsst	269	*r	*					*	4.8					2	**PM3**
/4	1276	166.0	R	carb vfsst	s														**n/d**
/5	1305	167.6	R	dirty coal	180		*											3	**PM2**
/6	1277	176.7	R	carb mst	175	*	*						2.3					1	**PM2**
667 /1	1288	102.2	Gt	fsst	129		*						29.5					4	**PM3**
/2	1289	110.0	R	fsst	s								*						**n/d**
/3	1290	120.5	R	fsst	139							*	12.2					2	**PM3**
/4	1291	129.0	R	fsst	s								*						**n/d**
697 /5	1217	249.85	G	silty mst	263							*	30.0	*		*		2	**PM3**
/6	1216	261.85	G	silty mst	264							*	36.7	*	*			2	**PM3**
/7	1215	273.83	G	silty mst	261								27.6	*				4	**PM3**
/8	1214	283.2	G	silty mst	298							*	20.8	*		*		2	**PM3**
/9	1213	292.25	R	carb mst	119								2.5					7	**PM2**

Table A5.2 Sample details (drillhole, UCP no., depth), total pollen count, diagnostic pollen and spore occurrences, zonation group and interpreted age for study sample suite.
UCP = University of Canterbury Palynology collection number.
Depths in metres from drillhole collar.
Units: G = Goldlight Fm., Gt = Goldlight Transitional Member, R = Rewanui CMM.
"s" = sample scanned but not counted, "*" = taxon present, "r" = reworked specimen, "n/d" = age not determinable.
Taxa are as follows:

TL	*Tricolpites lilliei*
NK	*Nothofagidites kaitangataensis*
GR	*Gambierina rudata*
TO	*Trilites ohaiensis*
TMo	*Trilites morleyi*
BE	*Beaupreaidites* sp.
TS	*Tricolpites secarius*
TM	*Triorites minor* (% total)
Tm	*Triorites minisculus*
MY	*Myrtaceidites* sp.
MA	*Malvacipollis* sp.
MH	*Myricipites harrisii*

assemblage. Moderate amounts (4.8%) of *T. minor* in 666/3, plus 1 specimen of *T. secarius*, may indicate a PM3 age. Conversely, the presence of *T. lilliei* and *N. kaitangataensis* would support assignment of 666/3 to Zone PM2. The damaged nature of the single specimen of *T. lilliei* indicates reworking, hence 666/3 is assigned to Zone PM3.

Group 3: Eleven samples contain *N. kaitangataensis* and/or *T. morleyi* and/or *T. ohaiensis*, but no *T. lilliei*. Key PM3 taxa *T. secarius* and *T. minor* are absent from Group 3 samples, except from 635/5, which contains 1 specimen of *T. minor*. Three samples (623/5, 623/6, 643/3) contain *Malvacipollis sp.* pollen, which are regarded as indicating a Cenozoic age (Raine 1984). However, *Malvacipollis sp.* is also present in Group 1 (Haumurian) samples 626/3 and 626/4, and is an unreliable age indicator.

Eight of the Group 3 samples are coals or dirty coals, and the absence of certain taxa indicates facies control on the palynoflora. *T. lilliei* occurs rarely at the margins of the "D" seam of Strongman Mine (Ward et al. 1995). No coal or dirty coal from the study suite contains more than 1 specimen of *T. minor*, indicating this species is absent or very rare in the coal-forming environment. However, the absence of *T. secarius* is not likely to reflect facies control, because *T. secarius* is present (and *T. minor* absent) in Paleocene (PM3) coal (Dunollie Fm.) from Tiller Mine (UCP1306). Absence of *T. secarius* therefore indicates Group 3 samples are most consistent with Zone PM2.

Group 4: Four sediment samples (619/1, 635/2, 667/1, 697/7) with high *T. minor* percentages (>28%) lack *T. secarius*. All samples are characterised by low angiosperm diversity (7 or fewer taxa) and low abundance of angiosperms other than *T. minor*. High *T. minor* percentage supports assignment of these samples to Zone PM3, though rare Haumurian forms *N. kaitangataensis*, *T. morleyi* and *T. ohaiensis* are also present.

Group 5: Samples 636/1, 640/1 and 640/2 contain *T. secarius*, rare *T. minor*, and rare Malvaceae and/or *T. minisculus*. Angiosperm diversity is moderate (9 –14 taxa), but abundance is low (9 – 11%). Consistent presence of *T. secarius* and the absence of Haumurian index taxa supports assignment of these samples to Zone PM3. These three samples are coaly or coals, and low *T. minor* abundance reflects facies control (see above).

Group 6: Five sediment samples (633/1–4, 643/6) with moderate–high angiosperm diversity (12 – 20 taxa) and high proportions of pteridophyte spores contain taxa typical of Zones PM2 and PM3, in particular both *T. lilliei* and *T. secarius*. Rare occurrences of *T. secarius* are known from Zone PM2 material (Ward et al. 1995), and range overlap between *T. lilliei* and *T. secarius* is discussed below. These samples have low proportions of *T. minor*, whereas Paleocene (PM3) sediment samples would contain a moderate–high proportion of *T. minor*. Group 6 samples are therefore assigned to Zone PM2. The sample from DH631 at 188.0m (UCP1221), which was assigned a PM2 age (Table A5.1), is very similar.

Group 7: Six samples (619/5, 623/3, 628/5, 628/6, 636/2, 697/9) contain no age diagnostic taxa other than 3 specimens of *T. minor* in 697/9 and 1 dubious *T. minor* in 636/2. The latter two samples are sediments, hence low *T. minor* percentage is tentative evidence for assignment to Zone PM2. The remaining 4 samples, which are coal or dirty coal, cannot be directly dated, however all coaly samples designated PM3 (Group 5) contain *T. secarius*, thus the absence of this species provides tentative evidence for assignment of these samples to Zone PM2.

Criteria for assigning ages to Greymouth Coalfield palynological samples are summarised in Table 5.1. Application of the criteria to the study drillholes, and the location of the KTB in Greymouth Coalfield, is discussed in detail in Chapter 5.

A5.5 Facies and floral controls on key species occurrence

The occurrence of key age-diagnostic pollen taxa within the samples described above (summarised in Table A5.4) is influenced by floral variation (e.g. diversity), facies variation (coal, dirty coal or sediment) and sample age (Zone PM2 or Zone PM3). To have confidence in age assignment based on the presence, absence or abundance of these taxa, the influence of facies and flora (i.e. paleovegetation) on key palynomorph occurrence must be assesed. Further discussion of abundance variation of all spore and pollen taxa within Greymouth Coalfield palynofloras is presented in Appendix 6.

Species	Haumurian sediments n = 12	Haumurian dirty coals n = 6	Haumurian coals n = 12	Teurian sediments n = 22	Teurian dirty coals n = 2
T. lilliei	**rare–absent** *in 9 samples*	**rare–absent** *in 3 samples.*	**trace/absent** *in 3 samples*	**absent**	**absent**
T. secarius	**rare–absent** *in 5 samples*	**absent**	**absent**	**moderate–absent** *in 18 samples*	**rare/trace**
T. minor	**rare–absent** *in 6 samples*	**trace/absent** *in 2 samples*	**trace/absent** *in 2 samples*	**abundant–rare** *abundant in 13, common in 6, moderate 1, rare in 2.*	**trace** *in both samples*
Beaupreaidites sp.	**rare–absent**	**absent**	**absent**	**absent**	**absent**
Tricolpites sp. F	**In 3 samples**	**in 1 sample**	**absent**	**absent**	**absent**

Table A5.4 Summary of occurrence data and lithological associations for the key age-diagnostic taxa.

A5.5.1 *Tricolpites lilliei*

One to four specimens of *T. lilliei* are present in the majority of Haumurian sediment samples, and in 3 of the 6 dirty coal samples. The species occurs at trace levels in 3 of the 12 Haumurian clean coal samples (628/8, 633/5, 628/1) and is absent from the remaining nine. The presence of *T. lilliei* in some Haumurian coals in the present study may indicate lateral proximity of the sample sites to mire margins, as observed within the "D" seam of the Strongman area (Ward et al. 1995).

The damaged nature of the two specimens of *T. lilliei* in samples interpreted as Teurian (628/3, 666/3) indicates probable reworking. Alternatively, structural disruption present in DH628 (Appendix 2) could have caused intermixing of Haumurian and Teurian lithologies, which may account for the occurrence of *T. lilliei* in sample 628/3. Age is therefore the primary control on the occurrence of *T. lilliei*, though a secondary facies control favours the occurrence of this palynomorph in sediments rather than coals.

A5.5.2 *Tricolpites secarius*

T. secarius is present in 18 of the 22 Teurian sediments and the two Teurian dirty coals (640/1, 640/2), and is also present in 5 Haumurian sediments. The species occurs in moderate amounts in 619/4 (6.6%), is rare in 10 samples and present as trace amounts in 13 samples, and was also observed in the additional scans of 697/8 (i.e. not included in count data). *T. secarius* is absent from 4 Teurian sediment samples (619/1, 635/2, 667/1, 697/7, comprising Group 4, see above) which are characterised by below average (<8.5)

angiosperm diversity (3 to 8 taxa), but otherwise have a similar overall composition to other Teurian palynofloras. Three of these are from basal Goldlight Fm. sediments, and the remaining one (635/2) is from 12m below the top Rewanui CMM contact, indicating that depositional environment is not controlling *T. secarius* occurrence.

The presence of *T. secarius* in 5 Haumurian sediment samples (Group 6) is associated with atypical floras with above average (>10.3) angiosperm diversity and high spore proportion (Cyatheaceae dominant). Twelve to 16 angiosperm taxa, and 11 to 14 spore taxa are present in these samples. Four of the five Haumurian sediment samples containing *T. secarius* are from DH633 (633/1–633/4), in which a thin sequence of Rewanui CMM comprises fine carbonaceous sediments, coal and thin crevasse splay sandstone units (Figure 5.2; map pocket).

Rapahoe Sector Main Seam coal in DH633 is atypical, with highly elevated volatile matter values and a transported assemblage of fragmented macerals, which together indicate very wet mire conditions (Newman 1987). The single palynological sample from the Main Seam in DH633 (633/5) is dominated by *P. mawsonii,* which also favours wet conditions (Ward et al 1995). The high proportion of Cyatheaceae spores and diverse angiosperm flora found in DH633 suggests a wet site which is regularly disturbed by flooding. Thus, palynological and other data from DH633 highlight the presence of localised variation in paleoenvironment within Greymouth Coalfield and the environmental influence on occurrence of age-diagnostic taxa.

Occurrence of *T. secarius* is therefore controlled by both age and floral association. This species is generally present (up to moderate proportions) in Teurian samples, and absence from certain samples reflects low angiosperm diversity. In contrast, the presence of *T. secarius* in Haumurian samples correlates with above average angiosperm (and spore) diversity. Occurrence of *T. secarius* is not facies dependent.

A5.5.3 *Triorites minor*

The majority of Teurian samples, including those from fluvial Rewanui CMM, lacustrine Goldlight Fm., Goldlight Transitional Members and fluvial Dunollie Fm., contain >c.10% (average 19.5%) *T. minor*. The exceptions are the two Teurian dirty coals (640/1, 640/2), a coaly mudstone (636/1) and 666/3, which has an atypical flora with high angiosperm and

spore diversity (Appendix 6.3.3). In contrast, *T. minor* is a rare or trace component (1–4 specimens) of 9/30 Haumurian samples, including coals, dirty coals and sediments, and is absent from the remainder. *T. minor* is also absent from the Teurian coal from Tiller Mine (UCP1306, Dunollie Fm.). The primary control on the occurrence of *T. minor* in the various clastic lithofacies is therefore age. However, this species is not present in either Haumurian or Teurian coal/coaly facies, which indicates a strong preference for inorganic substrates, inducing significant facies control.

A5.5.4 *Beaupreaidites* sp. and *Tricolpites* sp. F

The occurrence of *Beaupreaidites* sp. is restricted to Haumurian sediments, and *Tricolpites* sp. F to Haumurian sediments and dirty coals. These taxa occur in Groups 1, 3 and 6 (see above), which are confidently assigned to Zone PM2. Occurrence of these taxa is therefore primarily age-controlled, though both are absent from mire floras.

A5.5.5 Overlap of Haumurian and Teurian taxa

Previous studies (Appendix 5.4.1) have demonstrated overlap in the ranges of *T. lilliei* and *T. secarius*, which is believed to represent short-term survival of *T. lilliei* across the KTB, or reworking (Helby et al. 1987; Raine 1994a). In this study, the presence of *T. lilliei* in two Teurian samples (which contain *T. secarius*) is believed to represent reworking or structural intermixing. However, *T. secarius* is present in five Haumurian sediment samples, and trace amounts of *T. secarius* were also observed in a coal sample c.20m below the KTB (UCP1346; Ward et al. 1995).

T secarius was therefore present in palynofloras prior to the KTB, though only as a very minor component, and mostly in atypical floras with high angiosperm diversity (Appendix 6.3.2). Raine (1984) defined the lower boundary of Zone PM3 as the first appearance datum of *T. secarius*, however the present study indicates this bioevent is not a reliable palynostratigraphic indicator for the KTB, and other criteria, such as *T. minor* abundance and the absence of typical Haumurian forms must be applied for confident recognition of Teurian palynofloras.

Appendix 6. Description and analysis of Greymouth Coalfield palynofloras

A6.1 Introduction

The objectives of this appendix are:

- to describe the various angiosperm pollen, gymnosperm pollen and spore components of the Greymouth Coalfield palynofloras sampled in the present study
- to recognise floral associations
- to investigate the controls exerted on flora by facies
- to compare Haumurian and Teurian floras and assess floral change across the Cretaceous–Tertiary Boundary (KTB).

All 54 drillhole samples with count data (see Appendix 14) are utilised in discussions about pollen and spore abundance and diversity. Palynomorph abundance classes used throughout this appendix are as follows:

Abundant	>20.0%
Common	10.0 – 19.9%
Moderate	5.0 – 9.9%
Rare	1.0 – 4.9%
Trace	0.1 – 0.9%
Absent	0% in count

Taxa recorded in additional scans after counting was completed are not included in the pollen abundance measurements, but their presence is noted where appropriate and these taxa are included in measurements of diversity. Only qualitative and basic quantitative comparisons between floras from different lithologies and ages were possible, because of small sample size and non-normal distributions of most taxa. Though an unconventional means of displaying palynology data, ternary diagrams are used to portray overall proportions of angiosperm pollen, gymnosperm pollen and spores. Such diagrams are useful for reconstructing patterns of vegetation dynamics where absolute abundance data are absent (Taggart & Cross 1995). All ternary diagrams were constructed with the *TECHBASE TRIPLOT* application.

A6.2 Description of pollen and spore flora components

Identification of palynomorphs followed standard practice. Key sources included Couper (1953, 1960), McIntyre (1965), Dettmann & Playford (1968), Stover & Partridge (1973) and Warnes (1988). Where possible, topotypes of NZGS type specimens held in the Department of Geological Sciences, University of Canterbury, were inspected. Related or morphologically similar taxa of angiosperm and gymnosperm pollen, or spores, are discussed together, though certain common taxa are treated individually. All recorded taxa and their groupings are listed in Table A6.1.

A6.3 Description of Greymouth Coalfield palynofloras, present study

In order to describe Greymouth Coalfield palynofloras, the sample set was subdivided according to sample age and lithology, as these variables are known or have been determined elsewhere (Appendix 13, Section 5.3). The subsets distinguished were Haumurian (Zone PM2) clean coals, dirty coals (generally seams <1m thick) and sediments, and Teurian (Zone PM3) coals and sediments. Within each subset, floral variables included proportion and diversity of the various pollen and spore components (Table A6.1), and the dominant elements of the flora. Stated diversity must be regarded as a minimum value, as some common forms have not been differentiated to species level (Gleicheniaceae, Cyatheaceae) and un-named forms have been grouped together in the relevant genus or form-genus (e.g. *Podocarpidites*, *Tricolpites*, *Trilites*).

A6.3.1 Haumurian palynofloras

Haumurian palynofloras, derived from 12 coals, 6 dirty coals and 12 sediments, are variably dominated by spores (average = 45.3%) and gymnosperm pollen (average = 46.5%). Angiosperm pollen comprise the smallest component (average = 8.2%) in all but 2 samples (633/3, 643/6). Overall floral composition of these samples is presented in Figure A6.1, and occurrence of the various floral elements and dominant gymnosperm and spore components in each lithotype is summarised below in Tables A6.2–A6.4.

Angiosperm pollen group	Taxa represented
Monosulcate	Liliacidites spp.
	Liliacidites variegatus
	Monosulcites cf. granulatus
	Monosulcites cf. minima
	Monosulcites granulatus
	Monosulcites spp.
Tricolpate	Concolpites leptos
	Peninsulapollis gillii
	Tricolpites cf. pachyexinus
	Tricolpites lilliei
	Tricolpites reticulatus
	Tricolpites secarius
	Tricolpites sp. A–H
	Tricolpites spp.
Tricolporate	Myrtaceacidites
	Rhoipites
	Tricolporites spp.
Triorate	Gambierina rudata
	Myricipites harrisii
	Triorites minisculus
	Triorites minor
	Triorites spp.
Proteaceae	Beaupreaidites
	Proteacidites amolosexinus
	Proteacidites parvus
	Proteacidites scaboratus
	Proteacidites spp.
	Proteacidites subpalisadus
	Proteacidites subscabratus
Nothofagidites	Nothofagidites kaitangataensis
	Nothofagidites spp.
	Nothofagidites waipawaensis
Other angiosperms	Inaperturate
	Malvaceae
	Polycolpites
	Polyorites
	Quadraplanus brossus
	unidentified

Gymnosperm pollen group	Taxa represented
Araucriaceae	Araucariacites spp.
M. antarcticus	Microcachryidites antarcticus
P. mawsonii	Phyllocladidites mawsonii
Podocarpidites	Podocarpidites cf. ellipticus
	Podocarpidites major
	Podocarpidites marwickii
	Podocarpidites spp.
T. subgranulatus	Trichotomosulcites subgranulatus
Other gymnosperms	Dacrydiumites praecupressinoides
	Ephedra notensis
	Phyllocladidites paleogenicus
	Podosporites microsaccatus

Spore group	Taxa represented
Gleicheniaceae	Clavifera rudis
	Clavifera triplex
	Gleicheniidites circinidites
	Gleicheniidites spp.
Sphagnaceae	Cingutriletes regium
	Cingutriletes spp.
	Stereisporites antiquasporites
Cyatheaceae	Cyathidites cf. minor
	Cyathidites major
	Cyathidites spp.
Other trilete	Baculatisporites spp.
	Ceratosporites equalis
	Leptolepidites sp.
	Osmundacidites spp.
	Rugulatisporites mallatus
	Trilites cf. verrucatus
	Trilites microfoveolatus
	Trilites morleyi
	Trilites ohaiensis
	Trilites sinuatus
	Trilites spp.
	Trilites tuberculiformis
	Trilites verrucatus
Laevigatosporites	Laevigatosporites major
	Laevigatosporites ovatus
Other monolete	Monoletes spp.
	Peromonolites bowenii
	Peromonolites densus
	Peromonolites sp.
	Polypodiites spp.
Other spores	Lycopodiumsporites spp.

Table A6.1 Pollen and spore groups used in the discussion of Greymouth Coalfield palynofloras, and corresponding taxa and morphotypes

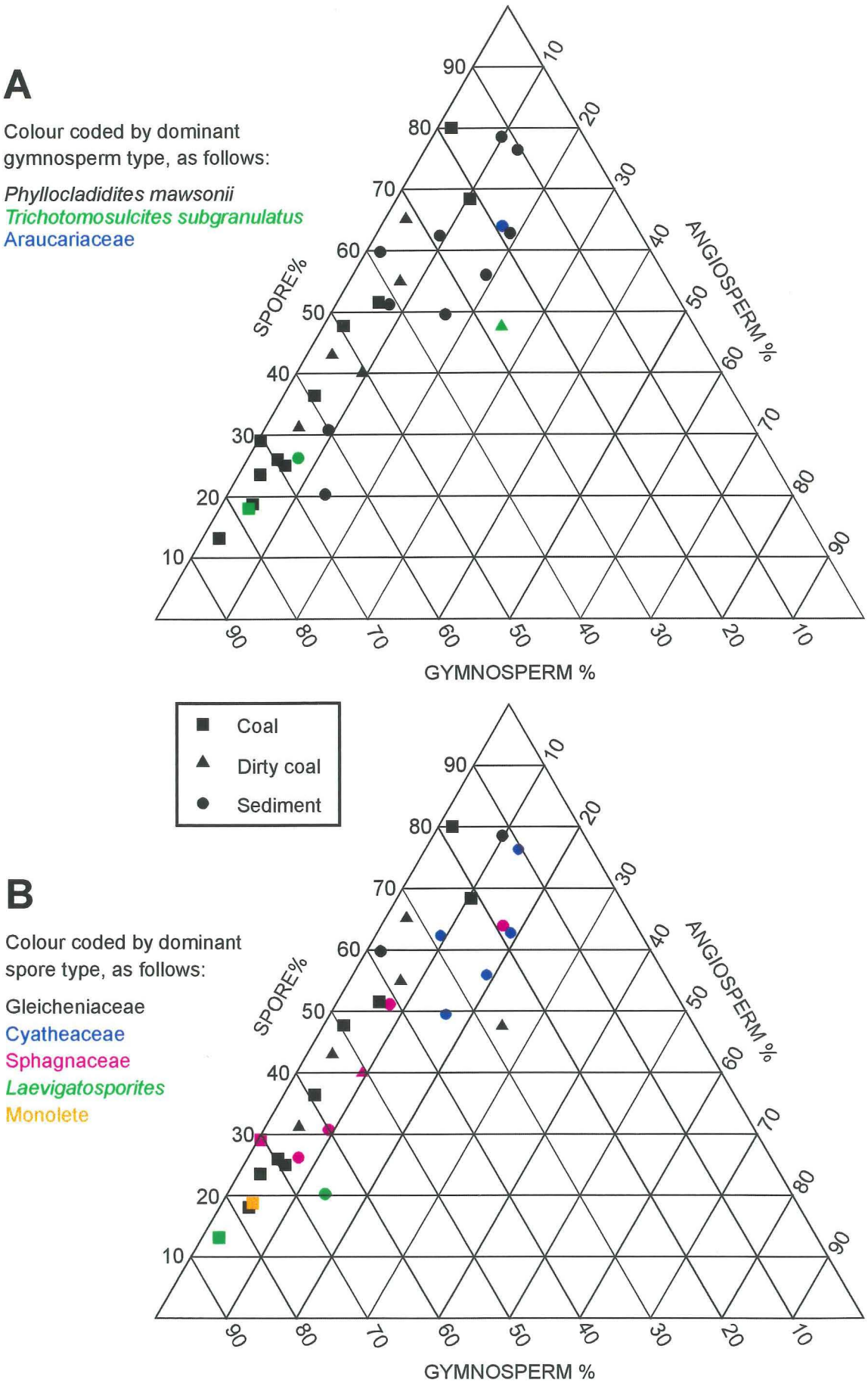

Figure A6.1 Ternary plot of pollen and spore proportions, all Haumurian samples
A = colour coded by dominant gymnosperm type, B = colour coded by dominant spore type

Pollen group	coals (n = 12)	dirty coals (n = 6)	sediments (n = 12)
Monosulcate	rare in 5 samples, trace in 4, absent from 3	rare in 4 samples, trace in 1, absent from 1	moderate in 633/2, rare in 8 samples, trace in 1, absent from 2
Tricolpate	rare in 7, trace in 5	common in 626/4, rare in 4, trace in 1	moderate in 5, rare in 6, trace in 1
Tricolporate	rare in 2, trace in 1, absent from 9	moderate in 626/4, trace in 1, absent from 4	moderate in 633/1, rare in 5, absent from 6
Triorate	rare in 1, trace in 2, absent from 9	trace in 1, absent from 5	rare in 1, trace in 3, absent from 8
T. minor	trace in 2, absent from 10	trace in 1, absent from 5	rare in 3, trace in 3, absent from 6
Proteaceae	rare in 4, trace in 5, absent from 3	rare in 2, trace in 3, absent from 1	rare in 8, trace in 3, absent from 1
Nothofagidites	trace in 3 samples, absent from others	rare in 2, absent from others	moderate in 666/6, rare in 1, trace in 2, absent from 8
Other angiosperms	trace in 2 only	trace in 2	rare in 3, trace in 3, absent from 6

Table A6.2 Summary of angiosperm pollen occurrence, Haumurian samples.

Pollen group	coals (n = 12)	dirty coals (n = 6)	sediments (n = 12)
P. mawsonii	**11** abundant in 10, common in 2	**5** abundant in 4, common in 1, moderate in 1	**10** abundant in 6, common in 2, moderate in 2, rare in 2
Podocarpidites	moderate in 635/5 & 633/6, rare in 9, absent from 1	moderate in 666/5, rare in 4, trace in 1	common in 633/2 & 636/2, moderate in 4, rare in 6
M. antarcticus	rare in 8, trace in 3, absent from 1	moderate in 666/5, rare in 3, trace in 2	common in 626/3, rare in 4, trace in 2, absent from 5
T. subgranulatus	**1** abundant in 628/1, moderate in 2, rare in 2, trace in 4, absent from 3	**1** common in 2, rare in 2, absent from 2	**1** abundant in 636/2, common in 1325, moderate in 2, rare in 6, trace in 2
Araucariaceae	trace in 7, absent from 5	moderate in 623/3, rare in 1, trace in 3, absent from 1	**1** common in 623/5, moderate in 2, rare in 7, trace in 2
Other gymnosperms	rare in 4, trace in 5, absent from 3	rare in 3, trace in 2, absent from 1	rare in 3, trace in 4, absent from 5

Table A6.3 Summary of gymnosperm pollen occurrence, Haumurian samples. Bold numbers indicate the number of samples in which the group comprises the dominant gymnosperm form(s).

Spore group	coals (n = 12)	dirty coals (n = 6)	sediments (n = 12)
Gleicheniaceae	**9** abundant in 4, common in 4, moderate in 2, rare in 2	**5** abundant in 4, common in 2	**2** abundant in 623/1 & 633/4, common in 1, moderate in 6 and rare in 3
Sphagnaceae	**1** common in 628/5, moderate in 4, rare in 4, trace in 2, absent from 1	**1** common in 623/2, moderate in 2, rare in 1, trace in 1, absent from 1	**4** abundant in 697/9 & 666/6, common in 6, moderate in 2, rare in 2
Cyatheaceae	moderate in 619/5, rare in 4, trace in 3, absent from 4	moderate in 1305, rare in others	**5** abundant in 4, common in 3, rare in 3, rare in 1, trace in 1
Trilete	moderate in 2, rare in 4, trace in 4, absent from 2	common in 1319, rare in 4, trace in 1	common in 3, moderate in 4, rare in 3, trace in 2
Laevigatosporites	**1** common in 619/5, moderate in 4, rare in 7	common in 623/4 & 626/4, moderate in 1, rare in 3	**1** common in 633/2 & 633/4, moderate in 5, rare in 5
Monolete	**1** common in 623/7, moderate in 3, rare in 5, trace in 2, absent from 1	common in 666/5, moderate in 1, rare in 4	rare in 8, trace in 1, absent from 3
Other spores	rare in 1, trace in 1, absent from others	rare in 1, trace in 1, absent from others	rare in 1, trace in 4, absent from others

Table A6.4 Summary of spore occurrence, Haumurian samples. Bold numbers indicate the number of samples in which the group comprises the dominant spore form(s).

Haumurian coals: Haumurian coal palynofloras are characterised by variable proportions of spores and gymnosperm pollen, and low angiosperm abundance (Table A6.2; Figure A6.1, squares). Angiosperm pollen contributes generally <6% of the Haumurian coal flora, the exception being sample 623/7 (10.4%, dominantly *Rhoipites* and monosulcate forms). The average angiosperm proportion is 4.2%, comprising between 1 and 8 taxa.

Most variation in Haumurian coal palynofloras is attributable to the proportions of *P. mawsonii* pollen and Gleicheniaceae spores, the combined total of which constitutes 33.8%–80.8% of the floras (average = 66.4%). The gymnosperm fraction of 11 of the 12 samples is dominated by *P. mawsonii* (average = 47.5%), whereas *T. subgranulatus* is the dominant form in 628/1 (Figure A6.1A). Moderate amounts of other gymnosperm taxa are present in all samples, with the exception of 628/6, which contains few gymnosperm pollen. Gymnosperm diversity ranges from 3 to 9 taxa, and averages 6.3 taxa.

Spore diversity in Haumurian coals varies from 5 to 12 taxa, and averages 8.8 taxa. Gleicheniaceae are the dominant spore taxa in nine samples (average = 18.8%) (Figure A6.1B). However, the combined total of other spores, which contribute 5.8%–30.8% of the flora (average = 17.7%), exceeds the Gleicheniaceae total in 7 samples. In 3 samples,

Gleicheniaceae abundance is low, and Sphagnaceae, *Laevigatosporites* and other monolete taxa dominate the spore flora in one sample each (Figure A6.1B). Five samples contain >10% total monolete spores (*Laevigatosporites* plus other taxa), though there is no relationship between total spore and total monolete proportion. Cyatheaceae, in all samples other than 619/5, are rare or absent, and other trilete forms are rare in most samples. Two samples (619/5, 623/7) with common total monolete spores also contain moderate–common trilete spores. Sphagnaceae are common in 628/5, and moderate amounts are present in 4 samples.

Haumurian dirty coals: Six samples of dirty coals (Figure A6.1, triangles) have been assigned a Haumurian age (Table A5.2). Five of these contain 5–10 angiosperm taxa which contribute <10% of the palynoflora, and plot within the area of typical Haumurian coal composition on Figure A6.1. The remaining sample (626/4) contains a high proportion of angiosperm pollen (13 taxa, total 25.2%) in addition to 14.4% of the gymnosperm *T. subgranulatus*, which is also common in 623/4 (12.6%). Other gymnosperm taxa are generally rare, though Araucariaceae, *M. antarcticus* and *Podocarpidites* occur in moderate amounts in one sample each.

Spore taxa follow the trends observed in the coal samples, with Gleicheniaceae dominant in most samples (Figure A6.1B). Sphagnaceae are dominant in 623/2, and abundance varies from common to absent in the other samples. Trilete spore forms are common in 623/4, *Laevigatosporites* is common in 623/4 and 626/4, and monolete forms are common in 666/5. Spore diversity varies from 6 to 14 taxa, and averages 11.5 taxa.

Gleicheniaceae have similar abundance in dirty coals and coals, though other spores (trilete forms and *Laevigatosporites*) occur in greater amounts in dirty coals (average = 17.7% coals, 25.8% dirty coals). Dirty coals also contain slightly more pollen from gymnosperms other than *P. mawsonii* (notably Araucariaceae) than do clean coals (average other gymnosperms = 7.7% coals, 11.6% dirty coals). Angiosperm pollen are more abundant in dirty coals (average = 8.9%) than coals (average = 4.2%), though the difference is reduced when the samples with anomalously high angiosperm proportion (623/7, 626/4) are disregarded (coals = 3.7%, dirty coals = 5.6%). Overall, differences between coals and dirty coals (with the exception of 626/4) are slight.

Haumurian sediments: Haumurian sediment palynofloras (Figure A6.1, circles) are dominated by spores (average = 53.2%). Spore assemblages are dominated by Cyatheaceae (average = 15.8%) and Sphagnaceae (13.2%) and Gleicheniaceae are the most abundant spore forms in only 2/12 samples (Figure A6.1B). Average Gleicheniaceae abundance is approximately half of that observed for Haumurian coals and dirty coals.

Samples in which Cyatheaceae are the dominant spores (633/1–3, 643/5–6) plot within a small area on Figure A6.2B, encompassing c.10–20% angiosperm pollen (approximately twice the normal Haumurian abundance), 10%–35% gymnosperm pollen (*P. mawsonii* dominant) and c.50–80% spores. All the Group 6 Haumurian samples (Appendix 5.4.3) lie within this area of Figure A6.1, and have above average spore diversity (11–14 taxa). *Laevigatosporites* is the dominant spore form present in 626/3, which has the lowest spore proportion (20.3%) of the Haumurian sediments. Trilete forms are common in 3 samples, and monolete forms comprise <5% of the spore flora.

P. mawsonii is the dominant gymnosperm in nine Haumurian sediment samples (Figure A6.1A), though the average abundance (16.8%) is lower than that for coals or dirty coals. Equal amounts of *P. mawsonii* and *Podocarpidites* are present in 633/2 (11.6%), and the total proportion of gymnosperm taxa other than *P. mawsonii* exceeds *P. mawsonii* abundance in 6 samples. Araucariaceae, *Podocarpidites*, *M. antarcticus* and *T. subgranulatus* all occur in trace to common proportions, and the average occurrence of these forms (18.1%) is slightly higher than for coals and dirty coals. *T. subgranulatus* and Araucariaceae are the dominant gymnosperm forms in one sample each. Gymnosperm diversity varies from 4–9 taxa (average = 6.6), similar to that of coals and dirty coals.

Angiosperm pollen average 11.9% of the Haumurian sediment palynoflora, and the angiosperm proportion is greater than that observed in coals for all but one sample (623/1, 2.0%). When recalculated without this value, average angiosperm abundance is 12.8%, which is significantly higher than the average (without outliers: see above) for coals or dirty coals. Angiosperm diversity (average = 10.7) is also greater than that of coals or dirty coals, and between 5 taxa (697/9) and 16 taxa (633/2) are present. Group 6 samples (Section 7.3.5) are characterised by above average angiosperm diversity (12–14 taxa). Sample 623/1 is a coaly mudstone, and has a flora which resembles that of a coal, however the angiosperm proportion of other coaly sediment samples (626/3, 633/2, 636/2) is

greater than that observed in coals and dirty coals. Angiosperm pollen in Haumurian sediment samples are mostly tricolpate forms (average = 4.8%), with isolated common occurrences of monosulcate forms (633/2) and *Nothofagidites* (666/6).

A6.3.2 Summary of Haumurian palynofloras

Palynofloras of most Haumurian coals and dirty coals are dominated by variable proportions of *P. mawsonii* and Gleicheniaceae, and contain <c.10% angiosperm pollen. In contrast, floras of sediments fall in discrete compositional clusters. Some contain 20%–30% spores and 60%–70% gymnosperm pollen, whereas others contain >50% spores and up to 20% angiosperm pollen. The dominant gymnosperm form is *P. mawsonii,* and most spore floras in sediments are dominated by Sphagnaceae and Cyatheaceae. Those sediments containing dominant or elevated Cyatheaceae proportions, are also characterised by high spore and angiosperm diversity. Other distinctive Haumurian samples include 626/4, which contains a high proportion and diversity of angiosperm pollen and high *T. subgranulatus*, and 623/1, a coaly sediment which resembles a coal in floral character.

The trends in spore and pollen occurrence from coal to dirty coal to sediment are summarised in Table A6.5. Decline in total gymnosperm proportion from coal to sediment samples results from decreasing *P. mawsonii* proportion, whereas there is a slight increase in the abundance of other gymnosperm forms. There is a progressive increase in angiosperm diversity from coals to sediment samples, largely reflecting the increased abundance of angiosperms (Figure A6.2). Spore diversity is slightly higher in dirty coals (average = 11.5) than coals (average = 8.8) or sediment samples (average = 10.4).

Lithotype	Angio-sperms	Total gymnos.	*P. mawsonii*	Other gymnos.	Total spores	Gleich-eniaceae	Other spores	Total trilete*
Coal	**4.2** 5.4	**59.3** 6.3	47.5	11.8	**36.5** 8.8	18.8	17.6	3.7
Dirty coal	**8.9** 8.3	**44.1** 6.2	30.8	13.4	**47.0** 11.5	21.3	25.8	8.0
Sediment	**11.9** 10.7	**34.9** 6.6	16.8	18.1	**53.2** 10.4	9.9	37.4	21.6
Total	8.2	46.5	31.9	14.6	45.3	15.8	29.5	11.7

Table A6.5 Summary of average pollen and spore abundances (bold) and diversity, Haumurian samples. * total trilete = Cyatheaceae plus trilete forms, excluding Gleicheniaceae.

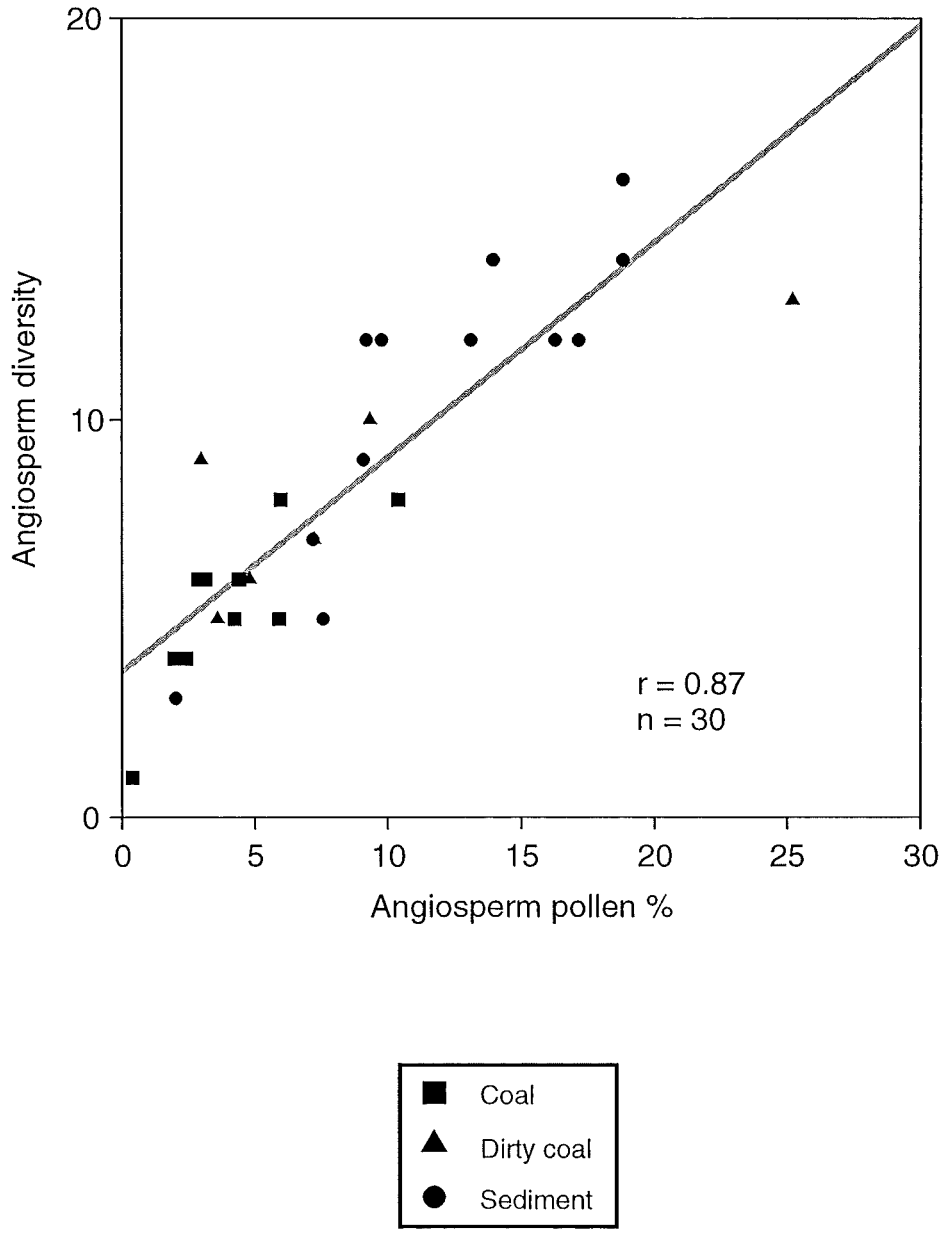

Figure A6.2 Angiosperm proportion vs. diversity, Haumurian samples

A6.3.3 Teurian palynofloras

Teurian samples consist of 22 sediments and 2 dirty coals. Clean coals were not sampled. The occurrence of angiosperm pollen, gymnosperm pollen and spores is summarised in Tables A6.6–A6.8 and Figure A6.3.

Pollen group	dirty coals (n = 2)	sediments (n = 22)
Monosulcate	**1** rare in 2	moderate in 666/1 & 667/3, rare in 7, trace in 9, absent from 4
Tricolpate	**1** moderate in 640/1, rare in 640/2	**2** moderate in 7, rare in 15
Tricolporate	rare in 640/2, trace in 640/1	trace in 4 only
Triorate	trace in 2	rare in 4, trace in 6, absent from 12
T. minor	trace in 2	**20** abundant in 13, common in 6, moderate in 1, rare in 2
Proteaceae	trace in 640/1	moderate in 666/3, rare in 10, trace in 7, absent from 4
Nothofagidites	absent	rare in 2, trace in 4, absent from 16
Other angiosperms	absent	rare in 5, trace in 6, absent from 11

Table A6.6 Summary of angiosperm pollen occurrence, Teurian samples. Bold numbers indicate the number of samples in which the group comprises the dominant angiosperm form (s).

Pollen group	dirty coals (n = 2)	sediments (n = 22)
P. mawsonii	**2** abundant in 2	**14** abundant in 6, common in 12, moderate in 2, rare in 2
Podocarpidites	common in 640/1, rare in 640/2	**5** abundant in 635/1 & 667/1, common in 7, moderate in 10, rare in 3
M. antarcticus	rare in 640/2, trace in 640/1	rare in 4, trace in 4, absent from 14
T. subgranulatus	common in 640/1, moderate in 640/2	moderate in 2, rare in 6, trace in 3, absent from 11
Araucariaceae	rare in 2	**3** abundant in 697/8, common in 4, moderate in 1, rare in 8, trace in 3, absent from 5
Other gymnosperms	rare in 2	rare in 13, trace in 1, absent from 8

Table A6.7 Summary of gymnosperm pollen occurrences, Teurian samples. Bold numbers indicate the number of samples in which the group comprises the dominant gymnosperm form(s).

Spore group	dirty coals (n = 2)	sediments (n = 22)
Gleicheniaceae	**1** abundant in 640/2, moderate in 640/1	**9** common in 7, moderate in 9, rare in 6
Sphagnaceae	**1** abundant in 640/1, common in 640/2	**3** common in 3, moderate in 6, rare in 7, trace in 2, absent from 4
Cyatheaceae	rare in 2	**3** abundant in 619/2, common in 6, moderate in 5, rare in 9, trace in 1
Trilete	trace in 2	**6** abundant in 635/2 & 667/3, common in 6, moderate in 3, rare in 9, trace in 2
Laevigatosporites	rare in 2	**1** common in 667/3, moderate in 11, rare in 10
Monolete	rare in 2	rare in 1340, trace in 6, absent from 15
Other spores	absent	rare in 3, trace in 4

Table A6.8 Summary of spore occurrences, Teurian samples. Bold numbers indicate the number of samples in which the group comprises the dominant spore form(s).

Teurian sediments: Teurian sediments (Figure A6.3, stars) are characterised by subequal proportions of spores and gymnosperm pollen (both average c. 35%) and a high proportion of angiosperm pollen, which ranges from 11.4% (636/1) to 47.0% (697/8), and averages 29.4%. 18 of the 22 samples contain >20% angiosperm pollen, and angiosperms contribute the greatest proportion of the palynoflora of three samples (697/6, 697/5, 667/1). Gymnosperm pollen are dominant in 10 samples, and spores in nine samples.

P. mawsonii is the dominant gymnosperm species (Figure A6.3A) in 16 samples (average = 17.0%), although other gymnosperm taxa collectively exceed the *P. mawsonii* proportion in 13 samples. *Podocarpidites* is the dominant gymnosperm genus in five samples, and Araucariaceae in three samples. Dominant gymnosperm form is independent of total gymnosperm proportion. Average gymnosperm diversity is 5.4 taxa.

Gleicheniaceae are the dominant spore taxa in nine samples (Figure A6.3B), trilete forms in six samples, and Cyatheaceae in three samples. Sphagnaceae are dominant in three samples (697/7, 697/5, 619/2). In all samples, non-gleicheniaceaen spores are present in greater amounts than Gleicheniaceae. There are no strong correlations between dominant spore taxa and proportions of angiosperm or gymnosperm pollen. Spore diversity ranges from 5 taxa (667/3) to 14 taxa (666/3), and the average is 8.9 taxa.

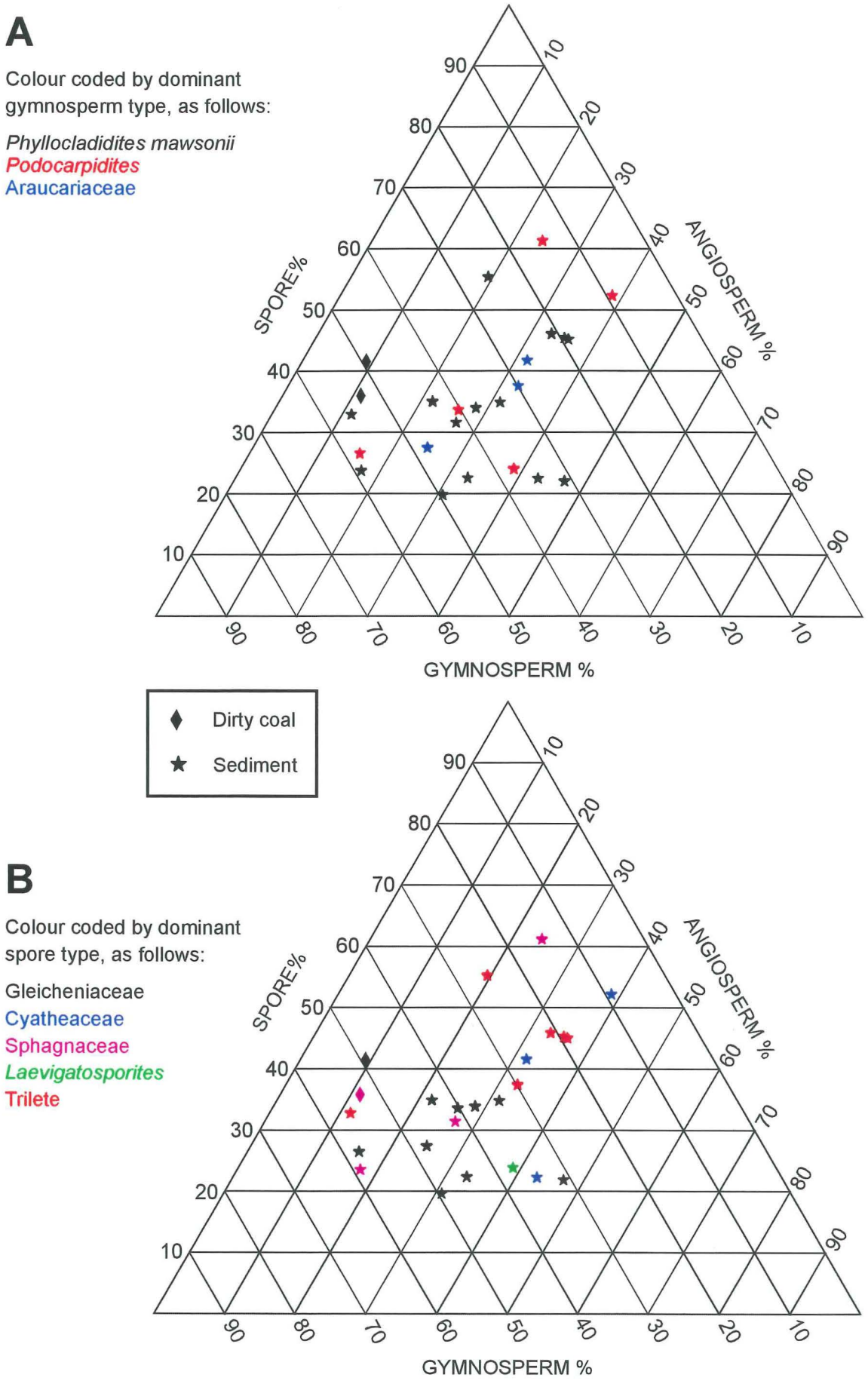

Figure A6.3 Ternary plot of pollen and spore proportions, all Teurian samples
A = colour coded by dominant gymnosperm type, B = colour coded by dominant spore type

The angiosperm flora in Teurian sediments is dominated by *Triorites minor*, which occurs in all samples (average = 21.3%), which varies from 3.1% (636/1) to 36.7% (697/6). Controls on the occurrence of *T. minor* are discussed in detail elsewhere (Appendix 5.x). Tricolpate forms are the dominant angiosperm pollen in 666/3 and 636/1, and are present in rare to moderate amounts in all samples. Moderate proportions of monosulcate forms are present in 666/1 and 667/3, and moderate Proteaceae in 666/3. Other angiosperms are rare to absent. Angiosperm diversity varies from three to 19 taxa, and averages 11.5 taxa.

Teurian dirty coals: The two Teurian coal samples (Figure A6.3, diamonds) are from the same upper Rewanui CMM seam in DH640 (640/1, 640/2). Ash contents are 21.8% and 8.1%, respectively, thus both samples are dirty coals. The gymnosperm proportion of both palynofloras is dominated by *P. mawsonii* (Figure A6.3A), though 640/1 also contains common *T. subgranulatus* and *Podocarpidites*. The spore component of 640/1 is dominated by Sphagnaceae, whereas Gleicheniaceae are dominant in 640/2. 640/1 contains a moderate amount of tricolpate angiosperms, and other angiosperm taxa are rare to absent in these samples. Sample 640/1 contains 14 angiosperm taxa, and 640/2 contains 9 taxa. Both samples contain 9 or 10 taxa each of gymnosperms and spores.

A6.3.4 Summary of Teurian palynofloras

Teurian palynofloras are summarised in Table A6.9. All Teurian samples contain >20% spores and <60% gymnosperm pollen, and most contain >10% angiosperm pollen (notably *T. minor*). Gleicheniaceae only occur as the dominant spore form where gymnosperm pollen exceeds 30%, and Cyatheaceae are dominant where gymnosperm pollen proportion is <c.35%. Sample 666/3 contains an atypical flora characterised high spore proportion, and the highest angiosperm diversity encountered in the present study (19 taxa).

Lithotype	Angio-sperms	*T. minor*	Total Gymnos.	*P. mawsonii*	Other gymnos.	Total spores	Gleich-eniaceae	Other spores
Dirty coal	**10.2** 11.5	**0.4**	**51.0** 8.5	**24.7**	**26.3**	**38.8** 10	**14.1**	**24.7**
Sediment	**29.4** 8.5	**21.3**	**35.3** 5.4	**17.0**	**18.3**	**35.3** 8.8	**8.1**	**27.1**
Total	**27.8**	**19.5**	**36.6**	**17.6**	**19.0**	**35.6**	**8.6**	**26.9**

Table A6.9 Summary of average pollen and spore abundances (bold) and total diversity, Teurian samples.

A6.3.5 Summary of Greymouth Coalfield palynofloras

Greymouth Coalfield palynofloras described in the present project comprise five floral associations (see below). No palynoflora contains >50% angiosperm pollen, whereas spores comprise c.20–80%, and gymnosperm pollen c.10–85%.

Association 1: Haumurian coals, and Haumurian and Teurian dirty coals, dominated by *P. mawsonii* and spores of Gleicheniaceae. Angiosperm pollen are rare, though slightly more abundant in Teurian than Haumurian floras.

Association 2: Haumurian sediments, similar in composition to Association 1, but with more abundant and diverse angiosperm pollen and more Sphagnaceae spores.

Association 3: Haumurian sediments, containing a high proportion of spores (dominantly Cyatheaceae) and high angiosperm diversity.

Association 4: Teurian sediments, containing abundant angiosperm pollen (notably *T. minor* and tricolpate forms). Gymnosperms are dominated by *P. mawsonii*, *Podocarpidites* and Araucariaceae, and spores by Gleicheniaceae, Sphagnaceae, Cyatheaceae, and trilete and monolete forms.

Association 5: As for Association 4 but with lower angiosperm diversity.

All floral associations are consistent with Southern Hemisphere Late Cretaceous and early Tertiary rain-forest vegetation (Askin & Spicer 1995). Differences between the associations reflect localised ecological conditions within the depositional environment (e.g. mire vs. non-mire settings), and changes in the vegetation which occurred across the KTB (see below). Comparison of Greymouth Coalfield palynofloras with correlative New Zealand and Southern Hemisphere material is discussed in Appendix 7.3.

A6.4 Floral change across the Cretaceous–Tertiary Boundary in Greymouth Coalfield

Differences between Haumurian and Teurian floras are readily apparent when pollen (angiosperm and gymnosperm) and spore proportions are plotted together (Figure A6.4). There is little overlap in the overall floral composition between the two ages of samples, and differences are discussed in detail below. In the following discussion, stratigraphic position refers to distance above or below the estimated KTB position (Table 6.1).

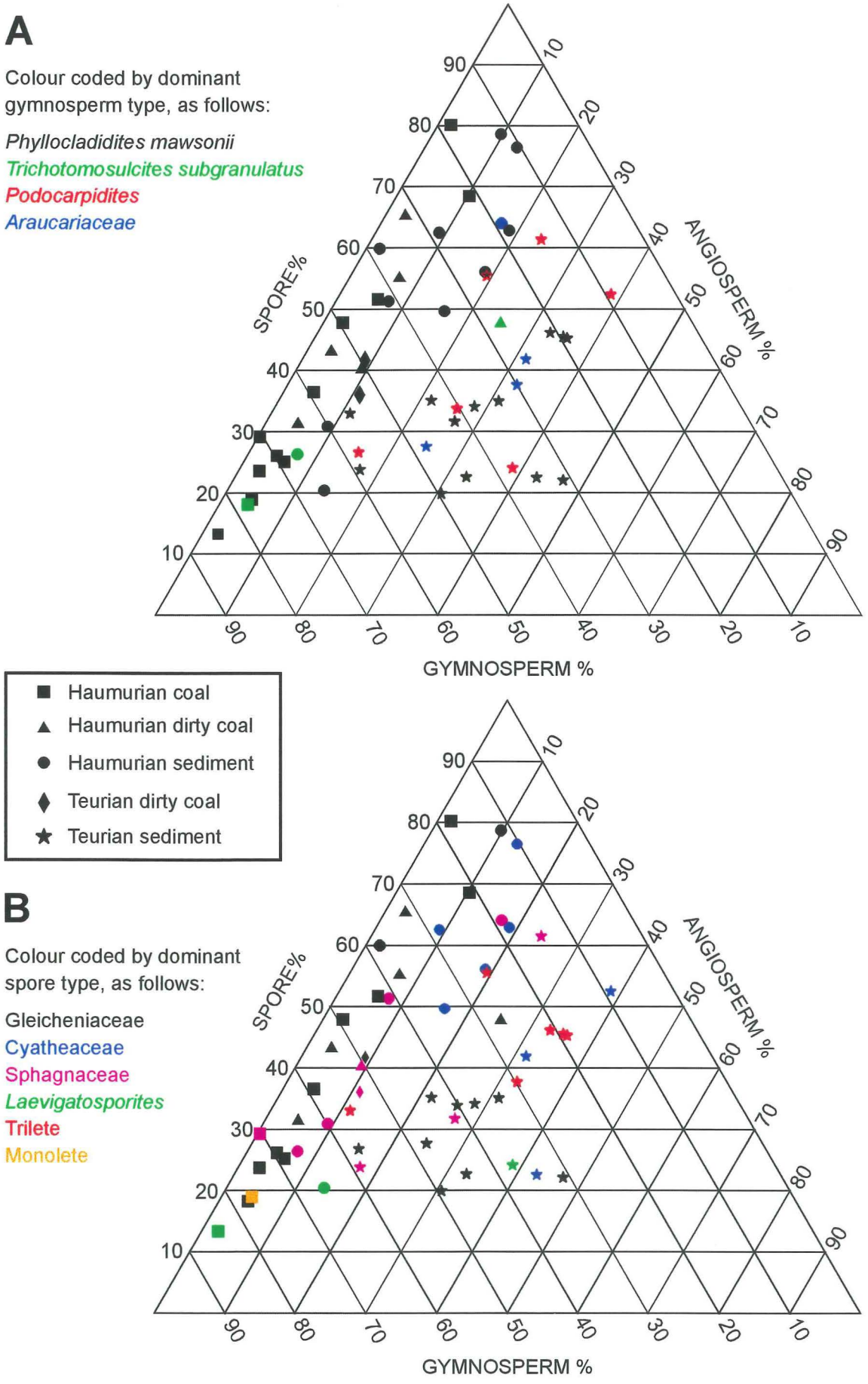

Figure A6.4 Ternary plot of pollen and spore proportions, all samples
A = colour coded by dominant gymnosperm type, B = colour coded by dominant spore type

A6.4.1 Angiosperm pollen

The proportion of angiosperm pollen in Teurian sediments exceeds 20% in 18/22 samples, and averages 29.4%, in contrast to the Haumurian average of 11.9%. Those Teurian sediment samples containing <20% angiosperms (635/1, 667/3, 636/1, 643/1) have similar overall palynofloral compositions to the Haumurian sediments with above average angiosperm proportion. In contrast, Teurian and Haumurian dirty coals contain similar proportions of angiosperm pollen.

There is a gradual change in angiosperm proportion with stratigraphic position (r = 0.76 for all sediment samples, and angiosperm proportion continues to increase for at least 30m above the KTB (Figure A6.5A). Although *T. minor* abundance exhibits the same overall relationship to stratigraphic position (Figure 8.5B), the identical correlation is coincidental, because *T. minor* occurrence always comprises <3% in Haumurian sediments, then abruptly increases to c.20% immediately above the KTB.

Diversity data for angiosperm pollen taxa in the study sample set are summarised in Table A6.10. Of the 43 identified angiosperm taxa, four are absent from Teurian samples and six are absent from Haumurian samples. Excluding the poorly represented Teurian dirty coals, the greatest collective number of angiosperm taxa (40) occurs in Teurian sediments, whereas Haumurian dirty coals contain the least (23). Maximum angiosperm diversity is present in Teurian sediments (up to 18 taxa), and Haumurian coals contain the fewest angiosperm taxa (6 taxa or less). Average angiosperm diversity is slightly higher in total Teurian samples than total Haumurian samples, though Haumurian sediments have the greatest average angiosperm diversity (excluding Teurian dirty coals).

Sample subset	Total angiosperm taxa present	Range of angiosperm taxa present	Average angiosperm diversity
All Teurian	**40**	**3 – 18**	**8.8**
Teurian sediments	40	3 – 18	8.5
Teurian dirty coals	17	9 – 14	11.5
All Haumurian	**38**	**1 – 16**	**7.9**
Haumurian sediments	34	3 – 16	10.3
Haumurian dirty coals	23	4 – 13	8.3
Haumurian coals	25	1 – 8	5.3

Table A6.10 Summary of angiosperm diversity and species occurrence, Greymouth Coalfield palynofloras.

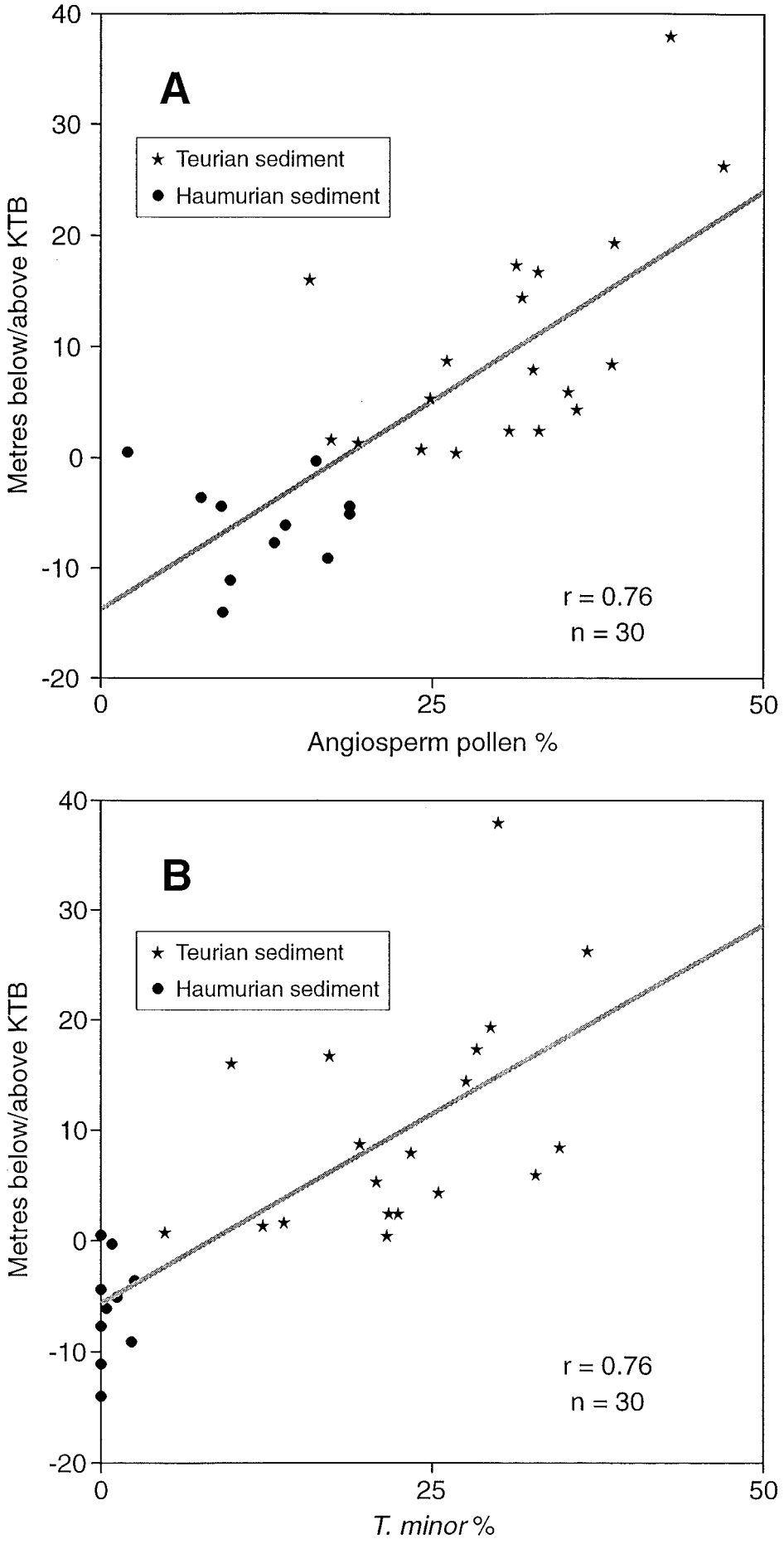

Figure A6.5 Relationship between angiosperm proportion (A) and *Triorites minor* proportion (B) and stratigraphic position, sediment samples

The relationship between angiosperm diversity (all samples) and stratigraphic position is illustrated in Figure A6.6A. Correlation between angiosperm diversity and stratigraphic position is poor. However, two populations of samples are evident in Figure A6.6A. Haumurian and earliest Teurian sediments (within 4m of the KTB) have variable angiosperm diversity (3–19 taxa), and there is no apparent correlation between diversity and stratigraphic position. A second population, of Teurian sediment samples which lie >4m above the KTB, exhibit a strong trend of increasing diversity with stratigraphic position above the KTB ($r = 0.83$). At c.4m above the KTB, angiosperm diversity declines abruptly to six or fewer taxa.

Angiosperm diversity trends across the KTB can be further determined by considering sediment samples alone and by distinguishing individual drillholes (Figure A6.6B). DH633, DH635 and DH666 define a pattern of increasing angiosperm diversity up to approximately the KTB, followed by rapid decline at c.4m above the KTB, and subsequent return of angiosperm taxa.. In contrast, angiosperm diversity in DH697 increases approximately linearly from the basal Rewanui CMM sample (697/9) to the uppermost of four Goldlight Fm, samples (697/5). No such trend is, however, apparent in DH619, though angiosperm diversity in this drillhole is similar to other drillholes spanning the same stratigraphic interval.

Angiosperm diversity suffered a rapid decline followed by recovery in the early Paleocene, but not precisely at the KTB. Possibly causes for diversity and abundance changes across the KTB are considered in Appendix 8.3.

A6.4.2 Gymnosperm pollen

Haumurian and Teurian sediment samples contain similar proportions of gymnosperm pollen, and there is no relationship between gymnosperm proportion and stratigraphic position (Figure A6.7A). The average occurrences of *P. mawsonii*, total other gymnosperms, and Araucariaceae differs by <0.5% between all Haumurian and Teurian samples. *Podocarpidites* pollen is more abundant in Teurian than Haumurian sediments (average = 10.8% vs. 6.2%), whereas the converse is true for *M. antarcticus* (0.4% vs. 1.5%) and *T. subgranulatus* (1.2% vs. 5.3%). Teurian dirty coals contain 7% more total gymnosperms, c.6% less *P. mawsonii* and c.13% more other gymnosperms than Haumurian dirty coals.

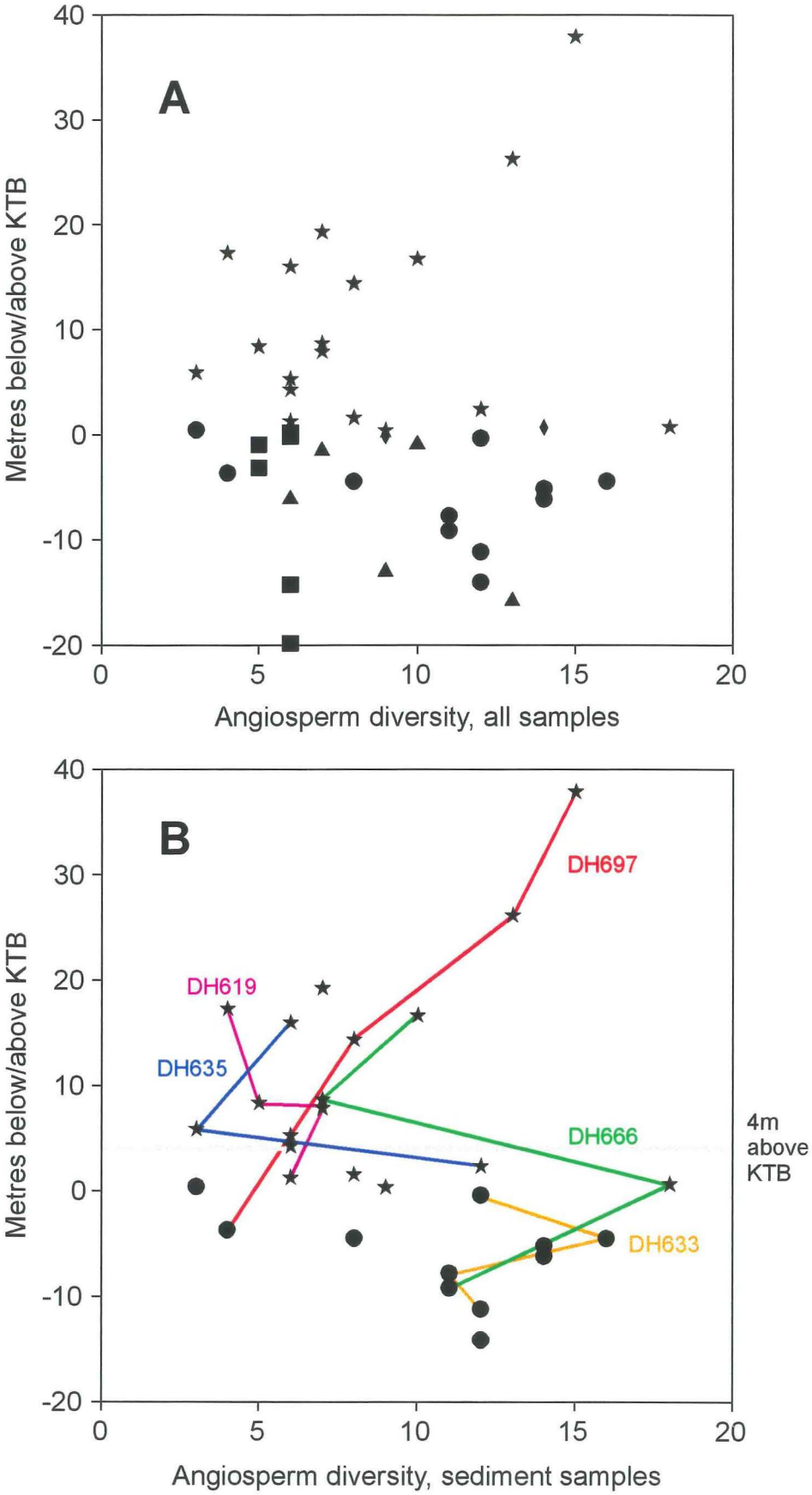

Figure A6.6 Angiosperm diversity vs. stratigraphic position (metres above or below KTB). A = all samples, B = sediments only. Drillholes discussed in text are indicated in colour in B. Symbols as in Figure A6.4

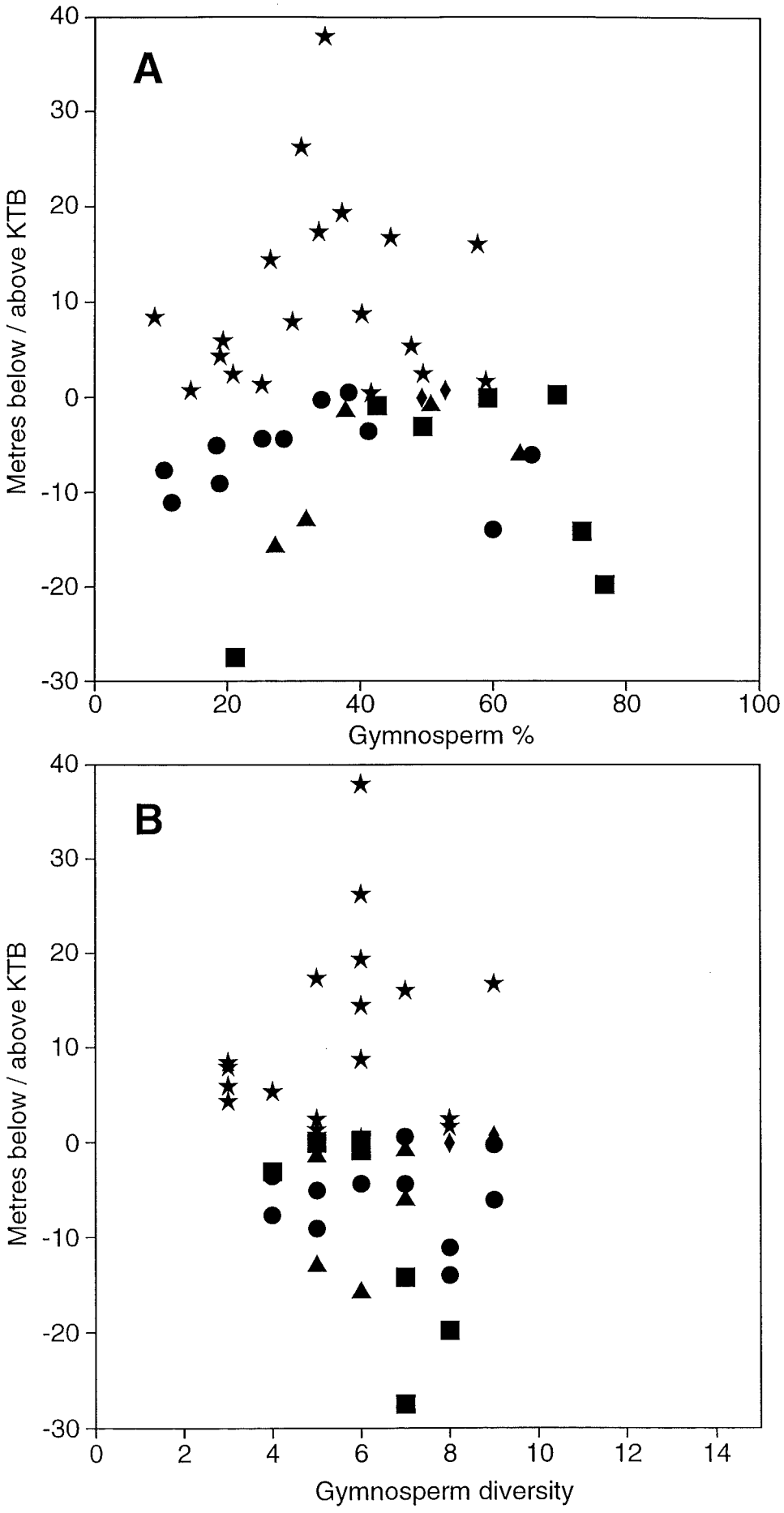

Figure A6.7 Gymnosperm proportion (A) and diversity (B) vs. stratigraphic position. Symbols as in Figure A6.4

Average gymnosperm diversity is slightly lower in Teurian sediments (5.4 taxa) than Haumurian sediments (6.6 taxa), and occurrences of the rare taxa *Dacrydiumites praecupressinoides* and *Ephedra notensis* are restricted to Haumurian sediments. All seven other gymnosperm forms occur in all lithologies and ages of samples. When plotted against stratigraphic position (Figure A6.7B), gymnosperm diversity exhibits no apparent trend, however minimum diversity is present in samples c.4–10m above the KTB, which corresponds to the interval containing minimum angiosperm diversity (Figure A6.6).

A6.4.3 Spores

The proportion of spores in Teurian sediment samples (average = 35.3%) is substantially less than in Haumurian sediments (average = 53.2%), and there is a modest negative relationship (r = -0.43) between spore proportion and stratigraphic position relative to the KTB (Figure A6.8A). Most of the decrease is accounted for by reduction in Cyatheaceae and Sphagnaceae abundance. Trilete spores (notably *T. verrucatus*, *T. tuberculiformis,* and *T. microfoveolatus*) are more abundant in Teurian sediments. There are similar amounts of *Laevigatosporites* in both Haumurian and Teurian sediment samples, however other monolete forms (notably *Peromonolites* spp.) are only a trace component of Teurian sediments. Similar amounts of Gleicheniaceae occur in both ages of sediments, though they comprise the dominant spore form in more Teurian than Haumurian samples (see Tables A6.3 and A6.7). The two Teurian dirty coals contain c.8% fewer total spores than Haumurian dirty coals, though Gleicheniaceae proportions are similar, and Sphagnaceae spores are c.13% more abundant.

Average spore diversity declines slightly across the KTB (Tables A6.4, A6.8), however there is no notable reduction in spore diversity in the 10m interval above the KTB (Figure A6.8B). Of the 33 counted spore taxa, five are restricted to Teurian samples: *T. microfoveolatus* (in 5 samples), and *Peromonolites densus*, *Polypodiites cf. minima*, *R. mallatus* and *C. equalis* (in 1 sample each). Two uncommon forms, *Leptolepidites* and *Trilites sinuatus*, are restricted to Haumurian samples. There are, therefore, at least 23 spore taxa common to both Teurian and Haumurian sediments, however average spore diversity is lower in Teurian sediment (8.9 taxa vs. 10.5 taxa).

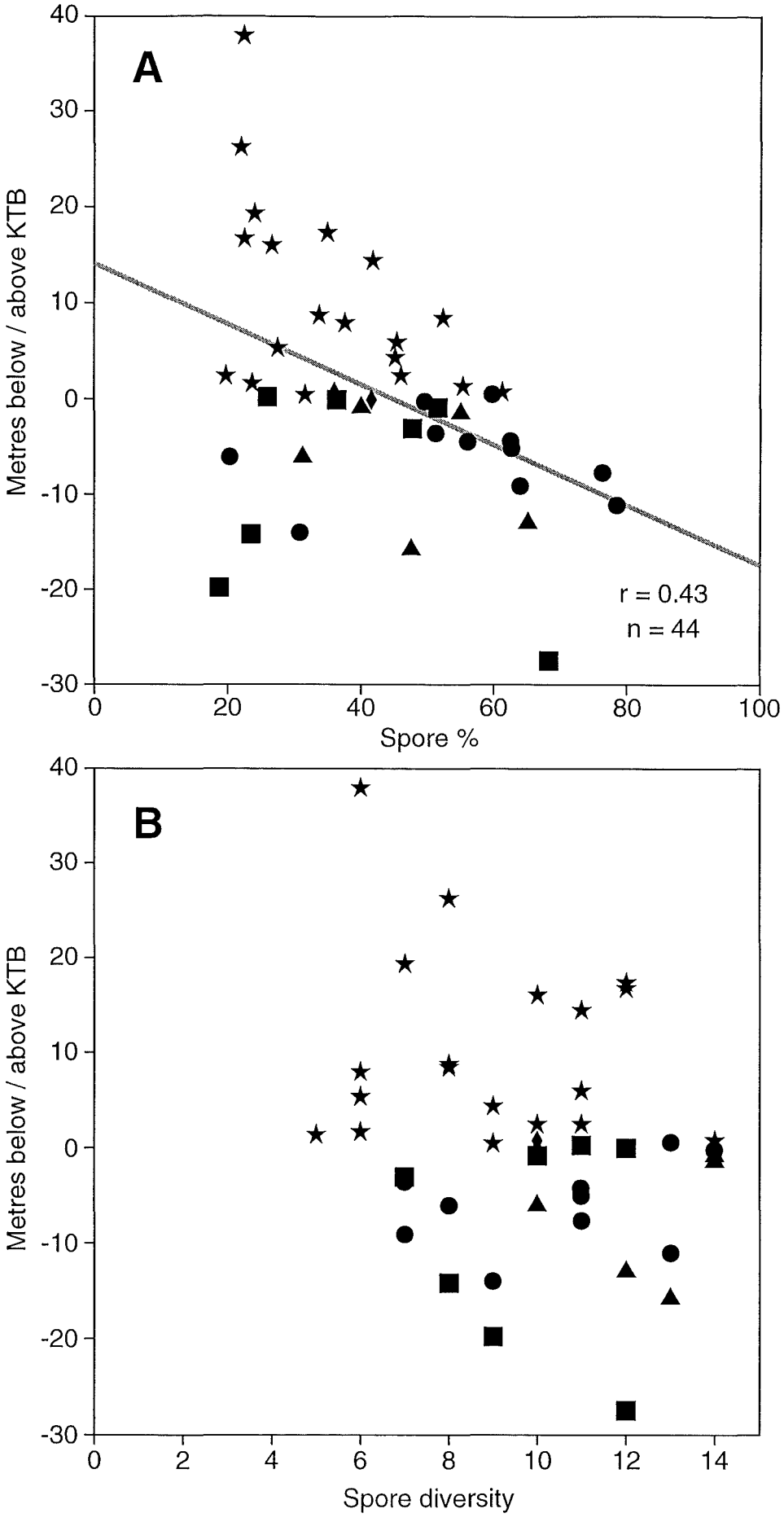

Figure A6.8 Spore proportion (A) and diversity (B) vs. stratigraphic position. Symbols as in Figure A6.4

A6.5 Summary

Floral change across the KTB in Greymouth Coalfield (summarised in Table A6.11) is characterised by a continuum of changing floral composition, whereby there is an increase in angiosperm proportion (especially *Triorites minor*) in Teurian samples at the expense of the spore component of the flora. First appearances of taxa outnumber last appearances (11 vs. 8), though most taxa which have first or last appearances at the KTB are rare/trace components of the flora. Of the four angiosperm taxa which became extinct at the KTB, three (*Beaupreaidites*, *T. lilliei*, *Tricolpites* sp. F) are large and/or ornamented forms.

	Angiosperms	Gymnosperms	Spores
PM3	High *T. minor* *T. secarius* usually present FAD of: *N. waipawaensis** *M. harrisii** Myrtaceae# *Q. brossus** polyorate# inaperturate* Increase in diversity after initial rapid decline above the KTB	Fewer *Podocarpidites* Araucariaceae More *M. antarcticus*, *T. subgranulatus* Slight decline in diversity especially 4- 10m above KTB	Fewer Sphagnaceae Cyatheaceae *Peromonolites* spp. More trilete FAD of: *T. microfoveolatus* *P. densus** *Polypodiites cf. minima** *R. mallatus** *C. equalis** Slight decline in diversity
	⇧	≈	⇩
PM2	*T. secarius* only in atypical floras LAD of: *T. lilliei* *Beaupreaidites* n.sp. *Tricolpites* sp. F *G. rudata**	LAD of: *D. praecupressinoides* *E. notensis**	LAD of: *Leptolepidites** *T. sinuatus**

Table A6.11 Summary of floral events across the KTB, Greymouth Coalfield. FAD = first appearance datum, LAD = last appearance datum. Arrows indicate direction of overall increase. There is little change in gymnosperm proportion across the KTB. Taxa marked * occur in one sample, those marked # occur in two samples.

There is no change in the average proportion of *P. mawsonii*, total other gymnosperms, or Araucariaceae across the KTB, though there are more *Podocarpidites* pollen and fewer *T. subgranulatus* and *M. antarcticus* in the Teurian. Gleicheniaceae abundance is also unaffected at the KTB, though other spores (Sphagnaceae, Cyatheaceae, *Peromonolites*) are less common in Teurian samples. A slight decline in average total diversity is evident between Haumurian and Teurian sediment samples (total taxa 27.8 vs. 23.0), though more taxa are present above the KTB. Angiosperm diversity declines very rapidly, and gymnosperm diversity slightly, in the earliest Teurian, however both indicators recover within c.10m above the KTB. Total Haumurian and Teurian average diversity for all pollen and spores present in all lithologies of samples is identical (23.5 taxa).

Appendix 7. Comparison of Greymouth palynofloras with other New Zealand and Southern Hemisphere palynofloras

A7.1 Introduction

The objectives of this review were

- to summarise all available palynological results from Greymouth Coalfield
- to define "typical" Haumurian and Teurian floras for the various sample lithotypes
- to compare Greymouth palynofloras with those of correlative deposits elsewhere in the South Island of New Zealand, and to identify regional differences in palynofloras
- to review palynofloral change at KTB localities throughout New Zealand and the Southern Hemisphere
- to estimate the significance of KTB floral change at Greymouth Coalfield.

Interpretation of the palynofloras is discussed in Appendix 8, and applications of this review to basin analysis within Greymouth Coalfield are presented in Chapter 6.

A7.2 Summary of Greymouth Coalfield palynofloras

A total of 335 samples with counted pollen and spore data are available for Greymouth Coalfield. Data comprise the present study (Appendix 6), 14 coals reported in Ward et al. (1995), unpublished data from Raine and Warnes for DH631 and 632 (Table A5.1), four analyses of miscellaneous coals (data in Appendix 14), and 242 samples from 12 drillholes analysed by Moore (1996a). Qualitative information is also available for Teurian–Kaiatan strata from selected sections in Greymouth Coalfield (Raine in Newman 1985, Appendix 3).

Moore (1996a) focussed on determining palynological and macroscopic banding profiles of coal seams in the central Rapahoe Sector as an aid to seam correlation, using the techniques developed in Ward et al. (1995). All samples analysed are Haumurian, and data comprise proportions of angiosperm pollen, gymnosperm pollen, spores, *P. mawsonii* and Gleicheniaceae abundance. Data from Moore (1996a) are summarised in Table A7.1 and Figure A7.1. Lithologies were assigned according to proximate analyses, with dirty coal containing 10–50% ash and sediments >50% ash.

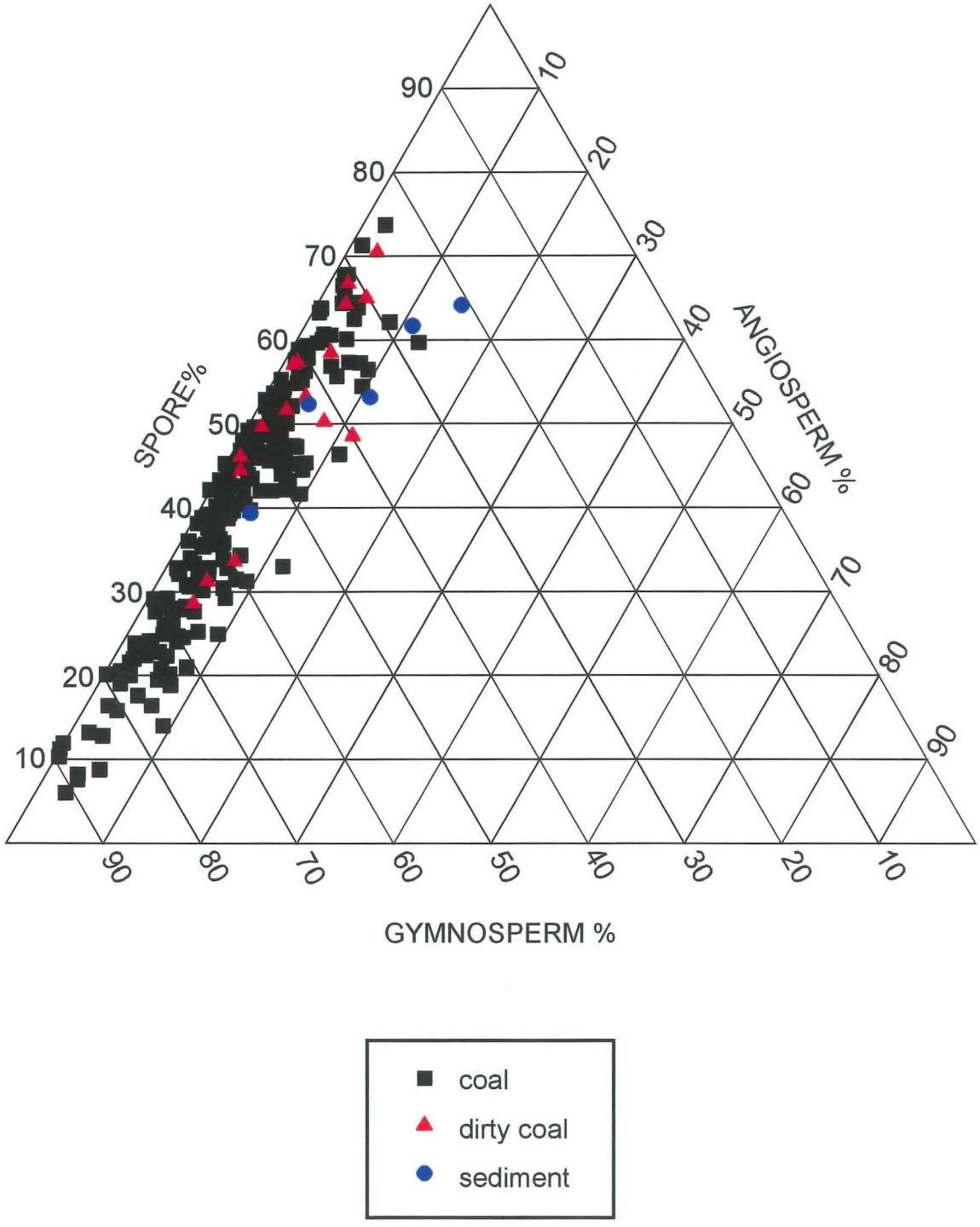

Figure A7.1 Summary palynology data, Rapahoe Sector Haumurian coal, dirty coal and sediments. From Moore (1996a).

Lithotype	Angiosperm %	Gymnosperm %	*P. mawsonii* %	Spore %	Gleicheniaceae %
Coal n = 220	3.5 0–12.8	56.3	53.0 24.0–83.7	40.3	9.6 0–50.4
Dirty coal n = 17	4.1 1.2–11.6	44.4	43.2 29.2–70.4	51.5	4.8 0–32.1
Sediment n = 5	9.6 5.1–15.0	36.3	34.9 15.8–55.4	54.1	2.3 0–8.0

Table A7.1 Summary of Rapahoe Sector Haumurian palynofloras, Moore (1996a). Abundance ranges are indicated for angiosperm %, *P. mawsonii* and Gleicheniaceae.

Findings from Moore (1996a) concur with those of the present study (Appendix 6.3.2). Samples of dirty coals and coal have similar floras, whereas most sediments contain a lower proportion of gymnosperm pollen. Moore (1996a) records a lower proportion of Gleicheniaceae in all sample groups than indicated by the present study, and maximum occurrence of these spores is restricted to the uppermost portions of the Rapahoe Sector "Main" seam. Angiosperms are generally <10%, and average abundance increases from coals to dirty coals to sediments, as described above in the present study (Appendix 6.3.2). Moore did not assess angiosperm diversity.

All palynology data for Greymouth Coalfield are shown on Figure A7.2A–D. Fields (coloured areas) are drawn around the major clusters of floral composition, and these fields are used for subsequent comparisons with palynofloras from other localities. Average composition of the various sample groups is summarised in Table A7.2.

Age/lithology	Angiosperm %	Gymnosperm %	*P. mawsonii* %	Spore %	Gleicheniaceae %
Haumurian coal n = 250	3.9	55.7	51.7 (10.5–78.0)	40.6	10.8 (0.8-60.8)
Haumurian dirty coal n = 23	5.3	44.4	40.0 (5.2–54.4)	50.3	9.1 (10.5–33.1)
Haumurian sediment n = 24	11.7	34.4	18.5 (3.4–40.7)	53.9	7.4 (1.5–14.9)
Teurian coal/dirty coal n = 4	7.0	60.2	44.0 (20.0–67.6)	32.8	17.6 (7.6–27.2)
Teurian sediment n = 34	25.9	41.8	18.2 (3.6–36.4)	32.3	7.0 (2.3–10.0)

Table 9.2 Summary of all palynology data, Greymouth Coalfield.

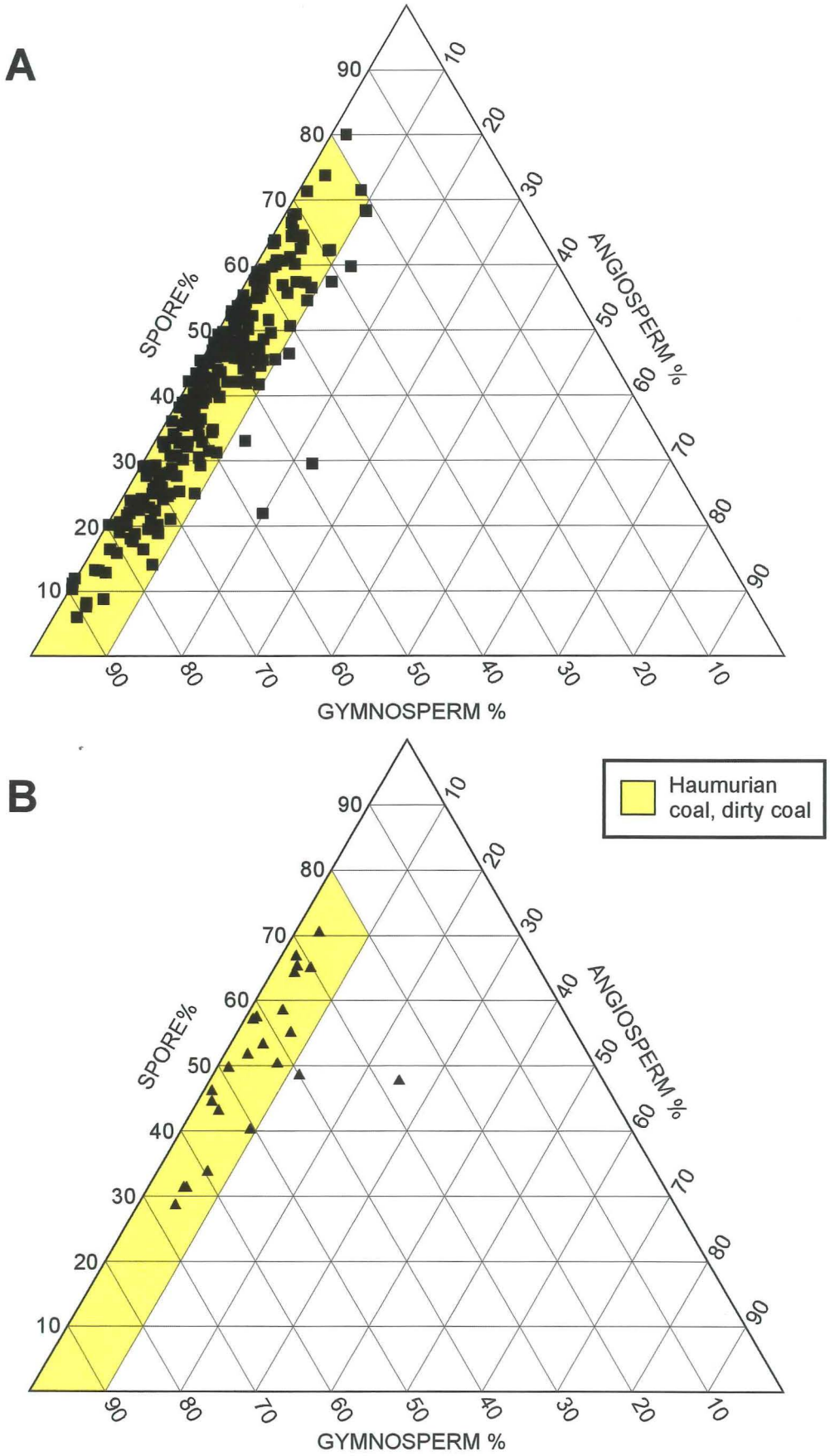

Figure A7.2 Summary palynology of Greymouth samples.
A = all Greymouth Haumurian (Zone PM2) coal.
B = all Greymouth Haumurian (Zone PM2) dirty coal.
Coloured area is field of typical palynofloras for sample group.

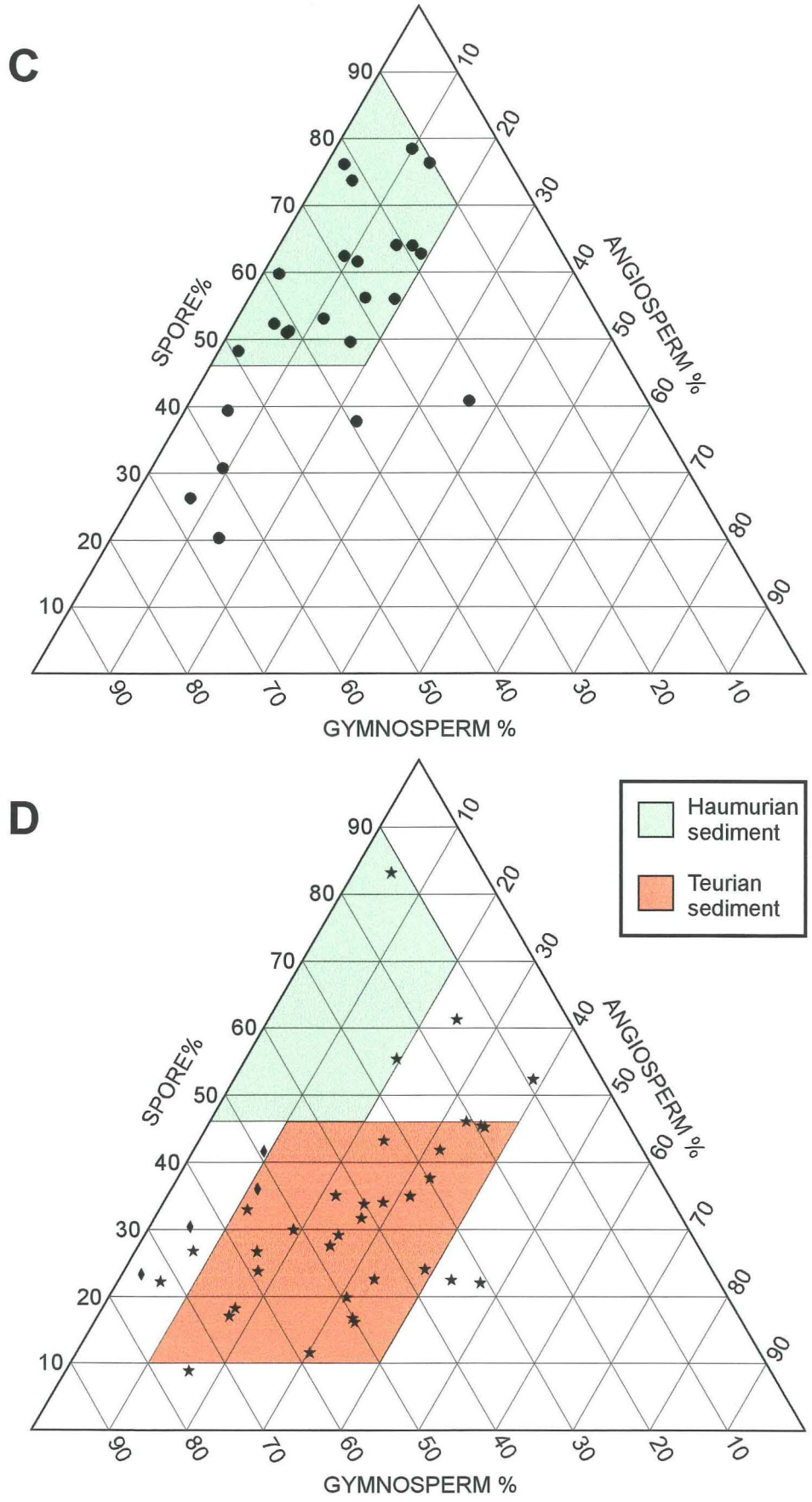

Figure A7.2 (cont.) Summary palynology of Greymouth samples.
C = All Greymouth Haumurian (Zone PM2) sediment samples.
D = all Greymouth Teurian (Zone PM3) coal/dirty coal and sediment samples.

Inclusion of all material reinforces conclusions from the present study (Appendix 6.3.5). Haumurian coal floras plot in a distinct cluster on Figure A7.2, and all but seven contain <10% angiosperm pollen. Two coals (UCP 1356, 1357) contain c.20% angiosperms, and the taxa present are indicative of a mire–marginal setting (Ward et al. 1995). Haumurian dirty coal floras plot within the same area as coals (Figure A7.2B), with the exception of two samples (UCP1326, 1399) with elevated angiosperm proportion. Teurian coals and dirty coals have similar palynofloras to Haumurian coals.

The majority (80%) of Haumurian sediment palynofloras contain <20% angiosperms, >45% spores and 10–50% gymnosperms (Figure A7.2C). Six sediment floras lie outside the field defined by these proportions, and all are from coaly and carbonaceous lithologies. Four have floras similar to Haumurian coals, and the remaining two (UCP1221, 1224) contain an atypically high proportion (>20%) of angiosperm pollen (notably *T. lilliei*, *N. kaitangataensis* and *Beaupreaidites* sp.).

Floral compositions of Teurian sediments are distinct from other samples, generally containing more angiosperm pollen (notably *Triorites minor*) and fewer spores. Data for Teurian sediments from Raine (pers. comm. 1989) and Warnes (pers. comm. 1992) indicate greater floral compositional variety than observed in the present study. Two Teurian sediment samples (from DH631) contain <10% angiosperms, which may reflect processing bias (Appendix 5.4.2). Only atypical Haumurian sediment, dirty coal and coal samples with high angiosperm proportions (Figure A7.2A,B,C), plot in the area of Teurian sediments on Figure A7.2D.

Palynofloras dominated by *T. minor* and gymnosperm pollen and lacking *Nothofagidites* persist throughout Zone PM3 (Teurian–early Waipawan) sediments of the Dunollie Fm. at Greymouth Coalfield (Raine, in Newman 1985, Appendix 3). However, quantitative information, with which to make a full comparison with the present data set, is unavailable for these samples.

A7.3 Comparison of Greymouth Coalfield palynofloras with other New Zealand Haumurian and Teurian floras

A7.3.1 Introduction

There is no comprehensive account of New Zealand Haumurian or Teurian palynofloras, and available literature concentrates on aspects of palynostratigraphy (e.g. Raine 1984) or paleobiogeography (e.g. Mildenhall 1980). Palynomorph occurrence information is generally limited to the presence and/or abundance of biostratigraphically useful taxa. In order to compare Greymouth Coalfield palynofloras with those of other localities, quantitative data (i.e. counts for all taxa, or major components) must be available.

There are detailed published analyses of selected palynofloras from Ohai Coalfield (Couper, in Bowen 1964), Mt. Somers (Raine & Wilson 1988), and Greymouth Coalfield (Ward et al. 1995). Otherwise published material is limited to a few samples (e.g. Bal 1994; Shearer & Moore 1994). In contrast, there is a large body of unpublished palynological data (>400 samples) residing in theses and unpublished or limited-circulation reports completed by researchers within the Department of Geological Sciences, University of Canterbury. Data sources are summarised in Table A7.3, and locations are indicated in Figure A7.3.

A total of 421 samples from localities other than Greymouth Coalfield has been assembled for this review. All pollen and spore occurrence data have been collated and angiosperm, gymnosperm and spore proportions were recalculated to 100% to correct for the inclusion of dinoflagellates, algae and fungi in some original counts. Where data were available, proportions of *P. mawsonii* and Gleicheniaceae have been determined. Comparisons with Greymouth Coalfield material are made using average abundance and diversity information, ternary plots, and the fields of typical Greymouth floral compositions, as defined above. Additional preliminary (qualitative) data are available for some localities, and these are discussed where relevant.

Location	Source	Intention of project	No. of samples
OHAI (Southland)	Couper in Bowen 1964 (Appendix 2)	Zonation of Morley CM, distinction of Beaumont CM from Morely CM	87
	Browne, unpublished report, 1986a	Application of Couper scheme	9
	Warnes, M.Sc. thesis 1988	Refinement of Couper scheme, establishment of new correlations	93
	Ward, B.Sc. (Hons.) project 1990*	Distinction of Morley and Beaumont CM	7
	Warnes, unpublished report, 1992; also in Shearer (1992, Appendix L)	Analysis of coal-forming vs. floodplain flora	112
KAITANGATA (Otago)	Browne, M.Sc. thesis 1986b Browne, unpublished report (MoE) 1987 Browne & MacKinnon 1989	Palynostratigraphy, location of KTB	79
	Crouch, unpublished report (IGNS) 1994	Review of Browne palynostratigraphy	–
	Raine, unpublished report (IGNS) 1994b	Palynology of outcrop material	–
	Ward, unpublished results 1996	floral analysis, palynostratigraphy	–
PIKE RIVER (Westland)	Raine 1984; Newman 1985, Figure 9	Palynostratigraphy	–
	Ward in Ferguson M.Sc. thesis 1993, Appendix 1*	Palynostratigraphy, coal-forming flora	8
PAKAWAU (Northwest Nelson)	Raine, unpublished report (NZGS) 1989	Palynostratigraphy	–
	Warnes in Bal B.Sc. (Hons.) thesis 1992, Appendix C*; Bal 1994	Palynostratigraphy, marine vs. non-marine	9
	Warnes in Kennedy M.Sc. thesis 1993, Appendix E*	Palynostratigraphy, floral analysis	7
	Ward, unpublished scan data, 1996 (in support of Stark (1996) M.Sc. thesis)*	Palynostratigraphy	–
Mt. SOMERS (Canterbury)	Raine & Wilson 1988	Palynostratigraphy, environment and climate	9
GREY RIVER (Canterbury)	Raine, unpublished report (NZGS), 1979	Palynostratigraphy	–

Table A7.2 Palynological data sources, South Island, New Zealand Late Cretaceous and early Tertiary coal measure sequences. Unless otherwise indicated, all unpublished sources are from Department of Geological Sciences, UoC. Other sources as follows:

NZGS = New Zealand Geological Survey (now IGNS)
IGNS = Institute of Geological and Nuclear Sciences Ltd.
MoE = Resource Management and Mining Group, Ministry of Energy (now Resource Information, Ministry of Commerce).

* indicates data were compiled from original count or scan records held in archive.

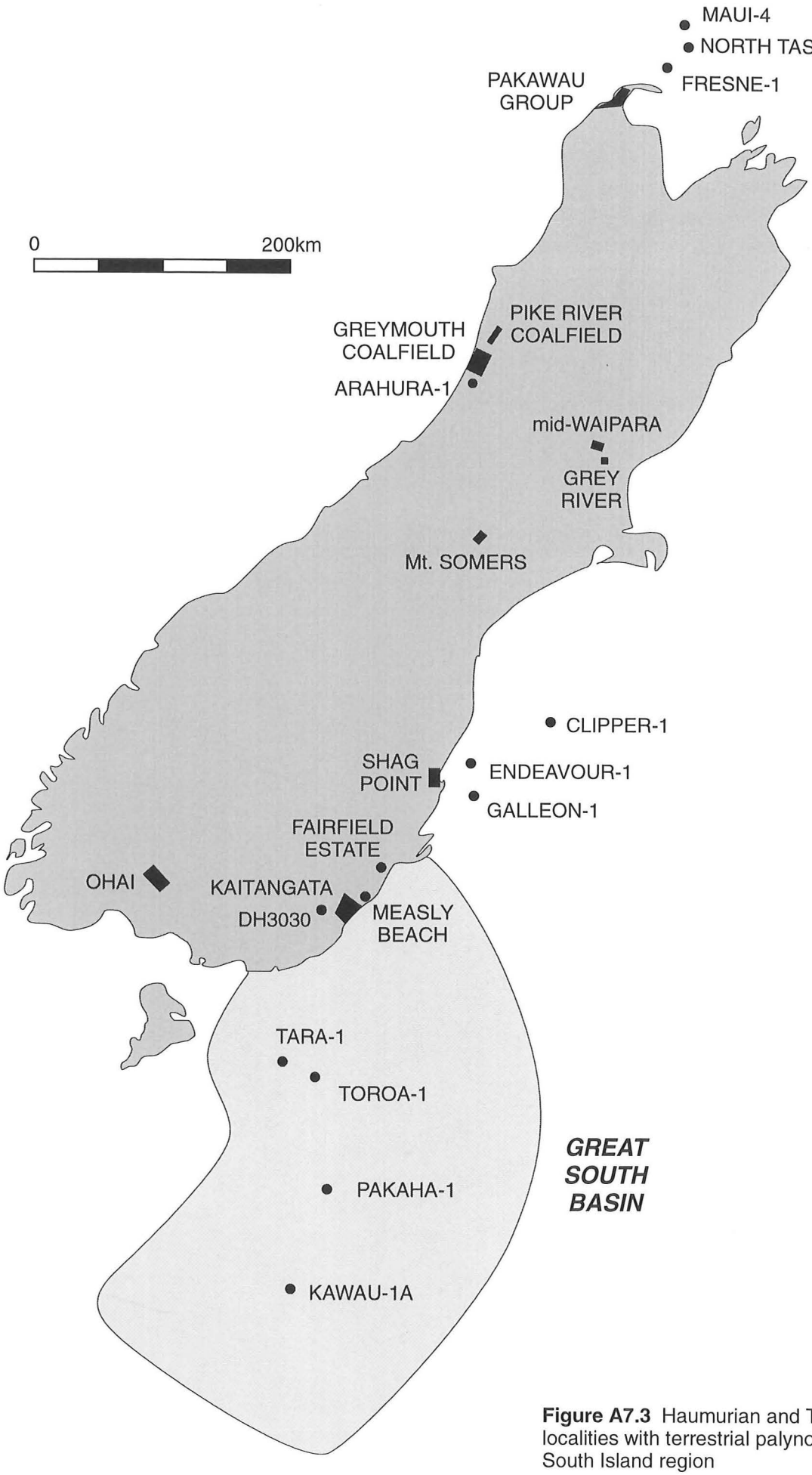

Figure A7.3 Haumurian and Teurian localities with terrestrial palynology, South Island region

A7.3.2 Ohai Coalfield

Palynological investigations at Ohai Coalfield (Southland) have addressed Haumurian zonation, distinction of Haumurian Morley Coal Measures from Bortonian–Runangan (Mid–Late Eocene) Beaumont Coal Measures, and analysis of coal-forming and regional vegetation. All data prior to 1992 were obtained from sediment samples, whereas Warnes (1992) utilised coals and associated sediments from eight mostly thick and clean seams. Dirty coals are those containing >10% ash (dry basis), and were identified from proximate analyses presented in Shearer (1992, Appendix D).

Warnes (1992) determined the proportion of *P. mawsonii* by an initial count of 250 palynomorphs (Pollen Sum 1), then recorded a further 250 pollen grains or spores, excluding *P. mawsonii* (Pollen Sum 2). Pollen Sum 2 enabled the occurrence of less abundant taxa to be quantified where *P. mawsonii* was overwhelmingly dominant. In this analysis, Pollen Sums 1 and 2 were recombined to give the overall proportion of angiosperms, gymnosperms, and spores.

All recent data from Ohai Coalfield are presented in Figures A7.4A–D and summarised in Table A7.4. As at Greymouth Coalfield, angiosperm pollen proportion increases from coals to dirty coals to sediments. Overall, angiosperm pollen are more abundant at Ohai than Greymouth Coalfield (Table A7.2).

Lithotype/data source	Angiosperm %	Gymnosperm %	*P. mawsonii* %	Spore %	Gleicheniaceae %
Coal (n = 69) Warnes 1992	11.5	64.7	44.8 (0.8–88.4)	23.8	3.7 (0–15.1)
Dirty coal (n = 21) Warnes 1992	18.4	53.2	30.3 (4.8–92.4)	28.4	1.6 (0–5.8)
Sediment (n = 131) Browne 1987; Warnes 1988, 1992 Ward 1990	33.2	34.8	11.7* (0–67.5)	32.0	1.0* (0–12.2)
Sediment (n = 87) Couper 1964	27.9	63.4	36.2** (16–64)	8.7	0.8** (0.8-8.8)

Table A7.4 Summary of Haumurian palynology data, Ohai Coalfield.
% range for *P. mawsonii* and Gleicheniaceae given in parentheses.
Notes: * does not include data from Ward (1990).
** *P. mawsonii* count from Couper (in Bowen 1964) includes *Dacrydiumites ruei* for 67 samples.

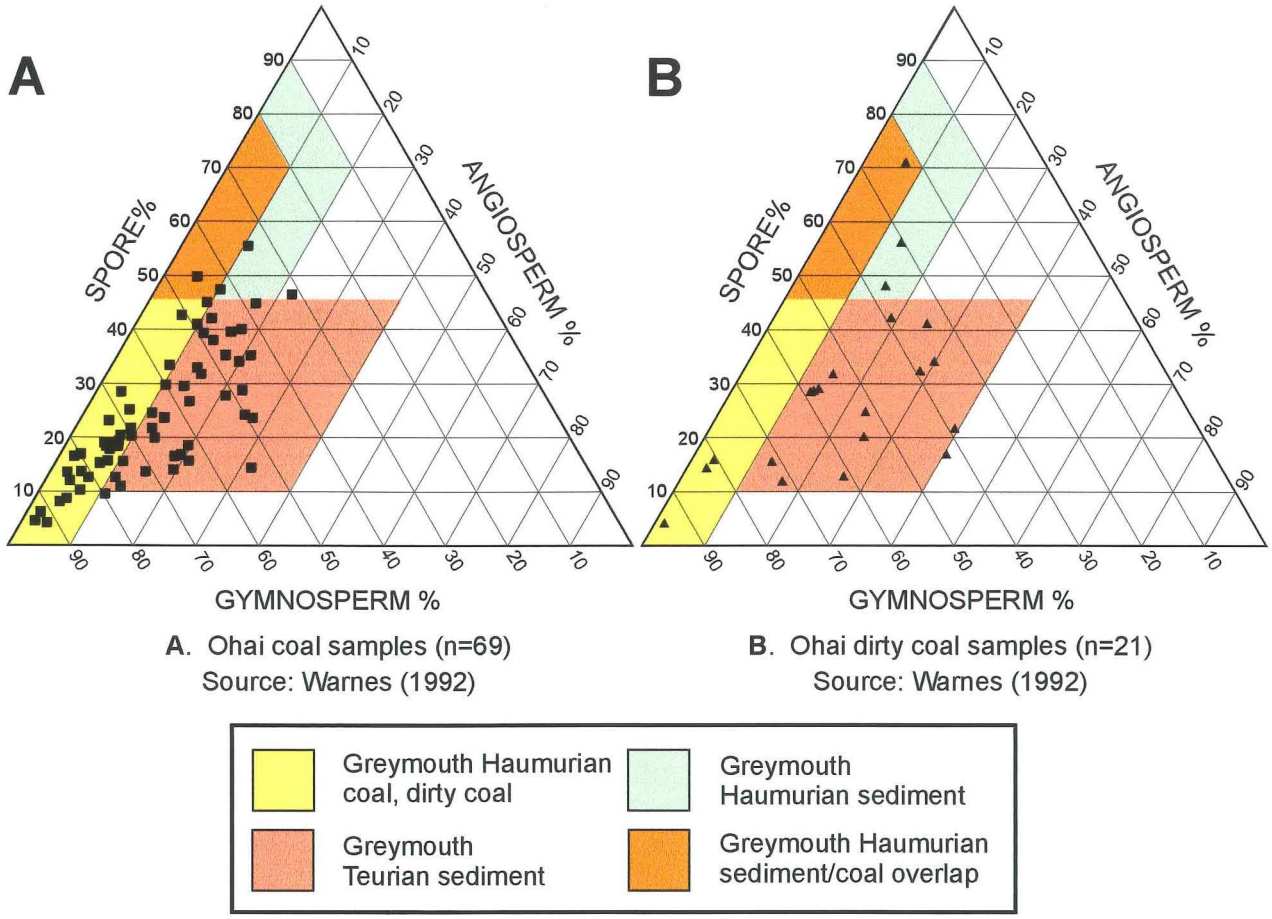

A. Ohai coal samples (n=69)
Source: Warnes (1992)

B. Ohai dirty coal samples (n=21)
Source: Warnes (1992)

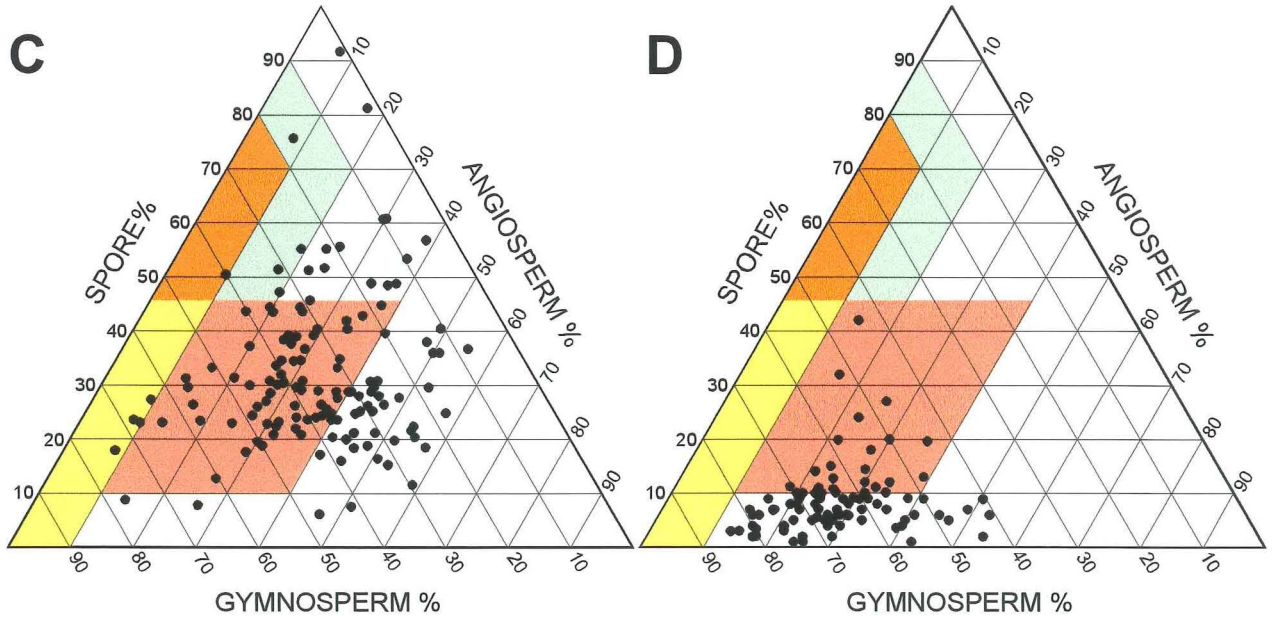

C. Ohai sediment samples (n=131)
Sources: Browne (1986a),
Warnes (1988, 1992), Ward (1990)

D. Ohai sediment samples (n=87)
Source: Couper *in* Bowen (1964)

Figure A7.4 Summary palynology data,
Haumurian Morley Coal Measures, Ohai Coalfield.
Average Greymouth fields shown for comparison.

Analyses by Couper (in Bowen 1964) contain fewer spores and more gymnosperm pollen than any subsequent determinations from Ohai sediment samples (Figure A7.4D). Couper also presented combined abundance data for *P. mawsonii* and *Dacrydiumites ruei* for 67 samples, and for these reasons, the data are reported here but excluded from the average sediment flora calculations.

Coal (Figure A7.4A): Ohai coals with a low proportion of angiosperms (<10%) and spores (<30%) have similar floral compositions to Greymouth Haumurian coals. However, as spore proportion increases in Ohai coals, angiosperm pollen proportion also increases. Tricolpate pollen are the dominant angiosperm forms in these coals, with lesser monosulcate pollen and Proteaceae, and *Triorites minor* is absent. Similar compositions are only present in the two mire-margin coals from Greymouth (Section 9.2). Ohai coal floras are also distinguished from Greymouth coals by the absence of high (>60%) spore proportions, and the presence of very high (>80%) gymnosperm proportions in 12 samples.

The differences between Ohai and Greymouth coals are reflected in the average composition values (Table A7.4), with Ohai material containing a greater proportion of angiosperm pollen and gymnosperm pollen and fewer spores than Greymouth coals. *P. mawsonii* is more abundant, and Gleicheniaceae much less abundant at Ohai Coalfield.

Dirty coal (Figure A7.4B): Dirty coals from Ohai Coalfield overlap in floral composition with coals. All but four dirty coals contain >10% angiosperm pollen, in contrast to Greymouth material which generally contains <10% angiosperm pollen. Dirty coals from both localities contain the same proportion of *P. mawsonii*, but Gleicheniaceae spores are much less abundant at Ohai.

Sediments (Figure A7.4C): Pollen and spore proportions in Ohai sediment samples are variable, though non contains >60% angiosperm pollen. The majority of samples contain more angiosperm pollen and fewer spores (including Gleicheniaceae) than Greymouth sediment samples, and only five Ohai samples plot within the Greymouth Haumurian sediment field. However, there are samples with high (>60%) gymnosperm pollen at both Ohai and Greymouth (which resemble coal floras), and the abundance of *P. mawsonii* is similar at both localities.

A7.3.3 Kaitangata Coalfield

Drillhole material from paralic coal measures (Taratu Fm.) of the Kaitangata Coalfield in southeastern Otago has been investigated palynologically by Browne (Browne 1986b, 1987; Browne & MacKinnon 1989). Data comprise full count information from Browne (1986b, also Browne and MacKinnon 1989), and summary and selected abundance data from Browne (1987). Raine (1994b) presented occurrence (but not abundance) data for Haumurian outcrop samples. Thus far, palynomorph assemblages have been described in detail only from sediment samples. Preliminary data for three samples from a thick, clean coal seam of probable Haumurian age suggests coal-forming floras at Kaitangata Coalfield contained similar floral components to Greymouth coals (e.g. common *P. mawsonii*) except that angiosperm pollen (notably Proteaceae) are common–abundant, and spores relatively rare.

The overall floral composition of all Kaitangata samples is presented in Figure A7.5 and summarised in Table A7.5. Teurian samples have been selected in accordance with the re-evaluation of the KTB position in DH3030 (Section A7.5.3).

Lithotype	Angiosperm %	Gymnosperm %	*P. mawsonii* %	Spore %	Gleicheniaceae %
Teurian sediment (DH3030, 184.1m and above) n = 8	36.6	31.8	13.4 (0–61.0)	31.6	6.7 (0–15.9)
Haumurian sediment n = 71	40.8	37.7	14.3 (0–46.8)*	21.6	3.6 (0–12.1)*

Table A7.5 Summary of palynology data, Kaitangata Coalfield.
* Haumurian *P. mawsonii* and Gleicheniaceae data from Browne (1986b), n = 26

Haumurian sediments: Haumurian sediments from Kaitangata exhibit a wide variation in floral composition, though most samples contain <40% spores (Figure A7.5). Only one Kaitangata sample falls within the field in which the majority of Greymouth Haumurian sediments lie, however those samples from Greymouth with a lower spore proportion fall within the compositional domain of the majority of Kaitangata sediment samples.

Dominant angiosperm taxa described by Browne (1987) are commonly unidentified tricolpate/tricolporate forms, which are abundant in 7 samples and range up to 46%, Proteaceae (abundant in 2 and up to 28%), *N. kaitangataensis* (abundant in 4 and up to

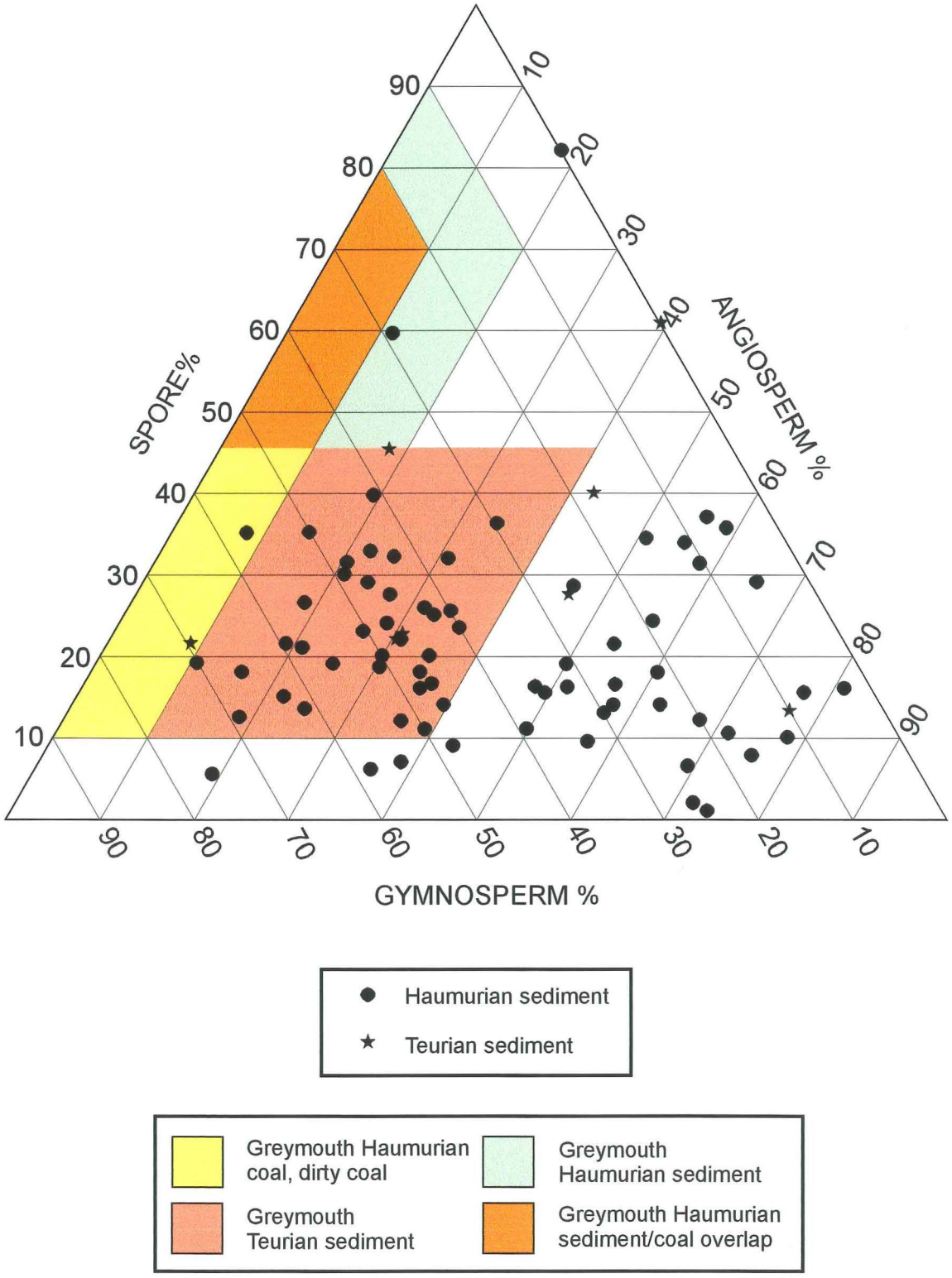

Figure A7.5 Summary palynology data, Kaitangata Coalfield (n = 79)
Sources: Browne (1986b, 1987), Browne & MacKinnon (1989).
All samples are sediments.
Average Greymouth fields shown for comparison.

48%) and *Peninsulapollis gillii* (common in 5 samples). Spore floras are dominated by *Laevigatosporites.* Average abundance of Gleicheniaceae is less than at Greymouth, though the range of occurrences is similar. Gymnosperm floras at Kaitangata are dominated by *P. mawsonii*, (average and range similar to Greymouth) and *Podocarpidites*, *T. subgranulatus* and *M. antarcticus* are present in moderate to common proportions in some samples.

Teurian sediments: Teurian sediment samples from Kaitangata (Figure A7.5) mostly have similar compositions to Haumurian samples, though one contains no gymnosperm pollen and has a high proportion of spores (Cyatheaceae and *Laevigatosporites*). The remaining samples have lower spore abundances (c. 15–45%), and overall composition is similar to some Greymouth Teurian samples (Figure A7.2). UCP369, a carbonaceous mudstone, contains an atypical flora (61% *P. mawsonii*, 12.9% Gleicheniaceae) which resembles that of a coal. Average *P. mawsonii* abundance (excluding UCP639) is 6.6%.

9.3.4 Pike River Coalfield

Limited palynofloral information is available for the Paparoa Group at Pike River Coalfield, which is located c.25km NE of Greymouth Coalfield (Figure A7.3). Ward (in Ferguson 1993, Appendix 1) presented summary data for four Teurian sediments and four thick, clean Haumurian coals (Figure A7.6A, Table A7.6).

Lithotype	Angiosperm %	Gymnosperm %	*P. mawsonii* %	Spores %	Gleicheniaceae %
Teurian sediment	64.3	20.0	3.6	15.7	3.0
n = 4	(40–83)	(4–42)	(0–7.8)	(9–25)	(0–7.8)
Haumurian coal	11.2	75.8	59.5	13	2.4
n = 4	(3–23)	(65–80)	(41–75)	(10–17)	(0–5.2)

Table A7.6 Summary of palynology data, Pike River Coalfield.

Two of the Pike River coal samples (Figure A7.6A) are comparable to typical Greymouth Haumurian coal, whereas the remaining two contain >10% angiosperms (notably *Tricolpites* cf. *pachyexinus*) and have similar overall composition to the two angiosperm–rich Greymouth coals. Similarly, two of the Pike River Teurian sediments plot close to equivalent Greymouth material, whereas the other two samples contain a very high proportion of angiosperm pollen (>80%, dominated by >60% *T. minor*),

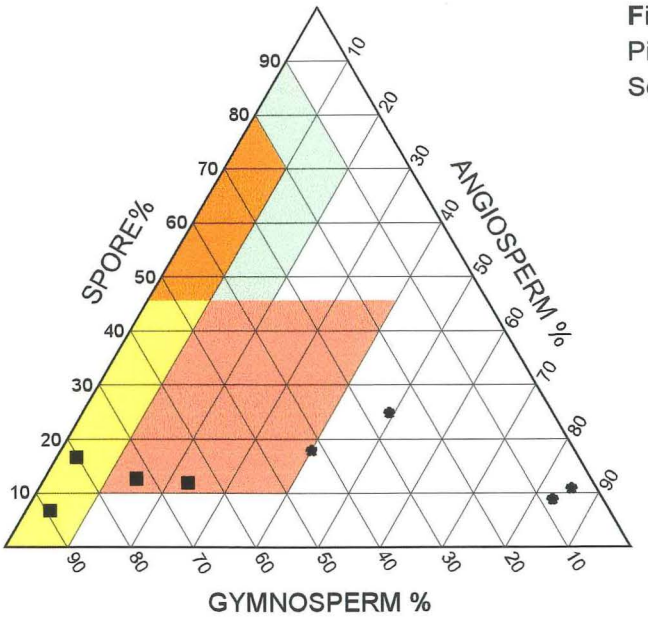

Figure A7.6A Summary palynology data, Pike River Coalfield (n = 8).
Source: Ward *in* Ferguson (1993).

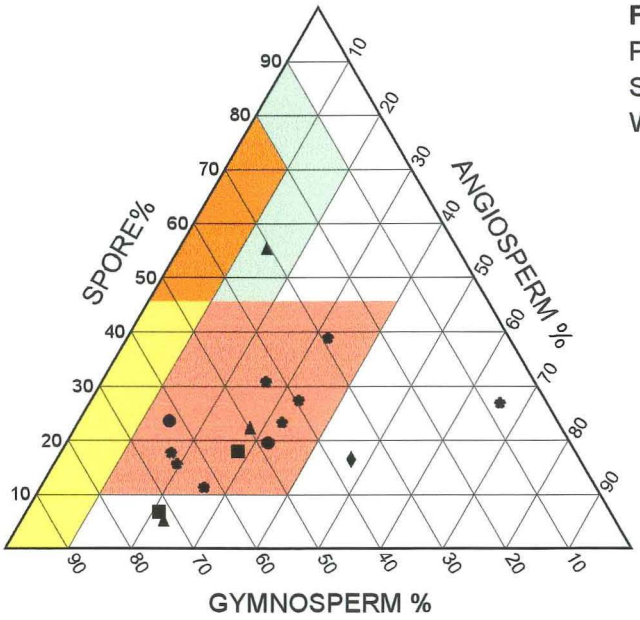

Figure A7.6B Summary palynology data, Pakawau Group, Northwest Nelson (n = 16).
Source: Warnes *in* Bal (1992), Bal (1994), Warnes in Kennedy (1993)

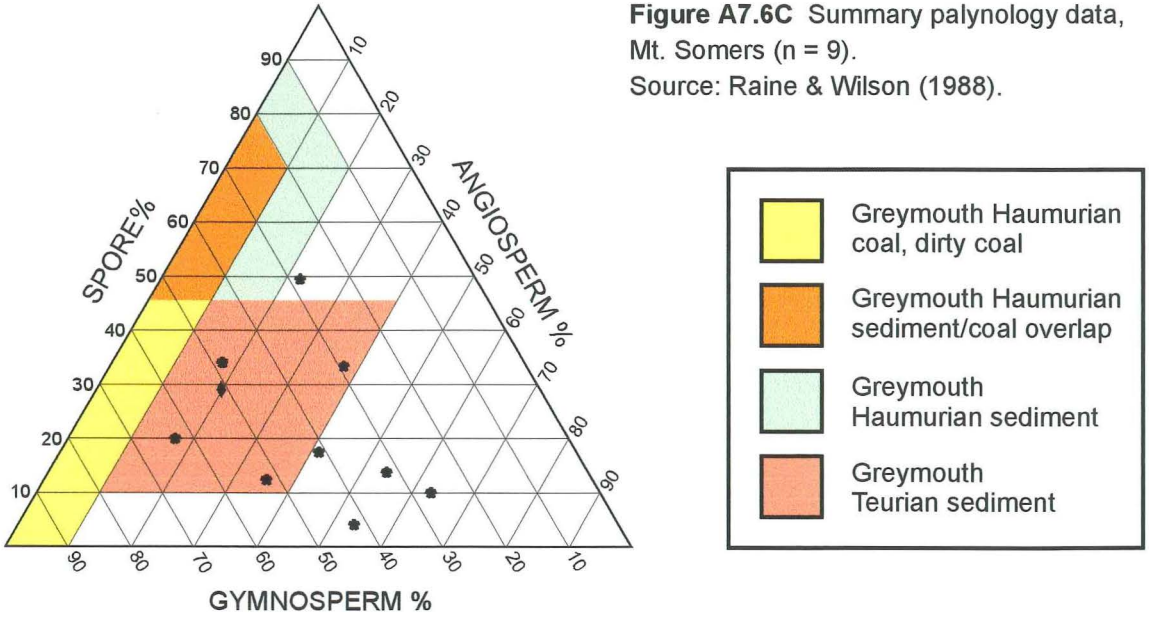

Figure A7.6C Summary palynology data, Mt. Somers (n = 9).
Source: Raine & Wilson (1988).

Figure A7.6 Summary palynology data for Pike River Coalfield, Pakawau Group and Mt. Somers.

which was not observed at Greymouth Coalfield. Collectively, the eight Pike River Coalfield samples contain a lower proportion of spores than are present at Greymouth Coalfield, though the data set is too small to yield any firm conclusions.

A7.3.5 Pakawau Group

Haumurian–Teurian coal measures and associated paralic deposits of the Pakawau Group are found at the northern tip of the South Island (Figure A7.3), and are the onshore equivalent of thick basal Late Cretaceous–early Tertiary strata of the greater Taranaki Basin (Thrasher 1990). Material includes thin coals (Puponga Mine), thin dirty coal (Moki "coal") and sediments (Figure A7.6B, Table A7.7) which have yielded both Haumurian and Teurian ages (Warnes in Bal 1992, Appendix C; Bal 1994; Warnes in Kennedy 1993, Appendix E). Ten additional samples of Haumurian and Teurian sediments (UCP1683–1692) have only been scanned for key taxa, and lack complete count data (Ward, unpublished data, 1996). J.I. Raine (IGNS) has also reported scan data for 15 outcrop sediment samples (Raine 1989) and has undertaken further collection in this area, however no data are yet available (Raine 1994a).

Lithotype	Angiosperm %	Gymnosperm %	*P. mawsonii* %	Spore %	Gleicheniaceae %
Haumurian coal n = 2	24.7	63.0	38.5	12.4	0.0
Haumurian dirty coal n = 3	21.5	50.9	15.9	27.6	5.5
Haumurian sediment n = 2	23.3	55.1	24.0	21.6	0.6
Teurian coal n = 1	47.1	36.4	10.3	16.5	0.8
Teurian sediment n = 8	31.6 (19.6–65.8)	44.4 (7.4–64.8)	24.6 (2.7–42.4)	21.0 (11.2–38.9)	3.2 (0.5–7.6)

Table A7.7 Summary of palynology data, Pakawau Group samples.

Haumurian coal/dirty coal: Summary data for five samples of Haumurian coal and dirty coal from Pakawau are presented in Figure A7.6B. All samples are from thin (<50cm) seams, and assignment to dirty or clean lithotypes is on basis of proximate analyses presented by Bal (1994, Table 1). Angiosperm floras contain conspicuous *T. lilliei* (up to 6.5%), *T. reticulatus* (up to 6.7%) and monosulcate forms (up to 12.5%). Gymnosperm floras are variably dominated by *P. mawsonii*, *P.* cf. *ellipticus* or *T. subgranulatus*, and *M. antarcticus* and *Podocarpidites* spp. are rare to common

components of the floras. Average gymnosperm proportion is similar to Greymouth material, though the average proportion of *P. mawsonii* is lower at Pakawau. Overall, Pakawau Haumurian coal floras are similar to the two mire–margin coal floras from Greymouth, but unlike the typical Greymouth Haumurian coal floras.

Sample UCP1683 is a thin dirty coal which yielded an Haumurian palynoflora, including both *T. lilliei* and *T. secarius* but lacking *T. minor*. Though not counted, this sample contains more abundant angiosperm pollen than equivalent Greymouth material.

Haumurian sediments: The two Haumurian sediment samples with full count data from Pakawau (UCP1263, 1264) contain palynofloras dominated by *P. mawsonii* and various species of *Podocarpidites*, *Laevigatosporites* and tricolpate angiosperm pollen. Rare to moderate amounts of *T. minor* are also present. UCP1264 plots close to the cluster of Greymouth Haumurian sediment samples with >60% gymnosperms, whereas UCP1263 contains more angiosperm pollen than Greymouth Haumurian samples, and is similar to Teurian material from Greymouth. Three other (uncounted) Haumurian sediment palynofloras (UCP1690–1692) contain similar floral components to equivalent Greymouth Coalfield material.

Teurian dirty coal: Sample UCP1240 ("Moki Pt. coal") is a thin (50–60cm) Teurian dirty coal. The palynoflora is notable for a high proportion (29.2%) of *N. kaitangataensis*, and the high total angiosperm pollen proportion (47.1%) distinguishes this sample from Greymouth Teurian dirty coals. *T. minor* is a trace component. Another Teurian dirty coal (UCP1686) contains conspicuously abundant Proteaceae pollen, which was not observed from Greymouth material.

Teurian sediments: There are eight counted Teurian sediment floras from Pakawau seven of which lie within the same compositional area as equivalent Greymouth samples. Floras are dominated by *T. minor* (7.2–21.2%), *P. mawsonii* (14.4–32.0%) and *Podocarpidites* spp. (10.8–30.4%), and only one sample contains more than a trace proportion of *Nothofagidites* (UCP1245, 5%). Average *P. mawsonii* abundance is slightly higher at Pakawau than Greymouth, and the reverse is true for Gleicheniaceae. The remaining sample (UCP1243) contains a higher proportion of angiosperm pollen than Greymouth or other Pakawau samples, and is dominated by *T. minor* (56.4%).

Four additional uncounted Teurian sediment samples from Pakawau Group (UCP1685–1688) contain similar floras to those samples described above, though diversity is generally low. Proteaceae are the dominant angiosperm form in UCP1688, and *T. minor* abundance is variable.

A7.3.6 Mt. Somers

Raine and Wilson (1988) described dinoflagellate and spore/pollen floras from Teurian–Waipawan coal measures and overlying marginal marine strata at Mt. Somers, inland mid-Canterbury (Figure A7.3). All samples were assigned to Zone PM3, and the age of the uppermost material is upper Zone PM3 (early Waipawan stage).

Overall floral compositions for six of the nine sediment samples (Figure A7.6C, Table A7.8) are similar to Greymouth Teurian sediments. Floras are dominated by *P. mawsonii*, *Podocarpidites,* Gleicheniaceae, Proteaceae, *T. minor* (up to 14%) and unidentified angiosperm pollen. The average proportion of spores is greater at Greymouth, though a higher proportion of Gleicheniaceae are present at Mt. Somers. The remaining three floras, which are dominated by angiosperms and contain dinoflagellates, are unlike any Teurian sediment from Greymouth. The single Teurian coal from Mt. Somers is similar to Greymouth Teurian dirty coals, though with more angiosperm pollen.

Lithotype	Angiosperm %	Gymnosperm %	*P. mawsonii* %	Spore %	Gleicheniaceae %
Teurian sediment n = 9	38.0 (17–63)	40.4 (27–63)	14.1 (3.0–43.0)	21.6 (4.1–49.5)	10.2 (0–31.3)
Teurian coal n = 1	19.8	51.2	23.3	29.0	11.6

Table A7.8 Summary of palynology data, Mt. Somers.

A7.3.7 Grey River, Canterbury

Four Teurian palynofloras from the West Branch of the Grey River in North Canterbury were described by Raine (1979). Conifer pollen and *T. minor/T. minisculus* are the dominant palynomorphs present, though no abundance data are given. Associated samples have been dated by K-Ar methods (Field & Odin 1981), and yielded ages of c.55.7Ma ± c.1.5Ma, which places these samples in the upper Teurian.

A7.4 Summary of New Zealand Haumurian and Teurian floras

Palynofloras from all localities described above are largely composed of the same common taxa as Greymouth Coalfield floras, however there are some significant differences in proportion of the various angiosperm, gymnosperm and spore components.

Haumurian coals: The predominant flora of Haumurian coals found at Greymouth Coalfield, which contains a high proportion of *P. mawsonii*, and c.10% angiosperm pollen, also occurs at Ohai and Pike River. However, a significant number of coals from these latter localities, and also Pakawau, contain >c.10% angiosperms and <40% spores, and only two Greymouth samples from a riparian setting have this composition. Coals with >60% spores and low angiosperm proportion occur mostly at Greymouth Coalfield, though one is also known from Pakawau. Average composition data for all Haumurian coals indicate Greymouth samples contain the least amount of angiosperm and gymnosperm pollen and the greatest proportion of spores.

Haumurian dirty coals: Comparison is only possible between Ohai and Greymouth material. There is little overlap between the respective samples, with Ohai material generally containing more angiosperm pollen.

Haumurian sediments: The majority of Greymouth Haumurian sediment samples contain <20% angiosperm pollen and >50% spores. A small number of samples from Ohai (6) and Kaitangata (2) have a similar composition, but the majority contain more angiosperm pollen and/or fewer spores. Floras of these compositions are present at Greymouth Coalfield, but are a minority. As with Haumurian coals, Greymouth material contains the lowest average amount of angiosperm and gymnosperm pollen and the greatest proportion of spores.

Teurian coals/dirty coals: Only 2 samples of Teurian coal (Mt. Somers, Pakawau) are available for comparison with Greymouth material (4 samples). Both contain a much higher proportion of angiosperm pollen than Greymouth samples, and neither contains more than trace amounts of *T. minor*.

Teurian sediments: Teurian sediments have similar palynofloras in all the deposits, with moderate to abundant *T. minor*. However, average angiosperm abundance at Greymouth is lower than at other localities, and Greymouth material also contains slightly more abundant spores than elsewhere.

Despite difference in absolute magnitude between the various sites, the general trend of increasing angiosperm proportion (and diversity) from coals to dirty coals to sediment samples is present in all localities, though best expressed at Greymouth and Ohai Coalfields where there is sufficient data for all lithotypes. At other localities, the range of angiosperm pollen proportion, rather than average abundance, illustrates the trend.

There is nothing exceptional about the diversity of pollen and spore taxa present at Greymouth Coalfield, though some widespread angiosperm pollen taxa (e.g. *Tricolpites phillipsii*) have not been observed in the present study. What is notable in Haumurian samples from Greymouth Coalfield, however, is the low overall angiosperm abundance, the rarity of certain angiosperm taxa (e.g. *T. lilliei*, *P. gillii*, *Nothofagidites*), and the high abundance of Gleicheniaceae and other spores. Possible explanations for the difference between Greymouth Coalfield and other floras are discussed in Appendix 8.1.

A7.5 Review of Cretaceous–Tertiary Boundary floral change in New Zealand and the Southern Hemisphere

The purpose of this review is to identify the floral events (first and last appearances, changes in abundance, dominance and diversity) which occur at the KTB in sections throughout New Zealand and elsewhere in the Southern Hemisphere, in order to determine whether the floral change recorded at Greymouth Coalfield reflects a localised, regional or widespread event.

A7.5.1 Other Paparoa Group sections

Pike River Coalfield: Preliminary establishment of the palynostratigraphy at Pike River Coalfield was by Raine (1984) who reported palynological zonation of three sections (see also Newman 1985, Figure 9). Further work by Ward (in Ferguson 1993) confirmed the presence of Teurian sediments, however there is no section in which the KTB has been

precisely located. Palynostratigraphy helps confirm stratigraphic relationships between the Paparoa Group members present at Pike River and the formations and members of Greymouth Coalfield (Figure A1.1C).

In Teurian sediments from Pike River Drillhole (PRDH) 1, *T. minor* increases from 30.6% to 61.2% over 20m towards the floor of the (Brunner CM) seam (Figure A7.7). *T. minor* is also abundant (71.2%) in UCP1206 from PRDH7, which is stratigraphically lower (but still Teurian) than samples from PRDH1 (Ferguson 1993). These samples are similar to Teurian material described by Raine (in Newman 1985) from Greymouth Coalfield.

Eight taxa plus two rare forms are restricted to Teurian samples, and four taxa occur only in Haumurian samples. There is less *P. mawsonii*, *M. antarcticus* and *P. marwickii*, and more *Podocarpidites* spp. in Teurian samples than Haumurian material. Angiosperm proportion increases markedly from Haumurian to Teurian samples (Table A7.6), at the expense of gymnosperm pollen. However, differences between the two ages of samples partially reflect facies controls on floral occurrence, as all Haumurian samples are coals, in which *T. minor* is absent (Appendix 5.5.3).

Arahura–1: A KTB section was identified in thin Paparoa Group strata in the oil exploration well Arahura–1, located 10km east of Hokitika (McIntyre 1964; Officers of the Geological Survey, 1974; Raine 1984 p. 80; Nathan et al. 1986). The KTB lies between 1704m and 1711m in the uppermost Rewanui CMM or lowermost Goldlight Fm. No palynological data have been published.

A7.5.2 Pakawau Group

The KTB lies within the paralic Puponga Coal Measure Member of the North Cape Formation in the Whanganui inlet area (Bal & Lewis 1994). Teurian ages are indicated by moderate to abundant *T. minor* (up to 56%, UCP1243), *T. minisculus* (which is sometimes common), *T. secarius*, *T. phillipsii*, *P. densus*, *R. mallatus* and possible *Concolpites leptos*. Haumurian samples contain *T. lilliei*, *N. kaitangataensis* and rare *Beaupreaidites*. *T. secarius* and *T. lilliei* occur together in four samples. Angiosperm pollen proportion is greater in Teurian sediments and coal than corresponding Haumurian samples, whereas gymnosperm pollen proportion declines (Table A7.7). Total spore and *P. mawsonii* proportion is, however, identical in Haumurian and Teurian sediments.

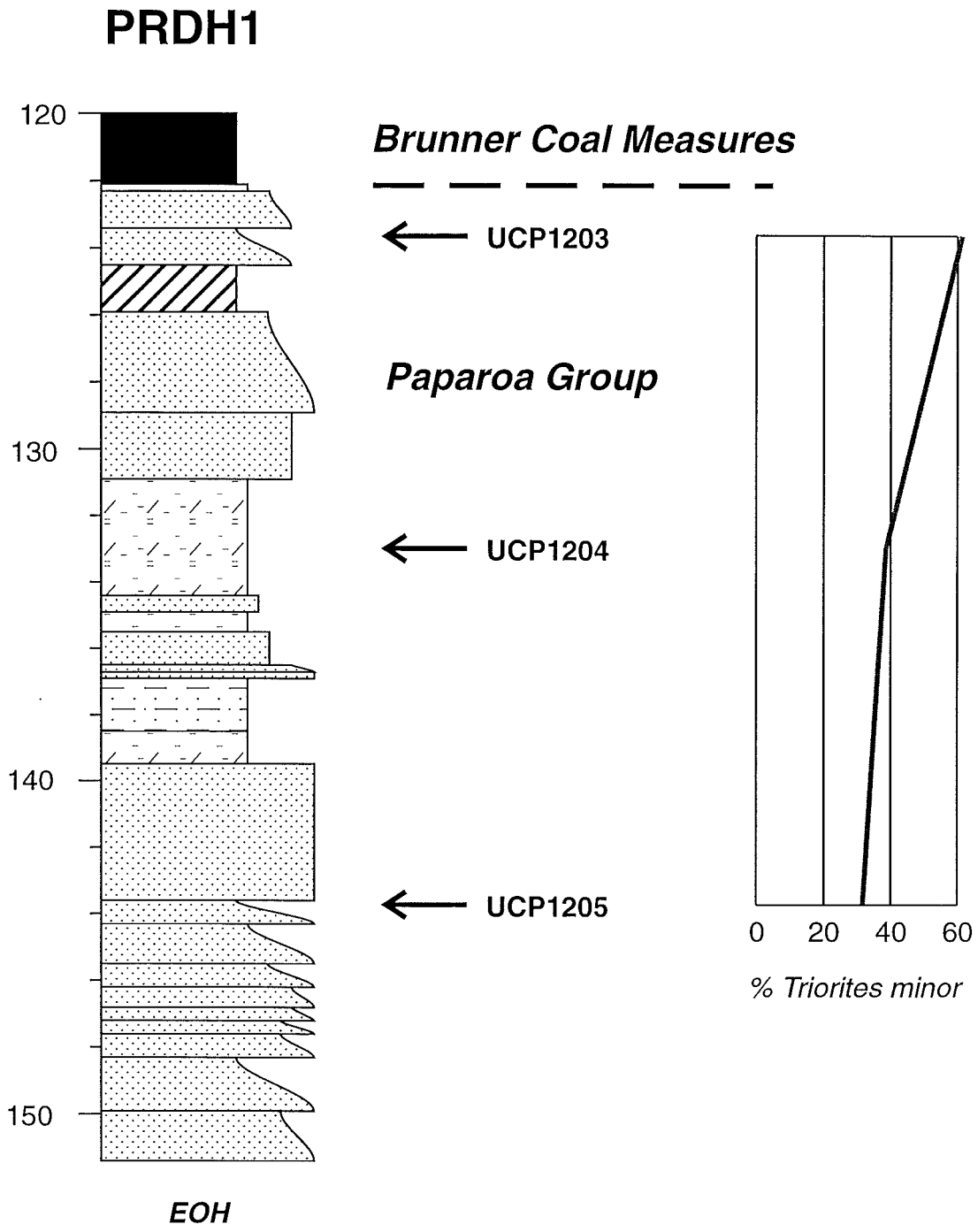

Figure A7.7 Lithostratigraphy and *Triorites minor* abundance, Pike Rive Drillhole PRDH1.
Lithology data from Ferguson 1993 (Figure 6A), palynology from Ward *in* Ferguson 1993.
All pollen samples are Teurian.

Raine (1989) reported both *T. secarius* and *T. lilliei* were rare within outcrop Pakawau Group samples, and that *T. phillipsii* was an alternative indicator species for Zone PM3. In contrast, the KTB was determined palynologically in sections from the Taranaki Basin petroleum exploration wells Fresne-1, Maui–4 and North Tasman–1 (Figure A7.3) from the presence of *T. secarius* (PM3) and *T. lilliei* (PM2).

A7.5.3 Kaitangata Coalfield

Browne (1986b, 1987) located the KTB using pollen, spores and dinoflagellates in DH3023, DH3030, DH3036, and DH3068, and subdivided Zone PM3 into 3 subzones on the basis of first appearances of taxa. These data have been recently re-evaluated by Crouch (1994), who indicates many of Browne's dinoflagellate identifications were erroneous, particularly those used to indicate early Teurian ages. Crouch (1994) placed the KTB higher up section than determined by Browne (1986b), and some sections (e.g. DH3029) reported as Teurian are now regarded as Haumurian.

DH3030 (Figure A7.8) is now the only drillhole from Kaitangata Coalfield with a confirmed KTB section, though the exact location remains uncertain. Browne (1986b) located the KTB between 212.2m (UCP305) and 213.35m (UCP460), citing the first appearance of *T. secarius*. Crouch (1994) placed the KTB between 140.0m (UCP351, containing *T. phillipsii*) and 143.2m (UCP404, uppermost occurrence of *T. lilliei*).

Application of zonal criteria from Greymouth Coalfield (Appendix 5.4.3) indicate the KTB in DH3030 is located within the interval 167.0m (UCP358) to 184.1m (UCP416). There is a pronounced but irregular increase in *T. minor* abundance above 184.1m (Figure A7.11), and angiosperm proportion increases markedly from UCP304 (197.3m) to UCP358 (167.0m). Browne (1986b) reports Teurian *M. harrisii* in UCP416 and samples above. Overlap in the occurrence of *T. lilliei* and *T. secarius* in DH 3030 (UCP346, 404) is consistent with findings from Greymouth Coalfield (Appendix 5.5.5), and was also reported by Browne (1986b) in nearby drillhole DH3011.

Angiosperm diversity data from DH3030 (Figure A7.8) shows a marked decline at 197.3m (UCP304), which correlates with low angiosperm abundance (as at Greymouth: Figure A6.2). If this decline in angiosperm diversity is equivalent to that observed near the KTB in Greymouth, the KTB in DH3030 should be placed at or above UCP304. The likely

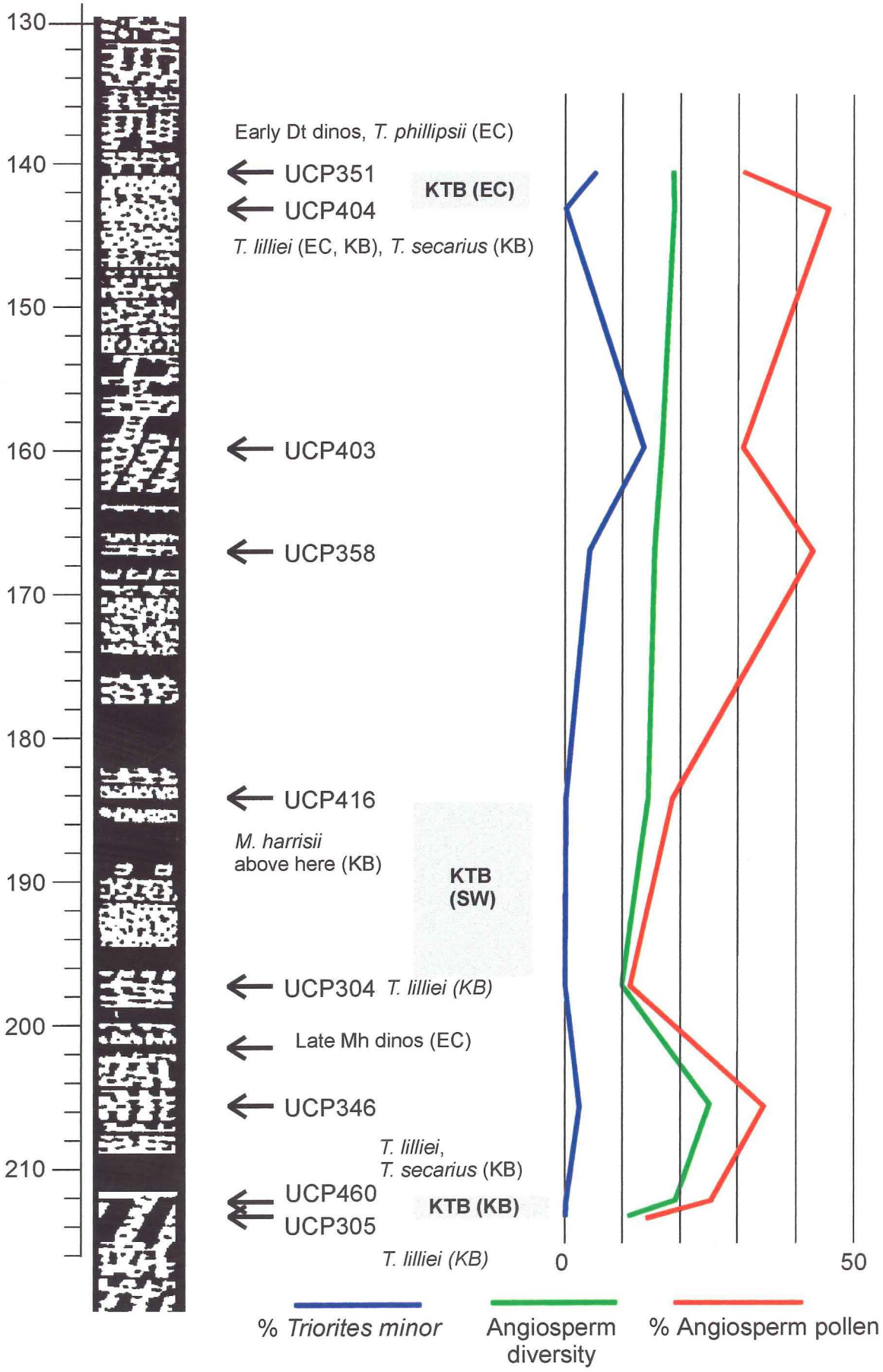

Figure A7.8 Summary of biostratigraphic data, DH3030, Kaitangata Coalfield
Compiled from **KB** = Browne (1986b) and **EC** = Crouch (1994).
Stippled areas show choices for KTB placement.

position for the KTB indicated on Figure A7.8 is between UCP304 and UCP416. Kaitangata strata represent different depositional environments from those in Greymouth Coalfield, and exact correspondence of floral events at the KTB is unlikely between the two sites. The decline in angiosperm abundance near the KTB in DH3030 is responsible for the slightly lower average angiosperm proportion in Kaitangata Teurian samples in comparison to Haumurian samples (Table A7.5).

Elsewhere in Otago (Figure A7.3), the KTB is preserved in marine sediments which overlie Taratu Fm. near Milton (Bishop 1994), and at Fairfield Quarry (McKellar 1990), though no palynological data is presently available (Raine 1994a). Dinoflagellate biostratigraphy of the Fairfield Estate drillhole (McMillan 1995) indicates lowermost Teurian strata are present within the Abbotsford Fm., though terrestrial palynofloras have not been studied. Equivalent strata are upper-most Teurian or younger in the Measly Beach Drillhole (Lindqvist 1995), and are underlain by mid-late Teurian Wangaloa Fm. strata. Terrestrial palynomorphs have yet to be investigated.

A7.5.4 Offshore Canterbury and Great South Basins

The KTB has been located in seven offshore petroleum exploration wells (Figure A7.3) in the southern Canterbury Basin (Clipper–1, Endeavour–1, Galleon–1) and the Great South Basin (Kawau–1A, Pakaha–1, Toroa–1, Tara–1), and is also present in the onshore Shag Point section in North Otago (Raine et al. 1993, 1994). Precision of KTB identification is variable, and ranges from +/-1.5m (Endeavour–1), to +/-120m (Shag Point). The KTB lies within coal measures in Tara–1, nearshore sediments at Shag Point, and inner shelf marine sediments in the remaining holes.

Where pollen and spores are present, Haumurian samples contain *T. lilliei* and *N. kaitangataensis*, and rare *Tricolpites pachyexinus*, *Tricolpites fissilis*, *Q. brossus* and *Beaupreaidites* n. sp. Early Teurian samples contain *Gambierina edwardsii*, *T. phillipsii*, *Nothofagidites* aff. *fusca*, *Proteacidites hakeoides*, *Proteacidites annularis*, *Tetracolporites similis*, *T. secarius* and *N. waipawaensis*, though the stratigraphic position of first appearance of these taxa varies from well to well. Later Teurian samples also contain *M. harrisii*. In Endeavour–1, *T. minor* is abundant in early Teurian samples, and common in late Teurian samples.

A7.5.5 Other New Zealand Cretaceous–Tertiary Boundary sections

There are numerous sections in which the KTB has been located in north Canterbury, Marlborough and the east coast of the North Island. However, these sections contain exclusively marine strata, and biostratigraphy is based on foraminifera, dinoflagellates and radiolaria rather than terrestrial palynomorphs. Limited information is available for the Middle Waipara KTB locality (Couper 1960; Hornibrook et al. 1962; Helby et al. 1987) (Figure A7.3) and the occurrence of age-diagnostic taxa in this section is discussed elsewhere (Appendix 5.4.1). Key palynostratigraphic events documented at the KTB are the demise of *T. lilliei* and the arrival of *M. harrisii* and *N. waipawaensis*.

A7.5.6 Australia

The KTB is preserved in the subsurface La Trobe Group of the Gippsland Basin in Bass Strait (Stover & Evans 1973; Stover & Partridge 1973; Macphail 1994), and spore and pollen ranges have been confirmed with dinoflagellates. Key floral events at this KTB locality are the demise of *T. lilliei*, *Q. brossus* and rare large/ornamented triorate and tetrad angiosperm forms, and a sharp decline in the proportion of *Gambierina rudata*. Small psilate/scabrate angiosperm taxa, especially Proteaceae, are abundant in the earliest Paleocene. Diversity declines across the KTB, though all but 11 of the c.70 taxa recognised in Maastrichtian material survive into the Danian. Floras are dominated by long-ranging gymnosperms and small proteaceous taxa.

A7.5.7 Antarctic Peninsula

The only known KTB section in Antarctica is preserved on Seymour Island, on the northern end of the Antarctic Peninsula (Askin & Jacobson 1996). The KTB is defined with marine microfossils, marine vertebrate fossils and dinoflagellate floras, and occurs in shallow shelf siliciclastic sediments (Elliot et al. 1994). These sediments were deposited in a back-arc basin at a paleolatitude of 63°S (Lawver et al. 1992). Presence of an iridium anomaly confirms the location of the KTB (Elliot et al. 1994).

Floras are dominated by podocarpaceous conifer pollen (40–65%), angiosperm pollen contributes 20–45% and spores are the least common component (6–15%). The dominant species throughout the Campanian–Paleocene is *P. mawsonii*, and there is little change in gymnosperm abundance or diversity across the KTB (Askin 1990). Many latest Maastrichtian angiosperm taxa were endemic to the Antarctic region (Askin 1989), and

there was constant change in the angiosperm flora (both first appearances and last appearances) across the KTB interval (±100m), perhaps reflecting the increased availability of lowland environments as regression continued (Askin 1990), or the effects of nearby volcanism (Askin 1992). *T. lilliei* and *Q. brossus* only occur below the KTB.

A7.6 Summary of Cretaceous – Tertiary Boundary floral change

Many of the floral events which occurred at the KTB in Greymouth Coalfield also occurred in other New Zealand and Southern Hemisphere localities. There is a strong trend of increasing angiosperm pollen proportion from Haumurian to Teurian sediment palynofloras, notably at Greymouth Coalfield, Pike River Coalfield and in Pakawau Group strata. The exception is Kaitangata Coalfield, where the pattern is reversed, though sampling Teurian material is limited and may be unrepresentative.

The demise of *T. lilliei* at the KTB is widespread, and is commonly associated with last appearances of *Beaupreaidites* and other large/ornamented proteaceous angiosperm taxa. The sparse occurrence of *Q. brossus* in Teurian samples at Greymouth is inconsistent with data from other localities, though reworking may have occurred. Throughout boundary intervals there is constant change in the angiosperm flora, and many taxa first appear at or near the KTB. *T. secarius* is only reported from the New Zealand region, where its range overlaps with *T. lilliei*. Occurrence of *T. secarius* alone is insufficient for the assignment of Zone PM3 to a sample, and the definition of Zone PM3 by the first appearance of this taxon (Raine 1984) should be revised.

Abundant occurrences of *T. minor* or similar small proteaceous forms are known from early Cenozoic strata throughout the South Island of New Zealand, and in Australia. Collapses in angiosperm diversity occured at or near the KTB in Greymouth Coalfield and Kaitangata Coalfield, but have not been reported elsewhere. In all localities, floral change is limited to less common taxa, predominantly angiosperms, and there is limited change in diversity or abundance of dominant, long–ranging gymnosperm or spore taxa.

Appendix 8. Discussion of palynology results: controls on paleovegetation

Two related issues must be addressed. Firstly, what controls might be responsible for the differences between Greymouth Coalfield palynofloras and those of other Haumurian and Teurian localities. The second key issue is to identify the cause(s) of floral change at the KTB, both at Greymouth Coalfield, and more widely throughout the Southern Hemisphere. Resolution of these two issues highlights the significance of palynofloras from Greymouth Coalfield in understanding floral change at the KTB.

A8.1 Greymouth Coalfield palynofloral differences

Greymouth Coalfield palynofloras are distinguished from all others described in Appendix 7.3.2–7.3.7 by the low average abundance of angiosperm pollen and the high average abundance of spores in coals and sediments of both Haumurian and Teurian samples (Appendix 7.4). Possible controls on these differences are discussed below.

A8.1.1 Sampling

All presently available samples from Greymouth Coalfield (n = 334) lie within ± c.50m of the KTB. Thick, clean coals are well represented in the sample set, however sampling of thin or dirty Haumurian coals is limited. Only two Haumurian coals from a mire margin setting, with >20% angiosperm pollen, have been described (Ward et al. 1995), and further sampling of mire margin settings may yield additional examples of these palynofloras. Sampling of Teurian coals is very limited. Palynofloras from samples stratigraphically further above or below the KTB have yet to be described, and there is no information on floral evolution throughout Paparoa Group strata. Limited data indicate all Paparoa Group strata below the Rewanui Fm. lies within pollen Zone PM2 (Raine 1984), but detailed count data, with which to make full comparison with the present sample suite, are unavailable.

Palynological sampling for localities other than Greymouth Coalfield varies from adequate (Ohai Haumurian coals and sediments, Kaitangata Haumurian sediments) to merely reconnaissance information from which only tentative conclusions can be reached. Thus, comparisons with Greymouth Coalfield are limited to available material which may not represent the true spectrum of palynofloras.

A8.1.2 Geological setting and depositional environments

Greymouth Coalfield is presently the only Southern Hemisphere locality in which the KTB has been located within a completely terrestrial stratigraphic sequence. There is no marine influence in the sedimentology (Chapter 2), palynology (Appendix 6) or petroleum geochemistry (Czochanska et al. 1987) in the late Haumurian or early Teurian of Greymouth Coalfield. Of the other deposits discussed in Appendix 7, exclusively terrestrial strata are present in the Haumurian and Teurian at Pike River Coalfield, and the Haumurian of Ohai Coalfield, yet floras at these localities differ from Greymouth Coalfield. At all other localities, sedimentation was influenced by marine processes.

Observed floral differences between Greymouth Coalfield and Ohai Coalfield may reflect differences in depositional environments. Morley Coal Measures (Ohai Coalfield) are characterised by alternating coarse sediment and fine sediment with mire deposits (Shearer 1992), and the coal seams have thin partings and consequently, variable flora (Warnes 1992). In contrast, Rewanui CMM seams have minimal clastic partings (e.g. Moore 1996a), and floras representing mire margin environments may be poorly developed (or inadequately sampled, see above). Coal seams from most other localities are thin and discontinuous, and floras more closely resemble regional vegetation than the distinct vegetation which developed in long-lived mires.

Extensive lacustrine deposits (e.g. Goldlight Fm.) are restricted to Greymouth Coalfield, and this may be reflected by floras which are not present elsewhere. There may also be pollen transport mechanisms which are unique to lacustrine settings, and lacustrine transgression at Greymouth Coalfield could have enhanced apparent floral change. However, similarity of Teurian palynofloras from fluvial, deltaic and lacustrine sediments at Greymouth Coalfield (Appendix 5.4.3) suggests such effects are negligible.

Palynofloras within the relatively small (c.100km^2) terrestrial basins at Greymouth, Pike River and Ohai Coalfields probably represent only the vegetation within the basin and its immediate hinterland. While all spore and pollen types would have been subjected to transport within the depositional environment (see Ward et al. 1995 for discussion of transport of *P. mawsonii* pollen and Gleicheniaceae spores), the likely effects within all basins would have been similar, and taphonomy is not regarded as a significant source of floral differences between these localities.

Marine strata occur near or at the KTB at Pakawau, Kaitangata, Middle Waipara, Gippsland Basin (Australia) and Seymour Island (Antarctic Peninsula), and these localities represent coastal depositional environments. At times of marine incursion, terrestrial palynomorphs were transported to these sites, and subjected to sorting or transport within the marine environment. Askin & Jacobson (1996) suggest multiple palynomorph transport and depositional events occurred between the upland source areas and the final palynomorph depositional site within the marine strata at Seymour Island, resulting in a reduction in palynostratigraphic resolution. Terrestrial palynomorphs extracted from marine strata may therefore represent a range of source area ecologies. The effects of sorting within the marine environment may be limited, as Macphail (1994) reports comparable floral change across the KTB within both non-marine and marginal marine sectors of the Gippsland Basin.

A8.1.3 Age

The samples described in the present study from Greymouth Coalfield all lie close to the KTB, whereas material from other deposits exhibits a wider range of ages. Mt. Somers samples (Zone PM3) are upper Teurian–Waipawan, and Grey River samples are upper Teurian (Appendix 7.3.6, 7.3.7). Zone PM3 sediments from Pike River Coalfield lie close below Waipawan–Runangan (Eocene) Brunner Coal Measures (Figure A7.8), and may also be upper Teurian.

The duration of the Haumurian stage is estimated to be between c.8My (Edwards et al. 1988) and c.16My (Crampton et al. 1995), and the stage is yet to be subdivided palynologically (Raine 1984). Thus, while Haumurian material from areas with known KTB localities is likely to be of comparable age to the present study material, the age of Ohai Coalfield Haumurian sediments, which are unconformably overlain by Runangan strata (e.g. Raine 1984), is poorly constrained. Some pollen samples from basal Morley CM and underlying Wairio CM at Ohai Coalfield contain possible lower Haumurian or upper Piripauan floras (Raine 1986), therefore Late Cretaceous strata at Ohai may be up to c.10Ma older than Haumurian strata from Greymouth Coalfield. Climate change throughout the Late Cretaceous (see below) could explain why floras of the generally similar Greymouth and Ohai basins are different.

A8.1.4 Climate

The late Haumurian paleoclimate of Greymouth Coalfield is estimated from foliar physiognomy of angiosperm leaf macrofossils to be humid microthermal–mesothermal with a mean annual temperature (MAT) of 12–16°C and 0–10°C during winter months (Johnson & Greenwood 1993). Greymouth Coalfield palynofloras (Appendix 7.2) are consistent with this interpretation, and the predominance of *P. mawsonii* and Gleicheniaceae suggest conditions were generally wet (Ward et al. 1995). Leaf diversity and morphology indicate the latest Haumurian paleoclimate at Pakawau was equable, cool–mild temperate with moderate rainfall and a MAT of 14°C (Kennedy 1993), though no estimate is given for minimum temperature.

Various angiosperm taxa present in the latest Cretaceous of Seymour Island (*Beaupreaidites*, *Bombacacidites*, *Cupanieidites*) have presumed modern analogues growing in upland, humid areas of New Caledonia, in equable tropical/subtropical climates (Pocknall & Crosbie 1988; Dettmann & Jarzen 1988), and are believed to indicate warm, frost-free conditions (Askin 1990). Askin & Spicer (1995) describe the latest Cretaceous Seymour Island climate as having a MAT of 8–15°C, a temperature range of 16°C, and a winter minimum temperature of >1°C. Such mild climatic conditions may reflect climate amelioration by proximity to the coast (Askin 1992). Askin (1989) acknowledged that the assemblages from Seymour Island are transported (see also comments above) and may therefore represent both coastal ("warmth-loving") and upland (i.e. "cool climate") floras.

Supporting evidence for equable latest Cretaceous climates comes from fossil wood found at various localities throughout the Antarctic Peninsula (Francis 1986). Woods of Podocarpaceae, Araucariaceae and *Nothofagus* represent trunks or branches of trees up to 40cm diameter, and exhibit distinct growth rings with rapid early-wood growth and thin latewood, reflecting polar winter darkness. Growth rings exhibit little annual variation, and false rings typical of frost or fire-influenced environments are absent. An everwet favourable climate with c.1000-2000mm/yr rainfall is proposed (Francis 1986).

There is general consesus that climate throughout the Southern Hemisphere deteriorated during the Late Cretaceous. Low latitude Pacific marine oxygen isotope data indicates cooling by 8-10°C from the early Campanian through the Maastrichtian followed by warming through the Danian (Christophel 1995). Paleofloral analysis in New Zealand demonstrates the same trends, with an estimated MAT of 23° in the Albian (Daniel & Lovis 1988), cooler temperatures (14°) in the upper Haumurian (Kennedy 1993) followed by a return to warmer conditions (23°) by the Eocene (Newman et al. 1993).

On the Antarctic Peninsula, palynomorph assemblages indicate increasing moisture from late Campanian to the end Cretaceous (Askin 1992; Askin & Spicer 1995), and the presence of "warmth-loving" taxa in the latest Cretaceous is regarded as indicating a brief period of warming superimposed upon the overall cooling trend (Askin 1990). Other evidence from the high southern paleolatitude marine realm points to declining late Maastrichtian temperatures, with cooling commencing at c. 71Ma (Barrera 1994).

Following the above interpretations of Seymour Island floras, the rarity of "warmth-loving" angiosperm pollen taxa (notably *T. lilliei*, *Beaupreaidites*, *Nothofagidites*) at Greymouth Coalfield indicates a climate which is cooler, or more variable, than a typical coastal setting. An increased occurrence of (winter?) frosts at Greymouth, resulting in the removal of frost-sensitive elements from the flora, could be the cause, and winter temperatures were estimated to be as low as freezing (Johnson & Greenwood 1993). The absence of a marine influence at Greymouth Coalfield until the Eocene suggests a more distal or upland setting is probable.

A8.1.5 Conclusions

Differences between Late Haumurian and early Teurian palynofloras from Greymouth Coalfield and contemporaneous floras from elsewhere in the Southern Hemisphere reflect many possible controls on flora. However, the dominant control appears to be climate, and the paleoclimate of Greymouth Coalfield is inferred to be cooler than other sites where there was the ameliorating influence of a coastal setting. The most comparable site to Greymouth Coalfield is Ohai Coalfield, however, greater angiosperm abundance at Ohai Coalfield indicates a warmer climate, which may reflect an older age (e.g. lower Haumurian) and milder paleoclimate for Morley Coal Measures.

A8.2 Causes of Southern Hemisphere Cretaceous–Tertiary Boundary floral change

High paleolatitude (c. 60–70°) Southern Hemisphere KTB sections are characterised by minor floral change rather than a catastrophic event typical of mid-latitude Northern Hemisphere sections (e.g. Nichols & Fleming 1990; Johnson 1992b). Most floral change occurred within proteaceous types (e.g. Dettmann & Jarzen 1991, Figure 17), which were diverse and common in many localities prior to the KTB.

Three theories have been proposed to explain the loss of large ornamented proteaceous taxa and other floral changes at the KTB: 1) climate change; 2) environmental change (e.g. volcanism, regression, change in drainage patterns); and 3) elimination of purported insect pollinators. Little emphasis has been placed on explaining the cause of first appearances of certain types, or why other types (e.g. *Triorites minor*, *Tricolpites secarius*) increase in abundance at or near the KTB.

A8.2.1 Climate change

Detailed estimates of climate change across the KTB at high southern paleolatitudes can be made from stable isotopes and marine (foraminifera) faunas, and these are supported by less reliable terrestrial sources data (e.g. from palynomorphs or plant macrofossils). Information from the marine realm is summarised in Figure A8.1, which indicates continuous climate change throughout the million year interval spanning the KTB. Significantly, the brief late Maastrichtian warming interpreted at Seymour Island by Askin (1990) is also recorded in marine stable isotopes, though this event had little effect on marine plankton (Kennett & Barker 1990).

Terrestrial information indicates the early Paleocene was cooler than the late Maastrichtian. Askin (1990) interpreted changes in Seymour Island pollen and spore assemblages to indicate cooling, but with no discernible change in moisture across the KTB. The result of cooling across the KTB was altitudinal shifts of the ecosystems and loss of temperature or moisture extremes (Askin 1990). A similar trend is evident in cuticle (Askin & Spicer 1995) and fossil wood (Francis 1986) material, though the presence of frost-sensitive epiphyllous fungi in the early Paleocene (Askin 1992) indicates no severe temperature deterioration.

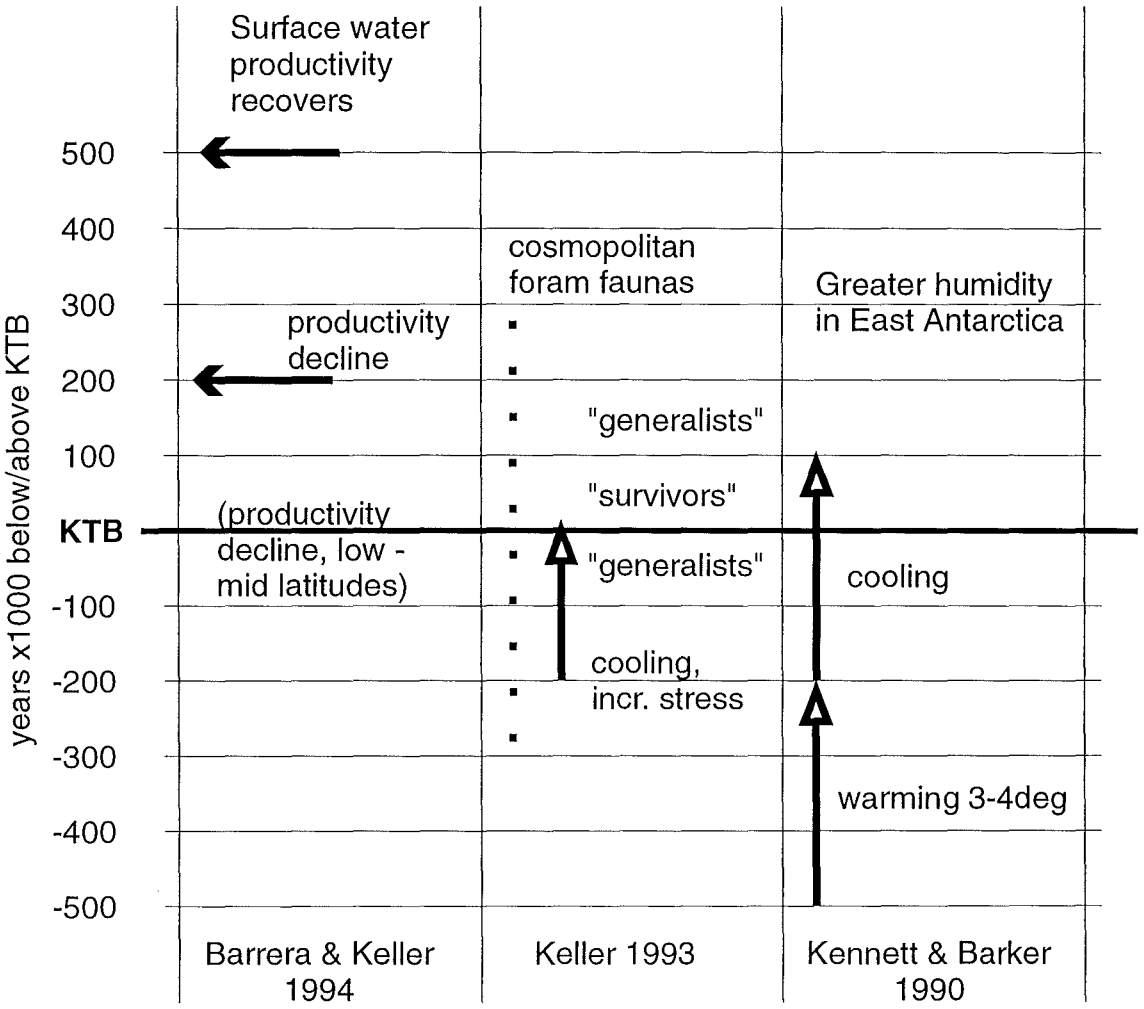

Figure A8.1 Summary of environmental changes and biological events from marine KTB sections in the Southern Hemisphere. Plot covers 0.5Ma above and below KTB.

No estimates of KTB climate change have been published for other Southern Hemisphere KTB sections, though synchronous extinction of proteaceous and other taxa in New Zealand, Australia and the Antarctic Peninsula suggests late Maastrichtian–early Danian climate change was a hemisphere-wide event. Floras, which were already adapted to winter darkness, were generally resilient to the effects of climate change (Macphail 1994).

A8.2.2 Environmental change

All KTB sections discussed here record late Maastrichtian environmental change which continued across the KTB, but no event which was coincident with the boundary. At Greymouth Coalfield, a lacustrine transgression occurred in the earliest Teurian, resulting in deposition of Goldlight Fm. mudstones and laterally equivalent fluvial and deltaic strata (Section 2.7.6). At Pakawau, progradation of the Puponga Coal Measure Member (North Cape Fm.) continued through the latest Haumurian and earliest Teurian (Bal & Lewis 1994), until termination by a lower Teurian erosional unconformity, related to cessation of sea floor spreading in the adjacent Tasman Sea (Bal 1994). An early Teurian transgression occurred at Kaitangata Coalfield (Browne 1986b).

The KTB in Australia (Gippsland Basin) is bracketed by two marine incursions (Macphail 1994), and regression continued across the KTB on Seymour Island (Askin 1990). Magmatic activity continued along the Antarctic Peninsula throughout the Maastrichtian and Danian, and volcanigenic sediments are present across the KTB at ODP Site 752 (Keller 1993), though ash layers do not correlate with the KTB iridium anomaly on Seymour Island (Elliot et al. 1994).

Danian first appearances of many taxa on Seymour Island are attributed to favourable environments for speciation or immigration, with regression making unvegetated land available for new plant species (Askin 1990). In contrast, Dettmann & Jarzen (1991) attribute the early Danian break in the fossil record of many proteaceous types to regression and consequent change in drainage patterns, which forced taxa to retreat temporarily from the depositional area.

A8.2.3 Loss of pollinators

The proteaceous pollen taxa which became extinct at the KTB most likely represented insect-pollinated, woody plants which were not part of the canopy vegetation, and similar pollen morphologies (larger/ornamented) in unrelated (non-proteaceous) taxa were also eliminated at the KTB (Macphail 1994). Many of these pollen types did not reappear until the Eocene, and others became extinct (Askin 1990; Dettmann & Jarzen 1991; Macphail 1994). Raine (1988, 1994a) and Macphail (1994) proposed that a reduction in insect (or other animal) pollinators at or near the KTB might be responsible for the removal of ornamented pollen taxa from the flora. Wind pollinated types (e.g. *Nothofagidites*, Podocarpaceae) were unaffected by extinction.

Raine (1994a) questioned the pollinator extinction hypothesis, observing that taxa which are represented in the fossil record may be able to survive by wind pollination even if the primary pollination mechanism requires insect vectors. Such a scenario was confirmed by Martin (1995), who proposed that early proteaceous taxa may have pollination mechanisms similar to certain modern taxa which, though insect pollinated, contribute significant pollen to the regional pollen rain in wooded areas.

A8.2.4 Discussion

Similar, subdued floral change occurred in all high latitude Southern Hemisphere KTB localities, suggesting a widespread external control. Both extinctions and first arrivals have been attributed to environmental change across the KTB. First appearances of many taxa at or near the KTB (present study; Raine 1984; Askin 1990) are more significant than the negligible extinctions. Loss of insect pollinators is an elegant hypothesis to explain the bias against certain pollen morphologies, though this mechanism was unlikely to have been solely responsible for the demise of certain taxa.

At many localities, floral (and faunal) change at the KTB occurred within the context of continuous Late Cretaceous and early Tertiary environmental and climatic change (e.g. Askin & Jacobson 1996). However, a similar pattern of KTB palynofloral change occurred throughout the Southern Hemisphere in many different depositional settings, and climate change (in particular, cooling) is the favoured control.

A8.3 Causes of Cretaceous–Tertiary Boundary floral change at Greymouth Coalfield

Floral change across the KTB in Greymouth Coalfield is summarised in Table A6.11. Climatic deterioration, with a reduction in mean annual temperature, is the most likely cause for extinction of certain palynomorph taxa at the KTB, and the precursor for floral change which persisted into the early Eocene. The magnitude of some components of climate change (e.g. precipitation, frost-free days) at Greymouth, however, must have been less than existing variation in those factors, as the dominant components of the flora (*P. mawsonii*, Gleicheniaceae) were unaffected by climate change.

Floral change is largely restricted to understory plants (Macphail 1994). Though the biological affinities of *T. minor* are unknown, high pollen abundance leads to speculation that this plant occupied a "weed" or coloniser niche which rapidly took advantage of the decline in abundance of other low-growing angiosperm and pteridophyte (Cyatheaceae, Sphagnaceae) taxa. In this respect, *T. minor* may be functioning like pteridophytes responsible for the "fern-spike" of Northern Hemisphere KTB sections (Nichols & Fleming 1990). A comparable marked rise in angiosperm pollen abundance, attributed to opportunistic species, occurred above the KTB at some Canadian boundary localites (Sweet et al. 1990). However, those abundance peaks were short-lived, whereas floral change at Greymouth Coalfield and elsewhere in the New Zealand region (e.g. high *T. minor* proportions) persisted for c.10Ma (Appendix 7.6).

An alternative hypothesis is that the parent plant(s) of *T. minor* and related type *T. minisculus* produced large amounts of very small pollen, and were wind pollinated. Taxa contributing very little pollen to the regional pollen rain (e.g. *T. lilliei*, *Beaupreaidites* sp.) were replaced by taxa contributing large amounts of pollen, which would dilute the contribution from spore-producers and other low-growing forms, thereby accentuating the impression of floral change. Replacement of Cyatheaceae and Sphagnaceae by *T. minor* may therefore be an apparent rather than real floral change.

Overall reduction in spore proportion from the Haumurian to Teurian at Greymouth Coalfield points towards a reduction in precipitation across the KTB. This hypothesis conflicts with the lack of observed change in the proportions of *P. mawsonii* and Gleicheniaceae, however these taxa are characterised by vegetative reproduction (Ward et al. 1995), and may have been tolerant of a wider range of environmental conditions than other plant types. Both were certainly tolerant of the low-nutrient, rainfed mire environment. Corroborative evidence from Teurian coals suggests drier conditions in the South Island region after the KTB (Newman 1994). Such coals are uncommon, and generally associated with lake margin (Dunollie Fm.) or coastal (Mt. Somers, Kaitangata) settings rather than riverine floodplains typical of the Haumurian (e.g. Newman 1987; Ward 1996). High inertinite content in these coals also points towards less saturated and more oxygenated conditions (Newman 1994).

The final aspect of KTB floral change at Greymouth Coalfield which requires explanation is the decline in angiosperm and gymnosperm diversity at c.4m above the KTB (Appendix 6.4.1, 6.4.2). A brief period of extreme climate variation followed by return to more average conditions could explain the observed trends, though the causal event(s) did not disrupt the general pattern of early to late Paleocene floras. The component of climate which changed may have been different from the component which exerted most influence at the KTB. There is no comparable trend in spore proportion or diversity throughout the lowest 10m of Teurian strata (Figure A6.8), suggesting that precipitation, at least, remained relatively constant.

To date, the present study of Greymouth Coalfield provides the most thoroughly documented non-marine record of change in terrestrial palynofloras across KTB from the Southern Hemisphere. However, palynology does not provide all the necessary clues to the cause(s) of floral change at the KTB in Greymouth Coalfield. Limited plant macrofossil evidence indicates more floral change than microfloras (Johnson 1992b), and no useful data has yet been obtained from fossil wood or paleomagnetic, isotope or geochemical analysis to support conclusions obtained from microfloras alone. Correlation of the floral events documented in Greymouth Coalfield and elsewhere with the KTB mass extinction event as recorded in the marine realm will only be confirmed when iridium anomalies have been located within Paparoa Group strata. As yet, there are no Southern Hemisphere terrestrial sites with such anomalies documented.

Part 3.

Data Tables

Appendix 9. Location data, drillholes used in thesis

Sources: DH001–DH269 Gage (1952)
DH270–DH598 NZGS coal drillhole record forms
DH599–DH618, DH629 State Coal Mines
DH619–DH668 (excluding DH629) Coal Resources Survey
DH686–DH694 Coal Corporation on NZ Ltd.
DH695–716, 725, 726 Greymouth Coal Operating Ltd.
DH717–719, 727–751 Coal Corporation on NZ Ltd.

Notes: all drillhole locations shown on Figure 1.3 (map pocket)
easting and northing in metres, NZ Map Grid
collar rl = elevation of collar above mean sea level (m)
td = total depth (m)
units: G = Goldlight Fm., R = Rewanui CMM, W = Waiomo MM, M = Morgan CMM, F = Ford Fm., J = Jay Fm., B = Basement

DH	easting	northing	collar rl (m)	td (m)	units
017	2366745.23	5870657.45		307.84	G
040	2367070.89	5865793.75		494.90	G R
086	2370927.91	5869643.43	367.89	256.64	R W M
088	2371493.15	5870699.52	357.22	70.10	W M
089	2371433.15	5870678.36	373.07	54.86	W M
090	2371718.60	5870461.98	369.41	64.92	W M
091	2370801.38	5868816.27	363.93	162.15	R
092	2371782.35	5871428.91	502.31	123.44	W M F J
093	2371925.25	5871310.65	508.40	63.70	W M
094	2371337.74	5871541.92	495.30	57.91	W
095	2371437.27	5871604.01	505.96	51.21	W M
096	2371580.16	5871485.77		102.72	W M
097	2372229.07	5871195.19	516.94	25.30	W M
098	2371448.40	5870960.33	420.31	124.36	W M
099	2370817.40	5871334.00		197.51	R
100	2370230.22	5868102.12	251.76	160.63	R
102	2369913.25	5867814.93	182.88	108.51	G
105				59.74	M
106	2368256.17	5872876.88	198.12	166.12	R
201	2369032.39	5872206.21	416.05	176.78	G R
202	2369232.16	5872290.16	428.85	143.26	G
205	2368781.33	5871598.22	263.65	262.13	R
212	2368487.96	5871110.22	232.56	160.32	G
213	2368770.62	5871054.75	311.50	190.20	G
214	2368605.17	5871313.46	338.93	228.30	G
215	2368243.79	5871266.96	165.81	136.55	G
226	2370314.86	5867862.14	111.86	243.84	R W M F J B
230	2369758.60	5867450.07	123.44	54.86	G
232	2371099.97	5869002.54	298.39	239.57	R W M F
233B	2371783.47	5870201.53	306.01	48.36	W M
241	2370927.29	5868516.63	245.36	395.63	R W M F J
246	2370862.77	5868756.96	324.61	544.06	R W M F J B

DH	easting	northing	collar rl (m)	td (m)	units
248	2371698.83	5870441.52	281.02	81.47	M F J
249	2371606.54	5871124.04	375.20	66.14	M F
250	2371871.86	5870907.30	380.08	47.24	M F
251	2371155.79	5869265.08	232.86	123.44	R M W
261	2371073.32	5868217.35	295.65	249.02	R W M F J
262	2370765.23	5869428.32	409.48	368.80	G R W M F J
265	2370774.99	5869177.99	383.43	341.68	R W M F
266	2372058.29	5862458.39	18.28	616.61	G R W M B
273	2371215.07	5863632.20		735.48	G R W M B
274	2368341.54	5867689.07	82.90	101.19	R
280	2368111.88	5867495.95	62.48	134.72	G R
282	2368219.14	5867576.28	76.50	136.09	G R
285	2368100.00	5867738.00	117.65	94.03	G
288	2368124.04	5867723.53	121.30	135.64	G R
289	2372466.51	5863985.91	320.00	605.94	G R B
291	2368318.24	5867930.53	173.43	184.40	G R
312	2371428.43	5869672.22		53.34	W M
313	2371273.00	5869468.31		54.86	W M
318	2372268.03	5868210.69		826.00	G R W M F B
336	2371873.36	5871519.02		50.29	M
338	2371795.38	5870443.19		44.20	M
339	2371965.68	5870543.73		44.29	M
341	2371934.65	5870186.04		42.67	M
342	2372663.48	5867811.91		676.19	G R W M
345	2371167.45	5871382.02		122.83	R
375	2371123.09	5870573.39	445.00	175.56	R W M
384	2371061.56	5868897.24	248.40	193.85	W M F
407	2372485.35	5871501.45	563.88	141.00	W M
408	2372485.35	5871501.45	563.88	69.49	W M
410	2371091.49	5869201.58	226.64	141.12	R W M
411	2371079.07	5869303.79	234.68	129.54	R W M
412	2371104.13	5869111.26	220.06	109.73	R W M
413	2370986.83	5869145.44	216.10	153.92	R W M
414	2369649.93	5871170.60	281.02	93.42	R
421	2372362.58	5871386.65	557.78	88.70	W M
426	2372605.14	5871555.84	618.74	86.87	W M
428	2372666.50	5871579.04	625.44	111.86	W M
429	2371093.25	5869007.44	115.82	42.67	W M
433	2367745.34	5867061.51	105.50	326.96	G R B
435	2371102.45	5869092.12	113.08	41.15	M F
443	2370849.38	5869297.99	237.74	152.40	R W M
446	2368728.98	5870321.61	134.41	133.41	R
449	2369109.43	5871010.33	149.96	214.12	R
454	2368323.45	5871314.61	140.20	140.36	R
456	2371156.41	5869927.07	363.32	197.82	R W M
463	2370884.89	5869106.45	207.56	197.82	R W M F
464	2370949.25	5868991.87	253.89	151.18	R W M F
467	2370926.25	5868833.12	238.01	243.23	R W M F
471	2370897.42	5868614.70	220.98	270.97	R W M F

DH	easting	northing	collar rl (m)	td (m)	units
475	2370936.56	5868911.16	245.97	232.56	R W M F
589	2370969.43	5869278.95	100.58	35.05	M
590	2371068.01	5869175.42	107.89	35.05	M
592	2372998.38	5869627.82	782.42	536.44	M
595				489.20	W M
600	2372469.35	5868623.18	725.00	808.90	W M
611	2368119.49	5871272.57	152.60	226.96	R
612	2368427.09	5871566.62	214.84	180.90	R
613	2368220.46	5871452.04	172.96	135.87	R
615	2368055.83	5870960.98	253.95	314.31	R
616	2373236.49	5868872.06	938.48	765.00	R W M F
617	2373128.64	5868205.38	808.86	750.00	R W M F
618	2372666.91	5869031.55	843.95	782.00	R W M F
619	2367305.87	5871393.33	93.97	608.00	G R F J B
620	2372775.47	5866191.33	698.40	800.90	G R W M F J
621	2367513.35	5872679.95	28.34	469.50	G R F J
622	2366379.30	5870591.04	86.50	429.00	G R F B
623	2368248.47	5867635.06	87.69	266.90	G R F B
624	2368499.06	5868919.76	241.50	317.30	G R F B
625	2371518.50	5866238.10	436.70	654.40	G R W M B
626	2365572.54	5869188.35	15.43	395.00	G R B
627	2370113.20	5864034.40	179.40	528.80	G R B
628	2367087.75	5866782.85	30.90	350.10	G R B
630	2370051.60	5866745.80	242.90	297.00	G R W M B
631	2368796.24	5869684.38	319.32	478.90	G R F
632	2369633.90	5869751.50	346.50	677.90	G R W M F J B
633	2365489.40	5868027.22	9.30	413.50	G R B
634	2366699.89	5872493.69	47.35	559.30	D R
635	2367842.99	5870599.04	343.10	720.00	G R F B
636	2366538.42	5867938.28	34.10	375.20	G R B
637	2365625.09	5869969.54	9.47	357.40	D R B
638	2367555.75	5868023.41	189.90	360.50	G R B
639	2366479.74	5871555.86	31.79	510.20	D R F B
640	2368238.95	5868341.95	310.60	442.30	G R F B
641	2367089.26	5870590.81	121.04	628.20	G R F
642	2366569.23	5868981.40	93.73	381.00	G R B
643	2367641.39	5868977.61	273.18	450.10	G R B
644	2366047.84	5866750.04	13.78	518.50	G R B
645	2367869.06	5869818.67	185.11	476.90	G R F
646	2366339.83	5867139.02	16.45	394.10	G R B
647	2366679.37	5869934.45	161.38	444.90	G R F B
648	2365714.07	5867542.01	11.06	354.30	G R B
649	2366961.91	5866272.96	27.49	384.40	G R B
650	2366062.27	5867979.55	21.80	314.26	G R B
651	2368620.04	5865474.90	76.60	687.20	G R F B
652	2365393.24	5866764.00	36.11	306.50	–
653	2364797.29	5867775.74	15.46	571.40	G R B
654	2368367.36	5863551.50	95.75	900.00	G R W M
655	2366889.73	5864250.51	30.60	641.70	G

Appendix 9. Drillhole locations

DH	easting	northing	collar rl (m)	td (m)	units
656	2370133.98	5872092.70	607.44	625.85	R W M F J
657	2369924.86	5871150.53	463.87	758.50	G R F J
658	2371750.77	5872461.17	768.81	375.15	R W M F J
659	2373281.97	5870906.37	802.61	517.00	R W M F J
660	2373089.89	5872185.20	855.70	478.00	G R W M F J
661	2374504.41	5872967.97	919.61	119.10	M F J B
662	2370201.67	5871552.27	570.90	256.90	G R
663	2370548.30	5872582.80	655.67	158.06	R
664	2369930.41	5870725.75	323.31	301.64	G R
665	2370428.89	5871922.17	599.37	294.40	G R
666	2370227.14	5871219.10	451.87	305.10	G R
667	2369786.70	5872054.92	547.89	194.05	G R
668	2373927.51	5871091.04	715.55	177.50	G R W M F
686	2370722.50	5872698.45	595.99	149.85	R
687	2370481.17	5872319.08	592.55	212.00	R
688	2370360.78	5872139.04	500.03	114.70	R
689	2369904.53	5872199.43	501.44	299.20	R
690	2369599.18	5872176.30	502.94	263.07	G R
691	2369616.10	5871915.69	471.98	302.52	G R
692	2370010.47	5871841.94	510.34	149.20	G R
693	2370243.44	5871778.64	524.72	236.00	G R
694	2370016.46	5871589.56	543.82	230.00	G R
695	2366509.61	5868357.99	39.45	200.00	G
696	2366470.41	5868418.07	54.20	330.80	G R B
697	2367060.90	5868446.40	90.00	373.30	G R B
698	2366933.39	5867521.30	51.00	358.60	G R B
699	2365965.11	5868812.02	68.41	415.40	G R B
700	2367799.41	5868624.78	197.46	304.60	G R B
701	2368219.60	5869457.91	288.94	391.40	G R F
702	2366112.00	5869578.11	138.47	355.45	G R B
703	2367148.51	5868984.36	121.75	376.70	G R B
704	2367071.72	5869495.90	98.75	418.50	G R F
705	2366667.05	5868638.42	80.50	427.50	G R B
706	2367372.70	5868681.95	198.59	409.40	G R B
707	2367326.50	5870050.01	184.82	532.00	G R F
708	2367630.20	5870995.37	160.53	475.40	G R F
709	2366767.56	5871115.95	100.11	499.40	G R F
710	2366981.12	5872017.96	45.85	493.40	D R F
711	2366298.32	5868704.76	19.24	295.30	G R B
712	2366759.00	5868373.00	80.70	412.00	G R
713	2367519.00	5868399.00	172.70	262.70	G R
714	2367408.00	5869002.00	248.90	373.70	G R
715	2367007.00	5868798.00	100.40	397.80	G R
716	2367266.00	5868299.00	139.10	334.80	G R
717	2372065.00	5869646.00	455.48	218.00	G R
718	2372134.00	5869916.00	537.08	246.60	G R
719	2372268.00	5872500.00	795.66	243.50	R W M F
725	2366613.00	5868382.00	81.74	384.30	G R
726	2366756.00	5869154.00	71.39	407.70	G R

Appendix 9. Drillhole locations

DH	easting	northing	collar rl (m)	td (m)	units
727	2372872.00	5868514.00	791.28	739.85	G R W M
728	2368231.00	5871358.00	184.95	148.70	G R
729	2368167.00	5871578.00	239.55	193.80	G R
730	2373377.00	5867699.00	817.26	756.65	G R W M
731	2367929.00	5870866.00	217.52	353.70	G R
732	2372201.00	5867889.00	491.33	591.55	G R W M F
733	2368251.00	5870787.00	379.12	374.02	G R
734	2373441.00	5868475.00	904.27	771.10	G R W M F
735	2368251.00	5871081.00	262.17	286.00	G R
736	2372582.00	5869656.00	579.22	433.65	G R W M F
738	2369588.00	5871782.00	431.99	28.80	R
739	2369550.00	5871775.00	421.77	30.50	R
740	2369981.00	5872038.00	557.09	76.80	R
741	2370128.00	5871951.00	586.36	67.60	R
742	2369763.00	5871763.00	455.31	30.50	R
743	2371176.00	5871986.00	649.90	280.65	R W M
744	2373555.00	5872701.00	801.56	109.55	R W M
745	2373706.00	5872308.00	843.09	222.45	R W M
746	2370742.00	5871441.00	570.27	446.80	R W M F
747	2369947.00	5871814.00	487.67	47.60	R
748	2370801.00	5871831.00	612.81	333.40	R W M
749	2371089.00	5871552.00	569.62	261.15	R W M
750	2370787.00	5872315.00	641.49	303.95	R W M
751	2371199.00	5868682.00	193.31	256.00	R

Appendix 10. Lithostratigraphic data

All lithostratigraphic data for drillholes used in this thesis are presented in the following Appendices. Thickness values (all in metres) are corrected to true thickness where possible.

Appendix 10.1 Lithostratigraphic data, Goldlight Formation

note: trans. = transitional lithosomes, mst = mudstone lithosomes

DH	thick-ness	mini-mum	top	base	upper trans.	mst	lower trans.	notes
017		61.0	246.9		yes	yes	yes	data poor
040		114.3	269.1	383.4	prob	yes	prob	contacts with trans. poorly defined
102		37.8		37.8		yes	poss	poss. thin lower trans.
201		96.6		99.7		62.8+	33.8	trans. previously in Rewanui Fm
202		106.7		108.5		71.3+	35.4	trans. previously in Rewanui Fm
212		117.6		119.5		59.4+	60.0	trans. previously in Rewanui Fm
213		110.9		110.9	poss	yes	prob	data poor
214		97.5	64.0	161.5	poss	yes	prob	data poor
215		34.5	9.1	43.6	poss	yes	prob	data poor
230		10.4		27.1		10.4+	0.0	
262		15.8		15.9		15.8+	0.0	
266	171.1		261.8	435.2	14.0	153.1	4.0	trans. units prev. in coal measures
273	171.7		411.5	569.4	16.1	141.8	13.8	trans. units prev. in coal measures
280		52.4		52.4		52.4+	0.0	
282		44.0		44.0		44.0+	0.0	
285		58.6		76.9		58.6+	0.0	
288		48.0		74.8		48.0+	0.0	
289	145.0		353.6	498.6	13.4	128.9	2.7	
291		64.7		70.1		64.7+	0.0	
318		130.1	268.2	398.5	poss	130.1+	0.0	data poor at top, close to full thickness
342		138.0	280.9	418.9	61.7?	138.0	0.0	too thick if upper trans. included, otherwise close to full thickness
433		71.7	104.1?	188.1	poss	71.7	0.0	data poor
619	6.0		236.0	241.8	0.0	6.0	0.0	only thin mst recognizable as Goldlight Fm.
620	140.0		367.5	507.5	0.0	140.0	0.0	
621	1.7		62.6	64.3	0.0	1.7	0.0	only thin mst recognizable as Goldlight Fm.
622	44.9		222.0	268.5	44.9	0.0	0.0	all trans.
623		39.2		45.6		39.2+	0.0	
624		46.8		52.0		46.8+	0.0	
625	138.4		304.0	443.0	44.0	94.4	0.0	base poss. faulted
626	59.5		242.0	302.4	59.5	0.0	0.0	all trans., caved open hole
627	133.3		311.4	446.8	38.6	94.7	0.0	
628		89.0	161.0	274.4	0.0	89.0	0.0	faulted (see Appendix 2)
630		73.0		73.0	25.0+	48.0?	?	open hole, unsure of correlations
631		84.2	63.0	148.5	18.2	66.0+	0.0	base faulted
632		41.9	209.0	250.9	0.0	41.9+	0.0	too thin, trans. lithosomes absent, possible fault at base

Goldlight Fm. cont.

DH	thick-ness	mini-mum	top	base	upper trans.	mst	lower trans.	notes
633	87.1		289.5	378.0	49.7	37.4	0.0	
634	0.0							absent, only Dunollie Fm
635	113.4		264.0	379.2	42.3	19.4	51.7	thickest mst bed in sequence designated mst lithosome
636	109.8		191.1	302.0	0.0	109.8	0.0	
637	0.0							no Goldlight Fm, Dunollie Fm is lateral equivalent
638	127.7		83.0	217.7	33.0	94.7	0.0	
639	0.0							no Goldlight Fm, Dunollie Fm is lateral equivalent, data poor
640		41.0	137.0	187.0	0.0	41.0+	0.0	fault at 137m
641		94.9	273.0	340.2	94.9+	0.0	0.0	close to full thickness, stratigraphy 242m–273m unclear
642	91.4		181.2	274.0	44.1	47.3	0.0	
643		86.2	195.0	281.2	18.0+	68.2	0.0	top faulted
644	86.6		371.2	457.8	23.8	62.8	0.0	
645	160.0		20.0	181.5	27.7	55.0	77.3	see Section 2.3 for correlation, thicker than minimum curvature model
646		71.3	244.0	337.5	13.8	57.5	0.0	poss. fault c.262m, dip of Goldlight Fm unknown. est 40°
647		34.7	249.0	284.2	34.7+	0.0	0.0	badly caved, no core
648		67.7	240.3?	308.0	0.0?	67.7	0.0	top uncertain, unusual log pattern
649	89.3		236.0	325.3	34.0	55.3	0.0	
650		79.5	186.0?	265.5	0.0?	76.5	3.0	top uncertain, close to full thickness
651	172.4		320.0	493.0	59.8	100.6	12.0	
653	58.3		498.0	557.2	10.3	48.0	0.0	minor sst in mst
654	158.1		449.0	672.3	80.2	61.0	16.9	60m dolerite intrusion
655		130.2	492.7		48.5	81.7+		eoh in Goldlight Fm
657		130.6		184.7		130.6+	0.0	dip c.45°
660		78.2		78.2		78.2+	0.0	
662		111.8		121. 5		118.0+	0.0	close to full thickness
664		138.5		160.0		138.5+	0.0	dip c.30°, close to full thickness
665		107.0		123.6		107.0+	0.0	
666		124.3		146.5		124.3+	0.0	close to full thickness
667		102.9		104.5		98.6+	4.3	occ. silt/vfsst i/b in mst
688		15.6		15.6		15.6+	0.0	summary data only
690		51.9		51.9		51.9+	0.0	summary data only
691		33.0		37.0		33.0+	0.0	summary data only
692		5.6		9.8		5.6+	0.0	summary data only
693		9.0		10.6		9.0+	0.0	summary data only
694		88.0		89.2		88.0+	0.0	summary data only
695		49.8	150.1		22.1	27.7+		abandoned, faulting 195.4m
696	134.1		144.5	280.6	17.7	116.4	0.0	thicker than minimum curvature model, c.30m higher than surrounding dh's in final model
697	107.2		176.7	286.7	19.8	87.4	0.0	
698	118.3		150.6	270.2	21.2	97.1	0.0	base poss. faulted

Goldlight Fm. cont.

DH	thick-ness	mini-mum	top	base	upper trans.	mst	lower trans.	notes
699	87.6		236.3	327.0	0.0	87.6	0.0	minor sandy i/b's
700		114.0		122.2	44.8+	62.8	7.1	close to full thickness
701	100.9?		67.6	169.0	6.5	94.4	0.0	c.30m thinner than final model
702		66.1	186.4	254.8	all	0.0	0.0	all trans., faults at 202m, 216m
703	98.8		163.5	265.8	35.7	63.1	0.0	
704	103.3		191.2	296.1	47.0	59.7	0.0	
705	98.2		192.8	297.2	16.7	81.5	0.0	prob. fault at 197m, 248m
706	113.4		168.4	283.0	45.6	67.8	0.0	poss. fault at base
707	113.6		213.6	329.3	113.6	0.0	0.0	all trans.
708	116.1		64.5	201.7	37.2	14.0	57.1	thickest mst bed in sequence designated mst lithosome, thicker than minimum curvature model
709	81.9		226.4	309.1	81.9	0.0	0.0	all transitional,thicker than minimum curvature model
710	0.0							no Goldlight Fm, Dunollie Fm is lateral equivalent
711		77.4	130.3	208.9	6.5+	71.8	0.0	top faulted, close to full thickness
712	101.2		241.5	350.5	11.7	89.5	0.0	
713	105.1		72.5	188.5	34.3	70.8	0.0	thinner than minimum curvature model, no e-log inspected
714	98.0		210.4	309.9	34.1	63.9	0.0	
715	103.1		184.2	298.0	42.6	60.5	0.0	
716	122.5		151.4	274.6	44.1	78.4	0.0	poss faults at 259m and 272m, possibly overthickened
717		173.8		183.5		173.8+	0.0	detailed data not available, no correction for dip, c.30m thicker than predicted by model
718	139.2		55.0	208.6	0.0	139.2	0.0	
725	97.0		210.0	317.0	15.0	82.0	0.0	
726	104.5		200.5	305.0	27.0	77.5	0.0	
727	142.5		294.2	436.7	?	142.5	?	summary data only
728		60.5		73.5		26.8+	33.7	
729		40.0	51.0?	91.0?	?	?	?	summary data only
730	141.8		281.4	423.2	?	?	?	summary data only
731		96.1	?171.9	268.1	32.2?	14.4	49.3	top uncertain, carb. i/b's in trans, bioturbation common
732	133.3		153.2	286.5	?	?	?	summary data only
733	103.2		160.9	264.1	32.6	24.8	45.8	*Hyridella* in upper trans.
734	138.8		305.0	443.8	?	?	?	summary data only
735		98.3	?74.4	184.2	?	9.6	88.4	top uncertain, prob fault at 140m, c.30m repetition. Close to full thickness.
736		86.0		128.1	?	?	?	summary data only

Appendix 10.2 Lithostratigraphic data, Rewanui CMM

DH	thickness	minimum	top	base
040		77.4	416.6	
086		188.4		188.4
091		142.3	19.8	
099		197.5		
100		131.7	26.2	
106		164.3		
201		77.1	99.7	
205		206.9	55.3	
226		92.0		99.7
232		147.5		156.1
241		189.5		192.5
246		235.6		251.1
251		73.8		73.8
261		135.9		141.4
262	233.8		15.9	249.6
265	234.7		5.5	243.8
266	107.1		435.2	544.0
273	109.4		569.4	678.8
274		101.2		
280		82.3	52.4	
282		92.1	44.0	
288		60.8	74.8	
289	102.1		498.6	602.3
291		114.3	70.1	
318	218.3		398.5	624.5
342		201.8	418.9	627.9
345		122.8		
375		91.3		92.7
410		73.8		72.5
411		82.3		79.9
412		64.0		64.0
413		74.7		71.0
414		92.4		
433	111.8		188.1	301.7
443		78.0		78.0
446		212.0		
449		174.0		
454		140.2		
456		124.1		124.1
463		77.7		77.7
464		125.0		125.0
467		154.5		154.5
471		164.3		164.3
475		125.0		125.0
611		189.6		
612		136.2		

DH	thickness	minimum	top	base
613		113.8		
615		133.5		
616		174.6		675.1
617		109.7		665.5
618		109.5		706.1
619	203.6		241.8	448.5
620	211.2		507.5	722.0
621	231.8		64.3	311.0
622	124.6		268.5	397.5
623	204.1		45.6	252.8
624	184.7		52.0	239.5
625	172.7		443.0	616.4
626	82.4		302.4	386.1
627	71.7		446.8	519.6
628		43.4	251.4?	310.3
630	168.1		73.0	247.1
631		207.3	148.5	387.9
632	165.5		250.9	419.0
633	31.1		378.0	409.6
634		188.0	319.0	513.0
635	222.6		379.2	605.2
636	87.0		302.0	370.2
637	97.8		252.0	351.9
638	136.6		217.7	356.5
639	172.7		272.8	456.6
640	201.9		187.0	396.0
641	199.8		340.2	547.0
642	103.6		274.0	379.2
643	156.1		281.2	438.6
644	50.7		457.8	508.5
645	224.1		181.5	407.6
646	38.8		337.5	388.1
647	130.4		284.2	416.6
648	21.0		308.0	329.0
649	51.6		325.3	376.9
650	38.5		265.5	304.0
651	151.5		493.0	648.2
653	7.6		557.2	564.9
654	181.3		672.3	860.2
656		231.8		246.7
657	223.9		184.7	494.9
658		155.1		189.4
659		208.0		229.4
660		90.0	78.2	171.5
662		122.8	121.4	
663		155.6		

Rewanui CMM cont.

DH	thickness	minimum	top	base
664		133.2	159.9	
665		148.0	123.6	
666		140.0	146.5	
667		92.5	104.5	
668		63.0		77.2
686		149.9		
687		234.7		
688		99.1	15.6	
689		202.2		
690		209.9	51.9	
691		265.5	37.0	
692		139.4	9.8	
693		225.9	10.6	
694		141.3	89.2	
696		38.2	280.6	320.1
697	67.5		286.6	355.6
698	71.9		270.2	344.6
699	75.2		327.0	404.9
700	158.6		122.2	297.2
701	186.9		169.0	362.5
702	86.8		254.8	344.7
703	96.4		265.8	365.6
704		115.7	296.1	415.9?
705	122.6		297.2	424.1
706	111.3		283.0	398.2
707	171.6		329.3	505.4
708	213.9		201.7	448.6
709	169.3		309.1	481.0
710	216.3		264.4	484.0
711	74.0		208.9	284.0
712		61.5	350.5	
713		74.2	188.5	

DH	thickness	minimum	top	base
714		63.8	309.9	
715		69.8	298.0	
716		60.2	274.6	
717		34.0	183.5	
718		34.4	208.6	
719		80.0		82.6
725		63.7	317.0	
726		102.7	305.0	
727	234.1		436.7	670.8
728		108.5	73.5	
729		102.8		
730	248.7		423.1	671.8
731		85.6	268.1	
732	239.7		286.5	526.2
733		109.9	264.1	
734	240.2		443.8	684.0
735		98.3	184.2	
736	230.8		128.1	358.9
738		28.8		
739		30.5		
740		61.3		
741		67.6		
742		33.5		
743		203.5		214.1
744		60.7		60.7
745		465.6		465.9
746		295.2		295.2
747		47.6		
748		275.2		275.2
749		209.0		218.6
750		218.5		252.3
751		250.0	6.0	

Appendix 10.3 Lithostratigraphic data, Waiomo MM

DH	thick-ness	mini-mum	top	base	notes
086	36.0		188.4	224.5	mudstone
088	29.3		18.0	50.3	mudstone
089	27.4		21.6	49.1	"shaley sandstone and mudstone"
090	29.9		16.5	46.3	"fine dark shaley sandstone" present at top, poss. transitional
092	27.1		18.6	45.7	"fine dark shaley sandstone" present at top, poss. transitional
093	27.1		27.7	54.9	"fine dark shaley sandstone" present at top, poss. transitional
094		40.2	17.7		thicker than surrounding holes, not all drilled
095	29.9		12.8	42.7	"fine dark shaley sandstone" present at top, poss. transitional
096	27.1		69.2	96.3	"fine dark shaley sandstone" present at top, poss. transitional
097		21.3		21.3	"fine dark shaley sandstone" present at top, poss. transitional
098	30.5		82.6	112.8	"fine dark shaley sandstone" present at top, poss. transitional
226	25.9		99.7	125.6	minor sandstone
232	25.9		156.1	182.0	mudstone
233B	28.0		12.2	40.4	hole not vertical, orientation unknown, therefore maximum
241	26.4		192.5	223.0	corrected for average 25° dip
246	25.2		251.1	277.7	mudstone
251	36.9		73.8	110.6	mudstone
261	37.2		141.4	178.6	mudstone, no dip correction
262	24.1		249.6	273.7	siltstone
265		20.4	243.8	264.4	mudstone
266	10.7		544.0	554.9	mudstone, included in Rewanui CMM by Newman (1985)
273	10.3		678.8	689.1	sandy mudstone, included in Rewanui CMM by Newman (1985)
312	21.0		24.4	45.4	data poor, may be up to 31.7m
313	31.7		13.7	45.6	mudstone with sandstone i/b's
318	33.2		624.5	657.8	mudstone
342	28.1		627.9	654.1	mudstone, sandstone at base
375	43.1		92.7	137.0	may be too thick
384	16.5		104.8	128.0	mudstone
407		13.1		13.1	mudstone
408		13.1		13.1	mudstone, same location as DH408
410	27.6		72.5	101.4	mudstone
411	30.5		79.9	82.3	mudstone
412	26.5		64.0	90.5	mudstone
413	24.7		71.0	98.2	mudstone + siltstone near base
421		3.7		7.6	mudstone
426	21.7		29.6	51.8	mudstone
428	19.2		52.1	71.3	mudstone
429	22.2		-25.9	-3.7	mudstone, hole drilled vertically upwards
443	30.0		78.0	107.0	could be greater, poss. transitional units present
456	26.7		124.1	138.4	may be up to 41.0m, poss. transitional units present
463		17.4	77.7	95.1	may be up to 37.0m, poss. transitional units present
464	24.8		125.0	149.8	may be up to 34.3m, poss. transitional units present
467	25.3		154.5	179.8	possibly faulted, therefore minimum
471		14.6	164.3	178.3	correlations unclear
475	27.0		125.0	158.0	mudstone
595	27.4				from SCM sections

Waiomo MM cont.

DH	thick-ness	mini-mum	top	base	notes
600	28.4				from SCM sections, stratigraphy unreliable
616	24.2		675.1	699.4	mudstone
617	27.2		665.5	692.7	mudstone
618	25.1		706.1	731.2	mudstone
620	34.0		722.0	756.0	not cored, all mudstone
625	22.6		616.4	639.0	not cored, all mudstone
630	20.2		247.1	267.3	not cored, all mudstone
632	22.7		419.0	442.1	see Appendix 2. Coarsening-upwards sandy interbeds
654	3.6		860.2	863.8	sandy interbeds, placed in Rewanui CMM by Newman (1985)
656	5.9		246.7	253.5	all transitional, 1 coarsening-upwards packet
658	57.6		189.4	252.9	top contact poss. faulted, 7.4m transitional at top, contains tuff
659	22.9		229.4	252.7	mudstone
660	51.6		171.5	223.9	16.3m transitional, 25.3m mudstone, 10.0m transitional
668	31.7		77.2	112.2	mudstone
719	33.6		82.6	117.0	7.9m transitional at top (prev. Rewanui CMM), 25.7m mudstone
727	25.5		670.8	696.3	mudstone
730	27.8		671.8	699.7	mudstone
732	26.5		526.2	552.7	mudstone
734	24.3		684.0	708.3	mudstone
736	24.2		358.9	383.1	mudstone
743	39.2		214.1	255.3	mudstone
744	25.4		60.7	86.1	mudstone
745	20.4		165.9	186.4	mudstone, possibly too thin
746	16.4		295.2	311.6	mudstone
748	34.9		275.2	310.7	mudstone
749	28.8		218.6	248.7	mudstone
750	17.7		252.3	272.7	mudstone

Appendix 10.4 Lithostratigraphic data, Morgan CMM

Note: Minimum values which are noted as being "close to full thickness" are included on Figure 3.19, other minimum values omitted for clarity.

DH	thickness	minimum	top	base	notes
086		32.3	224.5		
088		18.6	50.3		
089		5.8	49.1		
090		18.6	46.3		
092	38.7		45.7	84.4	value unreliable, too low
093		8.8	54.9		
095		8.5	42.7		
096		6.4	96.3		
097		4.0	21.3		
098		11.6	112.8		
105		18.3	41.5		
226	32.0		125.6	157.6	
232	50.0		182.0	232.0	
233B		7.9	40.4		
241	42.7		223.0	265.8	contains quartzose sandstone
246	36.7		277.7	314.3	
248		31.1	31.1		
249		25.8	25.8		
250		27.4	27.4		
251		12.8	110.6		
261	22.3		178.6	200.9	contains quartzose sandstone
262	43.3		273.7	317.0	transitional at base now in Ford Fm.
265	50.6		264.4	315.8	
266	58.5		554.9	613.2	placed in Rewanui CMM by Newman (1985), on basement
273	40.6		689.1	729.6	placed in Rewanui CMM by Newman (1985), on basement
312		7.9	45.4		
313		9.1	45.6		
318	45.4		657.8	703.2	
336		50.3			greater than nearby DH092
338		44.2			
339		46.9			
341		42.7			
342		20.2	654.1		
375		38.7	137.0		
384	57.0		128.0	185.0	
407		29.8	13.1		
408		56.4	13.1		close to full thickness
410		40.1	101.4		DH410–463 contain probable quartzose sandstones
411		16.7	82.3		
412		19.2	90.5		
413		54.6	98.2		close to full thickness
421		81.1			close to full thickness
426		30.5	51.8		

Morgan CMM cont.

DH	thickness	minimum	top	base	notes
428		40.5	71.3		
429		3.7			drilled vertically up
435		40.2	40.2		
443		45.4	107.0		
456		44.3	138.4		
463	55.2		95.1	149.8	
464	57.5		149.8	207.3	
467	41.8		179.8		
471	34.1		178.3	212.5	
475	52.6		158.0		
589		35.1			
590		35.1			
592	44.5				estimated from SCM sections, data poor
595	57.2				estimated from SCM sections, location unknown
600	42.0				estimated from SCM sections, data poor
616	62.2		699.4	761.6	
617	51.4		692.7	744.1	
618	47.5		731.2	778.7	
620		25.5	756.0	781.5	faulted lower contact (fractured, loss of circulation)
625	6.0		639.0	645.0	
630	26.0		267.3	293.3	
632	55.2		442.1	499.2	only WCS provenance
654		36.2	863.8		ECS sandstone, outlier of Morgan CMM
656	26.7		253.5	291.2	ECS sandstone, see Appendix 2 for new correlation
658	35.3		252.9	291.9	ECS sandstone
659	52.5		252.7	306.0	fault repetition of Morgan CMM (see Appendix 10.5)
660	28.7		223.9	252.6	
661		28.6	29.6		close to full thickness
668		45.8	112.2	161.6	fault at 120–122m
719	51.9		117.0	172.3	
727		43.6	696.3		close to full thickness
730		57.0	699.7		close to full thickness
732	30.7		552.7	583.4	
734	53.0		708.3	761.2	
736	38.8		383.1	421.9	
743		24.1	255.3		
744		23.5	86.1		close to full thickness
745		36.1	186.4		close to full thickness
746	71.9		311.6	383.5	
748		22.7	310.7		
749		12.4	248.7		
750		31.0	272.7		close to full thickness

Appendix 10.5 Lithostratigraphic data, Ford Formation

Notes: Data is poor for drillholes numbered <616.
trans. = transitional lithosomes, mst = mudstone lithosomes

DH	thick-ness	mini-mum.	top	base	trans.	mst	tuff	notes
092		22.6	84.4	106.7	–	all		value too low
226	23.5		157.6	181.1	–	all		
232		7.6	232.0		–	all		
241	89.9		265.8	383.4	–	all	poss.	
246	155.2		314.3	469.5	–	all	comm.	
248	43.1		31.1	77.7	–	all		sandy top/base. Thickness incorrect in Gage (1952)
249		40.5	25.8		–	all		
250		20.1	27.4		–	all		sandy interbeds
261	42.4		200.9		–	all		some Ford Fm. transferred to Jay Fm, sandy interbeds
262	51.5		317.0	368.5	19.2	32.3		trans. previously in Morgan CMM
265		25.5	315.8		–	all		sandy interbeds
318	116.7		703.2	819.9	–	all	none	on basement
384		8.8	185.0		–	all		
435		1.0	40.2		–	all		
463		25.9	149.8		?			white–lt. grey sandstone common in top c.15m, ?trans.
464		28.4	207.3		?			"
467		21.6	221.6		?			"
471		55.5	212.5		?			"
475		24.8	210.8		?			"
616		3.4	761.6		–	all		
617		6.0	744.1		–	all		
618		3.1	778.7		–	all		
619	115.0		448.5	564.8	58.1	56.9	poss.	occ. tuff may be present
620		14.4	781.5	796.1	–	all	yes	sandy throughout, top faulted
621	81.2		311.0	393.4	45.5	35.7	yes	pebble conglomerate in trans., base poss. faulted
622	18.7		397.5	416.2	all			on basement
623	10.7		252.8	263.5	all		yes	on basement
624	71.1		239.5	311.7	30.0	41.1	yes	on basement
631		82.5	387.9		38.6	43.9+	yes	basal 15.3m is volcanic cong.
632	152.2		499.2	653.7	61.2	91.0	comm.	
635	110.7		605.2	717.7	24.4	62.4	17.5m	tuff between trans.and mst, sandy at base, on basement
639	50.4		456.6	507.7	all	–	absent	on basement
640	37.1		396.0	433.6	–	all	comm.	volcanic agglomerate, cong. near base, on basement
641		25.0	547.0		yes	yes	yes	faulted
645		68.2	407.6		20.6	47.6+	yes	
647	23.2		416.6	440.2	all	–	yes	on basement
651	37.8		648.2	686.6	all	–	absent	on basement
656	185.6		291.2	489.0	36.1	111.8	yes	37.7m debris flow between trans. and mst

Ford Fm. cont.

DH	thick-ness	mini-mum.	top	base	trans.	mst	tuff	notes
657	180.8		494.9	679.6	52.5	128.3	yes	conglomerate and coal clasts in trans.
658		16.10	291.9	309.0	–	all	absent	faulted upper contact
659	118.2		306.0	490.2	7.5	110.7	yes	58.3m fault repetition of Morgan CMM and Ford Fm at 326m, debris flow conglomerate common
660	146.8		252.6	410.6	48.8	98.0	poss.	fault 304.4m–318.2m, also caving 390-410m, variable dip
661	36.8		29.6	67.7	–	all	yes	see Section 2.6.2 for recorrelation
668		14.4	161.6		8.0	6.4+		
701		30.5	362.5		24.9	18.0+	absent	?fault at c.382m
704		2.6	415.9		2.6+			hole abandoned in artesian
707		26.0	505.4		all	–	absent	gouge at 529.4m
708		23.6	448.6		all	–	absent	debris flow at c.469m
709		17.6	481.0		all		absent	top poss. faulted minor conglomerate in trans.
710		9.4	484.0		9.4+			include coal clasts
719		62.9	172.3		7.7	55.2+	absent	"Jay Fm" mud-supported cong. transferred to Ford Fm
732		8.2	583.4		–	all	?	no lithological or e-log inspected
734		9.9	761.2		–	all	?	no lithological or e-log inspected
736		11.8	421.9		–	all	?	no lithological or e-log inspected
746		63.3	383.5		–	all	?	no lithological or e-log inspected

Appendix 10.6 Lithostratigraphic data, Jay Formation

DH	thickness	min.	top	base	jay (iii)	jay (ii)	notes
092		16.8?	106.7				may only be conglomerate in Ford Fm.
226	56.7		181.1		18.0	38.7	probably on basement
241		20.0	283.4		12.5	7.5+	
246	4.0		469.5	473.4	2.6	1.4	top poss. faulted, on basement
248		7.3	77.7				interbedded coal measures and cong.
261		2.4	246.6		–	all	
262		0.3	368.5		–	all	
619	34.1		564.8	599.3	16.4	17.7	
620		4.8	796.1		–	all	may be volcanic conglomerate in Ford Fm
621		74.8	393.4		65.8	9.0+	probably close to full thickness
632	18.7		653.7	673.1	all	–	
656		132.0	489.0		52.7	79.3+	
657		77.8	679.6		40.3	37.5+	
658		62.2	309.0		37.1	25.1+	
659		26.4	490.2		24.0	2.4+	
660		65.1+	410.6		24.5	40.6+	poss. faulted at top (no core)
661	26.8		67.7	95.4	4.9	21.9	basal c.5m mudstone with fine pebbles, on basement

Appendix 11. Input data for burial analysis

Appendix 11.1 Vitrinite Reflectance (VR) data

Notes:
Calorific Value (CV) and Volatile Matter (VM) data are given where available.

Units **D** = Dunollie Fm., **R** = Rewanui CMM, **uR** = upper Rewanui CMM, **lR** = lower Rewanui CMM, **M** = Morgan CMM, **J** = Jay Fm.

Corrections **t** = type (vitrinite suppression)
d = depth below top Rewanui CMM
rm = conversion from Ro (random) to Ro (max)
(DH273 estimated from DH266).
Where sample depths span an interval, VR, CV and VM values are from composite sample representing full seam thickness.

Sources CRS = Coal Resources Survey data from CRA and ACIRL
CRS (map) = data from Bowman et al. (1984, Volume I, Plan 45)
JN 87 = Newman (1987)
JN pc = Newman (pers. comm. and unpublished CRL data)
RJB = Boyd (1993)
C&N = Cave and Newman (1995)

DH	source	depth (or unit)	VR value (original)	Calorific value MJ kg^{-1}	Volatile matter %	corrections	Ro_max top R	depth of burial (km)
266	JN 96	135.6 (D)	0.90			d +0.10	1.00	3.19
273	JN 96	573.0	0.87			rm +0.08	0.95	3.03
415	CRS (map)	uR	0.67				0.67	2.16
592	CRS (map)	lR/M?	1.20			d -0.08	1.12	3.56
596	CRS (map)	ditto	1.25			d -0.08	1.17	3.72
616	CRS (map)	ditto	1.25			d -0.08	1.17	3.72
617	CRS (map)	ditto	1.23			d -0.08	1.15	3.66
618	CRS (map)	ditto	1.14			d -0.08	1.06	3.37
619	JN 87	258.8-260.6	0.53	33.46	42.91	t +0.05	0.58	1.87
620	CRS (map)	M?	1.22			d -0.08	1.14	3.62
621	CRS	90.8-92.6	0.54	32.68	42.71	t +0.05 d -0.01	0.58	1.87
622	JN 87	280.4-285.4	0.43	32.99	42.05	t +0.04	0.52	1.69
623	JN 87	88.2-90.8	0.60	34.02	41.98	t +0.05	0.65	2.09
624	JN 87	97.0-99.8	0.63	34.27	40.33	t +0.04 d -0.01	0.66	2.13
626	CRS	357.9-359.0	0.51	31.96	43.56	t +0.05 d -0.02	0.54	1.75
628	JN 87	287.7-298.4	0.54	33.77	42.13	t +0.05	0.59	1.91
630	CRS	135.2-137.2	0.76	35.82	43.69	d -0.02	0.74	2.38
631	JN 87	223.4	0.62	34.21	42.66	t +0.06	0.68	2.19
632	JN 87	265.9	0.70	34.75	40.18	t +0.05	0.75	2.41
633	JN 87	391.1-400.8	0.38	33.51	48.66	t +0.16	0.54	1.75

VR data cont.

DH	source	depth (or unit)	VR value (original)	Calorific value MJ kg^{-1}	Volatile matter %	corrections	Ro_max top R	depth of burial (km)
635	JN 87	399.8	0.63	33.36	41.95	t +0.04	0.67	2.16
636	JN 87	306.5	0.55	33.09	45.66	t +0.07	0.62	2.00
638	JN 87	262.8	0.58	33.61	42.32	t +0.05 d -0.02	0.61	1.97
639	JN 87	333.4	0.54	32.31	39.93	d -0.02	0.52	1.69
640	CRS	248.0-249.9	0.58	33.93	43.87	t +0.07 d -0.02	0.63	2.03
641	JN 87	414.6-418.3	0.63			t +0.05 d -0.02	0.66	2.13
642	JN 96	284.1-286.1	0.47	32.86	43.07	t +0.10	0.57	1.84
643	JN 87	283.05	0.51	33.43	42.76	t +0.08	0.59	1.91
644		496.3	0.52	33.93	45.69	t +0.07 d -0.01	0.58	1.87
645	JN 87	226.7	0.59	33.67	45.44	t +0.07	0.66	2.13
646	JN 87	341.3	0.47	32.89	43.72	t +0.10	0.57	1.84
647	CRS	311.9-318.4	0.57	32.83	43.09	t +0.10 d -0.01	0.68	2.19
648	JN 87	312.0-314.6	0.54	32.18	42.14	t +0.02	0.56	1.81
650	JN 87	295.6	0.55	33.28	44.16	t +0.05	0.60	1.94
656	CRS	55.9-57.8	0.72	34.32	43.96	d -0.02	0.70	2.25
658	CRS	63.9-65.6	0.82	35.04	42.48	d -0.02	0.80	2.56
659	RJB	0.5	1.09				1.09	3.47
660	CRS	223.9-230.4	1.05	37.06	32.69	d -0.05	1.00	3.19
661	CRS (map)	J	1.17			d -0.08	1.09	3.47
662	CRS	140.2-141.9	0.72	35.35	43.58		0.72	2.31
663	CRS	15.8-16.2	0.67	34.55	41.59		0.67	2.16
664	CRS	182.2-183.2	0.77	34.91	39.79		0.77	2.47
665	CRS	147.4-149.0	0.80	34.78	39.70		0.80	2.56
666	CRS	192.6-193.7	0.75	34.77	39.94	d -0.02	0.73	2.34
668	C&N	IR?	1.38			d -0.06?	1.32	4.19
686	JN pc	140.6-145.3	0.75			rm +0.05 d -0.05	0.75	2.41
687	JN pc	222.2-228.5	0.74			rm +0.05 d -0.07	0.72	2.31
689	JN pc	42.5-57.5	0.62			rm +0.05	0.67	2.16
690	JN pc	77.6-83.1	0.63			rm +0.05	0.68	2.19
691	JN pc	60.5-65.6	0.65			rm +0.05	0.70	2.25
692	JN pc	32.8-42.1	0.63			rm +0.05	0.68	2.19
693	JN pc	27.9-32.5	0.70			rm +0.05	0.75	2.41
694	JN pc	109.5-114.9	0.69			rm +0.05	0.74	2.38
717	JN pc	208.0-212.0	0.96				0.96	3.06
718	JN pc	241.1-242.4	0.95				0.95	3.03
719	JN pc	117.2-121.7	0.97			d -0.10	0.87	2.78
727	JN pc	728.8-734.2	1.25			d -0.10	1.15	3.66
736	JN pc	383.1-386.8	1.08			d -0.08	1.00	3.19
740	JN pc	60.6-73.5	0.69				0.69	2.22

Appendix 11.2 Lithological proportions, coal measure units

Appendix 11.2.1 Rewanui CMM

Notes:

* = estimated thickness

Lithological proportions estimated as follows:

DH446 has base Rewanui CMM at 157.6m, lithologies above collar height (see Appendix 2) estimated as 15m coal, 35m mudstone and 4m sandstone.

DH628 faulted (Appendix 2), lithologies estimated from coal proportion trends (e.g. Ward 1996, Figure 5)

Lithologies for DH636 and DH696 estimated from Ward (1995, fig. 11)

DH662, 664 and 666 estimated from DH657

DH663, 665 and 667 estimated from DH656

DH668 estimated from DH659

DH704 faulted (Appendix 2), 15m of section added as 13m sandstone and 2m mudstone

DH	thickness (m)	coal %	mudstone %	siltstone %	sandstone %	conglomerate %	coarse:fine ratio
246	235.6	2.34	17.18	26.21	54.27	0.00	1.19
262	233.8	6.66	3.85	11.35	78.13	0.00	3.57
265	234.7	6.53	2.32	13.19	77.84	0.13	3.54
266	107.1	7.84	19.42	15.00	57.74	0.00	1.37
273	109.4	0.37	28.24	1.37	70.02	0.00	2.34
289	102.1	2.25	31.12	0.00	66.63	0.00	2.00
318	218.3	6.78	12.14	17.12	63.83	0.13	1.77
342	240.0*	5.12	16.65	37.88	40.35	0.00	0.68
433	111.8	5.25	31.62	30.37	32.76	0.00	0.49
446	220.0*	13.55	20.68	0.00	65.77	0.00	1.92
619	203.6	6.77	35.48	5.65	29.24	22.86	1.09
620	211.2	4.01	72.15	0.00	20.99	2.85	0.31
621	231.8	2.52	13.35	18.30	11.93	53.91	1.93
622	124.6	12.78	14.25	5.16	48.48	19.33	2.11
623	204.1	2.91	39.81	19.61	30.41	7.26	0.60
624	184.7	10.03	25.01	3.57	60.00	1.39	1.59
625	172.7	5.07	47.52	28.60	18.80	0.00	0.23
626	82.4	5.08	49.47	1.42	19.13	24.91	0.79
627	71.7	2.47	45.60	26.65	25.27	0.00	0.34
628	70.0*	19.18	48.63	0.00	32.19	0.00	0.47
630	168.1	6.15	13.33	10.11	64.22	6.20	2.38
631	207.3	11.17	19.61	17.56	42.59	9.07	1.07
632	165.5	17.55	17.73	14.04	49.38	1.31	1.03
633	31.1	29.75	39.87	9.81	20.57	0.00	0.26
634	200.0*	0.98	13.81	3.51	6.24	75.46	4.46
635	222.6	4.29	28.79	4.93	30.57	31.42	1.63
636	87.0*	21.84	36.32	7.47	30.34	4.02	0.52
637	97.8	0.00	14.41	3.20	16.42	65.97	4.68
638	136.6	16.49	54.82	1.16	26.74	0.80	0.38
639	172.7	6.06	15.94	0.49	20.14	57.37	3.45

Rewanui CMM cont.

DH	thickness (m)	coal %	mudstone %	siltstone %	sandstone %	conglomerate %	coarse:fine ratio
640	201.9	11.98	47.28	10.96	29.52	0.26	0.42
641	199.8	6.47	15.93	7.19	32.91	37.50	2.38
642	103.6	5.14	22.62	6.07	20.47	45.70	1.96
643	156.1	12.92	31.22	8.68	45.03	2.15	0.89
644	50.7	8.48	25.44	34.91	31.16	0.00	0.45
645	224.1	6.93	20.01	7.29	40.75	25.02	1.92
646	38.8	42.49	19.76	5.93	31.82	0.00	0.47
647	130.4	21.45	21.30	2.95	12.46	41.84	1.19
648	21.0	36.67	9.52	13.33	39.05	1.43	0.68
649	51.6	9.88	22.87	32.97	32.15	2.13	0.52
650	38.5	11.17	22.86	26.49	37.40	2.08	0.65
651	151.5	7.41	28.67	1.48	62.44	0.00	1.66
653	7.6	45.45	24.68	0.00	29.87	0.00	0.43
654	181.3	4.15	35.56	3.96	56.32	0.00	1.29
656	231.8	9.82	27.90	7.36	48.21	6.71	1.22
657	223.9	6.59	18.11	15.48	54.96	4.87	1.49
658	220.0*	4.58	15.23	16.44	63.75	0.00	1.76
659	220.0*	4.74	17.54	3.26	74.46	0.00	2.92
660	200.0*	3.11	15.65	2.36	71.06	7.82	3.74
662	230.0*	6.59	18.11	15.48	54.96	4.87	1.49
663	200.0*	9.82	27.90	7.36	48.21	6.71	1.22
664	210.0*	6.59	18.11	15.48	54.96	4.87	1.49
665	205.0*	9.82	27.90	7.36	48.21	6.71	1.22
666	225.0*	6.59	18.11	15.48	54.96	4.87	1.49
667	225.0*	9.82	27.90	7.36	48.21	6.71	1.22
668	200.0*	4.74	17.54	3.26	74.46	0.00	2.92
696	85.0*	23.53	27.06	0.00	9.41	40.00	0.98
697	67.5	38.80	29.63	17.91	13.52	0.15	0.16
698	71.9	34.95	44.87	1.59	18.58	0.00	0.23
699	75.2	21.94	15.66	9.81	10.45	42.14	1.11
700	158.6	9.85	28.16	5.48	48.24	8.27	1.30
701	186.9	9.57	23.54	12.25	40.18	14.47	1.20
702	86.8	4.10	24.95	9.15	34.74	27.05	1.62
703	96.4	23.18	30.01	1.53	35.66	9.62	0.83
704	130.0*	15.47	30.80	6.18	36.59	10.97	0.91
705	122.6	21.11	19.24	4.63	32.68	22.34	1.22
706	111.3	11.57	33.27	10.72	33.66	10.77	0.80
707	171.6	14.89	28.66	2.86	34.21	19.38	1.15
708	213.9	11.85	25.32	7.34	31.42	24.07	1.25
709	169.3	2.58	27.55	8.79	25.95	35.13	1.57
710	216.3	3.54	14.67	7.30	23.77	50.72	2.92
711	74.0	28.86	26.22	0.40	28.65	15.87	0.80

Appendix 11.2.2 Morgan CMM

Notes: * = estimated thickness
DH662–DH666 estimated from DH656.
DH668 faulted, missing section (18m) entered as sandstone

DH	thickness (m)	coal %	mudstone %	siltstone %	sandstone %	conglomerate %	coarse:fine ratio
246	36.7	23.22	25.67	22.67	28.43	0.00	0.40
262	43.3	8.43	17.67	18.91	54.99	0.00	1.22
265	50.6	4.77	2.08	25.22	67.93	0.00	2.12
266	58.5	28.94	33.09	0.00	30.75	7.22	0.61
273	40.6	0.00	36.30	0.00	61.48	2.22	1.76
318	45.4	10.09	53.70	0.00	36.21	0.00	0.57
342	40.0*	18.24	36.22	0.00	45.54	0.00	0.84
620	40.0*	0.00	28.63	20.78	50.59	0.00	1.02
625	6.0	0.00	0.00	100.00	0.00	0.00	0.00
630	26.0	4.71	23.92	0.00	67.45	3.92	2.49
632	55.2	13.31	3.33	11.91	58.49	12.96	2.50
654	36.2	7.72	40.00	2.34	49.93	0.00	1.00
656	26.7	7.43	14.85	5.04	51.19	21.49	2.66
658	35.3	17.69	24.18	2.56	53.90	1.67	1.25
659	55.4	7.58	3.03	23.48	65.91	0.00	1.93
660	33.5	27.70	44.43	0.00	27.87	0.00	0.39
662	20.0*	7.43	14.85	5.04	51.19	21.49	2.66
663	20.0*	7.43	14.85	5.04	51.19	21.49	2.66
664	10.0*	7.43	14.85	5.04	51.19	21.49	2.66
665	40.0*	7.43	14.85	5.04	51.19	21.49	2.66
666	30.0*	7.43	14.85	5.04	51.19	21.49	2.66
668	47.3	19.77	53.79	5.91	20.53	0.00	0.26

Appendix 11.2.3 Jay Formation

Notes: * = estimated thickness
DH446 estimated from DH632
DH662, 664 and 666 estimated from DH657
DH663, 665 and 667 estimated from DH656
DH668 estimated from DH659
DH710 estimated from DH619

DH	thickness (m)	coal %	mudstone %	siltstone %	sandstone %	conglomerate %	coarse:fine ratio
246	4.0	36.15	0.00	15.64	48.21	0.00	0.93
262	5.0*	0.00	0.00	0.00	0.00	100.0	∞
446	50.0*	0.00	0.00	0.00	0.00	100.0	∞
619	34.1	8.12	8.41	12.17	20.00	51.30	2.48
620	10.0*	0.00	0.00	0.00	0.00	100.0	∞

Jay Fm. cont.

DH	thickness (m)	coal %	mudstone %	siltstone %	sandstone %	conglomerate %	coarse:fine ratio
621	74.8	9.46	42.58	19.05	13.53	15.37	0.41
625	10.0*	0.00	0.00	0.00	0.00	100.0	∞
632	18.7	0.00	0.00	0.00	0.00	100.0	∞
634	60.0*	1.67	31.67	0.00	33.33	33.33	2.00
656	132.0*	0.66	9.50	5.77	27.91	56.16	5.28
657	77.8*	2.15	20.15	20.15	21.42	36.12	1.36
658	130.0*	0.00	17.98	1.97	21.23	58.91	4.04
659	105.0*	0.00	4.97	2.35	20.12	72.56	12.67
660	115.0*	0.00	6.12	4.03	16.86	72.99	8.85
662	100.0*	2.15	20.15	20.15	21.42	36.12	1.36
663	140.0*	0.66	9.50	5.77	27.91	56.16	5.28
664	40.0*	2.15	20.15	20.15	21.42	36.12	1.36
665	130.0*	0.66	9.50	5.77	27.91	56.16	5.28
666	70.0*	2.15	20.15	20.15	21.42	36.12	1.36
667	120.0*	0.66	9.50	5.77	27.91	56.16	5.28
668	130.0*	0.00	4.97	2.35	20.12	72.56	12.67
710	50.0*	8.12	8.41	12.17	20.00	51.30	2.48

Appendix 11.3 Decompaction input data

Notes: decomp. = decompaction coefficient
init. por. = initial porosity (%)
Rewanui CMM in DH637 split into two units as *BASIN.XLS* would not accept only two stratigraphic units (Rewanui CMM plus cover) as inputs.
Paleobathymetry and sea level columns set to zero for all units in all drillholes.

Units are as follows:

cover	Dunollie Fm. plus estimated overlying strata
G	Goldlight Fm.
G mst	mudstone lithosomes within Goldlight Fm.
UGTM	Upper Goldlight Transitional Member
GTM	Goldlight Transitional Member
LGTM	Lower Goldlight Transitional Member
R	Rewanui CMM
W	Waiomo MM
M	Morgan CMM
F	Ford Fm.
FTM	Ford Transitional Member
F mst	mudstone lithosomes within Ford Fm.
J	Jay Fm.

DH	unit	top (km)	base (km)	thickness (km)	decomp.	init. por. %	density kg m^{-3}	age Ma
246	cover	0.0	2.54	2.54	0.60	0.48	2660	20.0
	G	2.54	2.69	0.15	0.39	0.50	2650	62.0
	R	2.69	2.93	0.24	0.38	0.36	2620	65.0
	W	2.93	2.96	0.03	0.39	0.50	2650	68.0
	M	2.96	3.00	0.04	1.38	0.50	2310	69.0
	F	3.00	3.16	0.16	0.34	0.44	2650	70.0
	J	3.16	3.17	0.01	1.96	0.53	2130	73.0
262	cover	0.0	2.48	2.48	0.60	0.48	2660	20.0
	G	2.48	2.63	0.15	0.39	0.50	2650	62.0
	R	2.63	2.86	0.23	0.56	0.37	2550	65.0
	W	2.86	2.88	0.02	0.39	0.50	2650	68.0
	M	2.88	2.92	0.04	0.67	0.40	2530	69.0
	FTM	2.92	2.94	0.02	0.27	0.40	2650	70.0
	F mst	2.94	2.97	0.03	0.38	0.49	2650	71.0
	J	2.97	2.98	0.01	0.05	0.30	2650	73.0
265	cover	0.0	2.49	2.49	0.60	0.48	2660	20.0
	G	2.49	2.64	0.15	0.39	0.50	2650	62.0
	R	2.64	2.87	0.23	0.55	0.36	2560	65.0
	W	2.87	2.90	0.03	0.39	0.50	2650	68.0
	M	2.90	2.95	0.05	0.47	0.35	2580	69.0
	F	2.95	3.04	0.09	0.38	0.49	2650	70.0
	J	3.04	3.05	0.01	0.30	0.05	2650	73.0
266	cover	0.0	3.02	3.02	0.60	0.48	2660	20.0
	UGTM	3.02	3.03	0.01	0.36	0.48	2650	62.0
	G mst	3.03	3.18	0.15	0.39	0.50	2650	63.0
	LGTM	3.18	3.19	0.01	0.27	0.40	2650	64.0
	R	3.19	3.30	0.11	0.64	0.40	2540	65.0
	W	3.30	3.31	0.01	0.39	0.50	2650	68.0
	M	3.31	3.37	0.06	1.65	0.55	2230	69.0
273	cover	0.0	2.86	2.86	0.60	0.48	2660	20.0
	UGTM	2.86	2.88	0.02	0.30	0.42	2650	62.0
	G mst	2.88	3.02	0.14	0.39	0.50	2650	63.0
	LGTM	3.02	3.03	0.01	0.33	0.45	2650	64.0
	R	3.03	3.14	0.11	0.30	0.37	2640	65.0
	W	3.14	3.15	0.01	0.29	0.42	2650	68.0
	M	3.15	3.19	0.04	0.29	0.38	2650	69.0
289	cover	0.0	2.95	2.95	0.60	0.48	2660	20.0
	UGTM	2.95	2.96	0.01	0.31	0.44	2650	62.0
	G mst	2.96	3.09	0.13	0.39	0.50	2650	63.0
	LGTM	3.09	3.10	0.01	0.27	0.40	2650	64.0
	R	3.10	3.20	0.10	0.39	0.39	2620	65.0
318	cover	0.0	3.14	3.14	0.60	0.48	2660	20.0
	G	3.14	3.29	0.15	0.39	0.50	2650	62.0
	R	3.29	3.51	0.22	0.58	0.38	2550	65.0
	W	3.51	3.54	0.03	0.39	0.50	2650	68.0
	M	3.54	3.59	0.05	0.80	0.48	2500	69.0
	F	3.59	3.71	0.12	0.36	0.46	2650	70.0
342	cover	0.0	3.36	3.36	0.60	0.48	2660	20.0
	G	3.36	3.51	0.15	0.39	0.50	2650	62.0
	R	3.51	3.75	0.24	0.51	0.38	2580	65.0
	W	3.75	3.78	0.03	0.38	0.49	2650	68.0
	M	3.78	3.82	0.04	1.16	0.49	2390	69.0
	F	3.82	3.89	0.07	0.36	0.46	2650	70.0
433	cover	0.0	1.86	1.86	0.60	0.48	2660	20.0
	G	1.86	1.99	0.13	0.39	0.50	2650	62.0
	R	1.99	2.10	0.11	0.54	0.41	2570	65.0
446	cover	0.0	2.04	2.04	0.60	0.48	2660	20.0
	UGTM	2.04	2.06	0.02	0.33	0.45	2650	62.0
	G mst	2.06	2.18	0.12	0.39	0.50	2650	63.0
	R	2.18	2.40	0.22	0.92	0.44	2450	65.0
	FTM	2.40	2.45	0.05	0.27	0.40	2650	70.0
	F mst	2.45	2.52	0.07	0.38	0.49	2650	71.0
	J	2.52	2.57	0.05	0.05	0.30	2650	73.0
619	cover	0.0	1.87	1.87	0.60	0.48	2660	20.0
	G	1.87	1.88	0.01	0.39	0.50	2650	62.0
	R	1.88	2.08	0.20	0.57	0.42	2550	65.0
	FTM	2.08	2.14	0.06	0.27	0.40	2650	70.0
	F mst	2.14	2.19	0.05	0.39	0.50	2650	71.0
	J	2.19	2.22	0.03	0.54	0.37	2530	73.0
620	cover	0.0	3.48	3.48	0.60	0.48	2660	20.0
	G	3.48	3.62	0.14	0.39	0.50	2650	62.0
	R	3.62	3.83	0.21	0.53	0.47	2590	65.0
	W	3.83	3.86	0.03	0.39	0.50	2650	68.0
	M	3.86	3.90	0.04	0.28	0.37	2650	69.0
	F	3.90	3.91	0.01	0.39	0.40	2650	70.0
	J	3.91	3.92	0.01	0.05	0.30	2650	73.0
621	cover	0.0	1.87	1.87	0.60	0.48	2660	20.0
	G	1.87	1.88	0.01	0.39	0.50	2650	62.0
	R	1.88	2.11	0.23	0.28	0.35	2610	65.0
	FTM	2.11	2.16	0.05	0.27	0.40	2650	70.0
	F mst	2.16	2.20	0.04	0.37	0.48	2650	71.0
	J	2.20	2.27	0.07	0.73	0.45	2510	73.0
622	cover	0.0	1.65	1.65	0.60	0.48	2660	20.0
	GTM	1.65	1.69	0.04	0.28	0.41	2650	62.0
	R	1.69	1.81	0.12	0.83	0.42	2460	65.0
	FTM	1.81	1.83	0.02	0.30	0.42	2650	70.0

Appendix 11. Burial analysis input data

DH	unit	top (km)	base (km)	thickness (km)	decomp.	init. por. %	density kg m^{-3}	age Ma
623	cover	0.0	1.95	1.95	0.60	0.48	2660	20.0
	G	1.95	2.09	0.14	0.39	0.50	2650	62.0
	R	2.09	2.29	0.20	0.42	0.41	2610	65.0
	FTM	2.29	2.30	0.01	0.27	0.40	2650	70.0
624	cover	0.0	1.98	1.98	0.60	0.48	2660	20.0
	G	1.98	2.12	0.14	0.39	0.50	2650	62.0
	R	2.12	2.30	0.18	0.75	0.42	2500	65.0
	FTM	2.30	2.33	0.03	0.28	0.41	2650	70.0
	F mst	2.33	2.37	0.04	0.27	0.40	2650	71.0
625	cover	0.0	2.92	2.92	0.60	0.48	2660	20.0
	UGTM	2.92	2.96	0.04	0.34	0.46	2650	62.0
	G mst	2.96	3.06	0.10	0.39	0.50	2650	63.0
	R	3.06	3.23	0.17	0.55	0.43	2580	65.0
	W	3.23	3.25	0.02	0.39	0.50	2650	68.0
	M	3.25	3.26	0.01	0.24	0.32	2650	69.0
626	cover	0.0	1.69	1.69	0.60	0.48	2660	20.0
	GTM	1.69	1.75	0.06	0.30	0.42	2650	62.0
	R	1.75	1.83	0.08	0.51	0.43	2580	65.0
627	cover	0.0	2.57	2.57	0.60	0.48	2660	20.0
	UGTM	2.57	2.61	0.04	0.31	0.43	2650	62.0
	G mst	2.61	2.70	0.09	0.39	0.50	2650	63.0
	R	2.70	2.77	0.07	0.43	0.42	2610	65.0
628	cover	0.0	1.81	1.81	0.60	0.48	2660	20.0
	G	1.81	1.91	0.10	0.39	0.50	2650	62.0
	R	1.91	1.98	0.07	1.23	0.52	2370	65.0
630	cover	0.0	2.25	2.25	0.60	0.48	2660	20.0
	UGTM	2.25	2.28	0.03	0.31	0.44	2650	62.0
	G mst	2.28	2.38	0.10	0.39	0.50	2650	63.0
	R	2.38	2.55	0.17	0.54	0.38	2560	65.0
	W	2.55	2.57	0.02	0.39	0.50	2650	68.0
	M	2.57	2.60	0.03	0.49	0.39	2580	69.0
631	cover	0.0	2.04	2.04	0.60	0.48	2660	20.0
	UGTM	2.04	2.06	0.02	0.30	0.42	2650	62.0
	G mst	2.06	2.19	0.13	0.39	0.50	2650	63.0
	R	2.19	2.40	0.21	0.78	0.42	2490	65.0
	FTM	2.40	2.44	0.04	0.31	0.43	2650	70.0
	F mst	2.44	2.48	0.04	0.32	0.41	2650	71.0
632	cover	0.0	2.26	2.26	0.60	0.48	2660	20.0
	G	2.26	2.41	0.15	0.39	0.50	2650	62.0
	R	2.41	2.58	0.17	1.10	0.45	2400	65.0
	W	2.58	2.60	0.02	0.34	0.46	2650	68.0
	M	2.60	2.66	0.06	0.85	0.40	2460	69.0
	FTM	2.66	2.72	0.06	0.32	0.44	2650	70.0
	F mst	2.72	2.81	0.09	0.39	0.50	2650	71.0
	J	2.81	2.83	0.02	0.05	0.30	2650	73.0
633	cover	0.0	1.66	1.66	0.60	0.48	2660	20.0
	UGTM	1.66	1.71	0.05	0.33	0.45	2650	62.0
	G mst	1.71	1.75	0.04	0.38	0.49	2650	63.0
	R	1.75	1.78	0.03	1.72	0.56	2220	65.0
634	cover	0.0	1.73	1.73	0.60	0.48	2660	20.0
	R	1.73	1.93	0.20	0.16	0.34	2640	65.0
	FTM	1.93	1.97	0.04	0.27	0.40	2650	70.0
	F mst	1.97	1.98	0.01	0.39	0.50	2650	71.0
	J	1.98	2.04	0.06	0.30	0.38	2630	73.0
635	cover	0.0	2.05	2.05	0.60	0.48	2660	20.0
	UGTM	2.05	2.09	0.04	0.29	0.42	2650	62.0
	G mst	2.09	2.11	0.02	0.39	0.50	2650	63.0
	LGTM	2.11	2.16	0.05	0.28	0.41	2650	64.0
	R	2.16	2.38	0.22	0.43	0.39	2590	65.0
	FTM	2.38	2.40	0.02	0.25	0.37	2650	70.0
	F mst	2.40	2.46	0.06	0.39	0.50	2650	71.0
636	cover	0.0	1.89	1.89	0.60	0.48	2660	20.0
	G	1.89	2.00	0.11	0.37	0.48	2650	62.0
	R	2.00	2.09	0.09	1.33	0.51	2330	65.0
637	cover	0.0	1.81	1.81	0.60	0.48	2660	20.0
	R	1.81	1.91	0.10	0.14	0.33	2650	65.0
638	cover	0.0	1.84	1.84	0.60	0.48	2660	20.0
	UGTM	1.84	1.87	0.03	0.32	0.44	2650	62.0
	G mst	1.87	1.97	0.10	0.39	0.50	2650	63.0
	R	1.97	2.11	0.14	1.11	0.51	2410	65.0
639	cover	0.0	1.69	1.69	0.60	0.48	2660	20.0
	R	1.69	1.86	0.17	0.44	0.37	2560	65.0
	FTM	1.86	1.91	0.05	0.27	0.40	2650	70.0
640	cover	0.0	1.89	1.89	0.60	0.48	2660	20.0
	G	1.89	2.03	0.14	0.39	0.50	2650	62.0
	R	2.03	2.23	0.20	0.88	0.47	2480	65.0
	F	2.23	2.27	0.04	0.35	0.45	2650	70.0
641	cover	0.0	2.01	2.01	0.60	0.48	2660	20.0
	GTM	2.01	2.12	0.11	0.27	0.40	2650	62.0
	R	2.12	2.32	0.20	0.50	0.38	2560	65.0
	FTM	2.32	2.36	0.04	0.27	0.40	2650	70.0
	F mst	2.36	2.40	0.04	0.39	0.50	2650	71.0
642	cover	0.0	1.75	1.75	0.60	0.48	2660	20.0
	UGTM	1.75	1.79	0.04	0.32	0.44	2650	62.0
	G mst	1.79	1.84	0.05	0.37	0.48	2650	63.0
	R	1.84	1.94	0.10	0.43	0.38	2580	65.0

Appendix 11. Burial analysis input data

DH	unit	top (km)	base (km)	thickness (km)	decomp.	init. por. %	density kg m^{-3}	age Ma
643	cover	0.0	1.81	1.81	0.60	0.48	2660	20.0
	UGTM	1.81	1.84	0.03	0.33	0.45	2650	62.0
	G mst	1.84	1.91	0.07	0.39	0.50	2650	63.0
	R	1.91	2.07	0.16	0.90	0.45	2460	65.0
644	cover	0.0	1.79	1.79	0.60	0.48	2660	20.0
	UGTM	1.79	1.81	0.02	0.35	0.47	2650	62.0
	G mst	1.81	1.88	0.07	0.39	0.50	2650	63.0
	R	1.88	1.93	0.05	0.68	0.41	2530	65.0
645	cover	0.0	1.96	1.96	0.60	0.48	2660	20.0
	UGTM	1.96	1.99	0.03	0.29	0.42	2650	62.0
	G mst	1.99	2.05	0.06	0.38	0.49	2650	63.0
	LGTM	2.05	2.12	0.07	0.29	0.41	2650	64.0
	R	2.12	2.34	0.22	0.55	0.39	2550	65.0
	FTM	2.34	2.36	0.02	0.31	0.43	2650	70.0
	F mst	2.36	2.41	0.05	0.39	0.50	2650	71.0
646	cover	0.0	1.74	1.74	0.60	0.48	2660	20.0
	UGTM	1.74	1.75	0.01	0.34	0.46	2650	62.0
	G mst	1.75	1.84	0.09	0.39	0.50	2650	63.0
	R	1.84	1.88	0.04	2.29	0.60	2030	65.0
647	cover	0.0	2.10	2.10	0.60	0.48	2660	20.0
	GTM	2.10	2.19	0.09	0.29	0.42	2650	62.0
	R	2.19	2.32	0.13	1.21	0.47	2340	65.0
	FTM	2.32	2.34	0.02	0.27	0.40	2650	70.0
648	cover	0.0	1.73	1.73	0.60	0.48	2660	20.0
	UGTM	1.73	1.75	0.02	0.34	0.46	2650	62.0
	G mst	1.75	1.81	0.06	0.39	0.50	2650	63.0
	R	1.81	1.83	0.02	2.00	0.55	2120	65.0
649	cover	0.0	1.82	1.82	0.60	0.48	2660	20.0
	UGTM	1.82	1.85	0.03	0.32	0.44	2650	62.0
	G mst	1.85	1.91	0.06	0.39	0.50	2650	63.0
	R	1.91	1.96	0.05	0.74	0.42	2510	65.0
650	cover	0.0	1.84	1.84	0.60	0.48	2660	20.0
	G	1.84	1.94	0.10	0.39	0.50	2650	62.0
	R	1.94	1.98	0.04	0.80	0.43	2490	65.0
651	cover	0.0	1.99	1.99	0.60	0.48	2660	20.0
	UGTM	1.99	2.05	0.06	0.29	0.42	2650	62.0
	G mst	2.05	2.15	0.10	0.39	0.50	2650	63.0
	LGTM	2.15	2.16	0.01	0.31	0.43	2650	64.0
	R	2.16	2.31	0.15	0.64	0.41	2540	65.0
	FTM	2.31	2.33	0.02	0.27	0.40	2650	70.0
653	cover	0.0	1.63	1.63	0.60	0.48	2660	20.0
	UGTM	1.63	1.64	0.01	0.27	0.40	2650	62.0
	G mst	1.64	1.69	0.05	0.37	0.48	2650	63.0
	R	1.69	1.70	0.01	2.44	0.63	1990	65.0
654	cover	0.0	2.22	2.22	0.60	0.48	2660	20.0
	UGTM	2.22	2.30	0.08	0.31	0.44	2650	62.0
	G mst	2.30	2.36	0.06	0.39	0.50	2650	63.0
	LGTM	2.36	2.38	0.02	0.31	0.43	2650	64.0
	R	2.38	2.56	0.18	0.49	0.41	2590	65.0
	W	2.56	2.57	0.01	0.34	0.46	2650	68.0
	M	2.57	2.61	0.04	0.67	0.44	2540	69.0
656	cover	0.0	2.13	2.13	0.60	0.48	2660	20.0
	G	2.13	2.25	0.13	0.39	0.50	2650	62.0
	R	2.25	2.48	0.23	0.74	0.43	2510	65.0
	W	2.48	2.49	0.01	0.32	0.44	2650	68.0
	M	2.49	2.52	0.03	0.57	0.39	2540	69.0
	FTM	2.52	2.59	0.07	0.15	0.31	2650	70.0
	F mst	2.59	2.70	0.11	0.37	0.49	2650	71.0
	J	2.70	2.83	0.13	0.18	0.33	2640	73.0
657	cover	0.0	2.21	2.21	0.60	0.48	2660	20.0
	G	2.21	2.34	0.13	0.39	0.50	2650	62.0
	R	2.34	2.56	0.22	0.57	0.39	2550	65.0
	FTM	2.56	2.61	0.05	0.27	0.41	2650	70.0
	F mst	2.61	2.74	0.13	0.37	0.49	2650	71.0
	J	2.74	2.82	0.08	0.30	0.36	2620	73.0
658	cover	0.0	2.43	2.43	0.60	0.48	2660	20.0
	G	2.43	2.56	0.13	0.39	0.50	2650	62.0
	R	2.56	2.78	0.22	0.48	0.37	2580	65.0
	W	2.78	2.84	0.06	0.37	0.48	2650	68.0
	M	2.84	2.88	0.04	1.12	0.47	2390	69.0
	F	2.88	2.98	0.10	0.39	0.50	2650	70.0
	J	2.98	3.11	0.13	0.15	0.34	2650	73.0
659	cover	0.0	3.34	3.34	0.60	0.48	2660	20.0
	G	3.34	3.47	0.13	0.39	0.50	2650	62.0
	R	3.47	3.69	0.22	0.49	0.38	2580	65.0
	W	3.69	3.71	0.02	0.39	0.50	2650	68.0
	M	3.71	3.77	0.06	0.61	0.37	2540	69.0
	F	3.77	3.89	0.12	0.37	0.47	2650	70.0
	J	3.89	4.00	0.11	0.11	0.31	2650	73.0

DH	unit	top (km)	base (km)	thickness (km)	decomp.	init. por. %	density kg m^{-3}	age Ma
660	cover	0.0	3.06	3.06	0.60	0.48	2660	20.0
	G	3.06	3.19	0.13	0.39	0.50	2650	62.0
	R	3.19	3.39	0.20	0.40	0.36	2600	65.0
	W	3.39	3.44	0.05	0.34	0.46	2650	68.0
	M	3.44	3.47	0.03	1.63	0.56	2250	69.0
	FTM	3.47	3.52	0.05	0.30	0.43	2650	70.0
	F mst	3.52	3.62	0.10	0.39	0.50	2650	71.0
	J	3.62	3.74	0.12	0.11	0.32	2650	73.0
662	cover	0.0	2.18	2.18	0.60	0.48	2660	20.0
	G	2.18	2.31	0.13	0.39	0.50	2650	62.0
	R	2.31	2.54	0.23	0.57	0.39	2550	65.0
	M	2.54	2.56	0.02	0.57	0.39	2540	69.0
	FTM	2.56	2.59	0.03	0.27	0.41	2650	70.0
	F mst	2.59	2.74	0.15	0.37	0.49	2650	71.0
	J	2.74	2.84	0.10	0.30	0.36	2620	73.0
663	cover	0.0	2.04	2.04	0.60	0.48	2660	20.0
	G	2.04	2.16	0.12	0.39	0.50	2650	62.0
	R	2.16	2.36	0.20	0.74	0.43	2510	65.0
	M	2.36	2.38	0.02	0.57	0.39	2540	69.0
	FTM	2.38	2.40	0.02	0.27	0.41	2650	70.0
	F mst	2.40	2.50	0.10	0.37	0.49	2650	71.0
	J	2.50	2.64	0.14	0.18	0.33	2640	73.0
664	cover	0.0	2.32	2.32	0.60	0.48	2660	20.0
	G	2.32	2.47	0.15	0.39	0.50	2650	62.0
	R	2.47	2.68	0.21	0.57	0.39	2550	65.0
	M	2.68	2.69	0.01	0.57	0.39	2540	69.0
	FTM	2.69	2.74	0.05	0.27	0.41	2650	70.0
	F mst	2.74	2.85	0.11	0.37	0.49	2650	71.0
	J	2.85	2.89	0.04	0.30	0.36	2620	73.0
665	cover	0.0	2.44	2.44	0.60	0.48	2660	20.0
	G	2.44	2.56	0.12	0.39	0.50	2650	62.0
	R	2.56	2.77	0.21	0.74	0.43	2510	65.0
	W	2.77	2.78	0.01	0.37	0.48	2650	68.0
	M	2.78	2.82	0.04	0.57	0.39	2540	69.0
	FTM	2.82	2.84	0.02	0.27	0.41	2650	70.0
	F mst	2.84	3.00	0.16	0.37	0.49	2650	71.0
	J	3.00	3.13	0.13	0.18	0.33	2640	73.0
666	cover	0.0	2.21	2.21	0.60	0.48	2660	20.0
	G	2.21	2.34	0.13	0.39	0.50	2650	62.0
	R	2.34	2.57	0.23	0.57	0.39	2550	65.0
	M	2.57	2.60	0.03	0.57	0.39	2540	69.0
	FTM	2.60	2.63	0.03	0.27	0.41	2650	70.0
	F mst	2.63	2.76	0.13	0.37	0.49	2650	71.0
	J	2.76	2.83	0.07	0.30	0.36	2620	73.0
667	cover	0.0	2.10	2.10	0.60	0.48	2660	20.0
	G mst	2.10	2.19	0.09	0.39	0.50	2650	62.0
	LGTM	2.19	2.20	0.01	0.27	0.40	2650	64.0
	R	2.20	2.43	0.23	0.74	0.43	2510	65.0
	FTM	2.43	2.49	0.06	0.27	0.41	2650	70.0
	F mst	2.49	2.62	0.13	0.37	0.49	2650	71.0
	J	2.62	2.74	0.12	0.18	0.33	2640	73.0
668	cover	0.0	4.07	4.07	0.60	0.48	2660	20.0
	G	4.07	4.19	0.12	0.39	0.50	2650	62.0
	R	4.19	4.39	0.20	0.49	0.38	2580	65.0
	W	4.39	4.42	0.03	0.39	0.50	2650	68.0
	M	4.42	4.49	0.07	1.26	0.53	2360	69.0
	FTM	4.49	4.50	0.01	0.27	0.40	2650	70.0
	F mst	4.50	4.64	0.14	0.39	0.50	2650	71.0
	J	4.64	4.77	0.13	0.11	0.31	2650	73.0
696	cover	0.0	1.79	1.79	0.60	0.48	2660	20.0
	UGTM	1.79	1.81	0.02	0.32	0.44	2650	62.0
	G mst	1.81	1.92	0.11	0.39	0.50	2650	63.0
	R	1.92	2.01	0.09	1.32	0.50	2310	65.0
697	cover	0.0	1.80	1.80	0.60	0.48	2660	20.0
	UGTM	1.80	1.82	0.02	0.33	0.45	2650	62.0
	G mst	1.82	1.91	0.09	0.38	0.49	2650	63.0
	R	1.91	1.98	0.07	2.13	0.60	2090	65.0
698	cover	0.0	1.83	1.83	0.60	0.48	2660	20.0
	UGTM	1.83	1.85	0.02	0.31	0.43	2650	62.0
	G mst	1.85	1.95	0.10	0.39	0.50	2650	63.0
	R	1.95	2.02	0.07	1.97	0.60	2140	65.0
699	cover	0.0	1.73	1.73	0.60	0.48	2660	20.0
	G	1.73	1.82	0.09	0.38	0.49	2650	62.0
	R	1.82	1.89	0.07	1.23	0.47	2330	65.0
700	cover	0.0	1.83	1.83	0.60	0.48	2660	20.0
	UGTM	1.83	1.87	0.04	0.30	0.43	2650	62.0
	G mst	1.87	1.93	0.06	0.39	0.50	2650	63.0
	LGTM	1.93	1.94	0.01	0.27	0.40	2650	64.0
	R	1.94	2.10	0.16	0.74	0.43	2510	65.0
701	cover	0.0	2.00	2.00	0.60	0.48	2660	20.0
	UGTM	2.00	2.01	0.01	0.33	0.45	2650	62.0
	G mst	2.01	2.10	0.09	0.38	0.49	2650	63.0
	R	2.10	2.29	0.19	0.70	0.41	2510	65.0
	FTM	2.29	2.31	0.02	0.29	0.42	2650	70.0
	F mst	2.31	2.35	0.04	0.39	0.50	2650	71.0

Appendix 11. Burial analysis input data

DH	unit	top (km)	base (km)	thickness (km)	decomp.	init. por. %	density kg m^{-3}	age Ma
702	cover	0.0	1.84	1.84	0.60	0.48	2660	20.0
	UGTM	1.84	1.88	0.04	0.29	0.42	2650	62.0
	G mst	1.88	1.90	0.02	0.33	0.45	2650	63.0
	R	1.90	1.99	0.09	0.42	0.38	2590	65.0
703	cover	0.0	1.81	1.81	0.60	0.48	2660	20.0
	UGTM	1.81	1.85	0.04	0.32	0.45	2650	62.0
	G mst	1.85	1.91	0.06	0.38	0.49	2650	63.0
	R	1.91	2.01	0.10	1.37	0.51	2310	65.0
704	cover	0.0	1.99	1.99	0.60	0.48	2660	20.0
	UGTM	1.99	2.04	0.05	0.32	0.45	2650	62.0
	G mst	2.04	2.09	0.05	0.39	0.50	2650	63.0
	R	2.09	2.22	0.13	0.96	0.45	2430	65.0
	FTM	2.22	2.24	0.02	0.27	0.40	2650	70.0
705	cover	0.0	1.79	1.79	0.60	0.48	2660	20.0
	UGTM	1.79	1.81	0.02	0.29	0.42	2650	62.0
	G mst	1.81	1.89	0.08	0.39	0.50	2650	63.0
	R	1.89	2.01	0.12	1.23	0.47	2340	65.0
706	cover	0.0	1.80	1.80	0.60	0.48	2660	20.0
	UGTM	1.80	1.85	0.05	0.31	0.44	2650	62.0
	G mst	1.85	1.91	0.06	0.39	0.50	2650	63.0
	R	1.91	2.02	0.11	0.82	0.44	2480	65.0
707	cover	0.0	2.05	2.05	0.60	0.48	2660	20.0
	GTM	2.05	2.16	0.11	0.28	0.41	2650	62.0
	R	2.16	2.33	0.17	0.96	0.45	2430	65.0
	FTM	2.33	2.35	0.02	0.31	0.43	2650	70.0
	F mst	2.35	2.39	0.04	0.39	0.50	2650	71.0
708	cover	0.0	1.92	1.92	0.60	0.48	2660	20.0
	UGTM	1.92	1.96	0.04	0.29	0.42	2650	62.0
	G mst	1.96	1.98	0.02	0.39	0.50	2650	63.0
	LGTM	1.98	2.04	0.06	0.29	0.42	2650	64.0
	R	2.04	2.25	0.21	0.80	0.43	2480	65.0
	FTM	2.25	2.30	0.05	0.27	0.40	2650	70.0
	F mst	2.30	2.37	0.07	0.39	0.50	2650	71.0
709	cover	0.0	1.72	1.72	0.60	0.48	2660	20.0
	GTM	1.72	1.80	0.08	0.27	0.40	2650	62.0
	R	1.80	1.97	0.17	0.34	0.38	2610	65.0
	FTM	1.97	2.01	0.04	0.27	0.40	2650	70.0
	F mst	2.01	2.04	0.03	0.39	0.50	2650	71.0
710	cover	0.0	1.78	1.78	0.60	0.48	2660	20.0
	R	1.78	2.00	0.22	0.33	0.36	2600	65.0
	FTM	2.00	2.05	0.05	0.27	0.40	2650	70.0
	F mst	2.05	2.08	0.03	0.39	0.50	2650	71.0
	Jay CMM	2.08	2.13	0.05	0.54	0.37	2530	73.0
711	cover	0.0	1.77	1.77	0.60	0.48	2660	20.0
	UGTM	1.77	1.78	0.01	0.31	0.43	2650	62.0
	G mst	1.78	1.85	0.07	0.39	0.50	2650	63.0
	R	1.85	1.92	0.07	1.62	0.53	2230	65.0

Appendix 12. Results of decompaction analysis

Notes: All values in km.
Compaction listed in the cover column (lower right of tables) is total compaction of Paparoa Group strata (exluding Dunollie Fm.) by burial.
Units are as listed in Appendix 11.3.

DH246								
7	cover							2.54
6	G						0.24	0.15
5	R					0.32	0.31	0.24
4	W				0.05	0.04	0.04	0.03
3	M			0.08	0.07	0.06	0.05	0.04
2	F		0.23	0.23	0.23	0.21	0.21	0.16
1	J	0.02	0.02	0.02	0.02	0.01	0.01	0.01
	Tectonic subsidence	0.02	0.23	0.08	0.04	0.27	0.22	
	Compaction	0.00	0.00	0.00	0.01	0.05	0.02	0.23

DH262									
8	cover								2.48
7	G							0.23	0.15
6	R						0.32	0.30	0.23
5	W					0.03	0.03	0.03	0.02
4	M				0.06	0.06	0.05	0.05	0.04
3	FTM			0.03	0.03	0.03	0.03	0.02	0.02
2	F mst		0.05	0.05	0.05	0.05	0.04	0.04	0.03
1	J	0.01	0.01	0.01	0.01	0.01	0.01	0.01	0.01
	Tectonic subsidence	0.01	0.05	0.03	0.06	0.03	0.30	0.20	
	Compaction	0.00	0.00	0.00	0.00	0.00	0.02	0.03	0.18

DH265								
7	cover							2.49
6	G						0.23	0.15
5	R					0.32	0.30	0.23
4	W				0.05	0.04	0.04	0.03
3	M			0.07	0.07	0.06	0.06	0.05
2	F		0.14	0.14	0.14	0.13	0.12	0.09
1	J	0.01	0.01	0.01	0.01	0.01	0.01	0.01
	Tectonic subsidence	0.01	0.14	0.07	0.05	0.29	0.20	
	Compaction	0.00	0.00	0.00	0.00	0.03	0.03	0.20

DH266								
7	cover							3.02
6	UGTM						0.02	0.01
5	G mst					0.24	0.24	0.15
4	LGTM				0.01	0.01	0.01	0.01
3	R			0.17	0.17	0.15	0.15	0.11
2	W		0.02	0.02	0.02	0.01	0.01	0.01
1	M	0.12	0.12	0.10	0.09	0.08	0.08	0.06
	Tectonic subsidence	0.12	0.02	0.15	0.00	0.20	0.02	
	Compaction	0.00	0.00	0.02	0.01	0.04	0.00	0.16

DH273								
7	cover							2.86
6	UGTM						0.03	0.02
5	G mst					0.23	0.22	0.14
4	LGTM				0.02	0.01	0.01	0.01
3	R			0.15	0.15	0.14	0.14	0.11
2	W		0.01	0.01	0.01	0.01	0.01	0.01
1	M	0.05	0.05	0.05	0.05	0.05	0.05	0.04
	Tectonic subsidence	0.05	0.01	0.15	0.02	0.21	0.02	
	Compaction	0.00	0.00	0.00	0.00	0.02	0.01	0.13

DH289						
5	cover					2.95
4	UGTM				0.01	0.01
3	G mst			0.21	0.21	0.13
2	LGTM		0.01	0.01	0.01	0.01
1	R	0.14	0.14	0.14	0.14	0.10
	Tectonic subsidence	0.14	0.01	0.21	0.01	
	Compaction	0.00	0.00	0.00	0.00	0.12

DH318							
6	cover						3.14
5	G					0.25	0.15
4	R				0.32	0.30	0.22
3	W			0.05	0.05	0.04	0.03
2	M		0.09	0.09	0.07	0.07	0.05
1	F	0.19	0.18	0.18	0.17	0.16	0.12
	Tectonic subsidence	0.19	0.08	0.05	0.29	0.21	
	Compaction	0.00	0.01	0.00	0.03	0.04	0.25

DH342							
6	cover						3.36
5	G					0.25	0.15
4	R				0.35	0.33	0.24
3	W			0.05	0.05	0.04	0.03
2	M		0.07	0.07	0.06	0.05	0.04
1	F	0.11	0.11	0.11	0.10	0.10	0.07
	Tectonic subsidence	0.11	0.07	0.05	0.33	0.21	
	Compaction	0.00	0.00	0.00	0.02	0.04	0.24

DH433				
3	cover			1.86
2	G		0.19	0.13
1	R	0.16	0.15	0.11
	Tectonic subsidence	0.16	0.18	
	Compaction	0.00	0.01	0.10

DH446								
7	cover							2.04
6	UGTM						0.03	0.02
5	G mst					0.18	0.18	0.12
4	R				0.34	0.31	0.30	0.22
3	FTM			0.07	0.06	0.06	0.06	0.05
2	F mst		0.11	0.11	0.10	0.09	0.09	0.07
1	J	0.05	0.05	0.05	0.05	0.05	0.05	0.05
	Tectonic subsidence	0.05	0.11	0.07	0.32	0.15	0.02	
	Compaction	0.00	0.00	0.00	0.02	0.03	0.01	0.18

DH619							
6	cover						1.87
5	G					0.02	0.01
4	R				0.28	0.28	0.20
3	FTM			0.08	0.07	0.07	0.06
2	F mst		0.08	0.08	0.07	0.07	0.05
1	J	0.04	0.04	0.04	0.04	0.04	0.03
	Tectonic subsidence	0.04	0.08	0.08	0.26	0.02	
	Compaction	0.00	0.00	0.00	0.02	0.02	0.13

DH620								
7	cover							3.48
6	G						0.23	0.14
5	R					0.34	0.32	0.21
4	W				0.05	0.05	0.04	0.03
3	M			0.06	0.05	0.05	0.05	0.04
2	F		0.02	0.01	0.01	0.01	0.01	0.01
1	J	0.01	0.01	0.01	0.01	0.01	0.01	0.01
	Tectonic subsidence	0.01	0.02	0.05	0.04	0.34	0.20	
	Compaction	0.00	0.00	0.01	0.01	0.00	0.03	0.22

DH621							
6	cover						1.87
5	G					0.02	0.01
4	R				0.28	0.28	0.23
3	FTM			0.06	0.06	0.06	0.05
2	F mst		0.06	0.06	0.05	0.05	0.04
1	J	0.11	0.11	0.11	0.09	0.09	0.07
	Tectonic subsidence	0.11	0.06	0.06	0.25	0.02	
	Compaction	0.00	0.00	0.00	0.03	0.03	0.10

DH622					
4	cover				1.65
3	GTM			0.05	0.04
2	R		0.18	0.17	0.12
1	FTM	0.03	0.03	0.02	0.02
	Tectonic subsidence	0.03	0.18	0.03	
	Compaction	0.00	0.00	0.02	0.06

DH623					
4	cover				1.95
3	G			0.21	0.14
2	R		0.27	0.26	0.20
1	FTM	0.01	0.01	0.01	0.01
	Tectonic subsidence	0.01	0.27	0.20	
	Compaction	0.00	0.00	0.01	0.13

DH624						
5	cover					1.98
4	G				0.21	0.14
3	R			0.27	0.25	0.18
2	FTM		0.04	0.04	0.04	0.03
1	F mst	0.05	0.05	0.05	0.05	0.04
	Tectonic subsidence	0.05	0.04	0.27	0.19	
	Compaction	0.00	0.00	0.00	0.02	0.16

DH625							
6	cover						2.92
5	UGTM					0.06	0.04
4	G mst				0.16	0.16	0.10
3	R			0.26	0.25	0.24	0.17
2	W		0.03	0.03	0.03	0.03	0.02
1	M	0.01	0.01	0.01	0.01	0.01	0.01
	Tectonic subsidence	0.01	0.03	0.26	0.15	0.05	
	Compaction	0.00	0.00	0.00	0.01	0.01	0.16

DH626				
3	cover			1.69
2	GTM		0.08	0.06
1	R	0.11	0.11	0.08
	Tectonic subsidence	0.11	0.08	
	Compaction	0.00	0.00	0.05

DH627					
4	cover				2.57
3	UGTM			0.06	0.04
2	G mst		0.14	0.14	0.09
1	R	0.10	0.10	0.10	0.07
	Tectonic subsidence	0.10	0.14	0.06	
	Compaction	0.00	0.00	0.00	0.10

DH628				
3	cover			1.81
2	G		0.15	0.10
1	R	0.13	0.11	0.07
	Tectonic subsidence	0.13	0.14	
	Compaction	0.00	0.01	0.09

DH630							
6	cover						2.25
5	UGTM					0.04	0.03
4	G mst				0.16	0.15	0.10
3	R			0.24	0.23	0.23	0.17
2	W		0.03	0.03	0.03	0.03	0.02
1	M	0.04	0.04	0.04	0.04	0.04	0.03
	Tectonic subsidence	0.04	0.03	0.24	0.15	0.03	
	Compaction	0.00	0.00	0.00	0.01	0.01	0.14

DH631							
6	cover						2.04
5	UGTM					0.03	0.02
4	G mst				0.20	0.19	0.13
3	R			0.31	0.29	0.29	0.21
2	FTM		0.06	0.05	0.05	0.05	0.04
1	F mst	0.05	0.05	0.05	0.05	0.05	0.04
	Tectonic subsidence	0.05	0.06	0.30	0.18	0.02	
	Compaction	0.00	0.00	0.01	0.02	0.01	0.17

DH632									
8	cover								2.26
7	G							0.23	0.15
6	R						0.27	0.24	0.17
5	W					0.03	0.03	0.03	0.02
4	M				0.09	0.09	0.08	0.08	0.06
3	FTM			0.09	0.08	0.08	0.08	0.08	0.06
2	F mst		0.15	0.14	0.14	0.14	0.13	0.12	0.09
1	J	0.02	0.02	0.02	0.02	0.02	0.02	0.02	0.02
	Tectonic subsidence	0.02	0.15	0.08	0.08	0.03	0.25	0.19	
	Compaction	0.00	0.00	0.01	0.01	0.00	0.02	0.04	0.23

DH633					
4	cover				1.66
3	UGTM			0.07	0.05
2	G mst		0.06	0.06	0.04
1	R	0.06	0.06	0.05	0.03
	Tectonic subsidence	0.06	0.06	0.06	
	Compaction	0.00	0.00	0.01	0.06

DH634						
5	cover					1.73
4	R				0.22	0.20
3	FTM			0.05	0.05	0.04
2	F mst		0.02	0.02	0.01	0.01
1	J	0.08	0.08	0.08	0.07	0.06
	Tectonic subsidence	0.08	0.02	0.05	0.20	
	Compaction	0.00	0.00	0.00	0.02	0.04

DH635								
7	cover							2.05
6	UGTM						0.05	0.04
5	G mst					0.03	0.03	0.02
4	LGTM				0.07	0.06	0.06	0.05
3	R			0.30	0.29	0.29	0.29	0.22
2	FTM		0.03	0.02	0.02	0.02	0.02	0.02
1	F mst	0.10	0.09	0.09	0.08	0.08	0.08	0.06
	Tectonic subsidence	0.10	0.02	0.29	0.05	0.02	0.05	
	Compaction	0.00	0.01	0.01	0.02	0.01	0.00	0.12

DH636				
3	cover			1.89
2	G		0.16	0.11
1	R	0.16	0.14	0.09
	Tectonic subsidence	0.16	0.14	
	Compaction	0.00	0.02	0.10

DH637				
3	cover			1.81
2	R (upper)		0.06	0.05
1	R (lower)	0.06	0.06	0.05
	Tectonic subsidence	0.06	0.06	
	Compaction	0.00	0.00	0.02

DH638					
4	cover				1.84
3	UGTM			0.04	0.03
2	G mst		0.15	0.15	0.10
1	R	0.24	0.22	0.21	0.14
	Tectonic subsidence	0.24	0.13	0.03	
	Compaction	0.00	0.02	0.01	0.13

DH639				
3	cover			1.69
2	R		0.22	0.17
1	FTM	0.06	0.06	0.05
	Tectonic subsidence	0.06	0.22	
	Compaction	0.00	0.00	0.06

DH640					
4	cover				1.89
3	G			0.21	0.14
2	R		0.31	0.28	0.20
1	F	0.06	0.05	0.05	0.04
	Tectonic subsidence	0.06	0.30	0.18	
	Compaction	0.00	0.01	0.03	0.16

DH641						
5	cover					2.01
4	GTM				0.14	0.11
3	R			0.27	0.26	0.20
2	FTM		0.05	0.05	0.05	0.04
1	F mst	0.06	0.06	0.06	0.05	0.04
	Tectonic subsidence	0.06	0.05	0.27	0.12	
	Compaction	0.00	0.00	0.00	0.02	0.11

DH642					
4	cover				1.75
3	UGTM			0.05	0.04
2	G mst		0.07	0.07	0.05
1	R	0.13	0.13	0.13	0.10
	Tectonic subsidence	0.13	0.07	0.05	
	Compaction	0.00	0.00	0.00	0.06

DH643					
4	cover				1.81
3	UGTM			0.04	0.03
2	G mst		0.10	0.10	0.07
1	R	0.25	0.23	0.23	0.16
	Tectonic subsidence	0.25	0.08	0.04	
	Compaction	0.00	0.02	0.00	0.11

D644					
4	cover				1.79
3	UGTM			0.03	0.02
2	G mst		0.10	0.10	0.07
1	R	0.07	0.07	0.07	0.05
	Tectonic subsidence	0.07	0.10	0.03	
	Compaction	0.00	0.00	0.00	0.06

DH645								
7	cover							1.96
6	UGTM						0.04	0.03
5	G mst					0.09	0.09	0.06
4	LGTM				0.09	0.09	0.09	0.07
3	R			0.30	0.30	0.29	0.29	0.22
2	FTM		0.03	0.03	0.03	0.03	0.03	0.02
1	F mst	0.08	0.08	0.07	0.07	0.07	0.07	0.05
	Tectonic subsidence	0.08	0.03	0.29	0.09	0.08	0.04	
	Compaction	0.00	0.00	0.01	0.00	0.01	0.00	0.16

Appendix 12. Decompaction results

DH646					
4	cover				1.74
3	UGTM			0.01	0.01
2	G mst		0.13	0.13	0.09
1	R	0.09	0.07	0.07	0.04
	Tectonic subsidence	0.09	0.11	0.01	
	Compaction	0.00	0.02	0.00	0.07

DH647					
4	cover				2.10
3	GTM			0.12	0.09
2	R		0.21	0.20	0.13
1	FTM	0.03	0.03	0.02	0.02
	Tectonic subsidence	0.03	0.21	0.10	
	Compaction	0.00	0.00	0.02	0.10

DH648					
4	cover				1.73
3	UGTM			0.03	0.02
2	G mst		0.09	0.09	0.06
1	R	0.04	0.04	0.03	0.02
	Tectonic subsidence	0.04	0.09	0.02	
	Compaction	0.00	0.00	0.01	0.05

DH649					
4	cover				1.82
3	UGTM			0.04	0.03
2	G mst		0.09	0.09	0.06
1	R	0.08	0.07	0.07	0.05
	Tectonic subsidence	0.08	0.08	0.04	
	Compaction	0.00	0.01	0.00	0.06

DH650				
3	cover			1.84
2	G		0.15	0.10
1	R	0.06	0.06	0.04
	Tectonic subsidence	0.06	0.15	
	Compaction	0.00	0.00	0.07

DH651							
6	cover						1.99
5	UGTM					0.08	0.06
4	G mst				0.15	0.15	0.10
3	LGTM			0.01	0.01	0.01	0.01
2	R		0.22	0.22	0.21	0.20	0.15
1	FTM	0.03	0.03	0.03	0.02	0.02	0.02
	Tectonic subsidence	0.03	0.22	0.01	0.13	0.07	
	Compaction	0.00	0.00	0.00	0.02	0.01	0.12

DH653					
4	cover				1.63
3	UGTM			0.01	0.01
2	G mst		0.07	0.07	0.05
1	R	0.03	0.02	0.02	0.01
	Tectonic subsidence	0.03	0.06	0.01	
	Compaction	0.00	0.01	0.00	0.03

DH654								
7	cover							2.22
6	UGTM						0.11	0.08
5	G mst					0.09	0.09	0.06
4	LGTM				0.03	0.03	0.03	0.02
3	R			0.26	0.25	0.25	0.24	0.18
2	W		0.01	0.01	0.01	0.01	0.01	0.01
1	M	0.06	0.06	0.06	0.06	0.06	0.05	0.04
	Tectonic subsidence	0.06	0.01	0.26	0.02	0.09	0.09	
	Compaction	0.00	0.00	0.00	0.01	0.00	0.02	0.14

Appendix 12. Decompaction results

DH656									
8	cover								2.13
7	G							0.18	0.12
6	R						0.34	0.32	0.23
5	W					0.01	0.01	0.01	0.01
4	M				0.04	0.04	0.04	0.04	0.03
3	FTM			0.08	0.08	0.08	0.08	0.08	0.07
2	F mst		0.17	0.17	0.16	0.16	0.15	0.14	0.11
1	J	0.15	0.15	0.15	0.15	0.15	0.15	0.15	0.13
	Tectonic subsidence	0.15	0.17	0.08	0.03	0.01	0.33	0.15	
	Compaction	0.00	0.00	0.00	0.01	0.00	0.01	0.03	0.22

DH657							
6	cover						2.21
5	G					0.20	0.13
4	R				0.31	0.29	0.22
3	FTM			0.07	0.06	0.06	0.05
2	F mst		0.20	0.20	0.18	0.17	0.13
1	J	0.10	0.10	0.10	0.10	0.09	0.08
	Tectonic subsidence	0.10	0.20	0.27	0.28	0.16	
	Compaction	0.00	0.00	0.00	0.03	0.04	0.20

DH658								
7	cover							2.43
6	G						0.20	0.13
5	R					0.30	0.29	0.22
4	W				0.09	0.09	0.08	0.06
3	M			0.07	0.07	0.06	0.05	0.04
2	F		0.16	0.16	0.15	0.14	0.14	0.10
1	J	0.15	0.15	0.15	0.15	0.15	0.15	0.13
	Tectonic subsidence	0.15	0.16	0.07	0.08	0.28	0.19	
	Compaction	0.00	0.00	0.00	0.01	0.02	0.03	0.23

DH659								
7	cover							3.34
6	G						0.22	0.13
5	R					0.32	0.30	0.22
4	W				0.04	0.03	0.03	0.02
3	M			0.09	0.09	0.08	0.08	0.06
2	F		0.19	0.19	0.19	0.17	0.17	0.12
1	J	0.13	0.13	0.13	0.13	0.12	0.12	0.11
	Tectonic subsidence	0.13	0.19	0.09	0.04	0.27	0.20	
	Compaction	0.00	0.00	0.00	0.00	0.05	0.02	0.26

DH660									
8	cover								3.06
7	G							0.21	0.13
6	R						0.27	0.26	0.20
5	W					0.08	0.07	0.07	0.05
4	M				0.06	0.06	0.04	0.04	0.03
3	FTM			0.07	0.07	0.07	0.07	0.07	0.05
2	F mst		0.17	0.17	0.16	0.16	0.15	0.14	0.10
1	J	0.14	0.14	0.14	0.14	0.14	0.13	0.13	0.12
	Tectonic subsidence	0.14	0.17	0.07	0.05	0.08	0.22	0.19	
	Compaction	0.00	0.00	0.00	0.01	0.00	0.05	0.02	0.24

DH662								
7	cover							2.18
6	G						0.20	0.13
5	R					0.32	0.30	0.23
4	M				0.03	0.03	0.03	0.02
3	FTM			0.04	0.04	0.04	0.04	0.03
2	F mst		0.23	0.23	0.23	0.21	0.20	0.15
1	J	0.13	0.13	0.13	0.12	0.12	0.12	0.10
	Tectonic subsidence	0.13	0.23	0.04	0.02	0.30	0.17	
	Compaction	0.00	0.00	0.00	0.01	0.02	0.03	0.23

DH663								
7	cover							2.04
6	G						0.18	0.12
5	R					0.30	0.28	0.20
4	M				0.03	0.03	0.03	0.02
3	FTM			0.03	0.03	0.03	0.02	0.02
2	F mst		0.15	0.15	0.15	0.14	0.13	0.10
1	J	0.16	0.16	0.16	0.16	0.16	0.16	0.14
	Tectonic subsidence	0.16	0.15	0.03	0.03	0.29	0.14	
	Compaction	0.00	0.00	0.00	0.00	0.01	0.04	0.20

DH664								
7	cover							2.32
6	G						0.23	0.15
5	R					0.30	0.28	0.21
4	M				0.01	0.01	0.01	0.01
3	FTM			0.07	0.07	0.06	0.06	0.05
2	F mst		0.17	0.17	0.17	0.16	0.15	0.11
1	J	0.05	0.05	0.05	0.05	0.05	0.05	0.04
	Tectonic subsidence	0.05	0.17	0.07	0.01	0.28	0.20	
	Compaction	0.00	0.00	0.00	0.00	0.02	0.03	0.21

DH665									
8	cover								2.44
7	G							0.19	0.12
6	R						0.32	0.30	0.21
5	W					0.02	0.01	0.01	0.01
4	M				0.06	0.06	0.05	0.05	0.04
3	FTM			0.03	0.03	0.03	0.03	0.03	0.02
2	F mst		0.25	0.25	0.24	0.24	0.22	0.22	0.16
1	J	0.16	0.15	0.15	0.15	0.15	0.15	0.15	0.13
	Tectonic subsidence	0.16	0.24	0.03	0.05	0.02	0.28	0.17	
	Compaction	0.00	0.01	0.00	0.01	0.00	0.04	0.02	0.26

DH666								
7	cover							2.21
6	G						0.20	0.13
5	R					0.32	0.31	0.23
4	M				0.04	0.04	0.04	0.03
3	FTM			0.04	0.04	0.04	0.04	0.03
2	F mst		0.20	0.20	0.20	0.18	0.17	0.13
1	J	0.09	0.09	0.09	0.09	0.08	0.08	0.07
	Tectonic subsidence	0.09	0.20	0.04	0.04	0.29	0.18	
	Compaction	0.00	0.00	0.00	0.00	0.03	0.02	0.22

DH667								
7	cover							2.10
6	G mst						0.14	0.09
5	LGTM					0.01	0.01	0.01
4	R				0.34	0.34	0.32	0.23
3	FTM			0.08	0.08	0.08	0.07	0.06
2	F mst		0.20	0.19	0.18	0.18	0.17	0.13
1	J	0.14	0.14	0.14	0.14	0.14	0.13	0.12
	Tectonic subsidence	0.14	0.20	0.07	0.33	0.01	0.09	
	Compaction	0.00	0.00	0.01	0.01	0.00	0.05	0.20

DH668									
8	cover								4.07
7	G							0.21	0.12
6	R						0.30	0.28	0.20
5	W					0.05	0.05	0.05	0.03
4	M				0.14	0.13	0.10	0.09	0.07
3	FTM			0.01	0.01	0.01	0.01	0.01	0.01
2	F mst		0.25	0.24	0.23	0.23	0.21	0.20	0.14
1	J	0.15	0.15	0.15	0.15	0.15	0.15	0.15	0.13
	Tectonic subsidence	0.15	0.25	0.00	0.13	0.04	0.25	0.17	
	Compaction	0.00	0.00	0.01	0.01	0.01	0.05	0.04	0.29

DH696					
4	cover				1.79
3	UGTM			0.03	0.02
2	G mst		0.16	0.16	0.11
1	R	0.16	0.14	0.13	0.09
	Tectonic subsidence	0.16	0.14	0.02	
	Compaction	0.00	0.02	0.01	0.10

DH697					
4	cover				1.80
3	UGTM			0.03	0.02
2	G mst		0.13	0.13	0.09
1	R	0.14	0.12	0.11	0.07
	Tectonic subsidence	0.14	0.11	0.02	
	Compaction	0.00	0.02	0.03	0.09

DH698					
4	cover				1.83
3	UGTM			0.03	0.02
2	G mst		0.15	0.15	0.10
1	R	0.14	0.12	0.11	0.07
	Tectonic subsidence	0.14	0.13	0.02	
	Compaction	0.00	0.02	0.02	0.10

DH699				
3	cover			1.73
2	G		0.13	0.09
1	R	0.12	0.11	0.07
	Tectonic subsidence	0.12	0.12	
	Compaction	0.00	0.01	0.10

DH700						
5	cover					1.83
4	UGTM				0.05	0.04
3	G mst			0.09	0.09	0.06
2	LGTM		0.01	0.01	0.01	0.01
1	R	0.24	0.24	0.23	0.22	0.16
	Tectonic subsidence	0.24	0.01	0.08	0.04	
	Compaction	0.00	0.00	0.01	0.01	0.10

DH701							
6	cover						2.00
5	UGTM					0.01	0.01
4	G mst				0.13	0.13	0.09
3	R			0.28	0.26	0.26	0.19
2	FTM		0.03	0.03	0.03	0.02	0.02
1	F mst	0.06	0.06	0.06	0.06	0.05	0.04
	Tectonic subsidence	0.06	0.03	0.28	0.11	0.00	
	Compaction	0.00	0.00	0.00	0.02	0.02	0.12

DH702					
4	cover				1.84
3	UGTM			0.05	0.04
2	G mst		0.03	0.03	0.02
1	R	0.12	0.12	0.12	0.09
	Tectonic subsidence	0.12	0.03	0.05	
	Compaction	0.00	0.00	0.00	0.05

DH703					
4	cover				1.81
3	UGTM			0.05	0.04
2	G mst		0.09	0.09	0.06
1	R	0.18	0.16	0.16	0.10
	Tectonic subsidence	0.18	0.07	0.05	
	Compaction	0.00	0.02	0.00	0.10

DH704						
5	cover					1.99
4	UGTM				0.07	0.05
3	G mst			0.08	0.07	0.05
2	R		0.21	0.20	0.19	0.13
1	FTM	0.03	0.03	0.02	0.02	0.02
	Tectonic subsidence	0.03	0.21	0.06	0.05	
	Compaction	0.00	0.00	0.02	0.02	0.10

DH705					
4	cover				1.79
3	UGTM			0.03	0.02
2	G mst		0.12	0.12	0.08
1	R	0.20	0.18	0.18	0.12
	Tectonic subsidence	0.20	0.10	0.03	
	Compaction	0.00	0.02	0.00	0.11

DH706					
4	cover				1.80
3	UGTM			0.07	0.05
2	G mst		0.09	0.09	0.06
1	R	0.17	0.16	0.16	0.11
	Tectonic subsidence	0.17	0.08	0.07	
	Compaction	0.00	0.01	0.00	0.10

DH707						
5	cover					2.05
4	GTM				0.14	0.11
3	R			0.27	0.25	0.17
2	FTM		0.03	0.03	0.03	0.02
1	F mst	0.06	0.06	0.06	0.06	0.04
	Tectonic subsidence	0.06	0.03	0.27	0.12	
	Compaction	0.00	0.00	0.00	0.02	0.14

DH708								
7	cover							1.92
6	UGTM						0.05	0.04
5	G mst					0.03	0.03	0.02
4	LGTM				0.08	0.08	0.08	0.06
3	R			0.31	0.30	0.30	0.29	0.21
2	FTM		0.06	0.06	0.06	0.06	0.06	0.05
1	F mst	0.11	0.11	0.10	0.10	0.09	0.09	0.07
	Tectonic subsidence	0.11	0.06	0.30	0.07	0.02	0.04	
	Compaction	0.00	0.00	0.01	0.01	0.01	0.01	0.15

DH709						
5	cover					1.72
4	GTM				0.10	0.08
3	R			0.21	0.21	0.17
2	FTM		0.05	0.05	0.04	0.04
1	F mst	0.05	0.05	0.04	0.04	0.03
	Tectonic subsidence	0.05	0.05	0.20	0.09	
	Compaction	0.00	0.00	0.01	0.01	0.07

DH710						
5	cover					1.78
4	R				0.27	0.22
3	FTM			0.06	0.06	0.05
2	F mst		0.05	0.05	0.04	0.03
1	J	0.07	0.07	0.07	0.06	0.05
	Tectonic subsidence	0.07	0.05	0.06	0.25	
	Compaction	0.00	0.00	0.00	0.02	0.08

DH711					
4	cover				1.77
3	UGTM			0.01	0.01
2	G mst		0.10	0.10	0.07
1	R	0.13	0.12	0.11	0.07
	Tectonic subsidence	0.13	0.09	0.00	
	Compaction	0.00	0.01	0.01	0.07

Appendix 12. Decompaction results

Appendix 13. Palynological sampling and processing details

Notes: UCP = University of Canterbury Palynology collection number, given to all samples collected including those not processed or with poor results. Full locality information for field samples is held in the UCP master catalogue (Dept. of Geological Sciences, University of Canterbury)
CRA nos. are Coal Research Association catalogue numbers.
s = scanned
n/p = not processed
n/f = no flora recovered
The Bleach and Short. cent. columns indicate number of repeats of light oxidation with bleach and short centrifuging (Appendix 5.1.2).
A tick in the "HM" column indicates removal of heavy minerals.

DH	UCP	DEPTH	Lithology	CRA no.	Count	HF (days)	HNO_3 (mins)	Schulze (mins)	KOH (mins)	Bleach	Short cent.	HM
619 /1	1266	241.5	lam zst/mst		169	3			5	2	5	✓
/2	1300	250.6	vfsst		254	0.1				1	5	✓
/3	1267	251.1	vfsst-zst		141	3			5	2	5	✓
/4	1301	254.8	carb zst		259	0.1	5		5	3	12	✓
/5	1280	c.260	coal	26/069	254			10	5	2	10	
/6	1268	262.7	coaly mst		s	3		10	10	2	10	✓
/7	1269	271.1	vfsst		n/f	3						✓
623 /1	1316	47.1	coaly mst		249			12	5	1	3	✓
/2	1317	48.5	dirty coal		257			12	5	1	3	✓
/3	1318	54.0	dirty coal		250			12	5	1	3	
/4	1319	61.3	dirty coal		270			12	5	1	3	✓
/5	1320	62.4	carb zst		250	3		5	3	2	10	✓
/6	1321	68.1	carb zst		s	3		5	3	2	10	✓
/7	1322	76.6	coal		250			15	10	2	4	
626 /1	1323	301.8	carb zst		253	3		5	3	2	10	✓
/2	1324	303.6	phytoclast		n/f			15	10	1	1	
/3	1325	310.6	coaly mst		249			15	10	2	4	
/4	1326	320.7	dirty coal		250			15	10	2	4	
/5	1327	331.8	carb vfsst		s	3		5	3	2	10	
626A /6	1328	303.0	carb zst		n/p							
628 /1	1329	252.6	coal		260			15	5	3	13	✓
/2	1330	257.5	dirty coal		251			15	5	2	10	
/3	1331	259.6	mst		250	3	5			3	17	✓
/4	1332	274.2	mst		257	3	5			3	17	✓
/5	1333	275.0	coal		261			15	5	3	13	
/6	1334	280.2	coal		306			15	5	2	10	✓
/7	1335	284.9	coaly mst		n/p							
/8	1312	291.8	coal	26/365	268			15	10	2	10	
/9	1313	297.0	coal	26/372	250			15	10	2	10	
633 /1	1336	380.2	carb mst		246	4		10	3	1	2	✓
/2	1337	384.4	coaly mst		250	4		10	3	1	2	✓
/3	1338	387.8	zst		267	4	10		3	1	5	✓
/4	1339	391.2	carb mst		266	4			3	2	5	✓
/5	1314	394.3	coal	26/651	255			15	10	2	10	
/6	1315	400.0	coal	26/662	250			15	10	2	10	

DH	UCP	DEPTH	Lithology	CRA no.	Count	HF (days)	HNO_3 (mins)	Schulze (mins)	KOH (mins)	Bleach	Short cent.	HM
635 /1	1270	380.3	vfsst-zst		203	3		1	1	1	5	✓
/2	1271	390.7	carb f-vfsst		207	3		5	5		5	✓
/3	1302	394.3	carb vfsst		254	3hrs				1	5	✓
/4	1272	399.7	coaly vfsst		s	3		5	5	1	5	✓
/5	1304	400.0	coal	26/694	245			20	5	1	5	
/6	1273	410.5	fsst/carb zst		s	3		1	1	1	5	✓
636 /1	1340	302.0	coaly mst		255	6	5			6	25	✓
/2	1341	306.4	coaly vfsst		251	6	5			6	25	✓
640 /1	1342	188.2	coal	29/133	250			10	5	1	4	✓
/2	1343	189.0	coal	29/134	262			10	5	2	7	✓
643 /1	1362	281.5	mst		253	3	5		10	5	17	✓
/2	1363	282.7	carb mst		250	3	5		10	5	17	✓
/3	1344	282.9	coal	26/996	250			10	5	2	7	
/4	1345	283.2	coal	26/997	250		10	10	5	2	7	
/5	1364	287.5	carb zst		253	3	10		10	5	11	✓
/6	1365	288.2	carb zst		250	3			10	5	11	✓
666 /1	1274	146.8	carb mst		191	3			5	2	8	✓
/2	1275	156.0	carb vfsst		184	3			5	2	8	✓
/3	1303	165.4	fsst		269	3hrs	5		5		5	✓
/4	1276	166.0	carb vfsst		s	3			5	2	8	✓
/5	1305	167.6	dirty coal		180			20	5	1	5	
/6	1277	176.7	carb mst		175	3			5	2	8	✓
667 /1	1288	102.2	fsst		129	3				1	3	
/2	1289	110.0	fsst		s	3			15	2	9	
/3	1290	120.5	fsst		139	3				1	3	
/4	1291	129.0	fsst		s	3			15	2	9	
697 /5	1217	249.9	silty mst		263	3 days		2	1			
/6	1216	261.9	silty mst		264	3hr		1.5		1		
/7	1215	273.8	silty mst		261	3hr		1.5		1		
/8	1214	283.2	silty mst		298	3hr		5		1		✓
/9	1213	292.3	carb mst		119	3hr		5		1		✓
field	1278	Kiwi	coal		254			20	5	2	4	
	1279	Snowline	coal		254			20	5	2	4	
	1306	Tiller	coal		250			20	5	3	5	✓
	1307	Goldlight	coal		253			20	5	3	5	
	1360	S'man east "E"	coal		s			15	4	2	5	
	1361	S'man east "F"	coal		n/f			15	4	2	5	✓
field #1	1292	Ten Mile	carb fsst		n/f	5				1	5	✓
#2	1293	Ten Mile	carb zst		n/f	5				1	8	✓
#3	1294	Snowline	carb zst		n/f	5				1	6	✓
#4	1295	Snowline	carb zst		n/f	5				2	8	✓
#5	1296	12 Mile	carb fsst		n/f	5		10		4	8	
#6	1297	Ten Mile	silty fsst		n/f	5				3	4	
#7	1298	12 Mile	carb mst		n/f	5		10		4	8	
#8	1299	11 Mile	silty fsst		n/f	5				1		

Appendix 14. Palynology results for all analysed samples

Full sample details are given in Appendix 13.
Count data and summary (angiosperm %, gymnosperm % and spore %) are given where slides counted. * = taxa observed in additional scans where sample counted, or taxa observed but not counted where sample scanned (see Appendix 5.1.3).

DH619

Sample	619/1	619/2	619/3	619/4	619/5	619/6
UCP	1266	1300	1267	1301	1280	1268
ANGIOSPERMS						
Unidentified angiosperm						*
Concolpites leptos						*
Monosulcites granulatus			1		5	
Monosulcites spp.					5	*
Myricipites harrisii			1			
Nothofagidites kaitangataensis						*
Nothofagidites spp.	1			1		
Proteacidites scaboratus				1		
Proteacidites parvus		1		6		
Proteacidites subpalisadus					1	
Proteacidites subscaboratus		2			1	
Proteacidites spp.			5			
Tricolpites gillii	2	4	1	2		
Tricolpites reticulatus						*
Tricolpites secarius		3	3	17		
Tricolpites spp.	2		2		3	
Triorites minor	48	88	33	66		
GYMNOSPERMS						
Araucariacites spp.	2		19		2	*
Microcachryidites antarcticus					6	*
Phyllocladidites paleogenicus	5	2			2	
Phyllocladidites mawsonii	26	10	15	28	91	*
Podocarpidites cf. ellipticus	5			1	1	
Podocarpidites spp.	19	11	8	20	6	*
Trichotomosulcites subgranulatus						*
SPORES						
Cingutrileles spp.					1	
Clavifera rudis	6					
Clavifera triplex	2			4	48	
Cyathidites spp.	7	74	15	38	20	*
Gleicheniidites circinidites	4	8		12		
Gleicheniidites ssp.	11	9	12	6	3	*
Laevigatosporites major	2	2		2		
Laevigatosporites ovatus	10	10	4	12	38	*
Monosulcites spp.					3	
Osmundacidites wellmanii	1					
Stereisporites antiquasporites	3		5			*
Peromonolites bowenii					7	
Trilites morleyi						
Trilites verrucatus	2	2	14	7	2	*
Trilites microfoveolatus	2	8		1		
Trilites spp.			3		6	*
Trilites tuberculiformis	9	20		35		
Unidentified spore					3	
Angiosperm %	**31.4**	**38.6**	**32.6**	**35.9**	**5.9**	–
Gymnosperm %	**33.7**	**9.1**	**29.8**	**18.9**	**42.5**	–
Spore %	**34.9**	**52.4**	**37.6**	**45.2**	**51.6**	–

DH623

Sample	623/1	623/2	623/3	623/4	623/5	623/6	623/7
UCP	1316	1317	1318	1319	1320	1321	1322
ANGIOSPERMS							
Beaupreaidites sp.					*	*	
Malvacipollis spp.					1	*	
Monosulcites cf. granulatus		1			1		
Monosulcites cf. minima			3	2			3
Monosulcites granulatus		1					
Monosulcites spp.		3					3
Nothofagidites kaitangataensis	1	5			4	*	
Polycolpites clavatus		1		*			
Proteaceidites amolosexinus						*	
Proteacidites parvus				*	2	*	
Proteacidites scaboratus			1	*	5	*	3
Proteacidites subpalisadus	1						1
Proteacidites subscaboratus				1	3		
Rhoipites spp.							12
Tricolpites cf. pachyexinus						*	
Tricolpites gillii		2	4			*	1
Tricolpites lilliei	3	4		2			
Tricolpites reticulatus		4	1				
Tricolpites sp. A (tiny)			2	1	1		1
Tricolpites sp. B (tiny, granular/spinose)		2					
Tricolpites sp. C (tiny, clavate)					2	*	
Tricolpites sp. E (cf. reticulatus, smaller)					1	*	
Tricolpites sp. F (large,granular)					2		
Tricolpites spp.			1				2
Triorites minisculus					1		
Triorites minor		1		*			
Triorites spp.				2			
GYMNOSPERMS							
Araucariacites spp.	5	1	17		44		1
Microcachryidites antarcticus		9	3	5	6		3
Phyllocladidites paleogenicus	5	3	1	4	1		1
Phyllocladidites mawsonii	66	97	136	42	60	*	32
Podocarpidites cf. ellipticus	1		1		2		1
Podocarpidites marwickii		3	1		4	*	
Podocarpidites spp.	3	7	1	1	10		2
Podosporites microsaccatus	2						
Trichotomosulcites subgranulatus	13	10		34	23		13
SPORES							
Baculatisporites ssp.	2	3	1	5		*	2
Cingutriletes regium					1		
Cingutrilete ssp.					4		
Clavifera rudis	3	3		2			1
Clavifera triplex	16	1	7	10			11
Cyathidites major		1					
Cyathidites spp.	13	3	4	5	15		9
Gleicheniidites circinidites	69	23	27	64	16	*	73
Laevigatosporites major	1	6	3	12	2		9
Laevigatosporites ovatus	4	4	2	28	4		10
Leptolepidites major	1						
Lycopodiumsporites spp.	3			1			
Monosulcites spp.		1		1			
Osmundacidites wellmanii		17	12	29	1	*	9
Peromonolites bowenii	3	6	4	9	2	*	25
Peromonolites sp. (small)		2					
Stereisporites antiquasporites	32	32	17	10	32		20
Trilites morleyi							1
Trilites spp.	1	1					
Trilites tuberculiformis						*	
Trilites verrucatus	1		1				1
Angiosperm %	**2.0**	**9.3**	**4.8**	**3.0**	**9.2**	**–**	**10.4**
Gymnosperm %	**38.2**	**50.6**	**64.0**	**31.9**	**60.0**	**–**	**21.2**
Spore %	**59.8**	**40.1**	**31.2**	**65.2**	**30.8**	**–**	**68.4**

DH626

Sample	626/1	626/3	626/4	626/5
UCP	1323	1325	1326	1327
ANGIOSPERMS				
Beaupreaidites sp.		2		
Malvacipollis spp.	2	3	2	
Monosulcites cf. granulatus			2	
Monosulcites cf. minima	1	1	4	
Monosulcites granulatus		3	1	
Nothofagidites spp.	2			
Polycolpites clavatus	2			
Proteacidites scaboratus		1		
Proteacidites parvus	3	4	1	
Proteacidites subpalisadus		1		
Rhoipites spp.		7	22	*
Tricolpites cf. pachyexinus	1	1		
Tricolpites gillii	4	3	4	
Tricolpites lilliei		2	3	
Tricolpites reticulatus	3	4	3	
Tricolpites sp. A (tiny)	1	2	4	
Tricolpites sp. B (tiny, granular/spinose)			2	
Tricolpites sp. F (large, granular)			14	
Tricolpites secarius	2			
Tricolpites spp.			1	
Triorites minor	55	1		
Triorites spp.	2			
GYMNOSPERMS				
Araucariacites spp.	30	8	11	*
Microcachryidites antarcticus	4	27	2	
Phyllocladidites paleogenicus	5	4		
Phyllocladidites mawsonii	35	77	13	
Podocarpidites cf. ellipticus	3		2	
Podocarpidites major		1		
Podocarpidites marwickii	7	4		
Podocarpidites spp.	26	9	4	
Podosporites microsaccatus		5		
Trichotomosulcites subgranulatus	15	30	36	
SPORES				
Baculatisporites spp.			1	
Clavifera rudis			2	
Clavifera triplex	2	3	4	
Cyathidites spp.	7	3	7	*
Gleicheniidites circinidites	15	12	44	*
Laevigatosporites major	3	8	8	*
Laevigatosporites ovatus	9	8	25	
Monosulcites spp.			1	
Peromonolites bowenii	1	5	6	
Peromonolites sp. (small)			2	
Stereisporites antiquasporites	8	11	17	*
Trilites verrucatus	1	1	1	
Trilites tuberculiformis	2		1	
Unidentified spore	2			
Angiosperm %	30.8	13.9	25.2	–
Gymnosperm %	49.4	65.7	27.2	–
Spore %	19.8	20.3	47.6	–

DH628

Sample	628/1	628/2	628/3	628/4	628/5	628/6	628/8	628/9
UCP	1329	1330	1331	1332	1333	1334	1312	1313
ANGIOSPERMS								
Malvacipollis subtilis			3					
Monosulcites granulatus							2	1
Monosulcites spp.		3	2	2		3		1
Nothofagidites spp.							1	
Proteacidites scaboratus			3			1		3
Proteacidites amolosexinus							1	
Proteacidites parvus	5	3	3	1				
Proteacidites spp.		1					1	
Tricolpites gillii	1	1	6	9		1	5	1
Tricolpites lilliei	1		1				1	
Tricolpites reticulatus	1						4	
Tricolpites sp.C (tiny, clavate)			1		1			
Tricolpites secarius			2	3				
Tricolpites spp.	3		1					
Tricolporite sspp.		1						
Triorites minisculus			4	3				
Triorites minor			44	38			1	
Triorites spp.			1			1		
GYMNOSPERMS								
Araucariacites spp.	2	2	2	1	1		1	
Dacrydiumites praecupressinoides							5	
Microcachryidites antarcticus	12	1			1		5	5
Phyllocladidites paleogenicus	6	2	3	3	2	2	3	6
Phyllocladidites mawsonii	56	120	70	83	166	48	156	195
Podocarpidites cf. ellipticus							3	1
Podocarpidites marwickii	3	1			1		3	2
Podocarpidites spp.	3	3	16	23	11		7	1
Trichotomosulcites subgranulatus	120	5	3	1	2	5	2	1
SPORES								
Clavifera rudis							9	
Clavifera triplex	5	5				2	3	
Cyathidites spp.	2	4	15	4	1	15	1	
Gleicheniidites circinidites	27	78	38	37	17	184	15	7
Gleicheniidites spp.			1					
Laevigatosporites major	2			2			1	
Laevigatosporites ovatus	2	5	6	18	6	17	13	12
Lycopodiumsporites spp.			1	1				
Monosulcites spp.								1
Peromonolites bowenii	4	15	2		1		17	6
Stereisporites antiquasporites	3		17	25	51	25	7	4
Trilites verrucatus	1		2	1		2		1
Trilites morleyi		1	2					
Trilites ohaiensis								2
Trilites spp.							1	
Trilites tuberculiformis	1		1	2				
Angiosperm %	**4.2**	**3.6**	**28.4**	**21.8**	**0.4**	**2.0**	**6.0**	**2.4**
Gymnosperm %	**77.7**	**53.4**	**37.6**	**43.2**	**70.5**	**18.0**	**69.0**	**84.4**
Spore %	**18.1**	**43.0**	**34.0**	**35.0**	**29.1**	**80.1**	**25.0**	**13.2**

DH633

SAMPLE	633/1	633/2	633/3	633/4	633/5	633/6
UCP	1336	1337	1338	1339	1314	1315
ANGIOSPERMS						
Unidentified angiosperm			1			
Beaupreaidites sp.			*			
Gambierina rudata		1				
Liliacidites variegatus					1	
Monosulcites cf. minima	5	2				
Monosulcites granulatus		3				
Monosulcites spp.		12	8	6		
Nothofagidites kaitangataensis		2				1
Proteacidites scaboratus		1				
Proteacidites amolosexinus			1	*		
Proteacidites parvus	2	5	4	1	3	2
Proteacidites spp.	1			1		
Proteacidites subpalisadus					1	
Proteacidites subscaboratus					1	
Tricolpites gillii	2	5		3	1	2
Tricolpites lilliei	1	1	*	2	1	
Tricolpites reticulatus		2	6	2		1
Tricolpites sp. A (tiny)	4	5		3		
Tricolpites sp. E (cf. reticulatus, smaller)			3	2		
Tricolpites sp. F (large, granular)		1				
Tricolpites sp. G (small, granular)			2			
Tricolpites sp. H (cf. lilliei)	1		1	2		
Tricolpites secarius	4	1	3	1		
Tricolpites spp.	2	2	6	3		1
Tricolporites spp.	13	3				
Triorites minisculus		1				4
Triorites minor	2					
Triorites spp.	3					
GYMNOSPERMS						
Araucariacites spp.	3	1	5	2		
Dacrydiumites praecupressinoides	2				2	
Microcachryidites antarcticus	1		4	1	4	4
Phyllocladidites paleogenicus	1	2		1	4	2
Phyllocladidites mawsonii	50	29	9	18	165	171
Podocarpidites cf. ellipticus	1	1		2	3	1
Podocarpidites major						1
Podocarpidites marwickii	12	4		1	3	3
Podocarpidites spp.	10	24	6	5	6	9
Trichotomosulcites subgranulatus	4	2	4	1		1
SPORES						
Baculatisporites spp.	19	4	1			1
Cingutriletes spp.			1			
Clavifera rudis				*		2
Cyathidites cf. minor	17	5				
Cyathidites spp.	15	61	99	36		
Gleicheniidites circinidites	14	16			23	9
Gleicheniidites spp.	4		9	64		
Laevigatisporites major			1	1		
Laevigatosporites ovatus	17	32	14	35	8	10
Lycopodiumsporites spp.	1	0	2	*	1	
Monosulcites spp.		1		1		
Osmundacidites wellmanii			15	9	1	
Peromonolites bowenii	4	3		1	12	15
Peromonolites sp. (small)	1	4		8		
Polypodiidites cf. minimus		1				
Stereisporites antiquasporites	18	12	49	29	3	2
Trilites verrucatus	8	1		1	8	1
Trilites cf. verrucatus			11			
Trilites morleyi	1					1
Trilites spp.	1		2	24	4	6
Trilites tuberculiformis	2					
Angiosperm %	**16.3**	**18.8**	**13.1**	**9.8**	**3.1**	**4.4**
Gymnosperm %	**34.1**	**25.2**	**10.5**	**11.7**	**73.3**	**76.8**
Spore %	**49.6**	**56.0**	**76.4**	**78.6**	**23.5**	**18.8**

DH635

Sample	635/1	635/2	635/3	635/4	635/5	635/6
UCP	1270	1271	1302	1272	1304	1273
ANGIOSPERMS						
Unidentified angiosperm	1				1	
Concolpites leptos	1					
Malvacipollis subtilis			4			
Monosulcites cf. granulatus	3				1	
Monosulcites spp.		2	5			
Myrtaceidites spp.	1					
Proteacidites scaboratus					1	
Proteacidites amolosexinus			1			
Proteacidites parvus			2			
Proteacidites spp.			1			
Tricolpites gillii	5	3	2	*	1	
Tricolpites lilliei						*
Tricolpites reticulatus			1		2	
Tricolpites sp. D (med. size, gran-clav)			3			
Tricolpites sp. E (cf. reticulatus, smaller)			1			
Tricolpites secarius	1		5			
Tricolpites spp.			2			
Triorites minor	20	68	57	*	1	
GYMNOSPERMS						
Araucariacites cf. australis	4		5			
Microcachryidites antarcticus	5		1		2	
Phyllocladidites paleogenicus	10	3				
Phyllocladidites mawsonii	33	22	35	*	103	
Podocarpidites cf. ellipticus	12					
Podocarpidites major	13					
Podocarpidites marwickii					1	
Podocarpidites spp.	40	15	10		15	
Trichotomosulcites subgranulatus			2			
SPORES						
Clavifera rudis	1				3	
Clavifera triplex	5	1		*		
Cyathidites spp.	9	18	40	*		*
Gleicheniidites circinidites	6	5		*		
Gleicheniidites spp.	10	3	4	*	82	*
Laevigatosporites major			1		1	
Laevigatosporites ovatus	13	7	13	*	13	*
Lycopodiumsporites spp.	1	3				
Osmundacidites wellmanii			20			
Peromonolites bowenii					13	
Stereisporites antiquasporites	7		18			
Trilites verrucatus		1	1	*	3	*
Trilites cf. verrucatus			4			
Trilites microfoveolatus		1				
Trilites morleyi		2			2	
Trilites ohaiensis		2	*			
Trilites spp.	1		*			
Trilites tuberculiformis	1	51	16			
Angiosperm %	**15.8**	**35.3**	**33.1**	–	**2.9**	–
Gymnosperm %	**57.6**	**19.3**	**20.9**	–	**49.4**	–
Spore %	**26.6**	**45.4**	**46.1**	–	**47.8**	–

DH636, DH640

SAMPLE	636/1	636/2	640/1	640/2
UCP	1340	1341	1342	1343
ANGIOSPERMS				
Liliacidites variegatus			1	
Malvacipollis spp.	1			*
Monosulcites cf. granulatus		3		2
Monosulcites cf. minima			3	7
Monosulcites spp.	2			
Proteacidites parvus	1		1	
Proteacidites scaboratus			1	
Rhoipites spp.		3	1	5
Tricolpites gillii	10	4	3	4
Tricolpites reticulatus		1	1	
Tricolpites sp. A (tiny)			1	
Tricolpites sp. E (cf. reticulatus, smaller)	1			
Tricolpites sp. F (large, granular)		3	3	
Tricolpites sp. G (small, granular)			3	
Tricolpites secarius	2		7	2
Tricolpites spp.	2	3	1	
Triorites minisculus	2		1	2
Triorites minor	8	1	1	1
Triorites spp.				1
GYMNOSPERMS				
Araucariacites spp.		10	9	10
Microcachryidites antarcticus		3	2	3
Phyllocladidites paleogenicus	4	1	5	5
Phyllocladidites mawsonii	92	57	50	77
Podocarpidites cf. ellipticus			3	1
Podocarpidites major			1	
Podocarpidites marwickii	4	7	6	1
Podocarpidites spp.	26	31	18	7
Trichotomosulcites subgranulatus	16	58	38	25
SPORES				
Baculatisporites spp.	32	2		
Cingutriletes regium		4	6	10
Cingutriletes spp.		2	28	15
Clavifera triplex			2	7
Cyathidites spp.	8	2	4	9
Gleicheniidites circinidites	14	7	17	47
Laevigatosporites major			1	4
Laevigatosporites ovatus	20	8	4	5
Osmundacidites wellmanii		7		
Peromonolites bowenii	3	1		3
Peromonolites sp. (small)		2	3	
Polypodiidites sp. C		9		
Stereisporites antiquasporites	1	22	24	8
Trilites cf. verrucatus	1			
Trilites spp.	1			
Trilites tuberculiformis	4		1	1
Angiosperm %	**11.4**	**7.2**	**11.2**	**9.2**
Gymnosperm %	**55.7**	**66.5**	**52.8**	**49.2**
Spore %	**32.9**	**26.3**	**36.0**	**41.6**

DH643

Sample	643/1	643/2	643/3	643/4	643/5	643/6
UCP	1362	1363	1344	1345	1364	1365
ANGIOSPERMS						
Unidentified angiosperm					2	
Beaupreaidites sp.					1	1
Malvacipollis spp.			1			
Monosulcites cf. granulatus			2	4	2	
Monosulcites cf. minima	1	3	1		1	8
Monosulcites granulatus		1				
Monosulcites spp.	1	1				
Nothofagidites kaitangataensis				1		
Nothofagidites spp.				1		
Proteacidites scaboratus	1	2				
Proteacidites amolosexinus						1
Proteacidites parvus					5	3
Proteacidites subpalisadus	1					
Rhoipites spp.			2	3		
Tricolpites gillii	2	2		1		1
Tricolpites lilliei					1	1
Tricolpites sp. B (tiny, gran/spinose)			4			6
Tricolpites sp. D (med size, gran-clav)						6
Tricolpites sp. E (cf. reticulatus, smaller)		*			1	4
Tricolpites sp. G (small, granular)		2			4	
Tricolpites secarius	2	2				4
Tricolpites spp.	1			1	6	1
Tricolporites spp.						7
Triorites minisculus			1			
Triorites minor	35	54				3
Triorites spp.						1
GYMNOSPERMS						
Araucariacites spp.	8	9	1	2	4	9
Microcachryidites antarcticus			2	7	3	
Phyllocladidites paleogenicus	5					
Phyllocladidites mawsonii	92	74	149	125	50	24
Podocarpidites cf. ellipticus	9	3	1		1	1
Podocarpidites major	1					
Podocarpidites marwickii	4	1				
Podocarpidites spp.	21	12	8	4	7	8
Trichotomosulcites subgranulatus	9	5	13	10	7	4
SPORES						
Baculatisporites spp.					3	
Cingutriletes regium			1	5		
Cingutriletes spp.			2	3		
Clavifera rudis			2	1		
Clavifera triplex			2	12		
Cyathidites spp.	5	1	3	6	69	81
Gleicheniidites circinidites			26	35		
Gleicheniidites spp.	15	23			15	8
Laevigatosporites major		1	1		3	2
Laevigatosporites ovatus	5	14	9	10	9	22
Lycopodiumsporites spp.						1
Osmundacidites wellmanii				1	1	16
Peromonolites bowenii			1	7	1	1
Peromonolites sp. (small)				2	2	1
Polypodiidites cf. minimus						2
Polypodiidites sp. C		2				
Stereisporites antiquasporites	34	26	18	8	40	22
Trilites verrucatus	1	1				
Trilites microfoveolatus		1				
Trilites morleyi			*	1		
Trilites spp.					13	1
Trilites tuberculiformis	*	10			2	
Angiosperm %	**17.4**	**26.8**	**4.4**	**4.4**	**9.1**	**18.8**
Gymnosperm %	**58.9**	**41.6**	**69.6**	**59.2**	**28.5**	**18.4**
Spore %	**23.7**	**31.6**	**26.0**	**36.4**	**62.5**	**62.8**

DH666

Sample	666/1	666/2	666/3	666/4	666/5	666/6
UCP	**1274**	**1275**	**1303**	**1276**	**1305**	**1277**
ANGIOSPERMS						
Unidentified angiosperm						2
Inaperturate			3			
Liliacidites spp.						1
Malvacipollis spp.		2		*		
Malvacipollis subtilis	1					
Monosulcites cf. granulatus	10	4		*		
Monosulcites spp.			6			4
Nothofagidites kaitangataensis			4		2	10
Nothofagidites spp.					1	
Polyorites spp.			1			
Proteacidites amolosexinus			1			
Proteacidites parvus	4		10		4	2
Proteacidites spp.	1		1			
Proteacidites scaboratus		1	4	*	1	1
Proteacidites subscaboratus	2					
Tricolpites gillii	4		6	*	1	2
Tricolpites lilliei			1			1
Tricolpites reticulatus	1		2			1
Tricolpites sp. B (tiny, gran/spinose)			3			1
Tricolpites sp. D (med. size, gran-clav)			1		1	
Tricolpites sp. G (small, granular)			3			
Tricolpites sp. H (cf. lilliei)			1			
Tricolpites secarius	5	2	1			
Tricolpites spp.	2	2	3		3	1
Tricolporites spp.			1			
Triorites minor	33	36	13			4
Triorites spp.		1		*		
GYMNOSPERMS						
Araucariacites spp.	8		13		1	15
Ephedra notensis					1	
Microcachryidites antarcticus	1	2	1		9	
Phyllocladidites paleogenicus	5	2			1	
Phyllocladidites mawsonii	47	32	14		43	7
Podocarpidites cf. ellipticus	7	6		*		
Podocarpidites major	1					
Podocarpidites marwickii						1
Podocarpidites spp.	11	30	4		13	5
Podosporites microsaccatus	2					
Trichotomosulcites subgranulatus	3	2	7			5
SPORES						
Baculatisporites spp.					2	
Ceratosporites equalis	1					
Cingutriletes regium	1					
Cingutriletes spp.			1			
Clavifera rudis		1	2			
Clavifera triplex	8	9			15	
Cyathidites spp.	2	15	39	*	13	31
Gleicheniidites spp.	12	15	9		25	13
Laevigatosporites major			1		2	
Laevigatosporites ovatus	9	16	17		14	12
Lycopodiumsporites spp.	2				2	
Monosulcites spp.			1			
Osmundacidites wellmanii			9		1	
Peromonolites bowenii					7	
Polypodiidites cf. minimus	1					
Polypodiidites spp.					14	
Stereisporites antiquasporites	2	1	52	*	1	46
Trilites cf. verrucatus			16			
Trilites morleyi	2	1				
Trilites sinuatus					1	
Trilites spp.			3	*	1	9
Trilites tuberculiformis	2	4	7		1	1
Trilites verrucatus	1		8	*		
Angiopsperm %	**33.0**	**26.1**	**24.2**	**–**	**7.2**	**17.1**
Gymnosperm %	**44.5**	**40.2**	**14.5**	**–**	**37.8**	**18.9**
Spore %	**22.5**	**33.7**	**61.3**	**–**	**55.0**	**64.0**

Appendix 14. Palynology data

DH667

Sample	667/1	667/2	667/3	667/4
UCP	1288	1289	1290	1291
ANGIOSPERMS				
Liliacidites spp.	1			
Liliacidites variegatus			2	
Monosulcites granulatus			5	
Monosulcites spp.	1			
Nothofagidites kaitangataensis	1			
Nothofagidites spp.	1			
Proteacidites parvus			1	
Tricolpites gillii	6	*	1	
Tricolpites lilliei	1			
Tricolpites sp. D (med. size, gran-clav)	1			
Tricolpites secarius			1	
Triorites minor	38	*	17	*
GYMNOSPERMS				
Araucariacites spp.	1		2	
Microcachryidites antarcticus	3			
Phyllocladidites paleogenicus	2		2	
Phyllocladidites mawsonii	10	*	17	
Podocarpidites cf. ellipticus	4			
Podocarpidites marwickii			6	
Podocarpidites spp.	28	*	8	
SPORES				
Clavifera triplex	2		6	
Cyathidites spp.	3		21	*
Gleicheniidites spp.	2			
Laevigatosporites ovatus	11		21	*
Lycopodiumsporites spp.	2			
Stereisporites antiquasporites	2			*
Trilites tuberculiformis	9		3	
Trilites verrucatus			26	*
Angiosperm %	**38.8**	–	**19.4**	–
Gymnosperm %	**37.2**	–	**25.2**	–
Spore %	**24.0**	–	**55.4**	–

DH697

Sample	697/5	697/6	697/7	697/8	697/9
UCP	1217	1216	1215	1214	1213
ANGIOSPERMS					
Liliacidites spp.		1	1		
Malvacipollis spp.	1			1	
Myrtaceidites spp.		1			
Monosulcites spp.	1				
Nothofagidites waipawaensis		1			
Polyorites spp.			1		
Proteacidites parvus	6	4			
Proteacidites scaboratus	2		1		
Proteacidites spp.	2	3	1	7	1
Proteacidites subpalisadus		1			
Quadraplanus brossus	1				
Rhoipites spp.	2	1			2
Tricolpites gillii	2	7	2	2	
Tricolpites reticulatus	2	1			
Tricolpites sp. A (tiny)			2		
Tricolpites sp. B (small, granular)	1	4			
Tricolpites sp. D (med. size, gran-clav)	5				
Tricolpites sp. H (cf. lilliei)	1				
Tricolpites secarius	1	2		*	
Tricolpites spp.				1	3
Triorites minor	79	97	72	62	3
Triorites minisculus	7	1	3	1	
GYMNOSPERMS					
Araucariacites spp.	26	27	34	60	9
Microcachryidites antarcticus			1		
Phyllocladidites paleogenicus		4			
Phyllocladidites mawsonii	35	31	11	58	26
Podocarpidites major	2	1	3	7	
Podocarpidites marwickii	5	3	4	17	
Podocarpidites spp.	22	16	16		11
Trichotomosulcites subgranulatus	1				3
SPORES					
Baculatisporites spp.	1				4
Clavifera rudis	1		4		
Clavifera triplex		2			
Cyathidites spp.	23	7	33	25	10
Gleicheniidites spp.	8	19	24	26	13
Laevigatosporites major			3		
Laevigatosporites ovatus	8	3	10	7	4
Osmundacidites wellmanii			1		
Peromonolites densus			1		
Rugulatisporites mallatus		1			
Stereisporites antiquasporites	18	18	21	13	27
Trilites morleyi			2		2
Trilites spp.		2			
Trilites tuberculiformis			4	5	1
Trilites verrucatus		6	6	6	
Angiosperm %	**43.0**	**47.0**	**31.8**	**24.8**	**7.6**
Gymnosperm %	**34.6**	**31.1**	**26.4**	**47.7**	**41.2**
Spore %	**22.4**	**22.0**	**41.8**	**27.5**	**51.3**

MISCELLANEOUS COALS

Sample (Mine/sample site)	Kiwi	Snowline	Tiller	Goldlight
UCP	1278	1279	1306	1307
ANGIOSPERMS				
Monosulcites cf. granulatus	1	1		
Monosulcites cf. minima			*	
Monosulcites spp.	4	6		5
Nothofagidites spp.		1		
Polycolpites spp.		1		
Proteacidites parvus			1	
Proteacidites scaboratus			*	
Proteacidites subpalisadus			*	
Tricolpites gillii	2			
Tricolpites lilliei	2	2		
Tricolpites reticulatus	4	1		
Tricolpites sp. A (tiny)		1	*	
Tricolpites sp. B (small, granular)	2			
Tricopites sp. E (cf. reticulatus, smaller)			2	
Tricolpites secarius			8	
Tricolpites spp.	1	4		
Tricolporites spp.	1	1		
Myricipites harrisii				1
Triorites minisculus			2	
GYMNOSPERMS				
Araucariacites spp.		4	1	4
Microcachryidites antarcticus	8	4	4	
Phyllocladidites paleogenicus				1
Phyllocladidites mawsonii	88	86	147	171
Podocarpidites cf. ellipticus				1
Podocarpidites major			1	
Podocarpidites marwickii	15	18		
Podocarpidites spp.	1	3	7	7
Trichotomosulcites subgranulatus			1	4
SPORES				
Baculatisporites spp.		1		
Clavifera triplex	63	44	12	1
Cyathidites spp.	7	10	1	6
Gleicheniidites circinidites		8	56	37
Gleicheniidites spp.	1			
Laevigatosporites major	3	1		
Laevigatosporites ovatus	24	37		2
Lycopodiumsporites spp.		1		
Monosulcites spp.	1	2		
Osmundacidites wellmanii		1		
Peromonolites bowenii	15	3	1	
Peromonolites spp.	2		*	
Polypodiites spp.	4	7		
Stereisporites antiquasporites	1		6	10
Trilites morleyi	2	1		1
Trilites spp.	1	2		
Trilites tuberculiformis		1		
Trilites verrucatus	1	2		2
Verrucocosisporites kopukuensis			*	
Angiosperm %	**6.7**	**7.1**	**5.2**	**2.4**
Gymnosperm %	**44.0**	**45.3**	**64.4**	**74.3**
Spore %	**49.3**	**47.6**	**30.4**	**23.3**

Part 4.

Papers

Part 4. Papers

The following three papers were published during the course of the present project. All papers are presented here as published and with their original pagination.

Ward, S.D. 1995: Controls on sedimentology and coal occurrence in the Rewanui Coal Measure Member, western Greymouth Coalfield (Rapahoe Sector). *Proceedings, 6th New Zealand Coal Conference, Wellington, October 1995*: pp. 151–161.

Ward, S.D. 1996: Application of lithostratigraphic and chronostratigraphic analysis to seam modelling in the Rapahoe Sector, western Greymouth Coalfield. *Proceedings, Australasian Institute of Mining and Metallurgy, New Zealand Branch annual conference, Greymouth*: pp. 173–199.

Ward, S.D.; Moore, T.A.; Newman, J. 1995: Floral assemblage of the "D" coal seam (Cretaceous): Implications for banding characteristics in New Zealand coal seams. *New Zealand Journal of Geology and Geophysics 38*: 283–297

Statement of contribution:

All work presented in Ward (1995) and Ward (1996) was my own.

Contributions to Ward et al. (1995) were as follows:

- assisting with field work
- all palynological processing, data collection, reporting and discussion
- assembly of manuscript for submission
- all editing as required by the journal editor and external referee
- final editing of page proofs

CONTROLS ON SEDIMENTOLOGY AND COAL OCCURRENCE IN THE REWANUI COAL MEASURE MEMBER, WESTERN GREYMOUTH COALFIELD (RAPAHOE SECTOR)

Simon Ward

Geology Department, University of Canterbury, Private Bag 4800, Christchurch.

ABSTRACT

The Rewanui Coal Measure Member (RCM) in the Rapahoe Sector is a sequence comprising fluvial, floodplain and mire deposits in which substantial economic bituminous coal has accumulated. Isopach modelling reveals the location and orientation of the depocentres, and allows the effects of compaction to be differentiated from tectonic subsidence. Palynological identification of the Cretaceous-Tertiary boundary in 16 drillholes confirms the validity of using the contact between the RCM and the overlying Goldlight Mudstone Member as a correlation datum. Palynology also highlights variable subsidence rate in the upper RCM, and assists with the recognition of faulted strata. Principal sedimentary environments represented in the RCM include: high energy, braided river; low-moderate energy, sandy fluvial and crevasse splay; floodplain, which may be vegetated or ponded; and mire.

Greatest coal development occurs towards the southwest margin of the basin, where the RCM thins rapidly and is underlain by Paleozoic basement. Thick coals may overlie braided fluvial deposits, but are more commonly associated with floodplain sequences. The coals are split at their southwestern margin by crevasse splay sediments sourced from the adjacent basement, and are restricted to the north and east by increased fluvial activity in the more rapidly subsiding portion of the basin. In the central and northern Rapahoe Sector, coal formation may be attributed to variable clastic sediment supply, due to channel migration or overall reduction in sediment influx.

INTRODUCTION

The Rapahoe Sector of the Greymouth Coalfield (Fig. 1) contains significant resources of bituminous coal and has been a target for coal exploration and production for more than sixty years. Early mining was concentrated in the Brunner Coal Measures, but as these resources became depleted, emphasis has shifted towards the underlying Paparoa Coal Measures, and in particular the Rewanui Coal Measure Member (RCM). Exploration drilling in the 1930's led to the development of the Strongman Mine, which closed in 1994. The Coal Resources Survey programme (1979 – 1984) in Greymouth Coalfield (Ref. 1) identified significant resources in the previously un-drilled southern portion of the Rapahoe Sector, and led to research on paleoenvironment and coal properties (Ref. 2). Exploration has continued in both the southern Rapahoe Sector and the vicinity of the former Strongman Mine workings, and the Strongman No. 2 Mine has recently opened in the northeast of the Rapahoe Sector.

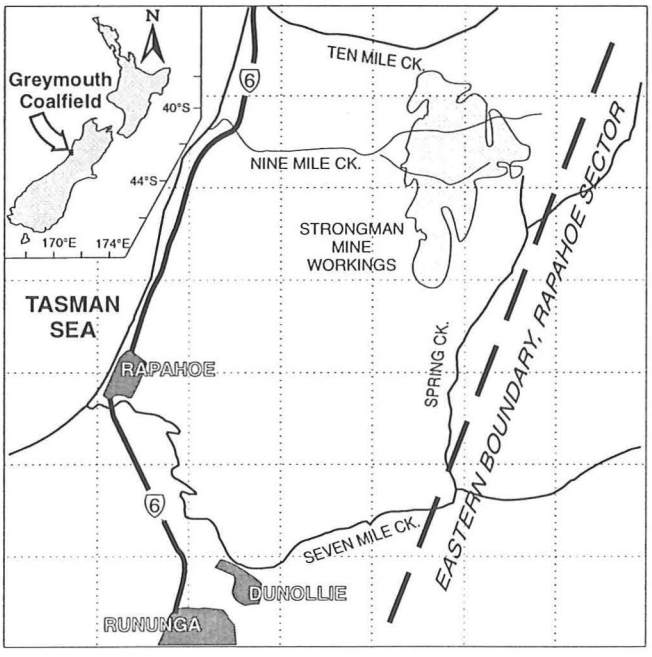

Figure 1.

Location map, Rapahoe Sector, western Greymouth Coalfield. The grid square on this and all subsequent figures is 1km.

The objective of the present study is to incorporate the wealth of drillhole data which now exists for the Rapahoe Sector into an integrated model for basin development and stratigraphy, and to investigate the controls on formation of thick, clean coals in the southern Rapahoe Sector.

DATA PREPARATION

A total of 62 drillholes, incorporating Coal Resources Survey, Greymouth Coal Ltd. and CoalCorp drilling, were investigated for this project, plus some older State Coal Mines holes where necessary (Fig. 2). Approximately 9500m of section through RCM has been drilled in the Rapahoe Sector for exploration purposes. Much of the lithological data is incorporated in the Greymouth Coalfield Drillhole Database (Ministry of Commerce/Ian R. Brown Associates), which was accessed via TECHBASE® software. Records for each drillhole were verified against the original lithological logs, then exported to RockWorks™ LOGGER® for production of graphic logs at 1:200 scale. These were manually annotated with sedimentological details (e.g. nature of contacts, graded bedding, sedimentary structures, fossils) and structural information (dips, shearing, faults). Where available, geophysical logs (e.g. natural gamma, long-spacing density and caliper) were used to accurately determine sedimentological boundaries and trends, and core was inspected as required. Lithological boundaries were picked by the application of consistent criteria (discussed below), and all isopach values have been corrected for dip and the effects of faulting (where this can be demonstrated).

Isopach maps were modelled with a grid composed of 250x250m cells, using a minimum curvature (spline curve) algorithm, which may be likened to fitting a flexible metal sheet through the data points. This process generally honours the data, but truncates anomalously high or low values, as the surface cannot deform to accommodate those values. Consequently, the isopach models may not exactly reflect the data. By comparing individual data values with the modelled surface, the reliability of data points may be assessed, and stratigraphic problems such as faulting-induced thinning or repetition of strata may be recognised.

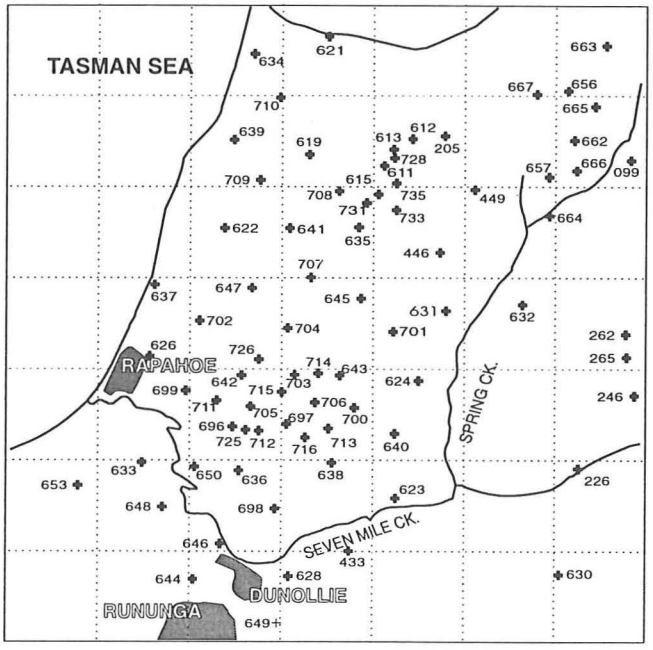

Figure 2.

Drillhole location map.
All drillholes used in this study are indicated. Drillholes east of Spring Ck., though outside the Rapahoe Sector, are required to constrain the isopach model.

STRATIGRAPHY

The stratigraphy of the Paparoa Coal Measures within the Greymouth Coalfield (Fig. 3) was originally determined by Gage (Ref. 3), and modified by Nathan (Ref. 4), who relegated Gage's Formations to Member status. Within the Rapahoe Sector there is significant variability in the stratigraphy due to the influence of the basin margins. In addition, the stratigraphic significance of packages of deltaic sediment between the fluvial and lacustrine members has not been previously determined.

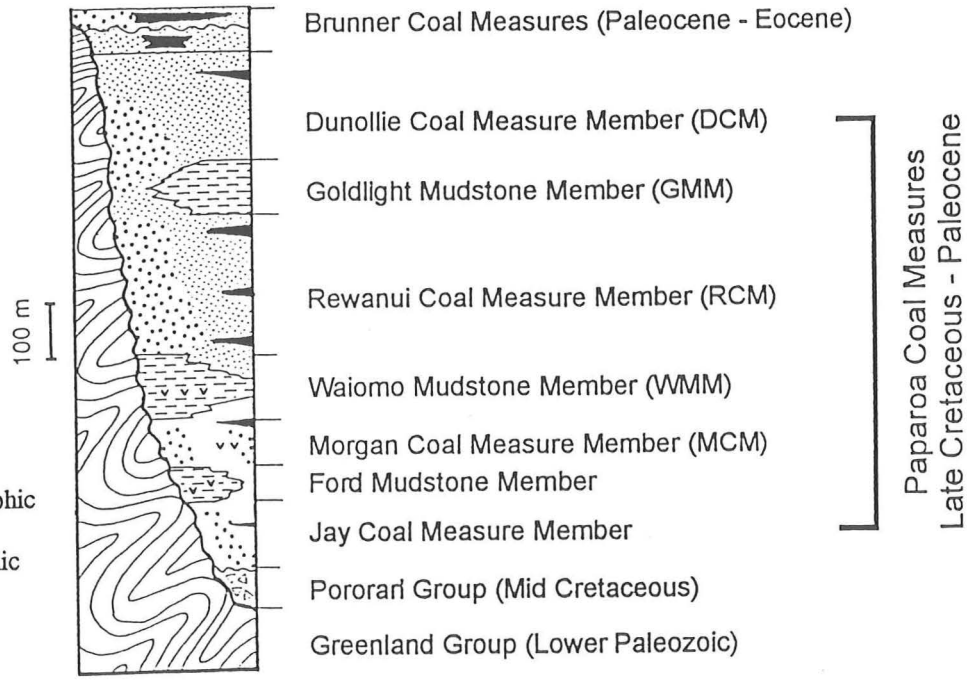

Figure 3.

Generalised stratigraphic column, Greymouth Coalfield. Stratigraphic abbreviations used throughout text are indicated.

Morgan, Ford and Jay Members

Morgan Coal Measures (MCM) and basal conglomerates are well developed (>75m) in the extreme NW of the Rapahoe Sector, while Ford Mudstone and Jay Coal Measures are absent. MCM occupy a narrow WNW-ESE trending basin which extends across the northern 2-3km of the Rapahoe Sector, approximately north of DH's 619 and 632. Isolated thin (0 – 40m) basal sands and conglomerates southwest of this line may represent lateral equivalents of the MCM, deposited by infilling of paleotopography.

Waiomo Mudstone Member

The distribution of Waiomo Mudstone Member (WMM) is indicated in Fig. 4. The lower boundary of WMM is generally recognised as the contact between MCM coals or carbonaceous mudstones and the overlying massive, lacustrine mudstones and siltstones, while along the SW basin margin, WMM onlaps onto basement.

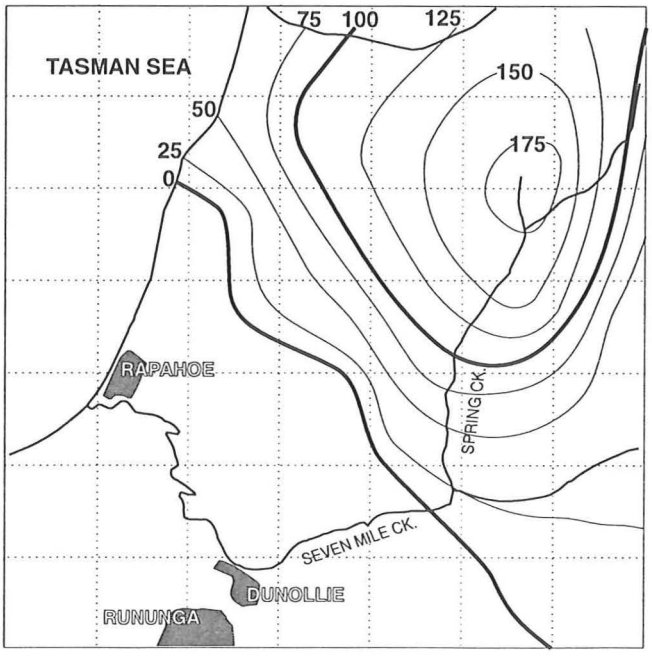

Figure 4.

Isopach map, Waiomo Mudstone Member

There are 3 components to the WMM: 1) massive lacustrine mudstones and siltstones, 2) tuffs and volcanic breccias and 3) deltaic sequences (some of which were formerly included in the overlying RCM). Lacustrine deposits vary from 0 – 128m, and generally follow the same thickness trends as the overall WMM isopach pattern. Tuffs are widespread, though best developed in the vicinity of DH's 635 – 632. Deltaic sequences are present between WMM and RCM throughout most of the Rapahoe Sector, but are absent in the southeastern area where WMM is entirely composed of 20 – 40m mudstone (Fig. 5). The deltaic sequences are composed of commonly thick (10 – 20m), coarsening-upwards packets of silts and sands, with soft sediment deformation features (e.g. slumping, flame structures), and occasional well preserved leaf fossils.

The WMM isopach model (Fig. 4) indicates an asymmetrical basin subsiding principally along a NNE/SSW oriented normal fault located approximately 1km east of Spring Creek. Magma probably rose to the lake floor as dykes along this fault surface, resulting in the tuffaceous deposits. The SW margin would also have been subsiding, possibly as a block tilting to the NE. The maximum thickness of WMM approximately coincides with the underlying MCM basin, though the two depocentres are at an orthogonal angle. Deltaic deposits result from deltas prograding from the NW toward the depocentre, but lacking sufficient sediment supply to completely infill the lake which persisted in the east.

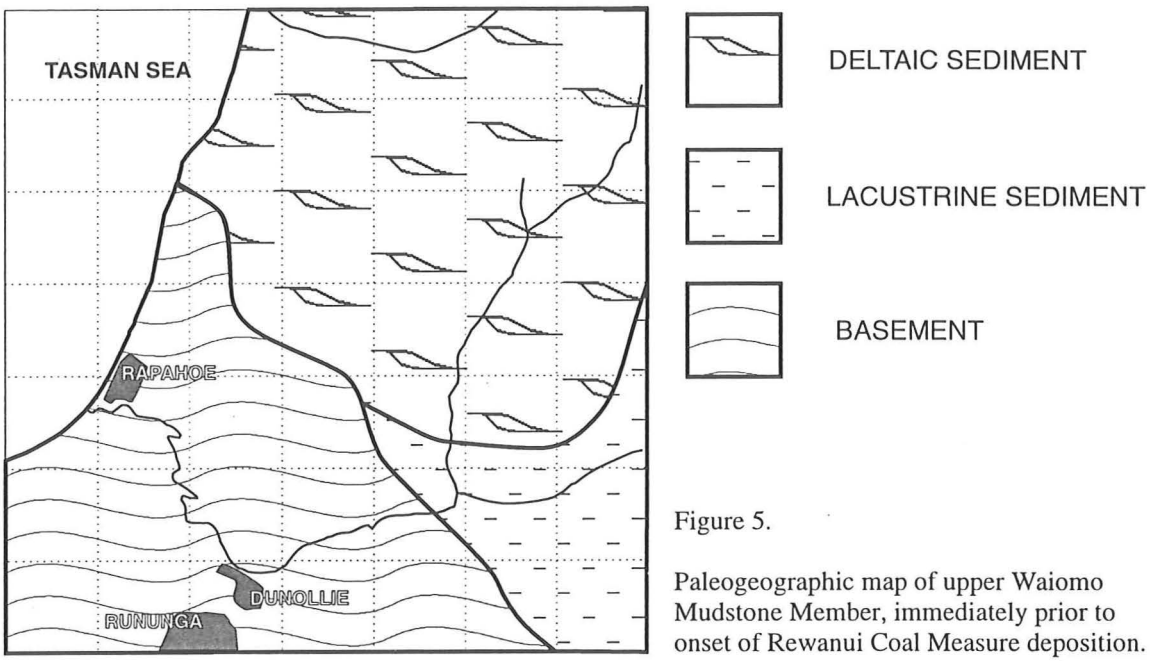

Figure 5.

Paleogeographic map of upper Waiomo Mudstone Member, immediately prior to onset of Rewanui Coal Measure deposition.

Rewanui Coal Measure Member

The Rewanui Coal Measure Member (RCM) lies either on basement, or conformably on WMM deltaic and lacustrine sediments (Fig. 5), in which case the first occurrence of coaly/carbonaceous muds, silts and sands, commonly in fining upwards packets, indicates RCM. The upper contact of RCM is generally placed at the transition from coaly/carbonaceous mudstones to deltaic sands or lacustrine mudstones and siltstones of the overlying Goldlight Mudstone Member (GMM). In the northwestern Rapahoe Sector, RCM is conformable with the overlying Dunollie Coal Measure Member (DCM), and GMM is absent.

The RCM occupies a broad (10+km) NW/SE oriented trough (Fig. 6) with a complex southwestern margin, where coal measures onlap basement. The 250m isopach, indicated on Fig. 6 as the "Strongman depocentre" is postulated from the presence of at least 250m of RCM in DH 449, and at least 245m in DH 205. The thickness of RCM in the northern Rapahoe Sector is poorly defined, partly because of difficulty in defining the upper contact in the northwest (discussed below), but also due to erosion of upper RCM and GMM, and structural complications in a number of drillholes. For example, at least 274m of RCM is present in DH 656, whereas the model (Fig. 6) indicates approx. 210m at this locality. Comparison with surrounding drillholes, and structural disruption evident in the core, indicates the sequence in DH 656 is anomalous, and this data point has been omitted from the model. In contrast, DH 641 (230m RCM) appears to perturb the modelled surface by 20 - 40m, but this data point has been retained as there is

little evidence for structural problems. These examples demonstrate the nature of the mathematical model, and the ease with which it may be influenced by the selective inclusion or omission of data points.

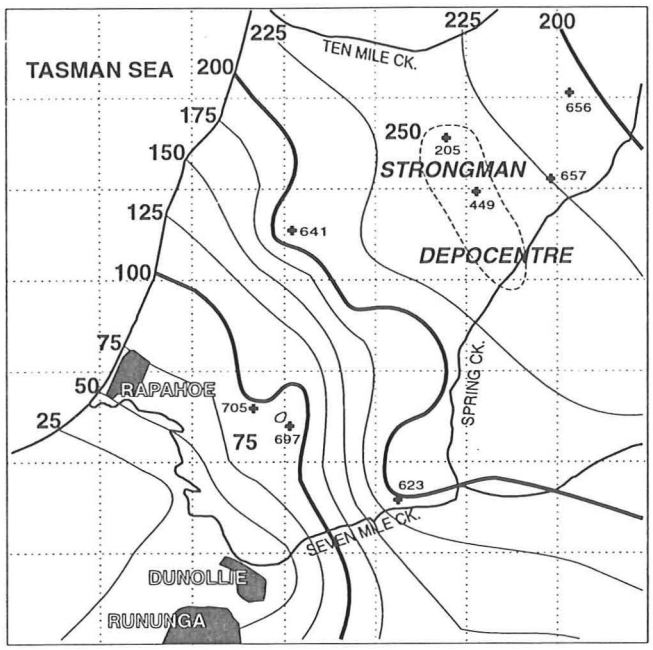

Figure 6.

Isopach map of the Rewanui Coal Measure Member. The 250m contour is postulated, all other contour lines are generated by a minimum curvature algorithm. Drillholes specifically referred to in text are indicated.

In the southern Rapahoe Sector, where the subsurface RCM overlies basement, the isopach model is better constrained, though up to 15 drillholes may be affected by post-depositional faulting. Rapid thickness variation in the vicinity of DH's 705 and 697 may reflect small-scale NNE/SSW oriented block-faulting of the basement, infilling of pre-existing topography, or structural complications in the RCM. The measured isopach value for DH 705 (122.6m) is approx. 20m greater than the modelled value, and the lithological log reports numerous faulted and sheared intervals. In this instance, the isopach model may have effectively compensated for the structural problems because of the mathematical constraints on the curvature of the modelled surface. The WMM zero isopach (Fig. 4) is relatively straight, suggesting only minor paleotopography. Discordance between the RCM isopachs and the WMM zero isopach indicates synsedimentary faulting within the basement block during RCM deposition is primarily responsible for the RCM thickness variation in the southern Rapahoe Sector.

The maximum thickness of RCM is coincident with that of the underlying WMM. The thickest RCM on basement (214.6m in DH 623) provides an estimate of the tectonic subsidence which occurred during RCM deposition. Decompaction analysis (Table 1) of the WMM mudstones in DH 657 suggests between 31m and 47m of subsidence by the end of RCM deposition may be attributed to compaction of underlying mudstones. This indicates that no greater tectonic subsidence is required in the Strongman depocentre than that which occurred at DH 623, suggesting platform-like subsidence in the northern Rapahoe Sector, and reduction of the extensional fault activity which influenced WMM deposition.

Rewanui - Goldlight Contact: Lithostratigraphy and Biostratigraphy

The contact between RCM and GMM has been traditionally used as a stratigraphic correlation datum for interpretation of the RCM seams (Ref. 1), principally because it is widespread and generally distinct. Problems arise in the northern Rapahoe Sector, due to lateral transition of the lacustrine facies into deltaic and fluvial sequences. The paleogeographic reconstruction of the initiation of GMM deposition (Fig. 7) indicates a northwestern sediment source, which resulted in continuous fluvial deposition, with an adjacent zone (1.5 – 2km) of deltaic sediments. A minor sand source also persisted in the southwest. The deltaic sediments comprise thick beds (8 – 10m) of fine to medium sands, conspicuously interbedded with lacustrine mudstones and siltstones (containing well-preserved leaf fossils and freshwater bivalve impressions). These sediments are readily distinguished from the underlying RCM by the lack of carbonaceous beds.

Drillhole 657
Stratigraphy:

116m "Upper" RCM
109m "Middle" RCM
53m deltaic WMM
128m WMM mudstone
78m+ MCM

	minimum porosity	maximum porosity
Maximum burial depth of mst (Ref. 5).	3.25km	3.25km
Assumed initial porosity (Ref. 6)	54%	68%
Decompaction to original thickness	185.6m Δth = 57.6m	199.7m Δth = 71.7m
Burial to 225m (average depth of mst at start of coal-bearing Upper RCM deposition)	165.7m (p = 42%) Δth = 19.9m	176.7m (p = 55%) Δth = 23m
Mst thickness at end of RCM deposition	154.7m Δth = 30.9m	152.4m Δth = 47.3m
Percentage of total RCM thickness attributable to WMM mudstone compaction	13.7%	21.0%

Table 1. Decompaction analysis, WMM mudstones, DH 657. Using maximum and minimum porosity/ depth relationships from Ref. 6. Change of thickness for each step indicated by Δth value.

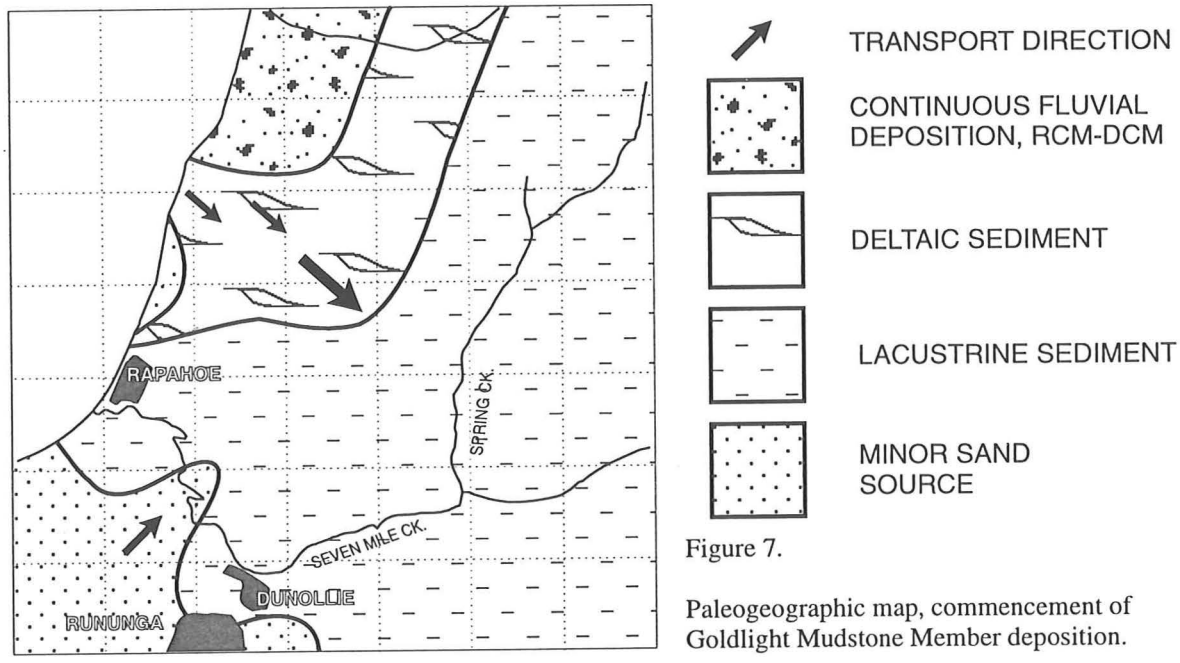

Figure 7. Paleogeographic map, commencement of Goldlight Mudstone Member deposition.

In the northwest, fluvial sedimentation appears to be continuous from RCM to DCM, and the lithostratigraphic boundary is poorly constrained. As a means of locating the contact, palynostratigraphy was applied to DH's 621 and 622 (Ref. 7). This indicated that the Cretaceous-Tertiary boundary (KTB), defined by the boundary between 2 spore/pollen zones (Ref. 8), is present within Greymouth Coalfield, and confirmed that thin mudstone beds within the conglomeratic sequences may be equivalent to GMM. Subsequent analysis of DH's 631 and 632 (Raine, unpublished data 1989) confirmed the proximity of the KTB to the RCM/GMM contact.

The KTB has been located in a further 12 drillholes as part of the present study (Fig. 8), which indicate the presence of two stratigraphic domains in the upper RCM. Southwest of a line through DH's 622 and 640 the KTB lies within c. 5m of the Rewanui/Goldlight contact, whereas northeast of this line, the interval averages c. 15m. Previous seam correlation models (Ref 2) have proposed significant diachroneity of the RCM/GMM contact, however these results indicate that within either domain, the RCM/GMM contact is approximately isochronous. This confirms the use of the lithological contact as a correlation datum, though care is necessary when correlating seams across the interface of the 2 domains. Palynostratigraphy also confirms the presence of fault repetition in DH 628, and is consistent with postulated fault-thinning of RCM in DH 636.

The sharp transition across the two biostratigraphic domains suggests rapid, and distinct, lateral variability in subsidence rate during late RCM deposition. Lacustrine sedimentation may have begun in the SW in response to locally increased subsidence rate, while fluvial sediments continued to accumulate in the NE. Alternatively, higher rates of subsidence in the NE would have permitted the accumulation of a thicker packet of fluvial sediment in this domain, prior to the regional onset of lacustrine and deltaic sedimentation. The coincidence of the boundary

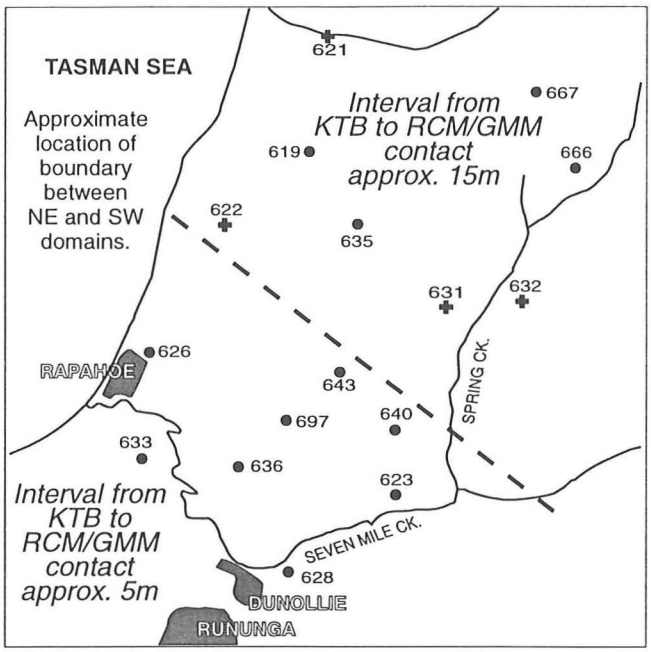

Figure 8.

Drillholes in which the Cretaceous/Tertiary Boundary has been located. Crosses are data from J.I.Raine (IGNS), circles are author's data. The approximate location of the boundary between the biostratigraphic subdomains is indicated.

between the two domains (Fig. 8) with the northwestern sediment supply feeding the deltaic region of the GMM (Fig. 7), the WMM zero isopach (Fig. 4) and the greater thickness of the RCM in the NE, supports the latter hypothesis.

Controls on Distribution of Coal in the RCM

The widespread distribution of coal in the Rapahoe Sector RCM is indicated in Fig. 9, which shows cumulative coal thickness for all seams over 1m. Coal occurrence varies from 1 thick seam (up to 28m) to multiple, thinner seams with fluvial or floodplain interseam sediments (Fig. 10), and greatest coal formation (as a proportion of the total RCM thickness) is restricted to the southwest (stippled area, Fig. 10). The occurrence of 1 thick seam (which is split to the southwest) is mostly restricted to the area of RCM underlain by basement, with the exception of DH 707. Relatively restricted coal development in the northern Rapahoe Sector can be attributed to the dominance of fluvial sedimentation in the Strongman depocentre, resulting in multiple and/or dirty seams.

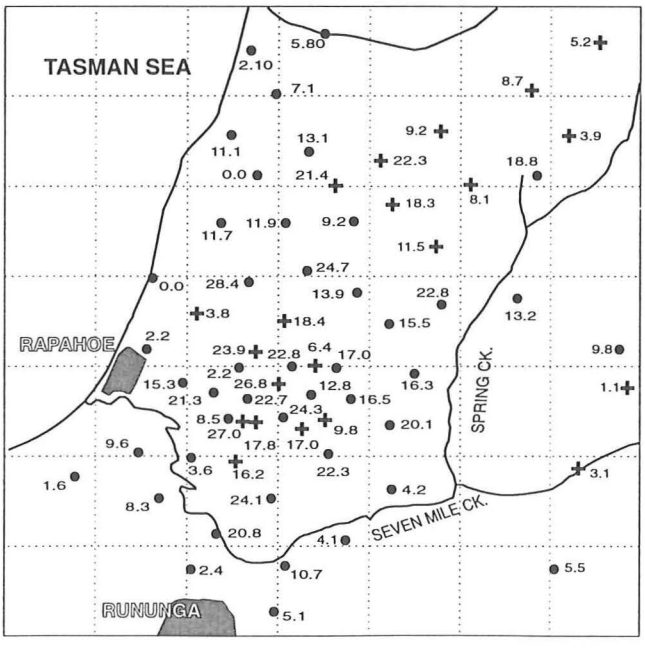

Figure 9.

Cumulative coal thickness, Rewanui Coal Measures. All seams >1m are included. Dots indicate precise data, crosses indicate minimum values where either the full thickness of RCM has not been drilled, or RCM is thinned by faulting.

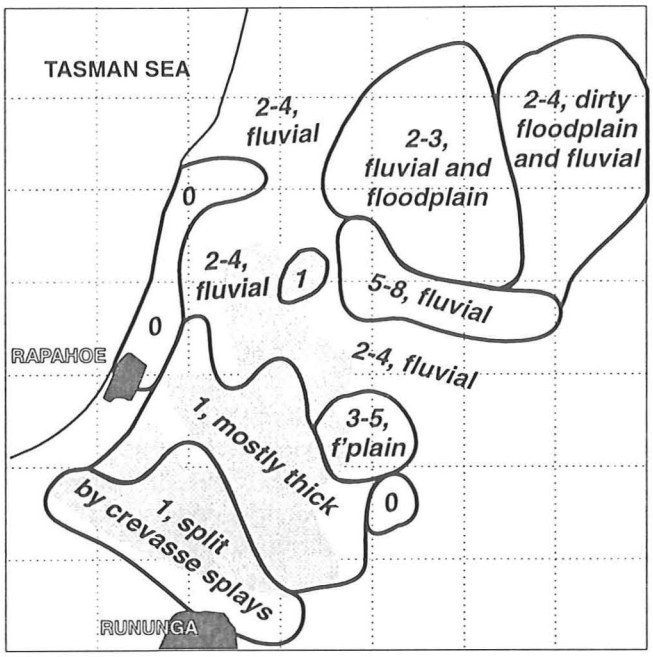

Figure 10.

Generalised character of zones of coal occurrence in the Rewanui Coal Measures. Numbers indicate the number of seams present, text refers to nature of interseam sediments. The shaded area represents >10% of total RCM thickness as coal.

A variety of fluvial, floodplain and mire paleoenvironments are represented by the lithofacies present in the southern Rapahoe Sector. These may be subdivided into 5 facies associations, which are summarised in Table 2. The distribution of these facies associations along 2 orthogonal sections (Fig. 11A) is indicated in Figures 11B and 11C. Drillholes 636 and 696 are significantly affected by faulting, and DH 712 does not penetrate the RCM to basement, thus the stratigraphy depicted at these locations has been adjusted to ensure conformity with the RCM isopach model (Fig. 6).

MIRE
varies from dull to semibright and bright coal
siderite nodules and chuckies often present in small amounts
seams may be dirty at or near roof and floor

VEGETATED FLOODPLAIN
varies from dirty coals (<2m) to carbonaceous mudstone and siltstone
coaly and minor fine sandstone interbeds, quartz granules, resin, some fine rootlets

FLOODPLAIN
mostly mudstone and siltstone with low-mod abundant carbonaceous fragments
minor rootlets, leaf fossils, coaly bands
massive, faintly laminated and occ. ripple cross-laminated
minor siltstone and vfine-fine sandstone interbeds

CREVASSE SPLAY AND MINOR CHANNEL
variable grainsize from rare granules and pebbles to vfine sandstone
variably fining upwards and coarsening upwards packets
variable lower contacts from gradational (often where finer) to erosional (cse sst)
massive (esp. where cse sst) to faintly laminated or wavy bedding
minor rootlets, carbonaceous frags, mudstone clasts (esp. at base of coarser beds)
coarser units often have vfine sandstone-siltstone interbeds

BRAIDED CHANNEL
conglomerates, vary from massive beds 10m+ to 1-4m i/b with thin sst
and carb mst/thin coal
commonly fining upwards, cobbles up to 25cm, more commonly <10cm.
clast supported (occ. matrix supported debris flow on basement
clasts mostly Greenland Group, subrounded-rounded, poor to moderate sorting

Table 2. Facies associations and key sedimentological features, southern Rapahoe Sector.

In section X – X' (Fig. 11B), splitting by crevasse splay sediments is responsible for the rapid reduction in coal proportion in the vicinity of DH 650, and similarly thinning of the major seam towards DH 643 (and overall reduction of coal proportion) may be attributed to persistent fluvial and crevasse splay deposition. Maximum coal development in section X – X' (DH's 636 – 706) is associated with persistent floodplain sediments, suggesting an area distal to major clastic sediment sources. In contrast, the seam in section Y – Y' (Fig. 11C) is not split by crevasse splays, but grades laterally at its margins into floodplain sediments. Again, coal development is associated with floodplain sediments, though in the northwest (DH 699 – 696), coal onlaps onto a wedge of braided fluvial deposits which has built out into the basin from the northwestern margin. Reduction of the proportion of coal towards the southern end of the section, and dominance of crevasse splay deposits, reflects greater fluvial activity in this vicinity.

The position of crevasse splays and minor channels which intersect the coal seam indicates the approximate location of sediment sources into the southern Rapahoe Sector, and similar information may be deduced from the sediment influxes into the basin during early GMM deposition (Fig. 7). Significantly, the sand wedge indicated in the southwest in Fig. 7 coincides with the area of seam splitting by crevasse splays indicated in Fig. 10. Thus, the southwestern sediment source remained active throughout the deposition of the RCM and the lower GMM, and was responsible for limiting of coal formation in this area. The sediment source may have been a NW/SE oriented fluvial system, located to the southwest of the study area. Crevasse splays during times of flooding would carry sediment laterally into the adjacent mire environment, though the extent of travel would be limited by the raised nature of the mires (Ref. 2).

The northern margin of abundant coal formation corresponds to the axis of the deltaic wedge in the lower GMM (Fig. 7), and the predominance of braided fluvial and crevasse splay lithologies in DH 643 indicates the presence of a fluvial system. In addition, the inferred boundary between the two palynostratigraphic domains (Fig. 8), and the WMM zero isopach (Fig. 4) are located in this vicinity, suggesting a persistent, probably structural, control which influenced a variety of aspects of basin development.

The eastern limit of the 10% coal zone (Fig. 10) is mostly a function of increased RCM thickness, and significant coal development in the central Rapahoe Sector is associated with fluvial lithofacies (Fig 10). Coal development in areas dominated by floodplain sediments is variable. For example, 15 – 20m of coal is generally present adjacent to Spring Creek (Fig. 9). Moderately thick (6 – 12m), clean coal is present as 2 – 3 seams in DH's 624, 631, 700 and 701, while split and dirty seams are present in DH's 623 and 640 (see Fig. 11A for location of these drillholes). There is a southwards transition from channel facies dominated sequences (DH 631, 701) to channel facies plus vegetated floodplain (DH 624, 700, 640), to DH 623 which has poor coal development and is dominated by floodplain and crevasse splay lithofacies.

Coal formation within the fluvial-dominated central Rapahoe Sector indicates variable clastic sediment supply at any depositional site, achieved either by channel belt migration towards the Strongman depocentre, or by extrabasinal variations in sediment input. The former scenario is likely in the central belt (labelled "2-4 fluvial" in Fig. 10) where coal is interbedded with braided channel lithofacies. In contrast, much of the coal in the northern Rapahoe Sector postdates fluvial (conglomerate) deposition and is associated with floodplain sediments, suggesting a regime of lower sediment influx from the northwestern basin margin. Restricted coal development in the northeast and east may reflect the influence of an axial fluvial system which is present to the east of the study area (Ref. 2).

SUMMARY

The Rewanui Coal Measures in the Rapahoe Sector accumulated in a tectonically active basin in the latest Cretaceous to earliest Tertiary. The basin was formed by platform subsidence and compaction of an older, lacustrine and deltaic extensional basin, and by block faulting in the Paleozoic basement to the southwest. Principal sediment sources were the western margin which shed coarse clastic material, and the southwestern basement block which provided dominantly sand. These sediment sources persisted throughout the deposition of the RCM and the subsequent Goldlight Mudstone Member. A wide range of fluvial and floodplain lithofacies are preserved in the RCM, and coal deposition was widespread. Greatest coal formation was in the Dunollie-Rapahoe area, where thick, clean coal is associated with floodplain sediments. This area was protected from clastic input by greater subsidence to the north and east, which constrained the location of major fluvial systems, and by mire topography to the southwest. Coal development in the central and northern Rapahoe Sector reflects variable sediment supply.

Figure 11A.

Location map of section X-X' (Figure 11B) and section Y-Y' (Figure 11C). Correlation datum for both section is the RCM/GMM contact, vertical exaggeration is 13x. Also indicated is the location of the drillholes west of Spring Ck., which are referred to in the text.

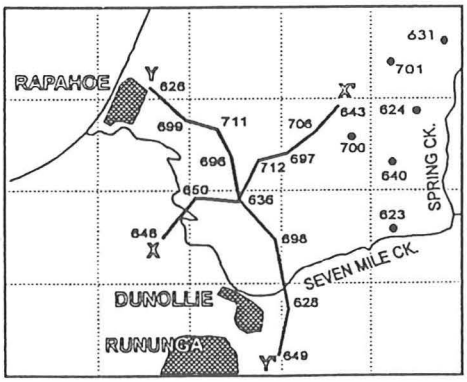

Figure 11B. Section X-X'

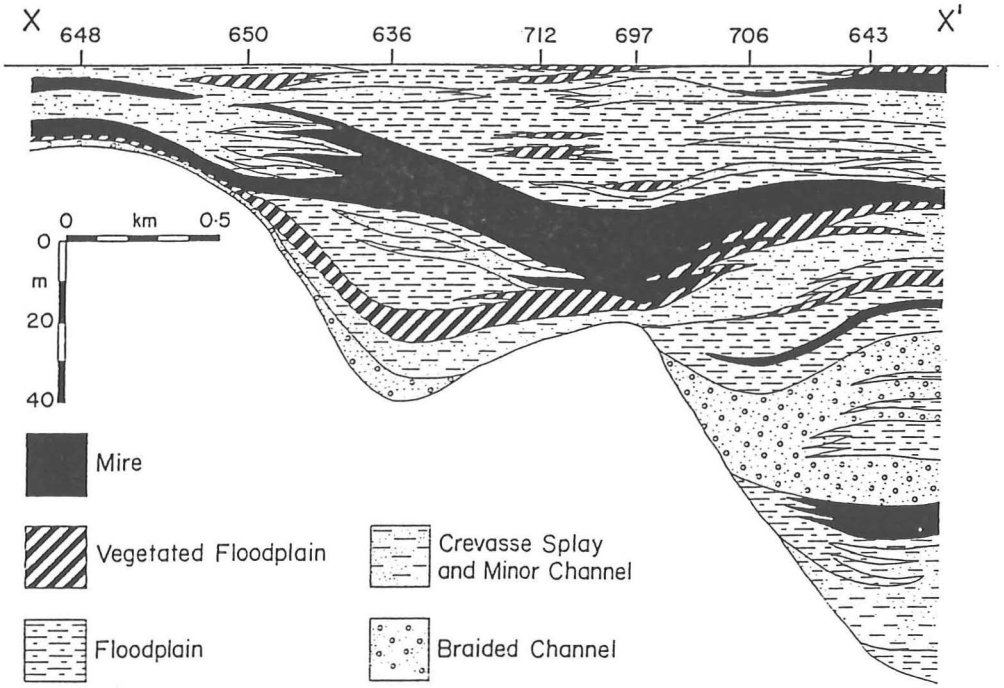

Figure 11C. Section Y-Y'

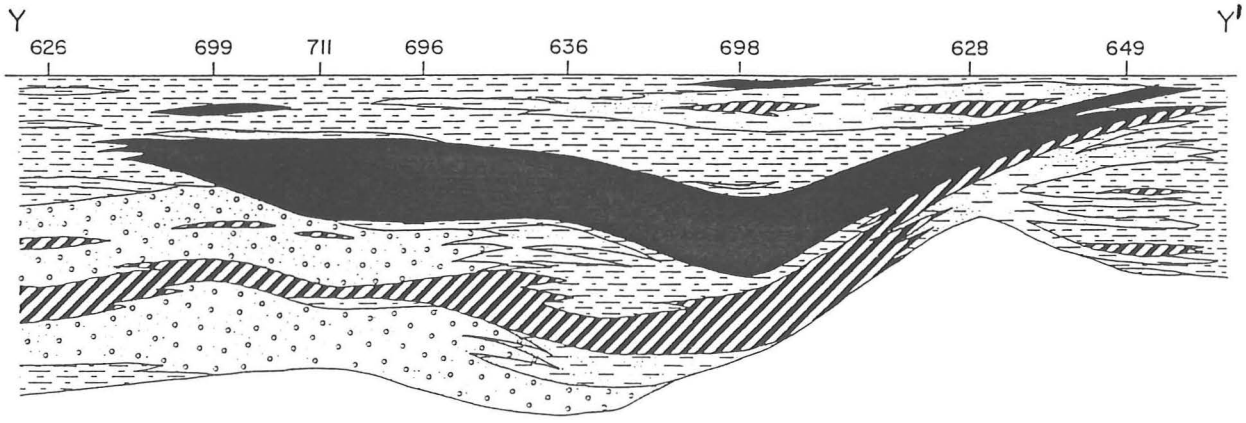

ACKNOWLEDGEMENTS

This paper is part of a Ph.D. study of the Rewanui Coal Measures, funded by a University of Canterbury Postgraduate Scholarship, the former Canterbury Coal Research Group and the Geology Department. The Mason Fund and Coal Research Ltd. contributed to logistic support, and CoalCorp provided valuable vacation employment. I am indebted to Murry Cave, Bill Leask and Pete Manning for creating the drillhole database and providing and supporting Techbase, and to the many geologists who logged the core. I am also grateful to Paul Caffyn, Stuart Henley (CoalCorp) and Frank Taylor (Greymouth Coal Ltd.) for their assistance, and contributing data. Lee Leonard kindly drafted Figure 11. Jane Newman has provided constant support and supervision of the study, and contributed valuable critical evaluation of this paper.

REFERENCES

1. Bowman R.G. New Zealand Coal Resources Survey, Greymouth Coalfield Report (1984) Parts I – V
2. Newman J. Resource Management and Mining, Coal Geology Report 3 (1987) 28
3. Gage M. New Zealand Geological Survey Bulletin 45 (1952) 232
4. Nathan S. Geological map of New Zealand 1:63 360 Sheet S44 Greymouth (1978)
5. Boyd R.J., Lewis, D.W. New Zealand Journal of Geology and Geophysics (1995) 38 333 – 349
6. Bond G.C., Kominz M.A. Geological Society of America Bulletin (1984) 95 155 – 173
7. Raine, J.I. New Zealand Geological Survey Report PAL 47 (1981) 11
8. Raine, J.I. New Zealand Geological Survey Report 109 (1984) 82

New Zealand Journal of Geology and Geophysics, 1995, Vol. 38: 283–297
0028–8306/95/3803–0283 $2.50/0

Floral assemblage of the "D" coal seam (Cretaceous): implications for banding characteristics in New Zealand coal seams

S. D. WARD
Department of Geology
University of Canterbury
Private Bag 4800
Christchurch, New Zealand

T. A. MOORE
Coal Research Limited
P.O. Box 31 244
Lower Hutt, New Zealand

J. NEWMAN
Coal Research Limited
c/- Department of Geology
University of Canterbury
Private Bag 4800
Christchurch, New Zealand

Abstract Two complete vertical sections were studied from the uppermost Cretaceous "D" coal seam near Greymouth, New Zealand. The thickest and most concentrated vitrain bands occur in the paleomire centre and bands are thinner and less abundant at the paleomire margin. Botanical analysis of the vitrain bands indicates they formed entirely from the secondary xylem (wood) of gymnosperms. Palynomorphs indicate that there is no consistent correlation between conifer pollen abundance and the degree of vitrain banding. However, maximum preservation of vitrain bands coincides with an inferred transition from a rheotrophic mire (as indicated by *Phyllocladidites mawsonii* pollen) to an acidic and possibly ombrotrophic system (as indicated by the abundance of Gleicheniaceae spores). This suggests that the presence/absence of gymnosperm secondary xylem as vitrain bands is controlled at least in part by mire chemistry.

Keywords coal; Late Cretaceous; palynology; vitrain bands; gymnosperm secondary xylem; *Phyllocladidites mawsonii*; Gleicheniaceae; paleomire; rheotrophic; ombrotrophic; petrology

INTRODUCTION

Coal seams generally represent thick in situ accumulations of plant material in a mire environment. Vertical and lateral variability of coal characteristics within any single seam can be related to a number of factors including original mire vegetation, proximity to contemporaneous fluvial channels, mire type (e.g., domed or low lying), and chemistry of the peat during accumulation. A number of process (i.e., facies) models have been developed to explain variability in coal seam characteristics (e.g., Teichmüller 1958; McCabe 1984; Cecil et al. 1985; Esterle & Ferm 1986; Hagemann & Wolf 1987; Anderson & Mackay 1990). However, these models commonly fail to differentiate between the effects of original vegetation and those of hydrologic and chemical controls on vegetative degradation. Or, more specifically, are plant remains in coal the result of plant tissue inherently resistant to fungal and bacterial decay, or do they represent a favourable chemical environment which depressed microbial degradation?

Plant tissues in coal are manifested most noticeably as bright, lensoidal bodies, generally >1 mm thick, referred to as vitrain or xylite bands (Stopes 1919; Thiessen 1937). Such structured plant remains can be a major component of coals, and their presence or absence can have implications for paleoenvironmental interpretations. Furthermore, banding characteristics may be a significant control on coal properties such as grindability and fluidity (Benedict et al. 1968; Moore 1990).

In order to investigate the degree to which original flora determined coal character, especially in relation to the presence or absence of vitrain bands, the latest Cretaceous "D" seam from the Strongman coalmine near Greymouth, New Zealand (Fig. 1), was macroscopically described and sampled for palynology and plant tissue analysis.

The "D" seam occurs close beneath the Cretaceous–Tertiary boundary within the Haumurian (latest Cretaceous) to Teurian (Paleocene) Paparoa Coal Measures at Greymouth Coalfield, which comprise an alternating sequence of fluvial and lacustrine members with a maximum original thickness of 1000 m (Nathan 1978; Sherwood et al. 1992). The Paparoa Coal Measures occupy a NNE-oriented half-graben, which is attributed to continued extension following the mid-Cretaceous separation of the Australian and Pacific plates (Laird 1993). At the time of coal measure deposition, New Zealand was located at a high southern paleolatitude, and megafloral studies indicate a humid microthermal-mesothermal climate (mean annual temperature 12–16°C) with winter darkness (Johnson & Greenwood 1993).

"D" seam is located near the top of the fluvial Rewanui Member of the Paparoa Coal Measures, and is one of several high-volatile bituminous rank seams in a sequence of fine floodplain sediments (Fig. 2). Early depositional models attributed the seams to a lake margin setting (Gage 1952), whereas later work has suggested a floodbasin located between western alluvial fans and a southward-flowing fluvial system in the east (Newman & Newman 1992). Sediment-filled paleochannels representing stream activity within the mires are a recurring feature in the upper Rewanui Member seams (Thorburn 1981).

G94042
Received 9 September 1994; accepted 18 May 1995

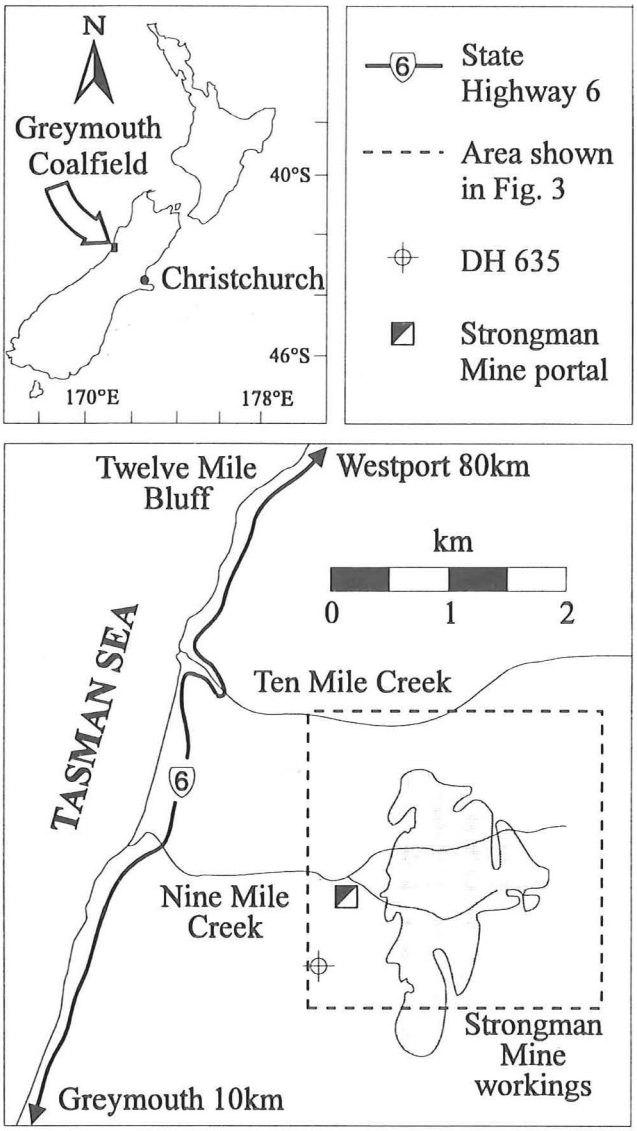

Fig. 1 Geographic location of the study area, showing the position of the workings of the recently closed Strongman mine.

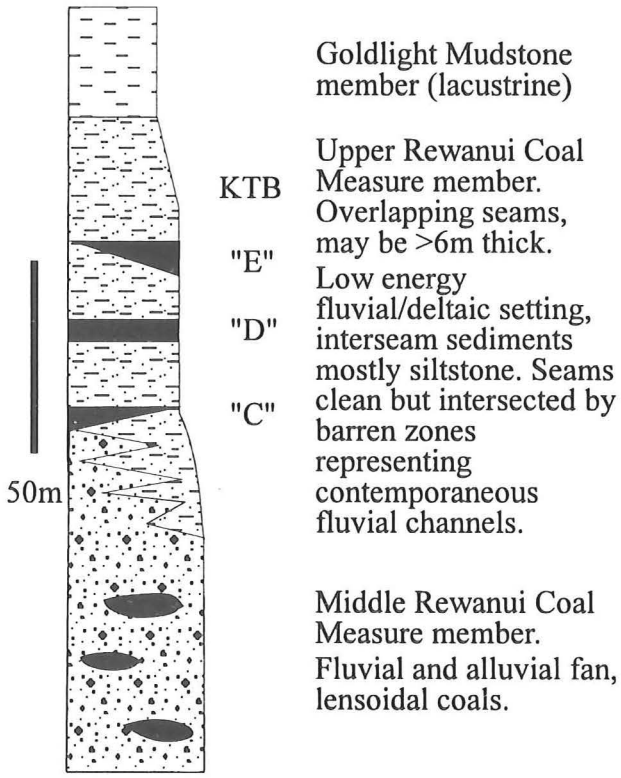

Fig. 2 Generalised stratigraphic section of the upper Rewanui Coal Measure Member, Paparoa Coal Measures.

Table 1 Macroscopic coal types observed from two localities in the "D" seam.

Matrix lustre	% Vitrain bands	Thickness of vitrain bands
Bright	Non-banded	–
	<30% bands*	<1 to 1 mm
	30–50% bands*	<1 to 1 mm
	30–50% bands*	>2 mm
Steely grey	Non-banded	–
	<30% bands	<1 to 1 mm
	30–50% bands	<1 to 1 mm
	30–50% bands	>2 mm

*Coal types which occur with greatest frequency in the "D" seam

METHODS

Sampling and description

To determine lateral variability of macroscopic, microscopic, and palynologic composition, the "D" seam was sampled at two localities within the underground Strongman mine (Fig. 3). The first locality (STM), along the East Heading, was chosen because of its proximity to the coal deposit margin and was sampled in 1978 as a consecutive series of oriented blocks. The second locality (ST-94) is within the thick central portion of the seam (Fig. 3) along the #2 North Heading, and was described and sampled in 1994 immediately before the closure of the mine. At both localities, samples were collected from fresh, unaltered coal sections.

Description of the coal seam sections was based on the lustre of the attrital layers and thickness and proportions of the vitrain bands. Attrital layers within coal are the fine-grained (<1 mm) groundmass in which the larger (>1 mm) plant parts (i.e., vitrain bands) are bound, and consist of particulate (fragments of cell walls, fillings, spores/pollen, resin, oxidised material) and amorphous (fossilised humic gels, bitumen) organic material. Vitrain bands are the preserved remains of secondary xylem or heartwood components of roots and stems.

Differentiation of macrolithotypes in the coal faces is the basis for selection of samples for palynological and petrographic analysis. Eight macroscopically recognisable types of coal were distinguished (Table 1). Seam sections and the corresponding macroscopic descriptions are shown in Fig. 4 and 5, as is the location of samples for palynology and tissue analysis.

At the STM locality, the macroscopic character of the coal was mostly fine grained (i.e. vitrain bands were generally <1 mm in thickness) with a bright attrital lustre. Because of the lack of sizeable vitrain bands in the coal, this location could be described only qualitatively (Fig. 4). The ST-94 locality contained numerous vitrain bands >1 mm

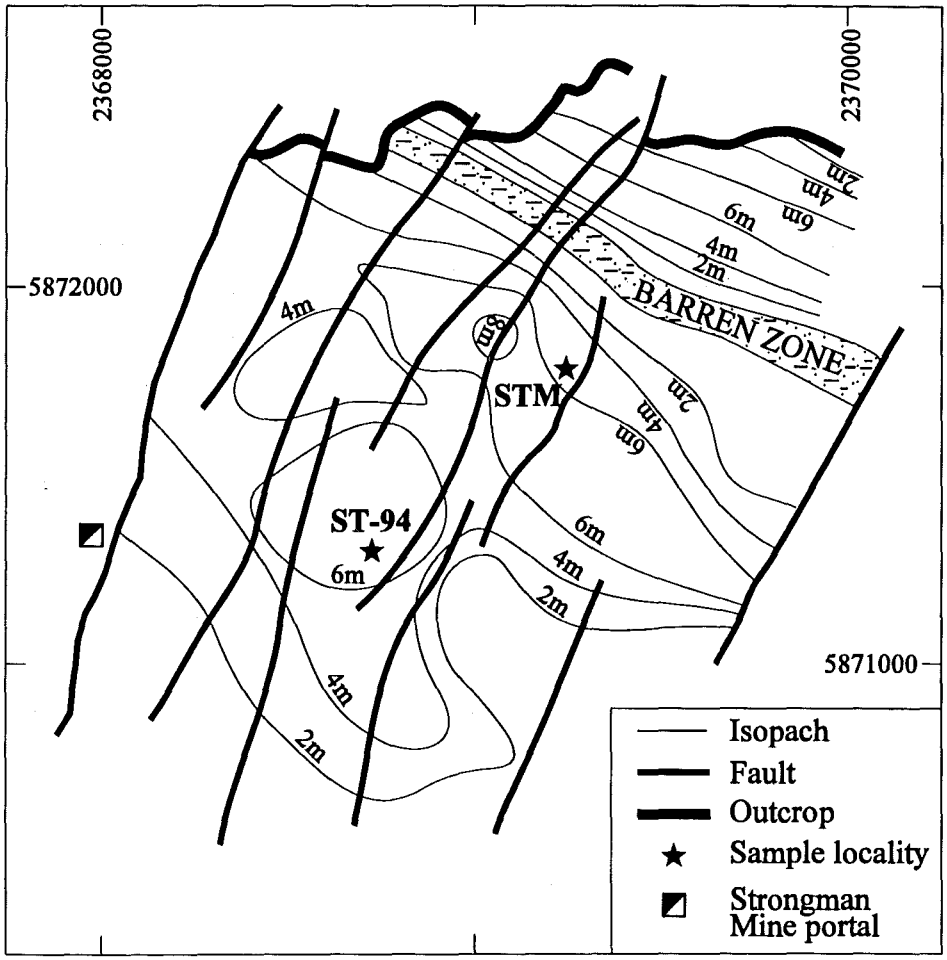

Fig. 3 Isopach map of the "D" seam, Strongman mine. Data are modified from Thorburn (1981) and collected from underground workings and drillholes within the Strongman mine and adjacent blocks. Grid references refer to map sheet NZMS 260, J31—Greymouth.

in thickness, and vitrain band proportions and size were quantified using a methodology described in Moore et al. (1993) and Shearer & Moore (1994a). Banding proportions for ST-94 are shown in Fig. 5.

Palynological sampling and preparation

Fourteen samples, six from the ST-94 section and eight from the STM section, were selected to encompass the range of lithotypes encountered (see Fig. 4, 5), and all were assigned University of Canterbury Palynology (UCP) numbers (Appendix 1). Samples from the STM locality were taken from individual blocks, whereas the ST-94 samples were collected from approximately the centre of the corresponding lithotype interval. All samples were ground and passed through a 1.5 ϕ (0.35 mm) sieve. Extraction of palynomorphs followed the wet Schulze process (see Traverse 1988, pp. 462–463), modified to suit the material. Each sample was reacted with concentrated $HNO_3/KClO_3$ for 10–15 min, followed by a wash step and the addition of 10% KOH solution for 5 min. All samples were passed through a 100 μm sieve, and unwanted fine material was removed by the addition of 10% bleach solution for 10 min, followed by "short centrifuging" (whereby the samples are accelerated from 0 to 2000 r.p.m. over 30 s), which was repeated as necessary. Mineral material was removed from UCP1357 by separation in ZnBr solution (specific gravity = 2.0). All samples were permanently mounted in glycerine jelly. Material, residue, and slides are held in the Department of Geology, University of Canterbury.

All slides were examined with a Zeiss KM microscope (GEOL876), using a scan interval of 0.6 mm and ×300 magnification. Higher magnifications were used to aid identification where needed. Approximately 250 pollen and spore grains were recorded for each sample, and where slides were only partially completed upon reaching this total, a further 10 tracks were scanned for the presence of key species. All samples yielded workable assemblages, though preservation and abundance were variable.

Petrographic analysis preparation

To determine the botanical origin of the vitrain, five vitrain bands were collected from the ST-94 section, and four block samples were collected from the STM section. Petrographic composition and texture were determined from six blocks of the fine-grained matrix, three from each section. Positions of the block samples for vitrain and matrix analyses are shown in Fig. 4 and 5.

All block samples were cut to c. 2.5 × 2.5 × 3 cm and embedded in epoxy resin, following procedures outlined in Esterle et al. (1991). The samples were polished perpendicular to bedding using a series of grit papers and diamond and silica slurries (see, e.g., Moore & Stanton 1985; Esterle et al. 1991). Finally, to reveal botanical structures and textures, all vitrain and matrix samples were chemically

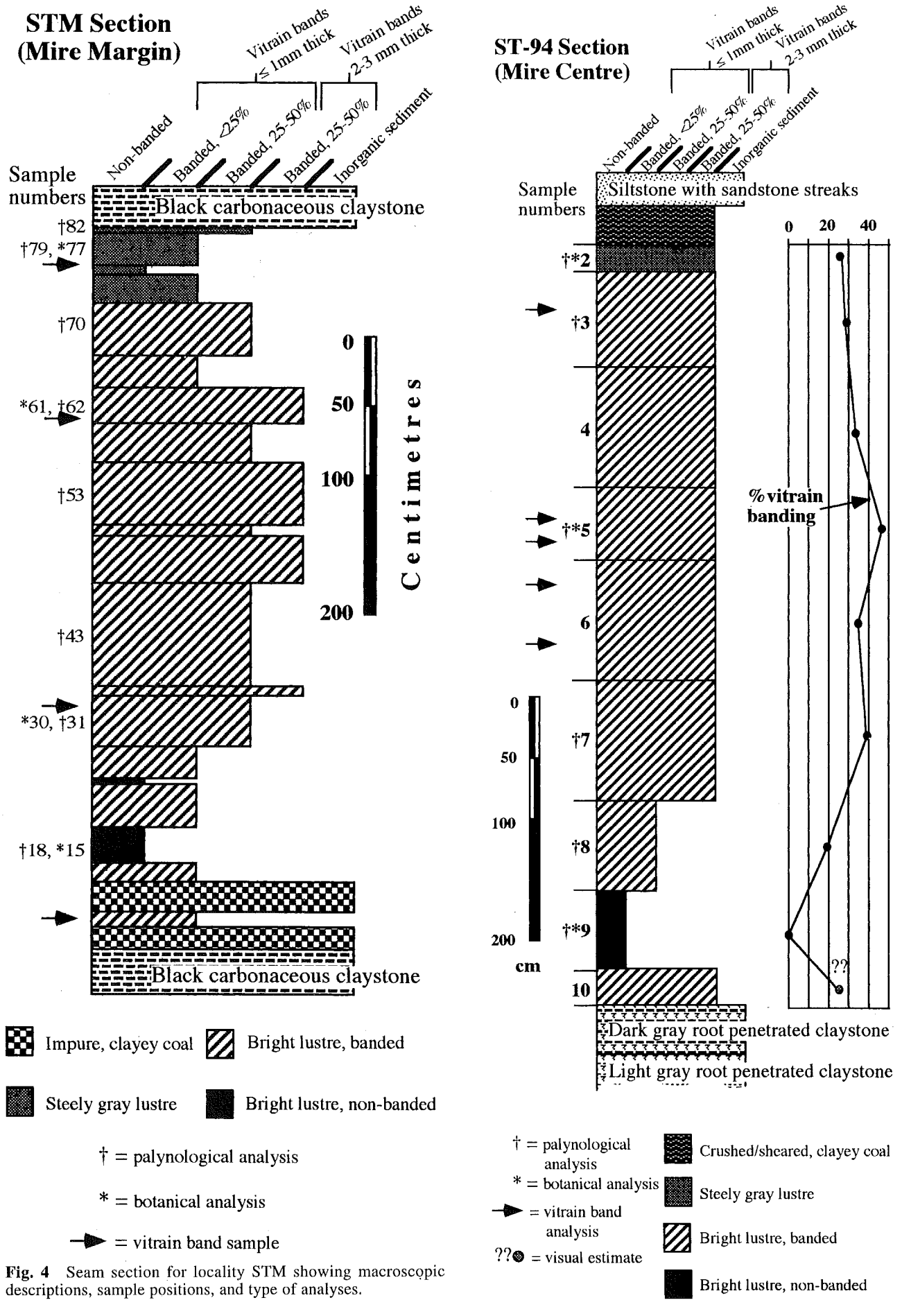

Fig. 4 Seam section for locality STM showing macroscopic descriptions, sample positions, and type of analyses.

etched with a solution of potassium permanganate and sulphuric acid (Stach et al. 1982; Newman & Newman 1988; Quick & Moore 1991).

Petrographic analyses of the matrix block samples were conducted as traverses perpendicular to bedding until 125 counts were reached, which Moore (1990) has demonstrated as sufficient to characterise the composition of oriented uncrushed coal samples. To give a representative modal analysis, no component was counted more than once. Point counts were conducted using white, reflected-light microscopy with a range of air objectives from ×5 to ×40. Most identifications and measurements were made at either ×200 or ×400. Classification of botanical consitutents in the matrix blocks followed the procedures of Moore & Ferm (1992), which have been successfully applied to New Zealand coals by Shearer & Moore (1994a). Maceral group identification follows that of ICCP (1971) and Stach et al. (1982).

RESULTS

Palynology

A total of 53 taxa and forms were recorded (Appendix 1), of which a large proportion are common Late Cretaceous to Paleocene taxa in the New Zealand region (see, e.g., Couper 1953, 1960; Pocknall & Tremain 1988 for illustrations). Similar palynomorph assemblages have been described from Late Cretaceous coals at Ohai Coalfield, Southland (Morley Coal Measures) (Warnes 1992; Shearer & Moore 1994a) and Puponga Coal Measures, northwest Nelson (Bal 1994). A number of undescribed taxa were encountered, most notably tricolpate forms (listed in Appendix 1 as *Tricolpites* sp. *A–F*), various forms of *Podocarpidites*, and trilete spores. Occurrences of the abundant and significant taxa are indicated in Fig. 6A, B.

Stratigraphic dating

The presence of *Nothofagidites kaitangataensis*, *Tricolpites lilliei*, and *Trilites morleyi* supports assignment of these samples to Zone PM2 of the *Phyllocladidites mawsonii* Assemblage (Haumurian, Late Cretaceous) of Raine (1984). However, two specimens of *Tricolpites secarius*, which is typically an indicator of Zone PM3 (Teurian, Paleocene; Raine 1984) were recorded from UCP1346 (see Fig. 6). The Cretaceous–Tertiary boundary is located c. 20 m above the "D" seam in nearby drillhole 635 (see Fig. 1 for location) (Ward unpubl. data), and minor overlap of key Haumurian and Teurian taxa is known from other nearby localities (Raine 1984).

Vertical and lateral trends in palynomorph abundance

The assemblages are variably dominated by pollen from conifers (gymnosperms) (20.3–73.2%) and pteridophyte spores (21.9–71.5%). The proportions of major types and taxa can be conveniently divided into five groups: (1) angiosperms, (2) the conifer *Phyllocladidites mawsonii*, (3) the remaining conifer species, (4) spores of the Gleicheniaceae (*Gleicheniidites circinidites* and the related species *Clavifera triplex* (Dettmann & Playford 1968)), and (5) spores other than Gleicheniaceae. These data are graphically represented in Fig. 7 and 8.

Most variation within the ST-94 locality may be attributed to opposing trends in the abundance of *Phyllocladidites mawsonii* and Gleicheniaceae (Fig. 7). *P. mawsonii* abundance increases from the floor to UCP1347, followed by a decline in the sample nearest the roof. The abundance of Gleicheniaceae is also variable but declines steadily from UCP1349 to the roof. Angiosperms exhibit virtually no change in proportion, being <10% in all samples, though there is a reduction in the abundance of *Tricolpites* sp. *A* from the floor to the roof. There is, however, a slight upward increase in angiosperm diversity. Conifers other than *P. mawsonii* (notably *Araucariacites* cf. *australis* and *Trichotomosulcites subgranulatus*) remain at c. 10% throughout the section. Non-Gleicheniaceae spores (in particular *Peromonolites* spp., *Laevigatosporites ovatus*, and *Cingutriletes* spp.) are most abundant, and most diverse, near the floor (UCP1351).

The STM section exhibits different patterns of abundance from those observed in the ST-94 section (Fig. 8). *P. mawsonii* generally increases in abundance towards the centre of the seam, though there are also slight increases at the roof and floor. Other conifers are most abundant in the basal two samples (UCP1356, 1357), which contain moderate amounts of *A.* cf. *australis*, *T. subgranulatus*, and *Podocarpidites* spp. Gleicheniaceae spores, which have low abundances relative to ST-94, increase consistently from the floor to UCP1354, then decline slightly towards the roof. The remaining spore flora remains at similar levels (10–20%) throughout the floor and centre of the seam, whereas *Peromonolites* spp. contribute to an increased abundance near (but not at) the roof (UCP1353). Angiosperms (notably *Monosulcites* spp., *Tricolpites* sp. *A*, and *Tricolpites reticulatus*) are conspicuously abundant, and have greatest diversity, at the base of the section (UCP1356, 1357), whereas abundance and diversity decline toward the centre of the seam.

Comparison of the two sections highlights similarities and differences between the sample sites. For example, the increase in *P. mawsonii* abundance in the centre of the STM section is absent in the ST-94 section. Spores of the Gleicheniaceae exhibit opposite abundance trends in each section; however, the remainder of the spores tend to increase toward the roof and floor of both sections. Angiosperms and conifers other than *P. mawsonii* maintain generally low abundances through both sections, the only exception being the floor of the STM section, where both components are moderately common.

Macroscopic analysis

The size distribution of vitrain bands for section ST-94 is shown in Fig. 9. Generally, the band thickness in section STM was <1 mm and thus not large enough to accurately measure visually. The measurements made on vitrain band widths in section ST-94 were converted to a $-\log_2$ scale (or phi [ϕ] scale) as it has been demonstrated that organic components tend to have a normalised distribution when sizes are transformed to a phi scale (Moore & Ferm 1992).

Although the average vitrain band thickness in the ST-94 section is 1.93 ϕ (SD = 0.93 ϕ, n =156), the distribution is skewed towards larger sizes (Fig. 9). In contrast, vitrain band size in coal elsewhere in New Zealand shows a normal distribution (Esterle et al. 1992; Shearer & Moore 1994a).

Fig. 5 Seam section for locality ST-94 showing macroscopic descriptions, sample positions, and type of analyses.

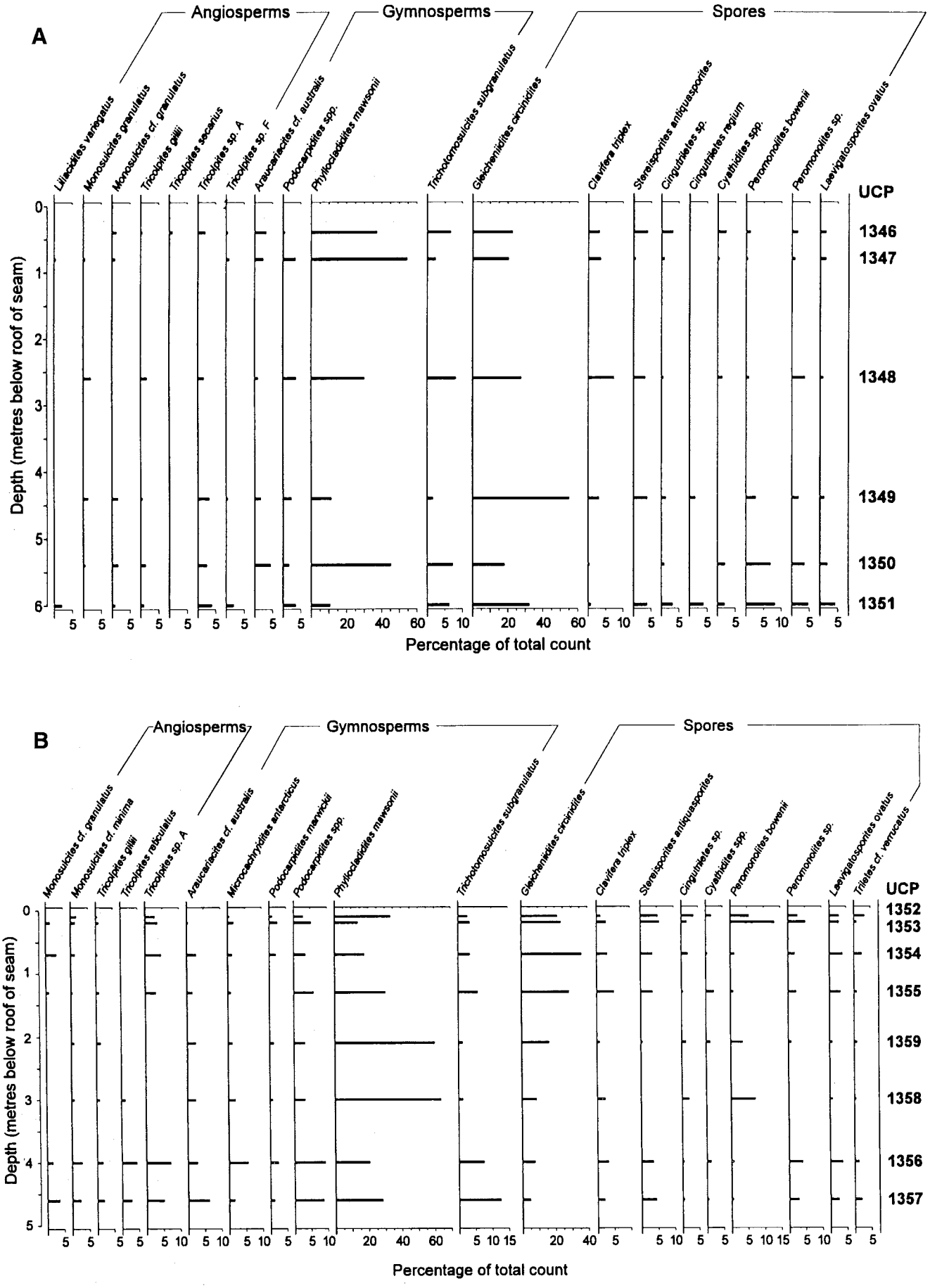

Fig. 6 Pollen diagrams indicating occurrences of abundant or significant taxa for locality ST-94 (A) and locality STM (B).

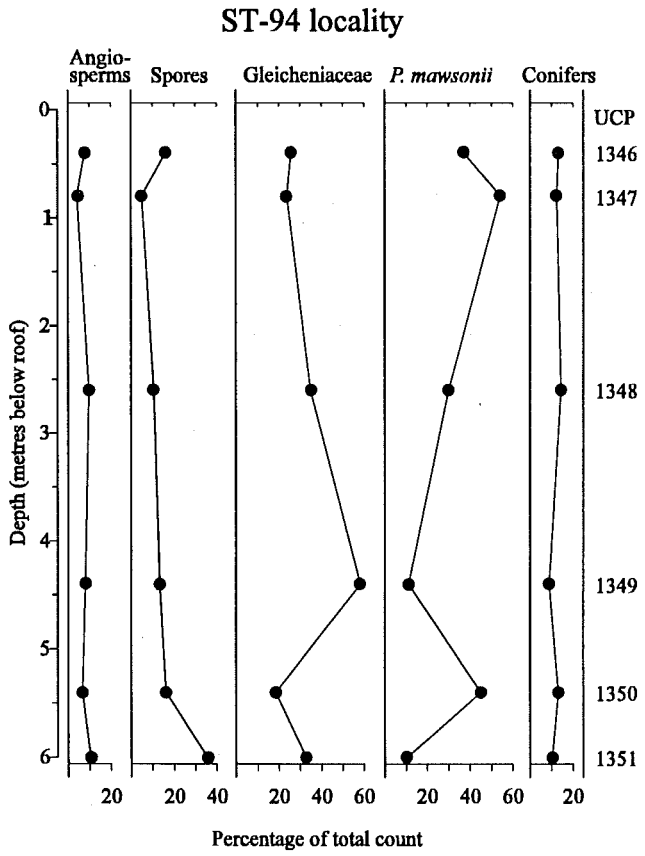

Fig. 7 Occurrence of major palynomorph groups, ST-94.

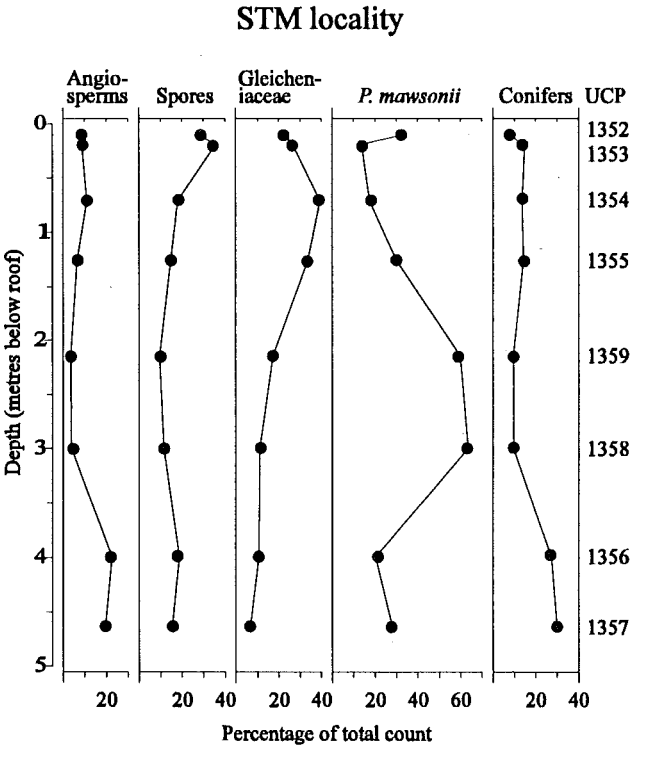

Fig. 8 Occurrence of major palynomorph groups, STM.

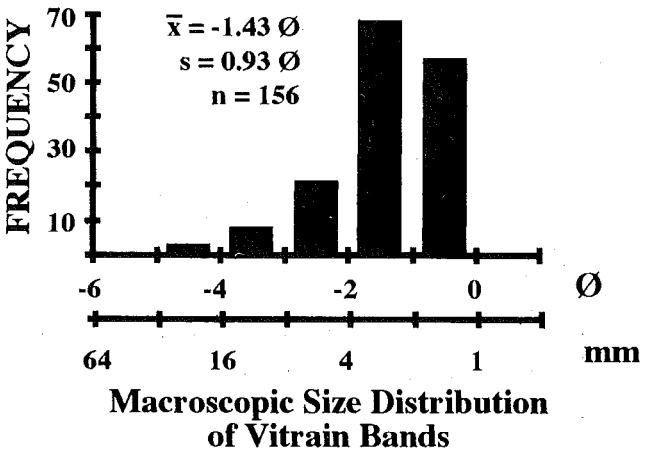

Fig. 9 Macroscopic size distribution of vitrain bands at section ST-94 (x = mean; s = standard deviation; n = number of measurements). Mean and standard deviation are calculated by methods of moments (Lewis 1984).

However, in the "D" seam, the distribution of vitrain band thickness extends significantly into the microscopic size fraction. To test this, further size measurements on microscopic plant material (i.e. <1 mm) would have to be performed, but that is beyond the scope of this paper.

Petrographic analysis

All vitrain samples collected from sections STM and ST-94 contain similar botanical structures. Cell wall structures were identified as xylem tracheids, and in most samples ray parenchyma was also recognised (Fig. 10A, B). This indicates that all the vitrain bands formed from secondary xylem tissue (i.e. wood) from either roots or stems. Only uniseriate ray structures were encountered, and there was a notable absence of any feature resembling vessel elements. Vessels, which are large vertical water-conducting tissue elements found in all but a small number of angiosperm genera, are absent from all gymnosperms except the gnetaleans (Esau 1965, p. 250). The presence of only uniseriate rays and the lack of vessels strongly indicate that vitrain bands in the "D" seam are of gymnosperm origin.

Petrographic analyses of blocks from the fine-grained matrix (i.e. attrital layers) of the "D" seam are given in Fig. 11 and 12. In the maceral group approximations for thickly banded coals (i.e. some samples from ST-94), proportions of matrix constituents were recalculated to incorporate macroscopic vitrain as vitrinite.

Although the small number of petrographic samples precluded detailed interpretations, some trends are worth noting. For example, the most significant difference is the upward decrease in well-preserved microscopic plant parts. Not only are the abundances lower at the top of the seam, but the cell walls of structured plant material appear less well preserved (Fig. 10C, D). The proportion of oxidised plant material (i.e. inertinite) also varies. In both the STM and ST-94 sections, the highest concentration of inertinite occurs in the upper portion of the seam. However, inertinite is generally higher in the ST-94 section. Most of this material is of "semifusinitic" reflectance (see Stach et al. 1982) and often occurs as fine particles (Fig. 10E, F).

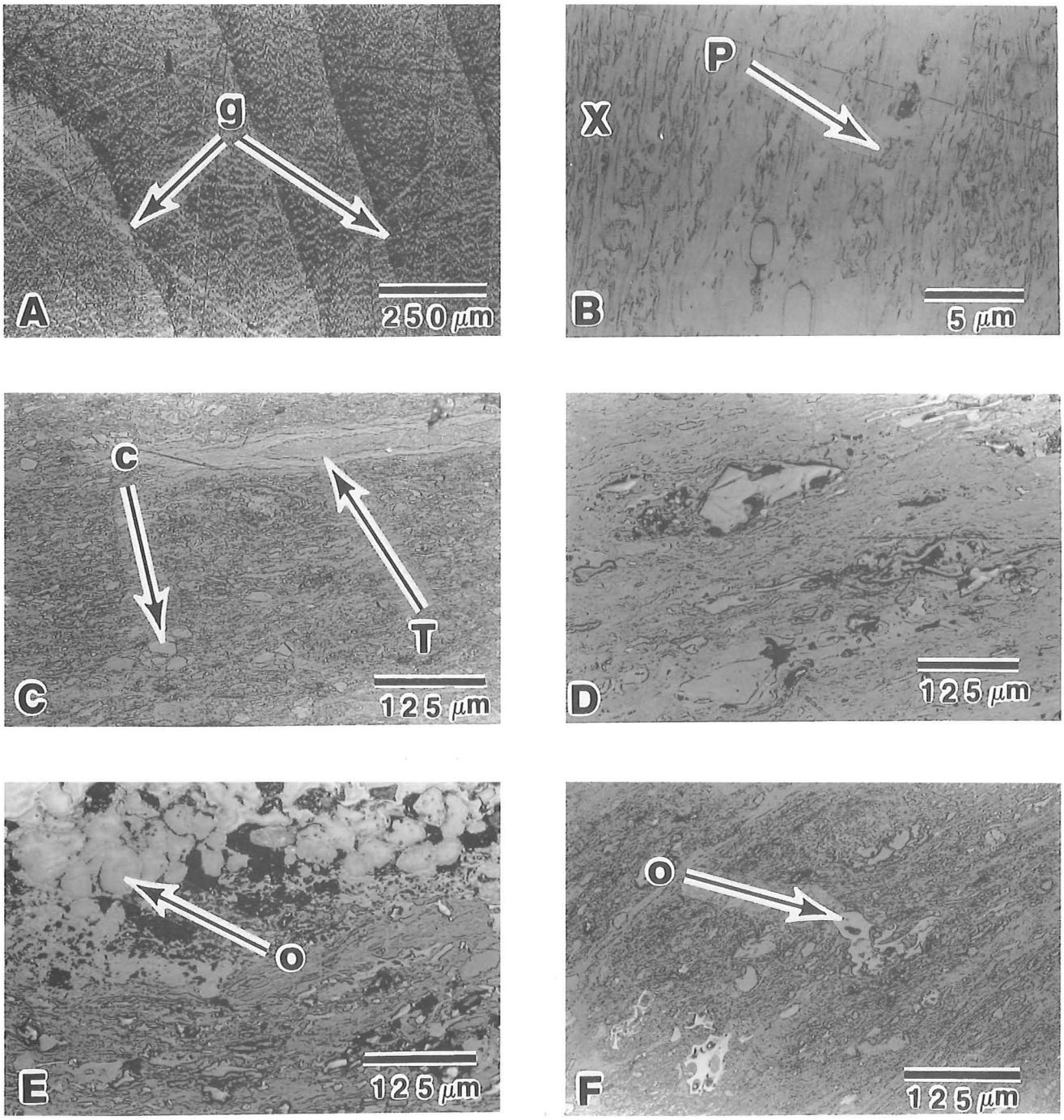

Fig. 10 Photomicrographs of botanical constituents in the "D" seam. **A**, Growth rings (g) in gymnosperm secondary xylem. Macroscopic manifestation is as a vitrain band. **B**, Vitrain band showing xylem tracheids (X) and uniseriate ray parenchyma (P), which indicate gymnosperm secondary xylem. **C**, Plant tissue (T) set in fine-grained matrix of amorphous gels, cell fillings (c), and fragments of cell walls. **D**, Fine-grained matrix, with lack of preserved plant parts. **E**, Oxidised plant cell fillings (o). **F**, Fragments of oxidised plant tissue (o) set in a matrix of fine-grained humic material. All photomicrographs were taken in white reflected light on a chemically etched surface.

DISCUSSION

Three significant variables described above shed light on the development and character of the "D" seam. These are the concentrations of the palynomorphs *Phyllocladidites mawsonii* and Gleicheniaceae, and the degree to which gymnosperm secondary xylem was preserved as vitrain bands. Palynomorph abundance provides insights into possible paleoecology of the mire, whereas the presence of gymnosperm secondary xylem can be used to make assertions about preservational/degradational chemistry of the paleomire. Each of these variables and their significance in interpreting the development of the "D" seam is discussed below.

Most of the palynological variation observed in this study can be attributed to two common forms, *P. mawsonii* and Gleicheniaceae (see Fig. 7, 8). As abundant palynomorphs

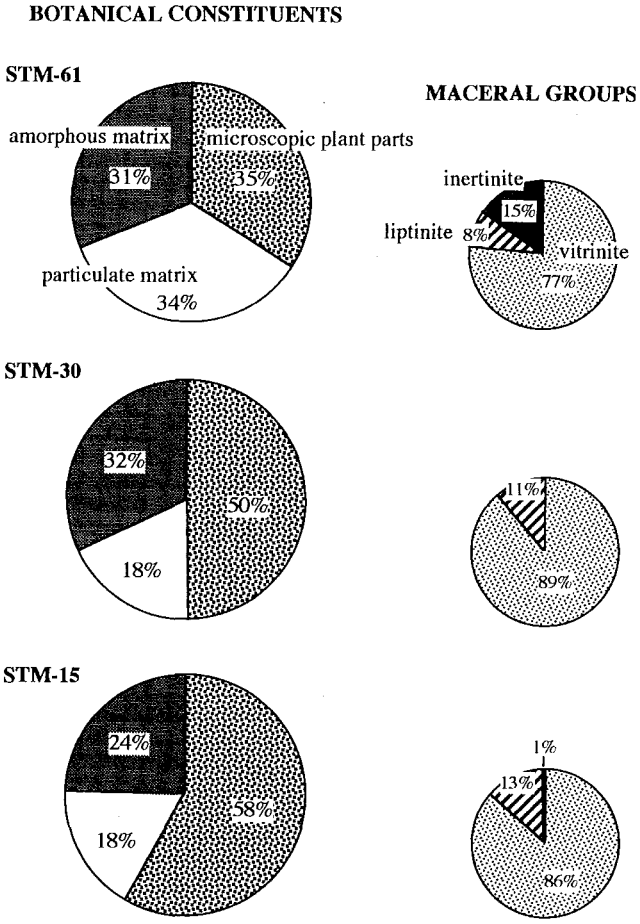

Fig. 11 Petrographic composition for samples from section STM.

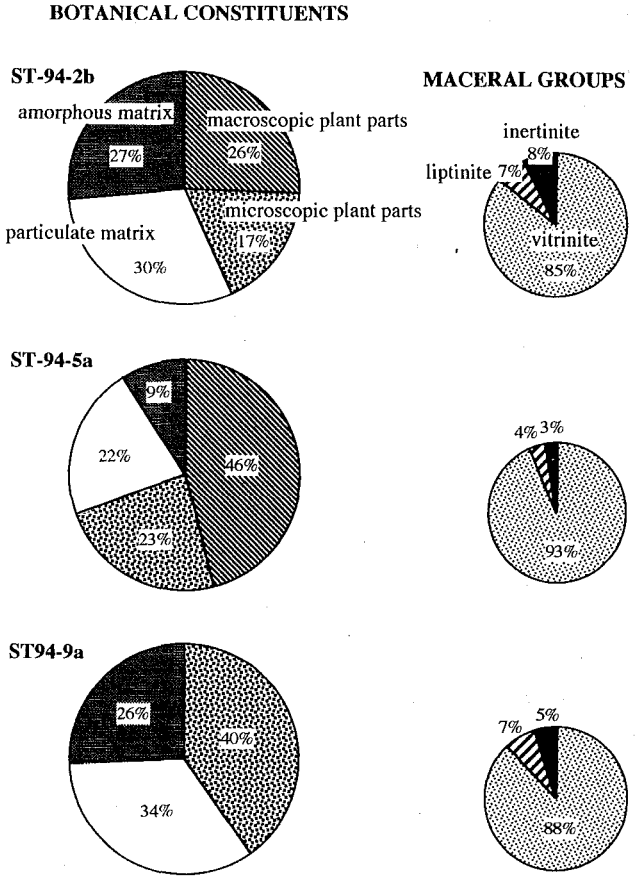

Fig. 12 Petrographic composition for samples from section ST-94.

can generally be regarded as representing plants growing at the site of deposition (Randall 1990), a brief consideration of the palynology and ecology of *P. mawsonii* and Gleicheniaceae is warranted to allow a useful interpretation of the "D" seam.

Phyllocladidites mawsonii is a common Southern Hemisphere Late Cretaceous and Tertiary palynomorph (e.g., Mildenhall 1980; Martin 1984; Kershaw 1988; Warnes 1992). Morphologically, *P. mawsonii* is distinctive owing to the presence of small proximal tubercles (Cookson 1947), and it is easily identified, even where the specimen is immature (e.g., Macphail et al. 1991; Gibson et al. 1991) or deformed. The lack of well-developed sacci (Cookson 1947) suggests a lower airborne transport potential than most other conifer pollen taxa (e.g., Luly et al. 1980). Water transport may be significant (MacPhail et al. 1993); however this is likely to be minimal within a poorly drained mire environment (Birks & Gordon 1985, p. 190). Thus, *P. mawsonii* is most likely to enter the fossil record at sites where the parent plant is growing, and decline rapidly away from these sites.

P. mawsonii has identical pollen morphology to the extant endemic Tasmanian podocarp species *Lagarostrobos franklinii* (Hook.f.) C.J. Quinn (Cookson 1953; Playford & Dettmann 1978). Macrofossil remains of *L. franklinii* have not been reported prior to the Pliocene–Pleistocene (Hill & Macphail 1985), though related material is known from Oligocene deposits (Wells & Hill 1989). It is therefore unlikely that *P. mawsonii* is taxonomically identical to *L. franklinii*, but the co-occurrence of unique pollen morphology would suggest strong botanical affinities.

L. franklinii (commonly known as the Huon Pine) generally grows within 10 m of river edges (Gibson et al. 1991), from which it disperses slowly. However, regular disturbance from flooding promotes vegetative reproduction, and *L. franklinii* may establish dominance over long time intervals (Gibson & Brown 1991). Larger stands (>200 ha) of Huon Pine include an area with an extensive reticulate drainage network (Gibson et al. 1991), and non-riparian stands in areas of high rainfall (2500 mm/yr) (Gibson 1988). The species has not been reported from mire (peat-forming) environments. *L. franklinii* has very low tolerance of fire, though a surviving seed source could easily enable a localised site to be recolonised (Gibson & Brown 1991). High abundances of *P. mawsonii* pollen can therefore be interpreted to indicate wet environments, though the water source may be either rivers or rainfall.

In contrast, spores of the Gleicheniaceae probably represent drier or at least better drained (i.e. absence of standing water) mire environments. Luly et al. (1980) correlated high abundance of *Gleichenia* spores with the development of a raised mire and drier swamp surfaces, and stated that *Gleichenia* spores are locally dispersed (i.e. within 100 m of the parent plant; Birks & Birks 1980, p. 252). However, the relationship between the abundance of the parent plant and the pollen count (see, e.g., Birks & Birks

1980, p. 196) is debatable. Luly et al. (1980, table 3) considered the genus is over-represented, whereas Macphail & McQueen (1983) reported that *Gleichenia* is under-represented in the Quaternary and Recent pollen record of New Zealand, despite being a common component of acid bog floras. Taxa with local dispersal of spores and pollen tend to exhibit high and irregular pollen counts (Janssen 1973), and the data from Macphail & McQueen (1983) are difficult to reconcile. Gleicheniaceae are clearly well represented in some samples reported in this study (e.g., UCP1349, 1354) and, although the parent plants must have been a significant component of the mire flora, the absolute abundance may be difficult to determine.

Extant *Gleichenia* in New Zealand is a rhizomatous fern with branching fronds, and it is ubiquitous on infertile wetlands (Wardle 1991, p. 322). *Gleichenia* inhabits a variety of ecological niches (Luly et al. 1980, table 4; Wardle 1991). In particular, it is common in New Zealand in the central areas of acidic swamps and bogs, away from drainage channels (Wardle 1991, p. 326), and is common on peat domes on the Chatham Islands (Wardle 1991, p. 442). In Australia, *Gleichenia* is commonly found in areas of moderate to high rainfall (>850 mm/yr), along streams, or in oligotrophic swampy areas with organic-rich substrates (Duncan & Isaac 1986; I. R. Sluiter pers. comm.). The genus is extremely tolerant of fire and may achieve temporary local dominance in burnt areas until competing species recover. Macrofossil Gleicheniaceae remains, with morphology strikingly similar to that of neighbouring extant material, are known from Late Cretaceous sediments in the Puponga Coalfield, northwest Nelson (Kennedy 1993; J. D. Lovis pers. comm.).

In comparison to the palynological assemblages, relatively little information is available on the origins and significance of vitrain banding in New Zealand coals. Banding in New Zealand coal seams has previously been ascribed to the occurrence of gymnosperms in the paleomire flora (Shearer & Moore 1994b). Because of the low chemical degradability of gymnosperm secondary xylem, Shearer & Moore (1994b) proposed that this tissue would be preferentially preserved over that of angiosperm secondary xylem in Cretaceous and Tertiary coal seams. To date, this inference has been supported by the virtually complete absence of angiosperm wood in coals that have been investigated, but insufficient palynological data have been available to determine whether band thickness and frequency relate primarily to floral assemblage or to mire chemistry.

INTERPRETATIONS OF VERTICAL SECTIONS

Application of the information implicit in the three key compositional variables discussed above (the abundances of the palynomorphs *Phyllocladidites mawsonii* and Gleicheniaceae as well as preservation of gymnosperm secondary xylem) aids in interpretation of the development of the "D" seam and sheds new insight into the controls of banding character in New Zealand coals, especially those of Cretaceous age.

Mire margin (STM) section

The STM section is located within 250 m of a "barren zone" (Fig. 3), where coal passes laterally into sediments at an inferred mire margin. The sediments have a lenticular geometry and are interpreted as an intra-mire channel which was contemporaneous with "D" seam peat accumulation. The basal interval of the STM section exhibits features consistent with a stream margin (riparian) location. For example, pollen of the angiosperm species *Tricolpites reticulatus* is common in the basal two samples (Fig. 6B). This form is referable to the extant genus *Gunnera*, an aquatic herb common near stream sides (Pocknall 1982). There is also a significant input from the regional conifer flora in these samples.

The dominance of *P. mawsonii* through the centre of the seam at this locality is interpreted to reflect competitive exclusion of other taxa, perhaps aided by the capacity for vegetative reproduction, rather than a major change in mire conditions. However, above UCP1359 (where the greatest development of vitrain bands occurs), the increasing dominance of Gleicheniaceae, and corresponding decline of *P. mawsonii*, suggests a change to drier and/or more acidic conditions.

Towards the top of the section, the replacement of Gleicheniacean spores by other spore taxa suggests a further change of mire regime (UCP1353). Other forms show little response until the final stage of peat accumulation (UCP1352), where *P. mawsonii* increases at the expense of other conifers and all spore taxa. These floral changes may reflect a return to disturbed (i.e. flooded) riparian conditions immediately before the death of the mire.

Petrographic analysis of the fine-grained matrix provides some supporting evidence for changes in the ecology of the mire margin (STM) section. The fine-grained matrix samples indicate that the basal layers of the section (STM 15 and 30, Fig. 11) were relatively water saturated and anaerobic (i.e. no significant accumulation of oxidised tissue or fragments). In contrast, in the upper portion of the section, just above where gymnosperm abundance begins to decrease, the fine-grained matrix is filled with abundant oxidised tissues and fragments. This observation corroborates the interpretation based on increased Gleicheniaceae abundance that the mire became drier or at least better drained in this interval. However, the uppermost interval (STM 77) has virtually no oxidised material, which supports palynological evidence for a brief return to wetter, less aerobic conditions.

Mire centre (ST-94) section

The overall floral development of the mire centre (ST-94) locality contrasts with that of the mire margin section. The initial peat-accumulating environment appears to have been dominated by spore-producing plants, though spore abundance may have resulted partly from water transport into the depositional site. *P. mawsonii* may be uncommon at the base of the section because of insufficient time to colonise from the mire margins. Slightly elevated inertinite levels at the floor and roof may reflect fire influences or water transport of oxidised material into the mire.

Toward the centre of the seam at the ST-94 section, the coal is dominated by Gleicheniaceae spores, indicating a drier or well-drained (absence of standing water) peat environment. Steadily increasing *P. mawsonii* abundance above UCP1349 suggests a gradual return to wetter conditions at this site. Vitrain bands, which suggest persistent acidity, are thickest and most abundant in the central portion of the seam, despite the change in flora through this interval. Maximum vitrain banding is not coincident with the

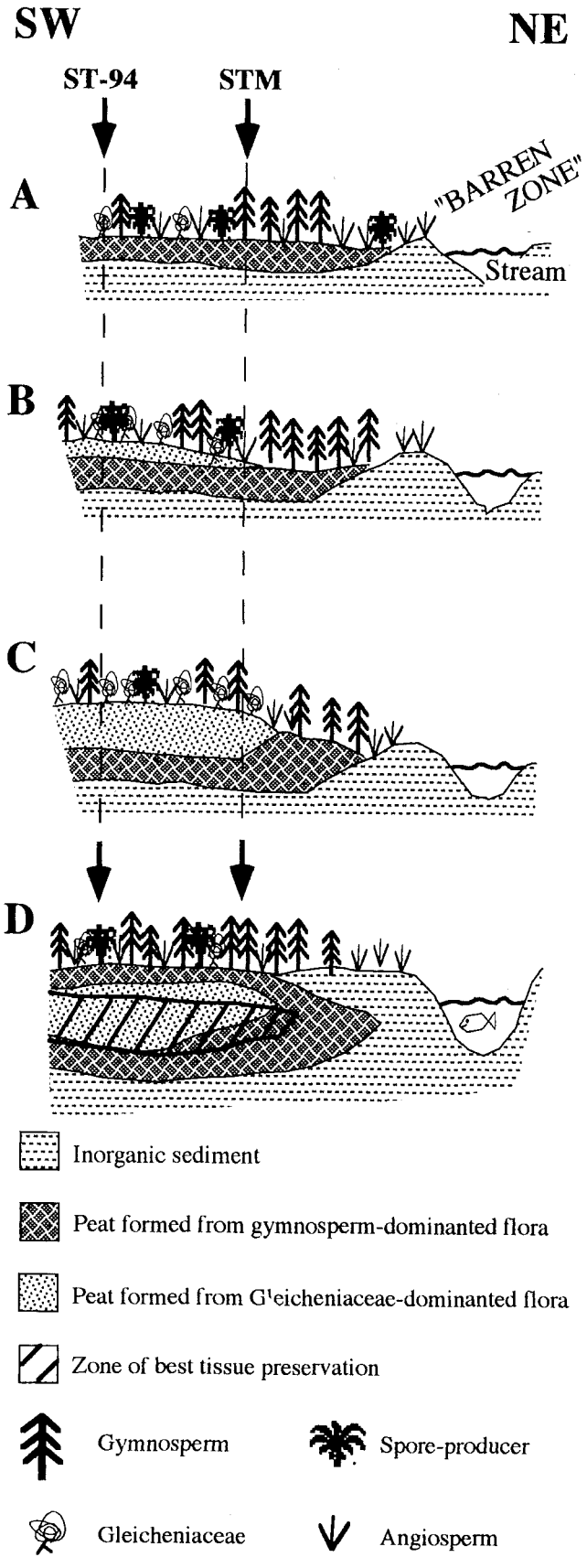

Fig. 13 Model for the development of the "D" seam (see text for explanation).

maximum abundance of either *P. mawsonii* or Gleicheniaceae. Low inertinite in the seam centre may also reflect increased acidity, and indicates that fire was not a significant factor in the mire ecology.

MODEL FOR "D" SEAM DEVELOPMENT

Combination of the palynological and petrographic data from the two sections, as well as seam thickness information (Fig. 3), allows a generalised model to be proposed for the development of the "D" seam (Fig. 13). In this model, the "barren zone" is assumed to represent a vertically aggrading fluvial channel system contemporaneous with the "D" paleomire. This model is preliminary, and more data localities and analyses are needed for confirmation.

Early peat accumulation was characterised by a dominant *Phyllocladidites mawsonii* (i.e. conifer) flora across the mire area (Fig. 13A). This phase of peat development was probably groundwater controlled (i.e. rheotrophic), as are similar environments in modern peatlands (Moore 1987). Continued peat accumulation resulted in a change of flora from *P. mawsonii* to Gleicheniaceae in the mire centre and eventually at the mire margin. This environment was better drained though still water saturated, as the water table must have been near the surface to prevent the peat from oxidising. Near-surface water tables in modern mires are maintained through precipitation (i.e. ombrotrophic), and these systems form mires with a topographically raised or domed surface (Anderson 1983). Therefore, Gleicheniaceae dominance may be coincident with the "D" paleomire developing from a groundwater, rheotrophic stage into a rain-fed, ombrotrophic peat-forming system (Fig. 13B), in which the lower pH enhanced the preservation of gymnosperm wood. The subsequent return to wetter conditions in the mire centre may reflect formation of a poorly drained central plateau (Fig. 13C) (see Sjörs 1983; Zoltai & Pollett 1983 for modern examples). The cause of mire termination is problematic; however, mire vegetation indicates a brief return to a riparian and probably rheotrophic mire environment, suggesting a rising water table, before the termination of peat accumulation by deposition of inorganic sediments (Fig. 13D).

IMPLICATIONS FOR CONTROLS ON VITRAIN BANDING

The major goal of this paper is to determine if there was a floral control on banding character in the Cretaceous "D" seam. The data presented suggest that there is no direct correlation between paleoflora and vitrain band frequency and thickness. We conclude, however, that if gymnosperms (conifers) are present in the paleomire flora, even in small amounts, only their secondary xylem tissue will be preserved as vitrain bands.

The vertical and lateral controls on abundances of vitrain bands may be related to local hydrologic and/or chemical environments within the paleomire. In this study, vitrain preservation coincides with the inferred development of an ombrotrophic mire. The higher acidity of these types of mires (Ingram 1983, p. 71) would reduce microbial degradation and favour preservation of plant material. Therefore, a high frequency of vitrain bands in the Cretaceous "D" seam indicates a period of low degradation related to an increase in acidity resulting from change of mire type.

The mire margin of the "D" seam is less banded than the more central regions, perhaps because of the continuous presence of oxygenated water. This is in contrast to the model proposed by Crosdale (1993) and Edbrooke et al. (1994) for Tertiary New Zealand coals, which suggests that the highest abundance of wood (i.e. vitrain banding) should occur at the margin of the deposit. The model for Tertiary coals is based largely on botanical and petrographic studies conducted on the domed, ombrogenous mires present in the Indo-Malesian Archipelago (Anderson 1964; Esterle et al. 1989; Brunig 1990; Moore & Hilbert 1992; Dehmer 1993) and on other models of overseas coal seams (Esterle & Ferm 1986; Warwick & Stanton 1988). Floral and climatic differences between the "D" seam depositional site and the locations used for the models mentioned above are the likely sources of divergence, and the preliminary results of this study suggest that caution should be exercised in extrapolating models of Holocene mires and Tertiary coals to Cretaceous deposits.

CONCLUSIONS

A combination of analytical techniques has permitted the "D" seam of the Strongman mine to be characterised from two localities, and controls on development to be assessed. Specifically, pollen analysis has allowed the floral development to be reconstructed, and botanical analysis of macroscopic and microscopic organic components has revealed characteristics of the original peat-forming environment. Integration of the palynological and botanical analysis has lead to an understanding of the controls on vitrain band occurrence in the "D" seam, which may have implications for the interpretation of other New Zealand coal seams.

Floral differences between samples and sections may be best explained by analogy to the ecology of the extant equivalents of the key pollen taxa, *Phyllocladidites mawsonii* and Gleicheniaceae. *P. mawsonii* is indicative of wet sites, whereas Gleicheniaceae suggest drier, acidic mire settings. Within each of the two studied sections, vertical floral trends reflect a change from rheotrophic to ombrotrophic mire conditions. This change occurs rapidly in the mire centre and more gradually at the mire margin. Mire termination was preceded by a return to rheotrophic conditions and riparian ecology.

Vitrain preservation (banding) within the seam is greater in the central sample site than at the margin, and is associated with the development of ombrotrophic conditions. All preserved vitrain is of gymnosperm origin. Because there is no direct correlation between banding abundance or thickness and the gymnosperm proportion in the palynoflora, inherent resistance to decay does not appear to have been the primary influence on preservation of the gymnosperm wood. Rather, the "D" seam study indicates that mire acidity was the key control on vitrain preservation. Less banding at the mire margin reflects the lower preservation ability of a riparian setting, which is continually influenced by oxygenated water.

ACKNOWLEDGMENTS

We are indebted to Coal Corporation of New Zealand Ltd. for permission to collect samples from the Strongman mine, and to G. Duncan (Mine Manager) and F. Taylor (formerly Mine Surveyor) for their assistance. J. D. Lovis (Plant and Microbial Sciences Department, University of Canterbury) and T. W. Matheson and A. H. Clemmens (Coal Research Limited) are thanked for their comments on earlier versions of the manuscript, and we thank I. R. Sluiter (Department of Conservation and Natural Resources, Victoria, Australia) for his thorough review. This project was partially supported by a grant from the Foundation for Research, Science and Technology.

REFERENCES

Anderson, J. A. R. 1964: The structure and development of the peat swamps of Sarawak and Brunei. *Journal of tropical geography 18*: 7–16.

Anderson, J. A. R. 1983: The tropical peat swamps of western Malesia. *In*: Gore, A. J. P. *ed.* Mires: swamp, bog, fen and moor. Ecosystems of the world 4B. Amsterdam, Elsevier. Pp. 181–199.

Anderson, K. B.; Mackay, G. 1990: A review and reinterpretation of evidence concerning the origin of Victorian brown coal. *International journal of coal geology 16*: 327–347.

Bal, A. A. 1994: Disparate hydrocarbon potential and maturation profiles of Pakawau Group source coals: implications for Taranaki Basin exploration. 1994 Petroleum Conference proceedings. Wellington, Energy and Resources Division, Ministry of Commerce. Pp. 332–337.

Benedict, L. G.; Thompson, R. R.; Shigo III, J. J.; Aikman, P. R. 1968: Pseudovitrinite in Appalachian coking coal. *Fuel 47*: 125–143.

Birks, H. J. B.; Birks, H. H. 1980: Quaternary palaeoecology. London, Edward Arnold. 289 p.

Birks, H. J. B.; Gordon, A. D. 1985: Numerical methods in Quaternary pollen analysis. London, Academic Press. 317 p.

Brunig, E. F. 1990: Oligotrophic forested wetlands in Borneo. *In*: Lugo, A. E.; Brinson, M.; Brown, S. *ed.* Forested wetlands. Ecosystems of the world Vol. 15. Amsterdam, Elsevier. Pp. 299–344.

Cecil, C. B.; Stanton, R. W.; Neuzil, S. G.; Dulong, F. T.; Ruppert, L. F.; Pierce, B. S. 1985: Paleoclimate controls on late Paleozoic sedimentation and peat formation in the central Appalachian Basin (U.S.A.). *International journal of coal geology 5*: 195–230.

Cookson, I. C. 1947: Plant microfossils from the lignites of the Kerguelen Archipelago. *British, Australian and New Zealand Antarctic Research Expedition 1929–1931 reports, series A, vol. 2, pt. 8*: 127–142.

Cookson, I. C. 1953: The identification of the sporomorph *Phyllocladidites* with *Dacrydium* and its distribution in southern Tertiary deposits. *Australian journal of botany 1*: 64–70.

Couper, R. A. 1953: Upper Mesozoic and Cainozoic spores and pollen grains from New Zealand. *New Zealand Geological Survey paleontological bulletin 22*: 77 p.

Couper, R. A. 1960: New Zealand Mesozoic and Cainozoic plant microfossils. *New Zealand Geological Survey paleontological bulletin 32*: 87 p.

Crosdale, P. J. 1993: Coal maceral ratios as indicators of environment of deposition: do they work for ombrogenous mires? An example from the Miocene of New Zealand. *Organic geochemistry 20*: 797–809.

Dehmer, J. 1993: Petrology and organic geochemistry of peat samples from a raised bog in Kalimantan (Borneo). *Organic geochemistry 20*: 349–362.

Dettmann, M. E.; Playford, G. 1968: Taxonomy of some Cretaceous spores and pollen grains from eastern Australia. *Proceedings of the Royal Society of Victoria 81*: 69–94.

Duncan, B. D.; Isaac, G. 1986: Ferns and allied plants of Victoria, Tasmania and South Australia. Melbourne, Melbourne University Press. Pp. 67–73.

Edbrooke, S. W.; Sykes, R.; Pocknall, D. T. 1994: The geology of the Waikato Coal Measures, Waikato coal region, New Zealand. *Institute of Geological & Nuclear Sciences monograph 6*: 236 p.

Esau, K. 1965: Plant anatomy. 2nd ed. New York, Wiley. 767 p.

Esterle, J. S.; Ferm, J. C. 1986: Relationship between petrographic and chemical properties and coal seam geometry, Hance seam, Breathitt Formation, southeast Kentucky. *International journal of coal geology 6*: 199–214.

Esterle, J. S.; Ferm, J. C.; Yiu-Liong, T. 1989: A test for the analogy of tropical domed peat deposits to "dulling up" sequences in coal beds—preliminary results. *Organic geochemistry 14*: 333–342.

Esterle, J. S.; Moore, T. A.; Hower, J. C. 1991: A reflected-light petrographic technique for peats. *Journal of sedimentary petrology 61*: 615–616.

Esterle, J. S.; Moore, T. A.; Shearer, J. C. 1992: Comparison of macroscopic and microscopic size analyses of organic components in both coal and peat. *26th Newcastle Symposium: Advances in the study of the Sydney Basin, Newcastle, N.S.W., Australia, April 3–5, 1992*. Pp. 143–149.

Gage, M. 1952: The Greymouth coalfield. *New Zealand Geological Survey bulletin 45*: 232 p.

Gibson, N. 1988: A description of the Huon Pine (*Lagarostrobos franklinii* (Hook. F.) C.J. Quinn) forests of the Prince of Wales and King Billy Ranges. *Papers and proceedings of the Royal Society of Tasmania 122*: 127–133.

Gibson, N.; Brown, M. J. 1991: The ecology of *Lagarostrobos franklinii* (Hook. f.) Quinn (Podocarpaceae) in Tasmania. 2. Population structure and spatial pattern. *Australian journal of ecology 16*: 223–229.

Gibson, N.; Davies, J.; Brown, M. J. 1991: The ecology of *Lagarostrobos franklinii* (Hook. f.) Quinn (Podocarpaceae) in Tasmania. 1. Distribution, floristics and environmental correlates. *Australian journal of ecology 16*: 215–222.

Hagemann, H. W.; Wolf, M. 1987: New interpretations of the facies of the Rhenish brown coal of West Germany. *International journal of coal geology 7*: 337–348.

Hill, R. S.; Macphail, M. K. 1985: A fossil flora from rafted Plio-Pleistocene mudstones at Regatta Point, Tasmania. *Australian journal of botany 33*: 497–517.

Ingram, H. A. P. 1983: Hydrology. *In*: Gore, A. J. P. *ed.* Mires: swamps, bog, fen and moor. Ecosystems of the world 4A. Amsterdam, Elsevier. Pp. 67–158.

International Committee for Coal Petrology (ICCP) 1971: International handbook of coal petrology—supplement to the second edition. Paris, Centre National de la Recherche Scientifique. Unpaginated.

Janssen, C. R. 1973: Local and regional pollen distribution. *In*: Birks, H. J. B.; West, R. G. *ed.* Quaternary plant ecology. New York, John Wiley and Sons. Pp. 31–42.

Johnson, K. R.; Greenwood, D. 1993: High-latitude deciduous forests and the Cretaceous–Tertiary boundary in New Zealand. *Geological Society of America abstracts with programs 25 (6)*: 295.

Kennedy, E. M. 1993: Palaeoenvironment of an Haumurian plant fossil locality within the Pakawau Group, north west Nelson, New Zealand. Unpublished M.Sc. thesis, lodged in the Library, University of Canterbury, Christchurch. 201 p.

Kershaw, A. P. 1988: Australasia. *In*: Huntly, B.; Webb, T. (III) *ed.* Vegetation history. Handbook of vegetation science, part 7. Dordrecht, Kluwer Academic Publishers. Pp. 237–306.

Laird, M. G. 1993: Cretaceous continental rifts: New Zealand region. *In*: Ballance, P. F. *ed.* South Pacific sedimentary basins. *Sedimentary basins of the world 2*: 27–49.

Lewis, D. W. 1984: Practical sedimentology. Stroudsburg, Pennsylvania, Hutchinson Ross. 229 p.

Luly, J.; Sluiter, I. R.; Kershaw, A. P. 1980: Pollen studies of Tertiary brown coals: preliminary analyses of lithotypes within the Latrobe Valley, Victoria. *Monash publications in geography 23*: 77 p.

McCabe, P. J. 1984: Depositional environments of coal and coal-bearing strata. *In*: Rahmani, R. A.; Flores, R. M. *ed.* Sedimentology of coal and coal-bearing sequences. *International Association of Sedimentologists special publication 7*: 13–42.

Macphail, M. K.; McQueen, D. R. 1983: The value of New Zealand pollen and spores as indicators of Cenozoic vegetation and climates. *Tuatara 26*: 37–59.

Macphail, M. K.; Hill, R. S.; Forsyth, S. M.; Wells, P. M. 1991: A Late Oligocene – Early Miocene cool climate flora in Tasmania. *Alcheringa 15*: 87–106.

Macphail, M. K.; Jordan, G. J.; Hill, R. S. 1993: Key periods in the evolution of the flora and vegetation in Western Tasmania I. The early – middle Pleistocene. *Australian journal of botany 41*: 673–707.

Martin, H. A. 1984: The use of quantitative relationships and paleoecology in stratigraphic palynology of the Murray Basin in New South Wales. *Alcheringa 8*: 253–272.

Mildenhall, D. C. 1980: New Zealand Late Cretaceous and Cenozoic plant biogeography; a contribution. *Palaeogeography, palaeoclimatology, palaeoecology 31*: 197–233.

Moore, P. D. 1987: Ecological and hydrological aspects of peat formation. *In*: Scott, A. C. *ed.* Coal and coal-bearing strata: recent advances. *Geological Society special publication 32*: 7–15.

Moore, T. A. 1990: An alternative method for sampling and petrographically characterizing an Eocene coal bed, southeast Kalimantan, Indonesia. Unpublished thesis, lodged in the Library, University of Kentucky, Lexington. 240 p.

Moore, T. A.; Ferm, J. C. 1992: Composition and grain-size of an Eocene coal bed in southeastern Kalimantan, Indonesia. *International journal of coal geology 21*: 1–30.

Moore, T. A.; Hilbert, R. E. 1992: Petrographic and anatomical characteristics of plant material from two peat deposits of Holocene and Miocene age, Kalimantan, Indonesia. *Review of palaeobotany and palynology 72*: 199–227.

Moore, T. A.; Stanton, R. W. 1985: Coal petrographic laboratory procedures and safety manual. *United States Geological Survey open-file report 85–20*: 68 p.

Moore, T. A.; Shearer, J. C.; Esterle, J. S. 1993: Quantitative macroscopic textural analysis. *The Society for Organic Petrology newsletter 9 (4)*: 13–16.

Nathan, S. 1978: Sheet S44—Greymouth. Geological map of New Zealand 1:63 360. Wellington, Department of Scientific and Industrial Research.

Newman, J.; Newman, N. A. 1988: Oxidative etching of high rank New Zealand coals. *Geological Society of New Zealand miscellaneous publication 41a*: 110.

Newman, J.; Newman, N. A. 1992: Tectonic and paleo-environmental controls on the distribution and properties of Upper Cretaceous coals on the West Coast of the South Island, New Zealand. *In*: McCabe, P. J.; Parrish, J. T. *ed.* Controls on the distribution and quality of Cretaceous coals. *Geological Society of America special paper 267*: 347–368.

Playford, G.; Dettmann, M. E. 1978: Pollen of *Dacrydium franklinii* Hook. F. and comparable early Tertiary microfossils. *Pollen et spores 20*: 513–534.

Pocknall, D. T. 1982: Palynology of late Oligocene Pomahaka Estuarine Bed sediments, Waikoikoi, Southland, New Zealand. *New Zealand journal of botany 20*: 263–287.

Pocknall, D. T.; Tremain, R. *comp.* 1988: Tour LB1, 7th International Palynological Conference, Brisbane, Australia, August 1988; New Zealand palynology and paleobotany. *New Zealand Geological Survey record 33*: 107 p.

Quick, J. C.; Moore, T. A. 1991: Microscopic analysis of some bituminous New Zealand coals: methods, uses and limitations. *Proceedings of the 4th New Zealand Coal Conference, Wellington, New Zealand, Coal Research Association of New Zealand.* Pp. 286–300.

Raine, J. I. 1984: Outline of a palynological zonation of Cretaceous to Paleogene terrestrial sediments in the West Coast region, South Island, New Zealand. *New Zealand Geological Survey report NZGS 109*: 82 p.

Randall, P. M. 1990: A study of modern pollen deposition, Southern Alps, South Island, New Zealand. *Review of palaeobotany and palynology 64*: 263–272.

Shearer, J. C.; Moore, T. A. 1994a: Grain-size and botanical analysis of two coal beds from the South Island of New Zealand. *Review of palaeobotany and palynology 80*: 85–114.

Shearer, J. C.; Moore, T. A. 1994b: Botanical control on banding character in two New Zealand coal beds. *Palaeogeography, palaeoclimatology, palaeoecology 110*: 11–28.

Sherwood, A. M.; Lindqvist, J. K.; Newman, J.; Sykes, R. 1992: Depositional controls on Cretaceous coals and coal measures in New Zealand. *In*: McCabe, P. J.; Parrish, J. T. *ed.* Controls on the distribution and quality of Cretaceous coals. *Geological Society of America special paper 267*: 347–368.

Sjörs, H. 1983: Mires of Sweden. *In*: Gore, A. J. P. *ed.* Mires: swamps, bog, fen and moor. Ecosystems of the world 4B. Amsterdam, Elsevier. Pp. 69–94.

Stach, E.; Machowsky, M-Th.; Teichmüller, M.; Taylor, G. H.; Chandra, D.; Teichmüller, R. 1982: Stach's textbook of coal petrology. 3rd ed. Berlin, Gebrüder Borntraeger. 535 p.

Stopes, M. C. 1919: On the four visible ingredients in banded bituminous coal. *Proceeding of the Royal Society part B 90*: 470–487.

Teichmüller, M. 1958: Rekonstruktionen verschiedener Moortypen des Hauptflözes der niederrheinischen Braunkohle. *Fortschritter in der Geologie von Rheinland und Westfalen 2*: 721 p.

Thiessen, R. 1937: Classification of coal from the viewpoint of a paleobotanist. *Transactions of the American Institute of Mining and Metallurgical Engineers 88*: 419–437.

Thorburn, D. F. 1981: Geology of the Strongman State Coalmine and environs, Greymouth coalfield, New Zealand. Unpublished report, Mines Division, Ministry of Energy. 17 p.

Traverse, A. 1988: Paleopalynology. Boston, Unwin Hyman. 600 p.

Wardle, P. 1991: Vegetation of New Zealand. Cambridge, Cambridge University Press. 672 p.

Warnes, M. D. 1992: Interpretations of coal forming vegetation of the Morley Coal Measures, Ohai coalfield. *Geological Society of New Zealand miscellaneous publication 63a*: 158.

Warwick, P. D.; Stanton, R. W. 1988: Depositional models for two Tertiary coal-bearing sequences in the Powder River Basin, Wyoming, USA. *Journal of the Geological Society London 145*: 613–620.

Wells, P. M.; Hill, R. S. 1989: Fossil imbricate-leaved Podocarpaceae from Tertiary sediments in Tasmania. *Australian systematic botany 2*: 387–423.

Zoltai, S. C.; Pollett, F. C. 1983: Wetlands in Canada: their classification, distribution and use. *In*: Gore, A. J. P. *ed.* Mires: swamps, bog, fen and moor. Ecosystems of the world 4B. Amsterdam, Elsevier. Pp. 245–268.

Appendix 1 Pollen count data.

	ST-94 locality						STM locality							
Sample (UCP number)	1346	1347	1348	1349	1350	1351	1352	1353	1354	1355	1356	1357	1358	1359
Total count	256	260	246	256	248	258	251	252	256	255	251	255	250	250
Depth (metres below roof)	0.43	0.93	2.62	4.42	5.30	6.00	0.03	0.18	0.70	1.26	4.00	4.64	3.00	2.14
Angiosperms														
Liliacidites variegatus	0	1	0	0	0	5	0	0	0	0	0	0	0	0
Monosulcites granulatus	0	1	5	3	1	0	3	1	0	0	1	0	0	0
Monosulcites cf. *granulatus*	3	2	0	4	4	2	0	3	8	2	4	9	0	0
Monosulcites cf. *minima*	1	0	4	1	1	0	4	3	3	1	7	6	2	2
Monosulcites sp. H	0	1	0	0	0	0	0	0	0	0	0	0	0	1
Tricolpites cf. *pachyexinus*	0	0	3	0	0	0	0	0	0	0	1	0	0	0
Tricolpites gillii	1	0	4	1	3	2	1	2	1	2	4	5	2	3
Tricolpites lilliei	0	0	0	0	0	0	0	1	0	0	1	0	1	0
Tricolpites reticulatus	1	0	0	1	0	0	0	0	0	0	11	7	3	0
Tricolpites secarius	2	0	0	0	0	0	0	0	0	0	0	0	0	0
Tricolpites sp. A	5	0	4	8	6	10	7	9	12	8	18	13	0	0
Tricolpites sp. B	1	0	0	0	0	0	0	0	0	1	0	0	0	0
Tricolpites sp. C	1	1	0	0	0	0	0	0	0	0	0	0	0	0
Tricolpites sp. D	0	0	0	0	0	0	3	0	0	0	0	0	0	1
Tricolpites sp. E	0	0	0	0	0	0	0	0	1	0	2	4	0	0
Tricolpites sp. F	1	2	0	1	0	5	3	1	3	0	4	3	0	0
Nothofagidites kaitangataensis	1	1	1	0	0	0	0	2	1	1	1	0	0	0
Rhoipites spp.	0	1	3	0	2	0	1	0	0	0	3	0	0	2
Tricolporites sp.	0	1	0	0	0	1	0	0	0	0	0	0	0	0
Proteacidites amolosexinus	0	0	0	0	0	1	0	0	0	0	0	0	0	0
Proteacidites scaboratus	2	0	0	2	0	1	1	0	0	1	0	1	2	0
Proteacidites sp.	0	0	0	0	0	0	0	0	0	0	0	2	0	0
Triorites minisculus	0	0	0	0	0	0	0	0	0	1	0	0	0	0
Unidentified inaperturate	1	0	0	0	0	0	0	0	0	0	0	0	0	0
Gymnosperms														
Araucariacites cf. *australis*	8	6	2	4	11	0	0	1	7	4	7	16	6	6
Microcachryidites antarcticus	2	3	3	2	0	1	1	4	3	2	14	4	5	3
Podocarpidites cf. *ellipticus*	2	2	0	4	0	0	0	2	1	1	0	0	0	0
Podocarpidites major	0	1	2	0	0	1	0	3	0	0	0	0	0	1
Podocarpidites marwickii	2	6	0	3	0	0	2	6	5	0	6	3	2	3
Podocarpidites spp.	1	9	9	6	4	9	7	13	9	15	23	22	8	8
Phyllocladidites mawsonii	95	141	74	29	112	27	84	35	45	77	51	72	159	150
Phyllocladidites paleogenicus	2	0	0	0	0	0	0	0	1	0	0	0	0	0
Trichotomosulcites subgranulatus	17	6	20	4	18	16	7	9	9	15	19	32	3	3
Spores														
Gleicheniidites circinidites	58	53	68	141	45	83	54	60	93	73	19	12	22	41
Clavifera triplex	8	9	18	8	1	2	3	7	8	13	8	5	6	2
Stereisporites antiquasporites	10	1	8	10	0	10	13	14	9	9	9	11	0	1
Cingutriletes sp.	8	2	1	3	2	8	9	4	5	1	1	1	5	3
Cingutriletes regium	0	0	0	4	0	10	0	3	2	1	0	0	2	0
Osmundacidites wellmanii	1	0	0	0	0	0	2	3	3	0	0	1	0	0
Cyathidites spp.	6	1	3	0	5	5	4	0	1	6	3	1	0	3
Peromonolites bowenii	3	1	2	7	17	21	14	33	3	2	2	1	18	9
Peromonolites sp.	4	2	9	5	9	12	7	13	5	6	10	7	0	2
Laevigatosporites ovatus	4	4	2	3	5	11	7	7	10	8	9	6	2	2
Laevigatosporites major	0	1	1	2	0	2	5	1	1	0	3	0	0	1
Trilites morleyi	4	0	0	0	1	3	0	6	0	1	1	1	0	1
Trilites cf. *verrucatus*	0	1	0	0	0	5	8	2	6	2	3	5	1	2
Trilites microfoveolatus	0	0	0	0	0	1	0	0	0	0	0	0	0	0
Trilites tuberculiformis	0	0	0	0	0	0	0	1	0	0	0	0	1	0
Trilites sp. A	0	0	0	0	0	3	1	0	0	0	0	0	0	0
Trilites sp. B	0	0	0	0	0	0	0	0	0	0	0	4	0	0
Baculatisporites sp.	0	0	0	0	0	0	0	3	1	2	4	1	0	0
Monosulcites sp.	0	0	0	0	1	1	0	0	0	0	2	0	0	0
Lycopodium (fast.-vol. group)	1	0	0	0	0	0	0	0	0	0	0	0	0	0
Totals (%)														
Angiosperms	7.8	4.2	9.8	8.2	6.9	10.5	9.2	8.7	11.3	6.7	22.7	19.6	4.0	3.6
Spores (not Gleicheniaceae)	16.0	5.0	10.6	13.3	16.1	35.7	27.9	35.7	18.0	14.9	18.7	15.3	11.6	9.6
Gleicheniaceae	25.8	23.8	35.0	58.2	18.5	32.9	22.7	26.6	39.5	33.7	10.8	6.7	11.2	17.2
P. mawsonii	37.1	54.2	30.1	11.3	45.2	10.5	33.5	13.9	17.6	30.2	20.3	28.2	63.6	60.0
Conifers (not *P. mawsonii*)	13.3	12.7	14.6	9.0	13.3	10.5	6.8	15.1	13.7	14.5	27.5	30.2	9.6	9.6

Application of Lithostratigraphic and Chronostratigraphic analysis to Seam Modelling in the Rapahoe Sector, western Greymouth Coalfield

by

S Ward

Department of Geological Sciences
University of Canterbury

Proceedings, The Australasian Institute of Mining and Metallurgy

New Zealand Branch 29th Annual Conference, Greymouth, August 1996

ABSTRACT

Seam correlation in the central Rapahoe Sector (Greymouth Coalfield) can be enhanced by detailed lithostratigraphy and chronostratigraphy. Rewanui Coal Measures are overlain conformably by lacustrine, deltaic and fluvial strata, and this upper contact can be located using lithological and geophysical log character. The Cretaceous–Tertiary Boundary (KTB) occurs near the top of Rewanui Coal Measures and has been identified palynologically in 16 drillholes. The Rapahoe Sector can be subdivided into two palynostratigraphic domains which adjoin along a basement normal fault which was downthrown to the north during coal measure deposition. The KTB provides an isochronous surface which is independent of the lithostratigraphic datum. Using the KTB as a datum, the "Upper", "Main" and "Submain" seams can be reliably correlated throughout the southern and central Rapahoe Sector. Similarly, the "Submain" seam can be correlated with "C" seam of the Strongman Mine area, though other Strongman seams are absent from the central and southern Rapahoe Sector.

INTRODUCTION

The Rapahoe Sector of Greymouth Coalfield (Figure 1) contains a large resource of high quality bituminous coal which has been defined by extensive, and ongoing, stratigraphic drilling (Figure 2). Mining is presently restricted to the northern and eastern portions of the sector (the former Strongman Mine, Strongman No. 2 Mine, Moody Creek Mine and independent mines in Ten Mile Ck.). The purpose of this paper is to illustrate the application of lithostratigraphy and chronostratigraphy to the understanding of coal seam distribution within the subsurface of the central Rapahoe Sector.

GEOLOGICAL SETTING

Geology of the Rapahoe Sector has been described by Bowman et al. (1984), Newman (1987), Newman and Newman (1992) and Ward (1995). The principal coal-bearing unit is the Rewanui Coal Measure Member (CMM) of the Paparoa Coal Measures (Figure 3). Rewanui CMM sediments in the Rapahoe Sector comprise mire, floodplain, crevasse splay, sandy fluvial and braided fluvial facies, which were derived from adjacent Paleozoic basement to the west and south of the present Rapahoe Sector (Ward 1995). These sediments were deposited in a broad NW / SE oriented trough, and overlie older lacustrine strata in the north and east of the study area, or onlap basement in the south (Figure 4). Deposition was largely controlled by basement faulting, though some subsidence in the north resulted from compaction of underlying strata (Ward 1995).

Coal seams occur throughout Rewanui CMM, except along a thin strip adjacent to the western margin (present coastline). Total proportion of coal (seams >1m thick) varies from zero to >30%, and maximum coal development occurs in the area between Runanga and Rapahoe (Figure 5). Coal seams are generally thick, clean and not split, however coal occurrence is variable and discontinuous, and fluvial, splay or floodplain sediments are present between seams. Primary controls on coal occurrence include subsidence and the location of clastic sediment sources (Ward 1995) which interact to limit coal occurrence at certain sites (Figure 6).

A generalised model is valuable for determining regional controls on coal formation, however such a model provides no detail suitable for recognition or correlation of individual seam horizons in the subsurface. The remainder of this paper presents a lithostratigraphic and chrono(bio)stratigraphic framework for the Rapahoe Sector, with which seam correlation models can be tested, and concludes with examples of the application of this framework.

LITHOSTRATIGRAPHY OF REWANUI CMM

The contact between Rewanui CMM and overlying Goldlight Mudstone Member (MM) (Figure 3) has traditionally been used as the lithostratigraphic datum for seam correlation within the Rapahoe Sector (e.g. Bowman et al. 1984). Correct identification of this contact is essential for reliable interpretation of stratigraphy, structure and seam correlation within the study area, however factors such as lateral facies changes, structural disruption and poor data (e.g. caved, uncored drillholes) can affect confidence in the location of the Rewanui CMM / Goldlight MM contact.

Gage (1952) originally described Goldlight MM as being massive mudstone which conformably overlies Rewanui CMM quartz-mica sandstones. This definition is applicable to the Mt. Davy Sector which lies east of the study area (Figure 1), however in the Rapahoe Sector, Rewanui CMM has different provenance, and Goldlight MM may incorporate 50% sandstone (Bowman et al. 1984). In the northwest of the coalfield, Goldlight MM grades laterally into coal measures, and the contact between Rewanui CMM and Dunollie CMM (Figure 3) has been arbitrarily located (Gage, 1952; Bowman et al. 1984). Newman (1985) considered that Goldlight MM deposition may have been contemporaneous with both Rewanui CMM and Dunollie CMM sedimentation.

Clear definitions for Goldlight MM and Rewanui CMM are required in order to correctly locate the contact between the units. Examination of geophysical logs (natural gamma, density and caliper) indicates that three lithofacies associations can be recognized (Figure 7). The lithological content and interpreted depositional environment of these associations is summarised in Table 1. The sandy transitional lithofacies association was deposited in a subaqueous environment, and is therefore incorporated into the lacustrine Goldlight MM. In contrast, Coal Measure members (e.g. Rewanui CMM, Dunollie CMM) contain exclusively terrestrial lithofacies. The conformable contact between Goldlight MM and Rewanui CMM is placed beneath lacustrine (mudstone or transitional) strata, at the first occurrence of carbonaceous beds.

Lithofacies association	lithologies	depositional environment
Coal Measures	poorly sorted v. fine to v. cse. sandstone and conglomerate with siltstone, mudstone and coal. Carbonaceous throughout.	terrestrial setting; fluvial, floodplain, floodbasin and mire environments
Transitional	well sorted, v. fine-med. sandstone, coarsening upwards packets (c.10m), interbedded with mudstone. Commonly slumped, bioturbated, with leaf and bivalve fossils. Rare carbonaceous material.	lacustrine setting; small sandy fluvial deltas
Mudstone	mudstone and silty mudstone, massive, with leaf and bivalve fossils. Rare carbonaceous material.	lacustrine setting

Table 1 **Major lithofacies associations and depositional environments, Greymouth Coalfield**

The isopach pattern and paleogeography of strata lying immediately above Rewanui CMM is depicted in Figure 8A. In the central Rapahoe Sector, up to 80m of transitional strata, with lacustrine mudstone above (as in DH635, Figure 7), are present. This package thickens westwards, and grades laterally into a zone where Goldlight MM is entirely composed of transitional strata, and the lacustrine lithofacies association is absent (see Figure 8B). Along the western margin (present coastline), transitional Goldlight MM grades into terrestrial Dunollie CMM (Figure 8B). In the northern Rapahoe Sector, the lacustrine lithofacies association persists westwards to the limit of Goldlight MM occurrence.

In addition to clarifying the location of the Rewanui CMM / Goldlight MM contact, recognition of transitional strata also permits identification of sediment sources which were active during the "lacustrine" periods of Paparoa Coal Measure deposition. Transitional strata were deposited by a river delta feeding from the NW into the Goldlight lake. A minor zone of transitional strata also occurs within lower Goldlight MM in the south of the Rapahoe Sector, representing a sand source from the southern margin of the basin.

Using the criteria given in Table 1, the upper Rewanui CMM contact can be accurately identified from geophysical logs and core in many drillholes. However, geophysical data is sometimes unreliable due to caving or the presence of casing. The relevant interval was uncored in a number of CRS drillholes (e.g. DH625, DH630, DH639, DH647), and caving produced anomalous density log patterns which were previously interpreted as indicating carbonaceous material. Data is poor for most drillholes drilled prior to 1979, for which only simple cuttings or core descriptions exists. In many older drillholes in the Strongman Mine area (e.g. DH201–205, DH611–615), transitional strata, logged as alternating sandstone and mudstone, were incorrectly placed within Rewanui CMM and not Goldlight MM.

Postdepositional structural disruption (faulting, shearing) also influences the expression of the upper Rewanui CMM contact. In most drillholes, carbonaceous material within upper Rewanui CMM is sheared due to mechanical anisotropy between these sediments, coarse clastic sediments and massive mudstones within Goldlight MM. Severe structural disturbance is present in DH628, in which there is thrust repetition of Goldlight MM. There are two Goldlight MM / Rewanui CMM contacts, both heavily sheared, and original stratigraphy cannot be reconstructed. Uppermost Rewanui CMM in DH631 is also structurally complex, with variable dip and fault gouge present in the upper 30m of Rewanui CMM.

Location of the upper Rewanui CMM contact in the northwest where Goldlight MM is absent remains difficult. No clear contact between Rewanui CMM and Dunollie CMM is present in coastal outcrop north of Ten Mile Ck. Similarly no contact can be located in DH634 which is dominated by conglomerates. Carbonaceous horizons beneath sandy and weakly carbonaceous Dunollie CMM mark the top of Rewanui CMM in DH637, DH639 and DH710. At the western margin of Goldlight MM occurrence, thin mudstone units but no transitional strata are present in DH619 and DH621.

LOCATION OF THE CRETACEOUS–TERTIARY BOUNDARY IN THE RAPAHOE SECTOR

In order to improve lithostratigraphic confidence in the northwestern area, the Cretaceous–Tertiary Boundary (KTB) was investigated palynologically in DH621 and DH622 (Raine 1981). The KTB has also been located near Moody Ck. mine (Raine 1984, 1994) and in DH631 (Raine 1990). These studies demonstrated that the biostratigraphic boundary lies close to the top of Rewanui CMM, and could be located across the coalfield. Newman (1987, Figures 29–32) proposed alternative seam correlation scenarios for the southern Rapahoe sector which depended on the degree of diachroneity of the Goldlight / Rewanui contact. Location of the KTB, which corresponds to 65 Ma, offers a means of testing the time significance of the lithostratigraphic contact.

Rather than being represented by mass extinction, slightly more fossil plant taxa have first appearances at the KTB than become extinct. The key floral event marking the KTB is an increase in the abundance of the small angiosperm pollen type *Triorites minor*, at the expense of the spore component of the flora. In addition, ornamented angiosperm pollen types disappear from the flora at the KTB. There is little change in abundance or diversity of the common conifer (podocarp) or spore (fern) elements of the flora. A similar pattern of floral change was experienced at other sites in New Zealand, Australia and the Antarctic Peninsula, suggesting that a hemisphere–wide climatic event was responsible for KTB floral change.

The position of the KTB has now been identified or constrained (Ward 1995; *in prep.*) in 16 drillholes (Figure 9), three of which (DH628, DH631, DH636) contain structural disruption in the upper Rewanui CMM interval. Projection of the remaining 13 drillholes onto a SW–NE cross-section (Figure 10) reveals that the interval between the KTB and the top Rewanui CMM is variable. In the southwest half of the section, the KTB lies within an interval of 1.5m–2.2m below the top Rewanui CMM contact. In the northeast, the corresponding interval is more variable but averages c.17m in all drillholes except DH632. Within either half of the section, the KTB is approximately parallel to the top of the Rewanui CMM, indicating that the lithostratigraphic datum is essentially isochronous.

Using the above results, the Rapahoe Sector can be divided into two palynostratigraphic domains. The location of the interface between these domains cannot be uniquely located from existing data, and may lie anywhere within the stippled area of Figure 9. A particular problem is the poor precision of KTB location in DH622 (±14m). Comparison of the lithostratigraphy of the drillholes which lie within the stippled area (diagonal crosses in Figure 9) allows the true position of the domain interface to be estimated (Table 2), and this is depicted by the heavy grey line in Figure 9.

Drillhole	domain	reasons
DH622	NE	Strat. more like DH619 & DH635 (NE) than DH626 & DH643
DH637, DH702	SW	Strat. more like DH626 (SW) than DH622 & DH647
DH647	NE	Strat. similar to DH622 (NE)
DH704	NE	Strat. (esp. top 20m) v. similar to DH622 & DH647
DH624	SW	Strat. comparable to DH640.
DH701	NE	Strat. unlike DH643 (congs. and cse ssts), v.similar to DH631 and comparable to DH645

Table 2 **Stratigraphic comparisons which constrain the position of the interface between palynostratigraphic domains.**

The greater interval between the KTB and the top Rewanui CMM contact in the northeastern domain indicates more rapid subsidence in the northeast during sedimentation of the uppermost Rewanui CMM. A normal fault, oriented along the domain boundary and downthrown to the northeast is the most likely cause for this variable subsidence. This fault is a persistent basement structure, which also formed the southern margin of the lacustrine basin underlying Rewanui CMM in the Rapahoe Sector (see Figure 4). The maximum thickness of transitional strata above Rewanui CMM (Figure 8) is located immediately north of this fault, indicating that fault movement persisted during early Goldlight MM accumulation.

Location of the KTB confirms the lithostratigraphic model presented above (Figure 8B). Samples from lacustrine Goldlight MM, transitional Goldlight MM and Dunollie CMM all lie above the KTB, indicating the three depositional environments (lake, delta and fluvial) were contemporaneous.

APPLICATIONS OF LITHOSTRATIGRAPHY AND CHRONOSTRATIGRAPHY TO SEAM CORRELATION, CENTRAL RAPAHOE SECTOR

The above discussions provide a means of correctly identifying the key lithostratigraphic datum in the Rapahoe Sector, and demonstrates that an isochronous surface can be located throughout the area. Within either palynostratigraphic domain, the position of the KTB can be simply modelled by determining the appropriate interval below the top Rewanui CMM contact and adjusting for dip where necessary. The resulting modelled KTB can be used as a basin-wide correlation datum. Four applications of this datum to seam correlation in the central Rapahoe Sector are discussed below.

a) Correlation across the domain interface

The immediate implication of the KTB datum model is that strata in the northeastern domain cannot be directly correlated with strata at the same relative lithostratigraphic position in the southwestern domain. However, when the known position of the KTB in DH643 is aligned with the modelled position in DH701, sensible correlations can be achieved (Figure 11). Likewise, DH714 and DH704 can be correlated. In either instance, incorrect correlations would be achieved if the lithostratigraphic datum was used.

b) Seam development coincident with the KTB: the "Upper" seam

Drillholes along the south of the domain interface (DH637, DH702, DH726) have only carbonaceous mudstone at the KTB location. In contrast, a thick (up to 21m) and often split seam, is developed immediately north of the domain interface, in DH622, DH647, and DH704 (Figure 11). This "Upper" seam is areally restricted (Figure 12), and developed in direct response to downfaulting of the northeastern domain. A minor, southern extension of the seam is present in DH643 (Figure 11). Elsewhere a variety of lithofacies are present at the modelled KTB location, with modest coal development in DH619 (4m) and DH632 (6m, clean and dirty). Coal formation coincident with the KTB also occurred in the south (DH633, DH646, DH648), and near Moody Ck. mine (Raine 1994).

c) Location of the "Main" and "Submain" seams

In many drillholes in the central Rapahoe Sector, the "Main" seam is located c. 35m below the modelled KTB, whereas the "Submain" seam is located c.60m below the modelled KTB. These positions are indicated in Figure 11. A notable feature is the interaction of clastic strata with coal formation in the "Main" seam interval in DH704 and DH714. The "Main" seam is partly represented by sandstone in DH714 and is absent from DH704. This correlation is supported by seam palynology profiles (N. Moore 1996, this volume). Sandstone interbeds within the "Main" seam in DH622 reflect proximity to the northwestern sediment source (Figure 5).

The "Submain" seam in DH701 falls c.12m below the predicted position. DH701 lies immediately north of the palynostratigraphic domain interface, and the greater depth to the "Submain" seam, in addition to the atypical thick sandstone unit above the seam, indicates a period of enhanced, but episodic, subsidence. Movement along the normal fault immediately postdated deposition of the "Submain" seam, but ceased prior to accumulation of the "Main" seam. Further movement occurred between "Main" seam deposition and the KTB.

DH631, at the north end of the section in Figure 11, is anomalous, and both the "Main" and "Submain" seams are higher than the seam model predicts. The interval above the "Main" seam is structurally disturbed, and the seam positions suggest c.15m of strata are absent from the section. Though the KTB has been located in DH631 (Raine 1990), the section is now believed to be unreliable (Raine 1994). Other drillholes in which the upper Rewanui CMM is structurally disrupted include DH636, DH696 and DH698, and modelling of the seam locations provides a useful tool for estimating the completeness of the stratigraphy. The seam correlation model also assists with the location of the top Rewanui CMM contact in DH639, in which Goldlight MM is absent.

Exact positions of the "Main" and "Submain" seams are influenced by Rewanui CMM thickness (Figure 4), localised subsidence and post-depositional structural disruption. However, the seam model presented above indicates the general stratigraphic position where seams would be expected, and allows correlation of seams across barren zones where coal is absent. The correlation model is particularly valuable for tracing seams across the palynostratigraphic domain interface. Correlations can be extended throughout the Rapahoe

Sector and the maximum extent of the "Main" and "Submain" seams can be determined (Figure 12), though barren zones which may lie within the seam limits are not depicted.

d) Correlation of central Rapahoe Sector seams with Strongman Mine area seams

The relationship between coal seams of the central Rapahoe Sector and those of the Strongman Mine area is poorly understood. The "Main" seam, which is present throughout most of the southern and central Rapahoe Sector (Figure 12), does not occur north of DH645 (Figure 13). In DH635 and DH708 (Figure 13), the uppermost seam is 5–10m below the modelled KTB position, and therefore does not correlate with the "Upper" seam further south, which spans the KTB (Figure 11). In DH708, the second highest seam occurs at approximately the same stratigraphic level as the "Submain" seam in DH641 (i.e. c.60m below KTB), and seam thickness and lithostratigraphy are comparable. The estimated position of the "Submain" seam in DH635 corresponds to an interval of dirty coal and carbonaceous mudstone, lying above thick sandstone and conglomerate beds.

The "Strongman area" log depicted in Figure 13 summarises lithostratigraphy in the Strongman West block, and is compiled from DH611-615, DH731, DH733 and DH735. A modest "D" seam occurs c.25m below the top of Rewanui CMM, and is separated from a thicker and often split "C" seam by c.30m of sandstone-dominated section. The "C" seam in the Strongman area occurs at the same stratigraphic level as the "Submain" seam of the central Rapahoe Sector, and the two seams can be correlated. In addition, the "Submain" and "C" seams have similar stratigraphy – both lie above conglomerate-dominated strata, both can exceed 10m in thickness, and both may be split by fine to coarse clastic beds.

The Strongman area "D" seam lies c.30m above the stratigraphic position of the "Main" seam, and is restricted to below the modelled position of the KTB. "D" seam does not therefore correlate with the "Upper" seam. "D" seam is present in DH635 and DH708, but does not extend as far south as DH645 or as far west as DH641 (Figure 13). Further north, "D" seam and a split "Submain" (= "C") seam are present in DH619 (see Figure 3 for location). There is also an interval of dirty coal in DH619 at c.30m below the KTB, which may correspond to the "Main" seam of the central Rapahoe Sector. Neither "Submain" nor "D" seams occur in the far north of the Rapahoe Sector (DH621, DH634, DH710) (Figure 12).

CONCLUSIONS

Seam correlations in the central Rapahoe Sector can be improved by optimising the data available from existing drilling. Enhanced sedimentological analysis provides more accurate criteria for locating lithostratigraphic contacts and describing lateral relationships between key units. Location of the KTB throughout the Rapahoe Sector provides an independent, isochronous surface which confirms the lithostratigraphic model and can also be used as a datum for seam correlation. Syndepositional basement faulting controls the location of the interface between two distinct palynostratigraphic domains, and the configuration of some coal seams. Recognition of the domain interface is essential for accurate seam modelling in the central Rapahoe Sector.

Three distinct seam horizons can be recognized within the central and southern Rapahoe Sector. The "Upper" seam is restricted to immediately north of the palynostratigraphic domain interface, and developed in response to enhanced subsidence. The "Main" and "Submain" seams are more widespread, and can be reliably correlated throughout the study area. Both seams are present in the central Rapahoe Sector, from which the "Main" seam extends southwards and the "Submain" seam extends northwards, correlating with "C" seam in the Strongman area. Other Strongman area seams are not found within the central Rapahoe Sector.

ACKNOWLEDGEMENTS

I thank Dr. Jane Newman (Coal Research Ltd.) for constant support and supervision of this project, and for commenting on this manuscript. Thanks also go to CRL for providing financial support via coal sampling and other casual work. Dr. Tim Moore (CRL), Dr. Ian Raine (IGNS) and Nick Moore have provided valuable discussion of seam correlation, palynology and the KTB in Greymouth. Ministry of Commerce Resource Information staff and Mr. Frank Taylor (Greymouth Coal Operating Ltd.) kindly supplied copies of geophysical logs.

REFERENCES

Bowman, R.G.; Caffyn, P.; Duff, S.W. 1984: Greymouth Coalfield. New Zealand Coal Resources Survey Report, Ministry of Energy, Wellington, New Zealand. Part 1, 211p.

Gage, M. 1952: The Greymouth coalfield. *New Zealand Geological Survey bulletin 45.* 232p.

Moore, N. 1996: Seam identification, correlation and coal quality prediction using in-seam variations in key palynomorph abundances. *Proceedings, AusIMM Conference, Greymouth, August 1996* (this volume).

Newman, J. 1985: Paleoenvironments, coal properties, and their interrelationships in Paparoa and selected Brunner Coal Measures on the West Coast of the South Island. Unpublished Ph.D. thesis, University of Canterbury.

Newman, J. 1987: Coal type and paleoenvironments in the Rapahoe Sector, Greymouth Coalfield. Resource Management and Mining Coal Geology Technical Report 3: 28p.

Newman, J.; Newman, N.A., 1992: Tectonic and paleoenvironmental controls on the distribution and properties of Upper Cretaceous coals on the west Coast of the South island, New Zealand. In McCabe, P.J.; Parrish, J.T. (eds), Controls on the distribution and quality of Cretaceous coals. *Geological Society of America Special paper 267*:. 347-368

Raine, J.I. 1981: Palynological correlation of the Dunollie/Rewanui Member boundary in drillholes 621 and 622, Greymouth Coalfield. *New Zealand Geological Survey Report PAL47:* 10p.

Raine, J.I. 1984: Outline of a palynological zonation of Cretaceous to Paleogene terrestrial sediments in West Coast region, South Island, New Zealand. *New Zealand Geological Survey Report 109:* 82p.

Raine, J.I. 1990: K/T boundary in New Zealand terrestrial sequences. *Geological Society of New Zealand Miscellaneous publication 50A (GSNZ 1990 Annual conference, programme and abstracts):* 110

Raine, J.I. 1994: Terrestrial K/T boundary studies in New Zealand. *Palaeoaustral* (PPAA Newsletter), December 1994: 9-12

Ward, S.D. 1995: Controls on sedimentology and coal occurrence in the Rewanui Coal Measure member, western Greymouth Coalfield (Rapahoe Sector). *Proceedings, Sixth New Zealand Coal Conference, October 1995*: 151–161

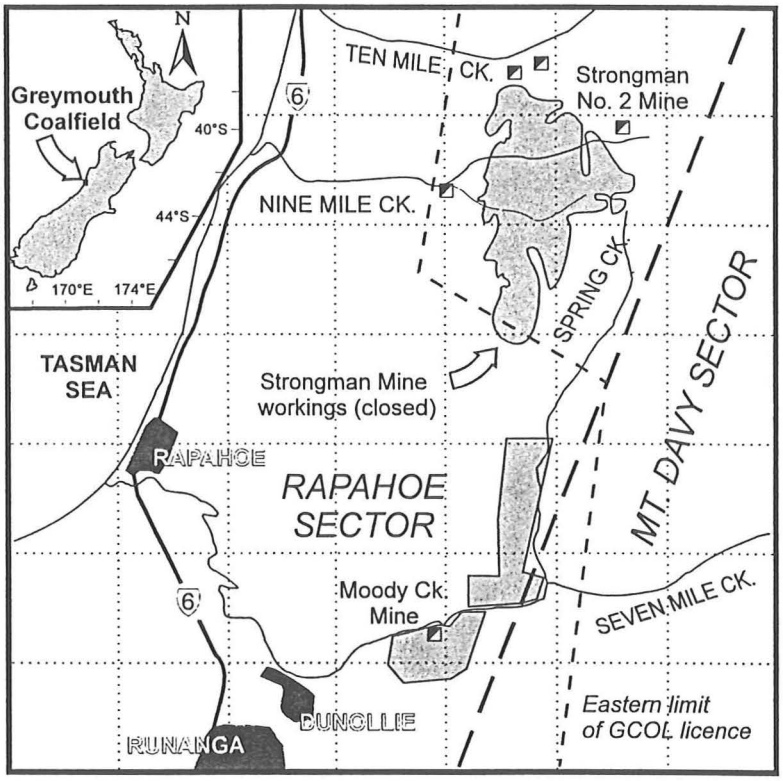

Figure 1
Location map of Rapahoe Sector.
Mined areas are stippled and
mine portals are indicated ◩
Grid square is 1km.

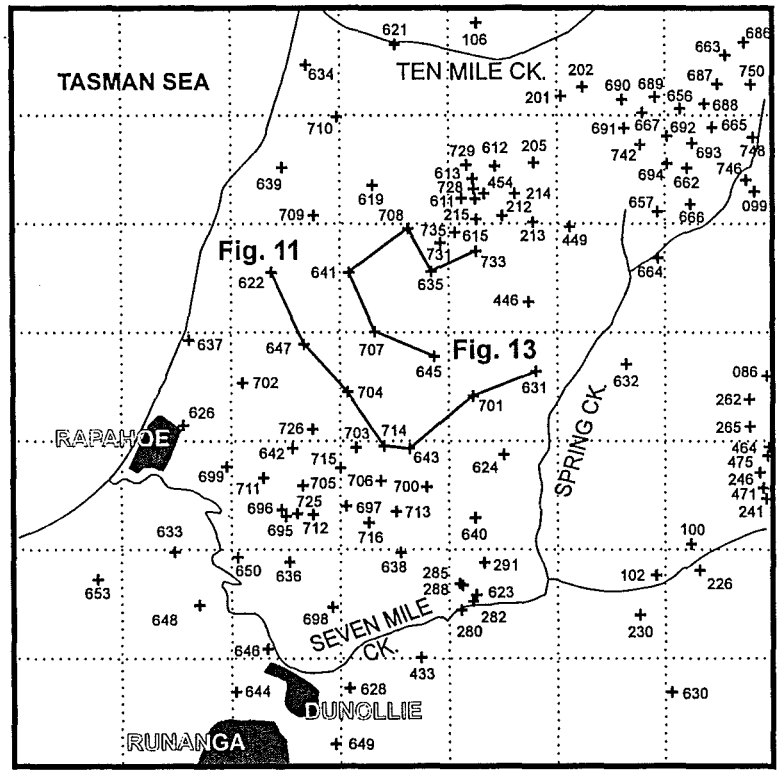

Figure 2
Location of stratigraphic drillholes. Sections illustrated in Figs. 11 and 13 are marked.
<619 = State Coal Mines
619-668 = Coal Resources Survey
>668 = modern exploration holes

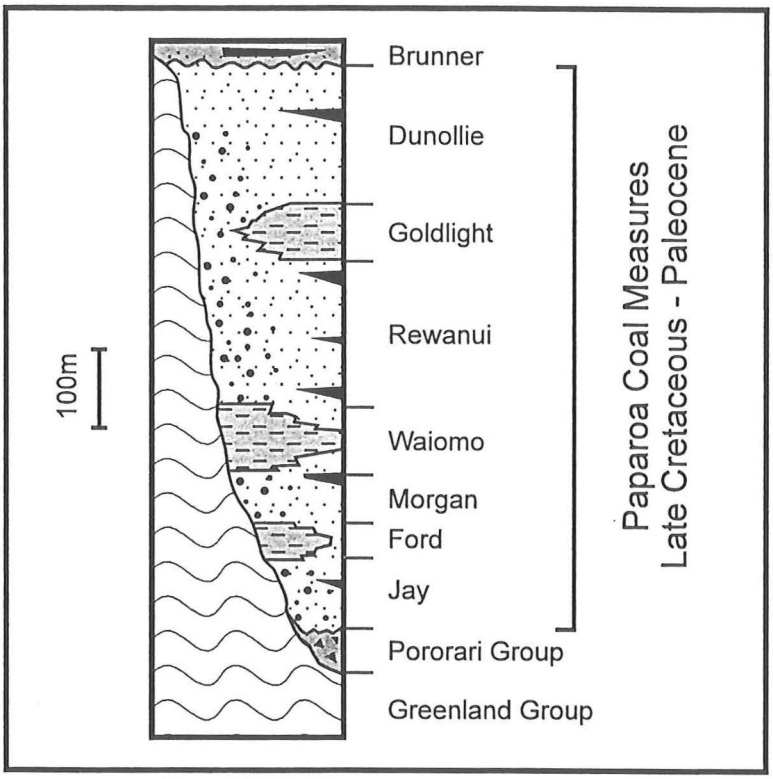

Figure 3
Generalised stratigraphic column, Greymouth Coalfield.
From Newman & Newman (1992)

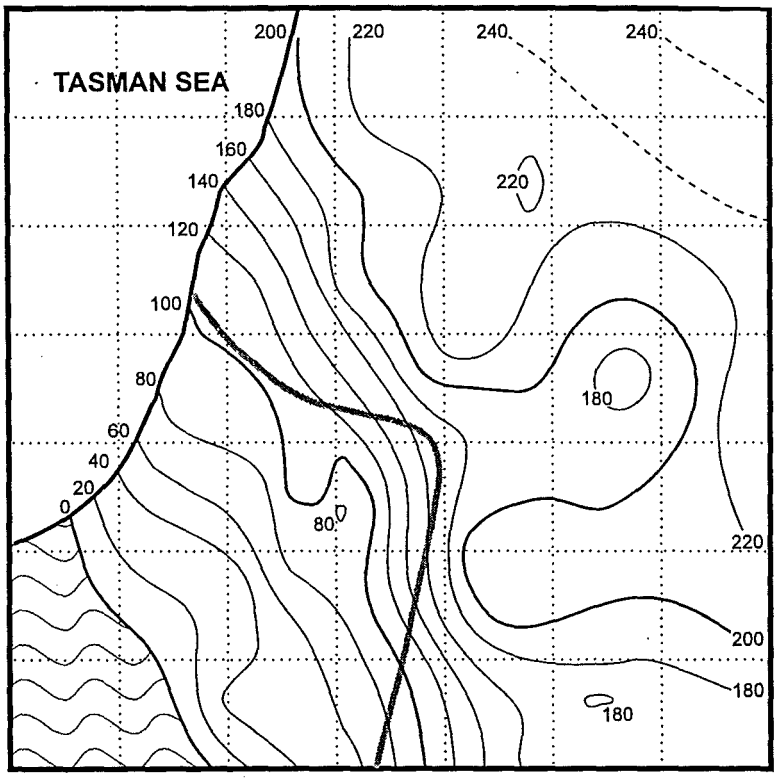

Figure 4
Isopach model, Rewanui CMM. Interval = 20m. 240m contour estimated, all others generated by geostatistical modelling. Heavy grey line is southwestern limit of underlying lacustrine basin. Pattern in southwest is basement, over which Rewanui CMM is inferred to be absent.

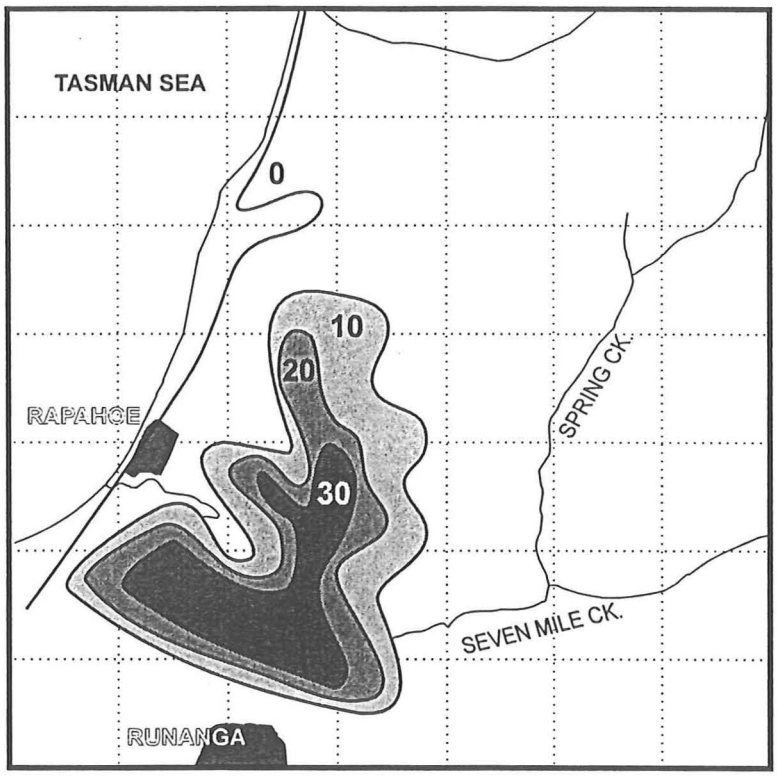

Figure 5
Cumulative coal percentage,
Rewanui CMM.
All seams >1m thick included.

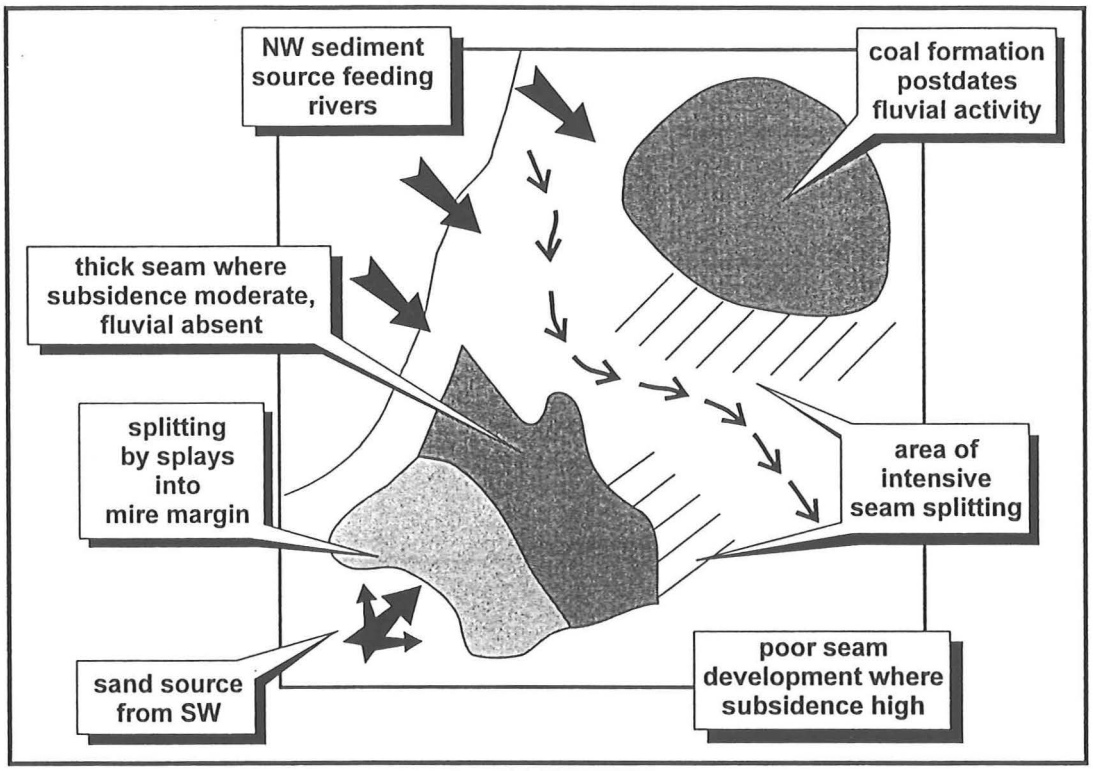

Figure 6
Generalised model for coal formation in the Rapahoe Sector, showing location of major sediment sources which affect coal dsitribution.

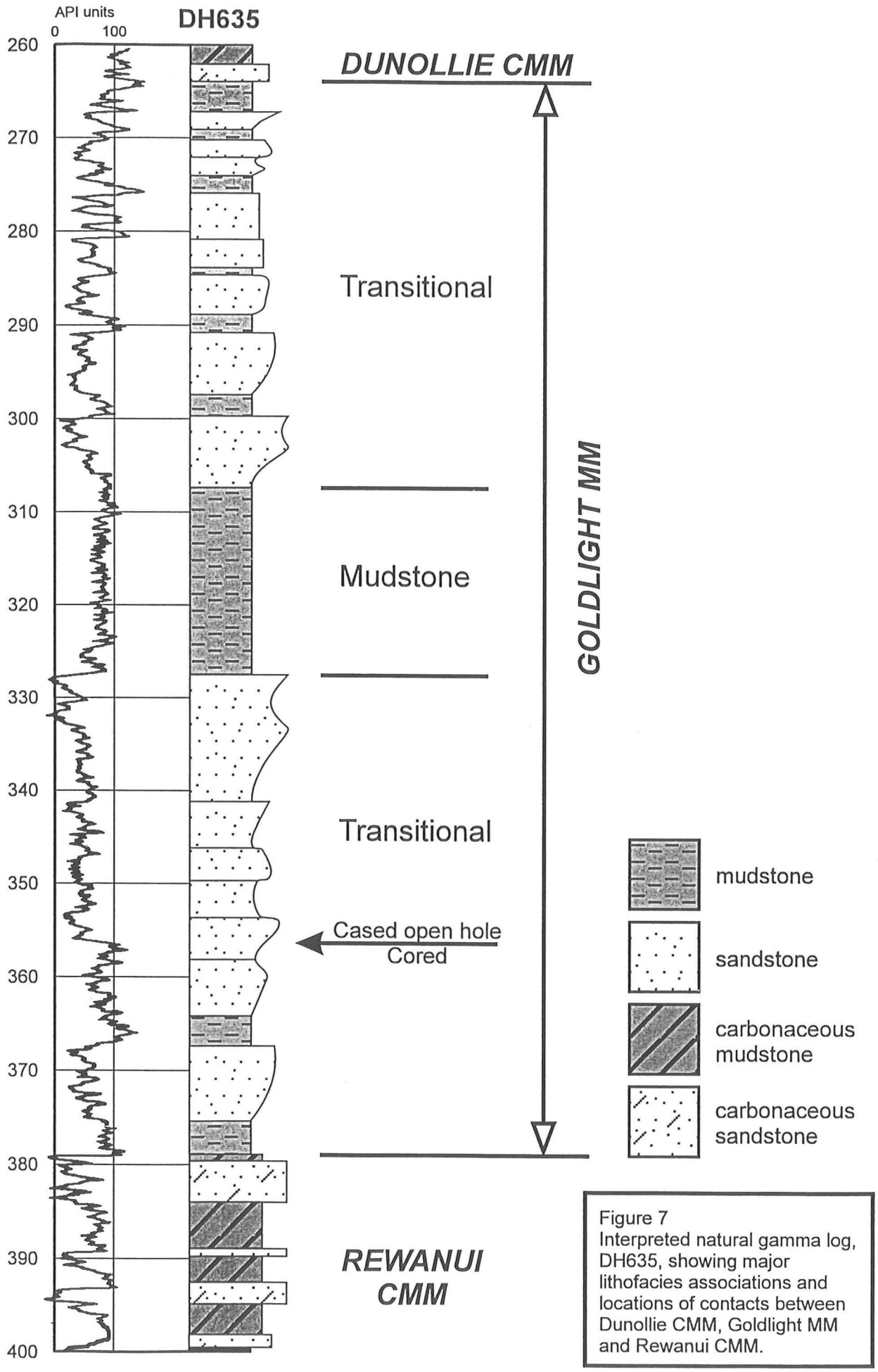

Figure 7
Interpreted natural gamma log, DH635, showing major lithofacies associations and locations of contacts between Dunollie CMM, Goldlight MM and Rewanui CMM.

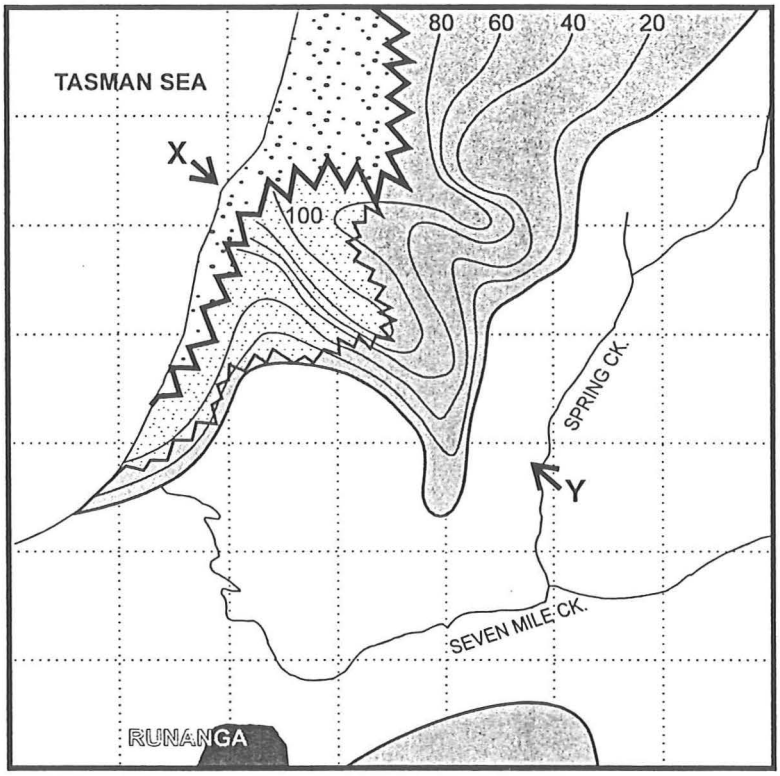

Figure 8 A
Isopach map and paleogeography of transitional strata above Rewanui CMM. Contour interval = 20m

Lacustrine Goldlight MM directly above Rewanui CMM

Sandy transitional strata with lacustrine mudstone above

Sandy transitional strata, lacustrine mudstone absent

Dunollie CMM, Goldlight MM absent

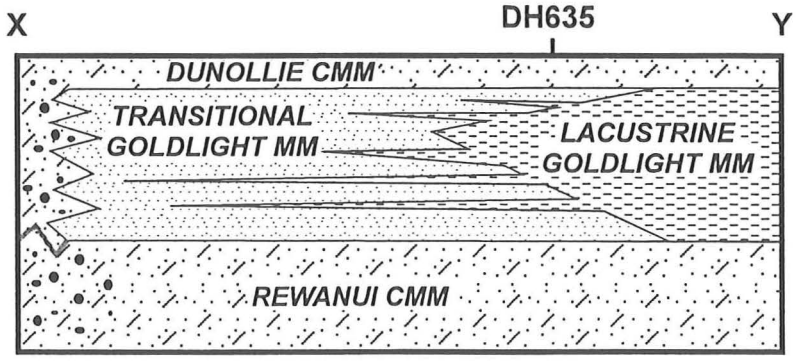

Figure 8 B
Schematic section along line X-Y showing relationship of Rewanui CMM to overlying strata. Note gradation between conglomeratic Rewanui CMM and Dunollie CMM in northwest. The approximate projected position of DH635 is indicated.

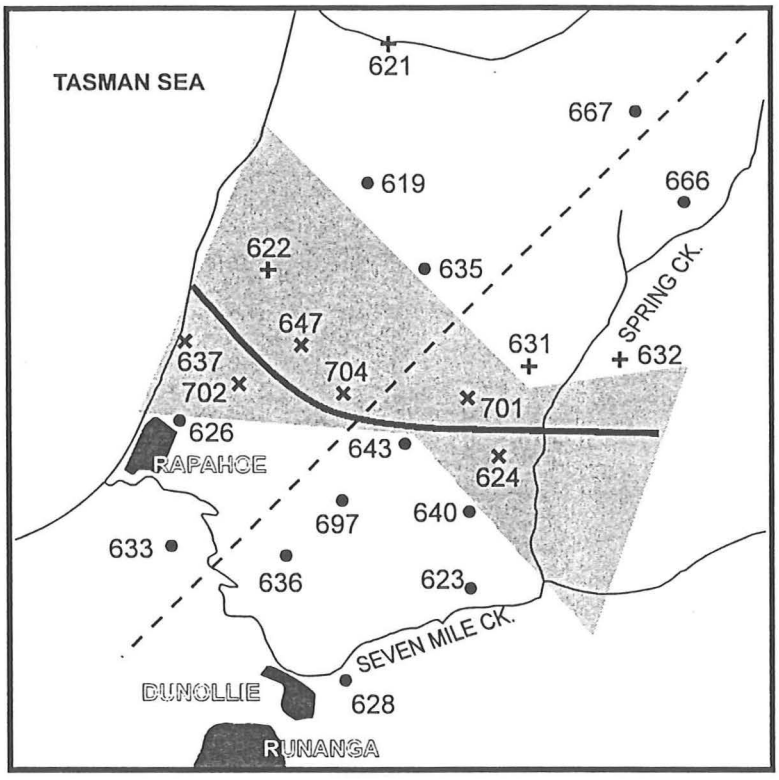

Figure 9
Drillholes in which KTB located:
+ = data from Raine (1981, 1990)
● = data from Ward (in prep.)
Palynostratigraphic domain interface falls within stippled area. Drillholes marked × are discussed in Table 2. Interpreted position of domain interface marked by grey line. Dashed line is line of section in Figure 10.

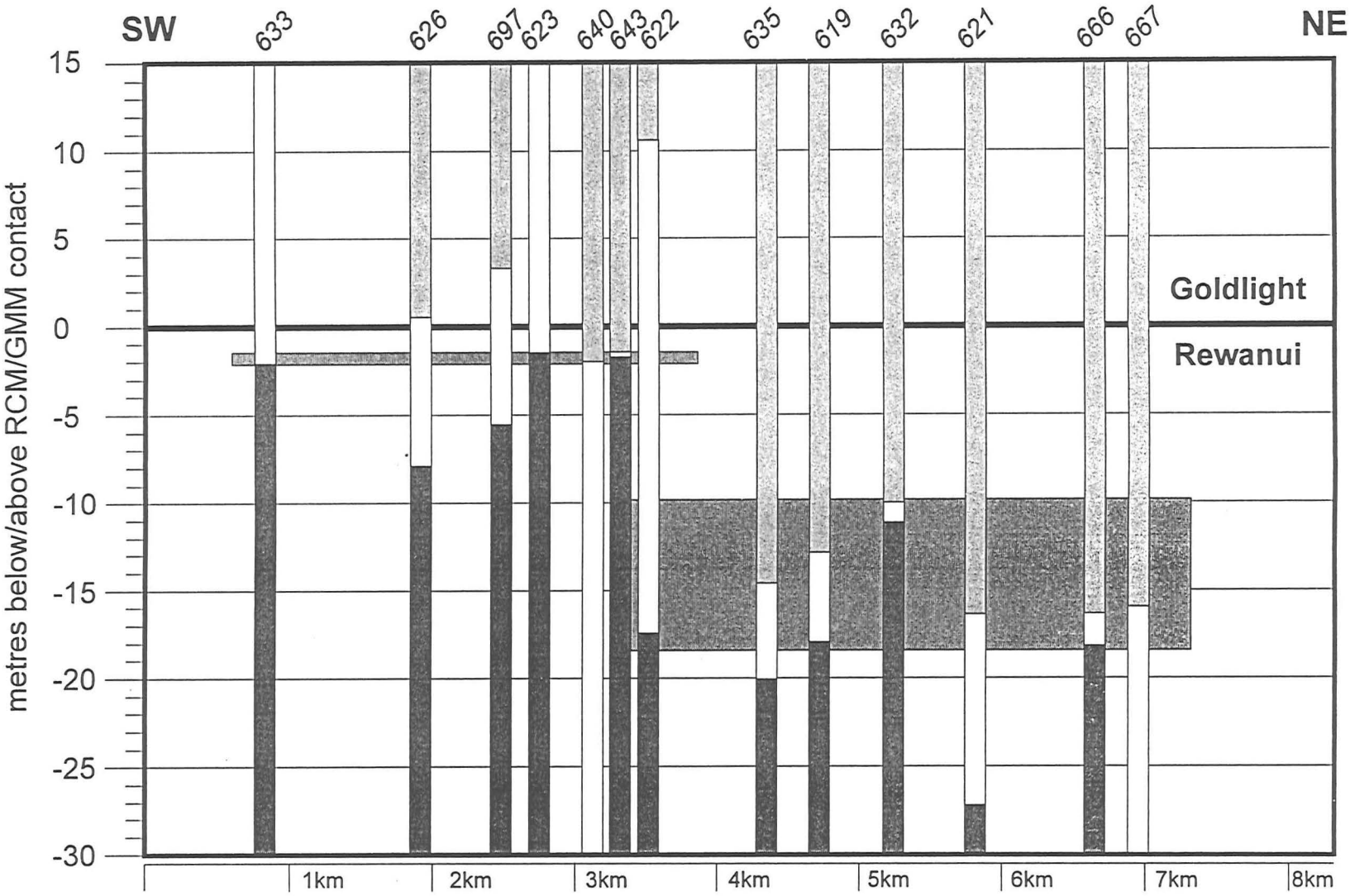

Figure 10
SW-NE cross-section through Rapahoe Sector, drillholes containing KTB projected onto line of section. Datum is Goldlight MM / Rewanui CMM contact.

Confirmed Tertiary strata

Confirmed Cretaceous strata

Interval with no age control

Zone in which Cretaceous - Tertiary Boundary occurs

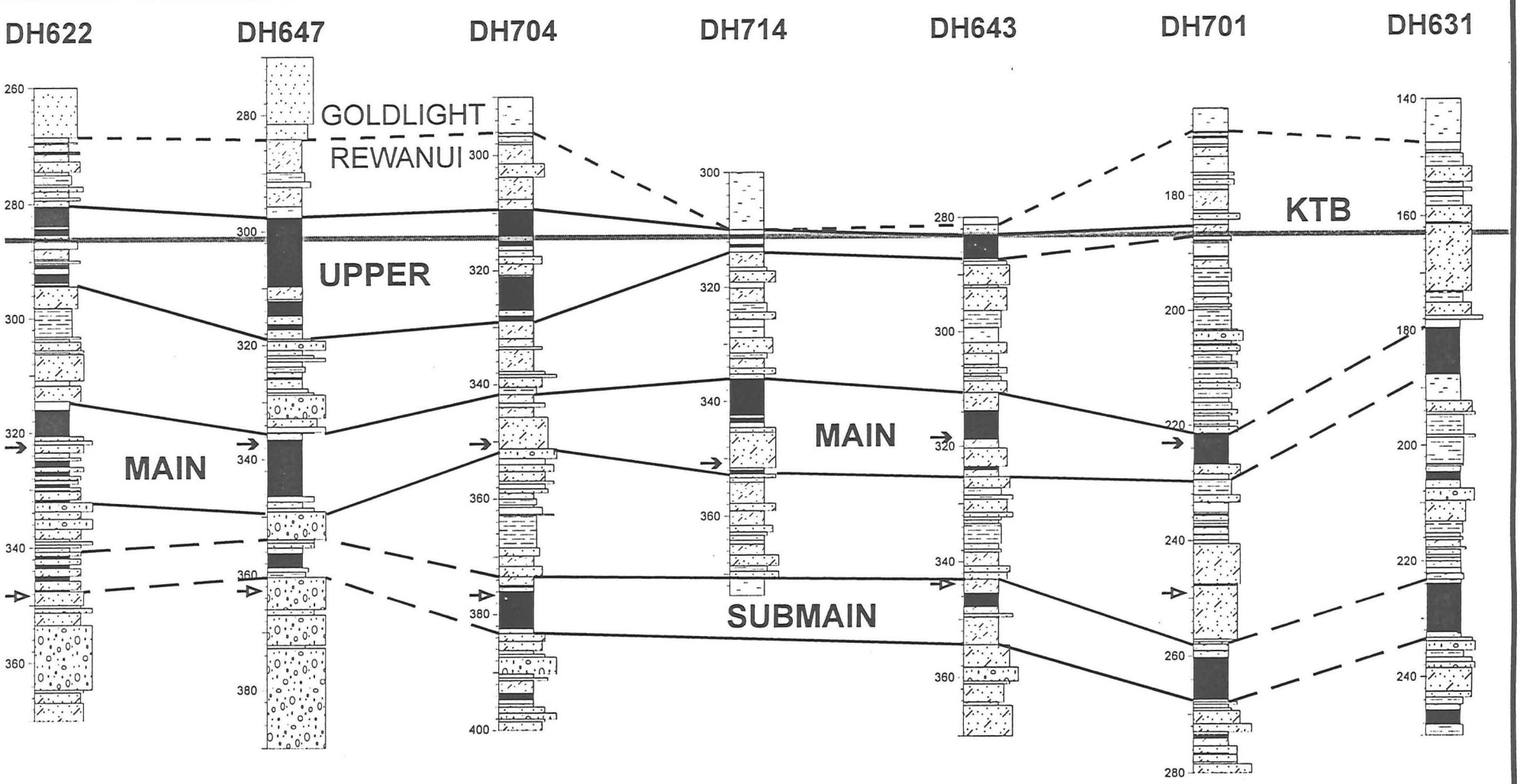

Figure 11
Seam correlation diagram, central Rapahoe Sector. Location of section given on Figure 2. Vertical scale = 1:1000, no horizontal scale implied. Datum is modelled position of Cretaceous-Tertiary Boundary (KTB).
→ = estimated position of Main seam
→ = estimated position of Submain seam

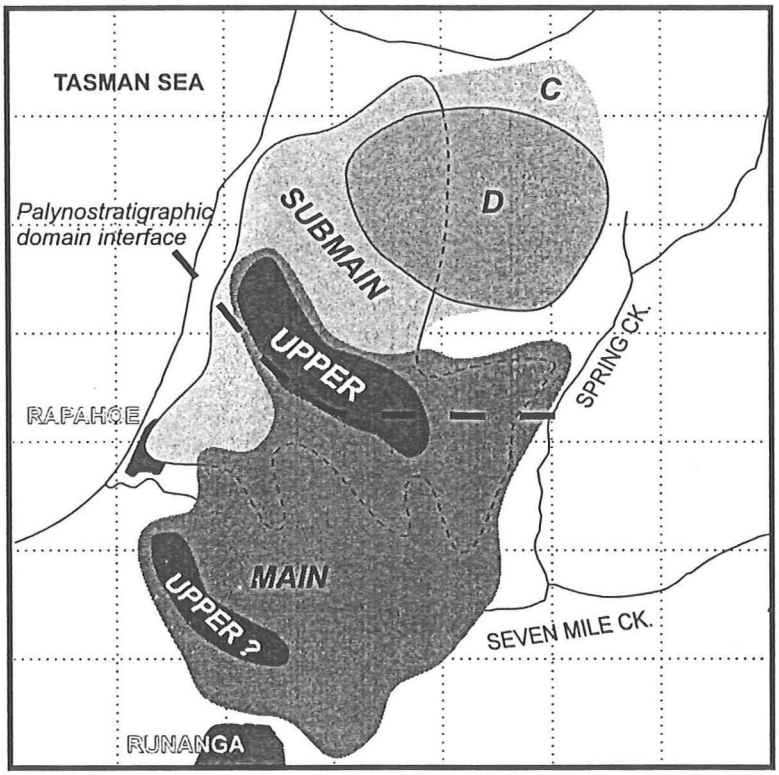

Figure 12
Schematic seam distribution map, Rapahoe Sector. Note that "C" seam is continuous with the "Submain" seam. Barren zones within individual seams are not depicted.

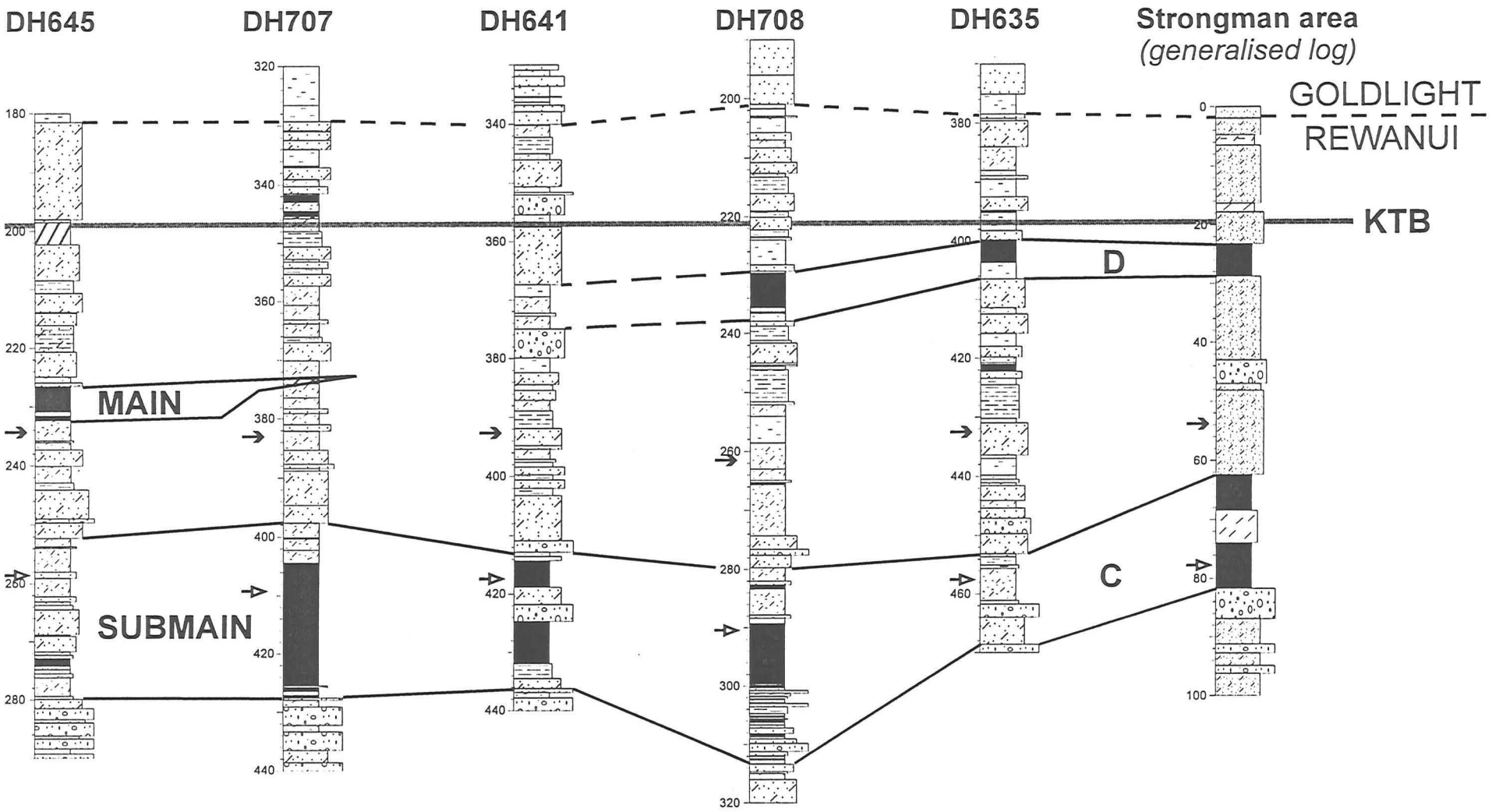

Figure 13
Seam correlations beween central Rapahoe Sector and Strongman area. Location of section given on Figure 2. Vertical scale = 1:1000, no horizontal scale implied. Datum is modelled position of KTB.
→ = estimated position of Main seam
↛ = estimated position of Submain seam